

BIRLA CENTRAL LIBRARY

PILANI (Rajasthan)

Class No:- 539.1

Book No:- 73 560

Accession No:- 47742

Acc. No.....

ISSUE LABEL

Not later than the latest date stamped below.

--	--	--

An Outline of

ATOMIC PHYSICS

An Outline of

ATOMIC PHYSICS

Collaborators on the Third Edition

OSWALD H. BLACKWOOD

Late Professor of Physics,
University of Pittsburgh

THOMAS H. OSGOOD

Dean of the School of Graduate Studies,
Michigan State College

ARTHUR E. RUARK

Temerson Distinguished Service
Professor of Physics, University of Alabama

Additional Collaborators on Earlier Editions

ELMER HUTCHISSON

Dean of the Faculty,
Case Institute of Technology

GEORGE A. SCOTT

Late Professor of Physics,
University of Pittsburgh

WILFRED N. ST. PETER

Late Professor of Physics,
University of Pittsburgh

ARCHIE G. WORTHING

Late Professor of Physics,
University of Pittsburgh

Third Edition

New York · JOHN WILEY & SONS, Inc.
London · CHAPMAN & HALL, Limited

COPYRIGHT, 1933, 1937, BY
OSWALD H. BLACKWOOD, ELMER HUTCHISSON,
) THOMAS H. OSGOOD, ARTHUR E. RUARK,
WILFRED N. ST. PETER, GEORGE A. SCOTT,
AND ARCHIE G. WORTHING

COPYRIGHT, 1955
BY
JOHN WILEY & SONS, INC.

All Rights Reserved

*This book or any part thereof must not
be reproduced in any form without
the written permission of the publisher.*

Library of Congress Catalog Card Number: 55-7788

PRINTED IN THE UNITED STATES OF AMERICA

Preface

This book grew out of a course of lectures given for some years to intelligent young men and women. All had completed a year's work in college physics. Most of them expected to devote their lives to professions other than physics, such as medicine, law, or chemistry. The course was organized in the belief that they would want to know what physical science has to say about the structure of atoms and molecules and the nature of radiation; that they would want to go to the frontiers of physics and see for themselves what manner of things must be done to take the next step forward.

The reception accorded to earlier editions of the book by professors and students in other universities has been most gratifying to us. In the earlier editions we acknowledged the helpful suggestions of many skillful teachers. The list of these suggestions has now grown so large that we must thank most of our friendly critics by this general acknowledgment. It is appropriate, however, that we record our indebtedness to Dean E. Hutchisson, an active collaborator on earlier editions, for a critical reading of the manuscript of this edition in the last stages of its development; and to Professors J. A. Bearden and E. Scott Barr for advice concerning Chapters 5 and 9.

The material in Chapters 1 through 10 of the present volume is a modernized version of the first three-quarters of the previous edition. It has been reorganized, rearranged, rewritten; parts have been amplified, parts discarded; but the simplicity of treatment characteristic of the first and second editions has been carefully preserved. There is no change in the level of difficulty of this portion of the book, which in itself provides a well-balanced year's course on the subject of atoms and molecules.

For two reasons it is inevitable that Chapters 11 through 14, which deal with elementary particles and the nucleus, should be considerably more difficult than those preceding them. First, much of the information they contain has been known for a decade or less; it has not had the benefit of the evolutionary process of simplification and clarification which time and discussion can provide. Second, the theoretical background has been and still is in such a state of flux that it is often dif-

difficult to justify the choice of one interpretation of observations in preference to another. To make room for this new physics, the long chapter on astrophysics has been omitted. A very simple account of the restricted theory of relativity has been retained.

Both professor and student will find that this *Outline of Atomic Physics* contains much more material than can be mastered in the time usually allotted to a course in "modern" physics at about the third-year university level. The selection of topics by the professor will naturally depend on his previous experience and his present scientific interests as well as on the preparation and background of his students. As a further help to the user, we have starred (★) certain paragraphs which may well be omitted in a first reading or in a brief course without destroying the continuity.

The tremendous advance of physics in recent years has led to extensive revision. Death deprived us of the help of our former colleagues, Professors Scott, St. Peter, and Worthing from the beginning of this task, and of Professor Blackwood in the final stages of writing. Only a few pages of the previous edition have escaped the knife. We have been guided by the desire to emphasize principles, not details. As we said in the first edition, "It is the hope of the authors that this book may awaken a love of physics and a respect for its achievements and that it will help to demonstrate that the academic research physicist is a disinterested advance agent of the progress of civilization."

January, 1955

THOMAS H. OSGOOD
ARTHUR E. RUARK

Contents

1. THE ATOMIC NATURE OF MATTER	1
1. Early Atomic Theories	1
2. Molecular Velocities	4
3. The Distribution of Velocities	6
4. Direct Experimental Determination of Molecular Speeds	8
5. Temperature and Molecular Energy	9
6. Molecular Heats of Gases	11
7. Real Gases	14
8. Mean Free Paths	16
9. Brownian Movements and Molecular Reality	17
2. THE ATOMIC NATURE OF ELECTRICITY	23
1. Early Electrical Theories	23
2. The Electronic Charge	25
3. The Mass of the Electron	30
4. Variation of Mass with Velocity	32
5. The Electromagnetic Nature of Mass	35
6. The Size of the Electron and of the Proton	37
7. Isotopes and Their Interpretation	38
8. The Whole-Number Rule	42
9. The Structures of Atoms	46
3. THE NATURE OF RADIANT ENERGY	51
1. Introduction	51
2. The Electromagnetic Conception of Radiation	53
3. Spectra	54
4. The Diffraction Grating	55
5. Types of Spectra	59
6. The Complete Electromagnetic Spectrum	60
7. Temperature Radiation	66
8. Black Bodies	68
9. Origin of the Quantum Theory	71
10. Early Observations on Photoelectricity	77
11. Experimental Results	78
12. Some Photoelectric Experiments	80
13. Theoretical Developments	85
14. Comparison between Theory and Experiment	87
15. The Significance of Einstein's Equation	88
16. Partial Reconciliation of the Wave and Corpuscular Aspects of Light	89
4. THE BOHR MODEL OF THE ATOM	93
1. The Hydrogen Spectrum	93
2. Bohr's Theory of the Hydrogen Atom	96
3. Extensions of the Theory	100
4. Insufficiency of the Bohr Model	107

5. X-RAYS	109
1. Production and Measurement of X-Rays	110
2. Absorption of X-Rays	114
3. Secondary X-Rays	116
4. The Wave Properties of X-Rays	117
5. Bragg's Law	122
6. Simple Crystals	126
7. Emission Spectra	134
8. Absorption Spectra	141
9. Scattering of Hard X-Rays and Gamma Rays	143
10. The Betatron	150
6. WAVES ASSOCIATED WITH MATERIAL PARTICLES	155
1. Introduction	155
2. De Broglie's Wave Theory of Matter	156
3. Verification of the Wave Nature of Electrons	158
4. The Electron Microscope	162
5. De Broglie's Quantization of the Hydrogen Atom	164
6. Frequency and Velocity of Matter Waves	168
7. Schroedinger's Wave Mechanics	169
8. Quantum Theory of a Particle in a Leak-Proof Box	172
9. The Penetration of a Potential Barrier	174
10. Born's Interpretation of the Wave Function	177
11. The Uncertainty Principle	179
12. Simple Harmonic Oscillator	185
13. Results of the Wave Theory of the Hydrogen Atom	189
14. Summary	190
7. ATOMIC SPECTRA AND THE PAULI PRINCIPLE	193
1. Spectra of the Alkalies	194
2. Electron Spin; the Explanation of Doublets in Alkali Spectra	198
3. Selection Rules	200
4. Atoms with Several Valence Electrons	202
5. Pauli's Principle	207
6. The Spectral Displacement Rule	209
7. Ionization Potentials	209
8. Resonance Radiation and Resonance Potentials	211
9. Collisions of the Second Kind	213
10. The Stern-Gerlach Experiment on Atomic Magnetic Moments	214
11. Magnetic Properties of Bulk Matter	215
8. THE PERIODIC SYSTEM	221
1. Classification of the Elements	221
2. Assignment of Quantum Numbers	225
3. Application of Pauli's Exclusion Principle to the Periodic Table	226
4. Chemical Properties of the Elements	229
5. Valence and the Formation of Molecules	229
9. MOLECULAR STRUCTURE AND RELATED TOPICS	234
1. The Number of Atoms in a Molecule	234
2. Specific Heats of Gases	234
3. Rotational Band Spectra	241
4. Vibration-Rotation Bands	244
5. Electronic Bands	249
6. Raman Spectra	252
7. Microwave Spectroscopy	253
8. Dipole Moments and Dielectric Constants	255
9. Energy Levels of Solids; Electrical Conduction	257

Contents

ix

10. RADIOACTIVITY	264
1. Brief Survey	264
2. The Discovery of Radioactivity	267
3. The Breakdown of Radioactive Elements	269
4. Statistical Character of Radioactive Decay	271
5. The Natural Radioactive Elements	272
6. Energy of Individual Particles and Gamma Rays	274
7. Magnetic Spectrographs	276
8. Alpha-Ray Spectra	278
9. Gamma-Ray Spectra	279
10. Beta-Ray Line Spectra	281
11. Continuous Beta-Ray Spectra	283
11. ELEMENTARY PARTICLES	287
1. The List of Elementary Particles	287
2. Detection of Individual Particles and Photons	288
3. Scattering and Absorption of Particles and Gamma Rays	297
4. Electrons and Positrons	309
5. The Neutrino	317
6. The Neutron	319
7. Pictorial Summary	334
12. TRANSMUTATION AND NUCLEAR STRUCTURE	337
1. Disintegration by Alpha Particles	337
2. Production of Fast Charged Particles	339
3. Transmutation Processes and Artificial Radioactivity	350
4. Reactions of a Few Light Elements	353
5. The Compound Nucleus	357
6. The Geiger-Nuttall Law and the Barrier Model	358
7. Regularities in Beta Decay	364
8. Yield Curves for Artificial Disintegration	364
9. Nuclear Spins and Magnetic Moments	368
10. The Deuteron	370
11. Proton-Proton Scattering	374
12. Specific Nuclear Forces	375
13. Regularities in Binding Energies	377
13. APPLICATIONS OF NUCLEAR PHYSICS	381
1. Foreword	381
2. Early Research on Fission	381
3. General Facts of Fission	383
4. Large-Scale Utilization of Fission	392
5. How a Pile Works	394
6. Recent Reactor Developments	400
7. Radioactive Isotopes in the Service of Science	401
14. COSMIC RAYS	405
1. Essential History	405
2. The Nature of the Cosmic Rays	407
3. Experimental Methods	415
4. The Behavior of High-Energy Particles and Photons	419
5. The Primaries	424
6. Pi and Mu Mesons	427
7. Other Unstable Particles	436
8. Showers	439
9. Geographic and Depth Distribution of the Cosmic Rays	441
10. Origin of the Rays	450

15. THE THEORY OF RELATIVITY	454
1. Introduction	454
2. Relative Motion	454
3. Uniform Motion through Space. The Michelson-Morley Experiment.	457
4. Pre-Relativity Explanations	461
5. Einstein's Solution	464
6. The General Theory of Relativity	469
7. Consequences of the Restricted Theory	471
APPENDICES	475
1. Electrical Units	476
2. Physical Constants and Conversion Factors	477
3. Properties of Elementary Particles	479
4. Behavior of Elementary Particles	480
5. Periodic System of the Elements	481
6. Properties of Light Isotopes.	482
7. Derivation of the Lorentz Transformation Equations	483
8. Derivation of the Length Transformation, $L = kL'$	484
9. Bibliography	485
INDEX	489

1

The Atomic Nature of Matter

1. Early Atomic Theories

The ultimate constitution of matter has fascinated thinkers for many ages. If a piece of clay is cut into smaller and smaller pieces, is there any limit to the sectioning process, apart from the restrictions which our crude instruments impose? Shall we, in imagination, at length reach a tiny particle of clay, which, when forcibly split, will cease to be clay, and shall we finally reach an ultimate particle which cannot, by any conceivable means, be further subdivided? From a philosophical point of view it is pleasanter to be able to halt somewhere; our minds, accustomed to dealing with objects whose dimensions are reasonably comparable with our own stature, cannot visualize an infinite process of subdivision with any more comfort than they can comprehend a universe which stretches out indefinitely in all directions. It is not surprising, therefore, that the hypothesis that gross matter is composed of tiny, indivisible entities is ancient. It was recorded in the works of Greek and Roman writers. For example, Democritus (400 B.C.) wrote: "Atoms are infinite in number and infinitely varied in form. They strike together and the lateral motions and whirlings are the beginnings of worlds.

"The varieties of all things depend upon the varieties of their atoms in number, size, and aggregation.

"The soul consists of fine, smooth, round atoms like those of fire. These are the most mobile of all. They interpenetrate the body, and in their motions the phenomena of life arise."

We treasure such statements because they correspond somewhat with modern views. Dozens of other guesses which were once equally plausible have been long forgotten. Furthermore, the ancient atomic hypotheses had no experimental justification. After Democritus, twenty-three sterile centuries elapsed before there was any appreciable progress in putting the atomic theory on an experimental basis. In the early years of the nineteenth century came the birthday of modern

chemistry. Since then the atomic theories of matter and of electricity have advanced hand in hand.

In 1803 the English chemist Dalton first stated an atomic theory approximately explaining the known facts. He thought of matter as constituted of a vast number of extremely small particles bound together by attractive forces. They were not, like the atoms conceived by Democritus, "infinitely varied in form," but belonged to a limited number of species.

Dalton's ideas were borne out by new experimental evidence as to the relative masses of substances entering into chemical combination. He realized the possibility that more than two atoms might combine to form a molecule, and therefore he studied the compositions of ethylene (which we now know to be C_2H_4) and of methane (CH_4). In the former substance, six grams of carbon combined with about *one* of hydrogen; in the latter, six grams of carbon combined with about *two* of hydrogen. Similarly, in forming gaseous oxide of carbon (carbon monoxide, CO) and carbonic acid gas (carbon dioxide, CO_2), if equal masses of carbon were taken, the masses of oxygen were as one to two. Such integral relationships were established for a number of other compounds, and in no case was the ratio non-integral. Upon such evidence, in 1804, Dalton stated the *law of multiple proportions*, which is in effect that, if two elements are able to unite in different proportions to form more than one compound, and if the mass of one element is constant in the different compounds, then the relative masses of the other element are representable by small integers. This law was simply explained by the atomic hypothesis. In forming a molecule of carbon monoxide, for example, *one* atom of carbon combines with *one* atom of oxygen; to form carbon dioxide, however, *two* atoms of oxygen are required for every *one* of carbon. Thus the amounts of oxygen in the two cases are in the ratio of one to two.

In 1808 Gay-Lussac established an important relationship for gases in chemical reactions. He found that, at constant pressure and temperature, one volume of oxygen combines with exactly two volumes of hydrogen to form two volumes of steam. Similarly, one volume of nitrogen combines with one of oxygen to form two volumes of nitric oxide (NO). In general, his law of volumes is that if gases *A* and *B* combine to form a gaseous product *C*, the three relative volumes can be represented by small integers. To explain this fact, Gay-Lussac suggested that equal volumes of different gases at the same pressure and temperature might contain equal numbers of "atoms" or, as we say, of molecules. In reply, Dalton pointed out that, according to this hypothesis, in forming nitric oxide a single volume of nitrogen uniting

with one of oxygen should form one of the compound, whereas, in fact, experiment produces two volumes.

A few years later, in 1811, the Italian physicist Avogadro showed where the inconsistency lay. Dalton had imagined that a "simple" molecule such as oxygen was identical with an atom. Avogadro suggested that atoms of the same element might cluster to form molecules. If, for example, each molecule of oxygen and nitrogen contained two atoms, the process of forming nitric oxide might consist of an interchange of atoms. In that event, one volume of oxygen and one of nitrogen would unite to form two volumes of nitric oxide, and the total volumes before and after the reaction would be the same.

It follows from Dalton's work that 2 gm of hydrogen, or 28 gm of nitrogen, or 32 gm of oxygen (the gram-molecular weight, or mole) each contain the same numbers of molecules. The volume that a mole of any gas occupies must therefore be the same under identical conditions, by virtue of Avogadro's law, viz., that equal volumes of gases at the same temperature and pressure contain equal numbers of molecules. This particular volume is therefore of universal importance in dealing with gases. Its value, according to the best measurements, is 22.415 liters.

As an application of these results we might consider the problem of finding the molecular weight of an unknown gaseous compound. To do this it is sufficient to find the mass of the gas (a mole) which would occupy 22.415 liters (the molar volume) under standard conditions of temperature and pressure (0°C and 76 cm of Hg).

The atomic hypothesis was greatly strengthened by Faraday's discovery (1833) that, if the same quantity of electricity traverses different electrolytes, the masses of material deposited at the electrodes are proportional to the *combining weights*, that is, the atomic weights divided by the valence, of the substances deposited. For example, if the same quantity of electricity traverses different solutions each containing univalent ions such as those of sodium, silver, or potassium, the masses of these substances set free at the electrodes are proportional to the respective atomic weights. This is easily explained by assuming that ions of the substances exist in the electrolytes, and that each ion bears the same charge e of electricity. Furthermore, when solutions containing *divalent* elements such as oxygen and copper are subjected to this process of electrolysis, the masses deposited are only *one-half* as great as they would be if the elements were univalent. Thus the mass associated with unit charge is also only half as great. Therefore we assume that each ion carries a charge $2e$.

Faraday's results strongly favored Dalton's hypothesis that matter is

composed of atoms. As is seen in Chapter 3, they also suggested that, in electrolysis, electricity appears in units, or small integral multiples of units, of the same size. In fact, some of the evidence for the atomic nature of matter is so closely related to the evidence for the atomic nature of electricity that the two cannot be profitably studied separately.

2. Molecular Velocities

A relation between gas pressure and molecular velocity. In 1738, before the birth of modern chemistry, the Swiss scientist David Bernoulli developed an equation for the pressure of a gas. He assumed that the pressure was due to the incessant motion of "atoms" or, as we would say, of molecules. To understand his method, imagine a swarm of flies of equal speed buzzing about in a cage. As they move to and fro, they strike against the door, tending to push it open. The average force which the door experiences depends upon the speed of the flies. If, in particular, the speed of each fly were doubled, it would make, on an average, twice as many impacts per second and would deliver twice as much momentum at each impact. Therefore, as will be shown later, the mean force on the door would be quadrupled, and the force is proportional to the square of the speed.

Now to be more precise: Bernoulli's mathematical treatment assumes that each molecule is a perfectly elastic sphere of mass m and that each has the same speed C . They are supposed to be "point" molecules, of

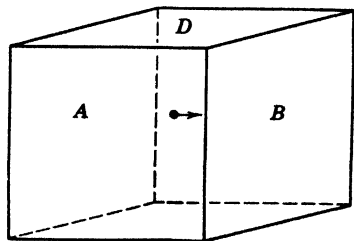


Fig. 1-1.

negligible volume, and to be far enough apart to exert no appreciable forces on one another. Let N of these molecules be enclosed in a cubical box, the length of each edge being l (Fig. 1-1). For simplicity we at first assume that one-third of the molecules move perpendicularly to A , one-third to B , and one-third to D . Let us fix our attention on a single particle striking B . As it bounces backward and forward in

the box, it must travel a distance $2l$ between successive impacts on the wall B , and thus will make $C/2l$ hits per unit of time. Since the impacts are perfectly elastic, when the molecule strikes B its velocity changes from positive C to negative C ; so the momentum delivered to the wall at each hit is $2mC$. The change in momentum per unit time, being the change per hit multiplied by the number of hits per second, will be

$$2mC \times C/2l = mC^2/l$$

Since we assume that one-third of the molecules strike B , the total momentum transferred to this wall per unit time is

$$\frac{1}{3} NmC^2/l \quad (1)$$

By Newton's second law of motion, the force acting on a body is equal to the time rate of change of its momentum. Thus the molecules striking the wall B exert on it a force $f = \frac{1}{3} NmC^2/l$. The area of B is l^2 ; hence the pressure of the gas is

$$p = \frac{\text{Force}}{\text{Area}} = \frac{1}{3} \frac{NmC^2}{l^3} = \frac{1}{3} \frac{NmC^2}{V} \quad (2)$$

where V is the volume of the box. Since Nm/V is the density ρ of the gas,

$$p = \frac{1}{3} \rho C^2 \quad (3)$$

so that the average speed of the molecules of a gas may be computed from its pressure and density. In Bernoulli's day little was known about the densities of gases; hence he did not estimate their speeds. Today, the densities are accurately known.

For hydrogen under standard conditions of temperature and pressure,

$$C = \left(\frac{3 \times 76.00 \text{ cm} \times 13.60 \text{ gm/cm}^3 \times 980.6 \text{ cm/sec}^2}{0.00008988 \text{ gm/cm}^3} \right)^{1/2} \\ = 1839 \text{ m/sec} = 1.16 \text{ mi/sec}$$

This is roughly the speed of a rifle bullet. Oxygen and carbon dioxide have larger densities and therefore smaller molecular speeds, namely, 459.7 and 392.1 m/sec, respectively.

★ **Conservation of kinetic energy in collisions.** For simplicity Bernoulli assumed that all the molecules have the same speed. In

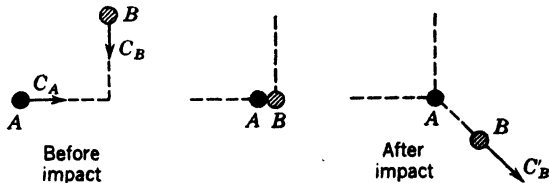


Fig. 1-2. Collision of two molecules. Momentum and energy are conserved.

fact, such a condition could not continue in an actual gas, even if it were initially established. At ordinary pressures, molecules collide with one another as well as with the walls of the containing vessel. A certain molecule A , for example, having a velocity C_A (Fig. 1-2) may strike squarely against another molecule B of the same mass moving

at right angles to A with speed C_B . In the interests of simplicity, we may quite legitimately suppose that the collision leaves A at rest. After the impact, A will have transferred all its kinetic energy to B , which has therefore an increased velocity C'_B . Since we assume the particles to be perfectly elastic, the energy after collision equals that before; that is,

$$\frac{1}{2}mC_A^2 + \frac{1}{2}mC_B^2 = 0 + \frac{1}{2}mC'_B{}^2$$

so that

$$C_A^2 + C_B^2 = C'_B{}^2$$

Thus, although the speeds of individual molecules change, the sum of the squared speeds, and therefore the mean of the squared speeds, remains constant. The same statement can be shown to be true for other impacts not at right angles. Thus equation 2 may be replaced by

$$p = \frac{1}{3}Nm\overline{C^2}/V \quad \text{or} \quad \overline{C^2} = 3pV/Nm \quad (4)$$

in which $\overline{C^2}$ represents the mean of the squared speeds of the molecules.

3. The Distribution of Velocities

As a result of random collisions, in an actual gas certain molecules, at a chosen instant, have very large velocities, others small ones, and still others intermediate values. Further, the velocities are distributed at random as regards direction. However, the magnitudes of the speeds are not distributed at random. By mathematical means too lengthy to be presented here, Maxwell has derived an expression (See Appendix 9, ref. 65, p. 81) for the most probable distribution of molecular speeds in a gas in thermal equilibrium. It is most simply written as

$$dn = (4N/S^3\sqrt{\pi})c^2e^{-c^2/S^2}dc$$

N being the total number of molecules, dn the number of these having speeds between c and $c + dc$, and S the most probable speed. The curves in Fig. 1-3 illustrate the Maxwell law of speed distribution for oxygen at two different temperatures, the abscissas being the molecular speeds. For convenience, the figure refers to 10,000 molecules, so that the area of each square represents 500 molecules. It will be seen that at any instant the relative numbers of molecules having very low speeds or very high speeds are vanishingly small. Of the 10,000 molecules, about 12 have, at 0°C , speeds between 600 and 601 m/sec.

The features enumerated below are also important.

(a) Since the number of molecules is constant the areas under the two curves should be equal.

(b) The average or mean speed \bar{C} at any instant is determined by finding the sum of the speeds of all the molecules and dividing by the number of molecules. The highest point on the curve represents the most probable speed S . (Notice that the number of molecules having speeds greater than S is larger than the number having smaller speeds. Thus the mean speed is greater than the most probable speed.)

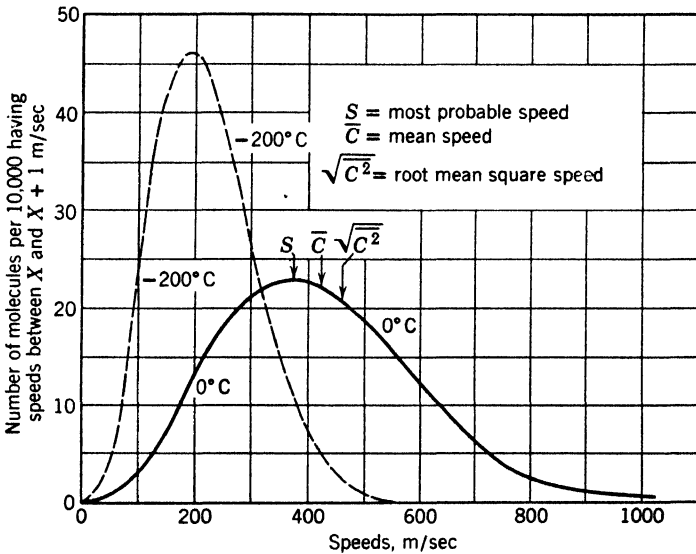


Fig. 1-3. Maxwellian distribution of speeds for oxygen at 0°C and at -200°C .

(c) In calculating the root-mean-square speed $\bar{C}^{2\frac{1}{2}}$ the speed of each molecule is squared, the average is found, and its square root is computed. In this process, molecules of high speed contribute more heavily than those of small speed; hence the value of $\bar{C}^{2\frac{1}{2}}$ is greater than the mean speed \bar{C} .

(d) Lowering the temperature decreases the values of S , C , and $\bar{C}^{2\frac{1}{2}}$. For example, at 0°C , the most probable speed S is 375 m/sec, whereas at -200°C it is a trifle below 200 m/sec.

(e) The speeds of most of the molecules do not differ greatly from the most probable speed. The diagram shows that, of the 10,000 molecules, about 400 have speeds greater than twice the most probable speed, $2S$.

It can be shown also that the probability of a chosen molecule having a speed greater than $4S$ is only 1 in 1,000,000.

★ The mean speed \bar{C} and the square root of the average of the squared speeds $\bar{C}^2{}^{1/2}$ are related to the most probable speed S by the following formulas, the derivations of which are beyond the scope of this book:

$$S = \bar{C}/1.128 = \sqrt{\bar{C}^2}/\sqrt{3/2} \quad (5)$$

Hence, from equation 4,

$$S = \frac{1}{\sqrt{3/2}} (3p/\rho)^{1/2} \quad (6)$$

so that S may be computed for a gas of known density and pressure.

4. Direct Experimental Determination of Molecular Speeds

The validity of the hypothesis that molecular speeds are distributed according to the Maxwell curve of Fig. 1-3 can be directly tested. We shall describe an apparatus developed by Zartman (Appendix 9, ref. 112). Suppose that bismuth is placed in the furnace E (Fig. 1-4a) in

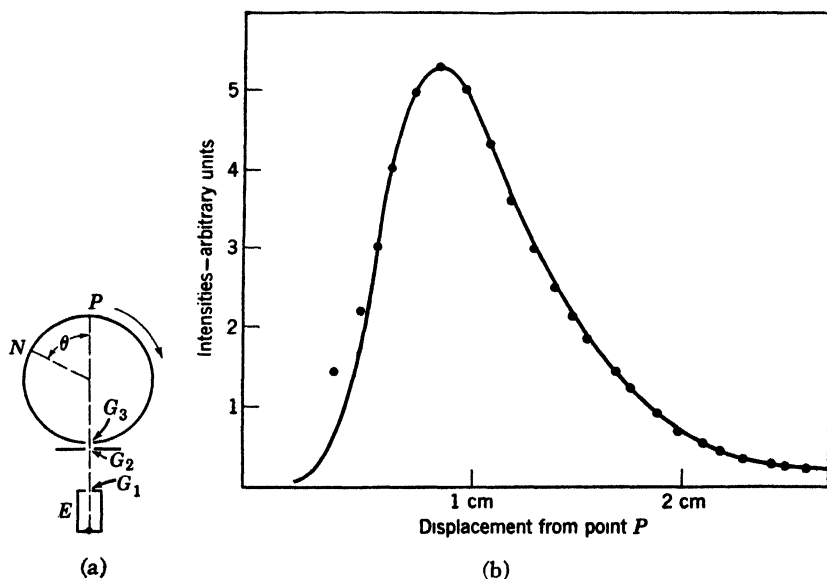


Fig. 1-4. (a) Diagram of Zartman's apparatus for measuring molecular velocities. (b) Observed intensity distributions (points) and theoretical distribution, assuming a vapor composed of 40 per cent Bi and 60 per cent Bi₂. $T = 851^\circ\text{C}$.

a highly evacuated enclosure which is heated so that the metal evaporates slowly. Some of the atoms pass through the slit G_1 . With the aid of G_2 a sharply defined, rectangular beam is formed. Let a cylinder, capable of rotating, and having a slit G_3 in its outer wall, be placed in the beam. If the cylinder is at rest and the slit G_3 is in the path of the molecular beam, a deposit forms at P diametrically opposite the slit.

If the cylinder rotates with an angular velocity ω , the time t required for it to turn through an angle θ is

$$t = \theta/\omega$$

During this time molecules of speed C travel a distance s across the cylinder and strike its wall at N . Thus

$$t = s/C$$

Eliminating t , we have

$$s/C = \theta/\omega$$

If θ and s are determined, C may be computed, since ω can be controlled and measured.

Since the atoms in the beam have different velocities some will arrive earlier and some later than the average, so the deposit will be spread out into a "velocity spectrum." Zartman finds that under his experimental conditions the distribution of the deposit accords with the Maxwell law within the limit of experimental error, as shown in Fig. 1-4b.

5. Temperature and Molecular Energy

When Bernoulli derived his gas-pressure equation the concept of kinetic energy was poorly understood and the kinetic theory of gases had little acceptance. He made no attempt to associate the average energy of gas molecules with the temperature of the gas. More than a century later, in 1853, James Prescott Joule showed that the molecular translational energy of a perfect gas is related to its absolute or Kelvin temperature.

A well-known expression combines the laws of Boyle and of Charles:

$$pV = RT \tag{7}$$

where p is the pressure of the gas, here expressed in dynes/cm², V is the volume per mole, T the absolute temperature, and R the so-called gas constant which has the value 8.314×10^7 ergs/(K° mole), or 1.986 cal/(K° mole).

The value of R is found as follows: From equation 7, $R = pV/T$, in which, under standard conditions of temperature and pressure,

$$p = 76 \text{ cm of Hg} = 1,013,200 \text{ dynes/cm}^2$$

$$V = 22,415 \text{ cm}^3/\text{mole}$$

$$T = 0^\circ\text{C} = 273^\circ\text{K}$$

Remembering equation 4, we have two forms for the product pV :

$$pV = RT \quad \text{and} \quad pV = \frac{2}{3}(\frac{1}{2}Nm\overline{C^2}) \quad (8)$$

Comparing these two expressions we see that the Kelvin temperature of a gas is proportional to the total translational kinetic energy of its molecules. Thus, the abstract concept of temperature is replaced by a physical picture. In particular it is easy to understand why no temperature lower than Kelvin zero is conceivable since kinetic energy may not have a negative value.

Avogadro's hypothesis that equal volumes of different gases at the same temperature and pressure contain equal numbers of molecules has been confirmed by numerous experiments. It may be combined with equation 8 to prove the significant theorem that *the mean translational kinetic energies of the molecules of all gases are the same at a given temperature*. To see this, consider a mole of gas a and one of gas b at the same temperature. From equations 7 and 8,

$$\frac{3}{2}RT = \frac{1}{2}N_a m_a \overline{C_a^2} = \frac{1}{2}N_b m_b \overline{C_b^2} \quad (9)$$

Since N_a and N_b are both equal to the Avogadro number, we have

$$\frac{1}{2}m_a \overline{C_a^2} = \frac{1}{2}m_b \overline{C_b^2} \quad (10)$$

which proves the theorem.

The Boltzmann constant. The average translational kinetic energy per molecule of a gas can be found by dividing the kinetic energy per mole ($\frac{3}{2}RT$) by the number of molecules per mole, that is, the Avogadro number N , which is 6.025×10^{23} molecules per mole. In other words the translational kinetic energy per molecule $= \frac{3}{2} \frac{R}{N} T = \frac{3}{2} kT$; k is called the Boltzmann constant and equals 1.380×10^{-16} erg/($^\circ\text{K}$ molecule).

6. Molecular Heats of Gases

Molar heat at constant volume. When a perfect gas is confined in a vessel of fixed volume and the temperature of the gas is raised, all the energy it receives goes into molecular energy, either translational, rotational, or internal. The heat absorbed per mole per Kelvin degree rise of temperature is called the *molecular heat or molar heat* at constant volume, C_v . Now if we are dealing with "point" molecules, incapable of rotation or of internal vibration, all the added heat must go into translational kinetic energy. By equations 8 and 9, the increase of this energy per mole, per degree rise of temperature, should be $\frac{3}{2}R$, or 2.98 cal/(K° mole). Joule tested this prediction by comparing the above value with the experimental values for hydrogen, water vapor, nitrogen, oxygen, and carbon dioxide. In every instance the experimental value was many per cent too high. Joule abandoned the investigation. A few years later, in 1857, the German mathematical physicist Clausius attacked the problem. First, he showed how to compute the molar heat of a gas when it is permitted to expand at constant pressure.

Molar heat at constant pressure. Since a gas expands while being heated at constant pressure, additional energy is required to do external work. Let us assume that a gas at pressure p is confined in a cylinder by means of a weightless frictionless piston, and let the initial volume be V and the Kelvin temperature T (Fig. 1-5). Let the area of the piston be A , and suppose that, when the temperature increase is ΔT , the piston moves through a distance Δy . The upward force on the piston is given by pA . But $A \Delta y$ equals the change of volume ΔV ; hence, work done by the gas = $p\Delta V = R\Delta T$. Moreover, if the rise of temperature is one Kelvin degree, the energy per mole expended in lifting the piston is numerically equal to R , or approximately 2 cal.

Thus the molar heat of a *monatomic* gas at constant pressure must be

$$C_p = \frac{3}{2}R + R = \frac{5}{2}R \cong 5 \text{ cal/K}^\circ \text{ mole}$$

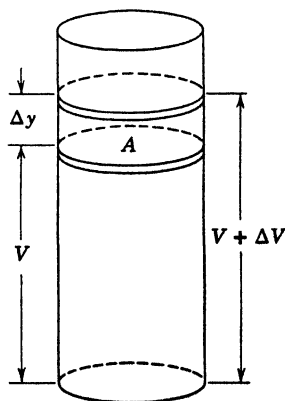


Fig. 1-5.

Experimental results. The ratio of the specific heats, $\gamma = C_p/C_v$, may be readily determined by measuring v , the speed of sound, in the

gas, and using the familiar formula

$$v = (\gamma p / \rho)^{1/2}$$

In deriving the expressions for the molar heats of a gas, we have assumed that all the energy absorbed by the molecules was utilized in increasing their speeds. Keeping this fact in mind, let us examine the experimental situation as revealed by Table 1-1.

TABLE 1-1. Experimental Values of Molar Heats of Gases at 15°C

Molecule	C_v in Calories per (K° mole)	Degrees of Freedom	C_p in Calories per (K° mole)	Ratio of Specific Heats C_p/C_v
He	2.98	3	4.95	1.66
A	3.01	3	5.03	1.67
Hg	2.98	3	4.98	1.67
Hydrogen (H_2)	4.83	5	6.81	1.410
Nitrogen (N_2)	4.94	5	6.94	1.404
Oxygen (O_2)	4.97	5	6.96	1.401
HCl	4.99	5	7.04	1.41
CO	4.94	5	6.94	1.404
CO_2	6.71	7	8.75	1.304
Ethyl ether (at 250°C)	25.7 40		27.7	1.08

We see from this table that the monatomic gases yield approximately the theoretical values for C_v and C_p for "point" molecules, namely, 3 and 5 cal/(K° mole), respectively. We conclude that the heat imparted to such gases is utilized solely in increasing the translational kinetic energies of the molecules. However, the molecular heats of diatomic, triatomic, and polyatomic gases are greater than the theoretical values for "point" molecules. We therefore conclude that their structures are such that a portion of the energy may be utilized in other ways.

Degrees of freedom. To explain these differences in molar heats, Clausius introduced the idea of *degrees of freedom*. The number of degrees of freedom possessed by any body is the *number of independent quantities which must be specified in order to describe its motion*. For example, a point sliding in a straight groove has one degree of freedom; if moving freely on a plane surface it has two; and in space it has three

degrees. A tennis ball, floating in water, has two degrees of translational freedom. It can rotate independently about three axes; hence it also has three degrees of rotational freedom. As an exercise, the reader may show that an airplane in flight has six degrees.

Assuming that an atom is rigid and cannot be made to spin faster or slower, we assign to it three degrees of translational freedom, as in Fig. 1-6a. If the x component of velocity is C_x , we may speak of $\frac{1}{2}mC_x^2$ as

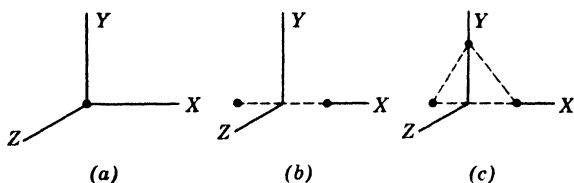


Fig. 1-6. (a) "Point" monatomic molecule. It has three degrees of freedom. (b) Rigid dumbbell molecule, aligned along the X axis. Rotation around the Y and Z axes assumed possible. This molecule has five degrees of freedom. (c) Rigid, triatomic molecule. It has six modes of motion, or degrees of freedom.

the kinetic energy associated with the x degree of freedom. By symmetry, the average value of this quantity must be one-third of $\frac{1}{2}mC^2$, and the same is true of the kinetic energies associated with motions parallel to the other two axes. In other words, *the energy per mole associated with each translational degree of freedom is $\frac{1}{2}RT$* . This is an instance of the *equipartition of energy*.

The fact that C_v for hydrogen is $\frac{5}{2}R$ instead of $\frac{3}{2}R$ leads us to suspect the existence of two additional degrees of freedom, and so we ask ourselves in how many independent ways a hydrogen molecule can move. We picture it (Fig. 1-6b) as a rigid dumbbell consisting of two "point" atoms joined together by a massless rod. Such a molecule can move translationally along three independent axes, and in addition to these motions it might be made to tumble or spin about any of these three axes so as to have three additional degrees of freedom. However, since the atoms are assumed to be points, the molecule cannot absorb or possess energy of rotation about the axis joining the atoms. It therefore has only 5 effective degrees of freedom; hence its molar heat C_v is $\frac{5}{2}R$, or 5 cal/(K° mole).

★ The values of C_v for triatomic gases are somewhat greater than $\frac{6}{2}R$. We conclude that they have three translational and three rotational degrees of freedom. The excess over the value $\frac{6}{2}R$ casts doubt on our working hypothesis that complex molecules are rigid, which enabled us

to neglect the absorption of energy by vibrational motions inside the molecule. In fact, molecules having three or more atomic constituents have specific heats corresponding to more than six degrees of freedom at room temperature and therefore cannot be considered rigid. In such molecules the vibrational degrees of freedom are gradually excited as the temperature rises; for this reason it is impossible to assign a definite integer representing the multiplier of $R/2$. For example, the molar heat C_v of ethyl ether at 15°C is $25.7 \text{ cal}/(\text{K}^\circ \text{ mole})$. At 250°C , C_v is $40 \text{ cal}/(\text{K}^\circ \text{ mole})$

★ At sufficiently high temperatures diatomic molecules also have molecular heats greater than $\frac{5}{2}R$. This is easily and quantitatively explained on the assumption that internal vibrations are excited at higher temperatures.

7. Real Gases

Thus far we have dealt with an “ideal” or “perfect” gas in which the molecules are negligibly small and exert no appreciable forces on one another. These conditions are approximately realized at ordinary temperatures for gases such as air and hydrogen which can be liquefied only at very low temperatures. Like most laws of physics, however, those of Boyle and Charles are approximations, holding true within certain limits. Boyle himself, in his pioneer experiments (1663), found that when the pressure was increased to a few atmospheres the product of pressure and volume for a given mass of air was larger than at 1 atm. A little consideration makes plain why this is true. As a gas is compressed more and more, the molecules, which have a finite though small volume, are crowded into closer and closer quarters, thereby occupying larger and larger fractions of the total volume. Thus the “free” volume in which the molecules may move becomes appreciably smaller than the total volume. Curiously enough, from this point of view, the part of the volume of a gas which obeys Boyle’s law is the *empty space* between the molecules.

For example, the total volume of the molecules in a mole of nitrogen is about 1.26 cm^3 , which under standard conditions is only 0.0056 per cent of the total volume. At 18 atm pressure the molecular volume is about 0.1 per cent of the whole. The resulting deviation in the product of pressure and volume is detectable by methods of fair precision. Equation 7 may be roughly corrected for this effect by the introduction of a constant B as follows:

$$P(V - B) = RT \quad (11)$$

The constant B cannot differ very much from the volume per mole of the liquid to which the gas may be condensed. This is perhaps three or four times the volume of the molecules.

Van der Waals' formula. The actual deviations are in general greater than those predicted by this formula, so that another factor must be considered, namely, the force, usually attractive, between molecules. As a gas molecule approaches a boundary it is retarded by the attraction of those behind it and therefore delivers a smaller impulse to the wall than if this attraction were zero. Thus the cohesion of the molecules causes a deficiency of pressure. If the gas density were doubled, the retarding force on a molecule would likewise be doubled as would also the number striking the wall per second. Hence the decrease of pressure due to this cause would be quadrupled. Thus the correction to be added to the observed pressure to make it equal to the theoretical value for zero attraction varies as the *square* of the density and hence inversely as the square of the volume. When we introduce a correction of this type, equation 11 becomes the celebrated Van der Waals' expression:

$$\left(p + \frac{A}{V^2}\right)(V - B) = RT \quad (12)$$

This equation holds in limited regions only, but it is a great improvement on equation 7. The evaluation of B is of considerable interest for, as we have seen, it is a measure of molecular volume. Some molecular diameters, determined experimentally, are shown in Table 1-2.

TABLE 1-2. Molecular Diameters and Mean Free Paths under Standard Conditions

The molecules are assumed to be spherical

Gas	Molecular Diameters in Centimeters $\times 10^{-8}$		Mean Free Paths in Centimeters $\times 10^{-6}$
	By Van der Waals' Equation	By Viscosity Measurements	
Hydrogen	2.76	2.72	11.25
Oxygen	2.91	3.62	6.4
Carbon dioxide	5.55	4.62	3.9
Mercury	2.37	3.64	

8. Mean Free Paths

If a bottle of ammonia is opened at one side of a room, several seconds elapse before the odor is detected at the other side. This slowness of propagation is surprising when we think of the rifle-bullet speeds of the molecules. It is explained by the fact that in quiet air a particle does not travel directly across the room, but bumps into other molecules every few millionths of an inch. Hence it darts hither and thither with random motion and makes comparatively slow progress in a definite direction. The distances traveled between successive collisions of a given molecule—the free paths—will be widely different, and will be distributed about an average value λ called the *mean free path*. Let us calculate the value of λ for a gas composed of spherical molecules of radius r and diameter d .

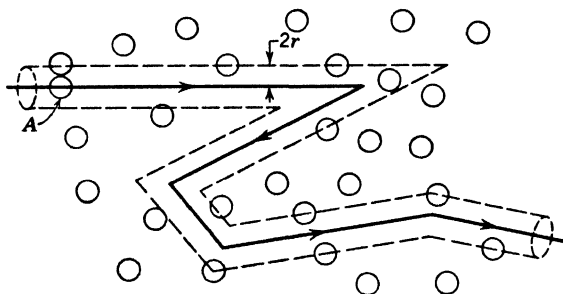


Fig. 1-7. Tunnel of exclusion. The molecule A will not hit any molecule whose center is at a distance greater than $2r$ from the path of its center.

Assume, for the present, that only one molecule A in a gas is moving. Let its center trace out the heavy line in Fig. 1-7. This molecule will just miss all other molecules whose centers are at a distance $d = 2r$ from the heavy line. While traveling a distance s , the molecule A sweeps out an imaginary "tunnel of exclusion" of radius d and volume $\pi d^2 s$. Let n be the number of molecules per unit volume. While moving through the distance s , A strikes all the $n\pi d^2 s$ molecules in the tunnel. It therefore hits $n\pi d^2$ molecules while traveling unit distance. The reciprocal of this value, the mean free path λ , is given by

$$\lambda = 1/n\pi d^2 \quad (13)$$

★ This simplified expression can be improved by taking into account the motions of the molecules. The derivation is too complicated to be presented here, but, if one assumes that the molecular speeds are dis-

tributed according to the Maxwellian theory, the equation becomes

$$\lambda = 1/\sqrt{2} \, n\pi d^2 \quad (14)$$

Experimental determination of mean free paths. One of the most direct methods of determining λ is essentially as follows: Silver is evaporated from a small region at the bottom of a quartz tube in a highly evacuated vessel. The molecules, after evaporating, pass through an orifice at the top of the tube and are deposited upon a horizontal glass plate which is cooled by liquid air. When the gas pressure is very low so that the mean free path is considerably greater than the distance from the orifice to the plate, the silver is deposited in a small region determined by the geometry of the system. As the gas pressure increases and the mean free path diminishes, more molecules are scattered before striking the plate and the patch of silver becomes wider. By measuring the sizes of the silver deposits obtained at several different distances, the pressure being constant, λ may be computed. Usually, however, the mean free path is obtained from an equation which connects it with the viscosity of a gas. Experimental values obtained by this method are given in Table 1-2. Note that under standard conditions molecules move only a few hundred-thousandths of a centimeter between collisions. In the highest vacua obtainable in our terrestrial laboratories the mean free paths may attain values of a few hundred kilometers. In some nebulae the mean free paths exceed 10^6 km.

After the mean free path in a gas has been determined experimentally, equation 14 may be used to compute the molecular diameter. The number of molecules per cubic centimeter may be found by dividing the Avogadro number by the volume of a mole of gas under the experimental conditions considered. Values of d obtained in this way are shown in Table 1-2. They are in fair agreement with those deduced from the equation of Van der Waals.

9. Brownian Movements and Molecular Reality

We have seen that the kinetic theory is successful in explaining the gas equation, and in giving consistent values for molecular speeds, energies, diameters, and mean free paths. These successes, and other evidence accumulating during the nineteenth century, made the molecular hypothesis very plausible. There was, however, no direct and compelling evidence based on the study of a small number of molecules. Even in 1908, Wilhelm Ostwald vigorously opposed the acceptance of the theory. But in that year researches of the French physical chemist Perrin were published which were so decisive as to silence all opposition.

He studied the so-called *Brownian movements* of colloidal particles suspended in a liquid. The chaotic dancings of these tiny specks of matter were first observed in 1827 by the botanist Brown. At the time of Perrin's experiments they were generally believed to be caused by unequal bombardment by molecules of the surrounding fluid. Perrin reasoned that if the average translational kinetic energy of a hydrogen or of a nitrogen molecule is equal to $\frac{3}{2}RT/N$, in accord with equation 10 and with the results of molecular heat determinations, the same value should apply to a relatively large protein molecule visible as a point of light in the ultramicroscope. It might even hold for colloidal particles consisting of billions of molecules and visible through an ordinary compound microscope. In other words, a colloidal particle should move about like a molecule, though with a smaller speed. If this were true, he reasoned, colloidal spheres in a liquid should behave like molecules of a gas, exerting forces on the walls of the container by their impacts. He decided to observe such particles through a microscope, to locate their positions at successive equal time intervals, and to estimate their average speeds. Then he planned to determine their average kinetic energies and to compare these with the value $\frac{3}{2}RT/N$ which had been computed for gas molecules. The wanderings of a certain particle were observed through a microscope, its positions being located at successive, equal time intervals. From these observations the average distance moved in the intervals between successive observations was determined, and the average speed was found using an equation derived by Einstein.

Experiments on translational energy of Brownian particles. In order to determine the mean kinetic energy of a particle, it was necessary to find its mass. At first sight this would seem to be easy since the density of the material was known and one should be able to estimate the diameters of the particles by the sizes of their images as formed by the microscope. Unfortunately, the globules were so small that they appeared as points of light, like stars, with no appreciable diameters. The most difficult part of the experiment was the determination of these diameters. To this end Perrin employed three methods, the simplest being as follows: To secure particles of about equal mass he dissolved a resinous substance called gamboge in alcohol. When the solution was mixed with water, a suspension of tiny spheres resulted, which was subjected to fractional centrifuging to separate out particles of about the same diameter. Part of the liquid was then evaporated, and some of the globules were found to lie in a row like the beads of a necklace. The length of such a row was measured, using the microscope; the number of "beads" was counted; the mean diameter was found by division; and the volume per particle was computed. To determine the

density the total mass of a large number of the spheres was found by weighing, and their total volume by water displacement. Using the density value thus secured and the volume of a single particle as found above, the average mass was calculated.

Having determined the masses of the spheres and their mean speeds, Perrin computed their mean kinetic energies, and the results were in fair agreement with the value $\frac{3}{2}RT/N$ as given by kinetic theory.

★ **Experiments on rotational energy of Brownian particles.** Some of the particles studied by Perrin were in chain-like clusters, and he could observe their positions in a horizontal plane. These bodies tumbled about because of bombardment by the molecules of the surrounding liquid. Perrin estimated their average angular speeds and their angular rotational kinetic energies. The values agreed nicely with those predicted by kinetic theory, and so the Maxwell theory of the equipartition of energy was again verified.

The value of the Avogadro number. Perrin's researches were useful in providing a more precise determination of the Avogadro number, N . As we have noted, he measured the average translational kinetic energy, $\frac{3}{2}RT/N$, of a molecule, and, since both R and T were known, N was readily computed. His values were within 17 per cent of the value which we use today.

The law of atmospheres. In addition to his work with individual colloidal particles, Perrin verified the kinetic theory by observing an "atmosphere" of the globules suspended in a liquid. He reasoned that, since they behaved like gas molecules, in the earth's gravitational field they should be present in greater concentration near the bottom of the vessel than at higher elevations. Further, if the concentration varied with elevation in the same way as do the molecules in the earth's atmosphere, the evidence would favor the reality of molecules.

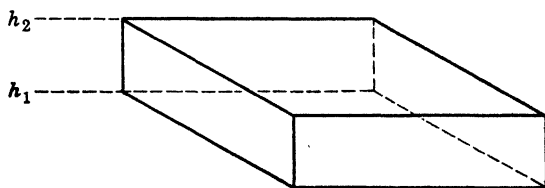


Fig. 1-8.

★ The variation of the pressure of a quiescent atmosphere with altitude may be derived as follows: Consider a parallelepiped with two horizontal surfaces, each of area A , at slightly different elevations h_1 and h_2 (Fig. 1-8). Let the pressures at these elevations be p_1 and p_2 ,

respectively. Then the up-force on the lower surface due to atmospheric pressure is $p_1 A$, while the down-force on the upper surface is $p_2 A$. Since the gas is in equilibrium, the resultant upward force equals the weight of the gas contained in the parallelepiped: that is,

$$(p_1 - p_2)A = \Delta h A \rho g \quad (15)$$

g being the acceleration of gravity and ρ the density of the gas.

★ The density of the gas varies with the altitude; hence it is desirable to eliminate ρ from the equation. If M is the gram-molecular weight, and V the volume per mole,

$$\rho = M/V \quad (16)$$

Also, by equation 7

$$p_1 V = RT \quad \text{and} \quad V = RT/p_1 \quad (17)$$

Thus, eliminating V ,

$$\rho = Mp_1/RT \quad (18)$$

Combining equations 15 and 18,

$$(p_1 - p_2)/p_1 = Mg \Delta h/RT \quad (19)$$

★ Relation 19 holds true only for small values of the left-hand member, since ρ was treated as a constant in equation 15. Subject to this restriction, if there were no convection, this equation might be used to find the molecular weight of nitrogen, for example, in our atmosphere. To do this it would be sufficient to measure the partial pressures p_1 and p_2 of the nitrogen at two heights h_1 and h_2 , provided that the temperature were the same at these two points. It might be more convenient to measure the concentrations n_1, n_2 of the nitrogen molecules rather than the partial pressures. Since these concentrations are proportional to the partial pressures, equation 19 may be rewritten

$$\frac{n_1 - n_2}{n_1} = \frac{Mg(h_2 - h_1)}{RT} \quad (20)$$

This equation will be true for all the particles in the atmosphere (assumed quiescent) that behave as molecules. It would be applicable, for instance, to fog particles. In this case, however, M represents the total mass in grams of a number of the fog particles equal to the Avogadro number N , just as, in the case of nitrogen, M represents the molecular weight. Equation 20 then shows that, if M is large, as for fog, then $n_1 - n_2$ is large, implying that the concentration of fog particles changes

rapidly with elevation; whereas if M is much smaller, as for nitrogen, the concentration of the gas decreases more gradually with increasing height. The above argument is equally applicable to the distribution at different heights of colloidal particles suspended in a liquid. In such a case, the quantities n_1 , n_2 , h_1 , h_2 , and T are observable, and, since g and R are known, a solution of equation 20 gives the value of M . This is equal to Nm , where N is the Avogadro number and m is the mass of one colloidal particle. To observe such an "atmosphere," Perrin placed a suspension of gamboge particles on the stage of the microscope just as before. Instead of observing the wanderings of a single globule, he counted the number that were visible through the eyepiece at a given elevation. Then he successively raised the microscope to higher levels, made other determinations, and found that the concentration varied with elevation in accord with equation 20. Moreover, the value of the Avogadro number thus determined was in good agreement with that found by the other method, and the truth of the kinetic theory was again verified.

The verification of the law of equipartition of energy and Perrin's success in determining the Avogadro number convinced everyone that the underlying assumption of the kinetic theory is true and that molecules do exist. Since then no prominent physicist has attempted to overthrow the molecular theory. Our faith in molecular reality is justified by the establishment of exact numerical relationships between results of observations with scientific instruments. And, indeed, such relationships possess a reality in no way inferior to those secured by direct observations, for, essentially, our eyes are optical instruments.

REFERENCES

In Appendix 9 is a long list of references designed to help the reader toward additional study. Some, at about the same level of difficulty as this book, may give him a new or clearer understanding of fundamental concepts; others will provide mathematical arguments and experimental evidence in full detail; a few are research papers—the ultimate authorities—in easily accessible journals.

References 12, 20, 29, 50, 52, 53, 55, 63, 74, 90, and 98, of a general introductory character, may be used to supplement nearly the whole of this book.

References 65 and 76 are particularly appropriate for Chapter 1.

PROBLEMS

1. In 1 min, 200 bullets from a machine gun strike a vertical wall normally. Each bullet has a mass of 10 gm and a horizontal velocity of 2 km/sec. On the assumption that each bullet rebounds with one-half its speed at impact, find (a) the momentum delivered to the wall per second, (b) the average force exerted against the wall.

2. Assume that molecules of oxygen are continually moving to and fro perpendicularly to the walls of a centimeter cube. Each molecule has a mass of 53×10^{-24} gm and a speed of 400 m/sec. The number of molecules per cm^3 is 2.7×10^{19} . On the assumption that each rebounds with undiminished speed at impact, find the pressure at the walls.

3. A billiard ball *A* moving eastward with a velocity of 40 cm/sec strikes another ball *B* of equal mass moving south with a velocity of 30 cm/sec. If, as a result of the collision, *A* loses all its momentum, find the speed of *B* immediately after the impact. Assume that no energy is dissipated as heat.

4. Consider $22,415 \text{ cm}^3$ of oxygen at 0°C and 76 cm of Hg. Find (a) the increase in volume due to a temperature increase of 1°C , if the pressure is constant, (b) the work in ergs done in causing expansion against the atmosphere, (c) the heat equivalent of this work, (d) the molar heat at constant pressure. (See Table 1-1.)

5. Given that the root-mean-square speed of hydrogen molecules at 0°C is 1839 m/sec, what are the corresponding molecular speeds of (a) helium and (b) oxygen? The molecular weights are 2.016, 4.003, and 32.000.

6. From Fig. 1-3, estimate roughly (a) the probable number of the 10,000 molecules having speeds greater than 1.8 times the mean speed, and also (b) the number having speeds less than one-half the mean speed.

7. Compute the translational kinetic energy per molecule for a gas at 27°C .

8. (a) At what Kelvin temperature would the average translational kinetic energy of a free electron be 1 electron volt (ev)? (b) What would be its average speed? (See Appendix 2, Energies and Speeds.)

9. (a) At what elevation in a quiescent atmosphere of hydrogen would the density be 99 per cent of that at sea level, if the temperature is 27°C ? (b) Consider the same question for an atmosphere of oxygen.

10. Assume that the Brownian particles used by Perrin were 10^{-4} cm in diameter, made of a substance of density 1.5 gm/cm^3 , and that the liquid was water. (a) What is the "molecular weight" of the colloidal particles? (b) What is their root-mean-square speed? Assume temperature = 27°C .

ANSWERS TO PROBLEMS

1. (a) 10^7 gm cm/sec^2 ; (b) 10.2 kg wt.
2. $0.763 \text{ megadyne/cm}^2$.
3. 50 cm/sec.
4. (a) 82 cm^3 ; (b) $8.31 \times 10^7 \text{ ergs}$; (c) 1.99 cal; (d) $6.96 \text{ cal/(mole } ^\circ\text{C)}$.
5. (a) 1304 m/sec; (b) 461 m/sec.
6. (a) 370; (b) 1000.
7. $6.17 \times 10^{-14} \text{ erg}$.
8. (a) 7740°K ; (b) $5.93 \times 10^7 \text{ cm/sec}$.
9. (a) 1260 m; (b) 79 m.
10. (a) 4.7×10^{11} ; 0.4 cm/sec.

2

The Atomic Nature of Electricity

1. Early Electrical Theories

The first attempt at a reasoned explanation of electrical phenomena appears to be that of the philosopher Thales (585 B.C.). He combated the popular view that the attraction of rubbed amber for light objects was of supernatural origin. Twenty-two hundred years later came the next advance, when William Gilbert, Queen Elizabeth's court physician, discovered that several other substances such as diamond, glass, and sulfur behaved like amber. He referred to them as "amberized" or "electrified," a term derived from *elektron*, the Greek word for amber. Throughout the seventeenth century there were other isolated discoveries and indications that the interest of scholars was being directed toward electricity. Somewhat later (1733) Dufay found that there are two kinds of electric charges: *vitreous*, appearing on glass rubbed with silk, and *resinous*, on wax rubbed with fur. In addition, he discovered the fundamental law that bodies similarly electrified repel whereas bodies dissimilarly electrified attract each other. No quantitative statement of this law was possible, however, until Coulomb (1785) had performed careful experiments with his newly invented torsion balance.

Benjamin Franklin suggested an atomic theory as to the nature of electricity. He surmised that a single kind of "electric fluid" or "electric fire" exists in all objects and thought of a positively charged body as containing more, and a negatively charged one as containing less, of this fluid, than an uncharged one. Franklin gave the name positive to what was previously called vitreous electricity. His choice was probably influenced by the fact that a candle flame is repelled by a positively charged ball as though something tangible—a "wind" of positively electrified particles—were emitted by the ball, while when it is negative the flame is attracted.

The following quotation shows that Franklin believed that electrical charges are atomic: "The electrical matter consists of particles extremely

subtile since it can permeate common matter, even the densest, with such freedom and ease as not to receive any appreciable resistance."

Since negatively charged bodies repel each other, Franklin's theory leads to the supposition that matter, stripped of the electric fluid, is self-repellent. Primarily to keep from entangling the problems of electricity and of matter, Symmer (1759) introduced the *two-fluid* theory. It assumes that an uncharged body contains equal quantities of two weightless substances, positive and negative electricity. The two rival theories were equally successful in explaining the facts known in that day, and both survived until late in the nineteenth century.

The first experimental evidence as to the atomic nature of electricity came with the discovery by Faraday of the laws of electrolysis (1833). We have already seen that these laws favored the atomic view as to the nature of matter. They also indicated that each ion in an electrolyte carries one or more elementary charges of electricity and that these elementary charges are numerically equal for all kinds of ions. Throughout the latter part of the nineteenth century it was widely believed that, in electrolytes at least, electric charges come in packages of the same size. Stoney (1874) first computed the magnitude of this "atom" of electricity by the following method:

The passage of 1 coulomb of electricity through a silver salt solution is accompanied by the deposition of 0.001118 gm of silver at the negative electrode. Hence 1 gram mole (107.88 gm) of silver would be deposited by 96,522 coulombs. The charge on each silver ion may be found by dividing this quantity by N , the number of molecules in a gram mole of silver. Stoney used a value of N determined by kinetic theory and obtained

$$e = 10^{-20} \text{ coulomb} = 10^{-21} \text{ abcoulomb} = 3 \times 10^{-11} \text{ statcoulomb}$$

(The electrical units used here are reviewed in Appendix 1.) This value is about one-fifteenth that found later by methods of great precision. The error of Stoney's determination is almost entirely due to inaccuracy in the value of N . Stoney suggested that the amount of charge on a univalent ion, whether positive or negative, be called the *electron*. However, it is now the accepted practice to assign this name to the negatively charged particle which plays such an important part in present-day physics. The positive part or *nucleus* of the most abundant type of hydrogen atom, which bears a charge equal in magnitude to that of the electron, we call a *proton*.

Now we shall enter on the study of electrons and of the positive ions which are produced when electrons are stripped away from atoms. For the sake of perspective, we suggest that the reader consult Appendix 3, which provides a census of the denizens of the atomic world.

2. The Electronic Charge

Precise information concerning the properties of electrons was obtained during the last quarter of the nineteenth century when a great deal of attention was devoted to the conduction of electricity through gases. The activity in this field resulted in the discovery of X-rays by Röntgen in 1895. This discovery was as important to the physicist as the invention of the telescope was to the astronomer. For the first time, the experimenter could readily ionize a gas without having to pass an electric discharge through the gas itself. The motions of the ions in an electric field could be studied with relative ease and precision. When the X-rays bombarding the gas were cut off, the oppositely charged ions combined and the conductivity slowly decreased.

The question then arose as to the magnitude of the charges on these particles. Was it the same for the positive as for the negative ions, and was it identical with that of the univalent ion of electrolysis? Pioneer attempts to answer these questions were made by Townsend (1897), Thomson (1898), and H. A. Wilson (1903).

During the years 1906–1916 Millikan modified and greatly improved their methods and evolved an apparatus (Fig. 2-1*b*) of great precision. A simplified diagram is given in Fig. 2-1*a*. A cloud of oil-fog particles was produced in the space *S* by means of a sprayer *A*. These fell slowly downward like mist, and a few entered the space between the horizontal metal plates *B* and *C*. When the droplets were strongly illuminated from one side, they were visible like motes in a sunbeam and could be observed through a low-power microscope *E*. The eyepiece of the microscope had a transparent millimeter scale, so that the elevation of a droplet could be accurately read. When the plate *B* was made positive with respect to *C* by means of a high-potential battery, some droplets moved upward, some fell slower, and others fell faster. This showed that some had been positively charged, and others negatively charged, either by the process of spraying or by contact with ions in the air. By carefully adjusting the potential of *B* so as to give a suitable field strength, a chosen droplet could be maintained at rest, like Mahomet's coffin, except for small agitations produced by the irregular bombardment of the air molecules.

★ Let g be the earth's gravitational field strength (force per unit mass), and m be the mass of the droplet. Let the electric field strength when the droplet is balanced be E , and the charge on the droplet be Q . Since the droplet is balanced, the downward force mg exerted on it by the earth's gravitational field is equal to the upward force exerted by the electric field; that is:

$$mg = EQ = (V/s)Q \quad (1)$$

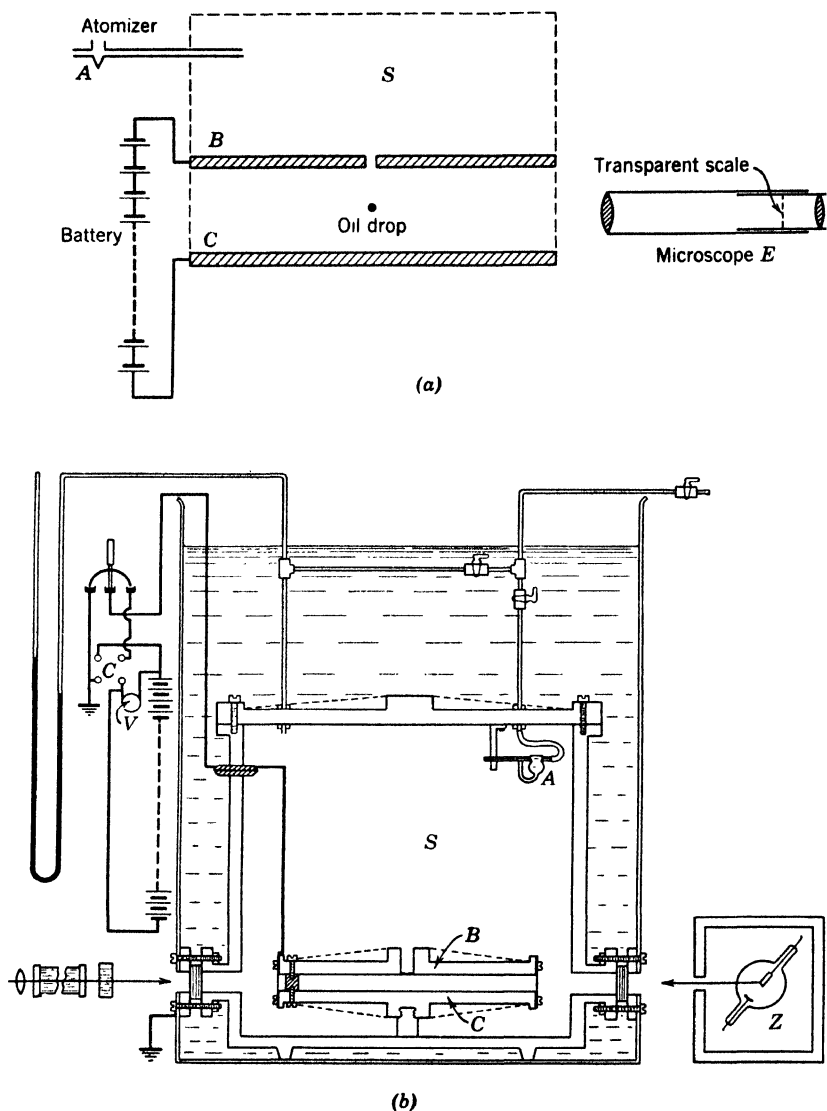


Fig. 2-1. (a) Millikan oil-drop apparatus, simplified diagram. (b) More complete diagram of the oil-drop apparatus. The atomizer *A* produced an oil fog, a few droplets of which entered the space between the plates *B* and *C*. An arc lamp illuminated the droplets from the left. To reduce convection currents between *B* and *C*, the light was passed through a heat-absorbing cell. The microscope was placed with its axis normal to the plane of the diagram. To change the charge on the droplets, a flash of X-rays from bulb *Z* was sent between plates *B* and *C*. (Courtesy of the University of Chicago Press.)

(The electric field strength between the plates is determined by dividing the potential difference V between them by the distance s . Thus a field strength of 1 dyne/abcoulomb is equal to 1 abvolt/cm. See Appendix 1.)

★ **Example.** An electric condenser consists of 2 horizontal plates 2 cm apart. The potential difference between them is 60,000 volts. What is (a) the electric field strength between the plates, (b) the charge on a pith ball, of mass 0.00204 gm, that is in equilibrium in the gravitational and electric fields?

$$(a) E = \frac{60,000 \text{ volts}}{2 \text{ cm}} = 3 \times 10^{12} \text{ abvolts/cm or dynes/abcoulomb}$$

$$(b) 3 \times 10^{12} \text{ dynes/abcoulomb} \times Q = 0.00204 \text{ gm} \times 980 \text{ cm/sec}^2$$

$$Q = 0.67 \times 10^{-12} \text{ abcoulomb} = 6.7 \times 10^{-12} \text{ coulomb}$$

★ The mass of the droplet was found by measuring its limiting “terminal” velocity v_g as it fell in the earth’s gravitational field alone. Since this velocity was constant, the upward resisting force of friction was equal to the downward pull mg of gravity. The force of friction was determined when the plates B and C were at the same potential by Stokes’ law, which states that the force f opposing the steady motion of a sphere of radius r through a homogeneous isotropic fluid is given by

$$f = 6\pi\eta vr$$

in which η is the viscosity of the fluid.

★ The resultant downward force acting on the droplet of density D is its weight minus the buoyancy of the air of density d . Thus

$$\frac{4}{3}\pi r^3(D - d)g = 6\pi\eta vr \quad (2)$$

From equation 2, r can be found; hence the mass of the droplet can be computed, and equation 1 then gives the charge.

★ In Millikan’s later work, the droplets were not balanced. The downward velocity v_g in the earth’s field alone was measured, then the velocity $v_{(g+E)}$ in the combined fields. Equation 1 was replaced by

$$\frac{mg}{mg + QE} = \frac{V_g}{V_{(g+E)}}$$

While a balanced droplet was under observation, Millikan noticed occasionally that it would suddenly begin to rise or to fall. This indicated that the charge had changed, presumably by contact with an atmospheric ion. After this change of charge, the electric field strength was altered to reestablish equilibrium, and a new value of E was determined. Long-continued observations showed that *for droplets of a*

given size the increase or decrease of charge caused by the picking up of an ion was always the same value within the limits of experimental error. This indicated that all the gas ions striking a certain droplet had numerically equal charges.

★ **Correction for the inhomogeneity of the medium.** However, when droplets of *different sizes* were used, the experimental values of e , the ionic charge, varied as shown in Fig. 2-2, being greater for small droplets than for large ones. Moreover, the experimental values of e for a droplet of given size increased when the pressure was reduced. The

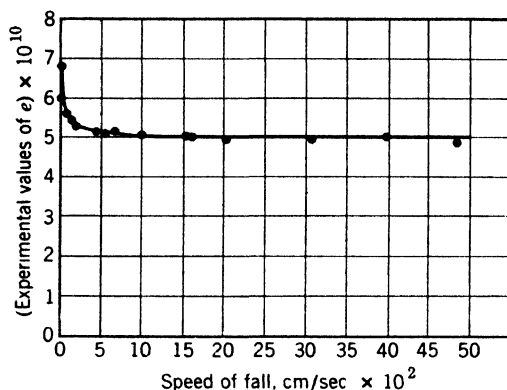


Fig. 2-2. Experimental values of the electronic charge as determined with droplets, which, having different sizes, fell with different speeds.

facts as to the variation with size might conceivably be explained by assuming that ions of many different charges were present in the gas and that for some mysterious reason the ions of larger charges were selectively attracted by the smaller droplets. However, a simpler explanation was possible; namely, that Stokes' law does not apply exactly to very small particles at normal pressures or even to larger particles at reduced pressures. One of the basic assumptions made in deriving the law is that the medium is *homogeneous* and contains no "holes" or discontinuities comparable in size with that of the sphere itself. The particle must move uniformly like a block sliding down a smooth inclined plane and not like one falling down a flight of stairs. If, then, in successive experiments we allow smaller and smaller spheres to fall through air at atmospheric pressure, eventually a condition will be reached in which Stokes' law no longer holds, since the distances between molecules become appreciable compared with the droplet's diameter. Because of these considerations, Millikan assumed that all

the ionic charges were equal. He therefore introduced into his equations a correction factor based on kinetic theory and finally brought about excellent agreement between all values of e determined by experiments at various pressures and droplet sizes in different gases.

As a result of researches by Millikan and his students covering a period of ten years, the value of the elementary charge of electricity was found to be

$$e = \pm 4.770 \times 10^{-10} \text{ esu (or statcoulomb)} = 1.591 \times 10^{-20} \text{ abcoulomb}$$

The most difficult part of Millikan's experiment was the determination of the viscosity of the medium. This was done for different gases, at different pressures, by several of Millikan's students. Despite this great effort, Millikan's value of the viscosity had an unsuspectedly large error. In consequence, his value of e was nearly 0.7 per cent too small. The error was finally detected and eliminated by Bearden. Today, the accepted value is

$$e = 4.802 \times 10^{-10} \text{ statcoulomb} = 1.602 \times 10^{-20} \text{ abcoulomb}$$

It follows that 6.25 billion billion electrons or protons equal 1 coulomb. The smallness of the charge may be illustrated by supposing that the electrons entering the filament of a 100-watt, 115-volt incandescent lamp in 1 sec are spread uniformly over the exposed land surface of the earth. If this were done there would be about one electron per square centimeter. The accurate determination of this quantity is indeed a remarkable achievement.

The numerical value of e has been found to be the same whatever the means used for the separation of electrons from their parent atoms. Among these we mention the irradiation of gases by alpha, beta, and gamma rays and by X-rays; the ejection of electrons from metals by heating to incandescence, or by illuminating them with ultraviolet rays. These results, together with other evidence, lead us to believe that the magnitude of the elementary charge is invariant in solids, liquids, and gases. To the best of our knowledge, it is a universal constant.

The Avogadro number. We have stated that Stoney in 1874 used electrolytic data and a very approximate value of the Avogadro number to determine the charge of the electron, or rather of the univalent ion of electrolysis. Now that the elementary charge has been determined by an independent method, it is possible, conversely, to determine N . Each silver ion has a charge $e = 1.602 \times 10^{-19}$ coulomb, and, if N atoms are deposited per coulomb, the charge transferred is Ne . This quantity is the faraday, and

$$N_e = \frac{107.88 \text{ gm/mole}}{0.001118 \text{ gm/coulomb}} = 96,500 \text{ coulombs/mole, approximately}$$

Using the most accurate data now available, we find $N = 6.025 \times 10^{23}$ molecules per mole.

A convenient unit of energy—the electron volt. In dealing with the energies of individual atoms, electrons, etc., it is convenient to use as a unit the *electron volt*, abbreviated as *ev*, which equals the work done when an electron is moved from one point to another differing in potential by 1 volt. Kinetic energy may be measured in electron volts. If a free electron moves without collisions from one place to another where the potential is different by 1 volt, then the electron's kinetic energy must change by 1 *ev*. Using numerical values from Appendix 2, we find:

1 electron volt	$= 1.602 \times 10^{-12} \text{ erg}$
The Boltzmann constant	$= 86.1 \times 10^{-6} \text{ ev/(K}^\circ \text{ molecule)}$
The average translational kinetic energy per molecule	$= 0.0353 \text{ ev at } 0^\circ \text{C}$
Rest energy (p. 34) of an electron	$= 0.511 \text{ Mev (million ev)}$

3. The Mass of the Electron

Discharges in gases. We have presented evidence that electric charges, whether positive or negative, are built up of indivisible units, all of the same numerical magnitude. We now consider the mass associated with the electron, which can be determined by experiments with discharge tubes. When the pressure is sufficiently reduced, the appearance of the discharge is very different from that of the disruptive, jagged spark which leaps the gap between the secondary terminals of an induction coil. Figure 2-3 shows the appearance of a discharge through a tube containing air at a pressure of 0.1 mm of Hg. The

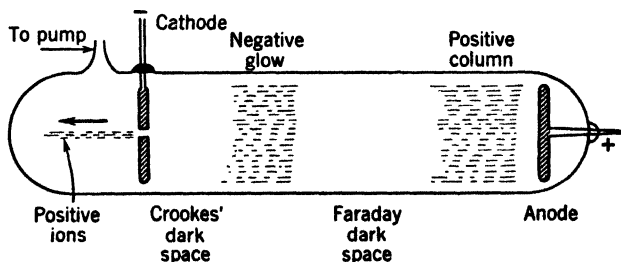


Fig. 2-3. Electric discharge at reduced pressure.

electric field near the cathode is very great. Positive ions, driven against the cathode, knock electrons out of the metal. The air pressure is so low that each ejected electron travels several millimeters before striking an air molecule in the *negative glow*. Then electrons move onward from the negative glow, and acquire enough energy to excite and ionize molecules in the *positive column*.

Notice the *Crookes' dark space*. In this region, electrons travel away from the cathode with speeds of thousands of miles per second. As the pressure in the tube is reduced, they travel farther on the average before striking the molecules; hence the dark space spreads outward from the cathode. At pressures of a few hundredths of a millimeter it fills the entire tube; the electrons strike the glass walls of the tube and make

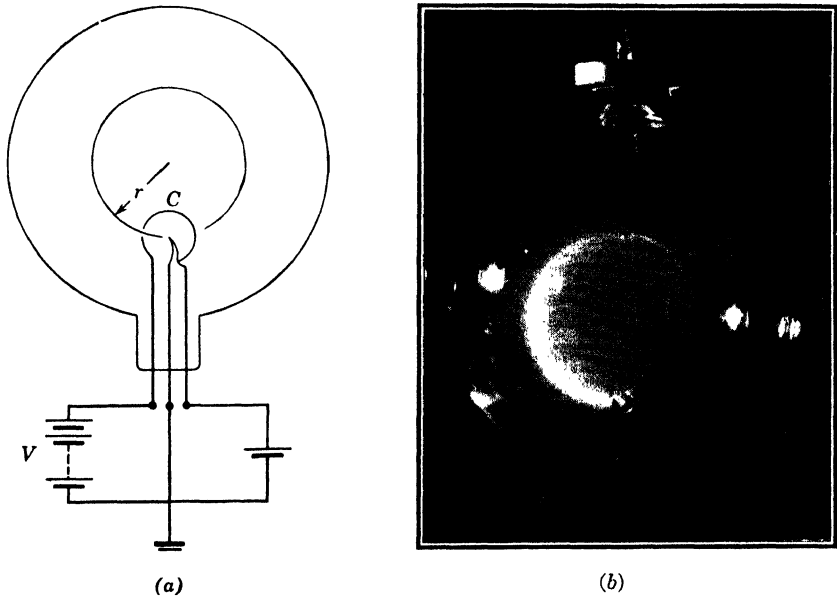


Fig. 2-4. (a) Diagram of tube for finding the electron mass. (b) Photograph (courtesy of Dr. K. T. Bainbridge). See *Am. Phys. Teacher*, 6, 35 (1938).

them fluoresce with a greenish-yellow light. Obstacles placed in front of the cathode cast sharp shadows on the walls, showing that the electrons travel in straight lines. The electrons may be deflected by electric or magnetic fields in such directions as to prove that they are negatively charged. A simple method of showing this, due to Bainbridge, is as follows:

Figure 2-4 shows a rather highly evacuated tube having as a cathode a wire mounted on the axis of a metal cylinder *C*. The cathode wire is

heated red hot so that it emits electrons. They are accelerated by the potential difference V between the wire and the cylinder, so that some of them pass through a slit in the cylinder. The tube is mounted between the poles of a strong magnet whose field of strength H causes a magnetic flux density $B = \mu H$. The force due to the magnetic field pulls the electrons sideways, causing them to travel on a circular path. This path is revealed by luminescence of the gas in the tube so that the radius of the circular path can be measured.

The work done in accelerating an electron from wire to cylinder is equal to the final kinetic energy of the electron:

$$Ve = \frac{1}{2}mv^2 \quad (3)$$

Each electron moves on a circle of radius r such that

$$mv^2/r = Bev \quad (4)$$

★ The radial force Bev is found as follows: Let a wire of length L carry a current I at right angles to a magnetic field of strength H , so that the flux density is B . The force F acting on the wire is given by

$$F = BIL$$

If the number of free electrons per unit length of wire is n , the current I equals nev , v being the forward drift velocity of the electrons. The number of electrons acted on by the field is nL , so that the force per electron is

$$f = F/nL = BnevL/nL = Bev \quad (5)$$

The velocity v can be evaluated by equation 3. Using this value in equation 4, and knowing e and r , we can compute the mass m of the electron.

Several other experimental methods have been employed, most of them involving the use of both electric and magnetic fields. The results indicate that the comparatively slow-moving electrons emitted from cathodes in discharge tubes, and from hot bodies, as well as those ejected by X-rays or by ultraviolet rays, all have the same mass, namely,

$$m_0 = 9.107 \times 10^{-28} \text{ gm}$$

which is approximately 1/1836 that of the hydrogen atom.

4. Variation of Mass with Velocity

This value of the mass holds only for electrons at rest, or moving with speeds small compared with that of light. For this reason we often call

it the "rest mass." When a sufficiently high voltage is applied to a discharge tube, so that the speed of the electrons becomes appreciable compared with that of light, the deflection produced by the magnetic field is less than that predicted by equations 3 and 4. This might be explained by assuming that either the charge or the mass of the electron depends on its speed, because only the ratio e/m occurs in the equations of motion. However, the observed variation of e/m with speed is accounted for by currently accepted theory which predicts variation of the mass, but not the charge. Lorentz derived an expression for the mass from electrodynamics, and Einstein derived the same formula from relativity theory (Chapter 15). The relation is

$$m = m_0 / \left(1 - \frac{v^2}{c^2}\right)^{1/2} = m_0 / (1 - \beta^2)^{1/2} \quad (6)$$

in which v is the speed, c the velocity of light, and $\beta = v/c$.

★ Assuming constancy of the charge, Bucherer and others determined the masses of electrons ejected from radioactive atoms with speeds approaching that of light. Zahn and Spees pointed out sources of uncertainty in the results of the early workers and made new measurements which support equation 6. Also, the results of Starke and Nacken, and of Lahaye support this relation. In Fig. 2-5, the upper curve shows the variation predicted by equation 6.

The relation between mass and energy. The importance of the experimental evidence that the mass of an electron depends upon its speed can be appreciated when we remember that for many years previous to the first experiments on this subject the law of conservation of matter had been considered well-nigh perfectly established. This opinion is not surprising since for ordinary speeds the variation of the masses of bodies is inappreciable.

Being loath to assume that mass can be created out of nothing, we ask ourselves, what must be expended in accelerating an electron, and what does it give up when it is retarded? The most obvious answer is energy. In confirmation of this view, the theory of relativity indicates that mass and energy are inseparable.

Any increase of the energy of any physical system is associated with an increase of its mass. In Chapter 15 we discuss the generally accepted view that a system of mass m contains energy

$$E = mc^2 \quad (7)$$

In view of equations 6 and 7, we can no longer uphold the law of conservation of mass as applied to an individual body. We replace it by

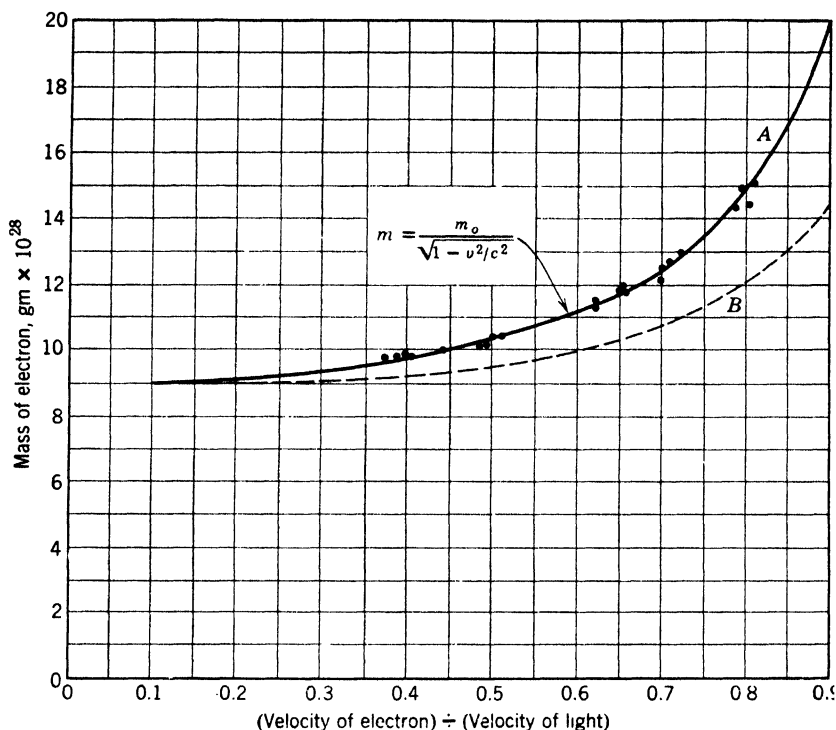


Fig. 2-5. Mass of the electron at different velocities. The solid curve, A, is computed from equation 6. The dotted curve is based on the assumption that half the mass is constant while the other half varies according to equation 6.

the law of conservation of energy and recognize the existence of a new entity, namely, mass energy. According to this view, an express train in motion has a greater mass than when it is at rest. (The increase is only a few micrograms.)

★ **Revised formula for the kinetic energy.** Consider a particle having mass m_0 , and energy m_0c^2 when at rest. If it moves with speed v , its energy will be a larger value, mc^2 , and the kinetic energy (K.E.) should be the difference between its total energy and its rest-mass energy. By equation 6,

$$\text{K.E.} = mc^2 - m_0c^2 = m_0c^2 \left[\frac{1}{(1 - \beta^2)^{1/2}} - 1 \right] \quad (8)$$

But if the speed is reduced to a value small compared with the speed of light, the kinetic energy must approach the familiar expression $\frac{1}{2}m_0v^2$. We shall show that the expression in equation 8 obeys this requirement.

The binomial theorem tells us that

$$(a - b)^n = a^n - \frac{na^{n-1}b}{1!} + \frac{n(n-1)a^{n-2}b^2}{2!} - \dots$$

Putting $a = 1$, $b = \beta^2$, and $n = \frac{1}{2}$, we obtain

$$(1 - \beta^2)^{-1/2} = 1 + \frac{1}{2}\beta^2 + \frac{3}{8}\beta^4 \dots$$

When β is so small that we may neglect β^4 and higher powers, equation 8 yields the *approximation*

$$\text{K.E.} = m_0 c^2 (1 + \frac{1}{2}\beta^2 - 1) = \frac{1}{2} m_0 v^2$$

as it should.

But even if an electron has mass, may we regard it as a form of matter? To decide this question it is necessary to agree as to what are the essential properties of matter. In particular, what do we imply when we state that the amount of matter in a piece of lead equals that in a pile of feathers? Certainly we do not mean that their weights are equal, for one might be on a mountain top and the other in a valley. What we really mean is that these two bodies, at rest or moving slowly, would experience equal accelerations when subjected to equal forces; in other words, their masses are equal. Mass is indeed an essential property of matter.

According to these views, both matter and radiation have mass. How then, do they differ? For one thing, a particle of matter cannot travel *as fast* as light, for if it did so, according to equation 6, its mass would become infinite.

5. The Electromagnetic Nature of Mass

A rather crude analogy from hydrodynamics may help to make clear how the mass of the electron can depend on its velocity. Consider a sailboat moving across a lake. It produces a disturbance, and some of the surrounding water is set in motion. Part of the inertia, and hence part of the kinetic energy, of the moving system is in the boat itself, and part in the surrounding water. Thus to impart a speed v to the boat we would need to supply energy such that

$$\text{K.E.} = \frac{1}{2}(M + m)v^2$$

In this equation M represents the mass of the boat and m the "effective mass" of the fluid which it drags along.

In considering electromagnetic mass, it is helpful to take the viewpoint of Faraday and think in terms of tubes or lines of force. When

a north magnetic pole is placed near an equal south pole, we picture magnetic lines as originating at the north pole and ending on the south pole. Usually, the field strength is represented by the number of lines per unit area. The lines act like elastic, mutually repelling strings. If the poles are moved apart, work must be done, and the energy is stored in the medium. Similarly, from a positively charged pith ball, electric lines emerge which find their way to negative charges. If the positive charge is moved away from the negative ones, work must be done, and energy is stored in the electric field.

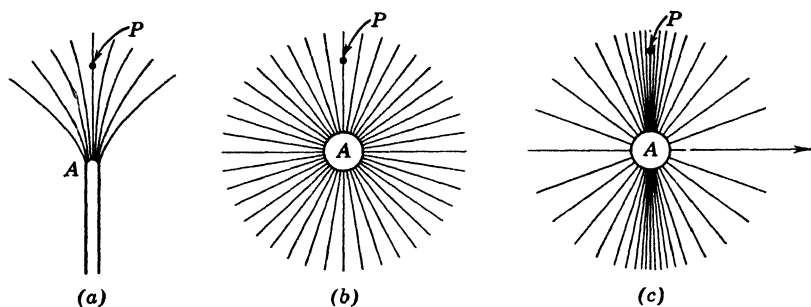


Fig. 2-6. (a) Magnetic lines from a magnet pole, moving sideways, generate an electric field perpendicular to the paper at point P . (b) Similarly, moving electric lines produce a magnetic field at P . (c) At high velocity the crowding of electric lines into the "equatorial" region produces an enhanced magnetic field.

We now consider the effect of the motion of such lines in causing magnetic or electric fields. Because of greater familiarity, we shall first deal with the magnetic lines. If a magnet pole A (Fig. 2-6a) is moved sideways, magnetic lines sweep past the point P and an electric field is established perpendicular to the plane of the paper. If a wire lay in this direction, the motion of the lines would produce an induced electromotive force. If the pole moves toward P , the magnetic line through P has no sideways component of motion and no electric field is established. In general, the strength of the electric field is proportional to the rate at which the magnetic lines sweep past P .

On the other hand, electric lines may be considered to exist in the region around an electrically charged pith ball, as in Fig. 2-6b. If they move sideways past P , a magnetic field is produced which is again proportional to the rate at which they pass. If, further, the velocity increases, the strength and hence the energy of this new field increase. Since the energy depends upon the velocity, it may be considered kinetic in nature. The energy of the system is thus in two parts, namely, that of the pith ball of mass M and that of the electromagnetic field.

Suppose that a very high velocity such as 150,000 mi/sec is imparted to the pith ball. From electrodynamic theory, it may be shown that the lines of electric force would be crowded together in the equatorial region (Fig. 2-6c). Thus the electric lines are shifted from the regions where their magnetic effect is small to ones where the effect is greater. As a result, the energy of the electromagnetic field becomes larger than if the distortion had not occurred. To explain this excess energy arising from the motion of the distorted field, we assume that the electromagnetic mass m increases with speed.

If we think of the electron as a tiny, negatively charged bubble of electricity, the question arises, "Is there a portion of the mass that does not increase with velocity?" We may call that hypothetical portion the "ordinary" mass. In dealing with this question the variation of electronic mass with speed is significant. In Fig. 2-5 the upper curve is plotted on the assumption that all the mass obeys the Lorentz equation (6). The lower curve shows the result to be expected if half the mass obeys equation 6, while the other half is of some nature such that it does not increase with velocity. The fact that the experimental points lie in the neighborhood of the upper curve has led to general belief that the electron has no "ordinary" mass. However, this matter deserves further investigation.

The relation between mass and electromagnetism has been considered here from the viewpoint of classical electrodynamics. The results are in accord with those of relativity (Chapter 15).

6. The Size of the Electron and of the Proton

★ In deriving an expression for the size of the electron, we are hampered by the fact that we know nothing of its shape or of the distribution of its charge. Let us arbitrarily assume that an electron is a bubble of electricity, the charge e being uniformly distributed over the surface of a sphere. Imagine that this sphere is caused to contract so that the charge on its surface is compressed. When this is done, energy is added to the sphere, and therefore its inertia and its mass are augmented. Moreover, the mass of the system can be made as large or as small as we wish by changing its radius. Suppose that, when the mass is equal to the value m_0 for the electron, the radius is r_0 . Then, when e is expressed in statcoulombs, the energy of the charged sphere is

$$E = \frac{1}{2} \frac{e^2}{r_0}$$

This result is obtained as follows: If we add a charge $-\Delta e$ to the electron, we must do an amount of work

$$(-\Delta e)(-e/r_0) = e \Delta e/r_0$$

because the potential at the surface is $-e/r_0$. If we "build" an electron by adding such charges, one by one, the average work required to put a quantity $-\Delta e$ in place is half the above expression because the potential gradually increases in magnitude from 0 to $-e/r_0$. Hence the work required to assemble all the charge on the surface of the sphere must be $\frac{1}{2}e^2/r_0$. Further, by Einstein's equation, this energy equals m_0c^2 ; hence

$$m_0c^2 = \frac{1}{2}e^2/r_0$$

$$m_0 = \frac{1}{2}e^2/r_0c^2$$

$$\text{that is, } 9 \times 10^{-28} \text{ gm} = \frac{(4.80 \times 10^{-10} \text{ statcoulomb})^2}{2(3 \times 10^{10} \text{ cm/sec})^2 r_0} \quad (9)$$

$$r_0 = 1.1 \times 10^{-13} \text{ cm}$$

★ Since the proton is more massive than the electron, this equation would lead us to believe that the proton "radius" is about 10^{-16} cm. This disagrees with known facts (p. 374) about the scattering of swiftly moving particles by hydrogen atoms. The proton does not act like a bubble of electricity. In many ways it behaves like a combination of a neutron and a positive electron whose properties are explained in Chapter 11.

7. Isotopes and Their Interpretation

The masses of positively charged particles may be determined by experimental methods similar to those used for the electron. In the discharge tube of Fig. 2-3, rays are indicated streaming to the left through the opening in the cathode. These rays, which are sometimes called *canal rays*, consist of atoms or groups of atoms each of which has lost one or more electrons in the intense electric field between the electrodes. Their masses were first carefully studied by J. J. Thomson. He found that the element neon is composed of two types of atoms, with atomic masses close to 20 and 22, respectively. Much later, a third variety of mass 21 came to light. These subspecies are called the *isotopes* of neon, from Greek words meaning "the same place," and signifying that they are varieties of one and the same chemical element.

Aston later developed apparatus of great precision, the essential parts of which are shown in Fig. 2-7. Positive ions, produced by an intense electric field near the cathode, were accelerated toward it. Some of these passed through very narrow slits, S_1 and S_2 . These positively charged particles were bent downward by an electric field between the plates P_1 and P_2 . Here a dispersion or separation occurred, the faster particles of a given mass and charge being less deviated than the slower

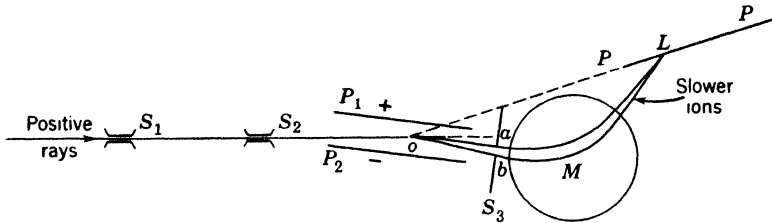


Fig. 2-7. Simplified diagram of Aston's mass spectrograph. (From Richtmyer's *Introduction to Modern Physics*, courtesy of the McGraw-Hill Book Co.)

ones. The resulting divergent beam entered M , where a magnetic field normal to the plane of the paper bent it upward. The application of two fields in this way caused all particles having a given ratio of mass to charge to converge in a certain region L on a photographic plate, regardless of their velocity. The focus points for particles having different values of this ratio lay on the straight line PP' , and therefore the photographic plate was placed along this line. When several types of ions were present, several regions were blackened and the result resembled an optical spectrum. For this reason, Aston called the instrument a *mass spectrograph*. The photographs obtained are called mass spectra.

The Dempster-Bainbridge type of mass spectrograph is diagrammed in Fig. 2-8. Suppose that the wire W is coated with a lithium salt. Positive lithium ions, given off by the heated wire, are driven across the enclosure, and some of them pass through a slit into the space between the plates M and N .

The purpose of the two parallel plates M and N is to make certain that ions of one velocity only pass through a second slit, S ; that is, the system serves as a "velocity filter." An electric field X between these plates deviates the ions toward the plate M . The force is opposed by one caused by a magnetic flux of strength B_1 perpendicular to the plane of the paper. If the two forces balance each other for a particular ion, that ion may pass through the slit S and enter a second chamber.

For such ions of charge e and velocity v ,

$$Xe = B_1 ev \quad \text{and} \quad v = X/B_1$$

In the second chamber, ions of mass m are deviated by a magnetic field H_2 and travel on a circle of radius r such that

$$B_2 ev = mv^2/r$$

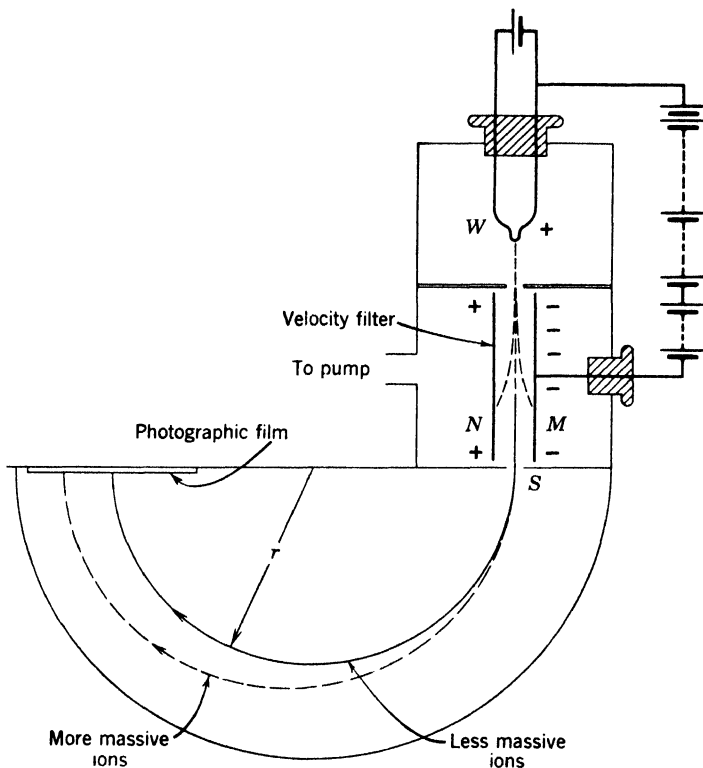


Fig. 2-8. Dempster-Bainbridge mass spectrograph. The curvature of the ion paths in the semicircular chamber is produced by a magnetic field applied to that region.

The value of e/m for different kinds of ions, traveling on circles of different radii, can be computed by using these two equations.

The kind of evidence afforded by the mass spectrograph is illustrated by spectra procured by Bainbridge. Figure 2-9a shows characteristic lines due to ions of beryllium, neon, and carbon, as well as those due to

compounds of carbon and hydrogen. In recording the lines indicated by letters below the spectrum, the fields were altered in a known way, so that the masses of the ions designated Be^9 and Ne^{20} could be more easily compared with that of carbon. Figure 2-9*b*, taken with higher dispersion of the masses, shows lines produced by the singly charged

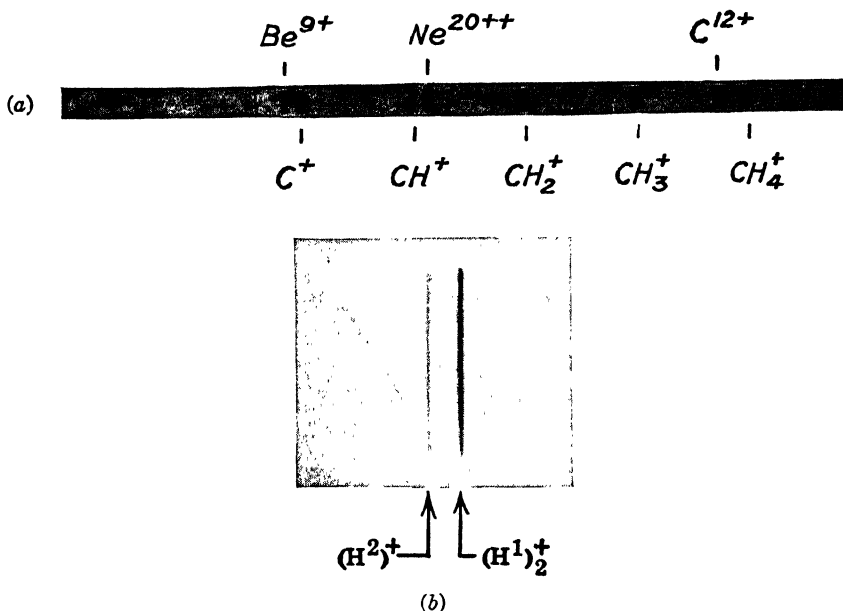


Fig. 2-9. (a) Mass spectra of beryllium (Be^9), neon (Ne^{20}), carbon, and carbon-hydrogen compounds. (b) Lines due to the molecular ion of ordinary hydrogen $(\text{H}^1)_2^+$, and the atomic ion of deuterium, or heavy hydrogen $(\text{H}^2)^+$. (After Bainbridge. (b) From Phys. Rev., **50**, 287, 1936.)

molecule of ordinary or mass-1 hydrogen, $(\text{H}^1)_2^+$, and by the singly charged atom of deuterium or heavy hydrogen, $(\text{H}^2)^+$. This shows that deuterium has a mass smaller than that of two ordinary hydrogen atoms.

Nature of the nuclear atom. These observations, and others like them, form part of the support for our present view of atomic structure, which is as follows: The atom of an element which occupies the Z th place in the periodic table (Appendix 5) has a nucleus with a charge $+Ze$, normally surrounded by Z electrons, each of charge $-e$. Z is called the *atomic number*. Most of the mass is concentrated in the nucleus, which is made up of protons and neutrons. The neutron

is a particle without electric charge, whose mass is slightly larger than that of the proton. The isotopes of any element are atoms which have the same number of protons but different numbers of neutrons. For example, the nucleus of deuterium is composed of one proton and one neutron.

Table 2-1 shows the masses of a few isotopes of several elements, as determined by the mass spectrograph and other methods.

TABLE 2-1. Some Isotopic Masses

Atom	Isotopic Masses*
Electron	0.000549
Neutron	1.00894
H	1.00813 2.01472
He	4.00389
Li	6.01695 7.01820
O	16.00000 17.00453 18.00491
Cl	34.97893 36.97755
Kr (there are 6 stable isotopes)	77.945 to 85.929
Pt (one of several)	198.044
U (one of several)	238.13

* Based on the value of exactly 16 for the isotope O^{16} . The "chemical" atomic weight scale is based on the value 16 for natural oxygen mixture. The masses in this table are about 1.8 parts in 10,000 higher than they would be on the chemical scale. In several instances the last digit is not trustworthy.

8. The Whole-Number Rule

As we shall see from detailed evidence presented through the remainder of this book, an atom consists of a tiny nucleus, surrounded by electrons. It is found that the masses of all atoms in terms of oxygen = 16.0000 are approximately whole numbers, to an extent which may be judged from Table 2-1. Whenever, as in the case of chlorine (atomic weight,

35.457), large deviations from whole numbers occur in the chemical atomic weights, the element under investigation has been shown to be a mixture. More than a century ago, Prout suggested that the heavier atoms are built up of hydrogen. At the time, the greatest barrier to the acceptance of Prout's hypothesis was that hydrogen itself was a trifle too heavy to fit into the scheme. However, this fact can be explained in terms of our present knowledge of nuclei. Imagine a proton near a neutron, and assume that the two attract each other when they are very close together. (This assumption is justified in Chapter 12.) If the neutron is carried farther away, work must be done; energy is stored in the "force-field," and the mass of the system increases. There is much evidence that in the nuclei (excepting ordinary hydrogen, of course) protons and neutrons are held intimately together. It is not surprising, therefore, that the mass of such a condensed unit is smaller than if its components were widely dispersed.

Instability of the elements. According to this view, the formation of heavier elements from hydrogen should be accompanied by the "annihilation" of matter and the liberation of energy. The amount of atomic energy transformed, ΔE , according to equation 7, is

$$\Delta E = c^2 \Delta m \quad (10)$$

in which Δm is the decrease of mass. Thus, if 1 gm of matter were converted into radiation, the amount of energy set free would be

$$\begin{aligned} \Delta E &= (3 \times 10^{10} \text{ cm/sec})^2 \times 1 \text{ gm} = 9 \times 10^{20} \text{ ergs} \\ &= 21 \text{ million million gm cal} \\ &= 25 \text{ million kw hr} \end{aligned}$$

According to this equation, if all the hydrogen in 100 cm³ of water could be converted into helium, the energy liberated would be about equal to that set free in the combustion of 3000 tons of coal or 500,000 gallons of gasoline. This energy would be sufficient to heat a small residence for about 400 years or to drive 100 automobiles several times around the world.

The discovery of atomic energy is welcomed by the astrophysicist, since it enables him to explain how the temperatures of the stars are maintained. In the sun and in other stars, hydrogen is converted into helium and heavier elements by a roundabout process described on p. 356. Such processes of agglomeration go under the name of "fusion." The sun emits about 4,000,000 tons of radiation per second. Its present mass is such that at this rate it could continue to supply energy for billions of years.

In physics, as in other fields, "laws" are often most interesting when they are not obeyed. The mass spectrograph reveals systematic deviations from the integral law throughout the entire periodic system. To indicate the trend of atomic mass values M , throughout the periodic system of the elements, we present Fig. 2-10. The abscissa represents the *mass number* A , the number of protons and neutrons in the nucleus. The ordinate shows the ratio of the atomic mass to the mass number M/A , since it would be impossible to plot M itself on any reasonable scale. The mass per particle minus 1 is called the *packing fraction*.

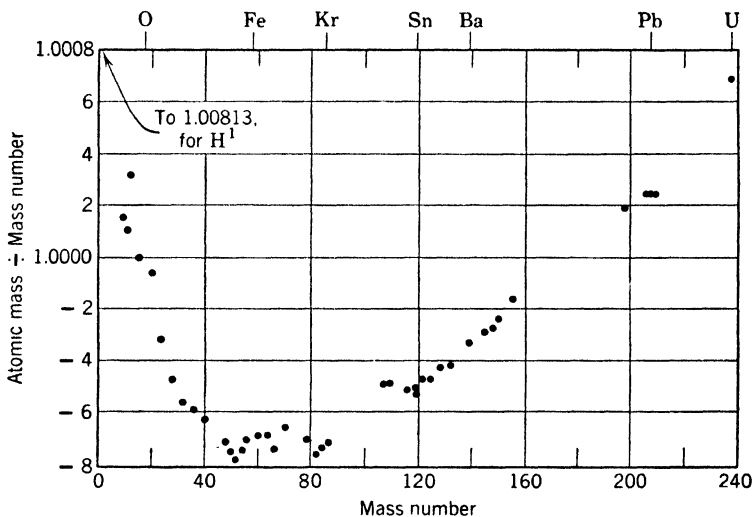


Fig. 2-10. Mass per nuclear particle, plotted against mass number (or number of particles in the nucleus).

In several parts of the periodic system, experimental difficulties have prevented the establishment of accurate atomic masses. The whole subject is under active study, and the values shown in Fig. 2-10 may in the future be considerably changed. (Appendix 9, ref. 27.) For values of the mass number less than about 12, the ordinates have interesting ups and downs; and many of them fall outside the range of the diagram. Figure 2-11 is a plot of this region, on a larger scale. (Many unstable varieties are omitted, for simplicity.)

A study of Fig. 2-10 will yield interesting hints regarding the stabilities of atoms if one keeps in mind that a minimum of potential energy in a system is usually associated with a maximum of stability. The middle part of the curve (Fig. 2-10) is lower than the ends, and therefore it is

to be expected that the elements of small or large atomic weights should be less stable than those with intermediate values.

If nuclei could react without hindrance, the material of this globe would be transformed to a single isotope. The data indicate that this isotope is Ni^{62} . A few heavy elements, located at the extreme right of Fig. 2-10, are unstable, subject to radioactive changes, and "fissionable."

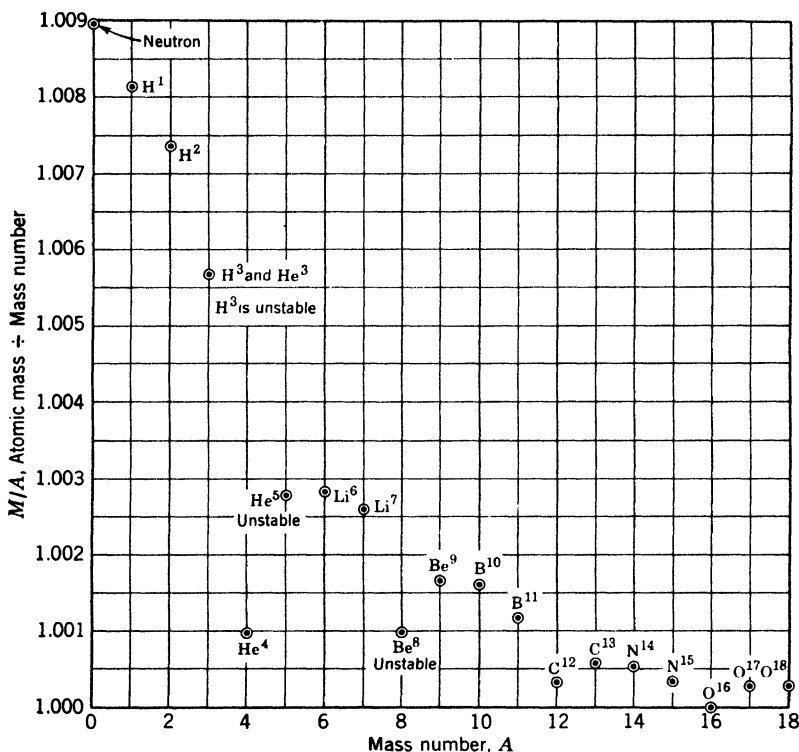


Fig. 2-11. Mass per nuclear particle for the light elements.

In Fig. 2-11, notice that at mass numbers 4, 8, 12, and 16 there are four "valleys" or points of great stability, three of which support the belief that the stable isotopes helium 4, carbon 12, and oxygen 16 are built up solely of particles of mass 4. Such nuclear building units are called alpha particles. Only two alpha particles, however, do not make a permanent nucleus, for beryllium 8, being unstable, breaks into two alpha particles. Lithium 6 and 7 and beryllium 9, at or near the tops of peaks in the curve, can be broken up rather easily.

Binding energy. The energy required to break up a nucleus and to disperse its protons and neutrons we call its *binding energy*. For example, when 1 gram atom of helium is thus broken up, the increase of mass is

$$\Delta m = 2 \times 1.00813 \text{ gm} + 2 \times 1.00894 \text{ gm} - 4.00389 \text{ gm} = 0.0303 \text{ gm}$$

The required energy input is $c^2\Delta m = 27.2 \times 10^{18}$ ergs.

This value, divided by the Avogadro number, gives the binding energy of helium, namely, 4.52×10^{-5} erg = 28.2×10^6 ev. Dividing this value by the number of protons and neutrons (nucleons) in a helium atom gives the binding energy per particle, 7.05×10^6 ev.

9. The Structures of Atoms

The discoveries described above agree with the view that all atoms contain protons, neutrons, and electrons, but give no information as to the arrangement of these entities. The atom as pictured by kinetic theory was a round, elastic billiard ball having a diameter of the order of a few times 10^{-8} cm. This value merely measures the nearness of approach of the centers of atoms colliding at ordinary temperatures. The questions may well be asked, "How closely will the atomic centers approach each other if the relative velocities of the atoms colliding are increased several thousand times? Does an atom have an impenetrable core?" Fortunately, the query is not idle since the means for the experiment are available. The gas radon is unstable, and occasionally

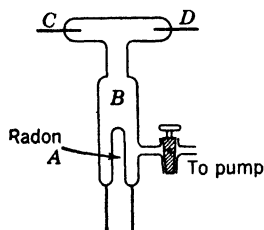


Fig. 2-12. Apparatus to demonstrate that alpha particles can penetrate thin glass.

an atom explodes, hurling out an alpha particle (helium 4 nucleus) with a velocity about 10,000 mi/sec. If some of this gas is enclosed in a thin-walled capillary tube *A* (Fig. 2-12), after a few hours helium may be detected in the evacuated space *B* by spectroscopic examination of an electric spark between the terminals *C* and *D*. If the space is again evacuated and helium instead of radon is enclosed in *A*, no trace appears in *B* during a period of many days. This proves that the thin glass walls, while impervious to gas molecules moving with speeds less than 1 mi/sec, are not an effective barrier

to alpha particles moving with very high velocities. From geometrical considerations, it may be shown that in plunging through the glass wall each alpha particle must have traversed hundreds of atoms of the size determined by kinetic theory. Thus, if impenetrable regions exist in the atoms forming the wall, they must be very minute.

Striking visual evidence for the penetrability of atoms and also for the existence of massive nuclei is afforded by the fog trails which form along the tracks of alpha particles moving through air supersaturated with water vapor. These fog particles form on ions produced by each alpha particle as it traverses the moist air (see Figs. 11-4 and 12-2). At ordinary speeds, gas molecules move only a few hundred thousandths of a centimeter between successive collisions, but the alpha particles move on fairly straight lines for several centimeters. In so doing, they must plunge through thousands of atomic systems. Furthermore, since the alpha particle is much less massive than an air molecule, it cannot proceed by shoving the air molecules aside as a rifle bullet does.

A glance at the figures referred to should remove all doubt as to the existence of massive nuclei. Some of the trails show abrupt bends, indicating sudden changes in the velocities of the particles. Each large deviation indicates that the alpha particle has encountered an obstacle whose mass is of the same order of magnitude as its own. An electron cannot deflect an alpha particle through a large angle.

Scattering of alpha particles. More direct evidence as to the sizes of the nuclei and the amounts of charge which they carry has been obtained through experiments on the scattering of alpha particles. If a parallel beam of alpha particles is incident upon a thin sheet of metal foil, most of the particles pass through without appreciable deviation. A few are deviated through small angles, and a very few rebound and emerge on the same side as that on which they entered.

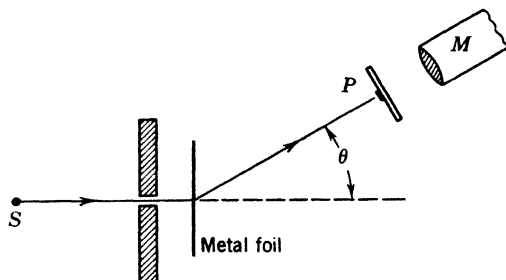


Fig. 2-13. Apparatus to detect alpha particles scattered by a foil.

★ Apparatus similar to that sketched in Fig. 2-13 has been used to determine the scattering produced by thin sheets of foil. A radioactive source *S* emits alpha particles, some of which pass through a slit and are scattered by the foil. Those deviated laterally through an angle θ fall upon a fluorescent screen *P* at the focal plane of the microscope *M*.

The impact of each particle causes a tiny flash of light, so an observer can count the number of hits in a chosen time interval. By repeating this process for other values of θ the distribution of the scattered particles may be determined.

★ In developing a theory of this scattering, Rutherford assumed that each alpha particle of mass M carried a positive charge $+2e$, equal to that of two protons, while the charge on each nucleus in the metal foil was $+Ze$. He assumed that the force exerted by any nucleus on the impinging alpha particle was due solely to the repulsion of their respective electric charges and that Coulomb's inverse square law was valid. The problem of determining the change of path of the alpha particle due to the influence of a single atom, say of gold, thus becomes similar to that of predicting the path of a comet approaching the sun, the significant difference being that in the case of the alpha particle the forces are repulsive rather than attractive. The problem is discussed in Chapter 11. We need only state that the fraction of all the incident particles that are deviated more than an angle θ is given by

$$G = \frac{4\pi NZ^2 e^4}{M^2 v^4} \cot^2 \frac{\theta}{2} \quad (11)$$

in which N is the number of atoms in 1 cm^2 of the foil and Mv^2 is twice the kinetic energy of an alpha particle.

★ A careful study by Geiger and Marsden resulted in experimental values for fairly heavy elements which were in agreement with equation 11. Since equation 11 is based on the inverse square law, this agreement indicates that the law holds when an alpha particle approaches a heavy nucleus as closely as 3 or $4 \times 10^{-12} \text{ cm}$. Therefore, the diameters of nuclei cannot be greater than one-ten-thousandth that of the atom of kinetic theory.

★ The scattering was found to be relatively greater for heavier atoms than for lighter ones. Numerical values of the atomic number Z , computed from the experiments by the aid of equation 11, were approximately one-half the atomic weights of the elements forming the foils. These experiments also indicate that the atomic number of an element, and not its atomic weight, is the fundamental quantity which determines its chemical properties.

Summarizing, we now think of atoms as complex structures somewhat resembling the solar system. The atoms of Democritus, "infinite in number and infinitely varied in form," are reduced to 90-odd elements, comprising several hundred isotopes. Finally, these particles seem to be manifestations of one fundamental entity, energy.

REFERENCES

Appendix 9, refs. 2, 44, 68, 70.

PROBLEMS

(See Appendix 1 for electrical units, and note that 1 dyne/abcoulomb = 1 abvolt/cm)

1. Using the accepted value of Avogadro's number, find the mass of (a) a silver atom and (b) a hydrogen molecule.
2. Given that the passage through an electrolytic solution of 96,500 coulombs of electric charge is accompanied by the deposition of 1 gram atom (107.9 gm) of silver, compute the mass of a silver atom.
3. (a) Find the vertical field intensity in dynes/abcoulomb such that a water droplet 0.0001 cm in diameter and carrying one electron will remain stationary in the field. (b) Also find the values if the droplet carries two, three, and four electrons, respectively. (c) Reduce these values to volts/centimeter (10^{-8} volt = 1 abvolt).
4. Using Stokes' law, compute the radius of a water droplet that falls in air at the rate of 0.3 cm/sec. The density of air may be neglected in comparison with that of the droplet. (The viscosity of air is 1.8×10^{-4} poises, and a poise is 1 dyne sec/cm².)
5. In a certain determination of the electronic charge by the oil-drop method the distance between the horizontal plates was 1.40 cm and the potential difference between them was 1500 volts. (a) Find the electric field in dynes/abcoulomb. (b) What is the mass of a water droplet whose weight would be balanced in this field if it carried one excess electron?
6. A potential difference of 10,000 volts was applied between the cathode and the anode or target of a certain X-ray tube. Find (a) the energy, and (b) the speed, of an electron when it struck the anode. (Neglect variation of mass with velocity.)
7. A certain trolley wire has a cross-sectional area of 1 cm², and the number of free electrons per cubic centimeter in the metal is assumed to be 10^{23} . If the current in the wire is 100 amp, (a) how many electrons pass any point in the wire per second, and (b) what is their average forward velocity?
8. An electron moving at right angles to a magnetic field of intensity 20 oersteds (dynes per unit pole) travels along a circle of radius 4 cm. Find the speed of the electron.
9. A singly ionized atom moves with a speed 9.56×10^7 cm/sec along a circle of radius 10 cm in a uniform magnetic field of intensity 1000 oersteds. Find the mass of the atom, and the ratio of its mass to that of a hydrogen atom.
10. If the mass of an electron at rest is 9.11×10^{-28} gm, find its mass when moving at speeds (a) 1/10, (b) 99/100 that of light.
11. (a) At what speed will the mass of an electron be twice its rest mass? (b) What fraction is this of the speed of light?
12. In Fig. 2-8, the distance between the plates *M* and *N* is 0.20 cm. The magnetic field strength between the plates is 100 oersteds. (a) What electric field in volts/cm is required so that a singly charged hydrogen ion may be undeflected if its speed is 3.0×10^9 cm/sec? (b) What potential difference, in volts, is required?
13. If 4.032 gm of hydrogen were converted into 4.004 gm of helium, find the energy liberated according to equation 10. Also find how many tons of coal must be burned to supply this energy if the heat of combustion is 8000 cal/gm.

14. Using masses from Table 2-1, find the energy, in Mev, liberated by the combination of (a) a proton and a neutron to form a deuterium nucleus; (b) 2 protons and 2 neutrons to form a helium nucleus. (1 atomic mass unit is equivalent to 931 Mev.)

ANSWERS TO PROBLEMS

1. (a) 178×10^{-24} gm; (b) 3.32×10^{-24} gm.
2. 178×10^{-24} gm.
3. (a) 3.21×10^{10} dynes/abcoulomb; (c) 321 volt/cm, etc.
4. 50×10^{-5} cm.
5. (a) 10.7×10^{10} dynes/abcoulomb; (b) 1.74×10^{-12} gm.
6. (a) 1600×10^{-11} erg; (b) 5.9×10^9 cm/sec.
7. (a) 6.25×10^{20} electrons/sec; (b) 0.0063 cm/sec.
8. 1.4×10^9 cm/sec.
9. 1.66×10^{-24} gm.
10. (a) 9.16×10^{-28} gm; (b) 64.6×10^{-28} gm.
11. (a) 2.6×10^{10} cm/sec; (b) 0.87.
12. (a) 3000 volts/cm; (b) 600 volts.
13. 25×10^{18} ergs can be provided by 75 megagrams or metric tons of coal.
14. (a) 2.19 Mev; (b) 28.2 Mev.

The Nature of Radiant Energy

1. Introduction

A partial reconciliation, effected in the period 1920–1930, between the corpuscular and the wave theories of light seems to mark the beginning of the final chapter of one of the longest controversies in the history of physics. The controversy arose among early Grecian philosophers, some of whom believed that light consisted of rapidly moving particles which were emitted in all directions by luminous bodies, while others thought of it as a disturbance in an assumed, intangible medium. However, it was not until the latter years of the seventeenth century that any real scientific progress was made. At that time, in opposition to the wave hypothesis of Hooke and Huygens, Newton enthroned a somewhat more successful corpuscular hypothesis. He believed that, on the basis of the wave theory, light should bend around corners, just as sound does. Grimaldi had perhaps observed the phenomenon of diffraction, but it appears that Newton did not know this. He was therefore faced with an apparent need for a corpuscular theory. He discussed both sides of the question, but those parts of his writings which favored the corpuscular theory impressed other scientists, and for more than a century its correctness was not seriously questioned. Then, as interest centered upon the phenomena of interference, diffraction, and polarization, it was found wanting and was displaced by an improved wave theory in the hands of Young and Fresnel. Foucault verified in 1850 the prediction of the wave theory that the velocity of light in water is less than in air. The corpuscular theories available at that time could not explain this result.

Lastly, Maxwell showed a definite connection between light and electricity and entrenched the wave hypothesis in an electromagnetic theory of radiation which was universally accepted.

Toward the close of the nineteenth century, however, it became apparent that the wave theory in its usual form was unable to explain ade-

quately the distribution of energy among the different wavelengths emitted by hot bodies. Conditions were again favorable for another radical change when Planck in 1900 introduced an important new concept. With its aid, he was able to predict accurately the characteristics of the radiation from "black bodies." His fundamental assumption was that the ultimate sources of radiation were intermittent rather than continuous in their modes of action. This did not deny that radiation, once emitted, was propagated as a wave motion, and in this respect Planck's views were not at variance with Maxwell's.

By the work of Einstein and others, later developments of Planck's theory led to the viewpoint that radiation, after leaving a source, traveled in bundles, called quanta, or, more commonly, photons, each containing a definite amount of energy, each retaining its individuality until it was absorbed by some obstruction in its path. It is scarcely fair, however, to allow these more spectacular modifications to obscure the tremendous importance of Planck's original ideas. Let us state at once that the directional effects which lead to the idea of photons did not receive a satisfactory explanation until the development of wave mechanics. Chapter 6 contains an introduction to the subject.

We shall now consider the wave picture of radiant energy, and shall describe the characteristics of the radiation emitted and absorbed by matter, in terms of that picture. Thereafter we shall discuss the facts which led to the recognition that radiation has both corpuscular and wave-like aspects. Finally, we shall present a composite description which reconciles in considerable degree the two aspects of radiation.

★ **Units of measurement.** In dealing with electromagnetic radiation we shall be concerned with various quantities describing wave motion. The most important for our present purposes are wavelength, usually denoted by λ , and frequency, commonly represented by ν . For some purposes, as we shall see in Chapter 4, the wave number $\bar{\nu}$ is convenient, representing as it does the number of wavelengths in 1 cm. The wave included in the symbol $\bar{\nu}$ distinguishes it from the frequency ν . Since, in free space, electromagnetic waves travel with the velocity of light c , it follows that $c = \nu\lambda$, and $\bar{\nu} = 1/\lambda$.

★ Units generally used in specifying wavelength are the centimeter, the micron, the angstrom unit, and the X-unit. The relationships between these units and the symbols used to denote them are shown below. All quantities in the same horizontal line are equal.

1 micron	1 μ	10^{-6} m	10^{-4} cm	10^4 A	
1 angstrom unit	1 A	10^{-10} m	10^{-8} cm		10^{-4} μ
1 X-unit	1 XU	10^{-13} m	10^{-11} cm	10^{-3} A	10^{-7} μ

In describing the energy coming from unit area of a surface, ergs/cm^2 or joules/cm^2 might be convenient at low and high temperatures, respectively. When the *rate* of radiation from a unit area is discussed, $\text{ergs}/(\text{cm}^2 \text{ sec})$ or watts/cm^2 are suitable combinations of units.

2. The Electromagnetic Conception of Radiation

A new physical interpretation of the vibratory nature of light was introduced in 1865 by Maxwell. Extending the ideas of Faraday, he deduced that electric and magnetic disturbances should propagate themselves through space in the form of a wave motion with a velocity equal to that of light. In 1887 Hertz discovered what we now call radio waves and showed that they obey the same laws of reflection and refraction as light waves. The conclusion was drawn that the differences between these Hertzian radiations and light are due only to their difference in wavelength. It was natural to ask, what medium carries the electric and magnetic waves? For a long time the view prevailed that these waves represent strains in an elastic ether. Finally it was recognized that it is not necessary to mention ether at all in describing the phenomena.

Certain advanced portions of the quantum theory are capable of giving the same results as the classical wave theory of light, but the details are not of a character that can be discussed here profitably. The advantages of a definite mental picture are, however, so great that we shall give further details of the propagation of an electromagnetic wave.

Let us imagine ourselves, therefore, stationed in free space in a stream of radiant energy, such as a parallel plane-polarized light beam. Further, let us assume that we are supplied with convenient devices for measuring magnetic and electric disturbances. We shall then detect the presence of variable magnetic and electric fields. These fields will be found traveling together with the velocity of light and in such a manner that, if we ourselves could move with the stream with the velocity of light, we should notice no changes in the fields whatever. In free space, the magnetic field, it is to be noted, is not associated with any magnet or current, in the ordinary sense, and the electric field has no accompanying charge. To be sure, these fields have their origins in the oscillations of some system of electric charges, but once the radiation has left the source a wavelength or two behind, it is substantially an independent entity and free from the electric charges which produced it.

In the case of plane-polarized light of a single color, a simple magnetic wave and a simple electric wave will be found traveling together in step.

Though the plane of the magnetic disturbance H is at right angles to that of the electric disturbance E (Fig. 3-1), the crests and the troughs of the one coincide with those of the other. Both disturbances possess the same frequency and the same wavelength. Usually, however, radiations from any real source are found to be quite complicated.

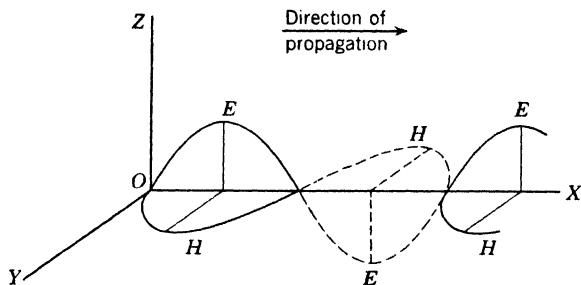


Fig. 3-1. Diagram of a plane-polarized electromagnetic wave. The electric field E and the magnetic field H are at right angles to each other and to the direction of propagation of the wave. The maxima occur simultaneously at the same place.

But even in such a case, the complex whole may be considered as a superposition of many simple waves of the kind described, which differ in wavelength, direction, and frequency.

3. Spectra

It has long been recognized that the ensemble of wavelengths, or *spectrum*, emitted or absorbed by any substance is determined by the atoms or molecules it contains. Naturally, the spectrum is modified by changes in the physical state of the material. It has been apparent, too, that it should be possible to infer from spectra not merely the presence of elements and compounds but something of the inner mechanism of the atoms or molecules by which different spectra are produced. Later chapters explain the methods that have succeeded, mainly since about 1900, in giving information of this "world within the atom." The spectroscope has done more than any other single instrument towards revealing the secrets of atomic structure. The great precision of the more refined spectroscopic methods has permitted advances which would otherwise have been impossible.

The early work of the spectroscopist was confined to the identification of elements in terrestrial and stellar bodies by means of visible and photographic spectra. Later the spectroscope became a source of much

valuable information for the astronomer in his efforts to extend our knowledge of the universe. It has given him a means of observing stars in the various stages of birth, growth, and decay, of determining their states of aggregation, their temperatures, and their relative motions, and in some cases even their diameters. Moreover, the vast laboratory of the stellar universe has supplied us with spectroscopic data which would be difficult or impossible to obtain in any terrestrial laboratory.

4. The Diffraction Grating

A useful and versatile instrument for spreading a beam of radiation into a spectrum is the diffraction grating. We shall discuss it here, omitting serious consideration of other types of spectrometers, partly because of the grating's intrinsic interest, partly because several of the arguments we use will be found helpful at a later time when studying X-rays, wave mechanics, and other topics.

The diffraction grating, invented by Fraunhofer in 1820, consists of a series of narrow identical slits separated by opaque regions, all of the

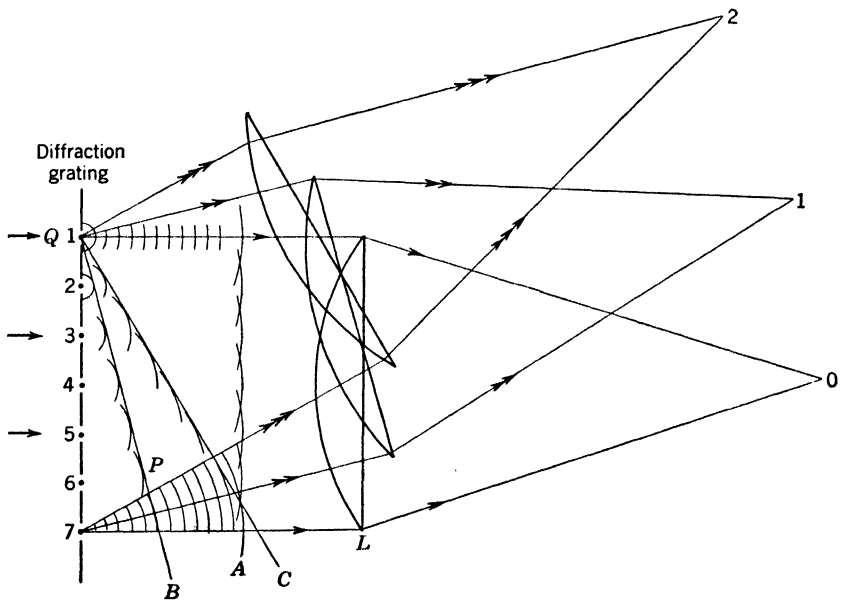


Fig. 3-2. Action of a plane diffraction grating. Radiation of one wavelength is incident normally on the grating. The direct beam is focused at 0. The first and second orders are at 1 and 2, respectively. In practice, one movable lens suffices.

same width. The whole may be mounted in place of a prism on the table of a conventional spectroscope with the slits or "lines" parallel to that of the collimator. Assume that parallel light of a single wavelength is incident normally from the left on the grating in Fig. 3-2. Neglecting the effect of the width of the apertures, each aperture becomes the origin of a train of wavelets in accord with Huygens' principle, all the wavelets being in phase at the apertures since the incoming wave front is plane. Regardless of the wavelength, the envelope of the wavelets marked A is a wave front and will produce the image 0 at the focus of the lens L . Let the small arcs whose envelope is marked B represent secondary wave fronts whose radii differ successively by one wavelength. Then B is a wave front corresponding to the wavelength of the incident beam. Its image 1 will then have the characteristic color corresponding to that wavelength. The wave front C is the envelope of wavelets that differ successively by two wavelengths, and its image 2 has the same color as 1. We have thus a series of images of the monochromatic slit source, the positions of all but the central image 0 depending on the wavelength. If the source contains other wavelengths each produces its individual set of images but there will be one common central image 0. From considerations of symmetry, there will be a similar set of images on the other side of 0. Neglecting the central image, the successive images are called images of the first order, second order, and so on.

If we consider the wave front B , the point P is five wavelengths ahead of the wavelet passing through the aperture Q . We see that

$$\sin \theta_1 = 5\lambda/5d = \lambda/d$$

where θ_1 is the inclination of the wave front B with respect to the grating face, λ is the wavelength, and d is the distance between successive apertures. Hence

$$\lambda = d \sin \theta_1 \quad (1)$$

Similarly, for the wave front C ,

$$2\lambda = d \sin \theta_2$$

and for the n th wave front,

$$n\lambda = d \sin \theta_n \quad (2)$$

Since the wavelength scale is indefinite in extent it is evident that a certain wavelength of one order may coincide with a different wavelength in some other order. To illustrate, a second-order image of wavelength 6×10^{-5} cm would coincide with the third-order image of wavelength

4×10^{-5} cm. Hence, a region of the spectrum in one order may overlap a different region of the spectrum appearing in another order. In general, the intensities of successive orders decrease very rapidly.

Resolving power. One of the most desirable characteristics of any optical instrument, whether it be a diffraction grating or a pair of binoculars, is adequate resolving power. This phrase is used to designate the ability of the instrument to distinguish fine detail, to resolve one image separately from another image close by. In the case of a diffraction grating, if λ is the wavelength of a spectrum line and $\lambda \pm \Delta\lambda$ is the wavelength of the closest line that can be distinguished as distinct from the first, the resolving power is defined as $\lambda/\Delta\lambda$. Theoretically, in the case of the diffraction grating, this resolving power is calculable from the relation

$$\lambda/\Delta\lambda = Nn \quad (3)$$

where N is the total number of apertures and n is the order of the spectrum. By way of illustration, suppose that a grating having 800 lines/cm is 4 cm wide, and that it is to be used to separate two lines whose wavelengths are 5800×10^{-8} and 5801×10^{-8} cm, respectively. From equation 3 it is found that the two can be resolved in the second-order spectrum. When the number of apertures is small the images are broad, and the overlapping of images very nearly identical in wavelength makes distinction difficult. Figure 3-3a is the diffraction pattern produced by a grating of two apertures, and Fig. 3-3c is that produced by a grating of six apertures, the space between adjacent ones being unaltered. In this case the slit width is approximately one-third of the grating space. The bright images are the ones predicted by equation 2. The secondary images between are not provided for in the simple discussion above. The reader may find their explanation in any advanced textbook on optics. We note that the change from two apertures to six narrows the bright images, and increases the number of faint secondary images. As the number of apertures increases, these secondary maxima diminish in intensity and the primary images become narrower and brighter. If we have a very large number of apertures, say 6000 instead of six, the primary images become correspondingly narrower, and the secondary images become so faint as to be practically unobservable. The spectrum lines are, therefore "clean," and conditions are more favorable for separating lines which are very close together. It is for this reason that in detailed work gratings are used with 100,000 apertures or more. It is not the number per centimeter but rather the total number that determines the resolving power, as we see from equation 3.

Modern diffraction gratings are ruled on metal or glass, and accurate ruling engines have been constructed which are capable of ruling as many as 30,000 parallel lines to the inch, though about 15,000 is the customary figure because it leads to practical advantages. Metal gratings produce spectra by reflection, but the principle is essentially the same as for transmission gratings. We may note that a metal grating with 15,000 lines/in. and a 4-in. ruled surface has a resolving power of about 60,000 for the first order of the visible spectrum. Equation 2 shows that if the light is incident normally the complete fourth-order visible spectrum cannot be observed with this particular grating.

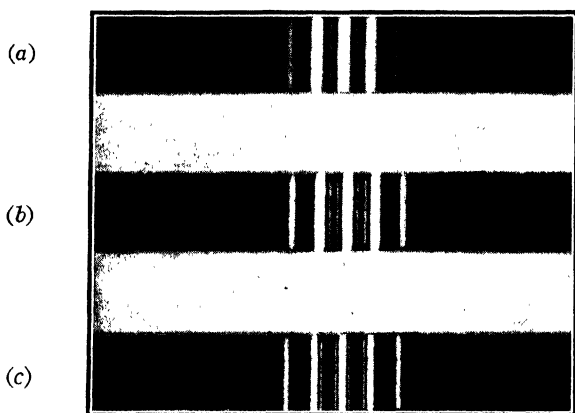


Fig. 3-3. Diffraction patterns of (a) two slits (b) four slits (c) six slits. The slit separation is three times the slit width, and is the same for all. As the number of slits is increased, the principal images grow narrower; subsidiary maxima appear in increasing numbers between the principal images; and these subsidiary maxima grow progressively fainter. (Courtesy of C. D. Hause and A. E. Smith.)

Sometimes the surface of the grating is made concave with parallel rulings; in this case the grating surface acts as its own collimator and collector. No lenses are needed at all; hence the concave grating is particularly useful in analyzing radiations to which ordinary glass is not transparent, such as the ultraviolet shorter than 3000 Å. Concave gratings having a radius of 20 ft or more are in use and may produce multiple-ordered spectra covering a length of about 30 ft. With such devices extremely high resolution is possible, but comparatively long exposures are required to record spectra satisfactorily on a photographic plate. In determining wavelengths in the near infrared, visible, or ultraviolet, the accuracy obtained with a large grating may readily be

of the order of 1 part in 1,000,000. By the use of suitable interference devices, it may be pushed to better than 1 part in 10,000,000, in favorable cases, that is, when the spectral lines are sufficiently narrow. Indeed, the body of accurate wavelength values now available constitutes the largest aggregate of precision data known to science.

5. Types of Spectra

Emission spectra. If the source is a solid, such as the filament of a lamp, a heated rod, or a furnace wall, the spectrum is generally continuous; that is, there is no interruption in the continuum of wavelengths. The same may be said of liquids such as molten metal or glass, though selective radiation from solids and liquids has been observed. Radiations of various wavelengths are emitted with unequal intensities, as can readily be observed in watching the change of color of a wire whose temperature is being slowly increased. In a general way, the distribution of intensities among the different wavelengths is a function of the temperature of the emitter, although each substance may have some selective emissivity.

When the source of radiation is a gas at normal or low pressure, the emission spectrum is usually discontinuous; that is, it consists of bright, isolated lines, or bands composed of lines, on an otherwise dark background. (Gases also emit *continuous* bands, but these are usually of subordinate intensity.) Such spectra may be observed in flames, when metallic salts are introduced; in the spaces between the electrodes of electric arcs; in spark discharges; in discharge tubes; in the chromosphere or outer gaseous envelope of the sun; and in nebulae.

The number of lines or bands emitted depends upon the nature of the source and upon the intensity of excitation. It is possible to excite the emission of a single spectral line in low-voltage discharges, while a slight increase in voltage may result in the sudden appearance of additional lines. The spectrum of a metallic *arc* may also differ in many respects from the high-voltage *spark* discharge between terminals of the same metal. The introduction of a foreign gas in discharge tubes will sometimes bring out lines that otherwise would not be observed.

Absorption spectra. When a substance is placed between the spectroscope and a source that emits a continuous spectrum, the otherwise continuous spectrum is broken up by dark spaces or regions of absorption. They do not necessarily lie in the visible spectrum. For solids and liquids they generally take the form of broad, structureless bands. With gases, they usually consist of dark lines or bands with well-defined structures. A line or band absorption spectrum is formed

when the absorbing substance is of such a temperature that its emissivity in that region is less than that of the continuous source. Should its emissivity be greater, its own emission conceals the effects of absorption. Occasionally an intense gas source may show emission lines with dark streaks at their centers. In such cases, radiation emitted by the central (and hottest) portion of the glowing gas is partly absorbed by the cooler

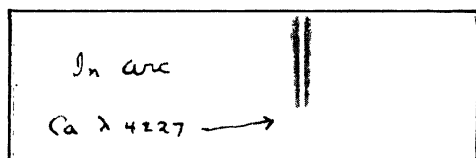


Fig. 3-4. A "reversed" line of the calcium spectrum (after F. A. Saunders). The (black) emission line is wide and fuzzy, the absorption line at its center narrower and sharper.

layers outside. Figure 3-4 shows such a "reversed" line. The photograph is reproduced from a negative, so that blackening corresponds to emission. It may be noted that the black emission line is much wider than the white absorption line which lies at its center. This is a normal expectation since the gas molecules in the cooler absorbing layers are in less violent motion than those in the hot interior region of the source. In general, the cooler the gas, the more strictly monochromatic is the line it emits. No actual spectrum line, however, is so narrow as to be truly of one frequency.

Experience has shown that line spectra are produced by atoms and band spectra by molecules. Under high dispersion the band spectra of gases have been shown to have a line structure. The bands occur in definite groups, and their arrangement always enables us to distinguish them from the spectra of atoms. The analysis of band systems (Chapter 9) has taught us much concerning the rotational, vibrational, and electronic motions within the molecule.

6. The Complete Electromagnetic Spectrum

Perhaps no single experimenter did more to advance the subject of spectroscopy in its early days than Fraunhofer, the inventor of the collimator and the diffraction grating. He observed and mapped the absorption spectrum of the sun, labeling the most prominent lines. These are still called the Fraunhofer lines. Kirchhoff (1859) explained

these as being caused by absorption in the sun's chromosphere. His conclusions were later verified by data obtained at times of total eclipse when the continuous emission of the sun was obscured and the relatively faint emission spectrum of the extreme edge or chromosphere could be observed.

As early as 1800, Herschel demonstrated that the spectrum of the sun extended to longer wavelengths than those of the visible red, but exploration was retarded by the lack of suitable recording instruments and by the high absorptivity of most optical materials in that region of the spectrum. The extension of the spectrum beyond the violet was demonstrated by Ritter (1801) and explored by Stokes (1852), who used quartz lenses and prisms and identified lines by means of fluorescent screens. Twenty years later, Liveing and Dewar introduced photography of the ultraviolet, as this region was called. These discoveries were followed by those of X-rays, and of gamma rays accompanying radioactive disintegrations, both lying in the domain of wavelengths shorter than the ultraviolet. At the other end of the scale occur the extremely long radiations used in radio communication. Since about 1930, six octaves of these, called the microwave region, comprising wavelengths approximately from 2 mm to 16 cm, have been well exploited scientifically.

The complete electromagnetic spectrum is thus arbitrarily separated into regions bearing definite names, because of the type of service they render or because of the specialized

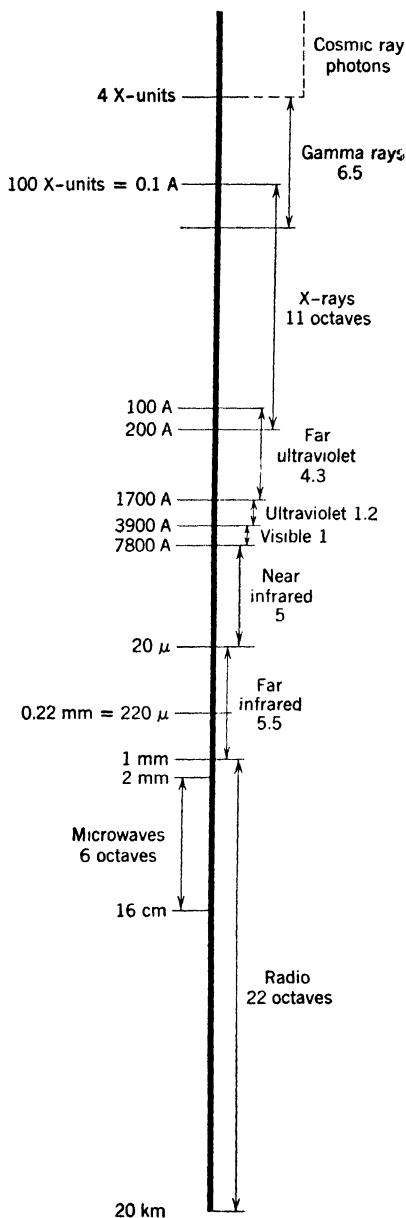


Fig. 3-5. The complete electromagnetic spectrum on a scale of octaves. Boundaries of the various regions are only approximate. Wavelengths corresponding to these boundaries are given.

methods used in their detection. Each region can make an important contribution to spectroscopy only as fast as suitable sources of radiation and appropriate instruments for analyzing the radiation are developed. The relative positions of various regions of the electromagnetic spectrum are shown in Fig. 3-5. Their extent is expressed in octaves of frequency since it is thus possible to represent the entire spectrum clearly in a limited space.

The radio and far infrared regions. The useful range of radio waves extends from about 20,000 m to 1 or 2 mm. These waves, and also the radiations of the far infrared are detectable by thermal devices. Nichols and Tear (1923) succeeded in measuring short radio waves both by radio and by optical methods, thereby furnishing a definite link between the two regions.

★ The far infrared may be considered as extending from the radio region to perhaps $50\ \mu$ (50×10^{-3} mm). For isolating and measuring monochromatic radiations in this region of the spectrum, Rubens and Nichols devised two methods. In the first method the change of focal length of a quartz lens with wavelength was utilized to block out all

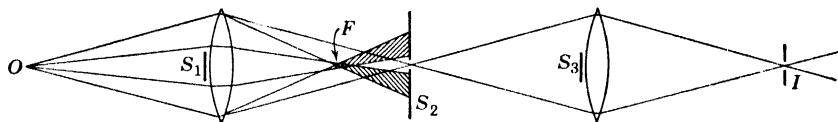


Fig. 3-6. Focal isolation method for the extreme infrared. *O* is the source; *S*₁, *S*₃ are screens to intercept the direct rays; *S*₂ is a slit admitting residual rays; *F* is the focus for sharply refracted rays; *I* is the image of *O* formed by the selected residual rays.

but the desired radiation. Figure 3-6 shows how this was accomplished. The shorter wavelengths focused and diverged before reaching the screen *S*₂, which was placed so as to transmit the desired wavelengths that focused at the screen. In the second method, Fig. 3-7, the radiation was reflected successively from a series of polished surfaces, for it had been found that crystals such as calcite and rock salt exhibit selective reflection especially in the far infrared. Other wavelengths are absorbed, so that after several reflections a beam comprising a few practically monochromatic components remains. These narrow selected bands of radiation are called residual rays, and their wavelengths are measured by means of reflection gratings, without the inconveniences due to the overlapping of multiple orders. Their study has yielded valuable information on the structure and dimensions of molecules.

The near infrared region. The near infrared extends from about $20\ \mu$ to the visible spectrum. Since photography in this region is limited to wavelengths less than about $1\ \mu$, it is necessary to depend chiefly upon the heating effects of the radiations for their detection and measurement.

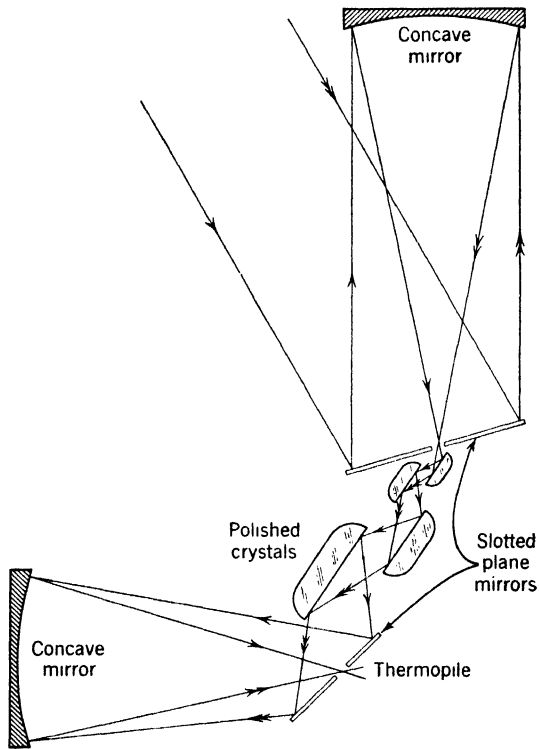


Fig. 3-7. Reflection method of isolating residual rays.

★ Until about 1940, the instruments most frequently employed for measuring the heating effects of radiation were: (a) Thermopiles, which consist of several very small thermocouples connected in series, with their hot junctions directly behind the receiving slit of the spectrometer. (b) Bolometers, which are platinum resistance thermometers of special design mounted in pairs in a Wheatstone's bridge, the radiation falling upon one of them and by the heating effect producing a change in resistance. Temperature changes of $4 \times 10^{-6}^{\circ}\text{C}$ have been measured with bolometers and thermopiles, with suitable galvanometers. (c) Radiometers, which are extremely light vanes mounted symmetrically in pairs

on a light rod supported by quartz fibers in a partially evacuated vessel. Radiation falling only upon one vane causes the system to rotate. Some of the best radiometers have been made from the wings of flies.

★ Two new instruments have contributed significantly to modern studies of the near infrared region. The first of these is a mechanical-optical-electrical device, the Golay cell. One side of a tiny closed gas-filled chamber, or cell, consists of a flexible membrane. Since the gas pressure inside the cell is greater than that outside, the membrane is convex, viewed from the outside. The membrane, acting as a convex mirror, forms part of a delicate optical system. If radiation is absorbed by the gas in the cell, the pressure increases, causing a change in the curvature of the membrane. This change, in turn, causes a change in the position of an image formed by the curved membrane, in conjunction with a converging lens. Finally, the change is recorded with the help of a photocell.

★ The second device, also called a cell, consists of a film (10^{-3} mm thick, or less) of lead sulfide, lead selenide, or lead telluride, deposited on an insulator, such as glass, between two electrodes, which may be carbon or metallic strips. These films are photoconductive; that is to say, when infrared radiation falls on the device, the resistance between the electrodes is lowered. The change of emf across the electrodes can be amplified and recorded by conventional electrical means.

Infrared radiation is absorbed by most optical materials; glass of ordinary thickness or a layer of water 0.1 mm thick is opaque beyond $2\ \mu$, and quartz is opaque from $4\ \mu$ to about $35\ \mu$. At longer wavelengths quartz again becomes transparent. Prisms and lenses of rock salt and fluorite are used between $11\ \mu$ and $20\ \mu$. Specially constructed diffraction gratings which concentrate a considerable portion of the reflected radiation in a definite direction have aided materially in the study of the infrared.

The visible and ultraviolet regions. The visible spectrum is the smallest in extent of all the designated regions, but owing to special sensory organs developed for its reception it plays a vital part in the economy of higher animals. The near ultraviolet apparently also plays an important role, and its effect on our lives continues to be given a very thorough survey. Its extent is from the visible violet to about 1700 Å, where it is almost entirely absorbed by 1 mm of air at normal pressure. Atmospheric absorption cuts off the sun's spectrum at about 2970 Å. Ordinary glass 2 mm thick absorbs all radiation whose wavelength is shorter than about 3100 Å, although some special glasses transmit to the sunlight limit. Quartz remains transparent down to about 1850 Å, and for this reason quartz spectrographs coupled with photographic

plates have been used extensively in the study of the near ultraviolet, although radiation in this region can also be detected by its ability to excite fluorescence and to ionize gases.

★ The region from 1700 Å to approximately 100 Å is called the far ultraviolet. The difficulties of exploring this region were partially overcome by Schumann (1893), who, using a fluorite prism in a vacuum spectrograph, was able to extend the spectrum to 1250 Å. He used special photographic plates containing very little gelatin. This portion of the ultraviolet is often called the Schumann region. Lyman (1916), using a reflection grating in vacuo, extended the spectrum to about 500 Å, and Millikan and Bowen, using very high vacua and high-tension sparks, were able to penetrate to nearly 100 Å. Techniques have advanced so rapidly that all parts of the spectrum between the visible and X-ray regions are now accessible to observation without great difficulty.

X-rays, gamma rays, and cosmic rays. Overlapping the extreme ultraviolet and extending beyond to 0.1 Å is the X-ray region, a span of about 11 octaves. That the ultraviolet and X-rays are continuous has been demonstrated by the use of X-ray methods to measure wavelengths of the order of 200 Å. All radiations classed as X-rays are usually produced by bombarding a metal target with high-speed electrons, artificially liberated and accelerated. They are capable of exciting fluorescence, of darkening photographic plates, and of ionizing gases. Their ability to penetrate many substances opaque to visible light is well known.

★ All the radiations so far discussed have their origin outside the atomic nucleus. Gamma rays, on the other hand, are connected with radioactive disintegration, and are known to arise within the nucleus (Chapter 10). The longer gamma rays overlap the X-rays. Their spectrum, however, extends at least four octaves on the high-frequency side, and probably further, beyond the radiations ordinarily classed as X-rays. Typically, an appreciable fraction of a gamma-ray beam can penetrate several centimeters of lead. Like ultraviolet and X-rays they can ionize gases, produce fluorescence, and blacken photographic plates. As early as 1900 evidence was found indicating the existence of naturally occurring rays having even greater penetrating power than gamma rays. At first, naturally enough, they were assumed to be similar to gamma rays, then the most penetrating radiation known. Later studies showed that these naturally occurring rays were almost entirely corpuscular in character. They have come to be called cosmic rays (Chapter 14) and have been extensively studied by means of ray tracks, Geiger counters, and electroscopes.

7. Temperature Radiation

A universal characteristic of matter. When radiation is emitted by a body in consequence of its temperature it is appropriately called temperature radiation. All bodies are sources of such radiation. For bodies cooler than 3000°K , more than 88 per cent of the temperature radiation is found in the invisible infrared regions of the spectrum. Consider the case of a body, hot or cold, suspended by a very fine thread or wire in an evacuated chamber with opaque walls maintained at a given constant temperature. Experience indicates that the body will eventually assume the temperature of the enclosing walls. This result is in no way dependent on the slight amount of heat which the thread may conduct from the body to the wall or in the reverse direction. To account for this attainment of thermal equilibrium, we find it necessary to assume that any body is at all times radiating energy to its surroundings; if initially cooler than its surroundings it heats up because its rate of radiating energy is then less than its rate of absorption. When equilibrium is reached, the rates of emission and absorption are equal.

Kirchhoff's law. A fundamental law of radiation may be inferred from an experiment with a piece of decorated crockery which has been heated to incandescence in a blast flame. If the room is sufficiently well lighted, that part of the decoration which appears darker when the crockery is at room temperature will also appear darker when it is hot.

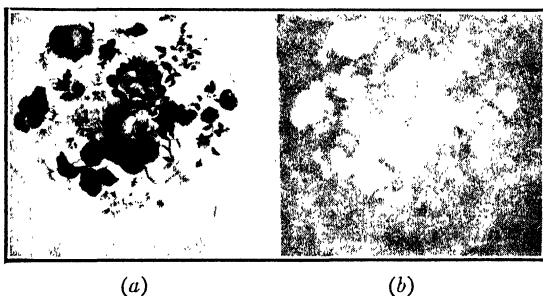


Fig. 3-8. Photographs showing how a piece of incandescent decorated crockery appears (a) by reflected light and (b) by its own emitted light.

However, when the incandescent material is viewed in a darkened room by its own light, the reverse is true. The parts normally darker now appear brighter (Fig. 3-8). Since the darker portions of a pattern or design are dark by reflected light because they absorb light incident on them, it follows from our simple experiment that bodies which are good absorbers of radiant energy are also good emitters of radiant energy.

If we test the radiating and absorbing properties of the hot piece of crockery with the aid of a radiometer or thermocouple, both of which are sensitive to the heating effects of the visible as well as the invisible radiations, we shall observe the same effect. The parts of the crockery that appear darkest, as it were, to the radiometer by reflected radiation will show the greatest heating effects when the instrument receives only the emitted radiations.

The fact that good absorbers are good radiators is implied by an important general relation known as Kirchhoff's law. It applies not only to the radiation as a whole but also to the radiation of any particular wavelength.

The exact statement of Kirchhoff's law follows from simple considerations. Assume two small opaque bodies supported by fine threads at a considerable distance from each other in a large evacuated enclosure with opaque walls which are kept at a constant temperature. Let one body be of any material, say tungsten, and the other of an assumed material capable of absorbing all radiation incident on it (see next section). In accord with what has been said, the equilibrium state is one of constant temperature throughout the enclosure, including its walls. When that state is attained, the rate of absorption of radiant energy by each body is necessarily equal to its emission rate. Letting A_1 and R_1 represent respectively those rates per unit of surface area for the tungsten, and A_2 and R_2 the corresponding values for the other body, we have

$$R_1 = A_1 \quad \text{and} \quad R_2 = A_2$$

or

$$R_1/A_1 = R_2/A_2 = 1 \tag{4}$$

This equation is known as Kirchhoff's law for total radiation from a body. It indicates, for example, that, at 1000°K , R_2 and A_2 are equal for a completely absorbing body, and that R_1 and A_1 are equal for tungsten at the same temperature. Kirchhoff's law states nothing, however, about the relationship between A_1 and A_2 or R_1 and R_2 .

Careful experimental measurements of the power radiated by different substances give the following typical results at 1000°K : tungsten, 0.65 watt/cm^2 ; Carborundum, 4.87 watt/cm^2 . These quantities correspond to the R 's discussed above. Carborundum being a much better emitter than tungsten, it must be a much better absorber than tungsten by virtue of Kirchhoff's law.

8. Black Bodies

Definition and experimental realization. In physics a black body is defined as a body that absorbs all radiation falling on it. In accord with the above statement regarding Kirchhoff's law, we shall expect that such a body, when heated to incandescence, will be brighter than any non-black body whatever which has been heated to the same temperature. This is so, as may be shown experimentally.

There is, however, no perfectly black substance, though lamp black, platinum black, and bismuth black possess extremely high absorptivities. They absorb about 99 per cent of the light incident on them; consequently they reflect only about 1 per cent of it; yet, so sensitive are our eyes that surfaces coated with these materials appear to be much less black than a small hole in the opaque wall of a large cavity. This might be expected because all radiations incident on the hole will enter and, with the exception of an insignificant amount, be entirely absorbed therein. How this is brought about by successive reflections and

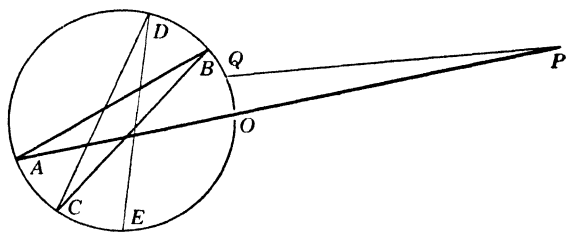


Fig. 3-9. Diagram to show (a) how the radiation entering a cavity through a small hole in its opaque wall is eventually absorbed, and (b) how the radiation coming from a small opening through the opaque walls of a large cavity heated uniformly is built up to give black-body radiation. The inner wall is assumed to be spherical and polished.

absorptions within the cavity is shown in Fig. 3-9. Because of the ease of obtaining practically complete absorption by such a device, small openings in uniformly heated enclosures constitute by far the most common means for realizing black bodies and their radiations.

★ Since any actual black-body cavity must be made from material whose brightness for any given temperature is less than that of the black body, a building up of brightness within the enclosure must take place. Just how this is accomplished may also be seen with the aid of Fig. 3-9. An eye which looks at the opening O along the line PO , if the walls of the cavity are incandescent, sees not only a portion at A with the normal brightness of the non-black material of which it is composed, but also

a portion at B once reflected, a portion at C twice reflected, etc. Let b_n be the brightness of the non-black wall material, as seen in free space, that is, as seen by the eye when directed towards Q . Let r be its reflectivity (the ratio of the intensity of a reflected beam of radiation to that of the incident beam) and b_0 the apparent brightness of the hole. Then, the building up of the brightness of the hole can be represented by the geometrical progression

$$b_0 = b_n + rb_n + r^2b_n + r^3b_n + \dots$$

whose sum can be shown by a simple method to be $b_n/(1 - r)$.

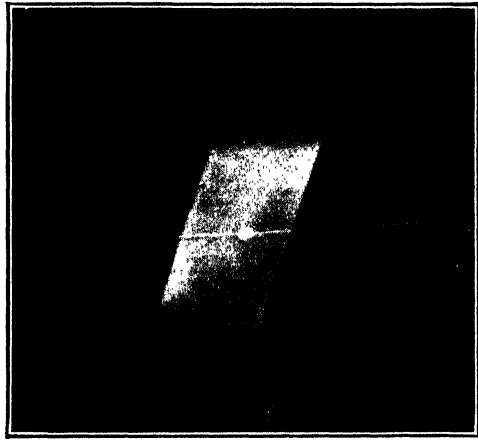


Fig. 3-10. Photograph of an incandescent tubular filament of tungsten with a small hole through its side wall. The brightness of the black-body cavity is seen to be greatly in excess of the normal brightness of the filament material. The bright cross line is an image of an additional filament used for making brightness comparisons.

For incandescent tungsten (Fig. 3-10) the r for red light is roughly 0.60. We see, therefore, that, while for a tungsten cavity the term b_n is only $(1 - 0.60)b_0$, the terms rb_n and r^2b_n are, respectively, $0.24b_0$ and $0.144b_0$, and that these are considerable contributions toward the brightness b_0 . For incandescent carbon, however, r is roughly 0.20. In this case the term b_n is $0.80b_0$, a quantity twice as large as that occurring for tungsten, but rb_n and terms involving higher powers of r are much smaller, in such measure, in fact, that the b_0 is the same for the two substances if the temperature is the same. If we should compare two such cavities, with walls of tungsten and of carbon, respectively, both heated to the same incandescent temperature, we should find that

the outer surface of the carbon enclosure is twice as bright as that of the tungsten enclosure and that the holes through the walls are of exactly the same brightness.

The black body is universally chosen as the standard radiator. Of the reasons therefor, we enumerate three:

1. At each wavelength, the intensity of its temperature radiation is greater than that from any other body at the same temperature.
2. Its radiations are independent of the material of which it is made.
3. The variations in its radiations with temperature and wavelength follow a known law, bearing the name of Planck. After some preliminaries, this is discussed in Section 9.

The fourth-power law. One of the firmly established laws of black-body radiation is the fourth-power law, often called the Stefan-Boltzmann law. It states that the radiancy R of a black body (i.e., the rate of emission of energy per unit area) varies as the fourth power of the absolute temperature T . Thus,

$$R = \sigma T^4 \quad (5)$$

where σ is a constant. When R is measured in watts per square centimeter and T in degrees Kelvin,

$$\sigma = 5.67 \times 10^{-12} \text{ watt}/(\text{cm}^2\text{K}^4)$$

Simple substitution shows that a black body with 1 cm^2 of surface at 1000°K radiates energy at a rate of 5.67 watts, and that at 2000°K the rate is 16 times as great, or 90.7 watts.

Any theory of black-body radiation, to be acceptable, must yield results in agreement with this law, because it can be derived from mechanics and thermodynamics alone (Appendix 9, ref. 82, p. 149).

Spectral energy curves. If the eyepiece of a spectrometer is replaced by a slit lying in the focal plane of the observing telescope, and a heat-sensitive device such as a radiometer is placed just behind it, the arrangement may be used to study the spectrum of a source from the standpoint of the heating effects of its radiation. It is to be noted that the spectrometers commonly used for this kind of work (Fig. 3-11) differ considerably from those used where the eye or the photographic plate is the sensitive instrument. Figure 3-12 shows how the spectral heating effects or relative amounts of power emitted at different wavelengths from a black body at certain high temperatures are distributed with respect to wavelength. The ordinates are proportional to the power emitted in a unit interval of wavelength. The curves show that:

1. For each temperature the heating effect of the radiation has just one maximum.

2. The wavelength at which this maximum occurs shifts toward the shorter wavelengths with increase in temperature, just as incandescent bodies on being heated to high temperatures change in color from red through orange to a yellowish white.

3. The total heating effect or total radiancy varies with temperature according to the fourth-power law, as may be verified by comparing areas under the curves.

It was in a theoretical attempt to explain the exact shapes of these spectral energy curves that the quantum theory had its origin.

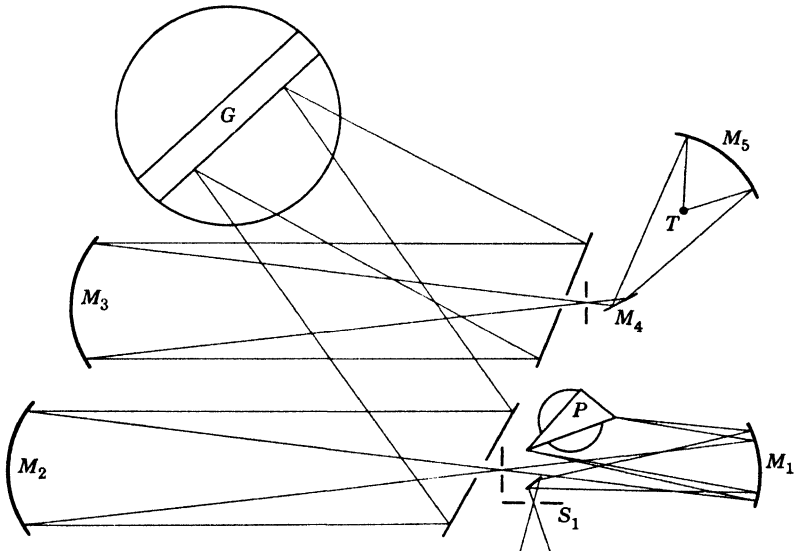


Fig. 3-11. Diagram of the optical system of an infrared spectrometer such as could be used in determining the distribution of energy in the spectrum of a black body. The incident radiation enters at slit S_1 ; after reflection at the curved mirror M_1 it is dispersed by passing twice through a rock salt prism P . This double passage is accomplished by having the back of the prism silvered. The radiation at different wavelengths, corresponding to various settings of the prism, is carried by a train of mirrors to a thermopile or other suitable detector at T . In the course of its travels, the radiation may be further dispersed by a grating G . For studying black-body radiation such additional dispersion might not be needed, in which case G would be replaced by a mirror. (Courtesy of Ohio State University and R. H. Noble.)

9. Origin of the Quantum Theory

The Wien and the Rayleigh-Jeans radiation formulas. The application of the laws of thermodynamics to radiation was first successfully carried out by Wien in 1896. He sought a relation to show how

the heating effect of black-body radiation varies with the wavelength, that is, an equation that would represent mathematically such curves as are shown in Fig. 3-12. He obtained one which gave accurately the changes occurring in the spectral energy curves of black bodies with change in temperature. As an illustration, he was able to predict the curve for 4000°K if given the curve for 3000°K. If, for instance, we

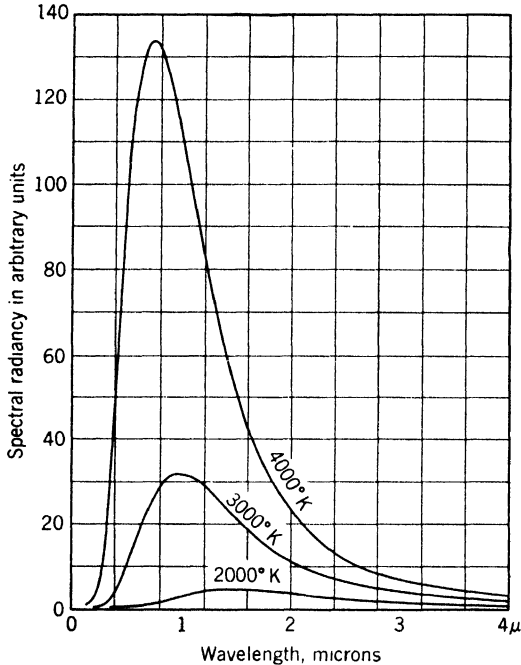


Fig. 3-12. Spectral energy curves for black-body radiation at temperatures 2000°K, 3000°K, and 4000°K.

contract the 3000°K curve of Fig. 3-12 laterally, in the ratio 3000/4000, and at the same time expand it vertically in the ratio $(4000/3000)^5$, we obtain the 4000°K curve. This procedure, illustrating what is known as Wien's displacement law, is in accord with the fourth-power law for the total radiation. This is easily seen, for the ratio of the area beneath the new 4000°K curve, by virtue of its manner of derivation from the 3000°K curve, is greater than that under the 3000°K curve by the product $\frac{3}{4} \times (\frac{4}{3})^5$, or $(\frac{4000}{3000})^4$. In the form of an equation, Wien's law is given by

$$R_\lambda = T^5 f(\lambda T) \quad (6)$$

where R_λ , the ordinate in Fig. 3-12, is termed the spectral radiance at

a specified wavelength. The equation states that, under circumstances so chosen that the product λT is constant, the spectral heating effects are proportional to T^5 , as just illustrated.

Another well-known application of Wien's displacement law concerns the wavelengths at which the maxima occur in curves like those in Fig. 3-12. If λ_m is the wavelength at the maximum of one of the curves, and T the temperature to which the curve corresponds, then the product $\lambda_m T$ is a constant with the value $0.290 \text{ cm}^\circ\text{K}$.

The displacement law, as derived by Wien, is undoubtedly exact and represents, with regard to spectral energy distributions, the limit of information attainable from thermodynamic considerations alone. It fails, however, to predict the actual shape of a spectral energy curve for any given temperature. In attempting to obtain a relation that would not fail, Wien made what seemed at the time to be a reasonable assumption. It was that a certain similarity existed between a perfect gas and black-body radiation, in particular that Maxwell's distribution law for molecular velocities for the gas also gave the distribution of radiant energy with respect to frequency for the radiation. The equation he obtained for R_λ , the rate of emission of energy per unit area per unit wavelength interval at wavelength λ , is

$$R_\lambda = c_1 \lambda^{-5} \frac{1}{e^{c_2/\lambda T}} \quad (7)$$

Here e is 2.718, the base of natural logarithms; c_1 and c_2 are constants whose cgs values are given in Appendix 2. This equation is in agreement with the fourth-power law. As may be seen from Fig. 3-13, Wien's law represents the experimental facts very well at wavelengths shorter than 3μ , and moderately well from 3 to 6μ . However, the law departs from the observed curve by about 25 per cent at 6μ , and the discrepancy is progressively greater at longer wavelengths, beyond the limits of Fig. 3-13.

Shortly afterward, in 1900, Lord Rayleigh perceived certain theoretical inconsistencies resulting from the use of Maxwell's distribution law. He was led to assume the applicability of a relation which had been found very important in the study of gases, namely, that of the equipartition of energy among the different degrees of freedom. A violin string capable of many modes of vibration furnishes a convenient illustration. At one time it may yield not only its fundamental but also its harmonics. The frequencies emitted correspond to vibrations of the string as a whole as well as in two segments, in three segments, etc. We may think of these modes of vibration as degrees of freedom, and say a single degree is associated with the fundamental frequency, and one

with each harmonic frequency. Were equipartition of energy associated with such a vibrating violin string, we should find that the energies associated with the fundamental, and with every other mode of vibration, would be equal to each other. Of course, such equipartition does not occur in a violin string which is bowed in the usual way. However, Rayleigh made such an assumption regarding the radiant energy

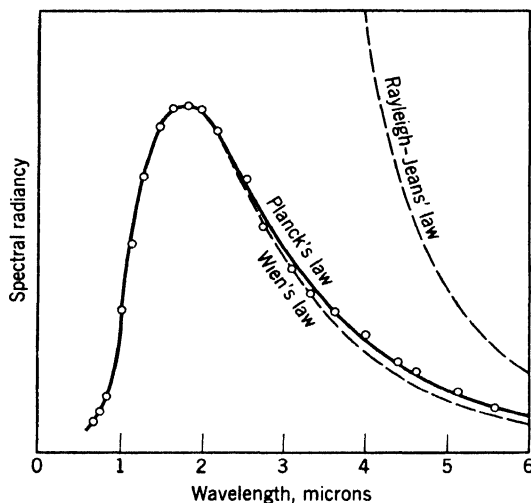


Fig. 3-13. A spectral energy curve for black-body radiation as determined by Coblentz, together with the curves giving distributions expected on the bases separately of Wien's, Rayleigh-Jeans', and Planck's equations. Open circles are experimental points.

that exists in a black-body enclosure, and Jeans contributed to the mathematical development of Rayleigh's idea. The equation that resulted is

$$R_{\lambda} = c_3 \lambda^{-5} (\lambda T), \quad (8)$$

where c_3 is a constant. This equation is in agreement with Wien's displacement law but *not* the fourth-power law. It fails badly in the region $0-6\mu$, but represents the facts accurately in the extreme region of the infrared, far beyond the range of Fig. 3-13. Thus, where Wien's law fails, the Rayleigh-Jeans law is valid, and vice versa.

Planck's radiation formula. The situation in 1900, as it appeared to Planck, showed two apparently well-founded relations for the spectral energy distribution of black-body radiation: Wien's and Rayleigh's. Both were founded in part on principles of classical mechanics. Both in part were in agreement, both in part inconsistent, with experiment,

the one agreeing where the other failed. Classical physics seemed powerless to proceed further.

In attempting to comprehend the cause for failure, Planck noticed that an equation which he had obtained during an attempted verification of equations 7 and 8 predicted values in agreement with Wien's equation where it was successful, and in agreement with Rayleigh's equation where it was successful. Looking for a moment at equation 7 and the corresponding curve, we notice that, to achieve good agreement with experiment at large values of λ , Wien's curve would have to be pushed up a little. A simple way to achieve this is to make the denominator smaller by subtracting a suitable constant. Indeed, if the denominator of equation 7 is changed to $(e^{c_2/\lambda T} - 1)$, the corrected equation will approximate equation 8 very closely for large values of λT . To see this, we write the series expansion

$$e^{c_2/\lambda T} - 1 = \left(1 + \frac{c_2}{\lambda T} + \frac{1}{2} \left(\frac{c_2}{\lambda T}\right)^2 + \cdots\right) - 1$$

When λT is sufficiently large, we need only the term $c_2/\lambda T$.

The new equation proposed by Planck is

$$R_\lambda = c_1 \lambda^{-5} \frac{1}{e^{c_2/\lambda T} - 1} \quad (9)$$

This equation checks with both the Stefan-Boltzmann fourth-power law and with Wien's displacement law. How well Planck's equation agrees with experiment may be seen from Fig. 3-13.

Having found an appropriate algebraic relation for R_λ as a function of λ , Planck tried to find the reason why equation 9 fitted the experiments, and to discover what changes in fundamental assumptions concerning radiation would be needed to derive it. The outcome was the quantum idea.

According to the physical theory current in Planck's time, the processes of emission and of absorption of radiant energy by their ultimate sources (the atoms or molecules composing the radiating body) were conceived as taking place in a gradual and random manner. The variation with time of the energy possessed by an atomic source in the midst of a large number of similar sources was believed to be continuous and smooth. In a body in thermal equilibrium with its surroundings, the energy of a single "ultimate source" was presumed to rise and fall gradually over a narrow range, the average value remaining always the same if the average is taken over a sufficiently long time.

Abandoning traditional ideas, Planck made the bold assumption that an ultimate source does not emit radiant energy in a continuous manner, but instead intermittently, and, what is more important, in packets—

quanta or photons—of very definite energy content. A photon was assumed to have, after emission, a definite wave structure with a frequency ν , and an energy content ϵ given by

$$\epsilon = h\nu = hc/\lambda \quad (10)$$

where h is called Planck's constant. It is in fact a universal constant comparable in importance with the constant of gravitation and the velocity of light in free space. Only in this way was Planck able to justify equation 9. From this point of view the variation with time of the energy content of an idealized elementary atomic source in thermal equilibrium with its surroundings would rise and fall, not smoothly, but in sudden little steps.

★ The constants c_1 and c_2 of equation 9 are not wholly independent. Instead they have a definite connection, through the velocity of light c and the Boltzmann gas constant k , with each other and with other fields of physics. Making appropriate substitutions without explaining them here, we may rewrite equation 9 in several ways. One of these is

$$R_\lambda = \frac{2\pi hc^2}{\lambda^5} \frac{1}{e^{hc/\lambda kT} - 1} \quad (11)$$

where the only new constant is h , the same h that occurs in equation 10.

★ Proof of equation 11 from theoretical principles lies outside the scope of this book, but we emphasize that this relation is a cornerstone of modern physics. The phenomenon of black-body radiation appears obscure and unimportant at first sight. However, proper understanding of this case of emission carries us to the very roots of physics, because electromagnetic radiation is the common carrier that transmits energy between electrons and nuclei. It is not the only carrier of importance. On the cosmologic scale, we have to deal with gravitational forces, and inside the nucleus there are forces that are not electromagnetic. Nevertheless, the science of atomic and molecular physics is mainly built on the study of interaction between charged particles.

Determination of Planck's constant h . A value for h may be computed by combining the experimental value of 1.439 cm K° for c_2 of equation 9 with the experimental values for k and c given in Appendix 2. The exponent of e in equation 9 is now to be identified with that in equation 11. When this is done, and appropriate numerical values are substituted, we find

$$\begin{aligned} h &= \frac{c_2 k}{c} = \frac{1.439 \text{ cm K}^\circ \times 1.380 \times 10^{-16} \text{ erg/K}^\circ}{2.998 \times 10^{10} \text{ cm/sec}} \\ &= 6.624 \times 10^{-27} \text{ erg sec} \end{aligned} \quad (12)$$

This is not, however, the method used for determining h when the greatest precision is desired.

Having determined the magnitude of h , we shall next find it of interest to determine for a particular case the magnitude of the quanta of energy (photons), as well as the rate of their emission. Consider a surface so faintly illuminated by a sodium flame that it is just visible against a completely black background. If the surface is sufficiently extended in the field of view, a radiancy from it of about 6.6×10^{-6} erg/(cm² sec) suffices. The energy ϵ contained in a photon of sodium light is given, to three significant figures, by

$$\begin{aligned}\epsilon = h\nu &= h \frac{c}{\lambda} = 6.62 \times 10^{-27} \text{ erg sec} \times \frac{3.00 \times 10^{10} \text{ cm/sec}}{0.589 \times 10^{-4} \text{ cm}} \\ &= 3.35 \times 10^{-12} \text{ erg}\end{aligned}$$

The approximate number of quanta, per unit area and time, for just perceptible vision, is accordingly,

$$R = \frac{6.6 \times 10^{-6} \text{ erg/(cm}^2 \text{ sec)}}{3.35 \times 10^{-12} \text{ erg/quantum}} \simeq 2.0 \times 10^6 \text{ quanta/(cm}^2 \text{ sec)}$$

For a different wavelength, of course, the energy per photon is different, being inversely proportional to the wavelength. It is quite apparent that the amount of energy carried by each quantum from ordinary light sources is extremely small and that the number of them radiated from any visible source is very large.

Another independent determination of Planck's constant is presented in the remainder of this chapter, together with some considerations regarding the changed point of view which has resulted from Planck's work on the spectra of black bodies. Before proceeding, however, we may well emphasize three things:

1. In his theory, Planck was primarily concerned with the emission process.
2. Although he was led to postulate corpuscular emission of radiant energy, the idea of propagation in corpuscular form did not seem required.
3. This idea of corpuscular propagation took firm hold only with the application of the quantum idea to the subject discussed in the following pages, namely, the photoelectric effect.

10. Early Observations on Photoelectricity

The earliest observation on the subject of photoelectricity appears to have been made by Hertz in 1887. He found that, under otherwise

identical conditions, an electric spark would jump a greater distance from one clean charged electrode to another when ultraviolet light was falling on the electrodes than when it was not. As a result of some simple experiments, he even suspected that the discharge was initiated by some process taking place at the negative electrode only. This view was soon substantiated by the work of other investigators. Another aspect was brought forward by Hallwachs (1888), who found that an insulated, uncharged zinc plate, exposed to ultraviolet light from a carbon arc, acquired a positive charge, as shown by a gold-leaf electroscope. He also found that a charge on it, if negative, began to leak away as soon as the light was turned on. If, however, the plate had a strong positive charge, the light from the arc had no effect on it. Hallwachs suggested, as the probable reason for this puzzling behavior, that the incident light caused the emission of negatively electrified particles from the zinc plate, and that they were prevented from escaping and revealing this effect when the plate had a considerable positive charge.

These early experiments were carried out before the isolation of the electron and the identification of its charge as the ultimate natural unit of negative electricity, and before any theory of ionization by collision had been developed to guide investigators in explaining the mechanism of the growth of an electric spark. We know now that the effect is due to the emission of electrons from the surface of the illuminated plate, and that these are the "particles" of which Hallwachs spoke, although he was necessarily unaware of their exact nature.

The term photoelectricity has been coined from two Greek words, *phōs*, light, and *elektron*, amber, the material used in the earliest recorded electrical experiments, as an appropriate term to cover the phenomena described. It is equally appropriate that electrons liberated in photoelectric experiments should be called photoelectrons.

11. Experimental Results

It was natural that the photoelectric effect should have been first investigated with a common metal, zinc, which shows the phenomenon very strongly. Subsequent work showed that all substances, solids, liquids, and gases, eject photoelectrons under the influence of light, provided that the light has a wavelength less than a certain value which depends on the nature of the substance. It is more in accord with modern practice to say that *each substance shows a photoelectric effect if the incident radiation possesses a frequency which exceeds a certain value, called the threshold (i.e., beginning) frequency*. For most substances this

threshold value lies in the ultraviolet region. Notable exceptions are the alkali metals, sodium, potassium, etc., and some of their alloys and compounds, whose threshold frequencies are in the red and in some cases the infrared region of the spectrum.

When X-rays or gamma rays are allowed to fall on any material, photoelectrons of considerable energy are emitted. This is shown beautifully in Fig. 3-14, which is reproduced from a photograph taken by C. T. R. Wilson. A narrow pencil of X-rays traverses and is partially



Fig. 3-14. Wilson cloud-chamber tracks of photoelectrons ejected from gas molecules by X-rays. A narrow beam of X-rays passes through the chamber horizontally. It can be seen that all the long tortuous tracks of the photoelectrons originate within the narrow region traversed by the beam. (*Photograph by C. T. R. Wilson, courtesy of The Royal Society, London.*)

absorbed by the gas in a Wilson cloud chamber. The long crooked tracks are the paths of photoelectrons set free from molecules of the gas. Notice that they all start in a narrow central band extending across the picture. The tiny isolated specks lying in this band are also formed by electrons; they do not, however, represent photoelectrons, but are probably "recoil" electrons set in motion according to the Compton process (p. 143).

Although we have chosen the production of photoelectrons by X-rays to illustrate the phenomenon, much of the fundamental experimental work on the photoelectric effect was performed with visible or ultraviolet light, mainly because the technical difficulties in making the necessary measurements are less than in work with X-rays. Three additional results deserve emphasis:

1. The number of photoelectrons emitted per unit area by a metal plate illuminated by light of a frequency above the threshold is exactly proportional to the illumination. This is a consequence of the conservation of energy.

2. With a constant monochromatic source of light, varying speeds of emission for the photoelectrons are found which range from extremely small values up to a certain maximum.

3. This maximum speed of emission is independent of the illumination but increases as the frequency of the incident light increases.

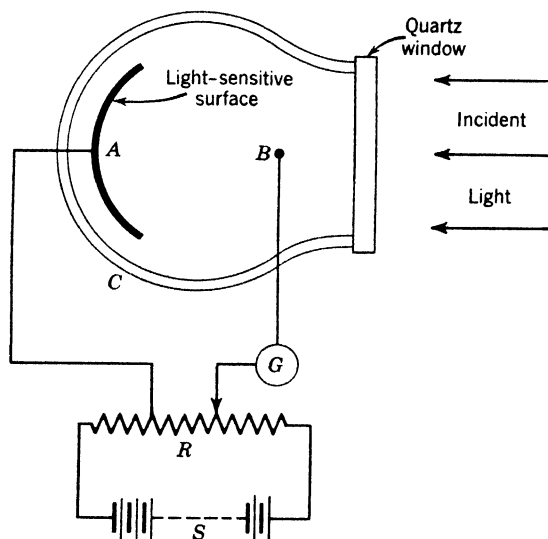


Fig. 3-15. Diagram of phototube and simple electric connections. The glass and quartz envelope is labeled *C*; *A* is the surface receiving the illumination; *B* is a collecting wire, *G* a galvanometer which measures the current. *R* is a potential divider connected to a battery *S*, so that any desired potential difference may be maintained between *A* and *B*.

12. Some Photoelectric Experiments

To illustrate the points mentioned in the preceding section, we shall consider an experiment in detail.

A rigid plate *A* of zinc, let us say, is enclosed in an evacuated glass envelope *C* (Fig. 3-15). Also sealed through the wall is a collecting wire *B*. A quartz window is provided to permit the use of wavelengths shorter than the cut-off point of glass at about 3000 Å. A potential divider comprising a battery *S* and resistance *R* is connected to *A* and

B in such a way that the potential of A with respect to B can be varied continuously from a negative value of several tens of volts to a positive value of a few volts. As soon as light is allowed to shine on A , photoelectrons are liberated from its surface. Helped by the electric field when A is negative, they move across the evacuated space inside the phototube to B , thence via the external circuit back to A . The photoelectric current is measured by a galvanometer G .

We shall be interested in the magnitude of the photoelectric current under a variety of circumstances. The dependence of the photoelectric current on three quantities may now be measured, in three distinct series of measurements. The three quantities to be varied are: (a) the intensity of the incident light; (b) the potential difference between A and B ; (c) the frequency of the incident light.

(a) As the intensity of the incident light is varied, (for example, by altering the distance of a steady source from A), the photoelectric current varies in direct proportion to the intensity of illumination on A .

(b) Turning to the next experiment, suppose the intensity of the incident light remains constant, and that, for the moment, the plate A is negative with respect to the collector B , to the extent of a few tens of volts. Under these conditions we observe a steady current flowing through the galvanometer and phototube. Now let the potential difference between B and A be reduced in convenient steps, making A

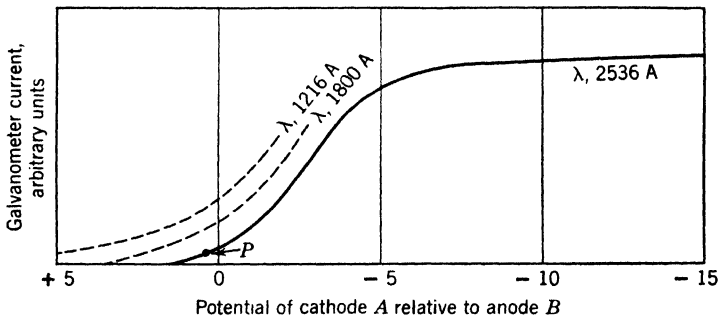


Fig. 3-16. Variation of photoelectric current with potential difference between collector B and illuminated surface A . The full line is approximately correct for zinc illuminated with light of wavelength 2536 Å. The dashed curves, also for zinc, show the results to be expected for higher frequencies, or shorter wavelengths, as labeled.

less and less negative. At first little change in the photoelectric current occurs; later, as the potential difference between A and B falls to 3 or 4 volts, a marked decrease in current is noticed as shown by the full line in Fig. 3-16. When both A and B are at the same potential, a

little current still flows. A small but measurable current continues to flow even when A is slightly positive with respect to B . When A is strongly positive with respect to B , no current flows at all.

In order to understand clearly what is happening, let us consider the point P on the curve, at which the plate A is slightly positive with respect to the collector B . An electron which happens to be at rest near A will, of course, be accelerated toward A and be caught by A . Another electron leaving A with a small amount of energy will proceed part of the way toward B and then return to A . Still another electron leaving A with more energy may proceed as far as B and be caught by B . Thus, the energy of each electron when it leaves the surface of A determines whether or not it will reach B . Some of these possibilities are illustrated in Fig. 3-17.

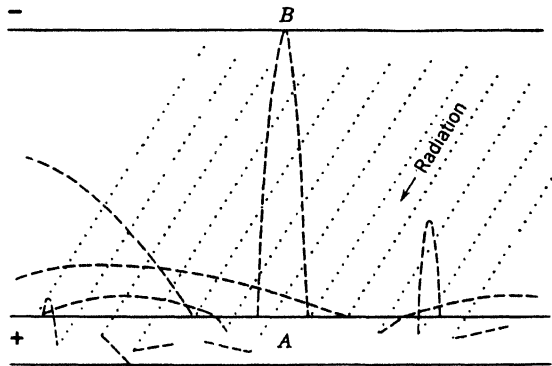


Fig. 3-17. Various imagined paths of photoelectrons liberated from a thin metal slab A subjected to a beam of monochromatic radiation. Between the slab and another plate B , in vacuo, there is applied a potential difference, just equal to the stopping potential corresponding to the material of the slab and the frequency of incoming photons.

A good analogy is offered by the case of a boy trying to throw stones over a high wall, the ground corresponding to A and the top of the wall to B . Before it can surmount the wall, a stone must be thrown with at least a certain definite velocity upward; all stones thrown upward with greater velocities will rise higher than necessary; all stones with smaller initial velocities will return to the ground without attaining the requisite height. In symbols, this means that, any stone having an initial kinetic energy greater than the potential energy that the stone at rest at the top of the wall would have, will pass over, and that all others will fail. Returning to the electrical case, it is clear that electrons, starting from A with sufficient kinetic energy, will be able to reach B despite the

potential difference which creates the opposing electric field. That is, if an electron leaving A has kinetic energy $\frac{1}{2}mv^2 \geq Ve$, it will reach B and contribute to the current through the galvanometer. Here m is the mass of an electron, e its charge, v its velocity, and V the potential difference between A and B . The product Ve represents the potential energy of an electron at the surface of B , just as height \times weight represents the potential energy of a stone at the top of a wall.

If now, starting from the point P (Fig. 3-16), the voltage V is increased, making A more positive with respect to B , the galvanometer will show a diminished current. A critical voltage V_0 can be found that will just prevent all the photoelectrons from reaching B . It is called the stopping potential. Our equation will then read

$$\frac{1}{2}mv_m^2 = V_0e \quad (13)$$

where v_m represents the maximum velocity with which photoelectrons can be ejected from the surface of A , under the given conditions.

(c) We now consider a series of experiments, allowing in each case a beam of light of different frequency to fall on the zinc plate. We determine for each frequency (Fig. 3-16) the minimum potential difference between A and B that will reduce the galvanometer current to zero; that is, we find, for each different frequency of the incident light, the value of V_0 that satisfies equation 13. Graphs representing three such determinations are shown in Fig. 3-16 for wavelengths 2536 Å, 1800 Å, and 1216 Å. These curves are to be taken as illustrative rather than actual. A modified arrangement would be necessary in dealing with wavelengths shorter than about 2000 Å. The results of a large number of such observations on zinc are next plotted to show the relation between the frequencies of the incident beams as abscissas, and the corresponding values of V_0 as ordinates. This graph is shown as a solid line in Fig. 3-18, for zinc. It turns out that all the experimental points lie on a straight line. (Actually, our graph shows the results after they have been corrected for contact difference of potential. The details of this correction are unimportant for the present argument.) This graph is dependent in no detail on the magnitude of the illumination of plate A , no matter how weak this may be. The diagram is interpreted as follows: Let PP' be any ordinate drawn at random. Then if the plate A were illuminated by light of frequency corresponding to the point P' (in the far ultraviolet as selected) the plate would have to be raised to the positive potential represented by PP' (3.60 volts) in order to prevent the loss of any of the photoelectrons. The region covered by the experiments is represented by the solid line. The dotted extension is an extrapolation, a continuation of the experimental line until it

cuts the horizontal axis. (Recent work shows that this would be justifiable only if the temperature of the metal were 0°K . For ordinary temperatures it is only approximately correct to do this.)

The straight line is represented by the equation

$$V_0 = a\nu - b$$

where ν is the frequency of the incident radiation and a and b are constants. For reasons which will be apparent later, this will be written

$$eV_0 = h\nu - W \quad (14)$$

where e is the charge of an electron and h and W are new constants.

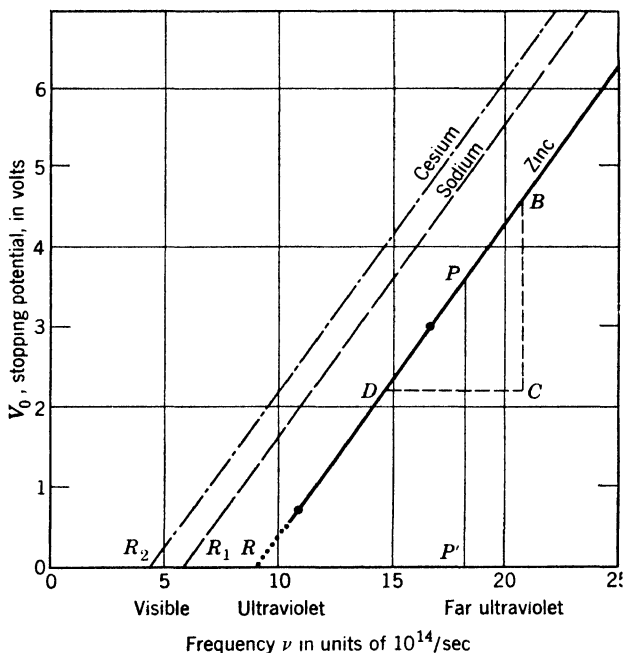


Fig. 3-18. Einstein's photoelectric equation $\frac{1}{2}mv_m^2 = h\nu - W$. The potential difference V_0 necessary to turn back the fastest photoelectrons is plotted as a function of the frequency ν of the incident light. Graphs are shown for zinc, sodium, and cesium. The points R, R_1, R_2 represent the threshold values from which the work functions W may be calculated.

When the plate A is illuminated by light of frequency represented by the point R , at which V_0 is zero, there is no tendency for photoelectrons to escape, since no retarding potential is required to keep them in. Hence,

the frequency corresponding to the point R (about $9 \times 10^{14} \text{ sec}^{-1}$) represents the threshold frequency for the emission of photoelectrons from zinc.

In Fig. 3-18, data for two additional metals, sodium and cesium, have been plotted. The new data fall accurately on two straight lines, one for each metal, which when extrapolated cut the horizontal axis ($V_0 = 0$) at R_1 and R_2 . For each of these metals, and indeed for any other, an equation can be written in the same form as equation 14. As the diagram shows, *the lines are parallel*, so that the ratios of the coefficients of ν and V_0 , in the equations representing the lines, must be the same for all three. Hence, we may write a series of equations for other metals, such as

$$eV_0 = h\nu - W_1$$

$$eV_0 = h\nu - W_2$$

These equations differ only in the term W .

13. Theoretical Developments

We now present the train of ideas that led to an interpretation of equation 14. Even though Planck had smoothed out the difficulties of understanding black-body radiation by assuming that energy was emitted intermittently from its source, yet this radiation, once emitted, was considered to obey all the rules of the classical wave theory, spreading out in spherical waves from its point of origin. By 1903, however, evidence had been gathered to show that theory and experiment were not always consistent. Radiation during its propagation through space or matter was considered everywhere as continuous; yet investigations of the photoelectric effect showed that enough energy could arrive on a minute spot on a metal plate to eject an electron with a high velocity, the magnitude of which depended in no way on the value of the illumination but only on its frequency.

In 1905 Einstein made a fundamental but radical contribution to the subject. He assumed, in extension of Planck's ideas, that radiation, having left its source, would travel through space, not in spreading waves, but in compact bundles. He postulated, in agreement with Planck, that when a source yields radiation of frequency ν , it emits this radiation only in units of magnitude $h\nu$, and also assumed that a similar restriction governed the process of absorption of radiation. Here h was a constant identical with Planck's constant, having the same value for all emitters and absorbers; and ν was a natural frequency of the

emitter or absorber. Since practically all known sources of radiation emit light of many different wavelengths, the implication was that they could emit quanta of various sizes—one size for each monochromatic spectrum line. In the emission (or absorption) of a continuous spectrum, there had to be a continuous range of sizes of quanta. The ejection of a photoelectron from an atom meant, therefore, that this atom had absorbed one of the photons of radiant energy, and hence had enough energy to emit a negative electron with considerable speed.

A monochromatic beam of light was no longer considered as a continuous stream of radiant energy, but as a swarm of discrete photons, following on one another's heels with the speed of light, each photon carrying an amount of energy $h\nu$. In a composite beam the ν 's would have a range of values.

Consider now what happens, according to Einstein's hypothesis, when a stream of these photons impinges on a metal plate. A particular atom near the surface of the metal may be struck by a photon, and absorb its energy $h\nu$. At once the excited atom rids itself of this excess energy by emitting an electron with kinetic energy $\frac{1}{2}mv^2 \leq h\nu$, the exact amount depending on how tightly the electron was bound to the atom. Since the incident light can penetrate the metal for a short distance, the emerging electron may have to make its way through several metallic atoms before reaching the surface of the metal (Fig. 3-17). In doing so it loses a little energy. Before it finally leaves the plate it must still have enough kinetic energy to accomplish the work necessary to free it entirely from the surface; this reduces still more the energy of the escaping electron. For those electrons that are most easily freed from their parent atoms and that have their origin very close to the surface of the plate, the following equation was proposed by Einstein:

$$\frac{1}{2}mv_m^2 = h\nu - W \quad (15)$$

Here W is interpreted as the work necessary to free one of the least firmly bound electrons from its parent atom and from the surface. It is most conveniently regarded as a kind of heat of evaporation of the electron from the metal and is often referred to as the work function for the metal considered. Further, v_m is regarded as a maximum velocity of emission of photoelectrons under the influence of monochromatic light of frequency ν . One would expect that the majority of the photoelectrons, coming from a small depth within the metal, should have energies somewhat less than that given by equation 15, which refers only to the maximum energy of emission.

14. Comparison between Theory and Experiment

The last experiment described in connection with Fig. 3-16, which led to equation 14, is obviously a test of the theoretical equation 15. Remembering equation 13, we may write

$$eV_0 = h\nu - W = \frac{1}{2}mv_m^2 \quad (16)$$

This is interpreted, reading from left to right, as follows: A stopping potential V_0 is necessary to prevent the escape of the fastest photoelectrons, whose kinetic energy on emerging is numerically equal to eV_0 . This energy has been provided by the absorption of a quantum of radiation of energy $h\nu$; but, since a definite amount of work W is required to free the electron from the metal surface, only the balance $h\nu - W$ appears as the kinetic energy $\frac{1}{2}mv_m^2$ of one of those photoelectrons.

★ The prime uses of the graph in Fig. 3-18 are to determine the values (1) of Planck's constant h , (2) of the threshold value of V_0 for any particular metal, and (3) of the work function W . Equation 14 shows that the slope of the line in the figure is $h/e = BC/CD$. This ratio can be computed from the figure, so that, if e is known, then h can be determined. BC represents 2.4 volts, or 2.4×10^8 abvolts; CD represents a frequency of $6 \times 10^{14} \text{ sec}^{-1}$. Using 1.60×10^{-20} abcoulomb for e , we find that

$$h = \frac{2.4 \times 10^8}{6 \times 10^{14}} \times 1.60 \times 10^{-20} \text{ erg sec} = 6.4 \times 10^{-27} \text{ erg sec}$$

One of the best determinations, based on methods much more complex than the above, is

$$h = (6.62363 \pm 0.00016) \times 10^{-27} \text{ erg sec}$$

★ The threshold frequency, represented by the point R , is found to have different values for a given metal, depending on the state of the surface as regards adsorbed gas, crystal structure, etc. For zinc, our graph gives the number $9 \times 10^{14} \text{ sec}^{-1}$, corresponding to a wavelength

$$\frac{3 \times 10^{10} \text{ cm/sec}}{9 \times 10^{14} \text{ /sec}} = 0.33 \times 10^{-4} \text{ cm} = 3300 \text{ \AA}$$

Various investigators have obtained results for zinc ranging from 3400 Å to about 3700 Å. However, the position of R does not affect the slope of the curve, so the experimentally determined values of h are unaffected by variations in the state of the surface.

★ Calling the threshold frequency ν_0 , we have $W = h\nu_0$. For zinc, we have

$$W = 6.4 \times 10^{-27} \text{ erg sec} \times 9 \times 10^{14} / \text{sec} = 5.8 \times 10^{-12} \text{ erg}$$

Expressing this in electron volts, we have

$$W = \frac{5.8 \times 10^{-12} \text{ erg}}{1.6 \times 10^{-12} \text{ erg/ev}} = 3.6 \text{ ev}$$

that is, the work required to remove the electron from the metal is equal to the work done on an electron when it falls through a potential drop of 3.6 volts. Experimental determinations yield values between 3.3 and 3.6 ev, depending on the circumstances.

★ **The thermionic work function.** It is known from the work of O. W. Richardson that the electron current from a unit area of a metal heated to an absolute temperature T , is, to a good approximation,

$$i = 120T^2 e^{-W/kT} \quad (17)$$

where i is in amp/cm², W in ergs, and k is the gas constant per molecule. In a few careful investigations it has been found that the value of W obtained from thermionic emission agrees well with that obtained from photoelectric studies. For example, Dubridge obtained the values 6.27 and 6.30 ev, for outgassed platinum, by the two methods, respectively.

15. The Significance of Einstein's Equation

In its broad outlines, the theory sketched above accounts admirably for the experimental results of photoelectric emission. The finer details of the process leave room for speculation.

Einstein's interpretation of equation 15 appeared to solve some problems, but raised other difficulties. As we have seen, he assumed not only the emission of a quantum of energy by an ultimate source, but in addition the continuation of this quantum intact like a projectile in its passage away from its source, and finally its complete absorption by some one atom or molecule. The experimental facts that seemed to force this point of view were the existence of the threshold frequency and the commencement of the photoeffect long before a single atom could be expected to accumulate the energy $h\nu$ from a spherical electromagnetic wave. The evidence relating to the low-frequency limit for the photoelectric effect indicated that absorption of energy leading to the ejection of an electron could not be gradual but must therefore be

sudden and complete in one act, for prolonged absorption of radiation of still lower frequency is entirely ineffective in releasing photoelectrons. This being granted, the facts relating to photoelectrons ejected from surfaces indicated that the radiant energy absorbed by an individual atom must have come to the atom in concentrated form as a single photon. Evidence from the scattering of X-rays (p. 143) reinforces this view. So convincing have been these considerations that, for a while, physicists seemed inclined to give up altogether the classical viewpoint. On the other hand, for all interference experiments the classical wave theory of light provides a simple interpretation. In Section 16 we present an attempt at reconciliation which gained considerable acceptance for a while but which, in view of more recent work of Dirac and others, probably cannot be accepted in the form given.

16. Partial Reconciliation of the Wave and Corpuscular Aspects of Light

Einstein's "ghost field." As a means of uniting the corpuscular and wave theories of light into one comprehensive scheme, Einstein reinterpreted the electric and magnetic fields accompanying a ray of light. It is well known that, according to the electromagnetic theory, the density of radiant energy at a point in space is proportional to $E^2 + H^2$, where E and H are the electric and magnetic field strengths at the point (Appendix 9, ref. 82, p. 53). Einstein suggested, however, that $E^2 + H^2$ is a measure of the average number of photons per unit volume. Otherwise expressed, we may consider this quantity as a measure of the probability that a photon is at the point in question. This idea that the electromagnetic field has no energy of itself but acts only as a "ghost field" to direct the particles was a little too strange to be enthusiastically accepted when it was first suggested. However, when, in 1926, Max Born showed the fruitfulness of a similar view with regard to matter waves and matter particles (Chapter 6) the idea was widely accepted at once, not only as the connecting link between the wave and corpuscular theories of light but also as that between the explanation of the nature of light and that of the nature of matter.

According to this "probability" theory of light, we must consider that, when a point source emits light, photons are sent out in all directions. Further, instead of saying in the language of spreading spherical waves that the illumination decreases inversely as the square of the distance, we must say that the average number of particles crossing a given area decreases as the distance from the source increases, simply because we have a definite number of photons which are spread over a larger area

the farther out we go. We can never specify just how many photons will strike on a given area in unit time, any more than we can predict exactly how many molecules of oxygen will be found in a particular cubic centimeter of that gas. In other words, although we cannot say that the illumination 2 m from a source will be exactly one-quarter of that at 1 m, we can say that the probability of a given surface area being struck by a photon at a distance of 2 m is just one-quarter of the probability that an equal surface will be struck at a distance of 1 m.

Weak-light experiments. In view of the sparser population of photons at large distances from a source, many investigators have tried experiments with very weak light in the hope that some irregular effects could be obtained. All experiments have shown, however, that any interference effects obtained with very weak light are exactly the same as those obtained with strong light. Other experiments indicate that the behavior of photons is not appreciably influenced by the presence of neighboring photons such as are present in a strong beam of light.

In some respects, Einstein's description of optical phenomena may appear quite artificial. We must remember, however, that the laws of physics are generalizations from experiments. For example, Newton's laws of mechanics were set up as a result of experiments and observations on objects of fairly great mass, and, though we would like to carry these same laws over to photons, we have no experimental justification for such procedure. Instead, we must try to generalize from observations of photons to establish laws for their behavior just as Newton did for objects of large mass. Einstein's probability theory does just this. It implies that one can never state in advance the complete story of what will happen to an individual photon. One can only predict the probability of its striking a given area, and observation tells us that this probability is proportional to $E^2 + H^2$, as calculated on the basis of a wave theory. The reader may be pardoned if he is inclined to recoil from this abandonment of exact law. It happens that we are dealing with an unavoidable lack of "resolving power," inherent in all our observations of physical phenomena.

As was mentioned on p. 89, the "ghost-field" interpretation is not completely satisfactory. Dirac and others in a series of research papers since 1927 have provided, with the aid of an extension of wave mechanics, a more acceptable reconciliation of the wave and corpuscular aspects of light.

REFERENCES

Appendix 9, refs. 18, 44, 51, 53, 55, 57, 82 (p. 53), 87 (p. 83), 106, 107.

PROBLEMS

1. What will be the angular positions of the various orders of a spectrum line at 5893 Å using a diffraction grating having 3000 lines/cm, at normal incidence?
2. A monochromatic source of light is recorded by an ordinary photographic plate after passing through a glass diffraction grating having 8000 lines/cm. The incident light falls normally on the grating. If an image is formed at an angle 33° from the central image, what are its possible wavelengths? How could you prove which of these it is?
3. A plane reflecting optical grating has 6000 lines/cm. Monochromatic light of wavelength 4860 Å falls normally on it. At what angle will the first-order spectrum appear? What is the maximum number of orders that might be observed?
4. Express the following wavelengths in centimeters, using powers of 10: 4 X.U., 20 μ , 75 Å, 7 mm, 3 km.
5. Carborundum, one of the best emitters of radiant energy that may be carried to incandescence in the open, has at 1000°K a radiancy R of about 4.87 watts/cm². Of the radiation from a black body at 1000°K that falls upon a piece of Carborundum, what is the fractional part that is absorbed?
6. How many reflections are required in (a) a tungsten cavity, (b) a carbon cavity, to reduce the intensity of an entering light beam to 5 per cent of its entering value?
7. A piece of incandescent carbon at 2000°K is seen reflected from a polished tungsten surface at 2000°K ; how does the sum of the normal tungsten and the reflected carbon brightness compare with that of a black body at 2000°K ? (Take the reflectivity of tungsten to be 0.6, and consider carbon to radiate 80 per cent of the power of a black body.)
8. Given that the operating temperature of a tungsten filament in a vacuum lamp is 2450°K and that its radiancy for visible light is 30 per cent of that for a black body at the same temperature, find the surface area of a filament of a 25-watt vacuum tungsten lamp.
9. The earth receives energy from the sun, on a surface normal to the incoming rays, at the rate of 1.94 cal/(cm² min). What is the temperature of a black body that radiates energy at this same rate?
10. The total surface of the earth is four times the projected surface which it offers to the sun's radiation. The average rate of incidence of solar radiation per unit of area on the earth is therefore just one-fourth of the maximum rate per unit of area, or 0.485 cal/(cm² min). Assuming that the earth, as a black body, reradiates energy back into space at this same average rate, what is its expected surface temperature?
11. Compute the number of photons of yellow light of wavelength 0.6 μ required to make an erg of energy.
12. Assuming that the average wavelength for the radiation emitted by a 25-watt vacuum tungsten lamp is about 1.2 μ , compute its rate of emission of photons.
13. Given that the rate of emission of energy by certain glowing (not flashing) fireflies is 10 ergs/sec and that most of the energy radiated is located within the visible limits of the spectrum with an average wavelength of about 0.57 μ , compute the rate of emission of photons by such a firefly while glowing.
14. A completely dark-adapted normal eye is just able to perceive against a dark background a point source of light whose radiation consists wholly of that which is most efficient in producing vision, when the rate of incidence of radiation on the retina is about 2×10^{-18} watt. Given that the wavelength of highest efficiency is

0.555 μ , compute the minimum necessary rate of incidence of photons on the retina to produce vision.

15. In a particular case, the fastest photoelectrons coming from an illuminated plate (plate *A*, Fig. 3-15) are just stopped from reaching *B* by a stopping potential of 2 volts. Compute (a) the initial kinetic energy possessed by them; (b) the temperature of a gas whose molecules have the same average translational kinetic energy.

16. For tantalum, the long-wavelength limit at which radiation is just able to produce photoelectrons is 2974 Å. Find the kinetic energy an electron must be given in order that it shall just be able to escape from the metal. Express the result in ergs and in electron volts.

17. What is the stopping potential necessary to prevent the passage of photoelectrons from *A* to *B*, Fig. 3-15, when plate *A* is composed of tantalum (see problem 16) and the light is the strong mercury arc line at 2536 Å?

18. Compute, on the basis of the outspreading wave theory, the length of time necessary for an atom on the surface of a piece of tantalum (see problem 16) to absorb enough energy from the radiation from a 25-watt light source at a distance of 10 m to eject one photoelectron. Assume that the atom absorbs all radiation incident normally on a circular area whose diameter is 3 Å.

19. If the photoelectric threshold for a particular metal is at 3600 Å, what will be the energy of an electron ejected by radiation of wavelength 1200 Å?

ANSWERS TO PROBLEMS

1. First order, $10^\circ 11'$; second, $20^\circ 42'$; third, $32^\circ 2'$; fourth, $45^\circ 0'$; fifth, $62^\circ 8'$.
2. 6808 Å (red); 3404 Å (ultraviolet).
3. $16^\circ 57'$; 3.
4. 4×10^{-11} cm; 2×10^{-3} ; 7.5×10^{-7} ; 7×10^{-1} ; 3×10^6 .
5. 0.85.
6. (a) 6; (b) 2.
7. 88 per cent.
8. 0.403 cm^2 .
9. 392°K .
10. 277°K (4°C).
11. 30×10^{10} photons.
12. 1.51×10^{20} per sec.
13. 2.9×10^{12} photons/sec.
14. About 600 photons/sec.
15. (a) 3.2×10^{-12} erg; (b) $15,500^\circ\text{K}$.
16. 6.7×10^{-12} erg; 4.2 ev.
17. 0.72 volt.
18. 475 sec.
19. 6.88 ev; 1.1×10^{-11} erg.

4

The Bohr Model of the Atom

1. The Hydrogen Spectrum

The Balmer series. From the positions and intensities of the innumerable spectral lines which his instruments record, the physicist endeavors to construct a theory of the mechanism within the atom and the molecule. To be truly acceptable, his theory must be able to survive any experimental test to which it can be legitimately subjected. As his experimental technique grows more searching, he may be forced to modify or even to discard his former hypotheses. As a starting point for theoretical work, it was of prime importance at first to discover empirical regularities in spectra. Toward the end of last century a few such regularities were found, but only one can be considered as the parent of modern theories. It was natural that the first successful attempts toward the solution of the whole problem should have dealt with the simplest of spectra, that of the hydrogen atom. Four of the most prominent lines in its visible spectrum correspond to Fraunhofer lines of the solar spectrum, and these, as a result of their regular spacing, have been designated as $H\alpha$, $H\beta$, $H\gamma$ and $H\delta$, respectively. Early researches in the ultraviolet extended this array to 11 lines, and later it was extended to 35 lines by the study of stellar absorption spectra.

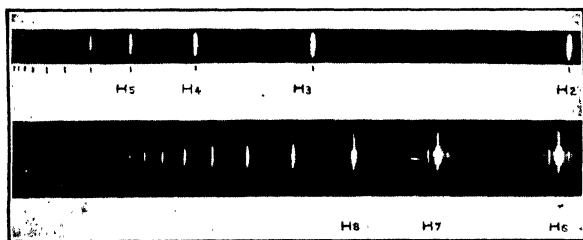


Fig. 4-1. Emission spectra of hydrogen (after Hulburt and Wood). The lower spectrum covers the same region as the left portion of the upper spectrum. In comparison, however, the lower spectrum is enlarged about 5 \times , and was obtained with a much longer exposure.

Figure 4-1 is a photograph of the emission spectrum of hydrogen, and Fig. 4-2 shows its absorption spectrum. Many attempts were made to find harmonic relations among these lines such as we find among musical sounds. The analogy with musical sounds was, unfortunately, in many respects misleading. In 1884, however, Balmer was able to devise an

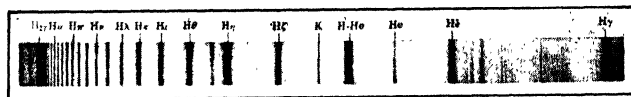


Fig. 4-2. The absorption spectrum of hydrogen (*after Curtiss*).

algebraic expression that represented a notable step forward. He found that the wavelengths of the hydrogen lines beginning with $H\alpha$ could be expressed by the formula

$$\lambda = \frac{3645.6n^2}{n^2 - 4} \quad n = 3, 4, 5, \dots \quad (1)$$

where λ is the wavelength in angstrom units and n takes successive integral values. The agreement between observed wavelengths and those calculated from the above formula is shown in Table 4-1.

TABLE 4-1. Wavelengths of Lines in the Balmer Series of Hydrogen

Line	n	Observed by Balmer (angstroms)	Calculated by Balmer (angstroms)	Observed by W. E. Curtis (1914) (angstroms)
$H\alpha$	3	6562.10	6562.08	6562.79
$H\beta$	4	4860.70	4860.80	4861.33
$H\gamma$	5	4340.10	4340.10	4340.47
$H\delta$	6	4101.30	4101.20	4101.74

We could designate a spectral line by its frequency as well as by its wavelength, but this would give us an enormous number. For theoretical purposes it is convenient to indicate a spectral line by giving its wave number, usually symbolized by the Greek letter $\tilde{\nu}$. We remind the reader that the wave above the symbol distinguishes the wave number $\tilde{\nu}$ from the frequency ν . Rydberg expressed the Balmer formula in terms of wave numbers, reducing it to the form

$$\tilde{\nu} = R_H \left(\frac{1}{2^2} - \frac{1}{n^2} \right) \quad n = 3, 4, 5, \dots \quad (2)$$

where $\tilde{\nu}$ is the wave number and $R_H = 109,678 \text{ cm}^{-1}$, approximately. The wave number increases with n for successive lines and approaches $(R/2^2)$ as a limit. A succession of related lines in a spectrum is called a *series*. In the Rydberg formula the wave numbers of the lines of a series are expressed as the differences between two quantities, or *terms* as they are called, one of which is constant for the series, while the other, involving $1/n^2$, varies from one line to the next.

The Lyman and Paschen series. Other series in addition to that carrying Balmer's name have been discovered in the hydrogen spectrum. Lyman found one in the extreme ultraviolet, which is accurately represented by a formula similar to that of the Balmer series, except for the constant term, namely,

$$\tilde{\nu} = R_H \left(\frac{1}{1^2} - \frac{1}{n^2} \right) \quad n = 2, 3, 4, \dots \quad (3)$$

A similar series discovered by Paschen in the infrared and named for him is represented by

$$\tilde{\nu} = R_H \left(\frac{1}{3^2} - \frac{1}{n^2} \right) \quad n = 4, 5, 6, \dots \quad (4)$$

Two more, named for Brackett and Pfund, respectively, are expressed by similar formulas, with 4^2 and 5^2 , respectively, replacing the number 3^2 . The Lyman, Balmer, and Paschen series are shown in Fig. 4-3.

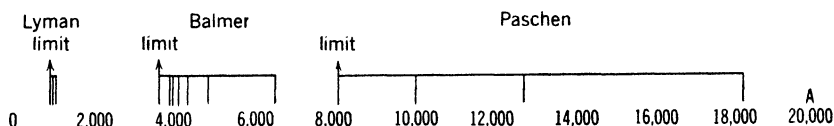


Fig. 4-3. The positions of some of the important lines of the Lyman, Balmer, and Paschen series of hydrogen, on a wavelength scale.

on a wavelength scale. The similarity of these series left little room for doubt that here lay a clue to the nature of the atom.

★ **The Ritz principle.** A general interrelation between the spectral series of a given atom or ion was postulated by Ritz (1908), who stated that lines were to be expected whose wave numbers were the sums or differences of those of any two lines already discovered. To illustrate, the difference between the wave number of the line $H\alpha$, $\tilde{\nu} = R_H[(\frac{1}{2})^2 - (\frac{1}{3})^2]$, and that of the $H\beta$ line, $\tilde{\nu} = R_H[(\frac{1}{2})^2 - (\frac{1}{4})^2]$, is the wave number of the first line of the Paschen series, $\tilde{\nu} = R_H[(\frac{1}{3})^2 - (\frac{1}{4})^2]$. The meaning and the limitations of this rule will become apparent from the discussion on p. 100.

The recognition of series in the hydrogen spectrum led to similar attempts on the spectra of other elements. Rydberg was extremely successful in analyzing the spectra of the alkali elements, for which he developed formulas similar in character to those of the hydrogen series. The development of these empirical formulas makes an interesting story, but in order to bring out the physical basis of these discoveries we proceed at once to Bohr's successful explanation of the spectrum of atomic hydrogen.

2. Bohr's Theory of the Hydrogen Atom

The nuclear atom. The identification of the electron and the proton, as well as experiments on the scattering of alpha particles by atomic nuclei have clearly shown that the most satisfactory mechanical model of the atom, at least from the physicist's standpoint, is that of a positively charged nucleus around which external electrons revolve. An atom, as pictured by Bohr, resembles our planetary system, with the nucleus as the sun and the electrons as the planets. For our present purpose these bodies may be treated as mass particles, since the distances between them are extremely large compared with their diameters. The hydrogen atom was thought of as having a single proton for a nucleus, and one planetary electron. A helium atom would then consist of a nucleus having a mass four times that of the proton and a charge twice that of the electron. It would have two planetary electrons.

Experimental basis of Bohr's theory. It is explained in Chapter 3 that, in order to account for the distribution of intensities in the continuous spectrum of a black body, Planck arrived at the conclusion that the interchange of energy between matter and radiation takes place in discrete amounts which he called quanta. The radiant energy involved is $h\nu$ per quantum, where ν is the frequency of the radiation and h is Planck's universal constant, 6.624×10^{-27} erg sec. This mechanism of radiation, as well as the nuclear model of the atom, is in direct contradiction to classical electrodynamic theory, which predicts that a charged body radiates when and only when it is being accelerated. Now an electron rotating about a positively charged nucleus has a centripetal acceleration, as a consequence of which it would, according to classical electromagnetic theory, emit radiation at the expense of its mechanical energy. Gradually it should spiral down into the nucleus. The frequency of the radiation should increase as the electron moves faster and faster until finally it falls into the nucleus.

Bohr's fundamental assumptions. In 1913, Bohr formulated a theory to explain the spectrum of atomic hydrogen wherein he made

two assumptions which were in direct contradiction to classical theory. He postulated the existence of a limited number of stable orbits or stationary states with respect to the nucleus, in which it is possible for an electron to reside without radiating. Each of these stationary states corresponds, of course, to a different total energy of the nucleus-electron system. When the atom in such a stationary state is subjected to a transient disturbance—a collision with an electron, another atom, or with a photon—its electron may (*a*) return to the original orbit, (*b*) pass to another stationary state, or (*c*) be removed entirely from the influence of the nucleus. Furthermore, an atom in a stationary state may shift to any available lower state by radiating a photon. In all these cases, the atom must absorb (or give up) an amount of energy equal to the energy difference between its initial and final states. Expressed as an equation, if E_1 and E_2 represent the energies of the lower and upper states, respectively, the amount lost or gained by the atom, according to the direction of the change, is given by

$$h\nu = E_2 - E_1 \quad (5)$$

The Bohr orbits. Bohr began by supposing, for simplicity, that the electron moves in a circle, and calculated the dimensions of its stationary orbits. Since the mass of the electron had been shown to be much smaller than that of the proton, he assumed at first that the nucleus is practically at rest with respect to the observer. The electron is maintained in its orbit by the electrostatic attraction between itself and the nucleus. This electrostatic force, indeed, is the centripetal force that is needed to keep the electron in a circular orbit as it moves around the nucleus; that is,

$$Ze^2/a^2 = m\omega^2a = mv^2/a \quad (6)$$

where Ze is the nuclear charge, $-e$ is the electronic charge, a is the distance between their centers, and ω is the angular velocity of the electron. For hydrogen the nuclear charge is $+e$; therefore $Z = 1$. As far as equation 6 is concerned, any radius, and therefore any energy, is possible. If this were so, spectral lines of any frequency whatever could be emitted by hydrogen, according to equation 5. This conclusion, of course, is in total disagreement with experiment; Bohr found that his model would yield the measured frequencies of atomic hydrogen if he chose fixed orbits such that the angular momentum $I\omega$ of the electron in any stationary state was always an exact multiple of $h/2\pi$, where h is Planck's constant and I the moment of inertia of the electron around the nucleus. That is, the angular momentum of the n th sta-

tionary state is

$$I\omega = m\omega a^2 = nh/2\pi \quad \text{or} \quad (mv)(2\pi a) = nh \quad (7)$$

where n is called the quantum number. The angular momentum is said to be quantized, and equation 7 is the quantizing condition. In general, any physical variable that is restricted (in Nature) to a definite set of separated values is said to be quantized. From equations 6 and 7 we can immediately determine the radius and the angular and linear velocities of the electron in each stationary state, in terms of universal constants which have been determined experimentally, and of the quantum number n . They are:

$$a_n = \frac{n^2 h^2}{4\pi^2 m Z e^2} \quad \omega_n = \frac{8\pi^3 m Z^2 e^4}{n^3 h^3} \quad v_n = a_n \omega_n = \frac{2\pi Z e^2}{nh} \quad (8)$$

We can now calculate the energy corresponding to the n th stationary state. Assuming that the potential energy V is zero when the electron is at infinity, the electric potential at distance a from the nucleus is Ze/a per unit (positive) charge. Hence, the charge of the electron being $-e$, its potential energy at a distance a from the nucleus is

$$V = -\frac{Ze^2}{a} = -\frac{4\pi^2 m Z^2 e^4}{n^2 h^2} \quad (9)$$

We also have, for the kinetic energy,

$$T = \frac{I\omega^2}{2} = \frac{2\pi^2 m Z^2 e^4}{n^2 h^2} \quad (10)$$

The total energy of the atom in the n th stationary state, obtained by adding the kinetic and potential energies, is

$$E_n = V + T = -\frac{2\pi^2 m Z^2 e^4}{n^2 h^2} \quad (11)$$

The change in energy when the atom passes between stationary states characterized by the quantum numbers n and n' is given by Bohr's second postulate as

$$E_{n'} - E_n = h\nu = \frac{2\pi^2 m Z^2 e^4}{h^2} \left(\frac{1}{n^2} - \frac{1}{n'^2} \right) \quad (12)$$

Rewriting this equation in terms of the wave number $\bar{\nu} = \nu/c$, we have finally

$$\bar{\nu} = \frac{2\pi^2 m Z^2 e^4}{h^3 c} \left(\frac{1}{n^2} - \frac{1}{n'^2} \right) \quad (13)$$

Substitution of the values of c , m , h and e (in electrostatic units) given in Appendix 2 shows that the quantity outside the bracket on the right has the numerical value $1.097 \times 10^5 \text{ cm}^{-1}$. This is substantially equal to the Rydberg constant R_H which occurs in equation 2. Bohr thus concluded that the terms of the Rydberg form of Balmer's equation are a measure of the energies of the atom in the successive stationary states (equation 5). The Ritz principle (p. 95) followed as a natural consequence. The student should compare equations 2 and 13, remembering that the former is deduced from an empirical study of the hydrogen spectrum, the latter from purely theoretical considerations.

Interpretation of the hydrogen spectrum. We are now in a position to visualize the process by which the various spectral series of hydrogen are called into being. Equation 8 shows that the radii of the successive orbits increase as the square of the quantum number, as indicated pictorially in Fig. 4-4a. The orbit marked $n = 1$ is called the normal orbit and represents the stationary state of the unexcited atom. By various processes, such as thermal agitation at high temperatures, or the impact of a rapidly moving electron or an alpha particle, the electron may be removed from the normal orbit and, upon reaching equilibrium again, may find itself in any of the other possible stationary states of higher energy. The atom, having more energy, is now less stable than before. Perhaps the approach of another atom or electron may be sufficient to ionize it or to cause it to pass to a stationary state of different energy. If, on the other hand, the excited atom is not disturbed, the electron will eventually fall toward the nucleus until it reaches either the normal orbit or some intermediate one. In so doing, the total energy of the atom is reduced, and this lost energy is radiated as a photon of frequency ν , according to equation 5.

Energy levels. Although Fig. 4-4a, with its circular orbits, is a reasonable picture of the hydrogen atom, it should be observed immediately that our specific knowledge of the atom is derived from energy emitted by the atom in the form of radiation; hence it will be helpful to have a representation of the atom in which the energy changes that it undergoes are depicted graphically in a clear and quantitative manner. Figure 4-4a might be considered misleading in that the tiny arrow joining orbits $n = 1$ and $n = 2$ actually represents a larger energy change than the longer arrow joining orbits $n = 4$ and $n = 3$. The larger energy changes occur between the lower orbits, because the electric field near the nucleus varies according to the inverse square of the distance, rather than according to a linear scale.

To represent energy changes in an atom on a linear scale, it is customary to set up what is known as an energy diagram, or energy-level

diagram, as in Fig. 4-4b. Here, the horizontal lines are drawn at positions, measured from the reference line labeled zero at the top, corresponding to the energies of the atom computed by equation 11. We notice that all the values are negative; that the lowest line (of greatest negative value) must be that for $n = 1$, since n^2 occurs in the denominator; and that, as n is given successively larger values, the energy E_n (equation 11) takes on values that are successively smaller in absolute magnitude. If we put n equal to infinity, meaning that the electron is very, very far from the nucleus, we obtain the value $E_\infty = 0$. The appropriate values of these negative energies, in electron volts, are recorded at the right of Fig. 4-4b.

The groups of arrows drawn from higher to lower states of energy represent the various series (Lyman, Balmer, etc.) of emission lines. Since the diagram was plotted on a linear vertical scale, the lengths of these arrows are quantitatively proportional to the corresponding energy changes. The energy of that line of the Lyman series which has the smallest energy is clearly $-3.40 - (-13.60)$, or 10.20 ev, approximately. Similarly the energy of that line of the Balmer series possessing the greatest energy, corresponding to the longest possible arrow, would be $0 - (-3.40)$, or 3.40 ev. As the remaining labels on Fig. 4-4b show, energy differences may also be indicated by means of wave numbers or wavelengths. Atomic energies are, however, most commonly expressed in electron volts; energy diagrams, on an electron-volt scale, will be used frequently in succeeding pages.

3. Extensions of the Theory

Elliptic orbits. We have reached these conclusions concerning the structure and behavior of the hydrogen atom on the basis of circular orbits only. However, we know that when a particle moves around a fixed center of force, under the inverse-square law of attraction, its orbit is an ellipse with the force center at one focus. A circular orbit is but a special case. Sommerfeld, using the Bohr assumptions, arrived at the same types of equations by the use of elliptic orbits in which the nucleus occupies one focus. In this case, however, it is necessary to use two quantum numbers in place of the one denoted by n in equation 7. The first of these is concerned with the angular momentum of the electron in its elliptic orbit. It restricts possible values of the angular momentum to integral multiples of $h/2\pi$, so that the angular momentum may be set equal to $kh/2\pi$, where k is an integer called the azimuthal quantum number.

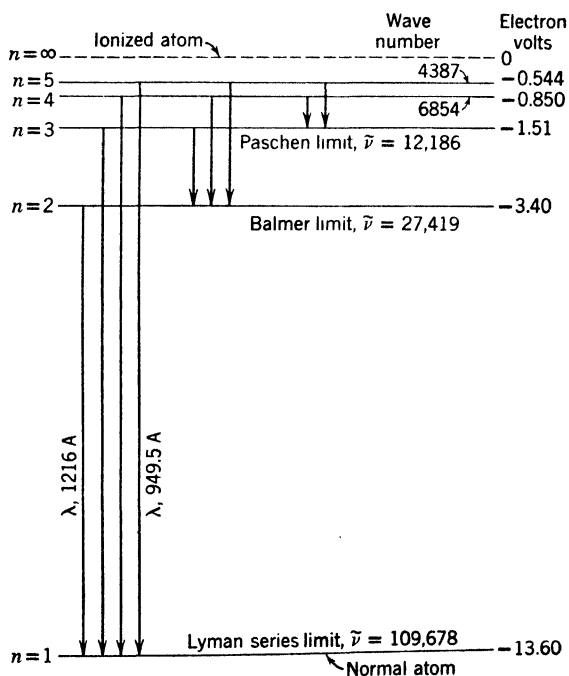
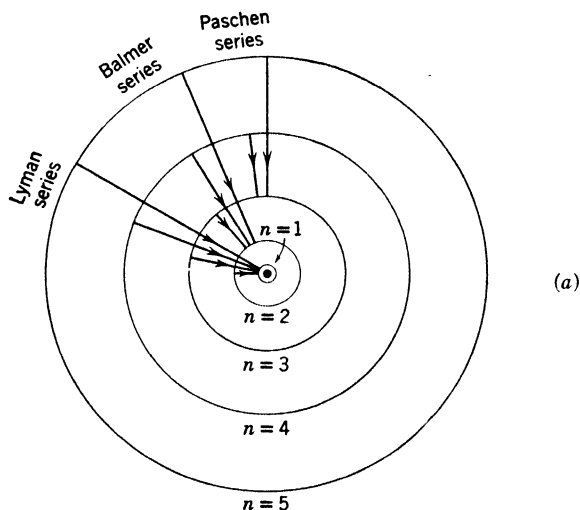


Fig. 4-4. (a) The circular Bohr orbits of hydrogen, showing the transitions that produce the Lyman, Balmer, and Paschen series. (b) An energy-level representation of the transitions shown in (a).

The second quantum number is introduced to place restrictions on the radial momentum of the electron. It is obvious, of course, that as an electron revolves in an elliptic orbit it must alternately approach and recede from the nucleus. If we multiply the average radial momentum by the whole amount by which the radius changes during a complete revolution (adding both the increase and the decrease), we obtain a quantity which is set equal to $n_r h$, where n_r is zero or an integer, and is called the radial quantum number. The sum of the azimuthal and radial quantum numbers is called the principal or total quantum number n , used in equations 7 to 13. This agrees with the simpler theory given above, because $n_r = 0$ for a circular orbit, and n is then identical with the azimuthal quantum number.

The effect of variable mass of the electron. Even with this refinement, the theory is not capable of explaining *all* the finest details of the hydrogen spectrum. On account of the change of mass with velocity of the electron (p. 32), every elliptic orbit in a hydrogen atom

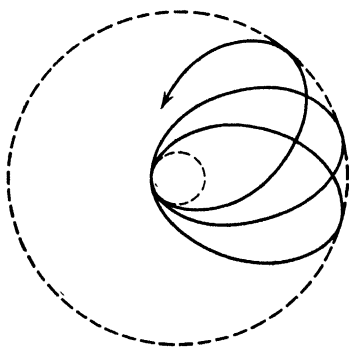


Fig. 4-5. The relativity precession of an elliptic orbit in the hydrogen atom.

undergoes a slow precession so that the major axis of the ellipse changes its position in space and the electron describes a so-called rosette orbit (Fig. 4-5). In fact, the effect of change of mass is the same as that of applying a small attractive force in addition to the inverse-square attraction. The average rate at which the axis revolves in the orbital plane depends on the value of the azimuthal quantum number k . Therefore, the energy depends on this quantum number to a slight extent. As a result, each of the terms described by equation 11 and characterized by a definite value of n is split

into several closely neighboring terms, except the lowest term $n = 1$, which remains single. Each line of the Balmer series is therefore replaced by a group of very closely neighboring lines. The Bohr atom model was thus highly successful in accounting for the spectral series of hydrogen described in Section 2.

Lamb and Retherford have uncovered another type of correction to the energy of the hydrogen atom. By microwave spectroscopy, they found slight shifts of spectral levels from the predicted positions, due to an interaction between the atom and the radiation field (see Appendix 9, ref. 40).

Spectral series of the helium ion. A series of the Balmer type but having as its variable term $R/(m + \frac{1}{2})^2$, where m is an integer,* was found by Pickering in certain nebulae; Fowler, using a mixture of hydrogen and helium, found a similar series in which the constant term was $R/(1.5)^2$.

Both were originally attributed to hydrogen, but do not fit the scheme described above, and the experimental value of R does not quite agree with the value found for hydrogen. Bohr therefore attacked the problem of the Pickering and the Fowler series, and showed that they are due to singly ionized helium, He^+ ; that is, a helium atom which has been deprived of one of its two electrons. This atom should have the same structure as a hydrogen atom, except that the nucleus has four times the mass and twice the nuclear charge. In calculating the energy values for singly ionized helium, equations 9 and 13 must be modified, since, for helium, $Z = 2$. The energy values are thus multiplied by 4. Equation 13 now takes the form

$$\nu = 4R \left(\frac{1}{n^2} - \frac{1}{m^2} \right) \quad m = n + 1, n + 2, \dots \quad (14)$$

The equation of the Pickering series can be written

$$\bar{\nu} = 4R \left(\frac{1}{4^2} - \frac{1}{(2m + 1)^2} \right) \quad m = 2, 3, \dots \quad (15)$$

It is, therefore, part of the series represented by the equation

$$\bar{\nu} = 4R \left(\frac{1}{4^2} - \frac{1}{m^2} \right) \quad m = 5, 6, \dots \quad (16)$$

The lines completing the series very nearly coincided with hydrogen lines and were, therefore, overlooked at first. The Fowler series is also due to helium and is explained in similar fashion.

Motion of the nucleus. Careful measurements show that there are slight differences between these less obvious lines of the Pickering series and those of the Balmer series. The discrepancies are explained when we return to one of the assumptions made in the development of the Bohr equations, that the nucleus is at rest with respect to the observer. It is evident that both must revolve about their common center of mass. To take this motion into account, we should replace the

* We have already used m to denote the mass of the electron, but this new use of the symbol should cause no confusion.

electron mass m by the effective mass of the system. This quantity is defined as

$$\mu = \frac{m}{1 + (m/m')} \quad (17)$$

where m' and m are the masses of nucleus and electron, respectively.

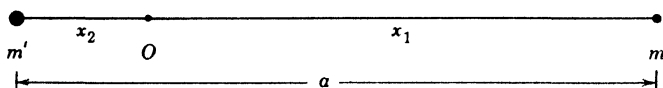


Fig. 4-6.

★ The effective mass may be calculated as follows: In Fig. 4-6, the electron and nucleus are at distances x_1 and x_2 from the center of mass O . By the law of moments, $x_1/x_2 = m'/m$, so that

$$x_1 = \frac{a}{1 + (m/m')}, \quad x_2 = \frac{m}{m'} \frac{a}{1 + (m/m')}$$

The total angular momentum of the system about O is, in terms of the angular velocity ω ,

$$mx_1^2\omega + m'x_2^2\omega = \frac{m}{1 + (m/m')} a^2\omega = \mu a^2\omega$$

Now equation 13 must be replaced by

$$\tilde{\nu} = Z^2 \frac{2\pi^2\mu e^4}{h^3 c} \left(\frac{1}{n^2} - \frac{1}{n'^2} \right) \quad (13a)$$

The combination
$$R = \frac{2\pi^2\mu e^4}{h^3 c} \quad (18)$$

is called the Rydberg constant for nuclear mass m' . The value it assumes when we make m' infinity is denoted by R_∞ and is called the Rydberg constant for mass infinity. The effect of change of nuclear mass on the wavelength is shown below for the so-called "missing" lines of the Pickering series and the corresponding ones of the Balmer series:

H α	6563.0 Å	He ⁺ ($m = 6$)	6560.1 Å
H β	4861.5	He ⁺ ($m = 8$)	4859.3
H γ	4340.6	He ⁺ ($m = 10$)	4338.7
H δ	4101.9	He ⁺ ($m = 12$)	4100.0

If the motion of the nucleus were neglected, the wavelengths of the lines would be the same in the two columns.

★ Equation 15 gives the wave numbers for only the odd values of m in equation 16. The above table supplies the spectrum lines corresponding to the even values of m which, as we said, were overlooked at first because of their proximity to the lines of the Balmer series, given here for comparison.

Heavy hydrogen. The discovery of deuterium or heavy hydrogen by H. C. Urey supplies further illustration of the change in value of the Rydberg constant due to the effective mass. The deuterium atom, with essentially two times the mass of the hydrogen atom, has a *larger* effective mass than the latter. Therefore, the wavelengths of the lines in the deuterium Balmer series (symbolized by $H^2\alpha$, $H^2\beta$, etc.) have wavelengths 1 to 2 angstrom units *smaller* than those of the correspond-

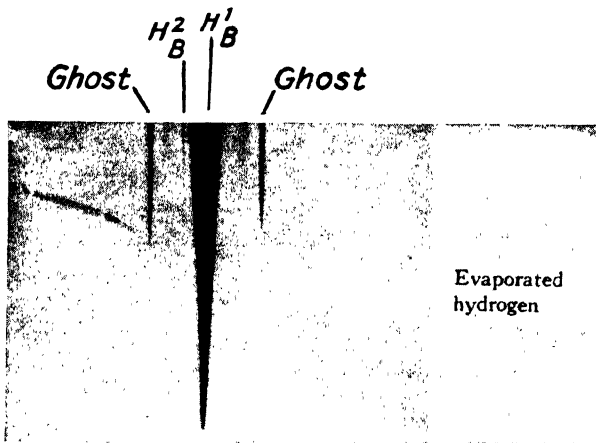


Fig. 4-7. Second-order grating spectrum of hydrogen, showing the second line of the Balmer series for the two isotopes H^1 and H^2 (after Urey, Brickwedde, and Murphy).

ing lines of the hydrogen series. Figure 4-7 shows the second-order spectrum of $H^2\beta$ taken with a 21-ft concave grating having a dispersion of 1.31 Å/mm. The $H^1\beta$ line of hydrogen is shown at the center, while on the left and very close to it is the $H^2\beta$ line of deuterium. The strong lines to the left and right are false or ghost lines. Figure 4-8 is a microphotometric graph of this spectrogram. The line marked $H^3\beta$ shows the position that line would occupy if hydrogen of mass 3 were present in sufficient quantity. This material, called tritium, is radioactive (see p. 353).

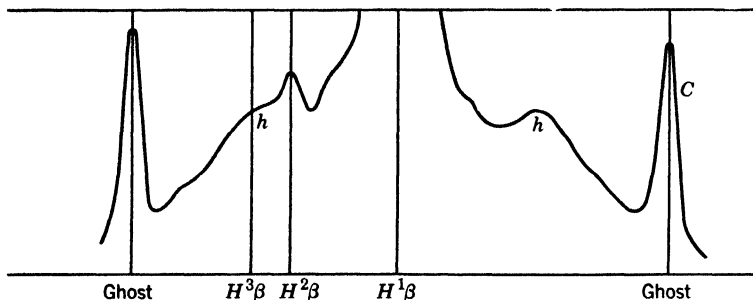


Fig. 4-8. Microphotometer record of Fig. 4-7 (after Urey, Brickwedde, and Murphy).

★ **Effects of external fields on the hydrogen atom.** Except for the introduction of the quantum conditions, Bohr's theory of the hydrogen atom made use of classical mechanics. It is possible, therefore, to calculate the effects of disturbing electric and magnetic fields. For simplicity we shall discuss only the latter. We may think of the atom as though it were a tiny magnet since the electron moving in its orbit is equivalent to a current flowing in a circular or elliptical loop of wire. When a uniform magnetic field is applied to the hydrogen atom, the electrons move just as they did in the absence of the field except that a uniform precession about the magnetic line of force through the nucleus is superposed. The situation is just like that encountered in the case of a frictionless spinning top. If the earth's gravitation were absent the top would continue to spin about the same axis in space; the effect of gravity on the top is to make the axis precess about a vertical line with constant angular velocity. Under these circumstances the vertical component of the angular momentum is constant. So it is also in the case of the atom. It executes a uniform rotation called the Larmor precession whose angular velocity is small compared to that of the electron in its undisturbed orbit. The frequency of this precession is proportional to the strength of the magnetic field. Since the direction of the axis of a magnet with respect to a magnetic field determines the energy of the magnet, so the orientation of the atom with respect to an external magnetic field in part determines the atom's energy. It is therefore necessary to introduce still another quantizing condition to describe the behavior of the atom whenever a magnetic field is present. According to an extension of Bohr's theory, this condition is expressed by specifying still another quantum number, the magnetic quantum number, denoted by m_k . The behavior of a hydrogen atom in a magnetic field is such that m_k can assume, at any one instant, only one of

the integral values from k to $-k$, inclusive. (See however, the discussion of electron spin, an added complication, in Chapter 7.)

This new condition states that the tiny magnet takes up only certain definite orientations with respect to the lines of magnetic force, so that the *component* of angular momentum parallel to the field is $m_k h/2\pi$. The possible orientations are shown for a typical case in Fig. 4-9. For each orientation the atom possesses a different potential energy with respect to the field, and this energy counts as a part of its total energy. In other words, each of the Bohr levels of the undisturbed atom is split into several levels by the magnetic field, and a single line of a hydrogen series is thus split up into several closely spaced lines, a phenomenon known as the Zeeman effect. The existence of this effect is to be considered a direct demonstration of the necessity of introducing this third, magnetic, quantum number.

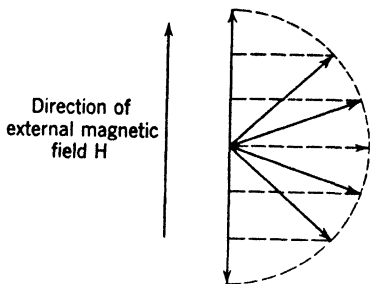


Fig. 4-9. Diagram showing the possible orientations of a hydrogen atom with respect to the lines of force of an external magnetic field, when $k = 3$. The spin of the electron (p. 198) is neglected.

Similar phenomena occur when an electric field is present, and the splitting of the spectral lines into several components is known as the Stark effect. In both cases the separations calculated from the Bohr theory are in good accord with experiment.

4. Insufficiency of the Bohr Model

The planetary atom thus yields correct results in systems where only a single electron is involved. When exact calculations are made of the energy required to remove an electron from neutral helium or from other more complicated atoms or ions, the results definitely disagree with observed data. Such failures have made it necessary to seek further for a complete solution. However, because of the value of the planetary model in explaining qualitatively many of the chemical and physical properties of atoms with several electrons, and because of its great convenience in picturing atomic processes, it is still used in discussing the origin of X-ray spectra and many other atomic problems.

REFERENCES

Appendix 9, refs. 40, 53, 55, 74, 82, 90, 94, 108.

PROBLEMS

1. Taking the wavelength of $H\alpha$ to be 6563 Å, calculate the Rydberg constant for hydrogen. Compare it with the value given in Appendix 2.
2. Calculate the wavelengths of the first three lines of the Paschen series, using the value of the Rydberg constant for hydrogen given in Appendix 2.
3. What are the radii of the second Bohr orbit of hydrogen and the velocity of the electron in this orbit?
4. What is the electric potential energy of (a) a positive charge of 1 electrostatic unit, (b) an electron at rest, at a distance 1 Å from a proton?
5. A tiny ball of mass 12 gm is whirled in a circle at the end of a string 8 cm long, at 3 rev/sec. (a) What is its moment of inertia about the center of the circle? (b) What is its linear speed? (c) What is its angular velocity? (d) What is its angular momentum? (e) What centripetal force is exerted on the ball?
6. Is the gravitational attraction between a proton and an electron 0.5 Å apart greater or less than 10^{-39} times the electric attractive force?
7. How much energy is necessary to remove an electron from the second Bohr orbit of hydrogen so that it is entirely beyond the influence of the nucleus?
8. The deuterium nucleus has twice the mass of the proton. Is the effective mass of the electron in a deuterium atom greater or less than the effective mass of the electron in a normal hydrogen atom?
9. Is the value of the Rydberg constant for the deuterium atom greater or less than the Rydberg constant for hydrogen?

ANSWERS TO PROBLEMS

1. 109,700/cm.
2. 1.8757μ ; 1.2821μ ; 1.094μ .
3. 2.11×10^{-8} cm; 1.092×10^8 cm/sec.
4. (a) $+4.8 \times 10^{-2}$ erg; (b) -2.3×10^{-11} erg.
5. (a) 768 gm cm^2 ; (b) 151 cm/sec; (c) 18.9 rad/sec; (d) $14,500 \text{ gm cm}^2/\text{sec}$; (e) 3.42×10^4 dynes.
6. Less.
7. 3.40 eV, or 5.45×10^{-12} erg.
8. Greater. The ratio is $2(M + m)/(2M + m)$, where M and m are the proton and electron masses.
9. Greater. The mass of the electron is a factor in the Rydberg constant; its reduced mass is greater in the deuterium atom.

5

X-Rays

The properties of the radiations which compose the whole electromagnetic spectrum (p. 61) change so rapidly as the wavelength increases or diminishes that it is customary to discuss a selected region as a subject in itself. This chapter deals with X-rays, with wavelengths in the range 10 Å to 0.1 Å. The reader should remember, however, that X-rays are known whose wavelengths are so long that they might equally well be classed as extreme ultraviolet radiations. X-rays are also known of such short wavelengths that they are indistinguishable from gamma rays, though it is customary to keep the name X-rays to describe rays produced artificially, the name gamma rays being reserved for the radiations emitted spontaneously by radioactive nuclei.

We know that visible light manifests its wave nature by such phenomena as refraction, interference, and diffraction. From observations of these effects the wavelengths can be found. So also it is with X-rays, although the shortness of the wavelengths usually demands a different experimental technique. At the same time experiments in photoelectricity compel us to attribute corpuscular properties to light, coexistent with its wave aspects. This duality finds its counterpart in X-rays. Indeed, the high energy of X-ray photons brings out strongly one important aspect of the corpuscular nature of radiation (see the Compton effect, p. 143). Therefore it will be well, throughout this chapter, to recognize that observations made in one region of the electromagnetic spectrum may clarify and amplify results obtained in another region.

It is found that under certain circumstances atoms can emit characteristic X-ray spectra which can be interpreted on the assumption that Bohr's theory is approximately true for electrons deep within the atom. These spectra will be used to throw light on the problem of atomic structure and on the periodic system of the elements.

1. Production and Measurement of X-rays

The X-ray tube and its operation. When electrons, moving with velocities of the order of 10^{10} cm/sec, are quickly stopped by collision with atoms, radiations are produced which can with peculiar facility pass through materials opaque to visible light. These radiations are X-rays. Conditions will be very favorable for production of the rays if an electron stream, moving through a well-evacuated space, impinges on a substance of high atomic weight, as in the Coolidge X-ray tube

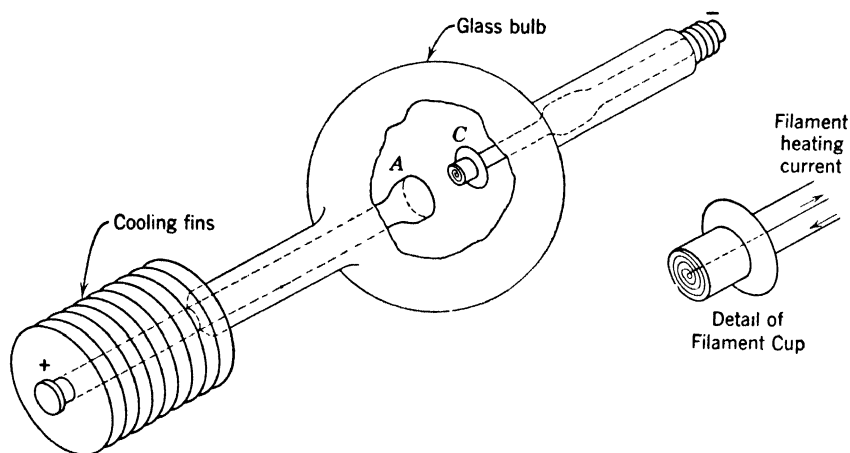


Fig. 5-1. The Coolidge X-ray tube. The cooling fins are attached outside the tube to the stem of the anticathode or target *A*. The filament, of tungsten, is usually wound in a nearly flat spiral just inside a molybdenum cup *C* which forms the cathode. The diameter of the glass bulb may be from 3 in. to 10 in., depending on the particular purpose for which the tube is designed.

(Fig. 5-1). Electrons are liberated thermionically from a hot tungsten wire cathode *C*; they are then accelerated toward the anticathode (or target) *A* by a high potential difference, perhaps 100,000 volts, applied in the direction shown by the plus and minus signs. Despite their high energy, the electrons penetrate at the first impact only a minute distance into the anticathode, whose surface becomes therefore a source of X-rays. If V is the applied potential and i the current (carried by the electrons), the electric power supplied is Vi . Of this only a small fraction of 1 per cent reappears in ordinary tubes as X radiation; the remainder heats the anticathode, which in many tubes is cooled by circulating water or by radiating fins. Thus, regarded as a machine for producing X-rays, such a tube has a very low efficiency.

Since X radiation in large doses is destructive to living tissue, precautions must be taken to protect the operator. The tube is often surrounded by a thick shield of heavy lead glass, or else totally enclosed in a lead box. The working beam of X-rays emerges through a hole in the side of the box, and is further limited, if necessary, by a series of lead slits.

To obtain from batteries a direct voltage of the magnitude required for the operation of an X-ray tube would be expensive and cumbersome. However, an alternating potential, from a step-up transformer, serves the purpose. From Fig. 5-1, it is clear that negative current can be carried by the electron stream in one direction only, from *C* to *A*. A high potential applied in the direction opposite to that shown would cause no current through the tube, even though the filament were heated. The application of an alternating potential difference to the tube results, therefore, in a pulsating current of electrons from *C* to *A*. The arrangement of the electric circuits for running an X-ray tube usually follows in its main features some such scheme as is represented

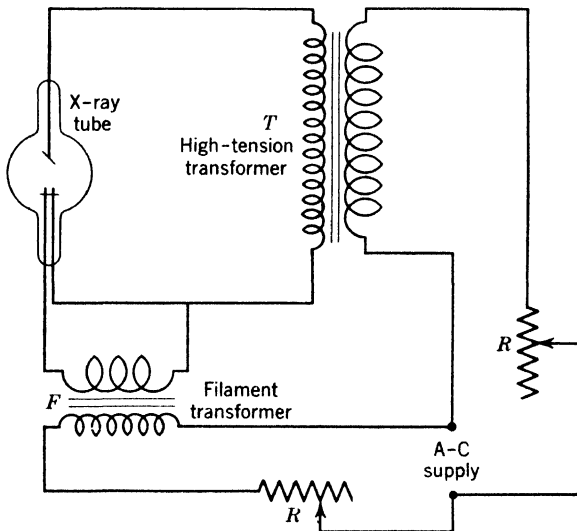


Fig. 5-2. Simple electric circuits for operation of an X-ray tube.

in Fig. 5-2, where *T* is the step-up transformer regulated by a resistance *R*, and *F* is a small step-down transformer, similarly regulated, providing the current for heating the filament. As we have just seen, in this simple outfit, the tube serves as its own rectifier. In practice, however, it is customary to include in the high-tension circuit some additional

thermionic rectifying device, to save the tube from unnecessary electrical strains. At the same time both halves of the alternating current wave may be utilized, so that the intensity of the radiation is increased. In addition, the regulating resistances R may be replaced by arrangements of choke coils, which insure more economical working conditions.

Measuring instruments. The fundamental effect of X-rays on matter is to produce high-speed electrons throughout the bulk of the material they traverse. Some of these are photoelectrons, others are recoil electrons produced by a phenomenon known as the Compton effect (p. 143). As the fast electrons are slowed down by collisions with atoms, they liberate slower ones, leaving some atoms temporarily as positively charged ions. In measuring X-rays, this chain of processes can be utilized conveniently in three different ways: (1) by causing ionization in a gas; (2) by affecting a photographic plate, and (3) by causing fluorescence on suitable screens. In (3) the X-rays penetrate the thin layer of fluorescent material supported on a glass backing, causing it to emit light in proportion to the energy per second that is absorbed. All three effects have their particular applications in the measurement of X-rays. Research problems generally require the detection of the rays by means of (1) or (2), whereas medicine and industry usually employ only (2) or (3).

★ The first method is by far the most sensitive of the three in detecting weak radiations, and merits detailed description. The detecting device may be a Geiger-Müller tube or an ionization chamber. In the latter case, shown in Fig. 5-3, C is the casing of the ionization chamber, often a cylindrical vessel, having an opening A through which pass rays from T , suitably restricted by lead slits S_1, S_2, S_3 . Air, or heavy vapor such as methyl iodide, is used to fill C ; the opening A may be covered by a thin sheet of celluloid to prevent the escape of the foreign gas. With an ionization chamber of given length, the denser the gas the more fully the X-rays are absorbed. Inside the chamber is an insulated electrode E , between which and the casing a potential difference of 100 or 200 volts is maintained by a battery B . The applied voltage causes a drift of the ions formed by the X-rays, the positive toward E and the negative toward C , or vice versa. It is important that this voltage be sufficient to sweep out the ions without appreciable recombination. The gathering of a charge on E constitutes a feeble electric current, which is usually so small that it has to be measured by a special electrometer, or by an amplifier connected to a recorder.

★ In certain cases it is convenient to substitute a photomultiplier tube or a crystal counter (p. 289) with appropriate electronic circuits in place of the ionization chamber and recording electrometer.

The intensity of a beam of X-rays is measured by the amount of energy which crosses a unit area placed perpendicular to the beam in 1 sec. Its absolute measurement is difficult. Relative intensities, which are usually sufficient in experimental work, can be found easily, either by measuring ionization currents or by studying the blackening of a photographic plate. Usually, the former method is preferable. Suppose, for example, that we wish to compare the intensities from the tube when operated at two different voltages. In an observation taken with the tube running at a voltage V_1 , let the deflection of the electrometer be d_1 , and, with the tube running at V_2 , suppose this changes to d_2 . The ratio of d_1 to d_2 gives us the desired intensity relation, provided that the relative absorption in the ionization chamber is the same at both voltages, a condition which is often difficult to obtain.

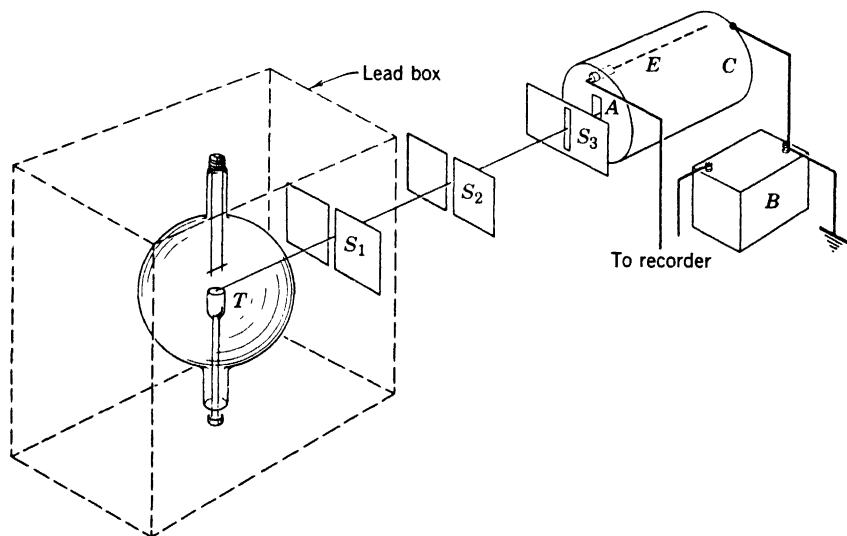


Fig. 5-3. An ionization chamber C arranged to measure relative intensities of an X-ray beam. The beam originates at the target T . Its geometrical dimensions are determined by the slits S_1 and S_2 and the aperture S_3 . If the ionization chamber is filled with a heavy gas such as methyl iodide, the window A is covered with a thin membrane, perhaps of plastic. Ions of one sign inside the chamber are collected on the insulated rod E .

In medical applications, a simple rule is used for determining X-ray dosage. It is approximately true, over the range of intensities commonly employed, that the effect of a given beam of X-rays acting on a specified area depends on the intensity multiplied by the time of exposure. If the intensity were halved, the time of exposure would have to be doubled

to produce the same result. The unit of dosage is the roentgen, or r unit. Special instruments are used to measure dosages of different types of radiation such as X radiation, or gamma radiation, or beta radiation. For people engaged in processing radioactive materials, the U. S. Atomic Energy Commission considers 0.3 r a limiting safe dose per individual worker per week. Over a period of a year this could accumulate to a maximum of 15 r. The safe limit for a brief single exposure is considered to be 25 r.

2. Absorption of X-Rays

The exponential law. Suppose, for the sake of simplicity (and contrary to fact) that the tube in Fig. 5-3 gives off radiations all of one wavelength. If the beam is intercepted by a thin metal foil placed between S_1 and S_2 , its intensity, as indicated by the ionization current, is found to be smaller than before.

★ Suppose that the monochromatic beam changes in intensity by a small amount $-dI$, in traversing a small thickness of material dx . The fractional change is $-dI/I$, where I is the intensity of the beam as it enters the element dx . This fractional diminution is proportional to the thickness of material traversed; hence $-dI/I = \mu dx$. Here μ is a constant, for the conditions given, called the linear absorption coefficient. By integration we obtain

$$I = I_0 e^{-\mu x} \quad \text{or} \quad I/I_0 = e^{-\mu x} \quad (1)$$

where I_0 represents the intensity of the beam when it is first observed, and e is the base of natural logarithms. This may be written in a form more convenient for computation, in terms of logarithms to the base 10:

$$2.3 \log_{10}(I/I_0) = -\mu x$$

As an example of the application of equation 1, let us find what fraction of a certain beam of X-rays will be transmitted through various thicknesses of aluminum, assuming that the value of μ in this experiment is 14 per cm.

When $x = 0$	0.05	0.10	0.15	0.20	0.30	0.40 cm
$I/I_0 = e^{-14x} = 1$	0.497	0.247	0.123	0.061	0.015	0.004

If these values are plotted in graphical form their meaning is at once apparent. To state this in another way: if $\mu = 14$ per cm, then a layer of material of thickness $\frac{1}{14}$ cm will reduce the X-ray beam to $1/e$ of its original intensity.

The second form of equation 1 means that the fraction of the original beam which penetrates more than a distance x through the absorber

is given by the exponential term $e^{-\mu z}$. The thickness of aluminum required to reduce a beam to (say) 10 per cent of its original intensity is much greater than the thickness of lead required to effect the same reduction; hence the absorption coefficients for aluminum and for lead must be different. Elements of high atomic number are much more effective absorbers than elements of low atomic number. For example, the absorption coefficient of lead per centimeter is 19.1 times as great as that for iron, at a wavelength 0.098 Å. Hence lead is almost universally used as shielding around X-ray tubes, to prevent radiation from going in significant quantities where it is not wanted.

★ If now we suppose that, by an increase in the operating potential, the tube is made to give off a shorter wavelength, it may be found that the absorption coefficient, measured in some one kind of foil, has decreased. In some cases, however, the coefficient increases. In Section 8, these effects are traced to their origin. Summing up, we see that the absorption coefficient depends on the natures of the absorber and of the X radiation, but is independent of the latter's initial intensity; therefore the values of μ , determined experimentally for some particular absorber, give valuable information as to the nature of X-rays from different sources. It should be remembered that equation 1 is valid only for homogeneous X-rays. In the case of a mixed beam, the expression is a sum of exponential terms involving different absorption coefficients.

Soft and hard X-rays. It is convenient to use the terms "soft" and "hard" X-rays to denote in a relative manner the distinction between radiations which are readily absorbed and those which are not so readily absorbed by the same substance, although there is no sharp dividing line between the two types. The former are produced with comparatively low exciting potentials, the latter with higher potentials. The distinction can be made, as we have seen, by the differing values of the absorption coefficient, or alternatively on the basis of wavelength—soft and hard radiations corresponding to long and short wavelengths, respectively.

It follows from the discussion in this section that, as a beam of X-rays which includes a range of wavelengths passes through or is "filtered" by an absorber of definite thickness, then the diminution of intensity caused by this definite thickness of absorber is not the same for all components of the beam. The soft components, characterized by large values of μ , suffer a greater fractional diminution of intensity than the hard components. Thus, in general, a heterogeneous beam becomes progressively harder as it traverses matter, although the intensity, of course, continually decreases.

3. Secondary X-Rays

Two kinds of secondary radiation. It has been mentioned that X-rays have the same nature as visible light, in that they consist of transverse electromagnetic waves. Their wavelengths, however, are some thousands of times smaller, of the order of 10^{-8} cm. A profound difference in the detailed properties of X-rays and of light is therefore to be expected. To obtain an adequate interpretation of the different properties of X-rays, the concept of X-rays as a wave motion is not always sufficient. It is often convenient to introduce the idea of photons or quanta. The quantum viewpoint frequently gives a rational explanation of facts which are unintelligible on the wave theory. However, for the description of several phenomena, we continue to regard X-rays as electromagnetic radiations of the same type as those with which we are familiar in the visible region of the spectrum.

Whenever a beam is intercepted by matter, this matter itself emits radiations known as secondary X-rays; therefore a metal foil placed in a beam as an absorber acts simultaneously as a secondary radiator. Of the energy removed by absorption, part increases the temperature of the absorber and the remainder reappears in the form of secondary X-rays. The relative proportions of the two parts depend on the shape, size, and material of the absorber. Secondary X-rays are of two types—scattered and characteristic (or fluorescent). The latter are emitted uniformly in all directions; the former are most intense in a general forward direction, within a small angular range including the primary beam.

Scattered X-rays. The beam from a searchlight pointing skyward is visible to an observer on the ground a long distance away. A small amount of light is scattered out of the beam in all directions, some of it toward the observer, thus revealing the path and shape of the main beam. The scattering in this case is principally due to fog and dust particles in the atmosphere, though the molecules of air are also scatterers. In much the same way, some scattered X-rays come in all directions out of a primary beam which is passing through matter. Their occurrence can be explained, though not always accurately, in a simple manner, without the aid of quantum theory. The extranuclear electrons in the scattering substance, under the influence of the alternating electric intensity of the primary waves, are set into forced oscillations, approximately simple harmonic, whose frequency is the same as that of the incident beam. The nuclei of the scattering atoms are too heavy in comparison with their attendant electrons to have any appreciable displacements. By analogy with the motion of the bob of a simple pendulum, it is evident that the scattering electrons are continuously

accelerated, first in one direction, then in the opposite, so that X-rays are emitted. The simplest conception is that the frequency of the scattered X-rays is the same as that of the oscillating electrons, which in turn keep time with the primary radiation; hence the scattered rays should have the same frequency, and consequently the same properties, as the primary rays. This similarity is borne out in respect to soft rays by an experimental comparison of their respective absorption coefficients in some such standard substance as aluminum; but for hard X-rays anomalous effects are found, as is explained in Section 9.

Characteristic X-rays. The other type of secondary X-rays, called characteristic, depends, as its name implies, on the specialized properties of the atoms composing the secondary radiator. Characteristic X-rays include various monochromatic radiations whose energies can be explained only by quantum theory. Experimental investigations on this subject were first reported about 1908. It was found, by measuring absorption coefficients, that for most scattering substances characteristic X-rays consist of two superposed radiations, one hard and one soft. These have been called the *K* and *L* characteristic radiations, respectively. For heavy elements, additional constituents have been observed, though not by the simple absorption methods used by early investigators. The letters *K*, *L*, *M*, *N*, and so on, denote the characteristic radiations in order of increasing softness. It is found further that the secondary X-rays from light substances, such as carbon, aluminum, or paper, are under ordinary conditions almost entirely of the purely scattered type. With increase of atomic number of the secondary radiator, the proportion of observable characteristic radiation increases, and at the same time the radiation becomes harder. The characteristic radiation will be discussed more fully in Section 7 in connection with X-ray spectra. In the meantime, it should be pointed out that it is intimately connected with the ejection of photoelectrons from the atoms of the secondary radiator. When atoms, under the influence of the primary X-rays, emit photoelectrons, they become positive ions. During the process of recombination of these ions, the characteristic radiations are emitted. For this reason they are classed as secondary radiations, although it is clear from the mode of their production that they must be present to a considerable extent in the primary radiation coming from the target of an X-ray tube.

4. The Wave Properties of X-Rays

Polarization. We have already assumed that X-rays are transverse electromagnetic waves. It is important to know how far this is justi-

fiable. Experiments on the polarization of scattered radiation by Barkla (1906) lent strong support to the idea. Imagine three mutually perpendicular axes drawn through a point O , in the directions north-south, east-west, up-down (Fig. 5-4). Let X radiation, coming from below, fall on a small block of carbon placed at O . The use of carbon, which

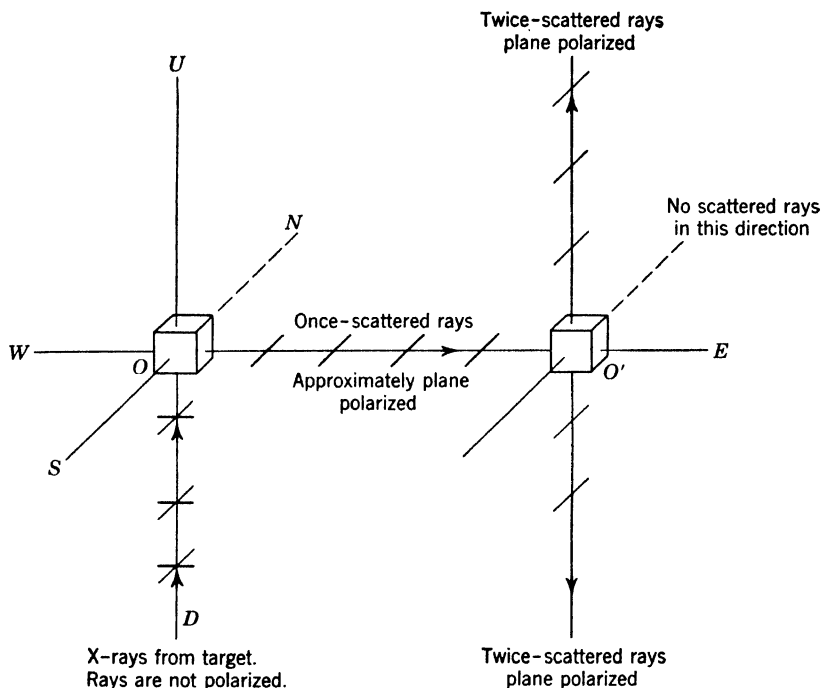


Fig. 5-4. Schematic diagram of an experiment on the double scattering of X-rays. The purpose of the experiment is to show that X-rays have the properties of a wave motion. The directions N , S , E , W , U , D are north, south, east, west, up, down. The absence of twice-scattered rays in the direction N from the carbon block O' is proof of the wave nature of X-rays. It should be remembered that an electron that is being accelerated in the direction of its motion does not radiate along the line of its acceleration, but sends out radiation in all other directions.

has a low atomic weight, insures that the secondary radiation is mainly of the scattered type. The accelerations of the electrons at O will be confined to a horizontal plane, if we assume tentatively that the radiation is of the transverse type, but will be distributed uniformly in all directions in this plane. Now since an electron radiates no energy along a line in the direction of its acceleration, a second small block of carbon placed at O' , a short distance east of O , will be acted on only by scattered waves

due to the north-south components of the accelerations of the electrons at O . This is equivalent to saying that the beam scattered eastward from O is plane polarized. The scattering electrons at O' can therefore be given accelerations only in a north-south direction. If now an ionization chamber well shielded from the rays scattered by O is placed above or below O' , it should detect the twice-scattered radiation; but, if it is placed north or south of O' , the intensity should be zero, since the electrons at O' have accelerations only in a north-south direction. Actually, Barkla found the ionization to be a minimum north and south of O' , and a maximum above and below. This agrees qualitatively with our tentative assumption as to the nature of X radiation. To be perfectly logical, the argument ought to have been set out in the reverse order; the conclusion, however, is the same, viz., that the experimental result bears out the original hypothesis that X-rays are transverse electromagnetic waves.

Diffraction by slits and ruled gratings. Soon after Röntgen's discovery of X-rays in 1895, attempts were made to verify their wave nature by passing a beam through a fine slit in the hope of obtaining a diffraction pattern from which the wavelength could be measured. The smallness of the wavelengths involved made such experiments difficult. Although they were afterwards repeated by many investigators, the results were rather inconclusive, even for many years after the whole question had been satisfactorily settled by other methods. They indicated, however, a wavelength of the right order of magnitude.

Since 1925 it has been found possible to obtain good X-ray diffraction patterns and spectra (as in optics) from ordinary reflection gratings, provided that the X radiation falls on the grating at a very large angle of incidence, nearly 90° . This technique has provided a new method of measuring X-ray wavelengths, largely superseding the older method employing reflection from crystals. It has at the same time made possible the study of X-rays of very long wavelengths, in a region of the spectrum formerly inaccessible to photographic work. On p. 56 the equation $n\lambda = d \sin \theta_n$ was derived for the diffraction of light by a plane grating, on the assumption that the incident light fell normally on the grating. There, λ was the wavelength of the spectrum line in question, d the grating space, and θ_n the angle of diffraction of the n th order, measured from the normal. An extension of the theory to cover the case when the incident light (or X-ray beam) makes an angle ϕ with the normal leads to the equation

$$n\lambda = d |\sin \phi - \sin \theta_n| \quad (2)$$

which is applicable to the X-ray case just mentioned. It should be

emphasized that, historically, wavelengths of particular radiations in the X-ray region were first determined by experiments involving reflection from crystals. Wavelengths so determined were, however, later found to be slightly in error. Ruled grating measurements are now the accepted ones (p. 134).

★ **Refraction by prisms.** Before 1924, all attempts to measure the refractive indices of prisms for X-rays (as in standard optical practice) showed only that this index differed from unity by an inappreciable amount. In that year, however, three Swedish physicists, Larsson, Siegbahn, and Waller, used the device of setting a prism not, as usual, in the position of minimum deviation but in a position where the deviation would be nearly a maximum. They obtained not only a measurable deviation of the original beam of X-rays but also a recognizable spectrum. From this and other work it can be stated without doubt that the refractive index of glass for ordinary X-rays is about 0.999995, which is slightly less than unity. (Compare this with the value for optical light, which is, in the visible region, considerably greater than 1.) The meaning is that X-rays, in passing through a prism, are deviated very slightly *away* from the base of the prism; ordinary optical light is bent in the opposite direction. This result must not be interpreted as indicating a dissimilarity between light and X radiation. There are sound theoretical reasons for this behavior. Making due allowance for the vastly different wavelengths, X-rays behave in the same manner as visible light.

Diffraction by crystals. The Laue diagram. The technical difficulties confronting the use of ordinary optical diffraction gratings in the

field of X-rays are due in the main to the shortness of the wavelengths. In 1912, Max von Laue suggested that a natural crystal might serve as a three-dimensional grating for X radiation. His idea was put to test by Friedrich and Knipping, with an apparatus such as is suggested in Fig. 5-5. Here T is the target of an X-ray tube, S_1 and S_2 are small circular holes, C is a thin crystal of (say) potassium iodide, and P a photographic plate. The experiment produced

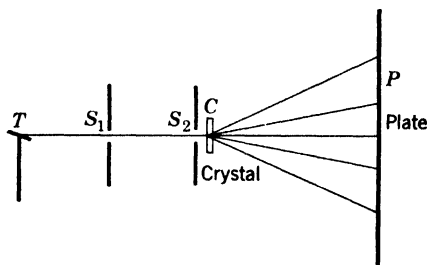


Fig. 5-5. Diagram of experiment for taking Laue photographs. X-rays from a target T pass through small holes S_1 and S_2 before traversing the crystal C .

on the plate a regular pattern of diffraction spots called a Laue diagram, of the type shown in Fig. 5-6. That a pattern of this kind should be

formed when X-rays pass through a three-dimensional grating like a crystal is conclusive proof that X-rays have the properties of waves. Thus many phenomena—polarization, diffraction by ruled gratings, refraction through prisms, diffraction by crystals—show independently that X-rays are electromagnetic waves.

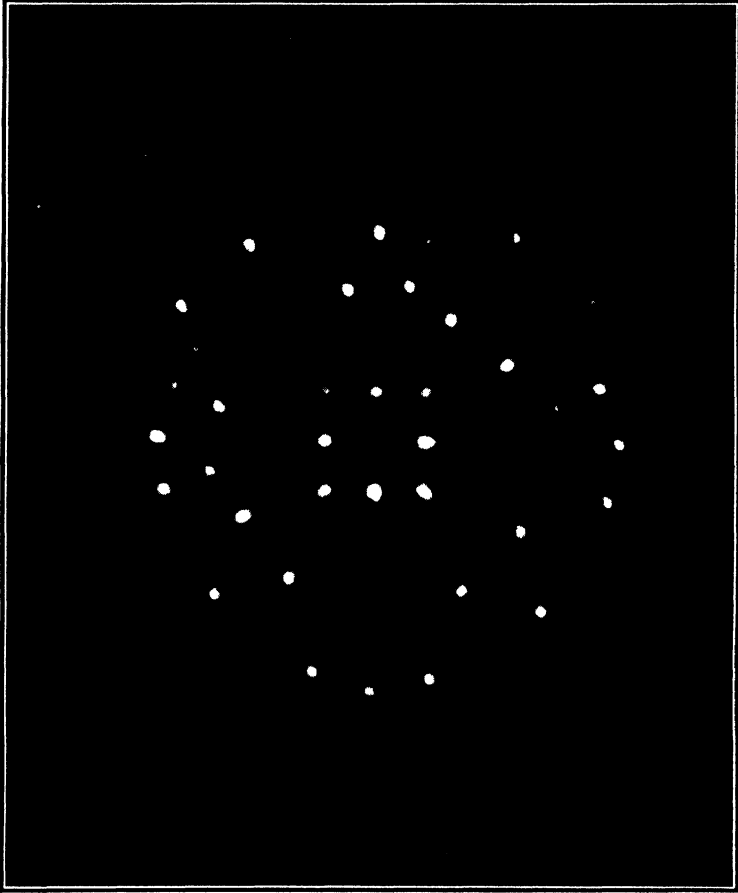


Fig. 5-6. Laue photograph of potassium iodide (*courtesy of S. S. Sidhu*).

The direct interpretation of such a photograph as Fig. 5-6 is somewhat complex, though the mechanism involved can be understood simply by the explanation offered by W. L. Bragg (1913). It is possible to draw various planes in a crystal, some passing through a large number, others passing through a small number, of atoms. Bragg showed that the

positions of the spots in the Laue diagram could be described accurately if it were supposed that the X-rays were reflected from such planes, the intensity of the spots being dependent on many factors including the number of atoms lying in any typical plane. This interpretation provided a convenient mental picture of the process; it did not deny that the phenomenon was actually one of scattering or diffraction. The

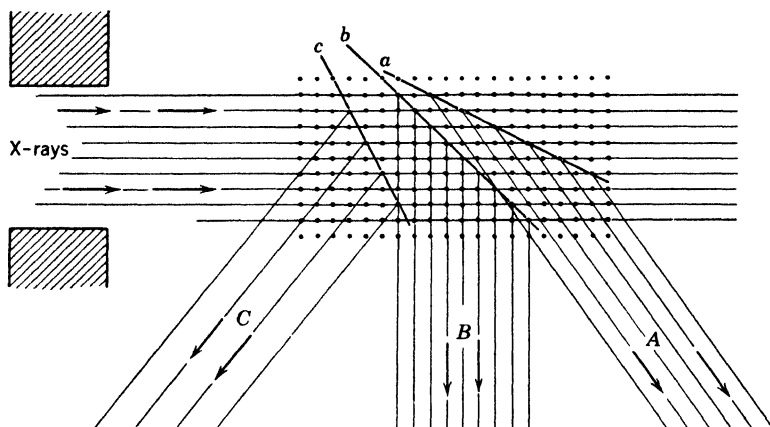


Fig. 5-7. Diagram to illustrate reflection of X-rays by planes of atoms inside a crystal. Although reflection is shown occurring only from single planes, simultaneous reflection also takes place from parallel planes. The main beam becomes less intense as it penetrates the crystal, for energy is being removed from it by reflection at the planes a , b , c , etc. The incident beam is assumed to contain a range of wavelengths. The reflected beams traveling away in the directions A , B , C , etc., are monochromatic.

mechanism is indicated in Fig. 5-7, where the incident beam is shown meeting planes a , b , c which reflect parts of the radiation to new directions A , B , C . Bragg reasoned that since the concept of *reflection* of X-rays from planes of atoms gave a simple justification of the result of the experiment of Friedrich and Knipping, then it ought to be applicable just as readily at an outside facet or a cleavage face of a crystal, since these faces are just as much planes of atoms as any of the interior planes a , b , c .

5. Bragg's Law

Diffraction of X-rays from crystal faces. First consider the matter theoretically. A cleavage plane, enormously magnified, is repre-

sented in cross section by the row of dots A in Fig. 5-8. Just as in the case of light, it might be expected that X-rays could be reflected from the surface layer, following the usual optical laws, whatever the angle of incidence, if diffraction could be neglected. But X-rays penetrate easily through matter; hence some radiation will be diffracted by layer A , the remainder will penetrate to layer B , part being diffracted there, part going still deeper. Hence, any actual diffracted beam will be made

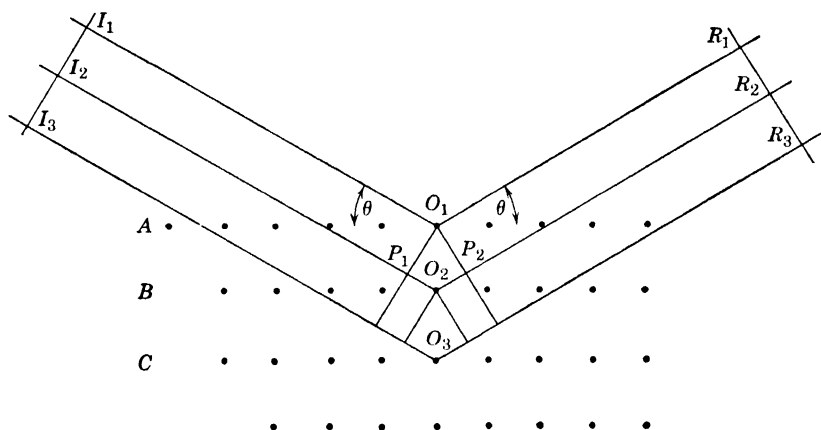


Fig. 5-8. Diffraction of X-rays from a crystal face. Radiation is diffracted not only from the top layer of atoms A but also from deeper lying layers, B , C , etc., to which the incident rays penetrate.

up of contributions, differing in intensity, coming from a very large number of layers. In the diagram, I_1O_1 , I_2O_2 , I_3O_3 represent parallel rays falling on the crystal at a glancing angle θ . This is the complement of the angle of incidence as employed in optics. The "reflected" rays O_1R_1 , O_2R_2 , O_3R_3 make equal angles θ with the crystal planes. It must not be assumed, however, that the effect of each crystal plane A , B , \dots can be observed independently of its neighbors. The resultant beam arises from the cooperative scattering from these different layers. The distance $I_1O_1R_1$ traveled by the first ray is shorter than $I_2O_2R_2$, which again is shorter, by the same amount, than $I_3O_3R_3$. A strong diffracted ray will be obtained at $R_1R_2R_3$ only if the waves arrive there in phase, so as to reinforce one another. This condition restricts the possible angles at which diffraction can occur. The requirement for a strong diffracted beam is that the path difference between successive rays be a whole number of wavelengths λ . This condition is $(I_2O_2 + O_2R_2) - (I_1O_1 + O_1R_1) = n\lambda$, where n is a whole number, called the order of

the spectrum. Using the obvious construction in the diagram,

$$P_1O_2 + O_2P_2 = n\lambda$$

i.e.,
$$2O_1O_2 \sin \theta = n\lambda$$

or
$$2d \sin \theta = n\lambda \quad (3)$$

where d , the grating space of the crystal, is written for O_1O_2 . This is known as Bragg's law. If $n = 1$,

$$\sin \theta_1 = \lambda/2d \quad (4)$$

This equation gives the smallest angle at which reflection can occur for particular values of λ and d . The similarity of Bragg's formula to that derived for a diffraction grating is obvious. It should be noted, however, that the d in equations 3 and 4 is measured perpendicular to the reflecting planes of atoms. In equation 2, p. 56, the symbol d , representing the grating space of an optical grating, is measured perpendicular to the lines of the grating, but in the plane of the grating. In the one case the diffraction is a volume effect, in the other a surface effect.

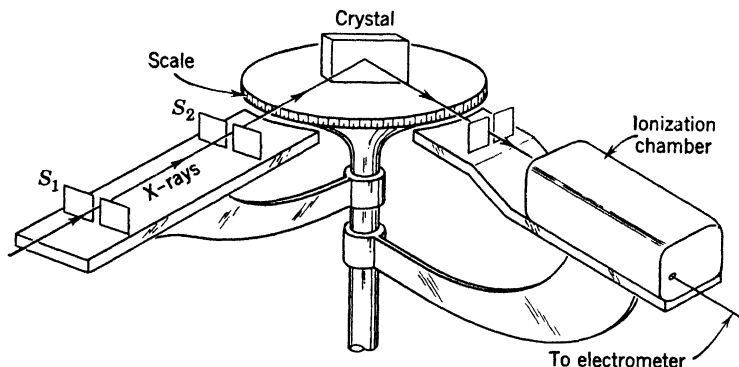


Fig. 5-9. Simplified drawing of X-ray ionization spectrometer. Since the source of X-rays is usually bulky and heavy, the arm carrying the slits S_1 and S_2 is ordinarily fixed in position. The table on which the crystal is mounted and the arm carrying the ionization chamber are independently rotatable. When observations are being made, both table and arm must be clamped at such positions that the glancing angles of incidence and of reflection at the crystal face are equal.

Spectra by the ionization method. An experimental investigation of the angles at which a beam of X-rays is intensely reflected from a crystal face is most conveniently carried out with the help of an ionization spectrometer. In its simplest form (Fig. 5-9) this resembles a spectrometer used for optical spectrum analysis, with the following modifi-

cations. The collimator lens and brass slit are replaced by two or more parallel lead slits; a crystal with its cleavage face vertical takes the place of the prism or grating; and an ionization chamber, its entrance guarded by still another slit, is substituted for the telescope. The ionization chamber, like the telescope, is capable of rotation about the axis of the instrument. Sometimes it is geared to the table on which the crystal is mounted so that the chamber turns through an angle 2θ while the crystal turns through an angle θ , thus automatically keeping the ionization chamber in a position where it will receive the beam reflected from the cleavage face. This is necessary, if, as is usually the case, the X-ray tube is fixed in position. Two typical ionization records

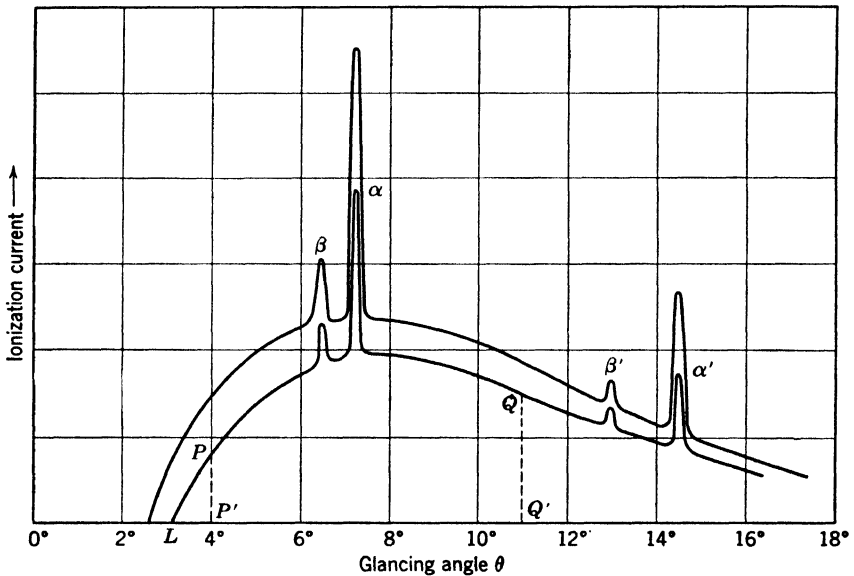


Fig. 5-10. Ionization spectra of X-rays from a molybdenum target, recorded after reflection from a rock salt crystal. The two curves correspond approximately to voltages of 40,000 and 50,000 applied to the tube. The peaks $\alpha\beta$ and $\alpha'\beta'$ are the K characteristic spectrum lines of molybdenum, shown in the first and second orders.

At L is the short wavelength limit of the continuous part of the spectrum.

obtained with such a spectrometer when X-rays from a molybdenum anticathode were reflected from a crystal of sodium chloride are shown in Fig. 5-10. They were obtained with different voltages applied to the X-ray tube. The ordinates represent intensities, plotted in arbitrary units; the abscissas, glancing angles. We interpret particular points on the diagram thus: under the conditions appropriate to the lower

curve, the relative intensities of the ionization currents when the glancing angles are 4° and 11° are given by the ratio of the ordinates PP'/QQ' . The graphs in Fig. 5-10 can obviously be considered as composed of smooth curves on which are superimposed several sharp peaks; the peaks correspond to spectrum lines, which make up the characteristic radiation, the curves to what is called the continuous spectrum. One of its most important features is the sharp short-wavelength limit at L . As the operating potential on the tube increases, the spectrum lines hold their positions and become more intense, while point L moves to still shorter wavelengths, that is, to smaller values of θ .

The dependence of the position of point L on the potential difference applied to the tube receives a simple explanation on the basis of the quantum theory. If a single electron of charge $-e$ in the X-ray tube falls through a potential difference V , its energy is Ve . Certainly not more than this energy can be transformed into an X-ray photon, so that the limiting conditions can be written $Ve = h\nu = hc/\lambda$, where ν and λ refer respectively to the maximum possible frequency and minimum possible wavelength of the X-rays. The equation shows that, if V is increased, λ diminishes, so point L moves to a shorter wavelength; that is, to a smaller value of θ . This regularity is often known as the Duane-Hunt law, after its discoverers at Harvard University.

The grouping of the peaks $\alpha\beta$ is the same as that of $\alpha'\beta'$; the latter group occurs at glancing angles whose sines are twice those of the former. These groups are therefore interpreted as first- and second-order spectra of the same group of lines; for, considering only the peaks α and α' , and using equation 4, $\sin \theta_1 = \lambda/2d$ for the first order, and $\sin \theta_2 = 2\lambda/2d = 2 \sin \theta_1$ for the second order.

It is obvious that, if the glancing angle is fixed at some particular value, the reflected beam will be approximately monochromatic. If such a beam is required for experimental purposes, it is customary, for the sake of intensity, to choose θ so that a prominent spectrum line, say α , is reflected. If the grating space d were known, it would be possible to measure the wavelength of this radiation; and conversely, if we have determined a single wavelength, we shall be able to find the grating space of any crystal. This cannot, however, be done rigorously until some knowledge is obtained of the structure of the crystal.

6. Simple Crystals

The crystal lattice. A natural crystal, or a fragment of a natural crystal, has recognizable features which are the same for all specimens; the plane faces intersect at angles which fall into a definite pattern—

such angles as one would expect when the supposition is made that the atoms are arranged in a regular array. It is this geometrical perfection that distinguishes a crystal from an amorphous substance like glass. Glass, when broken, takes on an infinite variety of different shapes, marked by edges of varying sharpness and surfaces that are seldom plane. The natural, and correct, conclusion is that, whereas the atoms of an amorphous substance are irregularly arranged, those of a crystal are built, one next to the other, according to a rigorous geometrical scheme. The fundamental units of which a crystal is composed may be simple atoms or complex groups of atoms. But always, this fundamental unit is repeated throughout the structure so that the situation of any one particular unit with respect to its neighbors is exactly the same as that of any other unit. In this chapter we shall confine our attention to the simplest of crystals, in which the fundamental unit is the atom. If the positions of the adjacent atoms in a crystal are joined by a suitable network of straight lines, a pattern of regular geometrical

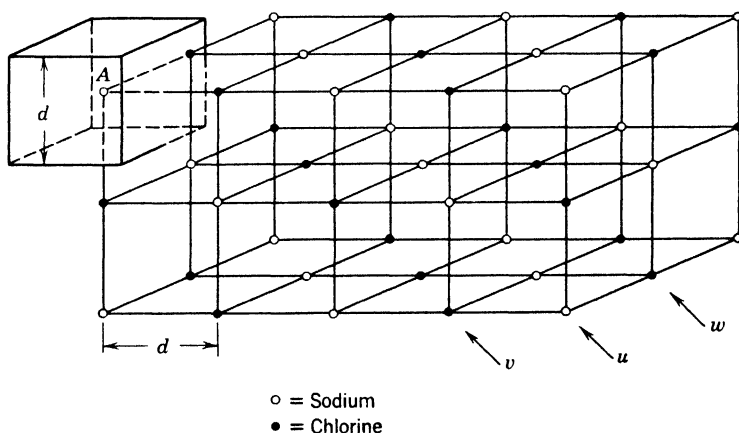


Fig. 5-11. Space lattice of sodium chloride (rock salt), oriented to show clearly that there are planes in the crystal that contain only sodium atoms, others that contain only chlorine atoms. The arrows u , v , w point to particular planes discussed in the text.

solids is formed, known as the space lattice of the crystal. An example of such a lattice is shown in Fig. 5-11, for the particular case of sodium chloride. One of the important scientific uses of X-rays is the discovery of the details of the lattices of crystals.

To develop the story in a logical fashion we ought to start with the observed external, large-scale properties of a crystal, such as its geo-

metrical shape, the positions of its natural cleavage planes and its density; couple these with the behavior of the crystal in reflecting or scattering X-rays; and deduce the true structure. To do this in a completely rigorous manner, discarding one false construction after another, would take more space than can be spared. We shall, however, do the next best thing, which is to show that the structure in Fig. 5-11 will behave towards X-rays as a crystal of rock salt (NaCl), or of sylvite (KCl), is observed to do.

A natural crystal of sodium chloride is cubical in shape; hence it seems probable that it is built up of unit cubes of atoms. Nowhere does X-ray evidence contradict this idea, which we may therefore assume for the moment to be correct. We shall *calculate* the grating space along the three perpendicular edges; but it should be pointed out that a rapid and convenient method for *measuring* grating spaces (p. 134) is now available.

One mole (58.5 gm) of NaCl contains 6.03×10^{23} molecules (Avogadro's number). The volume occupied by these is $58.5/2.17 \text{ cm}^3$, since the density of the crystal is 2.17 gm/cm^3 . Therefore, the volume occupied by 1 molecule is $(58.5/2.17) \div (6.03 \times 10^{23}) \text{ cm}^3$. However, 1 molecule contains 2 atoms; so the volume per atom is half this, or $22.4 \times 10^{-24} \text{ cm}^3$. But this volume represents an elementary cube whose side is equal to the grating space d , as indicated in Fig. 5-11 by the heavy lines that enclose the atom A . Hence, taking the cube root, $d = 2.81 \times 10^{-8} \text{ cm} = 2.81 \text{ \AA}$. If we were now to reflect a beam of X-rays from the top surface of the crystal, we could use equation 3 to find the wavelengths of the prominent lines in Fig. 5-10. Then, having determined the wavelength of some convenient, strong line, we could reflect that line from a face of any other crystalline substance, and thus find the grating space between similar planes of atoms all of which lie parallel to the outside face of that other crystal. In addition, a crystal could be broken along some of its natural cleavage planes, and the experiment could be done again for these new surfaces.

Miller indices. It happens that there are only three types of cubic lattices, that is, three different ways of arranging identical atoms in a cubical array, so that the surroundings of *any atom* have the symmetries possessed by a single geometrical cube, no more and no less. These three types are known by the names simple cubic, body-centered cubic, and face-centered cubic, all illustrated in Fig. 5-12. Here, for the moment, we are thinking of a crystal such as a pure metal, comprising only one kind of atom, and not of one like rock salt which is made of sodium and chlorine. It is now necessary to be able to describe similar planes of atoms by some shorthand notation. Parallel planes such as $DEAB$, $D'E'A'B'$ are obviously similar; hence we may take one of

these as typical. Instead of describing the directions of lines such as AB and AE in a particular plane, it is more convenient to consider the direction of a line drawn from the origin O , perpendicular to that plane, such as OF , which is perpendicular to the plane $DEAB$. The angles that it makes with the three principal axes are: with OA , 45° ; with OB , 45° ; with OC , 90° . The cosines of these angles are: $1/\sqrt{2}$, $1/\sqrt{2}$, 0 .

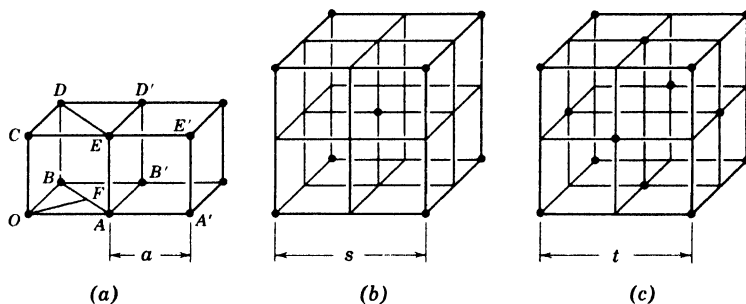


Fig. 5-12. Types of cubic crystals: (a) simple cubic; (b) body-centered cubic; (c) face-centered cubic. The edge of the unit cell, the distance along the x axis from one atom to the next identical atom, is marked in the three cases by the symbols a , s , t .

The simplest possible integers expressing the ratio of these three cosines are 1, 1, 0. These three numbers, called the Miller indices, describe the plane $DEAB$, and all others parallel to it, which are similar. In the same way, the plane $AB'D'E$ is a 100 plane; $DD'B'B$ is a 010 plane; CAB is a 111 plane.

Miller indices may be worked out geometrically for any more complicated planes. If a simple cubic crystal were cleaved along the 110 planes, the distance between adjacent layers of atoms parallel to the cleaved surfaces would be OF , which is less than a , the distance between adjacent atoms along the principal axes (Fig. 5-12a). Hence, in reflecting X-rays from a 110 face, the d in equation 3 must be given the appropriate value, namely, $OF = \sqrt{2}a/2$. The reader will find it an interesting exercise to check Table 5-1 where the symbols a , s , t are those appearing in Fig. 5-12. It should be noted particularly that the grating spaces a , s , t along the principal axes of the three types of cubic crystals describe the distances *along the axes*, from one atom to the next *identical* atom. There might possibly be other atoms, not on the principal axes, or not identical, in between.

TABLE 5-1. Spacings of Important Planes of Cubic Crystals

	Spacings between		
	100 Planes	110 Planes	111 Planes
Simple cubic	a	$a\sqrt{2}/2$	$a\sqrt{3}/3$
Body-centered cubic	$s/2$	$s\sqrt{2}/2$	$s\sqrt{3}/6$
Face-centered cubic	$t/2$	$t/2\sqrt{2}$	$t\sqrt{3}/3$
	Spacings, Relative to the 100 Spacing		
	100 Planes	110 Planes	111 Planes
Simple cubic	1	0.707	0.577
Body-centered cubic	1	1.414	0.577
Face-centered cubic	1	0.707	1.154

Recognizing the different types of planes is difficult if the patterns are merely drawn on paper. A little time may well be spent in handling crystal models such as are found in most laboratories, or in constructing models from wire and putty. Different planes are easily picked out if the model is held near a wall illuminated by a distant light. The planes of atoms show up clearly as rows of atoms in the shadow picture.

If now we can by any means measure the relative distances between the 100, 110, and 111 planes in a cubic crystal, we shall have a key to the distribution of points on the space lattice; that is, we shall be able to decide whether a cubic crystal is simple cubic, body-centered cubic, or face-centered cubic.

★ **The structure of NaCl and KCl.** The problem was first solved by W. H. and W. L. Bragg, who reflected X-rays from crystals of sylvite and of rock salt, cut with surfaces parallel to the 100, 110, and 111 planes in turn. The experimental results are shown, in somewhat idealized form, in Fig. 5-13. Looking first at the reflection from the 100 planes of KCl, it is seen that the X-ray beam includes two prominent lines of different intensities. These are labeled α and β . The lines appear in the same relative intensities in the second order, and a faint third order can be noticed. Confining our attention to the strong α line, we see that the positions of the peaks at $2\theta_1$, $2\theta_2$, $2\theta_3$, are given by equations $\lambda = 2d \sin \theta_1$, $2\lambda = 2d \sin \theta_2$, $3\lambda = 2d \sin \theta_3$, each of which is a special case of equation 3, in which d represents the grating space for the 100 planes of KCl. In the spectrum from the 110 planes of

sylvin, only two orders are recorded, the first occurring at a greater angle than the first reflection from the 100 planes.

★ Let us now compare the grating spaces for the 100, 110, and 111 planes of sylvin. The necessary information can be obtained from the positions of the strong α lines in the first order. These positions, as

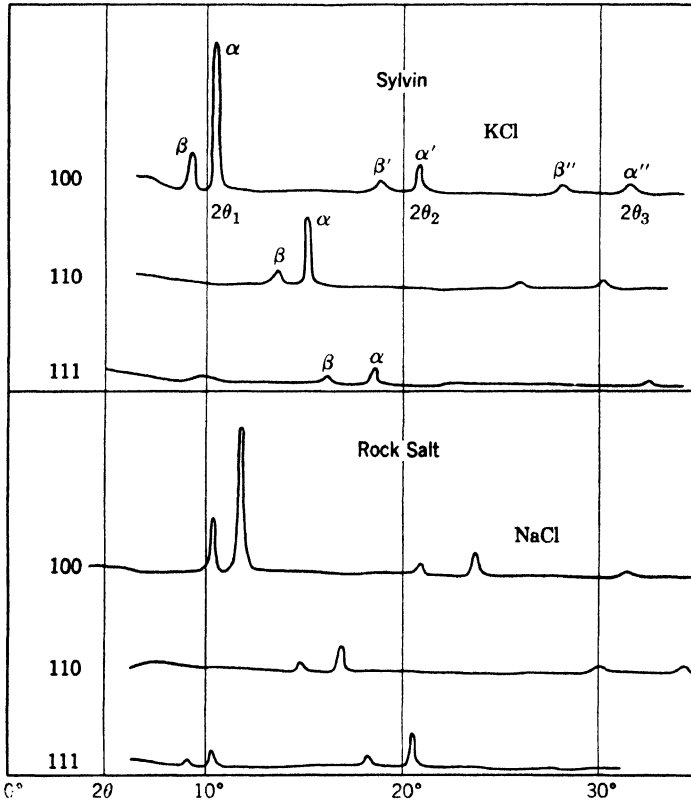


Fig. 5-13. Ionization spectra of X-rays (K -radiation of palladium) reflected from various planes of potassium chloride and of sodium chloride. Since the principal peaks occur at different angles in the various spectra, it is very obvious that the interplanar spacings are different. (After W. H. Bragg.)

measured by Bragg, are 5.22° , 7.30° , 9.05° . The corresponding grating spaces are almost exactly in the ratio $1:0.707:0.577$. The only row of Table 5-1 which suits these figures is that for a simple cubic crystal.

★ The same technique must now be applied to NaCl. If the positions of the three first-order α lines (Fig. 5-13) are measured, the corresponding

grating spaces for the 100, 110, and 111 planes turn out to be in the ratio 1.0:0.707:1.154, which agrees only with the last row of Table 5-1. In other words, NaCl is a *face-centered cubic crystal*. Remember that we have just found evidence indicating that KCl is a *simple cubic crystal*.

★ **An apparent contradiction.** Now this appears to be a very unsatisfactory conclusion. The chemical properties of NaCl and KCl are extraordinarily similar, and there is every reason to expect them to have the same crystal structure. Actually, our dissatisfaction need be only temporary, because there is a simple explanation of the difficulty. The confusion has arisen because we have not yet taken into account the fact that each of the crystals under discussion is made up of two kinds of atoms, sodium and chlorine in the one case, potassium and chlorine in the other.

★ A glance at Fig. 5-13 shows that, in NaCl, the first order of the strong α line from the 111 planes is actually found at a smaller angle than the first order from the 100 planes! This means that the distance between the planes which causes the first-order 111 peak is greater than that which causes the first-order 100 peak. An examination of Fig. 5-11 will show how this occurs. The 111 planes which give this weak first-order reflection are like those marked v and w . They are similar planes. In between them are other planes made entirely of different atoms. Now if the X-rays are reflected in the first order from planes like v , w , the radiation from v , let us say, lags 1 wavelength behind that from w . But when the crystal is in a position to give this reflection, the in-between planes (like u) are also able to reflect, and the radiation they reflect will lag only half a wavelength behind that from planes like w . Hence, the reflection from planes like u will to some extent neutralize the reflection from planes like v and w . In the second order of this type of reflection, however, the interplanar lag is 2λ in one case and λ in the other; the radiations are in phase, and the α line appears in greater intensity.

★ May it not be that the first-order reflection from the 111 planes of KCl is suppressed completely? We have just seen that the corresponding reflection in NaCl is comparatively weak because of destructive interference between radiations reflected from dissimilar parallel planes like u and w . If, in KCl, the first order is absent entirely, it must be concluded that planes like u and w reflect X-rays equally strongly and therefore cancel one another's effects exactly.

★ Although it is customary to regard a crystal as reflecting X-rays, a truer statement would be that the rays are selectively scattered, thus linking the phenomenon of crystal reflection with the scattering of X-rays, as described in Section 3 of this chapter. But the amount of

scattering by an atom depends on its number of electrons. A normal potassium atom has 19 electrons and a normal chlorine atom 17. These numbers are not equal, yet a plane of potassium atoms scatters just enough to cancel the scattering from an equally populated plane of chlorine atoms. The reasonable conclusion is that, in the crystal of KCl, the atoms exist as ions, K^+ and Cl^- , each of which possesses 18 electrons. No wonder KCl behaves as a simple cubic crystal! In NaCl, the ions have 10 and 18 electrons, respectively, and careful measurements have shown that the first-order reflection from its 111 planes has the relative intensity which would be expected from this distribution of scattering electrons.

To sum up, both KCl and NaCl have the structure shown in Fig. 5-11. The metallic ions alone form a face-centered cubic structure; so do the chlorine ions alone. The two lattices are interlocked, however, with the result that the face-centered structure is concealed in KCl, because of the equality of scattering power of the K^+ and Cl^- ions. In NaCl, on the other hand, the X-ray reflections reveal the true face-centered structure. It is worth noting that what appeared at first sight to be a difficulty in explaining the structures of NaCl and KCl has led to new knowledge, namely, that these particular crystals are ionic. This pattern is typical of scientific discovery.

Powder method of crystal analysis. The structure of a crystal is scarcely ever deduced by only one method of analysis. In practice, the Bragg method is less convenient and less frequently used than the Laue method; and though we describe it last, the powder method, frequently known by the names of its first users, Debye-Scherrer-Hull, is perhaps the most versatile of all. Often a crystal cannot be obtained conveniently in a large enough size to use the Bragg technique, but it may be available in powdered form, that is, in very tiny crystals. In this case a beam of X-rays of *one* wavelength is sent through a small pellet of the powder in the style shown in Fig. 5-5. There then appears on the photographic plate not an array of spots but a series of concentric rings, for there are always some of the tiny crystals lying by chance at just the correct angles for the reflection of the radiation which is used. From the diameters of the rings, the pellet-to-plate distance, and the known wavelength of the X-rays, interplanar distances in the little crystals may be calculated. These distances are the same as they would be in a large crystal of the same substance. A photograph of powdered tungsten is reproduced in Fig. 5-14. It was obtained, however, not on a flat photographic plate as in Fig. 5-5 but on a strip of film placed cylindrically, at a distance of a few centimeters round the crystal pellet. Thus, only portions of the circles are recorded. In Fig. 5-14, *B* is in

the straight forward direction. The spot *A* is 180° away from *B*, on the line between the target and the crystal pellet.

Absolute measurement of wavelengths. The calculation of the grating space of a sodium chloride crystal demanded a knowledge of the values of several constants of great importance in atomic physics. One of these was the Avogadro number which used to be determined from the charge of the electron coupled with other experimental measurements. It is obvious, therefore, that the grating space so determined and the wavelengths derived from it were at least as inaccurate as all the quantities that were included in the calculations.

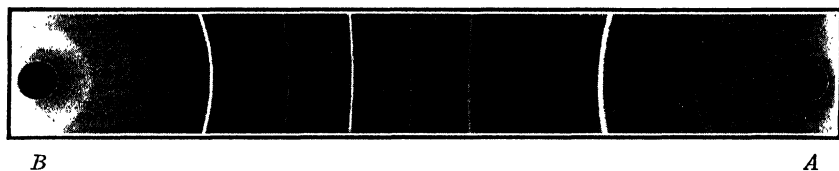


Fig. 5-14. A photograph of powdered crystalline tungsten taken by the Debye-Scherrer-Hull method. Monochromatic radiation from a copper target was used. The tiny powdered specimen was rotated continuously during the exposure. The film was placed along a cylindrical surface of 5.73-cm radius, at the center of which was the tungsten pellet. The circular patches *A* and *B* represent holes punched through the film, through which the X-rays entered and left the camera. Thus some of the lines shown represent reflections from the specimen at angles greater than 90° but less than 180° from the forward direction of the beam. (Courtesy of S. S. Sidhu.)

The optical way of measuring X-ray wavelengths by diffraction from ruled gratings (p. 119) involves no such uncertainty, since it depends only on equation 2. Indeed, so accurate are the wavelength measurements provided by ruled gratings that the historical process is now reversed. From the accurate wavelengths are deduced in turn (*a*) Avogadro's number, (*b*) the charge of the electron, and (*c*) grating spaces of crystals. The work of several investigators, notably Bearden, in the 1920's and 1930's, demonstrated that the value of *e* derived from ruled-grating measurements was about 0.2 per cent greater than that determined by the older, direct method of Millikan. The new value of *e* turns out to be 4.802×10^{-10} esu.

7. Emission Spectra

Moseley's law. If ionization spectra like those in Fig. 5-10 are determined with the same crystal for two elements close together in the periodic table (say tungsten and platinum), the curves are found to be

similar in appearance, but the characteristic peaks for the heavier element are shifted bodily towards smaller angles, that is, towards shorter wavelengths. The first systematic investigation of a series of neighboring elements was made by Moseley (1913). His results, recorded photographically instead of by an ionization chamber, are shown in Fig. 5-15. Here the wavelengths increase as we go toward the right. For each element the figure shows two spectrum lines, whose wavelengths increase with beautiful regularity as we go step by step up the diagram. Brass, an alloy of copper and zinc, shows four lines; the second and fourth are identical with those of copper; the other two are due to zinc, showing clearly that the X-ray spectrum depends to an excellent approximation on the atom alone, not on its environment. At the top of the figure there is a sudden jump between titanium and calcium. This shows unmistakably where the somewhat rare element scandium must be placed. It is clear from this example that X-ray spectra are an infallible guide in the classification of elements in the periodic table. In the

past they have supported chemical evidence in showing what elements were unknown. Since the time of Moseley's work, new elements, for example, hafnium, have thus been found and placed in their appropriate places in Mendeleef's table. In Fig. 5-15, nickel and cobalt are placed in wrong order, judging by their atomic weights, but obviously their inversion would destroy the harmony of the picture. Guided by such observations, Moseley stated, "We have here a proof that there is in the atom a fundamental quantity, which increases by regular steps as we pass from one element to the next. This quantity can only be the charge on the central positive nucleus," which has since been identified as the atomic number of the atom, discussed from a different point of view in Chapter 2.

A glance at Fig. 5-15 shows that the wavelength steps between successive elements become larger for lighter elements; the spectra lie on a curve. It is much easier to formulate a law mathematically from a graph that is a straight line than from one that is curved. Moseley

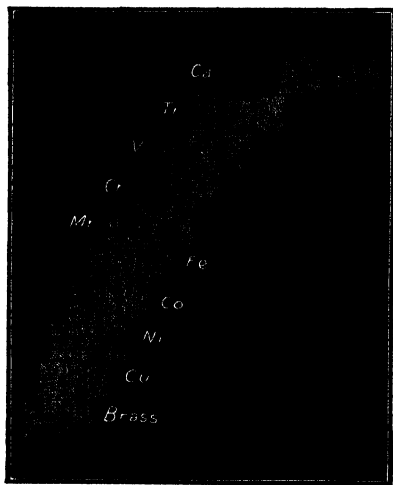


Fig. 5-15. *K*-series emission lines of elements from calcium (20) to copper (29). This is a reproduction of the original composite picture made by Moseley.

found that if the square root of the wave number $\tilde{\nu}$, or of $1/\lambda$, for each of the lines was plotted against the corresponding atomic number, the graph was linear. Evidence of the same kind as he found, but for a

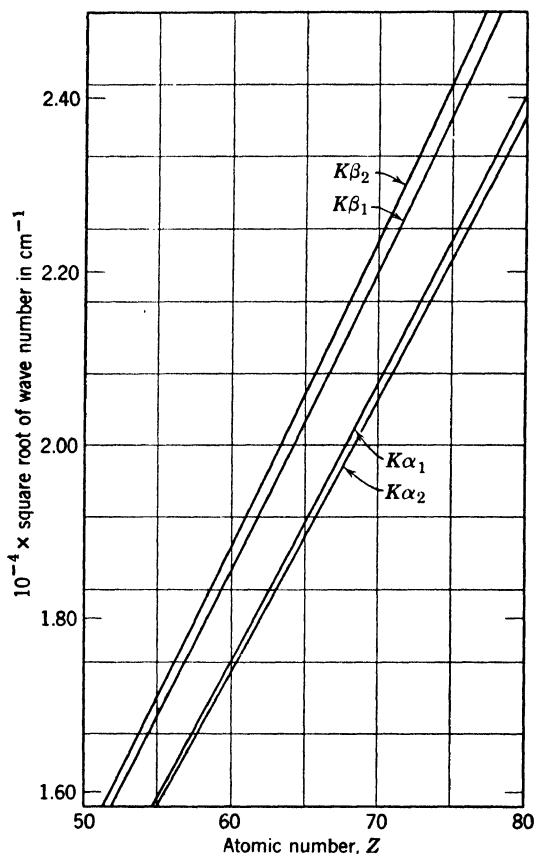


Fig. 5-16. A Moseley diagram. The square root of the wave number $\tilde{\nu}$ is plotted against the atomic number Z for the four K lines of the elements numbered 55 to 80. To make the ordinates convenient small numbers, the square roots of the wave numbers are multiplied by 10^{-4} . The linearity of the plots shows that the square root of the wave number is almost proportional to Z .

different part of the periodic table, is shown in Fig. 5-16. Each of the four graphs in Fig. 5-16 follows the variation of one particular spectrum line from element to element. Each is representable by an equation of the type

$$\tilde{\nu}^{1/2} = a(Z - b) \quad (5)$$

where Z is the atomic number, and a and b are constants, which differ slightly for each of the four graphs. For elements of low atomic number, at low resolution, the four lines merge into two, thus explaining why, in Fig. 5-15, there are only two spectrum lines for each element. A close observer will remark that the graphs are not quite straight. This deviation from linearity has been explained. It is due to the change of electron mass with velocity.

From equation 5 we obtain the emitted energy,

$$h\nu = hc\bar{\nu} = hca^2(Z - b)^2 \quad (6)$$

This is reminiscent of the formula for the frequencies emitted by hydrogenic atoms, presented in Chapter 4, except that the atomic number is replaced by an "effective" atomic number. For these lines, which are the K radiation mentioned on p. 117, b is about unity. This means that the electron which makes the radiative transition is partially screened from the attraction of the nucleus by its companion electrons.

The L , M , N radiations also consist of close groups of lines, which obey Moseley's equation 5, but with very different values of the constants a and b . Roughly speaking, the wavelengths of the K , L , M , N lines of a particular element are in the ratios of 1:7:30:100. In the same order the complexity of the series increases. A few prominent X-ray lines are listed in Table 5-2. The values quoted are based on measurements with ruled gratings, although only one or two of them represent direct experimental determinations by this method.

TABLE 5-2
Wavelengths of X-Ray Emission Lines, in Angstrom Units

Element	K series				L series		M series
	α_2	α_1	β_1	β_2	α_2	α_1	α_1
13 Al	8.3387		7.982				
29 Cu	1.5446	1.5408	1.3923	1.3813	13.335		
42 Mo	0.7137	0.7094	0.6323	0.6210	5.413	5.407	
47 Ag	0.5639	0.5595	0.4971	0.4871	4.163	4.155	
74 W	0.2138	0.2090	0.1844	0.1795	1.4876	1.4766	6.984
78 Pt	0.1905	0.1826	0.1641	0.1592	1.3244	1.3132	6.047

Interpretation of X-ray spectra. A simple explanation of X-ray spectra is possible by an extension of the Bohr theory. It has been deduced from simple experiments that there exist, within an atom,

shells of electrons of differing energy values. When a monochromatic beam of X-rays of frequency ν_1 falls on a thin metal foil, the partial absorption of the rays causes the emission of photoelectrons. These photoelectrons are found to have not a continuous range of energies but only certain definite values, none exceeding $h\nu_1$, where $h\nu_1$ is the energy of one photon in the X-ray beam. Suppose that E_1, E_2, E_3 , etc., are the observed kinetic energies of the emerging electrons. Then, since X-ray photons are absorbed whole by electrons within atoms, each emerging electron must originally, at the instant of absorption, have had an amount of energy $h\nu_1$. But as the observed energies are only E_1, E_2 , etc., varying parts of the original energies must have been used up by the electrons in escaping from their parent atoms. These amounts of used-up energy have the discrete values $h\nu_1 - E_1, h\nu_1 - E_2$, etc. This means that the energy which must be furnished to one particular electron to expel it from an atom is not necessarily the same as is required for another electron in the same atom. The logical conclusion is that, inside atoms, different electrons or groups of electrons exist normally in different energy states. These groups are known by the letters K, L, M , etc., in order of increasing distance from the nucleus.

We thus regard the planetary electrons of a normal atom as grouped round the nucleus in shells: two K electrons in a small shell, eight L electrons on a much larger one; next, the M electrons, and so on, until we arrive at the valence electrons, at the periphery. The number of complete shells depends on the atomic number of the atom. In carbon, the L electrons are also the valence electrons; in krypton the N electrons; and in uranium the P electrons play this part. The emission of a line of the K series takes place when an electron farther out from the nucleus falls into the innermost or K shell. This process naturally liberates energy, which appears in the spectrum line. But this process cannot occur unless there is a vacancy in the K shell, in accord with a general principle named after Pauli, explained on p. 207. The prime requisite, therefore, for the emission of a K -series line is that the atom shall have already lost an electron from the K shell; normally this "lost" electron has been ejected completely from the atom, that is, it is usually a photoelectron, though under suitable experimental conditions it may be carried to an outer orbit. To restore the atom to its normal state, an electron goes to the K shell from one of the outer groups, usually from the L shell; this leaves a space in the L shell which is filled in a similar fashion by the movement of a more distant electron. Finally the valence shell is completed by the usual process of recombination. Hence, the ejection of one photoelectron from the K shell can initiate the successive emission of a large number of spectrum lines.

Energy-level diagram. Since the various electron shells have differing energy values, it is convenient to represent them by an "energy diagram," in which vertical distances correspond to energy differences and have no direct relation to the geometrical dimensions of the atom. Such a diagram is given in Fig. 5-17*b*. We say that an atom is in the

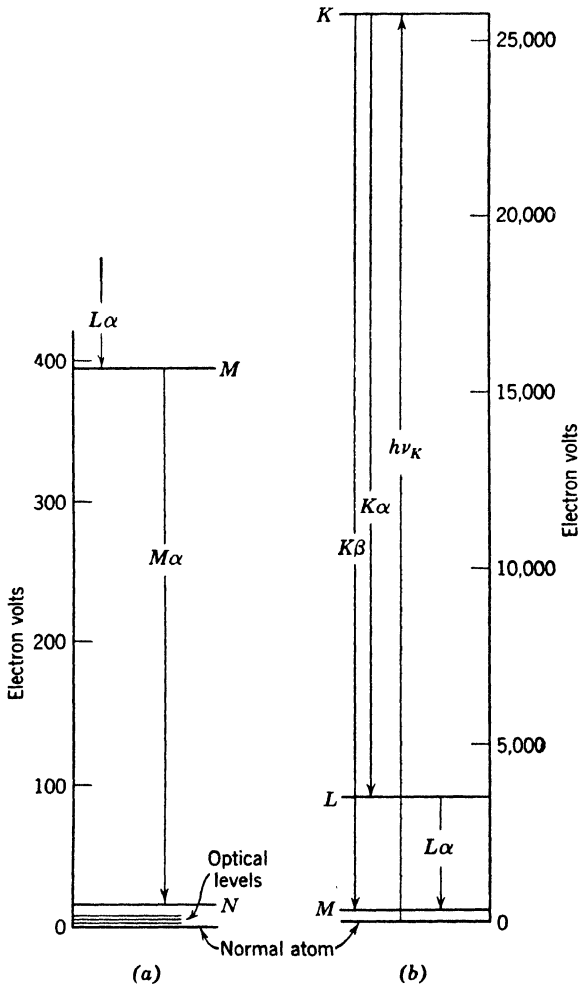


Fig. 5-17. X-ray energy-level diagrams, showing the relative positions of optical and X-ray levels. Numerical values are approximately correct for silver. The vertical scale of (a) is forty times as great as that of (b). Here the optical levels of an atom, like those depicted in Fig. 4-4*b*, p. 101, occupy a small region just above the level representing the normal atom.

energy state represented by the horizontal line K when it has lost a photoelectron from the K shell, thereby gaining energy. If an electron goes from the L shell to fill this vacancy, the atom is left in the L state of lower energy, represented by the line L . The change in energy we denote by the arrow $K\alpha$, meaning that the atom has changed from the K state of high energy to the L state of lower energy; the difference in energy is radiated as a spectrum line, the $K\alpha$ line, a member of the K series. Similar explanations apply to other arrows in the diagram. The length of an arrow obviously represents the amount of energy released and hence the energy of the photon emitted. If E represents the energy difference between the K and M states of the atom, it is also the energy emitted in the $K\beta$ line. Applying Bohr's quantum condition,

$$E = h\nu = hc/\lambda \quad (7)$$

where ν is the frequency and λ the wavelength of the $K\beta$ line. The student will easily see that it is of shorter wavelength than the $K\alpha$ line. The energy difference between the $K\alpha$ and $K\beta$ lines is the same as that between the L and M energy states; hence a study of the lines leads to a determination of the relative positions of the energy states.

Every heavy element has an optical spectrum, represented by an energy diagram like that of the light atom hydrogen, Fig. 4-4*b*, p. 101, but much more complicated, and an X-ray spectrum. The energy-level diagrams for these two spectra, and the relationship between them, are shown in Fig. 5-17*a* and *b*. Since the energies of X-ray spectrum lines are of the order of thousands of electron volts, while those of optical spectrum lines are but five or ten electron volts, it is difficult to represent the two sets of levels clearly in one picture. Figure 5-17*a* is, in fact, a forty-fold enlargement of the lowest part of Fig. 5-17*b*. The whole of the optical energy diagram is compressed into a small space at the bottom of Fig. 5-17*a*. It is too small to show at all in Fig. 5-17*b*. For simplicity, the zero of the scale has been put at the level labeled "normal atom." (When dealing with optical spectra alone, however, the zero is usually put at the top of the optical levels, as was done in Fig. 4-4*b*, and many writers adhere to this convention when dealing with X-ray levels.)

Actually, the X-ray diagram is complicated by the division of the L , M , N states, etc., into several close substates; the K state alone remains single. It is this finer structure that accounts for the wealth of X-ray spectrum lines in the various series. The occurrence of multiple substates will be easier to understand when it is shown (Chapters 7 and 8) that not one but a set of quantum numbers is required to specify the role of each electron in a complex atom.

8. Absorption Spectra

The mechanism of absorption. The absorption of X-rays is complicated by certain phenomena not mentioned in Section 2. Suppose that a beam is homogeneous and that its wavelength can be varied at the will of the experimenter. Suppose further that thin sheets of platinum are used as absorbers. The K -series emission lines of platinum have a wavelength about 0.16 Å. Suppose that we begin the experiment with an X-ray beam of wavelength 0.2 Å, and find, with the help of an ionization chamber, how much the intensity of the beam is reduced on passing through a fixed thickness of absorber. At 0.2 Å the rays do not have sufficient energy to ionize the K shell of platinum. Energy can therefore be removed from the beam only by scattering and by ionization of the L and M and outer shells of the absorbing atoms. If the wavelength of the primary beam is now reduced, the absorption coefficient μ decreases rapidly, approximately in proportion to λ^3 . However, at a value slightly less than 0.16 Å, the energy will be sufficient to ionize the K shell. This K ionization is an additional drain on the energy of the beam; so the platinum absorber shows a sudden increase in absorbing power. The result is easily shown graphically, if the absorption coefficient μ is plotted against λ . The processes we have been discussing cover the range $ABCD$ in Fig. 5-18*a*, the sudden increase BC taking place at a wavelength called the K absorption limit, λ_K , of platinum. Turning now to Fig. 5-18*b*, it will be seen that if platinum were used as an absorber of X-rays of wavelength 1.10 Å, the value of μ would be about 2000 per cm. On reducing the wavelength to 0.85 Å, μ would go up to about 4000 per cm, because the incident rays would now have enough energy to ionize the L shell of platinum. This ionization, which was not present at 1.10 Å, constitutes an additional drain on the energy of the primary beam. The L absorption limit of platinum lies between 0.85 Å and 1.10 Å. Actually, as the wavelength is reduced, the absorption increases suddenly three times at particular frequencies but apart from these discontinuities falls smoothly, following the λ^3 rule. These changes, as λ changes, demonstrate the existence of three L states.

The frequency ν_K of the original beam corresponding to the absorption discontinuity BC is given by the quantum relation $W_K = h\nu_K$, where W_K is the energy necessary to ionize the K shell. The characteristic K radiation cannot be emitted by an atom of the absorber until there is a vacancy in the K shell, that is, until the primary wavelength is reduced to λ_K . All the K lines, therefore, must have smaller energies, and longer wavelengths, than the K absorption limit λ_K . This is made clear by Fig. 5-17*b*. To raise an atom to the K state, an electron must

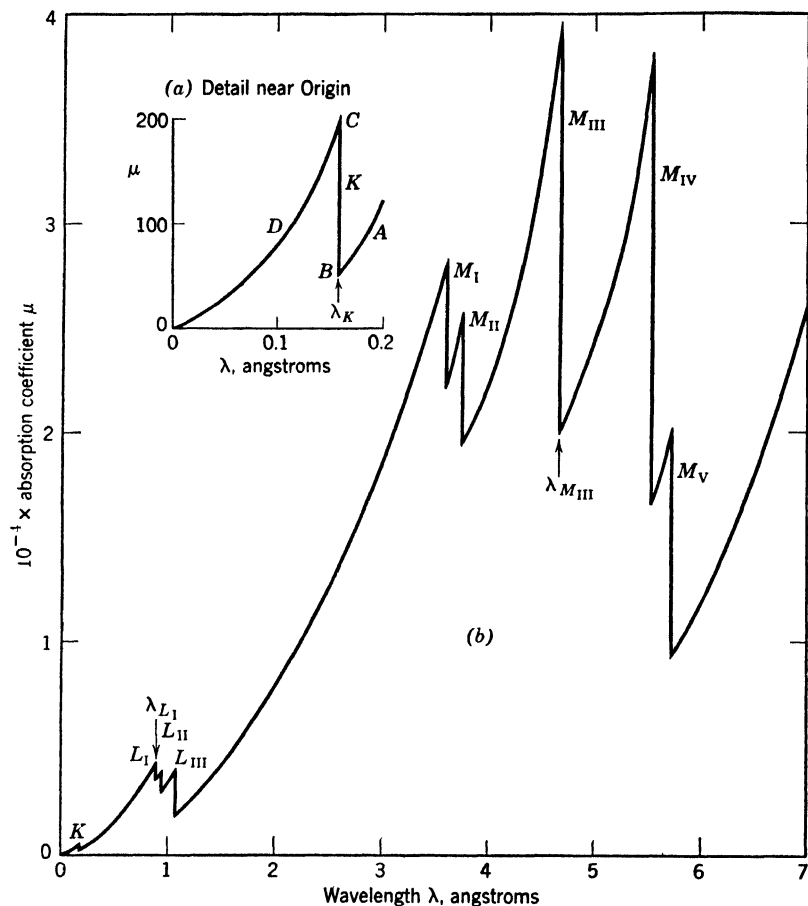


Fig. 5-18. X-ray absorption curve for the element platinum. The linear absorption coefficient μ is plotted against the wavelength of the radiation which is being absorbed. (a) shows a 10×50 -fold enlargement of detail near the origin in (b). Five M , three L , and one K absorption discontinuities are shown. The student will find it instructive to replot the curve, using wave number as abscissa.

be ejected from the K shell to beyond the range of influence of the atom, requiring an amount of energy $h\nu_K$. When a spectrum line is emitted, for example $K\beta$, not quite all of this energy is sent out as radiation.

Most prominent in Fig. 5-18b is the variation of the absorption coefficient μ of platinum in the region 6 Å to 3.5 Å, covering the M absorption edges. There are five of these, corresponding to the five subdivisions of the M state of the platinum atom. In a region of wavelengths that does not include any absorption discontinuities, the value of μ changes

approximately in proportion to the cube of the wavelength. This feature, denoted by curves sweeping rapidly upward, is especially easy to follow between the L_{III} and M_I discontinuities in Fig. 5-18b.

★ In Fig. 5-17b the emission line $L\alpha$ is shown as a consequence of the change of the energy of the atom from the L to the M state. This must not be taken to mean that transitions can occur between *every* L level and *every* M level. A few transitions do not occur. Those observed to take place can be predicted by applying a number of "selection rules," discussed for optical spectra in Chapter 7. It can be seen from Fig. 5-18b, however, why the L and M emission spectra of an atom are more complex than the K spectrum. There is only one K level from which an electron may start in the process of emitting a K line; but there are *three* L levels and *five* M levels as starting points for the L and M spectra.

9. Scattering of Hard X-Rays and Gamma Rays

The Compton effect; X-ray photons. As mentioned in Section 3, it has been found that the classical theory of scattering is inadequate to explain the experimental observations with hard X-rays and with gamma rays. The chief deduction from this theory is that the scattered radiation should have the same wavelength as the primary, whereas absorption measurements showed that it was, in part at least, definitely softer. In 1922 a satisfactory explanation was offered on the basis of quantum theory.

The experimental and theoretical work of A. H. Compton in that year showed that, when a beam of hard X-rays was scattered, the scattered radiation consisted of two parts; the "unmodified" part retaining its original wavelength, and the "modified" part having a slightly increased wavelength, corresponding to a smaller energy. The occurrence of the former is explicable on the classical theory; the latter requires the radiation to be considered as bullet-like photons. The collision of a photon and a free electron is depicted as roughly similar to the collision of two balls. If a white ball, representing a photon, is aimed to hit a red ball (an electron) a glancing blow, the white ball will be deflected, corresponding to a scattered X-ray; the red ball will recoil, acquiring kinetic energy at the expense of the other, whose energy must be decreased.

The process is illustrated in Fig. 5-19. The incident photon carries energy, in amount $h\nu_0$. It also carries momentum, as we see from the following argument: the energy that it carries endows the photon with a mass $h\nu_0/c^2$, in accordance with equation 7, p. 33. Since this mass

travels with the speed of light c , its momentum is c times its mass, or $h\nu_0/c$.

★ In working out this scattering problem, two principles must be observed: the conservation of energy and the conservation of momentum. We may suppose the scattering takes place in the xy plane, so there is no z component of momentum. Hence, three equations can be set up,

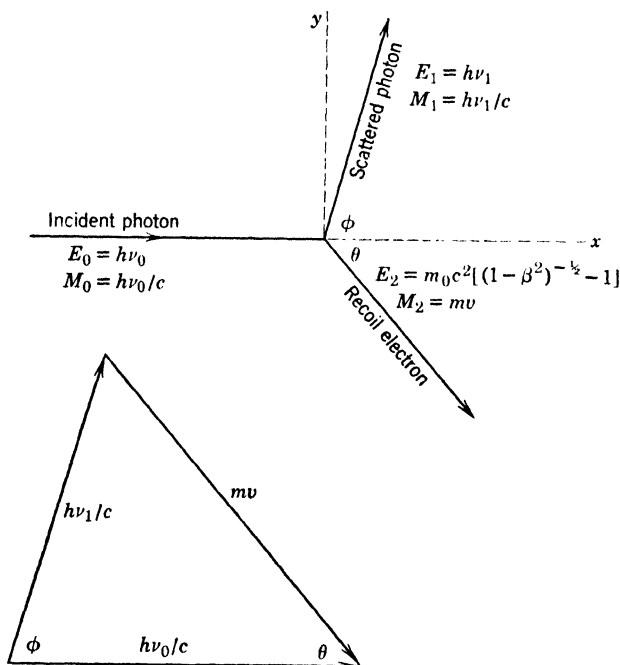


Fig. 5-19. Collision between a photon and an electron; the Compton effect. The E 's denote energies, the M 's are the momenta of the particles. The vector triangle shows the balance of momenta. The diagrams illustrate the case of an incident photon of tungsten $K\alpha$ ($\lambda = 0.21\text{\AA}$) scattered at 75° , so that the electron recoils at approximately 50° .

one for energy, and two for the two components of momentum in the x and y directions:

$$h\nu_0 = h\nu_1 + m_0c^2 \left(\frac{1}{\sqrt{1 - \beta^2}} - 1 \right) \quad (\text{Energy})$$

$$\frac{h\nu_0}{c} = \frac{h\nu_1}{c} \cos \phi + mv \cos \theta \quad (\text{Momentum, } x \text{ component}) \quad (8)$$

$$0 = \frac{h\nu_1}{c} \sin \phi - mv \sin \theta \quad (\text{Momentum, } y \text{ component})$$

Here $m = m_0/(1 - \beta^2)^{1/2}$ is the mass of the electron in motion, m_0 its rest mass, and v its recoil velocity; β is v/c ; ϕ is called the angle of scattering, that is, the angle at which an observer investigates the scattered radiation; ν_0 and ν_1 are the frequencies of the primary and scattered X-rays. These equations involve relativity expressions (p. 34) to take care of the high velocity of the recoil electron. The solution gives values of ν_1 , v , and θ in terms of the other quantities, which are known. As we are interested primarily in the scattered X-ray, we need only the result for ν_1 . From the values of ν_1 and the original ν_0 we can calculate the corresponding wavelengths, and thence the change in wavelength on scattering, $\Delta\lambda$. The result is

$$\Delta\lambda = \frac{h}{m_0c}(1 - \cos \phi) \quad (9)$$

This result indicates (a) that the change in wavelength $\Delta\lambda$ is independent of the primary wavelength; hence, the phenomenon is much more apparent for hard X-rays where the percentage change in wavelength is greater; (b) that the change in wavelength is greater, the greater the angle θ at which the scattered radiation is observed; it is zero in the straight forward direction (no scattering), h/m_0c at 90° , and $2h/m_0c$ at 180° . Figure 5-20 shows two ionization spectra of the $K\alpha$ line of molybdenum scattered at different angles from graphite. They bring out clearly point *b* above. For the scattered radiation from graphite observed at right angles to the primary beam, we should obtain a change in wavelength

$$\Delta\lambda = \frac{h}{m_0c}(1 - \cos 90^\circ) = \frac{h}{m_0c} = 0.0242 \text{ \AA}$$

If the radiation were scattered at 135° from the primary beam, the predicted increase in wavelength would be 0.0413 Å. The experimental results are obviously in good agreement with these figures.

It should be noticed that the change in wavelength suffered by radiation when it is scattered in the quantum manner is quite independent of the nature of the scatterer. The reason is that all substances contain some electrons, either free, or loosely bound to their parent atoms. It is the free or nearly free electrons that are able to take some energy from the primary photon, leaving less in the scattered photon. All elements except the very light ones also contain varying numbers of electrons tightly bound to their parent atoms, and these are responsible for the unmodified scattered radiation. To sum up, the proportions of modified and unmodified scattered X-rays vary from element to

element, but the wavelength change of the modified radiation depends only on the angle of scattering, aside from very small effects due to the binding energy of the nearly free electrons. In the case of molybdenum described above, the wavelength of the incident beam is about 0.7 Å, so the increase of 0.024 Å at 90° is not of great moment. However, if the wavelength of the primary beam were 0.1 Å—a hard radiation—the

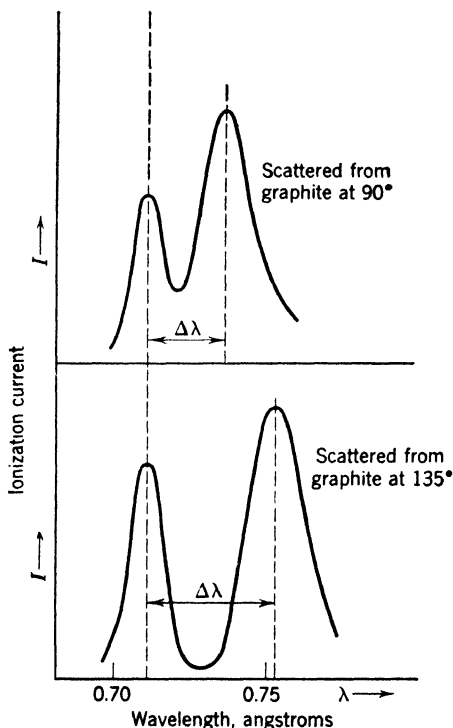


Fig. 5-20. Ionization spectra of molybdenum $K\alpha$ radiation scattered at different angles from graphite. The unmodified line holds the wavelength, 0.71 Å, of the incident radiation. The modified line appears at a longer wavelength, the change being determined by the angle of scattering.

change in wavelength of the modified part of the scattered beam would still be 0.0242 Å, which means that the scattered beam would have two components, of wavelengths 0.10 Å and 0.1242 Å. These differ by nearly 25 per cent, and if any considerable proportion of the modified radiation were present, the properties of the scattered beam would be very different from those of the primary beam. For instance, as is indicated by Fig. 5-18, changes in wavelength imply greater relative

changes in the value of the absorption coefficient μ , even when there are no absorption edges within the range considered. In this case, the change in μ is about 50 per cent. With gamma rays (Chapter 10), which are similar to X-rays but usually of much shorter wavelengths, the modification or partial softening of a scattered beam is even more pronounced. This difference in the qualities of primary and scattered radiations makes an accurate comparison of their intensities difficult.

Equation 9 has been amply verified by many investigators in the years since A. H. Compton's discovery. We are thus forced to ascribe to X-rays, as to visible light, a dual role. In Chapter 6 it is shown that even electrons possess the same peculiarities. Modern physics is often a game of give and take between corpuscles and waves.

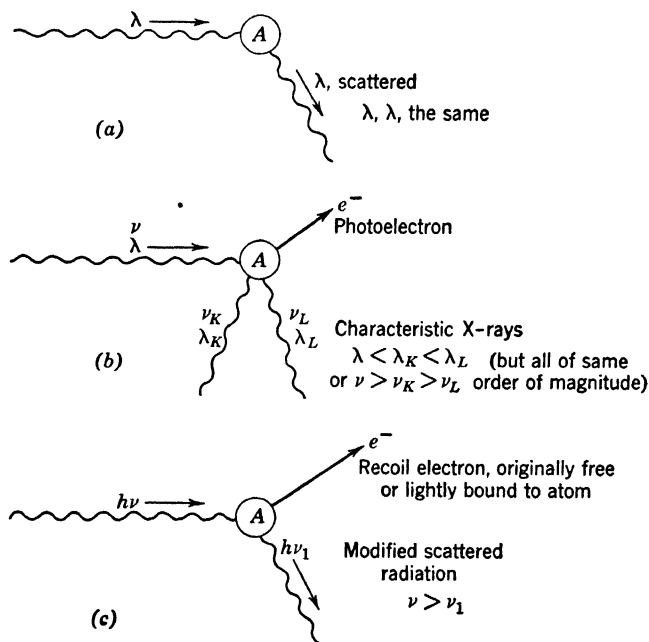


Fig. 5-21. Scattering of radiation by an atom A . The electrons do the scattering, the atom merely serving as a holder for the electrons. (a) applies to X-rays of long wavelength, such as were used in Fig. 5-4. (b) applies to rays of intermediate hardness, while the Compton process of (c) is especially prominent in the case of hard X-rays and gamma rays.

To summarize some of the important ways in which radiation interacts with an atom or an electron, several schematic diagrams are shown. In Fig. 5-21a, X-rays of wavelength λ impinge on an atom A . Scattered

radiation, also of wavelength λ is produced. This diagram is applicable especially to light elements and to radiation of long wavelengths.

In Fig. 5-21*b*, a photoelectron e^- is ejected. Consequently, as atom A readjusts itself, K , L , and perhaps other characteristic radiations are emitted. This diagram is applicable when λ is less than, but of the same order of magnitude as, the wavelengths of the K , L , etc., characteristic radiations.

In the third sketch, Fig. 5-21*c*, an X-ray photon $h\nu$ impinges on an electron that is free or lightly bound to atom A . The photon is scattered with loss of energy, so that the frequency after scattering is ν_1 , which is less than ν . The balance of energy is carried away by the recoiling electron e^- . This phenomenon is particularly likely to occur with very hard X-rays.

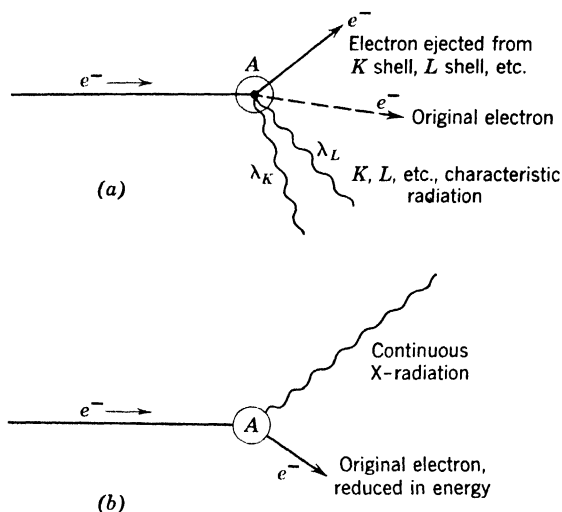


Fig. 5-22. Interaction between a moving electron and a stationary atom. The processes illustrated in (a) occur when the energy of the incident electron is greater than that required to eject some electron from the atom. (b) records, without specifying any detailed mechanism, the production of continuous X-radiation which always forms an important part of the emission from the target of a tube.

For the sake of completeness, a pictorial summary of possible common happenings when an electron impinges on an atom is given in Fig. 5-22. In Fig. 5-22*a* an electron e^- impinges on an atom A , ionizing it (that is, striking out another electron e^-). The original electron is likely to bounce away, as suggested by the dashed arrow. While the atom readjusts itself, characteristic X-rays, K , L , etc., are emitted. The picture describes what happens, especially with heavy elements, when the energy

of the impinging electron is greater than, but still of the same order of magnitude as, that of the characteristic K radiation. The picture should be compared with Fig. 5-21*b*.

Finally, in Fig. 5-22*b*, an electron e^- impinges on an atom, continuing on its way, with altered direction and reduced energy after the impact. The atom emits part of the continuous X radiation (see Fig. 5-10) or, using the common scientific German word, *Bremsstrahlung* (literally braking rays caused by the slowing down of the electron). In this chapter, little has been said concerning the mechanism of production of the continuous spectrum although it occurs over all ranges of energy of the incident electron (cf. p. 126). It is included in our pictorial summary because of its importance in high voltage X-ray tubes, from which the energy emitted in the form of characteristic radiation is usually negligible in comparison with the energy of the *Bremsstrahlung*.

★ **Very hard X-rays.** It is possible to produce X radiation much harder than the characteristic K lines of uranium by operating a tube at a high potential. Such radiation is part of the continuous spectrum whose high-frequency limit, or short-wavelength limit (Fig. 5-10) is determined only by the quantum relation $h\nu = eV$, where V is the voltage applied to the tube, e is the electronic charge, ν is the frequency of the radiation at the short wavelength limit, and h is Planck's constant. Ultrahard radiation is important in many ways; it is useful in therapeutic medicine—for example, in the treatment of some forms of cancer; in the metal industries it has wide applications in the detection of flaws in massive castings; and in fundamental scientific work it serves as artificial gamma radiation which is one tool for studying the creation of matter (p. 312) and the structure of the nucleus.

★ For the production of extremely hard X radiation, long tubes of unusual design like that in Fig. 5-23 are needed, and special arrangements are required to supply the necessary electric power. Up to something more than half a million volts, transformers can be used to provide the high potential difference in a more or less conventional manner. Beyond that point, giant electrostatic generators (Chapter 12) are satisfactory, and for voltages of the order of tens of millions, a new instrument, the betatron, has been developed.

★ The properties of X-rays produced in a tube operated at (say) 2,000,000 volts are in at least two respects different from those of ordinary X-rays. In the first place, the radiation emerges from the target of the tube mainly in the forward direction, that is, in the direction of motion of the electron beam. It is as though the momentum of the electron stream drove the X-rays forward—a point of view which is most easily comprehended if the radiation is considered as a collection

of photons. In the second place, the efficiency of production of the radiation is comparatively high. It was stated earlier that, in an ordinary tube, only a small fraction of 1 per cent of the input power reappeared in the form of X radiation. In a 2,000,000-volt tube, the efficiency may be 6 or 7 per cent.



Fig. 5-23. A 2,000,000-volt X-ray tube. Tubes designed to operate at extremely high or extremely low voltages depart considerably in shape and size from a simple Coolidge tube. (*Courtesy of Machlett Laboratories.*)

10. The Betatron

In 1941 D. W. Kerst reported the first successful construction of an instrument now known as the betatron. The purpose of the instrument is to accelerate electrons to very high energies, of the order of many millions of electron volts, without having available a potential difference of that magnitude. Instead, the electrons are accelerated repeatedly

by a much smaller emf. Although the use of the principle employed in the betatron was suggested in the 1920's, Kerst and Serber were the first to overcome the theoretical and technical difficulties involved in its design and operation.

The basic principle of the instrument is simple. Let us first imagine a circular loop of wire through which a magnetic flux passes, in a direction perpendicular to the plane of the loop. If the magnetic flux is increased or decreased, an induced emf is set up in the wire. Its magnitude and direction can be determined by simple rules. The important point is, however, that the induced emf is present whether the wire is there or not. If the emf will accelerate electrons in the wire, will it not also accelerate free electrons in a vacuum?

For Kerst's first betatron, a magnet was constructed with very flat conical poles about 20 cm in diameter. Between them lay an evacuated glass tube of the unusual shape shown in Fig. 5-24. The wedge-shaped cross section was necessary to let the tube fit the pole pieces rather snugly. In the picture, a part of the tube has been cut away to show clearly an electron injector I , and a target T . Suppose, now, that the

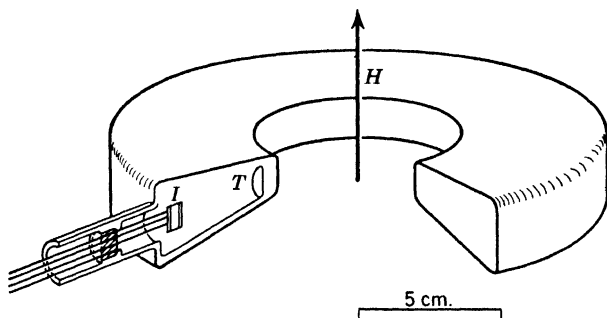


Fig. 5-24. Cutaway diagram of evacuated tube used in an early model of the betatron. The injector or source of electrons I and the target T are shown.

flux due to the magnet is increasing. Some electrons coming out of I will be accelerated by the induced emf and will, at the same time, be kept by the magnetic field H in approximately circular paths. The electrons will therefore stay inside the evacuated tube, going round and round faster and faster as long as the flux keeps increasing.

All this happens very quickly, for the electrons are soon traveling at almost the speed of light. In the first betatron, the increase in flux took place in 0.0004 sec, and during this brief time the electrons made about 100,000 circuits of the tube, picking up energy during every revolution. By special design of the magnet, and by other tricks of

electrical technique, the electrons were finally drawn inwards in a gentle spiral path so that they struck the target *T*.

In actual fact, the electromagnet was energized by an alternating current of frequency 600 per sec. What has been described above took place during the first quarter cycle. During the second quarter cycle, nothing occurred. During the third quarter cycle, new electrons were accelerated around the tube, but in a direction opposite to that taken

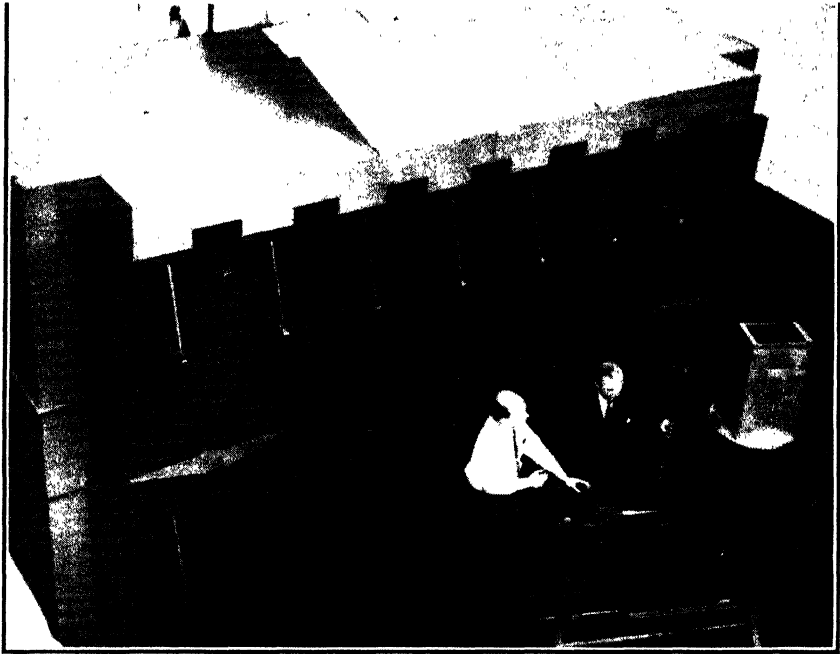


Fig. 5-25. The 100,000,000-volt betatron. The ring-shaped vacuum tube lies between the flat coils in the center of the picture. On the table is a much smaller betatron. (Courtesy of the General Electric Co.)

by the electrons during the first quarter cycle. The fourth quarter period was again one of inactivity. Thus the target *T* was bombarded by electrons first on one side then on the other, 600 times per sec on each side. X-rays were therefore produced intermittently. The original instrument gave about 1 microamp of electrons at 2.3 million volts. Several subsequent models, each larger than its predecessor, were designed for 20,000,000 to 300,000,000 ev. A photograph of the General Electric 100,000,000-volt betatron is reproduced in Fig. 5-25.

REFERENCES

Appendix 9, refs. 9, 10, 14, 16, 35, 36, 66, 83, 92, 96.

PROBLEMS

1. How much heat will be generated per second in the target of an X-ray tube operated at a steady potential of 20 kv with a current of 10 ma? Approximately how much power is sent out as X-rays if the efficiency is 0.2 per cent?

2. What fraction of a beam of X-rays will pass through a plate of aluminum 0.25 cm thick if $\mu = 0.42$ per cm? Repeat the calculation for lead, for which μ may be taken to be 40 per cm. What thickness of lead is equivalent in absorbing power to 0.25 cm of aluminum?

3. Make a calculation to show that an ordinary diffraction grating used at normal incidence cannot be used conveniently to produce X-ray spectra, on account of the shortness of the wavelengths. Assume a plane grating with 1000 lines/mm, and suppose the spectra are formed at a distance of 1 m from the grating. Compute the distance of the first-order spectrum from the central image, assuming $\lambda = 1 \text{ \AA}$.

4. Using the relation $eV = h\nu$, calculate the minimum voltage that must be applied to an X-ray tube to produce X-ray photons of wavelength 0.1 \AA , 3.0 \AA .

5. Calculate the smallest glancing angle at which the $K\alpha_1$ radiation of molybdenum ($\lambda = 0.71 \text{ \AA}$) will be reflected from calcite ($d = 3.036 \text{ \AA}$). At what angle will the fourth-order reflection take place? Repeat the calculations for the $K\alpha_1$ radiation of copper ($\lambda = 1.54 \text{ \AA}$).

6. A certain spectrum line *A* is reflected, in the first order, from a crystal face at a glancing angle of 30° . Another line *B* is reflected, in the third order, from the same crystal face at a glancing angle of 60° . Find the ratio of the wavelengths of *A* and *B*.

7. The $K\beta_2$ line of an atom is emitted when the atom undergoes an energy change from the *K* to the *N* state. Reading from Fig. 5-17*a* and *b*, what is the energy of the $K\beta_2$ line of silver, in electron volts? What is its wavelength? Check for reasonable correspondence with Table 5-2.

8. Rewrite equations 8 for the case in which the photon strikes the electron head on. In this case the photon is scattered through 180° , and the directions of motion of all the particles are along the X-axis. A solution of equations 8 can be found in Appendix 9, ref. 82, p. 516.

9. Prove the formula $n\lambda = d |\sin \phi - \sin \theta|$ for the diffraction of radiation by a plane grating. The symbols are defined near equation 2, p. 119.

10. Compute the wavelength of the most energetic photons emitted by an X-ray tube operated at a steady potential of 80,000 volts. At what glancing angle would these photons be reflected, in the first order, from the 100 planes of sodium chloride?

11. A magnetic field of 700 oersteds passes perpendicularly through a single circular loop of wire of diameter 16 cm. The field is reduced to zero in a time 0.01 sec. What emf is generated in the loop of wire?

12. Figure 5-14 is a powder crystal photograph of tungsten metal. What are the distances between successive planes which give the eight strong reflections on the photograph? Is there a possibility that some of these lines are second-order reflections? The following data are needed: Copper $K\alpha_1$ radiation was used, $\lambda = 1.54 \text{ \AA}$; the actual distance from the center of *A* to the center of *B*, measured along the cylindrical camera wall, was 18.0 cm. The radius of the camera was 5.73 cm. At

large glancing angles, the contribution of $K\alpha_2$ is resolved from that of $K\alpha_1$, which is stronger than $K\alpha_2$. The student is encouraged to proceed as follows: (a) make measurements along the middle of Fig. 5-14, noting the distance of every line from the center of A ; (b) adjust these readings to take care of the scale on which Fig. 5-14 is reproduced; (c) use the geometry of the circle to find the angles of reflection of the measured lines; then (d) apply Bragg's law.

13. Taking data as well as you can from Fig. 5-18, draw an energy-level diagram for platinum, showing the single K , the three L , and the five M levels in their proper relative positions.

14. A photon of molybdenum $K\alpha$ radiation, $\lambda = 0.71 \text{ \AA}$, is scattered at 90° by an electron. Calculate the momenta of the incident and scattered photons.

15. Draw vectors representing the momenta of the two photons in problem 14, remembering that their relative directions are already determined.

16. Add to the diagram of problem 15 a vector representing the momentum of the recoiling electron. (In Compton scattering, the momentum of the original photon is equal to the sum of the momenta of the scattered photon and of the recoiling electron.) From the geometry of the diagram calculate the electron's momentum, and its direction.

17. In the case of the rather slowly moving electron of problem 16, it is reasonable to omit relativistic calculations and to set the momentum of the electron equal to the product of its rest mass and its velocity. Find the velocity with which the electron recoiled. What fraction is it of the speed of light?

ANSWERS TO PROBLEMS

1. 48 cal/sec; 0.4 watt.
2. 0.90, 0.45×10^{-4} , 2.6×10^{-3} cm.
3. 0.01 cm; angular separation, 10^{-4} rad.
4. 124,000, 4130 volts.
5. $6^\circ 43'$; $27^\circ 55'$; $14^\circ 43'$; cannot occur.
6. 1.73.
10. 0.155 \AA ; $1^\circ 35'$.
7. 25,900 eV; 0.48 \AA .
11. 0.141 volt.
12. Approx. 2.15, 1.53, 1.25, 1.09, 0.98, 0.89, 0.83, 0.78 \AA . Of these the first and fourth may be first and second-order reflections, as may the second and eighth.
14. 9.3, 9.0×10^{-19} gm cm/sec.
16. 12.9×10^{-19} gm cm/sec, $44^\circ 8'$ from the direction of the incident photon.
17. 1.42×10^9 cm/sec; 0.047.

6

Waves Associated with Material Particles

1. Introduction

Although the planetary model of the atom had received wide acceptance by 1920, the Bohr theory had encountered difficulties. Successful in the case of hydrogen, it definitely disagreed with the observed energy levels of helium, or of any atom composed of more than two particles. There were also other difficulties, not appropriate for consideration here. Gradually, ideas involving the basic philosophy of physics, the proper interpretation of experiments, and the meaning of atom models were brought to bear on the problem. For example, it was generally admitted that it would never be possible to observe directly an electron traveling in an orbit about a nucleus. By degrees it came to be recognized that the properties of an atom must necessarily be inferred or deduced from indirect experiments most of which depend upon the interaction of light or other electromagnetic radiations with one or more of the electrons. Thus there could be no logical justification for dogmatic statements about the behavior of the electrons in an atom, unless the nature of radiation itself was well understood. It was somewhat disconcerting, therefore, to remember that there were two current theories of radiation: the classical wave theory, which provided a beautiful explanation of interference and diffraction effects; and the photon theory, well adapted to account for the photoelectric effect and the characteristics of radiation from black bodies.

Einstein's idea that the waves serve merely as guides for the photons (p. 89) was widely known, but many physicists felt that this suggestion merely brought in a new and difficult concept to explain away another.

However, in 1922, L. de Broglie suggested that, if photons were accompanied by waves, it would be reasonable to expect that what were thought of as *material* particles should have some type of companion wave motion associated with them. The same point of view was independently considered by Elsasser. De Broglie postulated that such

waves existed, calling them matter waves, and used this new point of view to explain the quantization of the hydrogen atom. The new theory reached its full development in the hands of Schroedinger, in 1925. His theory is called *wave mechanics*.

A capital advance was made in 1925, when Davisson and Germer discovered that electrons scattered from a crystal form a diffraction pattern. Their experiments show quite definitely that we must associate a system of waves with an electronic beam. Independently, G. P. Thomson found that electrons are diffracted in passing through thin foils, forming a pattern of the Debye-Scherrer-Hull type after the fashion of X-rays (p. 133). Thus electrons (and indeed all known particles) have both wave-like and corpuscular properties.

In this chapter, we shall present the essential ideas of de Broglie, and the above-mentioned experimental demonstrations of matter waves. Thus prepared, we shall describe wave mechanics, applying the matter-wave theory to the problem of atomic structure. Then we can show to what extent the wave and corpuscular pictures of matter have been blended, and finally, how close is the parallelism between our present concepts of light and of matter.

To guide the reader we summarize some relations between the theories of light and of matter in Table 6-1, which naturally will be better appreciated after the chapter has been read.

2. De Broglie's Wave Theory of Matter

In 1922, L. de Broglie was especially attracted by Einstein's suggestion that the laws of optics can be developed by assuming that light is composed of tiny corpuscles guided by "ghost fields." He was led to the following question: Since the behavior of photons, having zero rest mass, is decidedly different from the behavior of bodies having quite appreciable masses, is it not to be expected that particles having small but still finite masses will behave in some intermediate fashion? In other words, will not electrons and protons, because of their small masses, behave in a manner somewhat similar to light quanta? We have seen that the wave frequency and the photon mass are related as follows:

$$\nu = \frac{\text{Energy}}{\text{Planck's constant}} = \frac{W}{h} = \frac{mc^2}{h} \quad (1)$$

where m represents the actual mass of the photon, $h\nu/c^2$. The wavelength is therefore

$$\lambda = \frac{c}{\nu} = \frac{h}{mc} = \frac{h}{\text{Mass of photon} \times \text{Velocity of photon}} \quad (2)$$

TABLE 6-1. Parallelism of Physical Theories

Theories of Light	Theories of Matter
<p>1. <i>Simplified Corpuscular Theory</i></p> <p>Photons follow rays, whose paths can be derived from principles very like those of Newton's mechanics.</p>	<p>1. <i>Simplified Corpuscular Theory</i></p> <p>Particles obey Newton's laws of mechanics.</p>
<p>2. <i>Wave Theory</i></p> <p>Theory deals with continuous waves yielding interference and diffraction effects. Standing waves produced by interference correspond to quantization. No mention of photons.</p>	<p>2. <i>Wave Theory</i></p> <p>Theory deals with continuous waves yielding interference and diffraction effects. Quantization, as suggested by de Broglie and Schroedinger, corresponds to standing waves. No mention of particles in certain extreme forms of the theory.</p>
<p>3. <i>Evidence of Connection</i></p> <p>Experiment requires that, when the waves have frequency ν, the photon energy is $h\nu$.</p>	<p>3. <i>Evidence of Connection</i></p> <p>Experiment requires that when a particle has energy E, waves with frequency $\nu = E/h$ are associated with it.</p>
<p>4. <i>Einstein's "Ghost Field" Interpretation partially reconciles the corpuscular and wave theories</i></p> <p>Amplitude of electromagnetic waves determines the density of photons at any point in a statistical way. Behavior of an individual photon cannot be accurately predicted.</p>	<p>4. <i>Born's Probability Interpretation partially reconciles the corpuscular and wave theories</i></p> <p>Amplitude of matter waves determines the density of particles at any point in a statistical way. Behavior of an individual particle cannot be accurately predicted.</p>

If now we assume that particles of very small mass such as electrons behave in a manner similar to photons, we must recognize that these particles may be directed by "matter waves" having a wavelength which, by analogy to light, is given by

$$\lambda = \frac{h}{mv} = \frac{h}{\text{Mass of particle} \times \text{Velocity of particle}} \quad (3)$$

where m is the mass of the matter particle and v is its velocity. This is the entirely new assumption which L. de Broglie brought into physics in 1923. Examples of the wavelengths predicted for particles of different masses and velocities are given in Table 6-2. The wavelengths of the de Broglie waves associated with electrons having energies between 1 and 100 eV are of the same order of magnitude as those of X-rays.

TABLE 6-2. Wavelengths Associated with Material Particles

Particle	Mass m_0 (gm)	Velocity (cm/sec)	de Broglie wavelength
Slow electron	9×10^{-28}	1	7.27 cm
Slow electron	9×10^{-28}	100	0.0727 cm
1-volt electron	9×10^{-28}	5.94×10^7	1.22×10^{-7} cm = 12.2 Å
100-volt electron	9×10^{-28}	5.94×10^8	1.22×10^{-8} cm = 1.22 Å
100-volt alpha particle	6.6×10^{-24}	6.94×10^6	1.43×10^{-10} cm = 0.0143 Å
Alpha particle of radium	6.6×10^{-24}	1.51×10^9	6.56×10^{-13} cm
Golf ball in motion	45.9	2500	5.71×10^{-32} cm

3. Verification of the Wave Nature of Electrons

Davisson and Germer's experiments with slow electrons. We have seen that monochromatic X-rays are diffracted from crystal faces at definite angles only, while in a somewhat different fashion monochromatic optical light is diffracted by a ruled grating in certain selected directions. Davisson and Germer were the first to discover that electrons also are diffracted from crystal surfaces. The arrangement of the ingenious apparatus used in their experiments is shown in Fig. 6-1.

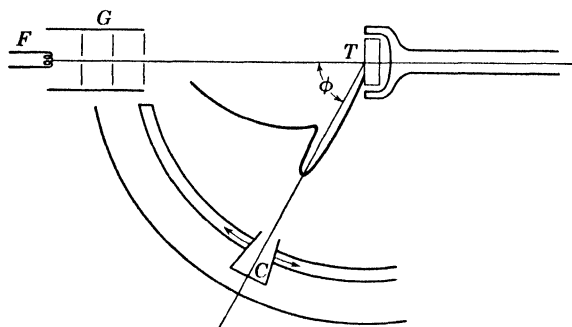


Fig. 6-1. Simplified cross section of apparatus used by Davisson and Germer to obtain diffraction of an electron beam.

The parts indicated are enclosed in a glass tube so that the space between the filament and the crystal may be evacuated. Electrons are emitted from the filament F and are accelerated while passing through the slits of the electron gun at G . The electrons then impinge upon the crystal face located at T . Those which are reflected or diffracted from the crystal are caught by the collector, which is connected to a sensitive

galvanometer. The apparatus is so arranged that the collector C can be moved within the vacuum to make any desired angle ϕ with the incident beam of electrons. The collector is also free to rotate about an axis collinear with the electron stream so as to sweep out practically all the space in the hemisphere which the crystal faces. The azimuthal angle about this axis which the collector makes with some given reference plane is called θ .

The procedure that Davisson and Germer followed was, first, to measure the current to the galvanometer while changing the azimuthal angle θ , but keeping everything else fixed. They found that the current varied in a periodic way. Second, they fixed the azimuthal angle at one of the positions at which a maximum current was obtained and with a fixed accelerating voltage varied the angle ϕ of the collector with respect to the incident ray and plotted the angle against the reading of the galvanometer. Thus they obtained the graph shown in Fig. 6-2a.

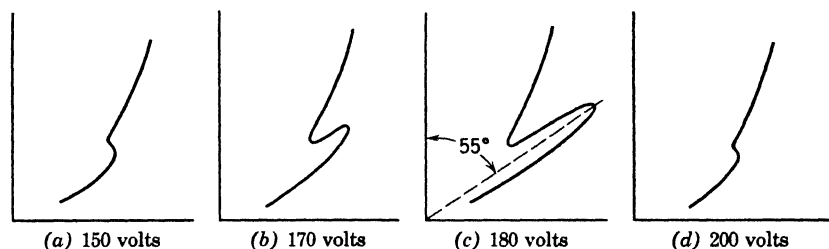


Fig. 6-2. Polar diagrams in which the radius vector is proportional to the electron current and the angle is that between the incident electron beam and the reflected beam. The voltage refers to the energy of the incident electrons.

The accelerating voltage was then varied and readings for a second graph were taken, giving Fig. 6-2b. Graphs were made for various voltages, and, for certain sharply defined voltages, peaks like those shown in Fig. 6-2c were obtained.

From the angles at which these finger-like peaks were obtained and the distance between the atoms in the crystal faces, Bragg's law ($n\lambda = 2d \sin \theta$) could be used to test whether the wavelengths for the reflected electrons calculated according to de Broglie's predictions agreed with those experimentally observed. At first it was thought that there was an important discrepancy in the wavelengths, but it was found later that the discrepancy arose from assuming that the refractive index for the matter waves in the crystal was very nearly unity, like that for X-rays. After the refractive index for the matter waves was properly evaluated, all of Davisson and Germer's peaks were shown to be exactly

in the right position for the wavelengths calculated by the relation $\lambda = h/mv$. Thus it is reasonable and necessary to speak of *electron diffraction*. Here, indeed, was a triumph for de Broglie's hypothesis that matter has a wave structure very similar to that of light.

Experiments with fast electrons. Independently, G. P. Thomson discovered the diffraction of electrons in another manner. He passed high-speed electrons through very thin metal foils and obtained the

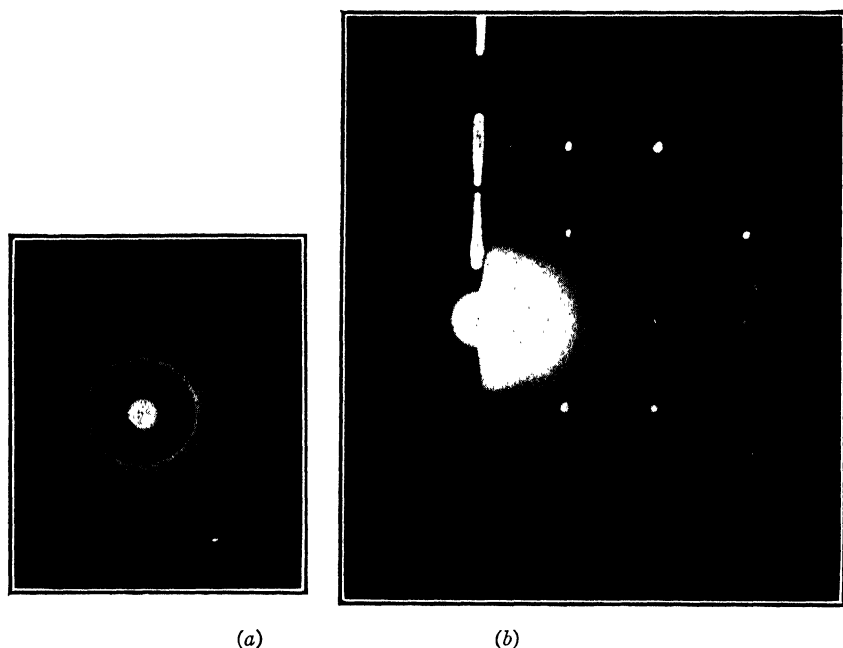


Fig. 6-3. (a) Diffraction pattern obtained by G. P. Thomson by passing a narrow beam of electrons through a thin gold foil. (b) Pattern obtained by reflection from a single crystal of copper.

pattern shown in Fig. 6-3a, using a gold foil. He also obtained the diffraction pattern shown in Fig. 6-3b from a single crystal of copper. The effect is very much the same as when one observes a distant light through a fine-mesh handkerchief. Kikuchi, working at Toyko, obtained magnificent Laue diffraction patterns (p. 120), by passing electrons through thin mica sheets as shown in Fig. 6-4.

★ **Diffraction of atoms and molecules by crystals.** At ordinary temperatures, the average velocity of a gas molecule of low atomic weight is such that its de Broglie wavelength, given by equation 3, is a

fraction of an angstrom. Thus it is to be expected that atoms or molecules suitably incident upon crystalline surfaces will yield diffracted beams in accordance with Bragg's equation. A short time after the discovery of electron diffraction the diffraction of atomic hydrogen from crystals was demonstrated by T. H. Johnson. The diffraction of neutrons in similar fashion is described in Chapter 11.

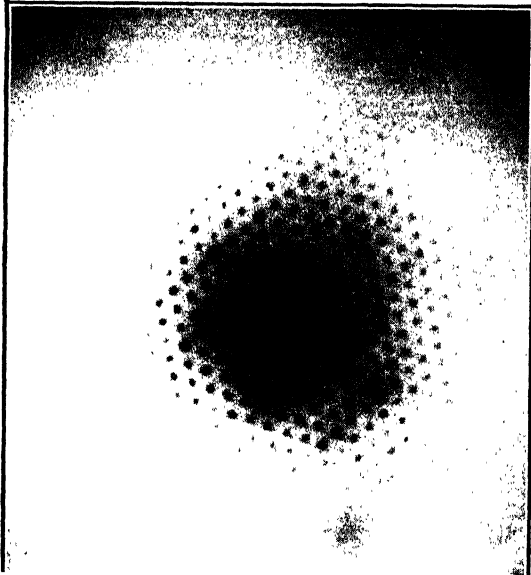


Fig. 6-4. Diffraction pattern obtained by Kikuchi by passing a narrow beam of electrons through a thin sheet of mica.

All these results bring us to a position in regard to matter which corresponds exactly to that which we attained in regard to light. Our everyday experiences proceed on a scale of size which completely masks the effects due to the wave properties of matter, but sufficiently refined experiments require that we associate waves with material particles—waves that interfere and are diffracted like sound waves or light waves. When the waves can be neglected, the motion of particles may be sufficiently well described by Newton's laws, or the extension of those laws given by Einstein's theory of relativity; but when the waves must be taken into account the motions are not predictable by ordinary mechanical laws. We are confronted with need for a new theory governing the behavior of matter waves.

4. The Electron Microscope

We turn aside from the main line of the argument to show how the minuteness of the wavelength of fast electrons has permitted the development of extraordinarily powerful microscopes. The theory of many optical instruments involves a concept known as resolving power (p. 57). A good telescope or microscope must possess not only high magnification but high resolving power for fine detail as well. The resolving power of an instrument is a measure of its ability to show, as distinct images, two points that are close together in the field of view. In a telescope, this property depends directly on the diameter of the objective lens, and inversely on the wavelength of light used. Without serious deviation from the truth, the same may be said of the resolving

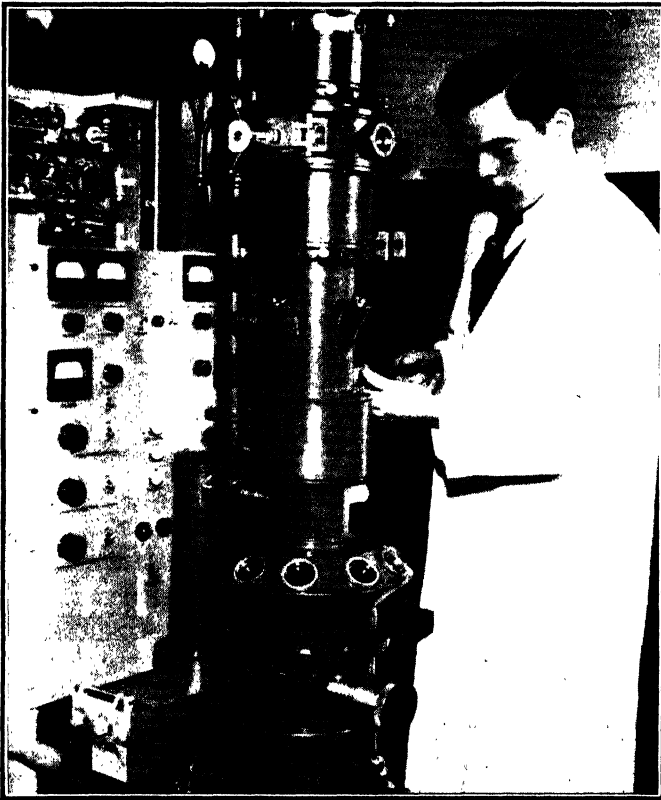


Fig. 6-5. An electron microscope. The inclined viewing ports near the bottom of the picture permit a visual examination of the final image on a fluorescent screen just before the photograph is taken. (Courtesy of the Radio Corporation of America)

power of a microscope. The limit of resolution of a microscope, beyond which it is impossible to go by any conceivable means, is of the order of magnitude of the wavelength of light. This means that the images of two points less than 1 wavelength apart, as seen through the microscope, merge into one image; and that no detail of shape or brightness less than about 1 wavelength in diameter can be detected. We have learned that X-rays have a wavelength $1/5000$ of that of visible light waves, or smaller. Therefore, if X-rays could be used in place of visible light for microscope illumination, a supermicroscope could be constructed with which objects more than 1 X-ray wavelength in diameter could

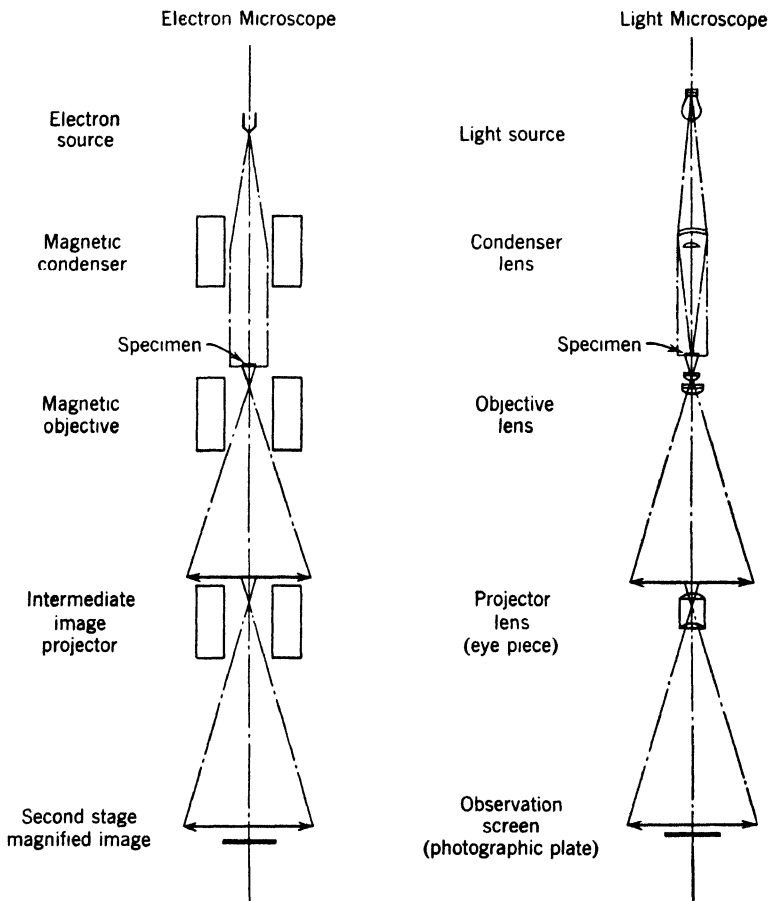


Fig. 6-6. Ray diagram of an electron microscope, with corresponding diagram of an optical microscope for comparison (modified from a diagram supplied by the Radio Corporation of America).

be clearly seen. Unfortunately, X-rays cannot be refracted through lenses like visible light. Theoretically, it is possible to devise an X-ray microscope using mirrors instead of lenses. Kirkpatrick has designed some instruments of this kind, but the practical difficulties of construction and adjustment are formidable.

However, we note from Table 6-2 that a 10,000-volt electron has a wavelength of about 0.1 angstrom; and such an electron can pass through, say, 50 layers of light atoms without suffering serious energy loss. Furthermore, such an electron can be deviated, or "refracted," by electric or magnetic fields. There is a possibility, therefore, of constructing a microscope that would use electrons instead of visible light, and that would have a resolving power as good as that of the X-ray supermicroscope discussed above. Such an electron microscope is now a standard instrument of physical, chemical, and biological research.

An electron microscope of American design is shown in Fig. 6-5. Referring to Fig. 6-6, we may follow the stream of electrons from what is practically a point source at the top of the picture. The divergent beam is first made parallel by the magnetic field of a coil which thus plays the part of a condensing lens. Then the beam falls on the specimen. Electrons pass through the thin parts of the specimen but are stopped or deflected by the thick parts. The resulting beam, carrying with it the pattern of the specimen, is first passed through a magnetic lens which produces a large intermediate image at the bottom of the object tube. There a small part of the image is selected for further magnification by the projection coil which focuses the electrons finally on a photographic plate. A preview of the final image is sometimes obtained by looking through the inclined ports (Fig. 6-5) at a fluorescent screen placed above the plate. The screen is then flipped out of the way while the photograph is taken.

A typical picture made by the electron beam has a magnification of 10,000 or 20,000. Often, the picture is so sharp, on account of the high resolving power of the instrument, that the original negative can be enlarged to give a total magnification of about 180,000. This is nearly a hundred times as much as can be obtained satisfactorily from an ordinary optical microscope. A picture of an interesting biological specimen is given in Fig. 6-7.

5. De Broglie's Quantization of the Hydrogen Atom

Prior to the discovery of electron-diffraction phenomena, it was realized by de Broglie that the method of quantization used in the Bohr theory was closely connected with wave properties of the electron. It

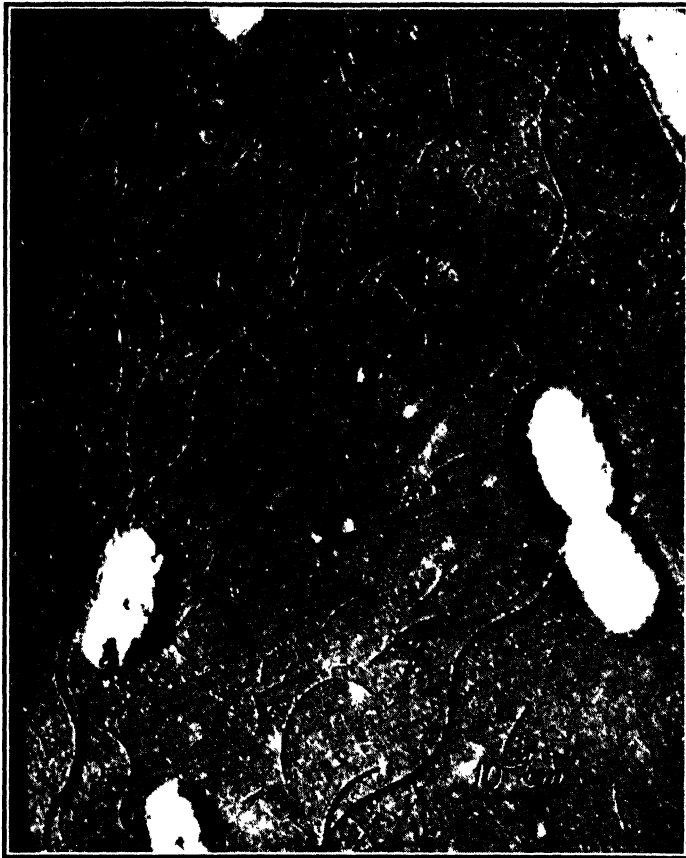


Fig. 6-7. Electron micrograph of bacilli of paratyphoid (*Bact. typhosum*). Magnification 10,000. The short straight line in the bottom right corner is 10^{-4} cm long. The long hair-like cilia are part of the bacteria. Broken cilia are seen scattered generally over the picture. The three-dimensional effect is produced by an experimental technique known as shadow casting. (Courtesy of Robley C. Williams and R. W. G. Wyckoff.)

was by a complete theoretical investigation of this connection that a new theory of the atom was developed. We saw on p. 98 that the radii of the various circular Bohr orbits are given by

$$a_n = \frac{n^2 \hbar^2}{4\pi^2 m Z e^2} \quad (4)$$

and that the velocity of the electron in its orbit is

$$v = \frac{2\pi Ze^2}{nh} \quad (5)$$

The wavelength of the corresponding matter waves is

$$\lambda = \frac{h}{mv} = \frac{nh^2}{2\pi mZe^2} \quad (6)$$

If now the circumference of the orbit is divided by the wavelength, we find

$$\frac{2\pi a_n}{\lambda} = n \quad (7)$$

where n is the quantum number used earlier. *Thus the stable paths of the Bohr theory are those whose lengths are an integral multiple of the de Broglie wavelength.*

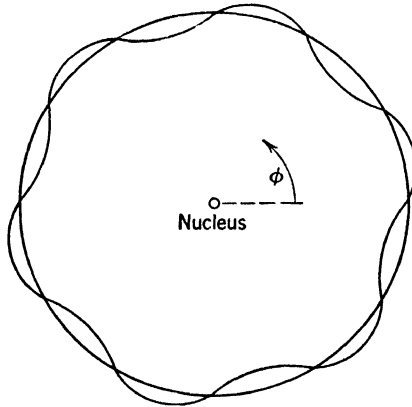


Fig. 6-8. Progressive, self-closing matter wave accompanying an electron around a Bohr orbit. The distance between the sinusoidal curve and the circular orbit indicates the amplitude of the wave.

This "tuning" of the matter waves with the length of the path (Fig. 6-8) suggests a very similar phenomenon in vibrating strings. If a string stretched between two points is plucked, the string may vibrate in one, two, three, or more segments in such a way that the double length of the string divided by the wavelength will be an integer just like the quantum numbers occurring in atomic systems. (As music

students know, the plucking must be done in particular ways if we desire to excite just one of these harmonics, analogous to a definite quantum state of the atom.) Here we are dealing with standing waves, and the distances between the nodes of these sinusoidal disturbances are determined by the obvious boundary conditions, namely, that the amplitude must be zero at the fixed ends of the string. However, in the case of the atom we should expect traveling waves, revolving around the nucleus in the same sense as the electron. The waves are not confined to an orbit as one might at first imagine from inspection of Fig. 6-8; they are three dimensional; they fill the space around the nucleus, somewhat like the waves excited by a paddle rotating in a bucket of water.

★ At any instant, the amplitude of the waves should be a single-valued function of the angle ϕ , measured around the orbit from any origin whatever. This can only be true if the circumference is an integral multiple of the wavelength. The symbol ψ_n is commonly used for the amplitude of the waves when the atom is in the n th quantum state.

★ We interrupt the argument for a moment to remind the student that the equation

$$y = A \sin 2\pi \left(\frac{x}{\lambda} - \frac{t}{T} \right)$$

discussed in many books on optics, describes a simple periodic wave of amplitude A . Here y is the displacement at any instant at position x , and T is the period. If the wave pattern is circular, surrounding the nucleus, a position on the wave is described by the length of an arc of the circle. This position is most conveniently specified by an angle ϕ at the center of the circle, subtending the arc of length x . If a is the radius of the circle, $x = a\phi$, and the equation becomes

$$y = A \sin \left(\frac{2\pi a\phi}{\lambda} - \frac{2\pi t}{T} \right)$$

For $2\pi a/\lambda$, the quantum number n may be substituted, by equation 7.

★ Thus, going back to the hydrogen atom, it is reasonable to write

$$\psi_n = A \sin (n\phi - 2\pi f_n t) \quad (8)$$

if the waves are “moving” counterclockwise. Here f_n is the frequency of the waves, which remains to be determined. Furthermore, since the waves are not confined to one plane, A may depend on the other two polar coordinates r and θ .

6. Frequency and Velocity of Matter Waves

De Broglie found an expression for the frequency of matter waves; it is the total energy of the particle divided by h . To make this result plausible, we remark that de Broglie's picture, in contrast to that of Bohr, gives us a means for visualizing a transition from one orbit to another, by emission of light, for example. Evidently the matter waves appropriate to the final state gradually build up, while the initial matter waves fade out of the picture. While this goes on, both are present, and it is not illogical to suppose that *the frequency of the light is simply that of the beats between the frequencies of the two sets of matter waves*. To understand this, and to reach an algebraic expression for the frequency of the *matter* waves, we remember that the beat note between any two frequencies f_1 and f_2 has the frequency $(f_2 - f_1)$. On the other hand, if a transition occurs between two states of energy E_2 and E_1 , we have, as usual, $E_2 - E_1 = h\nu$, where ν is the frequency of the *radiation* emitted. Since we consider $\nu = (f_2 - f_1)$ where f_2 and f_1 are now the frequencies of the *matter* waves, we must be sure that the two equations $E_2 - E_1 = h\nu$ and $f_2 - f_1 = \nu$ are simultaneously valid. This will be so if $f_2 = E_2/h + C/h$ and $f_1 = E_1/h + C/h$, where C is a constant, having the dimensions of energy, which generalizes the statements. Hence it is plausible to write, for the frequency of a matter wave, $f = E/h + C/h$, or $hf = E + C$.

De Broglie *assumed* that $E + C$ must be taken to represent the total energy of the electron, including its rest energy, its kinetic energy, and its potential energy. Therefore we may express the frequency of the matter wave of the electron as

$$f = E_T/h \quad (9)$$

where E_T is the total energy of the electron.

Observe that there can be no question of a *proof*; de Broglie was engaged in *constructing* a theory, and such proof as can be provided must come from experiment.

Now we may compute the velocity, u , of the matter waves, namely

$$u = f\lambda = (E_T/h) (h/mv) = E_T/mv$$

For a free particle,

$$u = c^2/v \quad (10)$$

since in this case $E_T = mc^2$. At first sight this result may excite suspicion; we have learned that "nothing" can go faster than light. But

u is only the phase velocity of a matter wave, not the velocity of a particle. (In textbooks of optics it is shown that the phase of a light wave has a speed greater than c , when the frequency is slightly less than an absorption frequency of the medium in which the wave travels. This is called anomalous dispersion, though there is nothing anomalous about it.) Thus we learn that the velocity of matter waves, in the hydrogen atom, for example, is *not* the velocity of the electron on its orbit, but is much greater and is inversely proportional to it. The waves slide past the electron, or the electron slides through the waves, whichever one prefers.

We can now construct a list comparing the properties of light waves, and of the matter waves of a free material particle. Let p and E be the momentum and energy of either the photon or the particle. Then we have:

Quantity	Light Waves	Matter Waves
Wavelength	h/p	$h/p = h/mv$
Frequency	E_T/h	$E_T/h = mc^2/h$
Velocity	$E_T/p = c$	$E_T/p = c^2/v$

7. Schroedinger's Wave Mechanics

The problem of determining the amplitude ψ of the matter waves remained to be solved. This was done by Erwin Schroedinger in 1926. The ensuing problem of seeing what ψ is, by examining its properties, was dealt with by Max Born shortly afterwards. Schroedinger recognized clearly that the waves belonging to an atom in a stationary state must be determined by boundary conditions, like those which enable us to pick out the various harmonics, or simple modes of motion, of a vibrating string or membrane, an organ pipe, or a radio antenna.

Wave equations. In all such cases there is a basic wave equation which tells us how to compute the shape of the wave. This is a differential equation, whose treatment lies beyond the scope of our book, but the nature of the service it renders to us can be explained as follows.

★ Figure 6-9a shows two instantaneous positions of a wave on a stretched uniform string, which happens to be vibrating in its second mode. These are sine curves, which differ only in amplitude y . Consider, on one curve, the values of ψ at three points separated by small intervals of length Δx . We wish to discuss the departure from linearity at any point, because a complete knowledge of this departure, at all points, amounts to a complete knowledge of the shape of the curve.

Between the points x_1 and x_2 , the average slope is approximately

$$S_{12} = \frac{y_2 - y_1}{\Delta x}$$

Similarly, between x_2 and x_3 , the average slope is approximately

$$S_{23} = \frac{y_3 - y_2}{\Delta x}$$

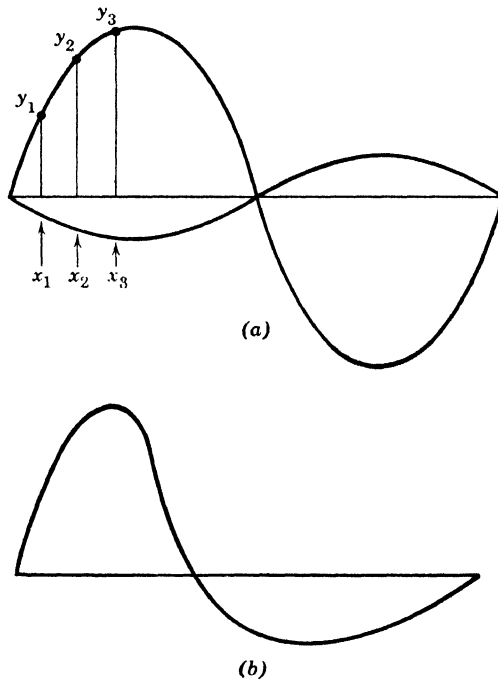


Fig. 6-9. (a) Shape of a possible standing wave on a uniform string, stretched between fixed end-blocks. The two curves show the configuration at two different times. (b) Shape of a possible standing wave on a non-uniform string. The thicker portions of the string lie toward the left, so the wave velocity and local wavelength are smaller there.

The change of slope in going a distance Δx is approximately $S_{23} - S_{12}$. Thus the change of slope per unit distance is

$$D = \frac{S_{23} - S_{12}}{\Delta x}$$

which we take as our measure of departure from a straight line. (It would be natural to call D the curvature, but the name has been applied for centuries to an allied quantity.)

★ Now we note that, for a sine curve of 'given height, an arbitrary decrease of the wavelength λ leads to greater D values all along the curve. Full analysis shows that D is inversely proportional to λ^2 . Also we note that $|D|$ is large where $|y|$ is large. Examination reveals that D is negative when y is positive, and vice versa. Full analysis shows that D is exactly proportional to y .

★ Indeed, if Δx is allowed to approach zero, D approaches a limiting value which is given by

$$D_L = -\frac{4\pi^2}{\lambda^2} y \quad (11)$$

This is the wave equation, from which y can be computed, as a function of x . It can be generalized. If we deal with a string of variable thickness, λ becomes a function of x ; that is to say, the "local wavelength" at any point depends on x . Then the waves are distorted from the sine shape, as in Fig. 6-9b. Still it can be shown that an equation very like 11 holds true. Again, if we deal with a membrane, or a vibrating solid body, equations very like 11 govern the motion.

★ **Schroedinger's equation.** To apply such ideas to matter waves, Schroedinger made certain assumptions:

★ 1. *Wavelength; Refractive Index.* He assumed that de Broglie's formula (equation 3) for the wavelength is correct for a particle moving in any field of force, with potential energy $V(x, y, z)$. The sum E of the kinetic and potential energies is $p^2/2m + V$. Therefore,

$$p = [2m(E - V)]^{1/2} \quad (12)$$

Thus the wavelength is

$$\lambda = \frac{h}{[2m(E - V)]^{1/2}} \quad (13)$$

We see that the presence of a potential field alters the wavelength. Where $E - V$ is greater the wavelength is shorter. Thus, where V has a minimum value the wavelength is also a minimum. By *analogy* with the change of length experienced by light waves in passing from one medium to another, it is customary to think of the potential as providing a "refractive index" for matter waves in empty space. Armed with this analogy, we may easily visualize the paths or rays of matter waves. They are like rays of light curving through some medium of variable refractive index, such as the lens of the human eye. It need not be a

surprise that the matter wave fronts wheel around a place of minimum potential energy, such as the nucleus of a hydrogen atom. Roughly, and only roughly, the rays, perpendicular to wave fronts, should be expected to parallel the directions of the particles moving on their orbits in the corresponding Bohr model.

★ 2. *The Wave Equation.* Schrodinger assumed that the amplitude ψ of the waves is governed by an equation of the type of 11. Thus, for a one-dimensional problem,

$$D_L = - \frac{8\pi^2 m}{h^2} (E - V)\psi \quad (14)$$

★ 3. *Boundary Conditions.* But what boundary conditions can be applied to “nail down” the standing-wave solutions which represent atoms in stationary states? For an atom in empty space, there is no boundary. Schrodinger’s ingenious answer for this case was: we need only require that the wave function, or wave amplitude ψ , be *finite*, *continuous*, and *single-valued* throughout all space. But there is another case. Sometimes it is convenient (Section 8) to deal with the idealized case of a particle shut up in an impenetrable box. Then, he assumed, the wave function must fall to zero at the walls.

To appreciate the theory, we must see it in action.

8. Quantum Theory of a Particle in a Leak-Proof Box

For simplicity we shall consider only one coordinate. Figure 6-10 shows the potential-energy diagram of a particle in a box having a

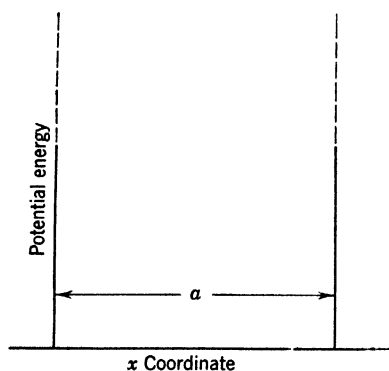


Fig. 6-10. Potential-energy diagram of a particle in a box of width a . The dashed lines are used to represent an infinitely high potential barrier.

width a . Inside the box, the potential energy is constant in accordance with the statement that the particle is free. Since the walls are assumed impenetrable, the potential energy makes a sharp rise to infinity (indicated by dotted lines) at the edges of the box. This potential energy diagram completely describes the problem. We know that ψ must be finite inside the box and zero outside. We conclude, therefore, that, at the edges of the box, where the potential energy goes to infinity, the ψ function must be zero. This restriction, however, is exactly the same one as

is applied to a uniform vibrating string with the ends clamped. Only those vibrations are allowed whose half-wavelengths fit into the width of the box (or the length of the string) an integral number of times n , as shown in Fig. 6-11. Since potential energy is only relative, we

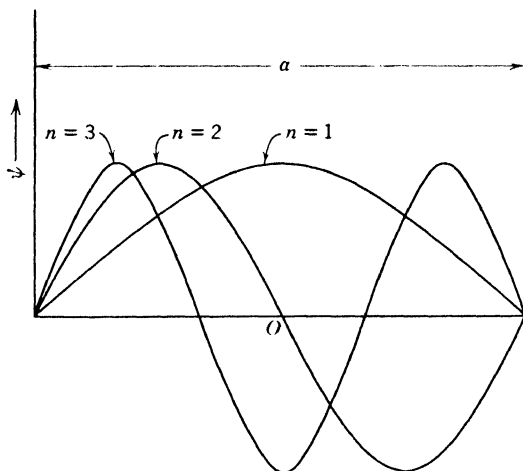


Fig. 6-11. Matter waves for three energy states of a particle held within the barriers shown in Fig. 6-10.

may call its value everywhere inside the box zero. The only energy of the particle is its kinetic energy. Its velocity is

$$v = h/m\lambda \quad (15)$$

However, the restriction above requires that

$$n(\lambda/2) = a \quad (16)$$

Therefore,

$$v = nh/2ma$$

and we have for the kinetic energy in the n th stationary state

$$E_n = n^2 h^2 / 8ma^2 \quad (17)$$

The boundary condition restricts n to an integer, and thus, in a very simple manner, wave mechanics leads to quantization.

One may justly ask, "Why is it that, if the energy of a particle in a box is quantized, this has not been noticed long before?" The answer is that we have never made direct observations on small enough particles.

With ordinary particles, the quantum numbers n are so high that the discrete differences between quantized states are not apparent. For example, let us assume that the mass is about 1/1000 that of a pin head, that is, about 10^{-6} gm, and that we give this small particle a velocity of 10^{-7} cm/sec so that, if the width of the box is 10 cm, it would require about 3 years to go across once. The energy would be

$$E = \frac{1}{2}mv^2 = \frac{1}{2} \times 10^{-6} \text{ gm} \times 10^{-14} \text{ cm}^2/\text{sec}^2 = 5 \times 10^{-21} \text{ erg}$$

We may now determine which quantum state this particle is in. From equation 17,

$$\begin{aligned} n &= \frac{\sqrt{8mE} a}{h} \\ &= \frac{(8 \times 10^{-6} \text{ gm} \times 5 \times 10^{-21} \text{ erg})^{1/2} \times 10 \text{ cm}}{6.6 \times 10^{-27} \text{ erg sec}} = 3 \times 10^{14} \end{aligned}$$

Thus, to be able to recognize the quantization of this particle by direct measurement, one must be able to distinguish between three hundred thousand billion and three hundred thousand billion and one! It is only when we deal with such small masses as electrons that quantization becomes important.

With the origin at the midpoint, the equations of the curves in Fig. 6-11 are

$$\psi_1 = A_1 \cos \pi x/a \quad \psi_2 = -A_2 \sin 2\pi x/a \quad \psi_3 = -A_3 \cos 3\pi x/a \quad (18)$$

It is perhaps more convenient to write them in the form

$$\psi_1 = A_1 \cos 2\pi p_1 x/h \quad \psi_2 = -A_2 \sin 2\pi p_2 x/h \quad \text{etc.} \quad (18a)$$

where p_n is the momentum of the particle in the n th quantum state.

9. The Penetration of a Potential Barrier

In Section 8 the potential energy barriers were assumed infinitely high for the sake of simplicity. In reality, no box has impenetrable walls; so we wish to see what happens when the potential barriers (or walls) have a height V_0 . Classical mechanics predicts that, if the total energy is less than V_0 , and the particle is inside, it stays inside; but, if the total energy is greater than V_0 , it rides off to infinity, with a kinetic energy smaller than the inside value by an amount V_0 . What, now, is the behavior of the wave function ψ in these two cases?

1. $E < V_0$. In the first case, the curves of Fig. 6-11 are modified in the way indicated in Fig. 6-12. The portion inside the box is still a sine or cosine wave, but the box contains less than half a wave. Each

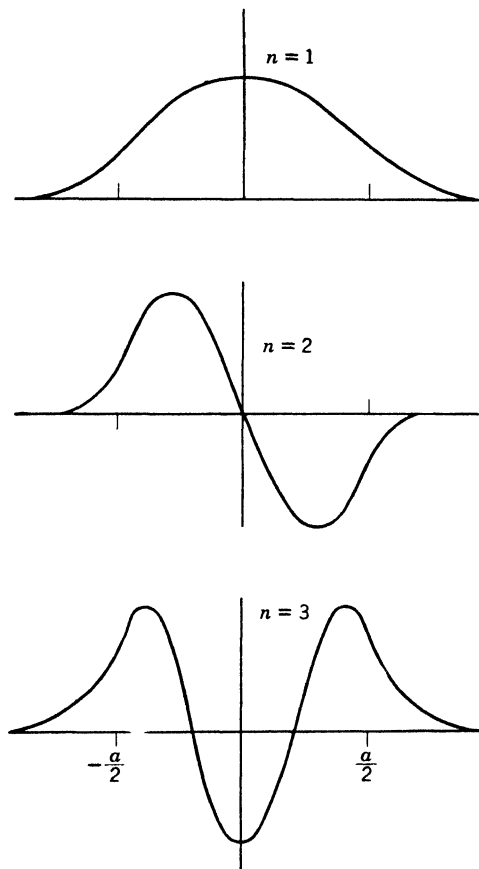


Fig. 6-12. Matter waves for three energy states of a particle influenced by potential walls of height V_0 and separation a . For $n = 1$ and $n = 3$, the curves are symmetrical. For $n = 2$, the curve is antisymmetrical.

curve is completed by adding tails, which drop off exponentially. The wave functions for the first quantum state are now as follows:

On the left (x always negative) $A_1 \cos (\pi p_1 a / h) e^{+\beta[x+(a / 2)]}$

In the box (x negative or positive) $A_1 \cos (2 \pi p_1 x / h)$

On the right (x always positive) $A_1 \cos (\pi p_1 a / h) e^{-\beta[x-(a / 2)]}$

Those for higher quantum states are similar, and β is defined by

$$\beta = \frac{2\pi}{h}[2m(V_0 - E)]^{1/2} \quad (19)$$

Thus, outside the box the wave drops off by a factor e in a distance

$$h/2\pi[2m(V_0 - E)]^{1/2}$$

But how is E determined? Merely from the common-sense conditions that (a) the first two of the above three expressions for the wave function must join together smoothly at the left wall, and (b) the last two must join together smoothly at the right wall. The reader will easily verify that they join; and some readers, familiar with calculus, will be able to show that the outside slope and the inside slope will agree at a wall, provided that

$$\tan(\pi p_1 a/h) = \left(\frac{V_0}{E_1} - 1\right)^{1/2} \quad (20)$$

Of course, $p_1 = (2mE_1)^{1/2}$, so this equation gives the energy. It is solved by trial, using a tangent table. The reader will note that there are several E values which satisfy it, because the tangent curve has a period π . In fact, the equation yields only the energy values for the odd-numbered quantum states, and the others have to be found from a similar equation in which the left side is replaced by $-\cot(\pi p_1 a/h)$.

2. $E > V_0$. When E is greater than V_0 , the wave functions are sine or cosine curves both inside and outside the box, but the momenta and therefore the wavelengths are different, inside and outside. The symmetry of the problem tells us that the inside wave function should be symmetrical or antisymmetrical (see Fig. 6-12) about the origin. As before, the curves must fit smoothly together at the potential walls (agreeing in height and in slope). Now, the business of fitting together two sine curves of different wavelength differs in detail from that of fitting together a sine curve and an exponential function. For the sine curves, this fitting can be done *whatever the value of E may be*, by merely adjusting the amplitude and phase of the outside wave function. Thus *the energy can have any value greater than V_0* . The process of fitting brings it about that the amplitude outside is somewhat smaller than the value prevailing in the box.

To summarize the points worthy of particular notice:

1. *Number of Energy Levels.* The number below V_0 is finite when the potential wall or box has the finite depth employed in this discussion. (For a potential valley of infinite depth, such as the Coulomb potential,

the number may be infinite, just as it is, by equation 17, for the potential of infinite height portrayed in Fig. 6-10.)

2. *The Leak Effect.* Even when E is less than V_0 , the waves "leak through" the potential barrier. This effect is like the behavior of light undergoing total internal reflection. Contrary to the statements of the elementary textbooks, light waves are found in the rarer medium, and they drop off exponentially as the distance from the boundary increases. They are seldom observed, because of the rapid drop of intensity, and because many people do not know where to look. In fact, the energy moves parallel to the surface, and conditions at the edges of the incident beam are curious and interesting; but we cannot pursue the subject here.

Where there are light waves there are photons. Should we not say that, where there are matter waves, there are material particles? If so, there must be some chance of finding a particle outside the potential walls, in the region where the wave amplitude is dropping off exponentially. *Contrary to classical mechanics*, this is indeed true. In certain cases (p. 362), the effect is readily observed, and it is a striking triumph for wave mechanics.

10. Born's Interpretation of the Wave Function

Now, what is ψ ? We have had many instances of the striking resemblance between the behavior of ψ and that of the electric or magnetic field of a wave of light. We have also seen (p. 89) that in optics the quantity $E^2 + H^2$ may be interpreted as a measure of the probability of finding a photon at a given place. Pursuing the analogy, Born assumed, in developing Schroedinger's theory further, that *the square of the amplitude ψ of the matter waves at a point in space gives the probability of finding a particle in a unit volume at that place.* Thus Schroedinger's theory cannot tell us where an electron is at any given time nor can it tell us exactly what paths the electrons follow in a given energy state. If we have a solution of Schroedinger's equation, we may calculate the time average of the positions that a given electron may occupy. The result is the same as we would obtain if we were able to photograph an atom using a long-time exposure. The motion of the electron is so fast that it would produce only a blur, but the darkening of the photographic plate at a given position would be proportional to the length of time that the electron spends in that position. The photograph would resemble that of a ball of mist, the mist being denser at the points at which the probability of an electron's presence is large. Those who work with Schroedinger's theory are accustomed to thinking of the atom as a misty ball of this kind. It is often convenient to reason in terms of such a

model, but in doing so we should remember that the model is only a picture of the statistical behavior of a single atom, or, if we prefer, of large numbers of atoms.

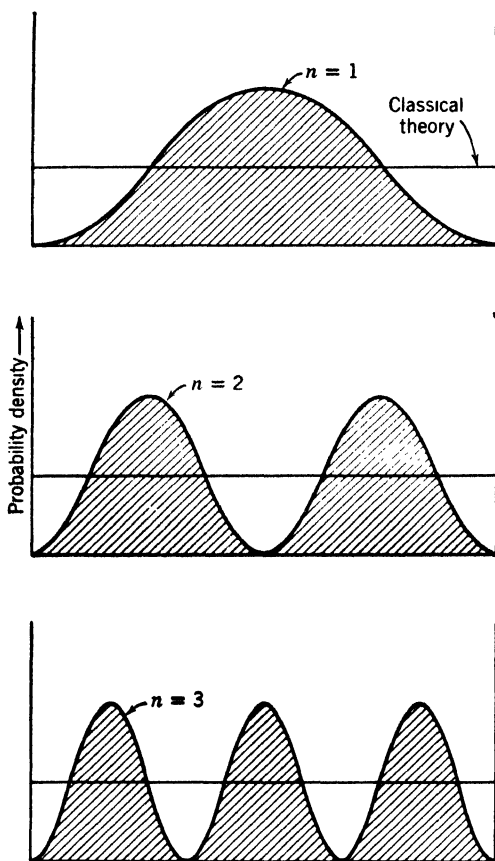


Fig. 6-13. Probability density distributions corresponding to the modes of vibration shown in Fig. 6-11.

An example. Figure 6-13 illustrates Born's ideas, showing the probability densities for the particle confined in the leak-proof box. Of course, in the classical theory, all positions in the box are equally probable, so that the probability density is a constant represented by the straight lines in Fig. 6-13. Thus, we arrive by means of wave mechanics at a result quite different from that of classical mechanics. In the lowest state $n = 1$, the probability density is a maximum at the

middle of the box and goes to zero at the edges. As the quantum number increases, new maxima appear and the maxima crowd closer together. In Section 8 we discussed numerically the case of a particle with a very high quantum number, 3×10^{14} . For this case, a diagram of the type shown in Fig. 6-13 would have 3×10^{14} peaks, all of the same height. Obviously it would be impossible to distinguish a probability distribution with such close array of peaks from the uniform one predicted by the classical theory. We see here the great resourcefulness of wave mechanics. Whenever we deal with large particles upon which accurate measurements can be made, wave mechanical results assume forms that are indistinguishable from those of the classical theory.

11. The Uncertainty Principle

It appears at first sight that the probability interpretations of both electromagnetic radiation and matter waves have fallen short of rendering the service we might expect since they do not describe the behavior of individual photons or material particles, respectively, in full detail. It remained for Heisenberg, in 1927, to put forward a point of view which indicates that this feature of the theory is not to be considered a fault, but rather an evidence of perfection. If the new mechanics is to furnish a faithful picture of nature, without excess or deficit, it should be able to make any statement which can be checked by experiment, and it should automatically *fail* to make any statement that cannot be checked by experiment.

The coupling between the object and the observer. Now it happens to be a fact that there are limitations on the amount of information we can obtain about a single particle by making measurements on it. This is true because every measuring device, when in use, disturbs the object it is designed to measure, and vice versa. With large objects the disturbance is negligible, but in the atomic world it assumes significant proportions. The very process of observation imposes on a measurement unavoidable limitations which make it experimentally impossible to obtain all the information in regard to an atom which would be required to predict its future individual behavior. In determining the position of an object, one of two fundamental methods (or else some combination of the two) must be employed: radiation may be allowed to fall on it, or other objects may be allowed to collide with it. For instance, suppose that we wish to turn on the electric light. First we try to find the switch. In daylight, a glance is sufficient to tell us where it is; in the dark, we grope about until one hand strikes it. The desired information is conveyed to us in the first instance by daylight which is

scattered by the switch into our eyes, and in the second by the behavior of a material probe (the hand) which collides with the object of our search. Similarly, the process of observing a very small particle such as an atom consists fundamentally in allowing that atom to scatter light or material particles. From the nature of the scattered radiation or particles, the original position of the atom is inferred. It is this scattering process which disturbs the atom during an observation. The discussion that follows deals almost entirely with the use of light in making measurements. The treatment for particles is very similar.

To approach the subject easily let us first set up a practical analogy. Big waves rolling toward the shore are not appreciably disturbed by a solitary wooden post fixed some distance out. The waves, divided as they pass the post, reunite and sweep on with unbroken crests toward the beach. Now suppose that the same post is fixed in a small pond on whose surface a breeze raises delicate ripples. Here the post occasions a relatively great disturbance, reflecting the ripples, bending them to new directions, creating small areas of calm and others of unexpectedly violent disturbance. Imagine some observer, sensitive only to the motion of water waves, and unable to perceive the post by any other means, who wished to determine its position. Would he gain more information from the ripples or from the heavy waves? Undoubtedly from the ripples. He would have to exercise nice discretion, however, in his choice of wavelengths. Waves that were very long would give him no information whatsoever; those that were too short, on the other hand, might offer him much detailed information (for example, whether the post were round or square) in which he had no interest. In general, the wavelength must be shorter than the greatest dimension of the details that are being studied. Having reached this conclusion, which is true also for all electromagnetic waves, let us forget the analogy of water waves, lest it lead us astray in the arguments that follow.

Example. Let us now see what experiment we would perform if we should wish to measure as accurately as possible both the position and the velocity of a small particle. To help in determining its position accurately, a microscope seems advisable. By using higher and higher magnifications, we might expect to be able to increase without limit the accuracy of our measurement.

Effects of diffraction. However, as every physicist knows, there is a size limit below which the images of particles become fuzzy and ill-defined, and one cannot hope to see clearly the shape of any particle which is much smaller than the wavelength of the light used. For this reason the physicist sometimes prefers blue light for illumination rather than red light. The source of this difficulty is that the images of points,

formed by the instrument, are not in fact points but rather diffraction patterns.

Textbooks on optics (Appendix 9, ref. 106, pp. 160-163) show that, if the light from a point source is imaged by a microscope objective, the central disk of the diffraction pattern has a width such that we cannot resolve two neighboring point sources when the distance between them is less than about $\lambda/2 \sin A$. Here $2A$ is the angle subtended by the objective at the point source. Suppose a photon were observed within the area of the central diffraction maximum pictured in Fig. 6-14. There is no certainty as to the place in the object plane from which it came, but there is a fair probability that it originated within a circular area whose radius is $\delta x = \lambda/2 \sin A$.

The maximum value of $\sin A$ is unity, so the only way in which the accuracy of locating the particle may be increased is by using light of shorter wavelength. In accordance with this reasoning, Heisenberg suggested a hypothetical experiment in which the particle would be observed with a "gamma-ray microscope."

Thus the wavelength would be very small and the position of the particle could be determined very accurately. However, a new difficulty then appeared. A photon that is scattered either receives from the particle or gives up to the particle some of its momentum. If we assume that the photon is originally directed parallel to the y axis, then, after being deflected, it will still pass through the microscope if its direction falls within the angle $2A$. All one knows, then, is that the photon passed through the microscope; one does not know exactly from which direction it came. In the present example, the photon will enter the microscope if its acquired component

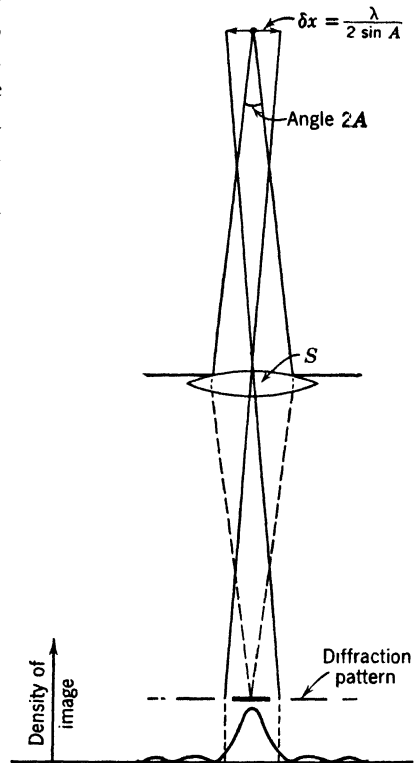


Fig. 6-14. Diffraction pattern produced when light from a point source passes through a microscope objective. The curve at the bottom and the horizontal bars above it show roughly the light intensity in the diffraction pattern formed in the image plane.

of momentum in the x direction is not greater than $\pm (h/\lambda) \sin A$ since the momentum associated with a photon is h/λ (p. 144). Thus, there is an uncertainty δp_x in the momentum of the particle equal to $(h/\lambda) \sin A$. Heisenberg pointed out that the difficulty which enters here is a general one. Whenever one attempts to increase the accuracy of a position measurement of a particle there is a corresponding decrease in the accuracy of measurement of its momentum or velocity. These uncertainties are related in a simple manner, thus

$$\delta x \delta p_x \sim \frac{\lambda}{2 \sin A} \frac{h}{\lambda} \sin A \sim h \quad (21)$$

$$\delta x \delta v_x \sim h/m$$

where m is the mass of the particle and the sign \sim is used to indicate approximate equality.

This statement was first formulated by Heisenberg and is known as the *uncertainty principle* or *principle of indetermination*. For positional coordinates it may be stated as follows:

If a coordinate x is measured with an error of the order δx , an uncertainty δp_x in our knowledge of the corresponding component of momentum p_x is introduced by the very process of measurement. The uncertainties δx and δp_x are connected by the relation

$$\delta x \delta p_x \sim h$$

where h is Planck's constant. Conversely, if p_x is measured with an error of the order δp_x , the value of x is made uncertain by an amount δx , satisfying this relation.

A closely related fact is that if we study a system during a time interval δt , we disturb its energy by an amount δE , such that

$$\delta t \delta E \sim h \quad (21a)$$

The shorter δt is, the more rapid the motions of our measuring devices must be; hence they induce larger changes of the energy.

The limitation (21) on the possible knowledge which we may acquire of the simultaneous position and momentum of a particle is in no way dependent upon the accuracy of our observing instruments. No instrument, however precise, can ever overcome the restrictions imposed by the uncertainty principle; they are inherent in Nature. What, then, is their significance?

Why Newtonian mechanics has been replaced by wave mechanics. If we cannot accurately specify both the position and the veloc-

ity of a moving body, we cannot exactly predict its position at a later time by employing the usual laws of motion. In this sense, the principle seems to rob ordinary dynamics of all significance, but it will be clear from one of the examples below that the limits set upon our knowledge by equation 21 cause no difficulty in problems of large scale dynamics, since the customary man-made errors of observation mask entirely the uncertainty limits set by nature. Difficulties will arise, however, if we overlook these uncertainty limits and attempt to predict, by Newtonian mechanics alone, the future behavior of atoms and electrons.

The uncertainty principle indicates that we should have a probability or statistical theory not only of *photons* but also of *material particles*. Thus, in developing a new mechanics we must have one which does not describe the motion of the individual particle or photon, since we cannot know both position and momentum with the requisite accuracy. As we said at the beginning of the discussion, no sensible system of atomic mechanics should try to furnish more information than we can verify by experiment. Heisenberg has stated the matter very clearly, as follows:

"It is *not* assumed that the quantum theory, as opposed to the classical theory, is essentially statistical, in the sense that nothing but statistical conclusions can be drawn from data which are given exactly. In the formulation of the causal law, namely, 'If we know the present exactly, we can predict the future,' not the conclusion, but the premise, is at fault." We cannot determine present conditions with the completeness necessary for the application of the classical theory. In this manner the uncertainty principle throws fresh light on the philosophic problems connected with causality and determinism. The extent of its ultimate influence in such fields cannot be properly appraised at present.

★ For the sake of clarity, two numerical examples of the application of the uncertainty principle will now be given.

★ 1. An electron moving along a discharge tube is known to have a velocity corresponding to some value between 20.00 and 20.01 electron volts. What is the greatest accuracy with which its position is known?

★ Here $\delta p_x = m \delta v_x$, where m is the mass of the electron and v_x its velocity along the tube. v_x is computed from the relation $\frac{1}{2}mv_x^2 = Ve/300$, where V is the applied voltage. We find $\delta v_x = 6 \times 10^4$ cm/sec. Hence

$$\delta x \sim \frac{h}{m \times \delta v_x} = \frac{6.6 \times 10^{-27}}{9 \times 10^{-28} \times 6 \times 10^4} \text{ cm} \sim 1.2 \times 10^{-4} \text{ cm}$$

★ 2. A 30-gm rifle bullet in flight is photographed by a mechanism set in operation by the bullet itself. The position of the bullet when it

actuates the mechanism is uncertain to the extent of 0.01 cm. What limitation does this set on our knowledge of the velocity of the bullet?

★ Here, $\delta x = 10^{-2}$ cm. Therefore

$$\delta p_x \sim h/\delta x = 6.6 \times 10^{-27} \times 10^2 = 6.6 \times 10^{-25} \text{ gm cm/sec}$$

$$\text{and } \delta v_x = 6.6 \times 10^{-25}/30 = 2.2 \times 10^{-26} \text{ cm/sec}$$

a quantity hopelessly beyond the limits of observation.

To avoid leaving a wrong impression, we must add a word concerning the predictions of wave mechanics in cases where some physical quantity is constant. Here the theory should provide a means for calculating the value of the constant quantity. Probability should give way to exactitude, as far as that quantity is concerned, and so it does. The energy of the isolated hydrogen atom is an example. True enough, we can only know what the energy is (or rather, *was*) by waiting until the atom radiates. By the time we have our knowledge, the energy has already changed, but this point should not disturb us because it is in good accord with our previous remarks about the disturbance that any system undergoes when a measurement is made. Ordinarily, *we* initiate a measurement and disturb the atom; in the present case, the *atom* takes the initiative, and thereafter we measure the wavelength of the light emitted.

★**Limits of accuracy in individual measurements.** It is commonplace to state that every measurement is affected by errors due to

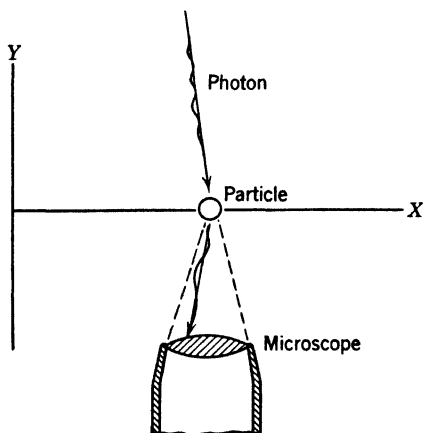


Fig. 6-15. Scattering of a photon into a microscope, on collision with a particle.

the imperfections of gross instruments, but it is reasonable to inquire whether the atomic nature of our tools introduces some fundamental limitation on the accuracy of measurement of a single quantity. It has been shown, by Flint and Richardson, and by Ruark, that there is a limit beyond which we cannot push the accuracy of our measurements of the position of a free particle. Suppose we wish to determine the x -coordinate of an electron, by allowing it to scatter a photon, Fig. 6-15. We attempt to make our determination of x as exact as possible, no matter how

great an uncertainty of the momentum is caused thereby. Obviously,

we must use light of very short wavelength, but nothing will be gained by using a wavelength much shorter than h/mc , because the measuring is done by noting the position of the scattered photon. This photon, having suffered a Compton collision, would have a wavelength greater than the incident one by an amount of the order h/mc , if the scattering angle were 90° . Much can be gained by reducing the scattering angle with a consequent decrease of wavelength; still, the microscope must have a finite angular aperture E , so the scattering angle and the scattered wavelength have a residual uncertainty. The uncertainty of the particle's x -coordinate turns out to be of the order of Eh/mc . Similar restrictions are met if we use a material particle as an exploring agent.

12. Simple Harmonic Oscillator

A problem that occurs very frequently in the atomic field is that of a particle held to an equilibrium position with a force proportional to its displacement from this position. On the basis of the classical theory, such a particle executes simple harmonic motion and is often referred to as a simple harmonic oscillator. A good example is a pendulum bob swinging with small amplitude. It passes through the center of the

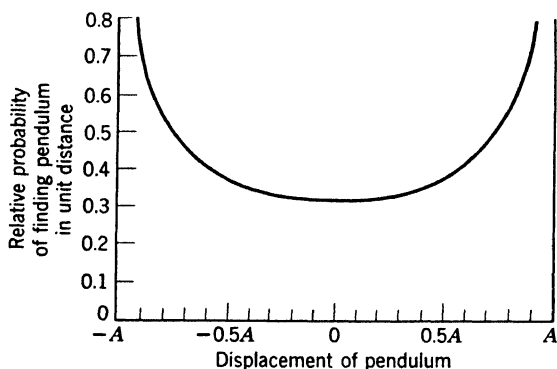


Fig. 6-16. The relative probability of finding a pendulum bob at different displacements, according to classical theory.

swing rather rapidly and then gradually slows down until it reaches the end of its swing, where it momentarily stops and reverses its motion. The pendulum bob spends most of its time at the ends of its path. Figure 6-16 shows the relative probability of finding the bob at any given point in its path.

★ Bohr's theory, applied to a harmonic oscillator of frequency ν_0 , states that the energy may have the values

$$E_n = n h \nu_0 \quad (22)$$

where $n = 0, 1, 2$, etc. It is natural to expect that the lowest energy value should correspond to a state of rest.

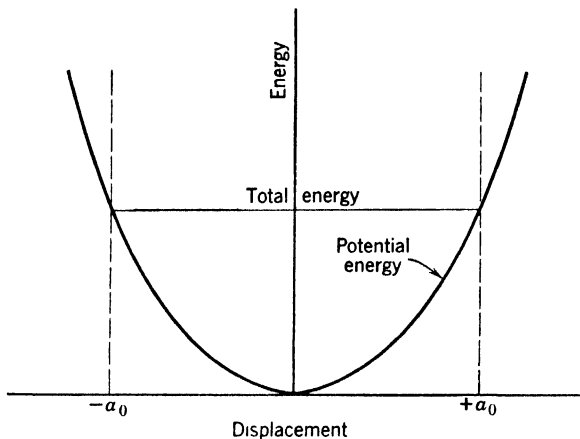


Fig. 6-17. Potential-energy diagram for a simple harmonic oscillator.

★ The potential energy, shown in Fig. 6-17, is given by

$$V = \frac{1}{2} k x^2 \quad (23)$$

where k is the restoring force called forth by unit displacement. We recall that $2\pi\nu_0 = (k/m)^{1/2}$, where m is the mass of the bob.

★ The problem of getting the energy values and the wave functions by wave mechanics cannot be dealt with here, but we shall state the results. The energy values are given by

$$E_n = (n + \frac{1}{2}) h \nu_0 \quad (24)$$

where $n = 0, 1, 2$, etc. This result disagrees with equation 22, and predicts that the oscillator has a finite energy, $\frac{1}{2} h \nu_0$, in its lowest state. Considering a solid body as a group of identical oscillators, there is a residuum of energy resident in it even at absolute zero.

★ It is known that, in emission or absorption, a harmonic oscillator changes its quantum number only one step at a time (p. 244). By equation 24, the frequency emitted or absorbed is always ν_0 .

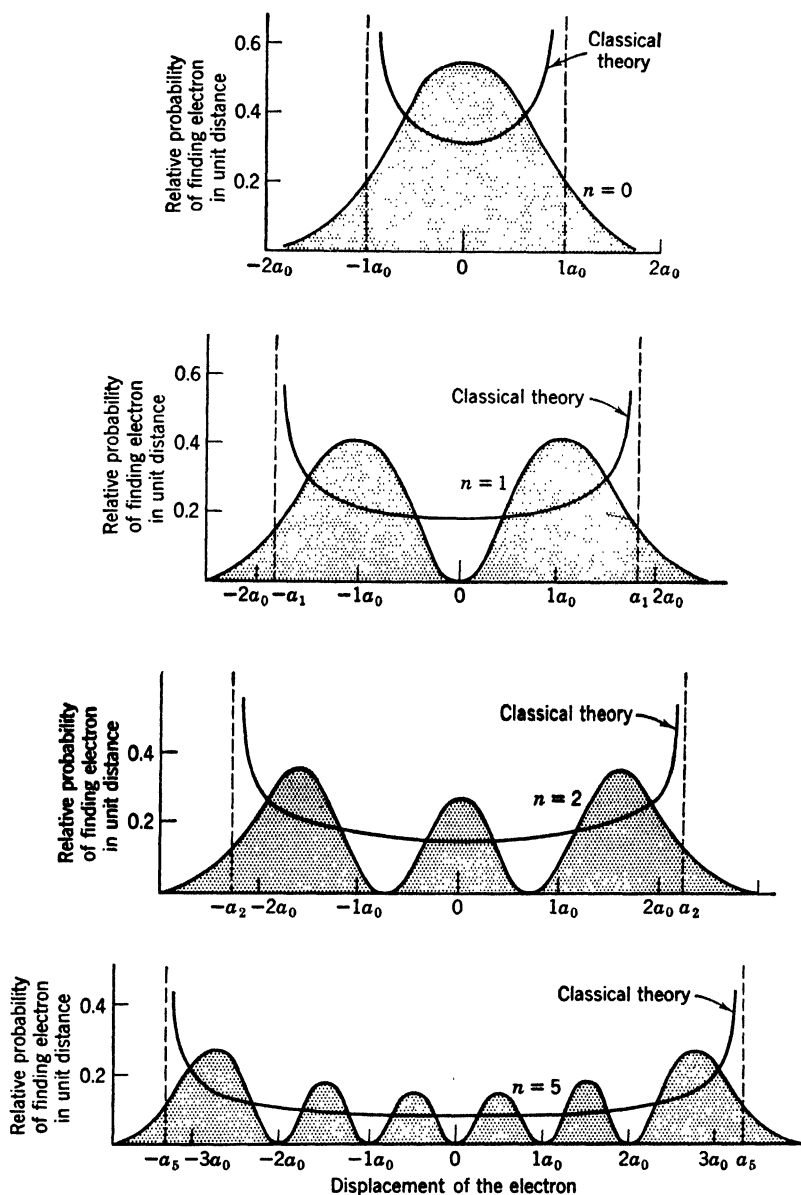


Fig. 6-18. Each diagram shows the relative probability of finding various displacements, for a particular state of a harmonic oscillator. n is the quantum number and a_n the amplitude of the corresponding classical motion.

★ The wave functions are of the form

$$\psi_n = C_n e^{-(x/a_0)^2/2} f_n(x/a_0) \quad (25)$$

where C_n is a constant, f_n is a polynomial, and a_0 is the amplitude that the oscillator would possess, on the basis of ordinary mechanics, if the energy were $h\nu_0/2$. In particular, the wave function for the lowest state is simply

$$\psi_0 = \frac{1}{\pi^{1/2} a_0^{1/2}} e^{-x^2/2a_0^2} \quad (26)$$

It is instructive to compare these results with those obtained for a particle in a leak-proof box. Consider the two potential-energy diagrams, Figs. 6-10 and 6-17. In both diagrams there is a deep valley, but in Fig. 6-17 there are no sharp corners. One can expect, therefore, that the wave functions will be of the same general shape but with less abrupt endings. Figure 6-18 presents the probability density curves for a simple harmonic oscillator corresponding to those of the "particle in a box" shown in Fig. 6-11, and the similarity will be noted. In the lowest state, just as before, the probability density is quite different from that of the classical theory, but, as the quantum number increases, the probability density tends toward that of the classical theory. If

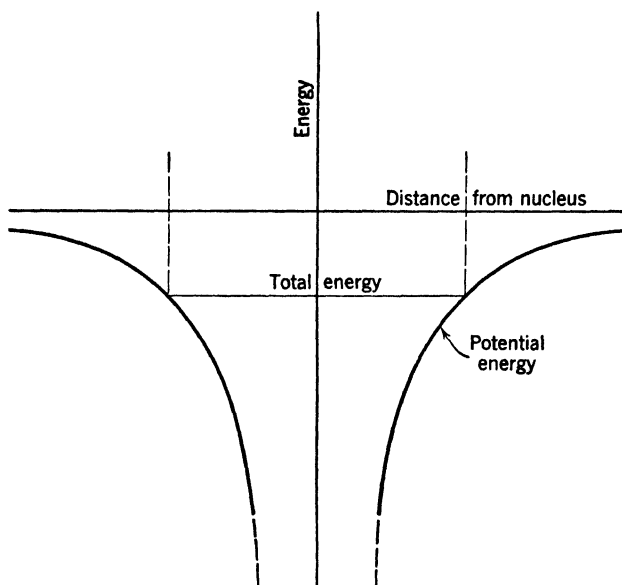


Fig. 6-19. Potential-energy diagram corresponding to an inverse square law of force.

one assumes a given total energy of the bob, the maximum displacement is very definite on the basis of the classical theory and occurs whenever the potential energy equals the total energy. In wave mechanics, however, this definiteness is lost, and we note in the diagrams a fairly large probability, in the lower states, that the bob will be beyond the classical amplitude.

13. Results of the Wave Theory of the Hydrogen Atom

The solution of the hydrogen problem begins with the potential energy diagram corresponding to the inverse square law of force (Fig. 6-19). As in previous problems, it has a valley; now, however, the curve goes to minus infinity at the origin. The right part of Fig. 6-20 shows that

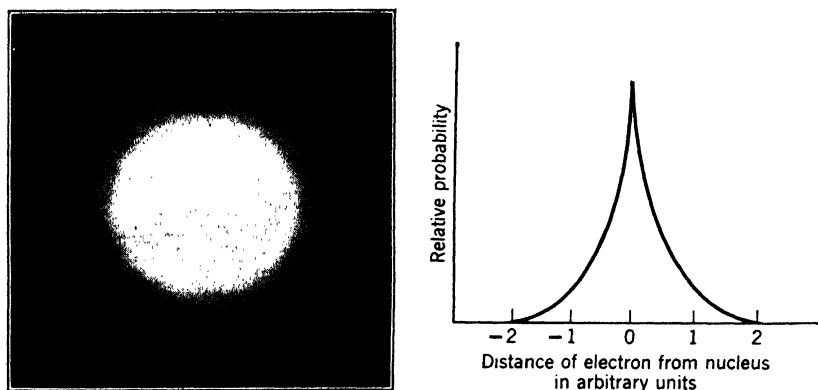


Fig. 6-20. Charge distribution in the lowest state of the hydrogen atom. In this state the probability distribution has spherical symmetry. (After H. E. White.)

the probability distribution in the lowest state resembles those obtained before, except for a sharp rise at the origin. There is, however, another difference, since the present problem is a three-dimensional one. The potential energy does not vary with the longitude or latitude of the electron with respect to the nucleus, so that, in the lowest state, the probability density will be the same in all directions. Thus, the average electron distribution for the hydrogen atom in the first quantum state is perfectly symmetrical in all directions around a point. In fact, the wave function for this state is

$$\psi_0 = \frac{1}{(\pi a_0^3)^{1/2}} e^{-r/a} \quad (27)$$

a being the first Bohr radius. There is no suggestion of an orbit; indeed, in contradiction to Bohr's theory, wave mechanics states that the angular momentum for the lowest state is zero. The probability of finding the electron at a given point, or the charge density if the average over a long time is taken, is large near the center and then gradually fades until it becomes imperceptibly thin at large distances from the nucleus. It is apparent from this diagram that, according to wave mechanics, the electron is more likely to be found coincident with the nucleus than at any other single point in space. This strange result may arise from the approximations made in obtaining a solution (inverse square law and non-relativistic mechanics).

The figure (6-20) shows the idealized concept of a time-exposure photograph of the hydrogen atom in which the average charge distribution is determined by the whiteness of the photograph. Figure 6-21

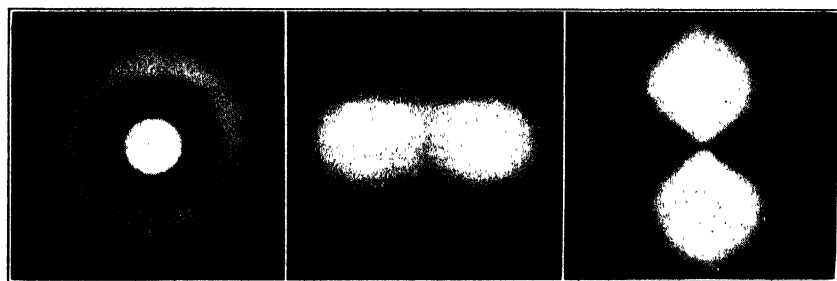


Fig. 6-21. The different charge distributions for the second state of hydrogen. There are four possibilities (two of which are alike), depending on the values of the orbital and the magnetic quantum numbers. See p. 226. Each distribution is symmetrical about a vertical axis. (After H. E. White.)

shows the three different charge distributions of the hydrogen atom for the state for which $n = 2$. The energies of these various distributions are very nearly identical so that for our present discussion they are indistinguishable.

14. Summary

We have traced the development of the wave and corpuscular theories of light and of matter and have seen how scientific opinion swayed from one extreme to the other. Gradually it has settled into a consistent intermediate position. The classical laws of mechanics which hold so well for large masses must be modified before they may be applied to bodies of very small mass. We are led to believe that we can never

predict exactly the paths which particles of protonic or electronic mass will take within the atom or molecule. Instead, we can merely express the probability that these particles will be found in a particular region at a given time. To obtain this probability we must solve the standard wave equations of optics for photons or the Schrodinger wave equation for electrons or other material bodies. Wave mechanics has been uniformly successful, giving correct energy values and other predictions in cases so numerous that today its basic principles are generally accepted. In all calculations, we may consider the waves alone, without even mentioning particles; but in experimentation we find that the gross physical effects are built up step by step, revealing the particle aspect of the phenomenon.

The reason behind this situation cannot be fully elucidated in this volume. It depends on an extension of wave mechanics, a quantum theory of the electromagnetic field itself. The interested reader will do well to consult ref. 28, Appendix 9; and he should be aware that a more thorough understanding of the self-energy of fundamental particles may alter the theory somewhat in the future.

REFERENCES

Appendix 9, refs. 13, 22, 23, 28, 42, 63, 101, 102, 106.

PROBLEMS

1. Determine the wavelength associated with a hydrogen atom moving with a velocity corresponding to 273°K .
2. Calculate the wavelength of the waves associated with a 50-volt electron.
3. Using equation 4, calculate the circumference of the ninth Bohr orbit. Using equation 5 to obtain the velocity, calculate the wavelength of an electron traveling in this orbit. What is the ratio of its circumference to the corresponding wavelength?
4. Find the velocity of the matter waves accompanying an electron whose speed is 6×10^7 cm/sec.
5. Using equation 13, show how the wavelength of the matter waves behaves in the first state of the hydrogen atom, as we pass inward, from the first orbit toward the nucleus.
6. Suppose an electron is trapped in a vacancy in an otherwise perfect crystal. Treat its x -component of motion, by assuming it is in a leak-proof cube whose side is 3 angstroms. What is the lowest possible velocity? The lowest energy?
7. Calculate the fractional part of the time in which the bob of a seconds pendulum is within 1 cm of the origin if the amplitude of swing is 4 cm.
8. Draw the potential-energy diagram of a 10-gm bob fastened to a string 20 cm long. Assume that the displacements are sufficiently small that the restoring force is proportional to the displacement.
9. Assume that Fig. 6-19 applies to the case of a point nucleus of charge $+Ze$ and a point electron of charge $-e$. (a) What is the potential energy when the

electron is at a distance $R_0, R_0/10$? (b) Find the equation of the curve using potential energy V and radial distance r as variables. (c) Within what volume is the potential, in absolute value, greater than at $R_0, R_0/10$?

10. A 1-volt electron is under the influence of potential walls whose height is 5 ev. Compare the chances of its residence (per unit length) for two points which are, respectively, 0.1 Å and 1 Å outside the walls. See Fig. 6-12 and equation 19.

11. Suppose we find the position of an electron with an accuracy of about 0.5 Å, the radius of the first Bohr orbit of hydrogen. What is the uncertainty of its momentum, caused by this measurement? And what can be said about the uncertainty of its kinetic energy?

12. If the electron of problem 11 was in the lowest state of a hydrogen atom, can we make a positive statement as to whether it will remain in the atom *after* the specified measurement is made?

13. Draw an energy diagram for a vibrating molecule (assumed simple harmonic) whose radiation has a wavelength of 3μ . Let the ordinate be in cm^{-1} , since wave numbers serve as well as energies for such a plot.

14. Draw the wave function for the first state of the H atom, with abscissas expressed in terms of the Bohr radius as a unit. (See Fig. 6-20.)

ANSWERS TO PROBLEMS

1. $1.53 \times 10^{-8} \text{ cm.}$

4. $1.5 \times 10^{13} \text{ cm/sec.}$

2. $1.73 \times 10^{-8} \text{ cm.}$

6. $1.2 \times 10^8 \text{ cm/sec; } 6.8 \times 10^{-12} \text{ erg.}$

3. $2.68 \times 10^{-6} \text{ cm; } 2.98 \times 10^{-7} \text{ cm; } 9.$

7. 16 per cent.

9. (a) $(-e)(+Ze)/R_0$, 10 times the preceding value; (b) $V + Ze^2/r = 0$; (c) $(4\pi/3)R_0^3$, 1/1000 of the preceding value.

10. The chance of residing in a very small range x in the neighborhood of 0.1 Å is only 0.16 as large as the corresponding chance for an equal range at 1 Å.

$$\psi(1 \text{ Å})/\psi(0.1 \text{ Å}) = e^{-\beta(10^{-8}-10^{-9})} = e^{-\beta(9 \times 10^{-9})}$$

Put $\beta = (2\pi/h)(2m[V_0 - E])^{1/2}$, with $V_0 = 5 \times 1.6 \times 10^{-12} \text{ erg}$ and $E = 1 \times 1.6 \times 10^{-12} \text{ erg}$. The ratio of the ψ 's is 0.397, and the ratio of the two values of ψ^2 is 0.16.

11. Uncertainty of the momentum = $1.3 \times 10^{-18} \text{ gm cm/sec.}$

12. No.

Atomic Spectra and the Pauli Principle

The Bohr theory gave a satisfactory account of the spectra of atoms with 1 electron, but failed for others. We saw in Chapter 5 that it applies fairly well in giving the energy levels of electrons deep within the atom, where the influence of neighboring electrons is slight compared with that of the nucleus. Its failure when applied to more complex systems showed that it was only an approximation to the truth, but it is a useful approximation. Although we shall use a few wave-mechanical values of angular momentum vectors, which differ slightly from the ones predicted by Bohr theory, the discussion in this chapter will be carried on in terms of particles and orbits. The model employed is often called the vector model of the atom. First we describe the spectra of atoms with only one outside electron, or valence electron, not belonging to a closed shell (see p. 229). These spectra are somewhat similar to that of hydrogen. The number and the arrangement of the spectral terms point clearly to the existence of an intrinsic or internal angular momentum of the electron. The magnitude of this angular momentum turns out to be $\sqrt{\frac{3}{4}}\hbar/2\pi$. In the case of hydrogen the influence of the electron spin on energy levels is so slight that we have neglected it, but for atoms with several electrons the spin becomes important.

Next, as we study the spectra of atoms with several valence electrons, a great generalization, the Pauli principle, comes into view. Together with the general principles of wave mechanics, it dominates the subject of atomic and molecular structure. This principle, in its simplest form, asserts that *no two electrons in an atom or molecule can have the same set of quantum numbers, including a quantum number for the electron spin.*

We then consider the verification of spectral theory by electrical and optical experiments. The remainder of the chapter is devoted to the magnetic properties of atoms.

1. Spectra of the Alkalies

Soon after Balmer's discovery of series relations in the spectrum of hydrogen (1885), Rydberg found similar relations in other spectra. The spectra of the alkalies and some other metals have many series which resemble the Balmer series. Even before Balmer's work, Hartley found groups of lines in the magnesium spectrum with constant frequency differences between their components. Using clues of this kind, Rydberg identified three separate groups of doublets in each alkali spectrum, and arranged them in series. As in the hydrogen spectrum, the lines of each series crowd closer together and approach a limit as we proceed toward the violet end of the spectrum (Fig. 7-1).

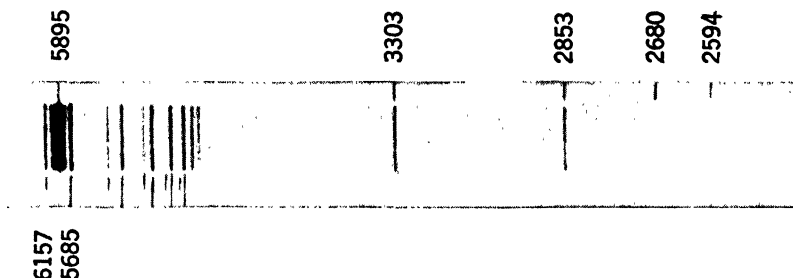


Fig. 7-1. The emission spectrum of sodium. The spectrum is in the central band; above and below are lines that are merely markers. The top row of markers indicates the principal series; below, the longer markers point to the diffuse series, the shorter ones to the sharp series. Wavelengths are approximate. (*Courtesy of Dover Publications, New York, from Atomic Spectra and Atomic Structure, by Dr. G. Herzberg.*)

The existence of Balmer-like series in the alkalies indicates that the structure of an alkali atom is somewhat similar to that of a hydrogen atom. In other words, an alkali atom behaves as though it consisted of a central region containing a distribution of positive charge, with a single valence electron moving in the field of that charge. We may suppose (Fig. 7-2) that the nucleus, carrying a positive charge Ze , is closely surrounded by $Z - 1$ electrons, leaving 1 electron in an orbit of relatively great size. However, the inner electrons are not completely effective in screening the nucleus. Hence the *effective nuclear charge* operating to guide the valence electron is greater than e . This effective charge varies as we pass from one orbit of the valence electron to another. In particular, for orbits with the same total quantum number n , the effective charge depends on the value of the angular momentum, that is, the value of the azimuthal quantum number. While all energy levels

with a given n coincide in the case of hydrogen, they are separated in the spectra of the alkalies. Corresponding to one spectral series of hydrogen, we have several series in an alkali. It must not be thought that the orbits are ellipses. In the field of a distributed positive charge, the valence electron will move somewhat as shown in Fig. 7-3.

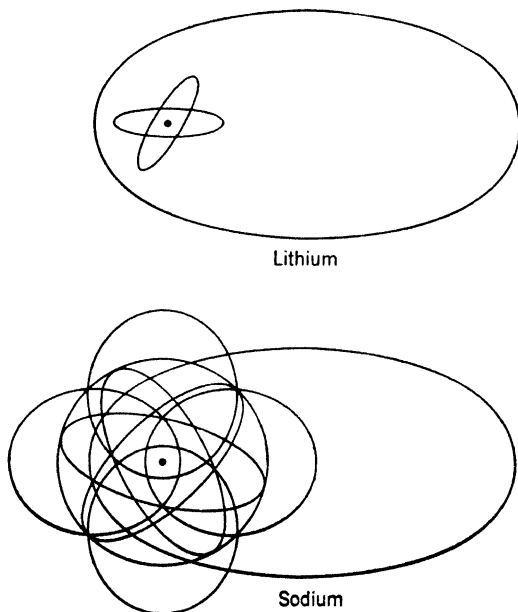


Fig. 7-2. Models of lithium and sodium. In sodium, the valence electron has a total quantum number $n = 3$. Two electrons have $n = 1$, and eight have $n = 2$. The ten inner electrons are called the core.

Spectral series of sodium; the Rydberg formula. Although each series in the spectrum of an alkali atom is composed of doublets it is simpler to consider them, for the present, as made up of single lines. Only the sodium spectrum will be discussed, for it is typical of the entire group. The series resulting from transitions to the lowest energy level of an alkali atom is called the principal series. It is marked in Fig. 7-1. The Fraunhofer D lines at 5890 and 5896 Å form the first doublet of this series. (In the early days of spectroscopy some of the most prominent Fraunhofer lines were designated by letters of the alphabet.) Two other prominent series are shown and are called the sharp and diffuse series because of the characteristic appearance of their lines. Rydberg originally expressed the wave numbers of the lines of each alkali series

by the formula

$$\tilde{\nu} = A - \frac{R}{(M + f)^2} \quad (1)$$

M is an integer which increases by unity when we pass from one line to the next in the series, going toward shorter wavelengths. A is called

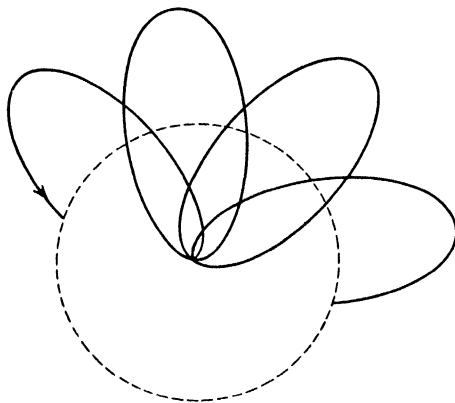


Fig. 7-3. A valence electron moving in the combined field of the nucleus and the other electrons of the atom.

the constant term, and the fraction following it the variable term, because it changes as we pass from line to line; and f is a proper fraction characteristic of the element and of the particular series. However, we prefer to write

$$\tilde{\nu} = A - \frac{R}{(n - a)^2} \quad (2)$$

where n is the total quantum number, already referred to on p. 102. The number a , usually positive, is called the “quantum defect,” that is, the amount by which the denominator falls short of the value it would have for a hydrogenic atom.

Figure 7-4 shows the energy levels of sodium. The spacings between the levels are not to scale, the better to show detail. For the levels with total quantum number $n = 3$, the Bohr theory suggests that the azimuthal quantum number k can be 1, 2, or 3. However, it is an important result of wave mechanics that the angular momentum differs from the value given by Bohr’s theory. Therefore we should introduce the *correct angular momentum value*

$$\sqrt{l(l+1)} \hbar/2\pi \quad (3)$$

where $l = k - 1$.

Spectral levels are now labeled either by giving n and l , or by writing n followed by a conventional letter, assigned in the following way:

l	0	1	2	3	4	5
Letter	S	P	D	F	G	H , etc.

This curious choice of letters is made for historical reasons. S , P , D , and F were originally used to designate the variable terms of the sharp, principal, diffuse, and fundamental series, although there was nothing

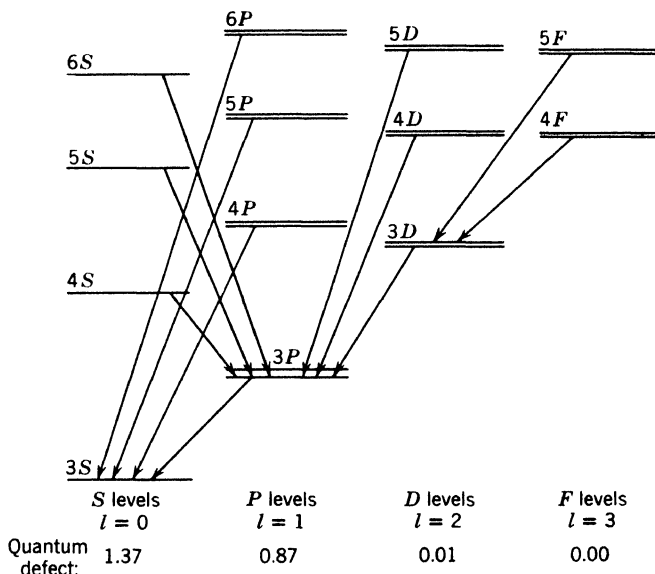


Fig. 7-4. Energy levels for sodium. For a given total quantum number, the S and P levels are lower than the D and F levels, because the electron penetrates closer to the nucleus. The P , D , and F levels are double on account of electron spin. For the S levels, the double character is lost because $l = 0$, as explained in the text. Still, they are called doublet S levels since they belong to a system of levels that are predominantly double.

particularly fundamental about the last. Afterward, the letters G , H , etc., were added to the sequence as needed. In Fig. 7-4, the *principal series* of spectral lines is the one in which the electron passes from the levels nP to the final level $3S$. It can be written

$$\tilde{\nu} = \frac{R}{(3 - S)^2} - \frac{R}{(n - P)^2} \quad (4)$$

where the numbers S and P in the denominator are particular values of the quantity a occurring in equation 2. Abbreviation became neces-

sary, and such formulas are generally expressed in a sort of shorthand. For sodium we write:

Principal series	$\tilde{\nu} = 3S - nP$	$n = 3, 4, \dots$
Sharp series	$\tilde{\nu} = 3P - nS$	$n = 4, 5, \dots$
Diffuse series	$\tilde{\nu} = 3P - nD$	$n = 3, 4, \dots$
Fundamental series	$\tilde{\nu} = 3D - nF$	$n = 4, 5, \dots$

For other alkalis, with different total quantum numbers for the ground state, the scheme is similar.

Figure 7-4 is worth detailed study. Notice that:

1. All the levels are double, except the S levels. This is an effect due to electron spin.

2. Electrons may transfer only from one column of the diagram to adjacent ones; that is, l changes by only plus or minus 1. (There are minor exceptions which we shall not discuss.) This is called a selection rule, written algebraically as

$$\Delta l = \pm 1 \quad (5)$$

3. The quantum defect decreases as l increases. For sodium the approximate values are shown at the foot of the figure. Each value is explained by considering the motion of the valence electron. In the D levels, the electron is thought of as moving on a "fat" orbit, and keeps far from the core, as the remainder of the atom is called. The actual charge of the core and its effective charge are then nearly equal. In the P levels, the orbit is thinner, and the electron moves closer to the core, or may penetrate it; so the quantum defect is greater. Finally, we think of the electron, in the S states, as moving through the core; the quantum defect is still greater.

2. Electron Spin; The Explanation of Doublets in Alkali Spectra

Up to this point we have considered the electron merely as a point charge revolving about a nucleus. To explain the doublet nature of the terms of the alkali spectra and similar phenomena in other spectra it is necessary to recognize that the electron behaves as though it were a finite body spinning around an axis through its center of mass. This concept was introduced by Uhlenbeck and Goudsmit, and by Urey and Bichowsky independently. A spinning electron of finite volume is equivalent to a system of circular electric currents. It behaves essentially like a tiny magnet. The angular momentum has the value

$$\sqrt{|s|(|s| + 1)}h/2\pi = \sqrt{\frac{3}{4}}h/2\pi = 0.866 h/2\pi \quad (6)$$

where s is called the spin quantum number and is either $\frac{1}{2}$ or $-\frac{1}{2}$, for reasons to be explained shortly. It can be proved that the magnetic moment of the electron is equal to its angular momentum times e/mc , with e in esu. Thus the magnetic moment is

$$\sqrt{\frac{3}{4}}eh/2\pi mc \quad (7)$$

The orbital motion of the electron produces a magnetic field in accordance with Ampère's law, but the magnetic moment due to spin cannot respond to this magnetic field. However, there is a mechanism by which *the self-magnetic moment of the electron becomes oriented* relative to its own orbital magnetic moment. From the standpoint of an observer riding on the electron, the nucleus and the charged core move in an orbit around it, and therefore produce a magnetic field at the position of the electron. On p. 106 we indicated that a hydrogen atom in an external magnetic field becomes oriented with respect to the lines of force. Similarly, in the present case, the electron's magnetic moment becomes oriented relative to the magnetic field produced by the nucleus and the inner electrons. But this field is perpendicular to the electron orbit, so it is necessary to include a term, the so-called spin-orbit term, in the energy of the system. This term depends on the orientation of the electron spin relative to the plane of its own orbit. A detailed discussion of this situation has been worked out by L. H. Thomas and by Frenkel; but suffice it to say that:

1. The component of angular momentum perpendicular to the plane of the orbit is always either $+h/4\pi$ or $-h/4\pi$. Calling this quantity $sh/2\pi$, we see that $s = +\frac{1}{2}$ or $-\frac{1}{2}$ in these two cases, respectively.

2. It has become customary to say that "the electron spin is $\frac{1}{2}$," meaning $(\frac{1}{2})h/2\pi$. This is merely a *convention*, useful in *enumerating* the various energy levels of complicated atoms. The actual angular momentum due to the spin is given by equation 6.

We shall employ this convention in discussing sodium. The doublets in Fig. 7-4 correspond to the two orientations of the electron relative to the plane of the orbit, as shown in Fig. 7-5. The total angular momentum of the atom is then said, conventionally, to be

$$jh/2\pi = (l + \frac{1}{2})h/2\pi \text{ when } l \text{ and } s \text{ are parallel}$$

or
$$jh/2\pi = (l - \frac{1}{2})h/2\pi \text{ when } l \text{ and } s \text{ are antiparallel}$$

The quantity j is called the *inner* quantum number, because it was erroneously supposed that it represented the angular momentum of the core, before the presently accepted theory was developed. We must

add that in reality the total angular momentum of the alkali atom is $\sqrt{j(j+1)}h/2\pi$.

★ One special case remains to be considered. If $l = 0$, as in the S states of the atom, the resultant of l and s has only one possible value,



Fig. 7-5. The two possible orientations of the spin-momentum vector s , with respect to the orbital angular momentum vector l . The energy depends on the angle between l and s . The representation of the electron as a spinning ball of electric charge should not be taken too seriously.

namely, $1/2$. The S energy levels are, therefore, single, as shown in Fig. 7-4. When $l = 1$, j may take the values $3/2$ or $1/2$. The P levels are thus doublets and are generally designated as $n^2P_{1/2}$ and $n^2P_{3/2}$, in which n indicates the total number, the superscript the multiplicity (doublet), and the subscript the quantum number j .

Table 7-1 shows the term designations and quantum numbers of the alkali spectra.

TABLE 7-1

Term Symbol	l	s	j	Terms
S	0	$1/2$	$1/2$	$n^2S_{1/2}^*$
P	1	$1/2$	$3/2$	$n^2P_{3/2}$
		$-1/2$	$1/2$	$n^2P_{1/2}$
D	2	$1/2$	$5/2$	$n^2D_{5/2}$
		$-1/2$	$3/2$	$n^2D_{3/2}$
F	3	$1/2$	$7/2$	$n^2F_{7/2}$
		$-1/2$	$5/2$	$n^2F_{5/2}$

* Although S levels are always single, the symbol 2S is used since there would be two levels if l were not zero.

3. Selection Rules

It might be expected that the lines of the diffuse series would appear in groups of four since there are two P terms and two D terms for each value of n . It is found that transitions are permissible only when the

change in j is ± 1 or zero. Consider the four possible transitions between a pair of D levels and a pair of P levels, shown in Fig. 7-6:

Line	Change of j in Emission	Situation
$3^2P_{3/2} - n^2D_{5/2}$	-1	Observed
$3^2P_{3/2} - n^2D_{3/2}$	0	Observed
$3^2P_{1/2} - n^2D_{5/2}$	-2	Not observed
$3^2P_{1/2} - n^2D_{3/2}$	-1	Observed

All these lines obey the selection rule for l , but the third would violate the selection rule for j and does not appear.

★ For the explanation of the selection rule for l , we must refer the interested reader to works on wave mechanics, but the selection rule for j can be understood by considering the angular momentum carried away by the emitted light. When Δj is zero, the electromagnetic field radiated by the atom is like that from a hypothetical linear oscillator whose motion is allowed to decay under the action of its own radiation. Such a field carries no angular momentum. On the other hand, if Δj is $+1$ or -1 ,

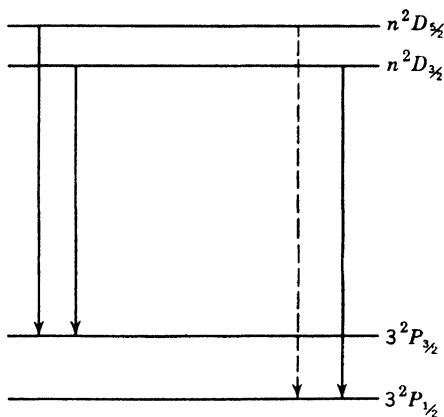


Fig. 7-6. Transitions between doublet levels. Three lines appear. The fourth is absent because j cannot change by 2 units.

the field is like that from a decaying circular oscillator. The light is circularly polarized, when viewed along a line perpendicular to the plane of motion of the oscillator, and passing through the center of its orbit. It can be shown that such a circularly polarized spherical wave, of energy W , carries an angular momentum equal to $W/2\pi\nu$. Putting $W = h\nu$, we see that the electromagnetic energy emitted by a single atom when $\Delta j = \pm 1$ has an angular momentum $h/2\pi$. Higher amounts of angular momentum cannot be associated with an energy $h\nu$ emitted by such an oscillator, so j should not change by 2 units or more. It is found that, in rare cases, transitions *do* occur in which j changes by 2 units, but this happens only when the atom is disturbed by the presence of neighbors, which are able to accept or to supply angular momentum.

Note on spectroscopic notation. Since spectroscopic terminology may be confusing to the beginner, we summarize here the broad ideas underlying it.

1. A particular *electron* is described as an *s*, *p*, *d*, *f*, etc., *electron*, according to its azimuthal number, just as we might describe a person as a Swede, or a Pole, or a Dane. When we desire also to show the total quantum number, we add it ahead of the letter, as follows: *ns*, *np*, etc. (An alternative scheme is to write n_l .) These symbols refer to electrons, not to spectral terms or energy levels.

2. Spectroscopic *terms*, without regard to their numerical values, are described by the capital letters *S*, *P*, *D*, *F*, just as we might describe a climate as temperate, without saying where that climate occurs.

3. A spectroscopic term *value* can be calculated from an algebraic expression. Two such expressions occur on the right-hand side of equation 4. (The second of these can assume a series of values for different integral values of *n*.) The *value* of a spectroscopic term gives its position on an energy-level diagram such as Fig. 7-4. In somewhat similar fashion we might specify the latitude of a temperate region where Danes live.

4. When we wish to give more detailed information about a term, we use the *complete* notation, of the type

$$n^2P_{3/2}$$

already described on p. 200.

4. Atoms with Several Valence Electrons

The spectra of many atoms with several valence electrons may be understood by easy extensions of the principles employed in our treatment of alkali spectra.

★ The second column of the periodic table contains the alkaline earths and Zn, Cd, and Hg, all of which have two valence electrons. These elements show spectral series arising from transitions of one electron. The energy levels occur as singlets and as triplets. Ruark showed that there are also lines arising from jumps of two electrons, but they will not be discussed because the same general principles apply. Figure 7-7 is a simplified energy diagram for mercury, not showing the threefold character of some levels. Many possible spectral lines are omitted to avoid confusion. The transitions between singlet levels give rise to spectral series, very similar to those of sodium when the doublet character of the latter is overlooked. The same can be said of transitions

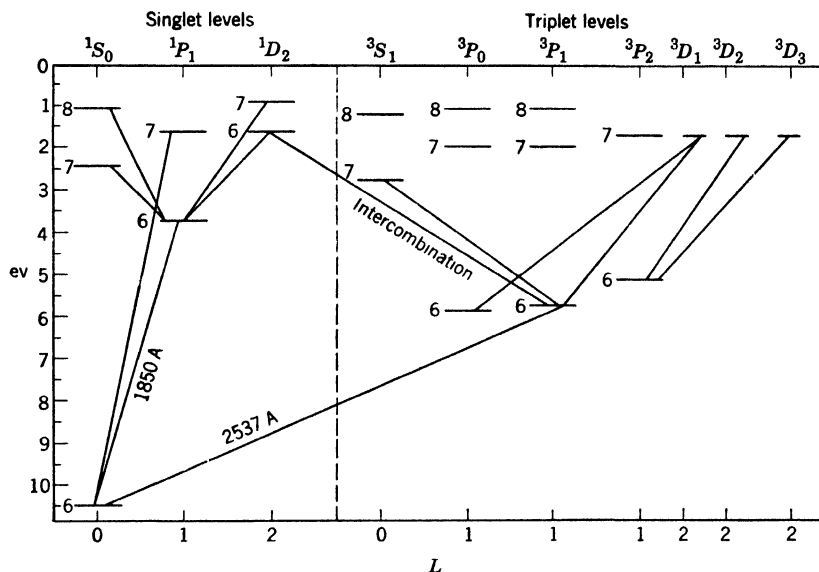


Fig. 7-7. The singlet-triplet energy levels of mercury. In the singlet system, the spins of the two valence electrons are opposed, and the resultant spin is zero. In the triplet system, the two spins are parallel, and the spin quantum number is 1. The spin and orbital vectors form a resultant which has three values, explaining the triplet levels.

between triplet levels when their threefold nature is overlooked. In addition, there are series arising in transitions from singlet to triplet levels, and from triplet levels to singlet levels, which are called intercombinations. Azimuthal numbers called L can be assigned to the singlet levels, and to the triplet levels. The usual selection principle,

$$\Delta L = \pm 1 \quad (8)$$

is operative. Passing to Fig. 7-8, we show the individual levels for some triplet terms separately. Lines that do not occur are dashed. They indicate the action of a selection principle for a quantum number J , analogous to the number j , introduced in our discussion of sodium. The explanation is as follows:

1. *Singlet Levels.* The normal mercury atom has two electrons with quantum numbers $n = 6$, $l = 0$, called $6s$ electrons to indicate their status briefly. Let one be excited to a higher state, such as $6p$ or $8d$. Suppose that their spins are opposed, so that the resultant spin is zero. Then the pair will have orbital angular momentum only. The levels will have no "fine-structure" due to spin; they will be singlets.

2. The orbital angular momenta l_1 and l_2 of the two electrons combine to yield a resultant, $Lh/2\pi$, in the fashion illustrated in Fig. 7-9. The rule is that for two electrons the resultant must be an integral multiple of $h/2\pi$.

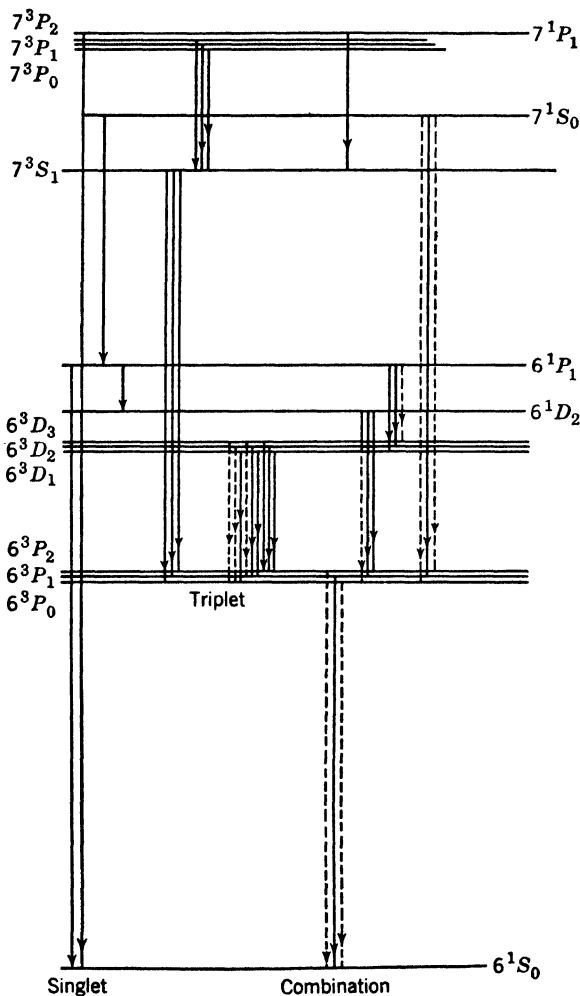


Fig. 7-8. Energy diagram of mercury, showing singlet series, triplet series, and combination series. The ordinates are not to scale.

3. *Triplet Levels.* Now suppose that the spins are parallel. Then the resultant spin, called S , will be 1. This combined spin vector now becomes oriented with respect to the vector L . The rule is that L and

S must form a quantized resultant J ; that is, by varying the orientation of S relative to L , J is made to take on the values from $L + S$ to $|L - S|$. For example, when $L = 2$ and $S = 1$, the possible values of J are 3, 2, and 1. In this case, if the total quantum number is 7, we designate the energy levels as 7^3D_3 , 7^3D_2 , 7^3D_1 , following the plan used in describing levels of the alkalis.

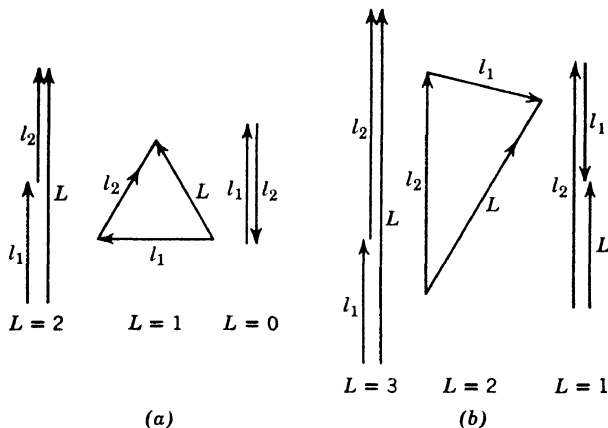


Fig. 7-9. Vector diagram showing the possible integral values of the vector L , in an atom with two valence electrons. The shortest vectors represent one unit of angular momentum, $h/2\pi$.

4. The selection principle for J is that it may change by ± 1 or zero, just as we found for j in the case of the alkalis. There is an additional restriction: terms for which J is zero do not combine with each other. This apparently insignificant addition to the selection rule bans the occurrence of the line $6^3P_0 - 7^3S_1$, which should lie at 2656 Å. Fukuda was able to observe the emission of this line in a strong discharge, but general experience supports the conclusion that for the well-isolated atom the upper state 6^3P_0 is *metastable*. An atom in this state, loaded with 4.68 eV, cannot leave the state save in collision with some partner, or through the intervention of some strong external field. This is not an isolated instance. There are many cases in which atoms (and nuclei) can exist in metastable states.

These matters are summarized in Table 7-2.

★ The extension of these ideas to atoms with any number of valence electrons is fairly obvious:

1. The individual electrons interact so that their orbital angular momenta combine to form a quantized resultant, $Lh/2\pi$, where L is

**TABLE 7-2. Terms and Quantum Numbers
for Alkaline Earths**

Term Symbol	l_1	l_2	L	s_1	s_2	S	J	Terms	Type
S	0	0	0	1/2	1/2	1	1	3S_1	Triplet
					-1/2	0	0	1S_0	Singlet
P	0	1	1	1/2	1/2	1	0	3P_0	Triplet
					1/2	1	1	3P_1	Triplet
					1/2	1	2	3P_2	Triplet
					-1/2	0	1	1P_1	Singlet
D	0	2	2	1/2	1/2	1	1	3D_1	Triplet
					1/2	1	2	3D_2	Triplet
					1/2	1	3	3D_3	Triplet
					-1/2	0	2	1D_2	Singlet

always an integer. For example, if we have

$$l_1 = 2 \quad l_2 = 1 \quad \text{and} \quad l_3 = 1$$

the possible L values associated with this configuration would range from 4 down to zero, the latter value being obtained by placing l_1 in opposition to the two other vectors.

2. The electron spins interact to form a quantized resultant, $Sh/2\pi$. If the number of electrons is even, this resultant takes on all the integral values from zero up to the value obtained by aligning all the spins in the same direction; if the number of electrons is odd, the resultant spin number S takes all the values in the sequence $1/2, 3/2$, and so on, up to the value obtained by aligning all of them in the same direction.

3. Finally, the vectors L and S take on such alignments that their resultant is $Jh/2\pi$. The allowable J values, separated by unity as usual, run downward from the maximum possible value, $L + S$.

4. Therefore, each value of S gives rise to a set of terms whose multiplicity is $2S + 1$. For example, if we have four valence electrons, S can be 2, 1, or 0, leading *respectively* to sets of quintuplet terms, triplet terms, and singlet terms.

★ These rules work well for approximately half the elements in the periodic table. The situation described is known as Russell-Saunders coupling. As we proceed toward the right of the table and to heavier elements, there is a progressive tendency toward another type of dynamical situation, in which the l and s of each electron form an individual

resultant j ; whereupon the j 's of the several electrons combine to form the total angular momentum $Jh/2\pi$. This is known as j - j coupling. It is indeed surprising that such simple principles suffice to describe the general features of all atomic spectra.

Additional remarks on spectroscopic notation. As we shall see in more detail on p. 227, to describe the n and l values for all the electrons of an atom, we put down a *sequence* of symbols of the kind ns , np , etc. For example, the normal state of boron ($Z = 5$) is described by

$$(1s)_2(2s)_22p$$

meaning that 2 electrons are in states with $n = 1$ and $l = 0$; 2 more are in states with $n = 2$ and $l = 0$; and just 1 in a state with $n = 2$ and $l = 1$. Often most of the early members in such a sequence are omitted because only the members describing the valence electrons are needed. For example, in mercury, the *group of states* 6^3P_2 , 6^3P_1 , 6^3P_0 , and 6^1P_1 all arise from the *configuration* $6s6p$.

The conflict between the use of s for the spin number of an electron and its use as an indicator that $l = 0$ for an electron will give no difficulty *if kept in mind*. The same is true of the conflict between the use of S as a resultant spin and as an indicator that $L = 0$.

5. Pauli's Principle

A great generalization concerning the quantum numbers of electrons in any isolated system was discovered by Pauli. He found from spectroscopic evidence that *no two electrons in a given atom can have the same set of quantum numbers*. It is necessary to note carefully that, in general, each electron has four quantum numbers, though we have worked with three in the discussion above. Our success was due to the fact that we did not consider space quantization (p. 106). As a matter of fact, practically all the levels discussed earlier in this chapter are *degenerate*, in the sense that application of a suitable external field is able to break them up into several sublevels. We met with such behavior in discussing the Zeeman effect of hydrogen on p. 107. The discussion on that page was incomplete because we neglected electron spin, in the interest of simplicity.

Now let us apply a very strong magnetic field to an atom with several valence electrons. By "very strong" we mean that the field is able to orient each electron, breaking up the coupling between the various angular momenta described above. For each electron, we now have four quantum numbers

$$n, l, m_l, \text{ and } m_s \quad (9)$$

The component of orbital angular momentum parallel to the field is $m_l h/2\pi$, and the component of electron spin parallel to the field is $m_s h/2\pi$.

For the normal state of mercury, both electrons have the same value of n , namely, 6, and the same l , namely, zero. Therefore m_l is zero for both of them. Therefore, according to Pauli, the values of m_s cannot be the same for both electrons. The two spins must point in opposite directions. On removing the field, they will still point in opposite directions. Therefore, the lowest state will have $S = 0$; it is, in fact, a singlet level. Because of Pauli's principle a *triplet* S state of total quantum number 6 is *completely banned*; for if the two electrons, each of the type 6s, had their spins parallel in the absence of the field, they would still be parallel after applying the field, and Pauli's rule would be violated. It is possible to show that, if the triplet state occurred, it would lie at lower energy than the existent ground state. In other words, the Pauli principle leads to having an ionization potential which is much smaller than we would find if the principle were *not* operative. This principle is in fact a dominant factor in determining the quantum numbers of all electrons in a normal atom, as we shall see in discussing the periodic system (p. 225).

The Pauli principle is an axiom based on universal experience. It cannot be derived from the laws of either ordinary mechanics or wave mechanics, as currently known. Actually, the principle imposes a condition on the wave function of the atom as a whole, stating that the wave function shall change its sign whenever the coordinates of any two electrons are interchanged. This matter is too complex for further discussion here. We wish to make it clear that wave mechanics does not *explain* Pauli's principle, but, on the other hand, is *limited by it*. There is a crude argument sometimes employed to make the principle plausible, as follows: Because of the inverse square law of electric force, and the inverse square repulsion of like "magnetic poles," we surmise that two electrons with parallel spins repel one another strongly on two counts and cannot be brought together. The Pauli exclusion principle arrives at the same conclusion. Also, the principle allows electrons to be very close together if the spins are opposite, and this might be "explained" as due to an attraction between two opposed "electronic magnets," overcompensating their electrical repulsion. It must be emphasized that the above description in terms of a definite model is *inadequate* and is given only to make the exclusion principle seem less abstract.

6. The Spectral Displacement Rule

We have seen that the spectrum of singly ionized helium resembles that of hydrogen. In general, the removal of a valence electron changes the type of a given spectrum to that of the element preceding it in the periodic table. This is known as the *law of displacement of spectra*. Thus the spectrum of singly ionized magnesium (Mg^+) has the same doublet structure as that of neutral sodium. Experiments have shown that this displacement rule may be extended to the loss of several electrons. Thus Si^{++} is like Al^+ or Mg , and Si^{+++} is like Al^{++} , Mg^+ or Na . With each successive ionization, the Rydberg constant is replaced by $4R$, $9R$, $16R$, etc., because the valence electron moves in an effective field whose magnitude is roughly proportional to $p + 1$, when p is the number of electrons removed to form the ion. Series representing such high degrees of ionization thus have large wave numbers and lie in the extreme ultraviolet.

7. Ionization Potentials

The general scheme for explaining atomic spectra described in the preceding pages is strongly supported by the direct determination of the energies required to remove electrons from atoms. If the energy required to ionize an atom of a certain gas or metallic vapor is I ev, then we say the ionization potential of that atom is I volts. To measure

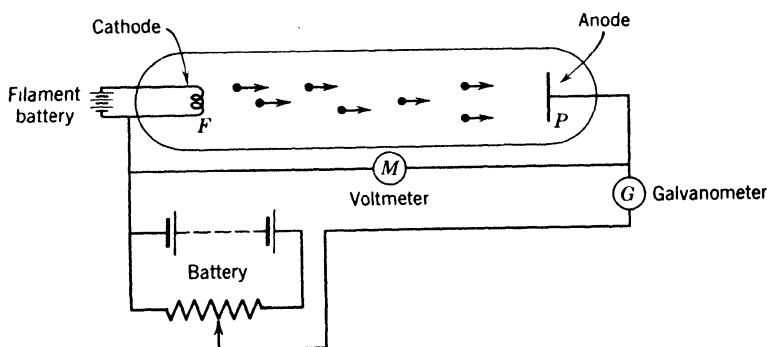


Fig. 7-10. Discharge tube for measuring ionization potentials.

the ionization potential of a gas or vapor, one bombards it with electrons of known and controllable energy, gradually increasing that energy until ionization occurs. The simplest type of tube which can be used for this purpose is shown in Fig. 7-10. A wire cathode, made incandescent by passing a current through it, serves as a copious source of elec-

trons. A voltage, which can be read on the voltmeter M , is applied between the cathode and the anode. At low voltages, the current is carried entirely by electrons from the cathode. When they strike against the gas atoms in the tube, the electrons may raise them to higher quantized states in which they emit light, but no ions will be produced until the voltage exceeds the value I .

At voltages below the ionization potential, the current is limited by the repulsive effect of the cloud of electrons present in the gas which drives other electrons back on the cathode and effectually limits the

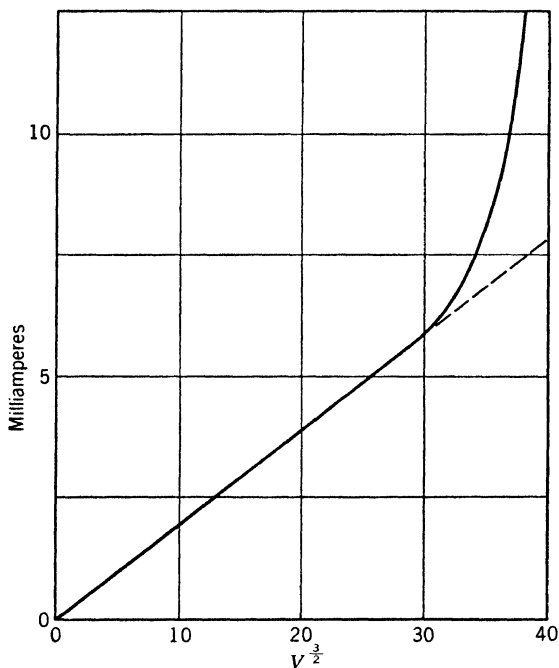


Fig. 7-11. Voltage-current curves for a hot-cathode discharge in mercury vapor. The departure of the current from the straight line found at low applied voltages indicates the beginning of ionization.

thermionic current. Under these conditions the current is proportional to the $3/2$ power of the impressed voltage. When ionization occurs, however, this effect is largely suppressed by the positive ions liberated from the gas atoms, so the current through the tube increases greatly. If we plot a curve showing the dependence of the total current on the $3/2$ power of the applied voltage, we obtain a result like that in Fig. 7-11, which was obtained by Found, using mercury vapor at a suitably chosen

density. The ionization potential of the gas is taken as the abscissa at which a sharp break occurs in the curve. For sodium, this break comes at 5.13 ev, after a proper correction is made for the initial energy with which the electrons leave the cathode. Referring to Fig. 7-4, it is seen that the lowest energy level is given by the limit of the principal series, at $41,449\text{ cm}^{-1}$. This limit corresponds in absorption to a jump from the normal state to an infinite orbit, that is, to a state in which the atom is ionized and the valence electron is at rest at infinity. The corresponding energy value is 5.116 ev, in excellent agreement with the voltage given above.

8. Resonance Radiation and Resonance Potentials

We saw on page 59 that atoms and molecules in the gaseous state are able to absorb certain wavelengths from a beam of white light. From the discussion in this chapter we should expect that the frequencies absorbed by a normal gas or vapor are those which carry the atoms from the ground state to higher levels. This is strikingly demonstrated by R. W. Wood's discovery of resonance radiation. He showed that the light of a Bunsen flame, made yellow by supplying it with any sodium salt, can excite the yellow *D* lines in an evacuated bulb, containing sodium vapor at a suitable pressure. He also excited resonance radiation in mercury vapor by illuminating it with the wavelength 2537 Å, corresponding to a photon energy of 4.9 ev.

Similarly, atoms can be excited by electrons so as to emit light without being ionized. The first resonance potential of an atom is defined as the lowest potential difference through which bombarding electrons must fall in order to excite the emission of light. Thus, an electron having an energy of 4.9 ev can raise a mercury atom with which it collides to the excited state 6^3P_1 from which it returns to the normal state 6^3S_0 with emission of the *resonance line* at 2537 Å. As the energy of the bombarding electrons is increased, other spectrum lines come out by groups and the potentials at which they appear are also referred to as resonance potentials. A discharge tube in which such effects can be studied, both spectroscopically and by electrical measurements, is shown in Fig. 7-12. Electrons are accelerated from the cathode toward the wire grid *G* by a potential V_1 . A small opposing potential, V_2 (about 1/2 volt), is applied between the grid and the plate *P*. A galvanometer is connected as shown to measure the current flowing through the plate *P*. The pressure in the apparatus is so chosen that the mean free path of an electron is small compared with the distance between the electrodes. As long as V_1 is less than the first resonance potential of the gas or vapor

in the tube the current increases with V_1 . All collisions of the electrons with the gas atoms are *elastic*; that is, an electron loses only a very small fraction of its energy in each collision. However, when V_1 exceeds the resonance potential, *inelastic* collisions occur. Suppose, for example, we are studying mercury vapor, and the potential between cathode and grid is 5.1 volts. After a collision in which 4.9 ev are lost, the electron may approach the grid, arriving there with the energy 0.2 ev, but if it

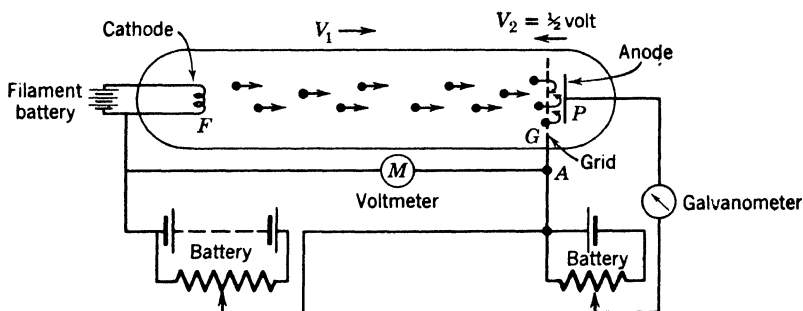


Fig. 7-12. Tube for measuring resonance potentials. When the applied voltage exceeds the first resonance potential, light is emitted. Also, each electron loses energy so that it cannot overcome the small opposing potential between grid and plate. Thus the plate-galvanometer current decreases.

passes through it will be thrown back by the opposing potential V_2 before it reaches the plate. Such an electron goes to the grid and through the metallic circuit GAF without being registered by the galvanometer. The net result is a drop in the galvanometer current, as we see from Fig. 7-13. As the voltage is further increased, electrons which have collided inelastically will have sufficient energy left over to fight their way uphill to the plate against the potential V_2 . Thus the current will begin to rise again. With still further increase, some of the bombarding electrons are able to make two resonance collisions and the current drops again. The peaks occurring at higher voltages are explained in similar fashion. The spaces between these peaks agree extremely well with the computed energy corresponding to the 2537 Å line, namely, 4.86 ev. By the use of various experimental refinements, G. Hertz was able to show that, while the green line of mercury at 5461 Å is absent from the spectrum at a certain potential, it comes out with considerable intensity at a potential only 0.2 volt higher, in close agreement with the theoretical excitation potential. The measurement of resonance and ionization potentials and experiments on the stepwise excitation of spectra have been very useful in determining atomic energy levels.

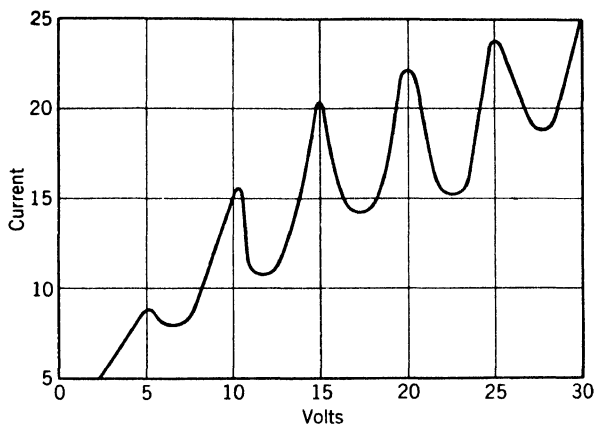


Fig. 7-13. Potential-current curves demonstrating inelastic collisions of electrons with mercury atoms (*after Mohler*). When the electrons are given sufficient energy, they excite atoms. The left-over energy is insufficient to force the electrons from grid to plate, so the current decreases.

9. Collisions of the Second Kind

★ Since electrons of sufficient speed can excite atoms with which they collide, emerging with lower speed, we may expect the converse, namely, that an excited atom, colliding with an electron, can return to a lower state without radiation; the internal energy is delivered to the electron, speeding it up, save for a small fraction which appears as kinetic energy of the recoiling atom.

★ Such an event is called a collision of the second kind. The type just described is difficult to demonstrate, but somewhat similar events were found by Franck and Cario. A bulb containing a mixture of mercury and thallium vapors was illuminated with the mercury resonance line, 2537 Å. Now the first resonance potential of Tl is much lower than that of Hg. Indeed, several different thallium lines can be excited by an energy of 4.9 eV. Thus an excited Hg atom should hand over some of its energy to a Tl atom. This energy will appear partly as internal energy of the Tl atom, later to be radiated, and partly as kinetic energy of the two collision partners. Franck and Cario found that the Tl atoms emitted just the lines expected and no others (Appendix 9, ref. 71). A host of phenomena of this kind are known. Whenever the reader studies an excitation process, he should ask himself, how will the stored energy be delivered back to the surroundings? We have no space for a study of photochemistry; but it is well to ponder the fact that the light of the

sun, falling on green leaves, sets into action a train of events which ultimately are responsible for production of most of the food consumed by ourselves and our fellow animals.

10. The Stern-Gerlach Experiment on Atomic Magnetic Moments

Further evidence of a non-spectroscopic character shows that an atom possesses angular momentum due to the orbital motion of its electrons and to electron spin. If an atom possesses angular momentum, it must behave like a tiny magnet, and it is possible to predict from spectral evidence just what the magnetic moment per atom should be. Stern and Gerlach devised an experiment which makes it possible to measure this magnetic moment. A metal, such as silver, is heated in a suitable electric furnace in a highly evacuated tube. A very narrow beam of metal vapor, formed by a slit system at the furnace mouth, is caused to pass through a highly inhomogeneous magnetic field produced by iron

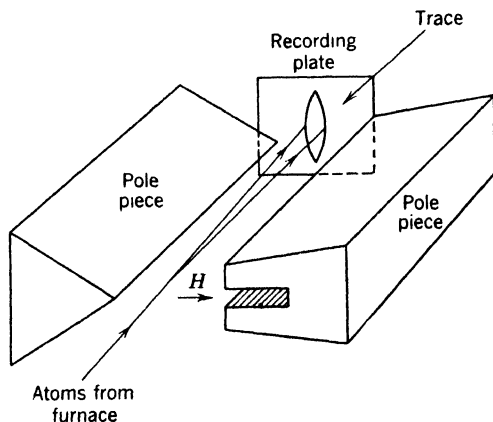


Fig. 7-14. Diagram of the Stern-Gerlach apparatus. A stream of silver atoms passes through the highly divergent magnetic field. Some atoms are pulled to the left and others to the right. (For clarity, the pole pieces are shown much farther apart than in actual practice.)

pole pieces of the form shown in Fig. 7-14. In the case of silver or any alkali atom, the angular momentum vector of each atom should be oriented either parallel or antiparallel to the external field. Atoms which have this vector parallel to the field are deflected toward one pole piece; those which have it antiparallel are deflected in the opposite direction.

The result is the formation of two distinct spots or lines of metallic deposit on a plate placed at the farther end of the magnetic field. From

the spacing of these spots, the magnetic moment of the silver atom can be computed. It is found to be 9×10^{-21} erg/oersted. Within the limits of error, this value agrees with the value predicted from the silver spectrum. For the normal state, $l = 0$, so the *component* of magnetic moment, μ_H , parallel to the magnetic field, is that due to the spin of the valence electron. We have

$$\begin{aligned}\mu_H &= \frac{1}{2} \frac{h}{2\pi} \frac{e}{mc} = \frac{1}{2} (1.05 \times 10^{-27}) (1.76 \times 10^7) \\ &= 9.25 \times 10^{-21} \text{ erg/oersted}\end{aligned}\quad (10)$$

This natural unit of magnetic moment is called the *Bohr magneton*.

11. Magnetic Properties of Bulk Matter

Suppose a long cylindrical homogeneous body is placed in a cylindrical coil (Fig. 7-15) which produces a magnetic field H_e in the absence of the body. The length of the body is supposed to be so great that

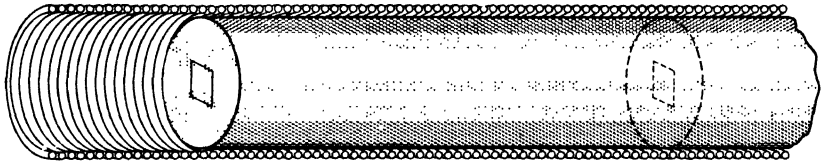


Fig. 7-15. Magnetic specimen in a long cylindrical coil. One unit area is indicated just outside the end of the specimen, and one near the middle of the solid, in its interior.

“poles” induced at its ends cannot appreciably weaken the field inside most of the body. Then:

1. The body acquires a moment I per unit volume.
2. The total number of lines of magnetic force, per unit area placed perpendicular to the field, will be

$$B = \mu H_e \quad (11)$$

where μ is called the permeability. No matter whether I is proportional to H_e or not, we *define* the *susceptibility* as

$$k = I/H_e \quad (12)$$

and it is easily shown that $\mu = 1 + 4\pi k$, or $B = H_e + 4\pi I$. The central problem in the study of magnetic materials has been to explain susceptibilities on the basis of our knowledge of atomic magnetic moments. The solution of this problem is reasonably well advanced at this time.

It is essential to recognize that the resultant magnetic field at the center of a molecule in our specimen is *not* B . While B lines of force pour out of each square centimeter at one end of the body, a glance at Fig. 7-16 shows that some neighbors of molecule M provide positive contributions to the resultant field at M , while others furnish negative ones.

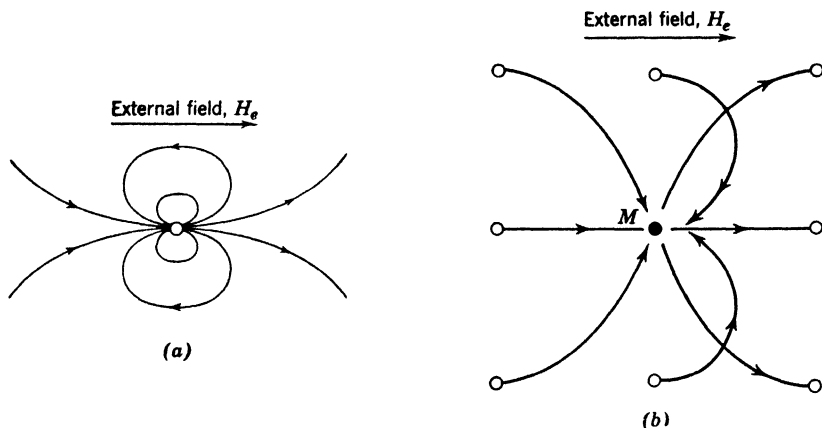


Fig. 7-16. (a) Sketch of the magnetic field due to a single isolated molecule. It is similar to that of a very short bar magnet. (b) The contributions to the magnetic field at an atom M produced by some of its neighbors in a simple cubic lattice. The resultant field is directed from left to right.

The field at M may, of course, be regarded as composed of two parts: first, H_e , due to the external coil; second, a field resulting from contributions made by all the neighboring molecules. The second of these does *not* have the value $4\pi I$. Its value depends, in part, on how the neighbors are arranged. For example, for gases and for simple cubic crystals, the neighbors' contribution is one-third of $4\pi I$. Hence, in these particular cases, the total field F_M at M is

$$F_M = H_e + (4\pi/3)I \quad (13)$$

Thus, from measurements of H_e and B , and the dimensions of the cylindrical object, we first obtain I ; then k ; and finally equation 13 tells us the field which acts upon an individual atomic magnet. Theory based on knowledge of these moments is able to explain most of the facts concerning diamagnetic and paramagnetic materials, in terms of the vector model of the atom. But when we deal with strongly magnetic

bodies, wave-mechanical ideas as to the interaction of the electron spins become essential.

Diamagnetism. When a field is being applied to any atom, there is an induction effect, which produces a relatively small magnetic moment oriented opposite to the applied field. In Fig. 7-17 we show electrons that cruise on Bohr orbits in opposite senses. Let us apply a magnetic field whose lines run perpendicularly into the paper. While this field increases, there is a counterclockwise induced emf around each orbit.

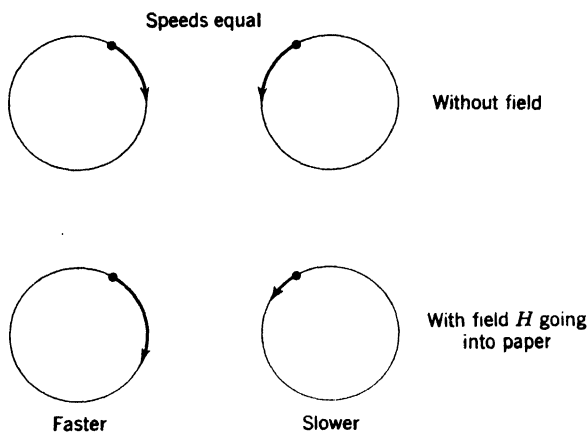


Fig. 7-17. How the speeds of electrons in circular orbits are affected by applying a magnetic field.

The negative electrons experience forces acting in a clockwise sense. The orbit diameters remain the same. Suppose that both electrons belong to an atom of helium. After the field ceases to grow, there will be a relatively small resultant current, *flowing counterclockwise*. At a distance, the field due to this current is like that of a tiny magnet with its north-seeking pole projecting *toward* the reader.

Thus even a closed-shell atom is endowed with a negative susceptibility by the action of the field, although the atom has no magnetic moment in the absence of the field. The diamagnetic susceptibility is very small compared with unity. The following values represent mass-susceptibility, or magnetic moment per unit mass (rather than per unit volume):

Helium	-0.47×10^{-6} cgs units
Bismuth	-1.35×10^{-6} cgs units

Indeed (Appendix 9, ref. 4), the magnetic moment per gram lies between -0.11 and -1.35×10^{-6} for all elements that show diamagnetic behavior. It can be shown that the diamagnetic moment of an atom in a field H is

$$\mu_D = -H \frac{e^2}{4\pi mc^2} A \quad (14)$$

where e is in electrostatic units and A is the sum of the average projected areas of the electron orbits, seen by an observer looking along H as in Fig. 7-17. The reader, knowing the magnitudes of atomic radii, can now check the order of magnitude of the mass susceptibilities given above.

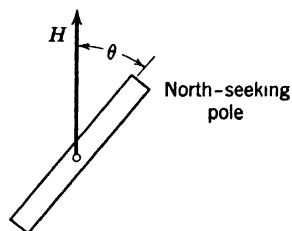


Fig. 7-18. The mutual energy of a small magnet and an external field in which it is placed.

Paramagnetism. Atoms that have a permanent magnetic moment become oriented in a magnetic field. In terms of the orbital model, the angular momentum vector J precesses around the lines of force of the magnetic field. The atoms are space quantized (p. 106). Now a magnet whose moment μ makes an angle θ with the field H (Fig. 7-18) is readily found to have a magnetic potential energy

$$V_{\text{mag}} = -\mu H \cos \theta \quad (15)$$

This means that the magnet can give up an amount of work $\mu H \cos \theta$ if it turns from a position perpendicularly athwart the field to the position shown. Figure 8-4 shows the orientations of the magnetic moment of an atom capable of five quantized positions. The atoms undergo thermal collisions, which switch them from one quantized orientation to another. When thermal equilibrium exists, there are more atoms with their equivalent north poles pointing downfield than there are pointing upfield. In fact, according to Boltzmann's law, the number having a magnetic energy E will be proportional to $\exp(-E/kT)$, or $\exp(\mu H \cos \theta/kT)$. The quantity in parentheses is small compared with unity for fields ordinarily available in the laboratory, and for T about equal to room temperature. Hence we may write a series expansion for the exponential and neglect small terms. Under these circumstances, if we deal with 1 gram-atom or N atoms, the number in a given orientation is proportional to $N(1 + \mu H \cos \theta/kT)$ and the excess of the number pointing downfield over the number pointing upfield is necessarily proportional to $N\mu H/kT$. Thus the magnetic moment per mole must be

of the order of μ times this expression. A rather simple calculation gives the result that

$$\text{Molar susceptibility} = N\mu^2/3kT \quad (16)$$

This is the Curie-Langevin law, which predicts great increase in the susceptibility of paramagnetic substances as the temperature is lowered. It is not an accurate law because of approximations made in its derivation; more accurate substitutes for equation 16 are very well verified by experiment. The magnitude of the paramagnetic effect is usually so large at ordinary temperatures that it swamps the diamagnetic contribution.

Ferromagnetism. Ferromagnetism is a wave-mechanical effect. Weiss proved that, in order to explain ferromagnets, one must assume that the field supplied by all the neighbors of a given magnetic molecule must be taken *thousands* of times greater than the value $(4\pi/3)I$, which we gave in equation 13. This tremendous field is called the Weiss field. Heisenberg showed that this field can be explained on a wave-mechanical basis. The energy connected with this field is commonly called exchange energy. When any electron spin is reversed, the energy of reversal calculated from the classical equation 15 is minute compared with other energy changes which arise from associated changes in the wave function of the system. We shall not attempt further explanation here, but refer the reader to the discussion of the forces that bind molecules together, on p. 230. The hydrogen molecule, for example, is held together by exchange forces. The important point for the reader to grasp now is that the individual atoms of a ferromagnet do not have moments which are exceptionally large. The strong orienting influences which come into play in iron and other strongly magnetic substances are a cooperative phenomenon. Let d be the distance between neighboring magnetic atoms, and r the radius of the incomplete electron shell which is responsible for the magnetic moment of the atom. It is found that ferromagnetism occurs only when d/r lies within a certain rather narrow range of values. This circumstance explains the relative scarcity of elements that are ferromagnetic.

REFERENCES

Appendix 9, refs. 4, 8, 46, 59, 71, 75, 87, 108.

PROBLEMS

Useful data:

Ionization potential of atomic hydrogen, 13.60 ev.

Wavelength of a 1-ev photon, 12,340 Å.

1. What is the energy in electron volts of a photon of yellow light with $\lambda = 5890 \text{ \AA}$? What is the wave number?
2. Using the following ionization potentials, compute the corresponding quantum defects: (a) Lowest state of hydrogen, 13.60 eV; (b) $2^2S_{1/2}$ state of Li, 5.38 eV; (c) $3^2S_{1/2}$ state of Na, 5.12 eV.
3. Using the quantum defects 0.415 for all the S levels, and 0.00 for all the P levels of Li, make an energy-level diagram like Fig. 7-4 for some of these levels with the ordinate in cm^{-1} .
4. Using the diagram of problem 3, determine the energies $h\nu$ and approximate wavelengths for the lines $2^2S - 2^2P$ and $2^2S - 3^2P$.
5. Using the diagram of Fig. 7-4, determine the energy $h\nu$ and the wavelength of the first line of the sharp series of Na.
6. Continue Table 7-2, p. 206, for F orbits, if $l_1 = 0$ and $l_2 = 3$.
7. Write the complete spectral symbols for the fundamental series lines $3D - 4F$, etc., of sodium. Make an energy diagram for transitions from a pair of F levels to a pair of D levels. Indicate which lines are forbidden, and state why.
8. Calculate the excitation potential for the mercury line $1^1S_0 - 2^1P_1$ at 1849 \AA . Compare your result with the experimental value, 6.73 eV.
9. Two resonance potentials, 1.89 volts and 2.92 volts, and an ionization potential, 6.08 volts, have been found for calcium. Find the approximate wavelengths of the corresponding lines, and the approximate wave number of the 1^1S_0 state.

ANSWERS TO PROBLEMS

1. 2.1 eV; $16,900 \text{ cm}^{-1}$.
2. (b) 0.42; (c) 1.37.
4. For $2^2S - 2^2P$, 1.84 eV; 6710 \AA . For $2^2S - 3^2P$, 3.76 eV; 3290 \AA .
5. 1.09 eV; 11,400 \AA .
6. 3F_2 , 3F_3 , 3F_4 arise from the vectors $L = 3$, $S = 1$; and 1F_3 arises from $L = 3$, $S = 0$.
7. $3^2D_{3/2} - n^2F_{5/2}$; $3^2D_{5/2} - n^2F_{7/2}$; $3^2D_{3/2} - n^2F_{7/2}$, with $n = 4, 5$, etc. The lines $3^2D_{3/2} - n^2F_{7/2}$ are forbidden by the j selection principle.
8. 6.67 eV.
9. 6540 \AA ; 4230 \AA ; $49,300 \text{ cm}^{-1}$.

The Periodic System

To classify the vast number of substances known in nature in terms of a few fundamental substances called elements was the goal of the early scientist. A chemist of the nineteenth century had a very definite meaning for the word "element," assigning it to somewhat fewer than the 100 primary substances which we know today.

In this chapter we shall discuss the reasons for the well-known similarities of physical and chemical behavior which lead to the periodic table of the elements. We shall see that the quantized behavior of planetary electrons described in Chapters 4, 5, and 7 leads naturally to a fairly complete understanding of both similarities and differences of behavior. Of course, we cannot do more than sample this vast field of study, which, in a broad sense, encompasses the whole of systematic chemistry. The structure of the nucleus need not yet concern us. We only need to know the atomic number, which dominates the situation. Periodic properties of the nuclei are discussed briefly on p. 44.

1. Classification of the Elements

Regularities in the atomic weights of the elements were first discovered about 1850. Many triads of elements with similar chemical properties were found in which the differences between the atomic weights were nearly constant. Examples are given below:

Lithium, 7	Sulfur, 32
Sodium, 23	Selenium, 79
Potassium, 39	Tellurium, 127

It was not, however, until 1869 that the periodic table, in approximately the form in which we now know it, was established. At that time both Mendeleef and Lothar Meyer published almost identical tables. Today it is a simple task to arrange the elements in order of their atomic weights and note the periodicities occurring in the list. It is easy to forget that,

at the time of these early tables, atomic weights had not been determined with the precision with which they are now known. Further, although the combining weights could usually be determined accurately there was often no way of knowing the number of atoms of one element associated with one atom of another element. For example, in the compounds of beryllium with some other element, say chlorine, it was not known whether the formula for the compound was BeCl_2 or BeCl_3 . In this case, 35.5 gm of chlorine were known to combine with 4.51 gm of beryllium, but before the periodic table was discovered there was no way of knowing whether the atomic weight of beryllium was 9.02 ($= 2 \times 4.51$) or 13.53 ($= 3 \times 4.51$). Also, there were several gaps in the periodic table, and there was no way of deciding whether a gap existed except by the periodicity of the properties of the elements. Mendeleef's great discovery was based upon his recognition of the valence of the elements as the periodic property that had most to do with their arrangement. Using valence and other properties as a guide, he was able to piece together the various parts of the puzzle, to find the correct atomic weight where only the combining weight was known, to choose the correct column for an element whose atomic weight was incorrectly determined, and to leave gaps where elements were yet to be discovered. The periodic table is presented in Appendix 5.

In the first column are the alkali elements lithium, sodium, potassium, rubidium, and cesium, which have closely similar chemical properties. All these metals have unit valence, p. 230, low melting points, and rather high boiling points. They have the property of combining very readily with water, liberating hydrogen and forming hydroxides such as NaOH and KOH . In the second column of the periodic table, the elements have a principal valence of 2. In the third, the valence is said to be $+3$ or -5 , depending upon whether the element acts as a metal or a non-metal. In the fourth, the valence is ± 4 ; in the fifth -3 or $+5$; in the sixth -2 ; and in the seventh -1 . On the right of the last column, the valence is 0; that is, the elements are very inactive. Here we have helium, neon, argon, krypton, xenon and radon, which are called "noble" gases to indicate that they do not associate with other elements. Below the third row it will be noticed that the number of elements in a period has increased. Here the columns are divided and the halves are designated as *a* and *b*. Thus in group I, below the third row, alternate elements have the same general chemical properties. Potassium, rubidium, and cesium form the subgroup *a* and exhibit the valence 1; copper, silver, and gold constitute the subgroup *b*, and have the valences 1 and 2. (See Table 8-1 for the differences between the outer electron structures of K and Cu, for example.)

The periodicity of the valence of the elements is well shown in Fig. 8-2, where the valence n of the element R in the oxide R_2O_n is plotted against the atomic number. Figures 8-1 and 8-3 illustrate other well-marked periodicities.

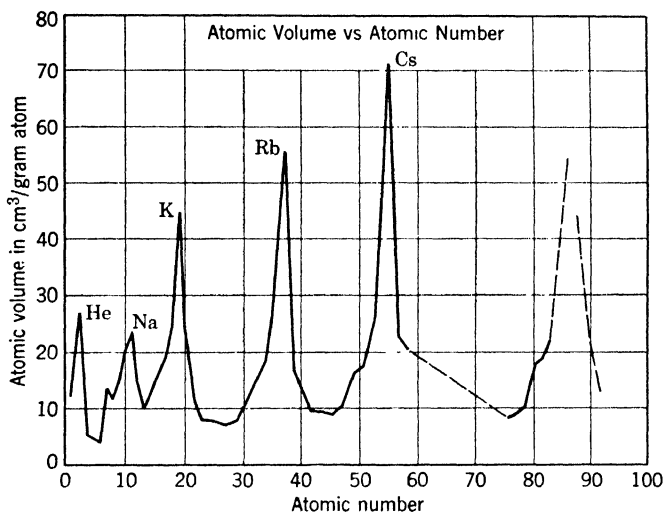


Fig. 8-1. Periodicity of atomic volumes (in the solid state) when plotted against the atomic number.

In spite of these outstanding evidences of order among the elements, certain irregularities occur when the elements are placed in rows and columns according to their chemical properties. Although as a rule the atomic weight increases from left to right, yet for such pairs as argon and potassium, cobalt and nickel, tellurium and iodine the order is reversed. However, Moseley's X-ray studies (p. 135) showed that the atomic number is more fundamental in determining the order than is the atomic weight.

The numbers of electrons surrounding the nuclei of the noble gases form a striking progression which is tabulated herewith. The most

He	Ne	Ar	Kr	Xe	Rn
2	10	18	36	54	86
$2(1^2)$	$2(1^2+2^2)$	$2(1^2+2^2+2^2)$	$2(1^2+2^2+2^2+3^2)$	$2(1^2+2^2+2^2+3^2+3^2)$	$2(1^2+2^2+2^2+3^2+3^2+4^2)$

remarkable property of these atoms is their lack of affinity either for atoms of their own kind or for other atoms. Evidently, when the atomic number can be written in one of the forms given in this table,

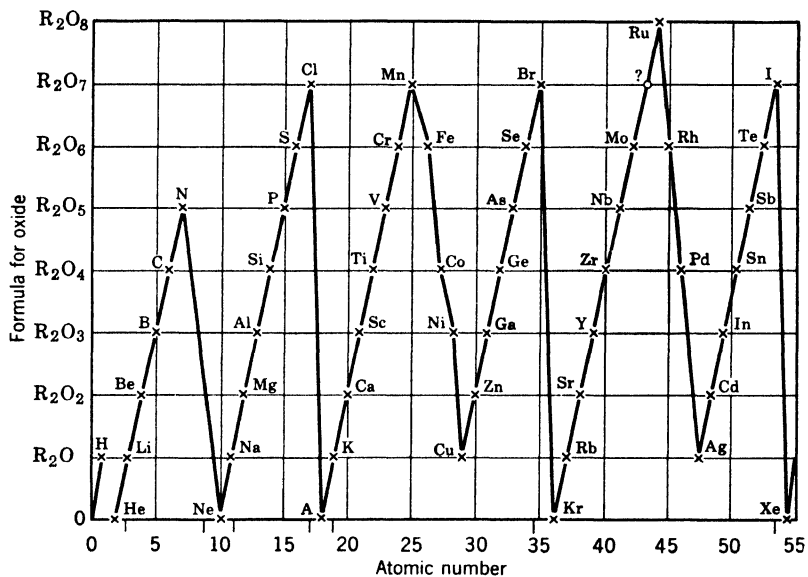


Fig. 8-2. Graph of the oxides of the form R_2O_n as far as atomic number 55. The subscript n is equal to the number of the column in the periodic table.

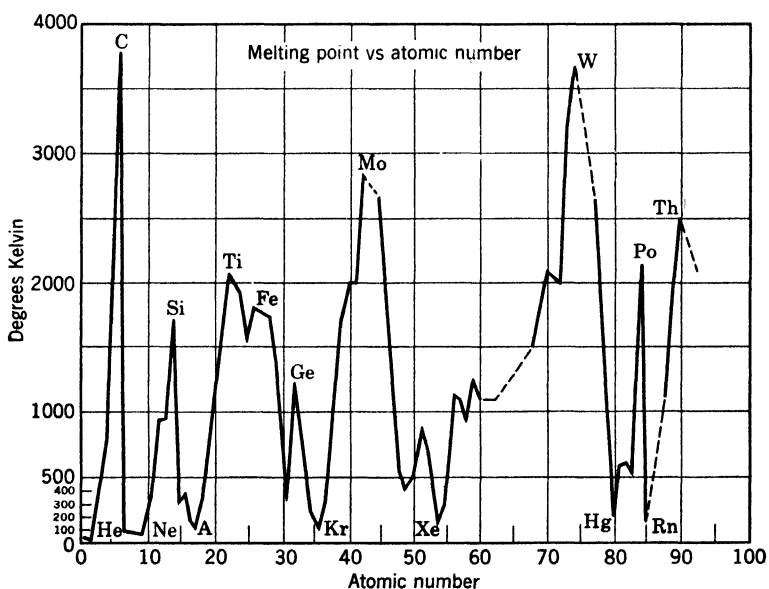


Fig. 8-3. Melting points of elements plotted against atomic numbers.

the element is unusually stable. These six elements are the only ones which display such a horror of chemical combination.

This situation supports the facts on X-ray spectra presented in Chapter 5. We consider the extranuclear electrons as arranged in "shells," each containing $2n^2$ electrons, where n can take the successive values 1, 2, 2, 3, 3, and 4. The reasons for the particular numbers found above will be clarified below.

2. Assignment of Quantum Numbers

As described in Chapters 4 and 7, the state of the extranuclear electrons in Bohr orbits may be specified in terms of quantum numbers. For a single electron, one particular orbit corresponds to each set of such numbers. However, from the point of view of wave mechanics, we should no longer think of definite orbits. We should think, instead, of different probability distributions. To each set of quantum numbers there now corresponds a particular distribution function which specifies the probability of finding the electron at any given point in space.

Making use of spectral data, chemical properties, and the Pauli principle (p. 207), it is possible to assign to each electron a set of four quantum numbers. In describing the spectra of elements with 1 or 2 valence electrons, we have made use of three of these: (1) the principal quantum number designated by n ; (2) the orbital quantum number l ; and (3) the spin quantum number s . Following the notation of Chapter 7, we use small letters to designate the quantum numbers of the individual electrons.

In the present discussion, it is necessary to assign quantum numbers to the electrons in the inner shells as well as to the valence electrons. Corresponding to the orbital angular momentum determined by l there is an orbital magnetic moment for each electron. Since the electrons are closely packed in the inner shells their interaction is appreciable. However, it is rather difficult, and not very convenient for our present purpose, to treat this interaction. If we place the atom in a sufficiently strong magnetic field, the field takes control to such an extent that we can neglect the interaction of the electrons. Each one is then conceived as feeling only the forces arising from the nucleus and the externally applied field. We have seen in the treatment of the Zeeman effect (p. 107) that the magnetic moment associated with the orbital motion of an electron can take only certain discrete directions with respect to an applied magnetic field. Similarly, in this case, the magnetic moment of each electron may take only a limited number of positions. These positions may be determined by finding those projections of l —upon a

line parallel to the direction of the field—which have integral values. Thus if l is 2, the projection of l may have any one of the five values 2, 1, 0, -1 , -2 , as is indicated in Fig. 8-4. The value of this projection is known as the “orbital magnetic quantum number,” or more simply as the “magnetic quantum number,” and is designated by m_l .

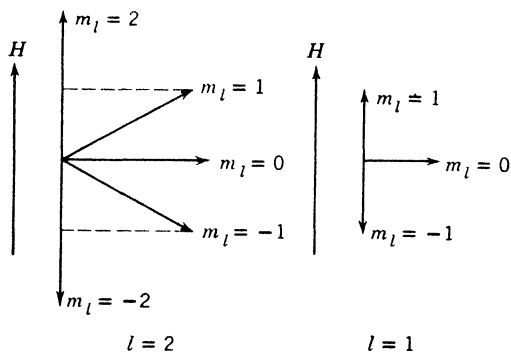


Fig. 8-4. Quantization of orbital magnetic moment.

Likewise, the electron spin which was found empirically to be $\sqrt{3/4}h/2\pi$ can have projections upon the direction of an external magnetic field of only $(\frac{1}{2})h/2\pi$ and $(-\frac{1}{2})h/2\pi$. The coefficients $\frac{1}{2}$ and $-\frac{1}{2}$ are called either the “spin magnetic quantum number” or for simplicity the “spin quantum number,” and are designated by m_s . The probability distribution of any particular electron in an atom, therefore, is determined when the four quantum numbers n , l , m_l , m_s are assigned to it.

3. Application of Pauli’s Exclusion Principle to the Periodic Table

Let us consider how Pauli’s rule (p. 207) may be applied in determining the distribution of electrons in a typical atom. We are interested in the electronic distribution for the normal state in which the electrons are in the lowest possible energy levels. For the hydrogen atom, the quantum numbers for the lowest energy state are $n = 1$, $l = 0$, $m_l = 0$, $m_s = -\frac{1}{2}$, and the Pauli exclusion principle has no significance because there is only 1 electron. However, for helium there is another electron, and we can have $n = 1$, $l = 0$, $m_l = 0$ provided we also have $m_s = +\frac{1}{2}$, which means a spin in the opposite direction. The spin quantum number is changed first because it has a smaller effect on the energy of the atomic system than a change of any other quantum number. If we wish to find the quantum numbers for the lithium atom we must

consider a third electron. Wave mechanics shows that the maximum value which l may have is $n - 1$, and the absolute value of m_l cannot be greater than l , so that there are no other states with $n = 1$ for which all four quantum numbers can be different. Making use of the nomenclature used in X-ray spectra we say that the first or K shell of electrons, for which $n = 1$, is filled when there are 2 electrons in it. If the energy of the third electron of lithium is to be as low as possible it must have $n = 2, l = 0, m_l = 0$, and $m_s = -\frac{1}{2}$. Continuing this building process, we find for the second or L shell ($n = 2$) the following possibilities:

n	l	m_l	m_s
2	0	0	$-1/2$
2	0	0	$+1/2$
2	1	-1	$-1/2$
2	1	-1	$+1/2$
2	1	0	$-1/2$
2	1	0	$+1/2$
2	1	1	$-1/2$
2	1	1	$+1/2$

Thus we see that the second shell is complete after 8 electrons are added.

This scheme serves well in showing what would happen in the presence of a strong magnetic field, but we are often more interested in knowing how the orbital and spin angular momenta will behave in the absence of an external field. This behavior depends on details of the atomic structure. Therefore, it was not found possible to predict the lowest spectral terms of *all* the elements, though success was had for most of the lighter ones. For example, the lowest terms of the elements boron to neon are as follows:

Element	Resultant L	Resultant S	Lowest Term
B	1	$1/2$	$^2P_{1/2}$
C	1	0	3P_0
N	0	$3/2$	$^4S_{3/2}$
O	1	2	3P_2
F	1	$3/2$	$^2P_{3/2}$
Ne	0	0	1S_0

Adding another electron (thus forming the next element, sodium) requires that a new value of the principal quantum number be chosen. The application of similar considerations to higher atoms gives the distribution of electrons shown in part in Table 8-1. This table indicates

TABLE 8-1. Distribution of Electrons

n, l		1, 0	2, 0	2, 1	3, 0	3, 1	3, 2	4, 0	4, 1	4, 2	4, 3
X-ray symbol		K	L		M		N				
Electron symbol		$1s$	$2s$	$2p$	$3s$	$3p$	$3d$	$4s$	$4p$	$4d$	$4f$
Element	Lowest Term										
H 1	$^2S_{1/2}$	1									
He 2	1S_0	2									
Li 3	$^2S_{1/2}$	Helium-like core	1	0							
Be 4	1S_0		2	0							
B 5	$^2P_{1/2}$		2	1							
C 6	3P_0		2	2							
N 7	$^4S_{3/2}$		2	3							
O 8	3P_2		2	4							
F 9	$^2P_{3/2}$		2	5							
Ne 10	1S_0	2	2	6							
Na 11	$^2S_{1/2}$	2	2	6	1	0					
Mg 12	1S_0	Neon like core			2	0					
Al 13	$^2P_{1/2}$				2	1					
Si 14	3P_0				2	2					
P 15	$^4S_{3/2}$				2	3					
S 16	3P_2				2	4					
Cl 17	$^2P_{3/2}$				2	5					
A 18	1S_0	2	2	6	2	6					
K 19	$^2S_{1/2}$	2	2	6	2	6	0	1			
Ca 20	1S_0	Argon-like core					0	2			
Sc 21	$^2D_{3/2}$						1	2			
Ti 22	3F_2						2	2			
V 23	$^4F_{3/2}$						3	2			
Cr 24	7S_3						5	1			
Mn 25	$^6S_{5/2}$						5	2			
Fe 26	5D_4						6	2			
Co 27	$^4F_{9/2}$						7	2			
Ni 28	3F_4	2	2	6	2	6	8	2			
Cu 29	$^2S_{1/2}$	2	2	6	2	6	10	1	0		
Zn 30	1S_0	Copper-like core						2	0		
Ga 31	$^2P_{1/2}$							2	1		
Ge 32	3P_0							2	2		
As 33	$^4S_{3/2}$							2	3		
Se 34	3P_2							2	4		
Br 35	$^2P_{3/2}$							2	5		
Kr 36	1S_0							2	6		

the numbers of electrons in the large groups or "shells" (determined by n) and in the subgroups (determined by l).

One notices that the electrons for which $n = 4$ and $l = 0$ are added before those for which $n = 3$ and $l = 2$. This is due to the fact that the energy of the 4, 0 state is slightly lower than that of the 3, 2 state in the elements K and Ca, though this is not true for higher atomic numbers.

Similar ideas may be used throughout the periodic table, and thus we obtain a distribution of the quantum numbers of the extranuclear electrons for most of the elements. In the remaining places in the table, other data, obtained from spectroscopy or chemistry, are needed to determine the distribution uniquely.

4. Chemical Properties of the Elements

The chemical properties of atoms are determined primarily by the outer electrons since they are the first to interact when two atoms are brought together. The fact that the chemical properties of the elements are periodic functions of the number of electrons comes therefore as a direct consequence of the distribution of electrons given by the Pauli exclusion principle. We notice in Table 8-1 that the outermost shells of lithium, sodium, and potassium are identical, thus accounting for the similar properties of the elements in the first column of the periodic table. We notice, too, that the inert gases such as helium, neon, and argon always occur at points in the periodic system at which a shell of 2 or 8 electrons is completed, and should have, therefore, very similar chemical properties.

The presence of only H and He in the first row follows from the fact that only 2 electrons can be present at the same time in the lowest or K shell. The fact that the L shell requires eight electrons before it becomes filled accounts for the fact that there are eight columns in the periodic table. The M shell requires 18 electrons for completion. We can also see how the period of 18 elements, beginning with potassium and ending with krypton, is accounted for. Similar principles apply for higher atomic numbers.

★ 5. Valence and the Formation of Molecules

Valence forces. The fact that some atoms combine to form stable molecules while others do not combine at all indicates that there must be rather strong forces between atoms when they are brought very close together. If the potential energy of a system containing two atoms

constantly increases as they are brought closer together, there is, of course, a repulsive force between the atoms. If the potential energy first decreases as two atoms are brought together, and then increases, as illustrated in Fig. 9-8 on p. 245, the force will first be one of attraction, then zero at an equilibrium position, and finally repulsion at distances closer than the equilibrium distance. The depth of the potential energy minimum as two atoms are brought together from a position of infinite separation to one of equilibrium separation varies greatly as we pass through the list of all possible pairs of atoms. On the one hand we have such loosely bound structures as Hg_2 , and on the other hand highly stable oxides, fluorides, sulfides, and chlorides, together with molecules like H_2 or N_2 . We recognize several categories of interatomic forces, the principal ones being as follows:

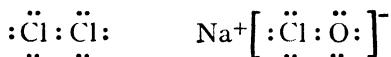
Electrostatic attraction between ions.

Exchange forces of quantum-mechanical origin, having no counterpart in classical mechanics.

Forces due to dipole moments (see p. 255).

The van der Waals force.

Both theory and experiment indicate the existence of all sorts of intergrades, and therein lies the difficulty of the subject. For a long time, a purely electrical theory of valence dominated the thinking of chemists. It was clear that electrostatic forces must play a large part in holding together such compounds as NaCl , constructed from one atom which easily gives up an electron and another which has an affinity for an extra electron. This view met with trouble in explaining molecules made of two atoms of the same kind, homopolar molecules such as H_2 , to say nothing of the vast class of organic compounds. About 1918, Lewis and Langmuir independently emphasized the idea that in homopolar compounds the forces may be associated with formation of a shared electron pair, or several such pairs. Such bonds are now called covalent bonds. Diagrams that show the electrons as dots, with shared electrons placed between the two atoms, are commonly used today because they help to visualize relations that might otherwise be quite puzzling. The following "structures" are good examples:



We note in the picture of sodium hypochlorite that the shared electrons help both the oxygen atom and the chlorine atom toward formation of a rare-gas shell of eight electrons. This is accomplished by robbing the sodium atom of one electron. The reader may construct similar dia-

grams for the series of singly negatively charged ions ClO_2 to ClO_4 , and will then no doubt feel that he understands them better. Forces depending on the cooperation of two electrons are by no means the whole story, but they do play a dominant part in the study of molecular bonds.

Heitler and London's theory of exchange forces. Such ideas were brought into a satisfactory state in 1930, when Heitler and London considered the formation of molecules on the basis of wave mechanics. They found that, if two neutral hydrogen atoms are brought close together, either an attraction or a repulsion is possible owing to the interaction of the electric fields of the nuclei and electrons. They found, however, that, when the atoms are in their *lowest* state, a stable molecule is formed only when the electron spins are in opposite directions or, in other words, when their spin quantum numbers have opposite signs. If the spin vectors are parallel, there is strong repulsion. It must not be supposed that this is an effect like the attraction or repulsion of two gross magnets. The magnetic potential energy of the two electron spins is relatively minute, but the *change* of spin directions carries with it a great change in the nature of the wave function of the molecule. Hence, the energy can be, and is, much lower than that of two separate atoms when the spins are opposite; the contrary is true when the spins are parallel. This has no analogue in classical mechanics. Hence the binding energy of two hydrogen atoms must be considered a wave-mechanical phenomenon.

In addition to furnishing methods of calculation of the interaction of two hydrogen atoms, wave mechanics makes possible a better understanding of the valence forces existing between other atoms. London's analysis shows that, in general, two atoms attract one another if the electron spins of one atom are oppositely directed to those of the other atom. In other words, a stable molecule is formed when the spin vectors are paired off. If one electron spin of one atom pairs off with one spin of the other atom, we say that the valence is unity. If two electron spins pair off, then the valence is 2. Thus, the maximum valence of an atom is the number of electron spins which are not paired off in the atom itself and are, therefore, available for pairing off with another atom.

In the case of normal helium atoms, the two spin vectors are paired off themselves so that there are no available spins and the valence is zero. Applying the same type of analysis as was applied to hydrogen atoms, Heitler and London found theoretically that there is no possibility of two helium atoms combining when they are in their lowest quantum states. Further, it is possible to calculate the actual repulsive force between the two atoms when they are near each other. When they are

far apart a slight attraction exists and theoretical values of the van der Waals constants (p. 15) may be calculated which are in fair agreement with experiment.

Since the outer electronic structure is repeated as we go through the periods of the elements, it will be sufficient to illustrate the application of the spin valence hypothesis with a few examples in the first row of the periodic table. Lithium has one electron which is outside the completed helium-like inner shell, and therefore, in agreement with experiment, we say that lithium can only have a valence of unity. In beryllium there are two electrons outside the helium inner shell. The spin vectors of these two electrons in the subshell for which $l = 0$ will be opposed, so that beryllium will not combine with other elements when cold. However, upon being heated, it burns to form BeO . In the language of spin vectors, heating excites one of the electrons to the subshell for which $l = 1$. The restriction arising from the Pauli principle that the spins must be opposed is therefore removed, and the two spin vectors may be parallel, which gives beryllium a valence of 2. Other compounds like BeF_2 and BeCl_2 also indicate that the dominant valence of beryllium is 2.

In the sixth column of the table, we find oxygen with four electrons in the $l = 1$ subshell of the L shell. In this subshell, as we see from the table on p. 227, it is only possible to have three electrons with $m_s = -\frac{1}{2}$; that is, with $m_l = 1, 0$, and -1 . Since we have four electrons for which $l = 1$, it is necessary according to Pauli's principle to have one spin in the opposite direction, balancing one of the spins for which $m_s = -\frac{1}{2}$. There are, therefore, two spin vectors left which are not paired off, and the valence of oxygen is 2, as in H_2O and Li_2O . One might expect all the spins of oxygen to pair off, giving a valence of zero. More complete calculations than can be attempted here show that such a configuration has higher energy than when three of the spins are parallel. The fact that the triplet levels of the oxygen spectrum are lower than the singlet levels is further evidence that this is true.

In the next column of the periodic table, headed by fluorine, we have five electrons in the $l = 1$ subshell. In this case it is necessary according to Pauli's principle to have four of the electrons paired off, leaving one free to combine in the formation of a molecule. We say, therefore, that the only possible valence for fluorine is unity, so that we have compounds such as HF , LiF and BeF_2 .

Although the linking of the available spin vectors with the possible valences of an atom gives a satisfactory explanation in most cases, there are many others in which it is not entirely satisfactory. For instance, boron usually has a valence of 3, whereas London's method would indicate a most probable valence of unity.

London's theory in its original form applies only when the molecule is formed by bringing two neutral atoms together. When two ions are brought together, then the electrostatic force between them is usually sufficient to hold them together even if the spins are not paired off and the theory requires relatively minor modifications. With this explanation of the binding forces of neutral atoms and the beginning of a theory of valence, wave mechanics made its debut into chemistry. It has now provided so many useful clarifications that physics and chemistry are gradually merging.

REFERENCES

Appendix 9, refs. 46, 47, 81, 100.

PROBLEMS

1. Making use of the periodic table, predict some of the properties of elements 43 and 85.
2. Construct a table showing the possible values that the quantum numbers n , l , m_l , and m_s may take for electrons in the M shell.
3. Making use of the Pauli exclusion principle, determine the probable distribution of electrons for krypton and for rubidium.
4. The common valences for sulfur are 0, 2, 4, and 6. Determine the probable distributions of electrons that will produce these valences.
5. Using only the periodic table and a general chemistry book, attempt to work out the electronic structures of the elements of the fifth period, Rb to Xe.
6. In similar fashion, attempt an explanation of the close similarity of the rare earth elements, 57 to 71.
7. Discuss the molecules ClO_2 and Cl_2O from the standpoint of Section 5.
8. Draw electronic structure formulas for C_2H_6 , ethane; for C_2H_4 , ethylene; for C_2H_2 , acetylene.

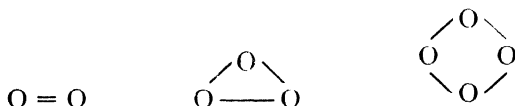
The problems do not have answers that can be summarized briefly.

9

Molecular Structure and Related Topics

1. The Number of Atoms in a Molecule

The spins of the outer electrons of an atom and their importance in determining its valences are discussed in Chapter 8. Valence, however, does not tell us definitely whether a molecule of oxygen, for instance, is made up of 2, 3, or 4 atoms. The valences can be satisfied in either case. One can see this by examination of the following structural formulas for ordinary oxygen, ozone, and the rare form O_4 .



The chemist usually determines the number of atoms in a molecule of a gas by making measurements on the gas as a whole. In accord with Avogadro's hypothesis it is known that equal volumes of different perfect gases under the same conditions of temperature and pressure contain the same number of molecules. In fact, we know that 22.4 liters of such a gas at 0°C and 76 cm of Hg contain 6.02×10^{23} molecules. It is only necessary then to divide the mass of the gas by the number of molecules in the volume used to obtain the mass of an individual molecule and, if the mass of one atom is known, the number of atoms in a molecule.

Besides the number of atoms in a molecule many other properties of molecules may be deduced by studying the gas as a whole. For instance, measurements of the specific heats of a gas are important since they enable us to determine independently the number of atoms in a molecule and also some of its physical dimensions.

2. Specific Heats of Gases

Classical theory. The kinetic theory of the specific heat of a gas has already been outlined (p. 11). It is desirable, however, to treat

the subject anew in order to emphasize the differences between the older classical theory and the new quantum theory. According to classical theory there is an equipartition of energy among the various degrees of freedom of the molecules. It follows that the energy per degree of freedom per mole is $\frac{1}{2}RT$, where R is the universal gas constant and T the temperature on the Kelvin scale.

To obtain the total energy of a mole of gas we need to consider in detail the number of degrees of freedom that a molecule possesses. Since practically all the mass of an atom resides in its minute nucleus, we regard for the present a diatomic molecule as consisting of two very small but comparatively heavy parts separated by a short distance. If the component atoms are considered rigidly bound in the molecule,

five quantities are required to specify completely the position of the molecule. Referring to Fig. 9-1, these may be the X , Y , and Z coordinates of the center of gravity, and the angles θ and ϕ which determine the orientation of the nuclear axis in space. If, instead of being rigidly fixed, the atoms are held in elastic equilibrium, another coordinate, specifying their separation, is needed. This coordinate corresponds to a vibration

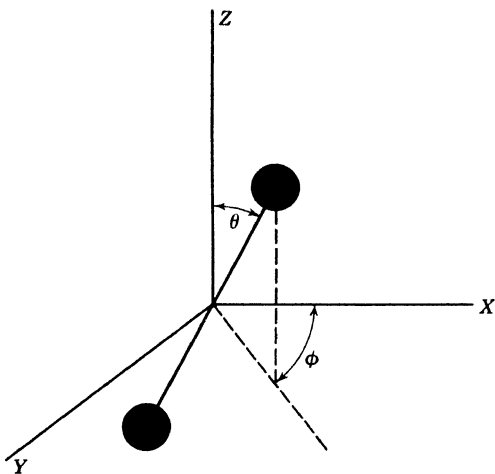


Fig. 9-1. Model of a diatomic molecule, showing the five coordinates needed to specify its position completely.

along the nuclear axis, which is then another degree of freedom. The kinetic energy per mole associated with this motion is $\frac{1}{2}RT$. But on the average there is an equal amount of potential energy, so the total added energy is the same as it would be if there were two extra degrees of freedom. At ordinary room temperature, the vibrational degrees of freedom of hydrogen, for example, do not come into play, and its energy per mole is $\frac{5}{2}RT$. If the vibrational degrees of freedom were excited, the energy per mole would be $\frac{7}{2}RT$.

Quantum theory. Nernst discovered in 1912 that the molar heat of hydrogen varies over wide ranges with temperature, in direct contradiction to the prediction of the classical theory. Figure 9-2 portrays

the temperature dependence of the molar specific heat of hydrogen at constant volume. At low temperatures the gas has the specific heat that might be expected for a monatomic gas. How is it that the rotation is so effectively suppressed up to about 100° K, and how shall we explain the exact shape of the curve as it rises from $\frac{3}{2}R$ to $\frac{5}{2}R$? The explanation of this discrepancy is another of the successes, first, of the early quantum theory, and later, to even a greater extent, of wave mechanics.

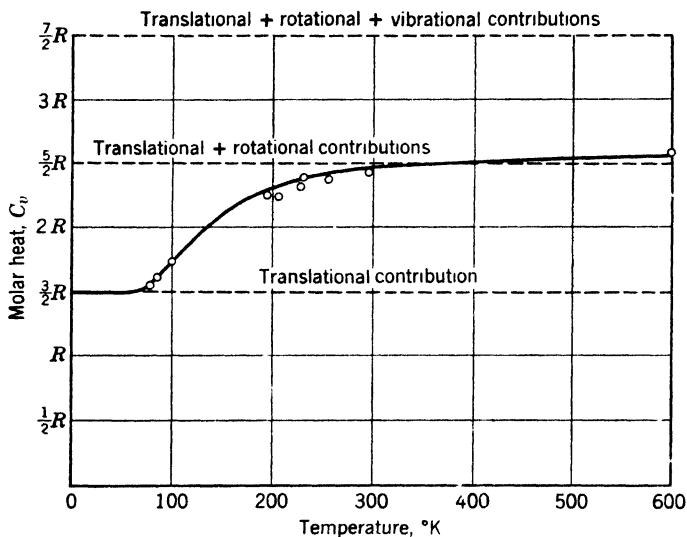


Fig. 9-2. Molar heat of hydrogen at constant volume. The horizontal dashed lines are the contributions according to the classical theory. The heavy full line is a curve obtained by the older quantum theory. Experimental points are shown by circles.

According to the classical theory discussed in the previous section, rigid diatomic gas molecules can rotate with any arbitrary angular velocity. As the temperature of a gas is increased, the molecules on the average rotate faster and faster, increasing their angular velocities in infinitesimal steps. Such behavior leads theoretically to a molar heat which is constant with changes of temperature.

The predictions of quantum mechanics are altogether different. Since the nuclei are very much heavier than the electrons, and since in collisions at ordinary temperatures electron quantum numbers are not changed, we restrict ourselves to a discussion of the motion of the nuclei alone. To apply wave mechanics, we must consider definite wave properties to be associated with the nuclei, and rotations with arbitrary angular

velocities are no longer expected. Only those are found which are consistent with the wavelength of the nuclear waves.

★ The solution of the wave equation is particularly easy in this case. Just as for a vibrating string, we have sinusoidal waves of the form

$$\psi = A \cos 2\pi\phi/\alpha + B \sin 2\pi\phi/\alpha \quad (1)$$

where ϕ is the azimuthal angle in the plane of rotation and α is the angle in which the wave repeats itself. However, it turns out that the special forms of ψ suited to our purpose are

$$\psi = A (\cos 2\pi\phi/\alpha + i \sin 2\pi\phi/\alpha) = A e^{i2\pi\phi/\alpha} \quad (1a)$$

and
$$\psi = A (\cos 2\pi\phi/\alpha - i \sin 2\pi\phi/\alpha) = A e^{-i2\pi\phi/\alpha}$$

Either one will serve our needs.

★ The reasoning behind this choice is as follows: In Chapter 6 we observed that ψ^2 is the probability density. In the present case, since no angle ϕ is preferred over any other, the probability density, which expresses the chance that the molecule be within a given angular range, must be independent of ϕ . Now there is no real combination of the form (1) such that its *square* is independent of ϕ ; but we notice that, if we employ equation 1a, then the product of ψ and its complex conjugate ψ^* is independent of ϕ (because $e^{ix}e^{-ix} = 1$). The product $\psi\psi^*$ may be considered a natural generalization of ψ^2 for the case where ψ is a complex number. It is $\psi\psi^*$, not ψ , that can be directly studied, so we do not hesitate to make the wave function complex, since with the increase in mathematical complexity we obtain a description of nature corresponding more closely with experimental knowledge.

To get the energy states, we note that the wave angle α as used here is exactly analogous to the wavelength λ in the theory of vibrating strings. For electron waves, as stated on p. 157, $\lambda = h/mv$. In the present case we have a similar expression except that now we must use angular quantities so that we have, in accord with quantum considerations, $\alpha = h/I\omega$ where I is the moment of inertia of the molecule and ω is its angular velocity about its center of gravity. The complete mathematical solution of this problem requires the introduction of boundary conditions which here are very simple because we are dealing with angular measurement. The only condition necessary is that ψ shall have the same value if ϕ is increased by 2π . In other words, ψ can have only one value for a given orientation of the nuclear axis. This requirement is fulfilled by setting $2\pi/\alpha$ of equation 1 equal to a whole number, say K . The physical significance of this condition follows: only those wave angles occur which fit into a complete circle

an integral number of times, just as in a vibrating string only those half wavelengths occur which fit into the length of the string an integral number of times. Since

$$2\pi/\alpha = K \quad (2)$$

$$\omega = Kh/2\pi I \quad (3)$$

All the energy of rotation of a rigid molecule model rotating about a fixed axis is kinetic and is given by

$$E_K = \frac{1}{2}I\omega^2 = K^2h^2/8\pi^2I \quad (4)$$

Thus, the wave-mechanical theory, in contrast to the classical theory, yields only discrete values of the angular velocity and of the energy.

Because the energy of an individual molecule is quantized, the effect of heat on a gas on the basis of the quantum theory is quite different from that predicted by the classical theory. Since the first energy step above zero for the rotational energy is $h^2/8\pi^2I$, it follows that this step is quite large for light molecules like hydrogen with small moments of inertia. Because of the small energy of motion at low temperatures a diatomic gas behaves as though the possibility of rotation did not exist and the molar heat at constant volume is $\frac{3}{2}R$. As the temperature is increased, however, more and more of the molecules are able to pass into states in which they rotate. When the average energy of a molecule becomes large compared with the change of energy in going from a non-rotational to the first rotational state, the effect of quantization becomes small and the gas then simulates the behavior predicted by the classical theory. The gas then has a molar heat equal to $\frac{5}{2}R$. The variation of the molar heat of hydrogen with temperature at low temperature as predicted by the quantum theory is shown by the curve in Fig. 9-2. The same type of curve is predicted theoretically for other diatomic gases, but on account of their larger moments of inertia the first energy step in question, as computed from equation 4, is very much lower than that for hydrogen. This means that the sloping part of the curve for other diatomic molecules occurs at a much lower temperature and is difficult to observe.

Para and ortho hydrogen. The quantization of energy levels as described in the preceding section is not complete because the nuclear spin has been neglected. In a more precise analysis it is necessary to consider this spin in the same way the electron spin was considered earlier (p. 198). For molecules like hydrogen the two nuclei are identical and are quantized together, giving only one quantum number K which is connected with the sum of the nuclear angular momenta about the common center of gravity. It can be shown that when K is even

the two nuclear spins can only be in opposite directions (Appendix 9, ref. 87, p. 695). When K is odd, there are three possibilities: (1) to have the nuclear spins parallel to K , (2) to have them antiparallel to K , and (3) to have one parallel and the other antiparallel, as in Fig. 9-3. When the nuclei spin oppositely, their resultant magnetic moment is zero, so that their energy is independent of orientation, like the situation found for the singlet levels of mercury on p. 203. When the spins are parallel, we can think of the resulting magnetic vector as having three orientations and three energy levels, as in the triplet levels of mercury. Each of these four possibilities is a priori equally probable, so that there will be three times as many molecules with K odd as there are with K even. According to quantum mechanics it is almost impossible in such a molecule to have transitions from a state with an even K to a state with an odd K . In other words, collisions at ordinary temperatures do not affect the spin properties of the nuclei. This means that, if a colliding molecule is in the state $K = 0$, only changes to the states $K = 2, 4, 6$, etc., can occur in appreciable numbers; similarly, a molecule with $K = 1$ can change with facility only to other states with odd K . Thus, two different types of molecules are normally present.

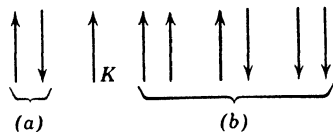


Fig. 9-3. Directions of nuclear spin for hydrogen, relative to the orbital angular momentum K , (a) para hydrogen; (b) ortho hydrogen.

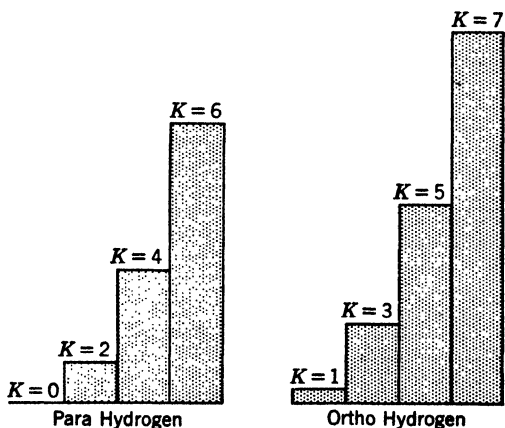


Fig. 9-4. Comparison of successive energy levels of para and ortho hydrogen.

In the case of hydrogen, the gas characterized by even quantum numbers is called para hydrogen and that by odd quantum numbers

ortho hydrogen. In the lower states, the changes of energy in passing from one state to another for para and ortho hydrogen are different, as may be seen from Fig. 9-4. The expected molar heats of these gases are consequently different. The computed variations with temperature are shown in Fig. 9-5. The solid curve of Fig. 9-5 represents the expected variation for hydrogen as it occurs naturally, the ortho compo-

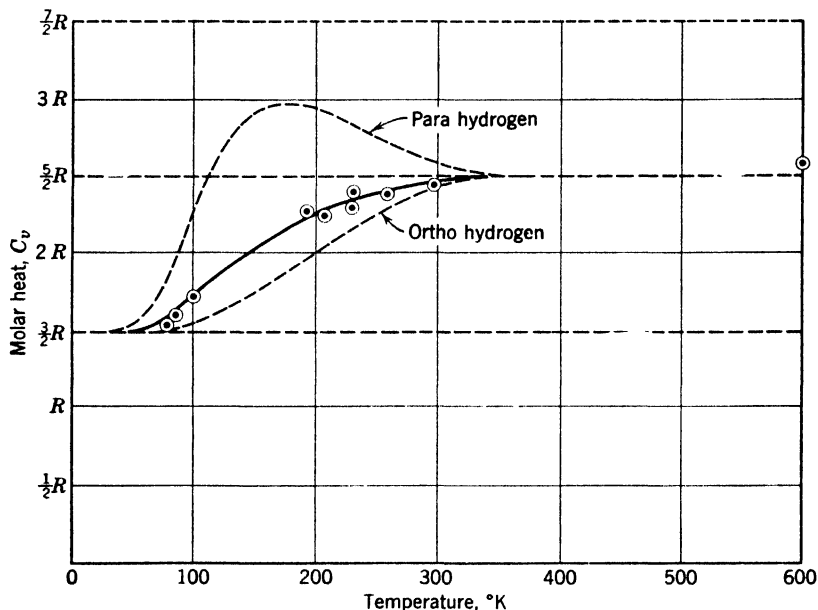


Fig. 9-5. Variation of the molar heats of para and ortho hydrogen. The heavy solid line represents the molar heat of the equilibrium mixture. Dots represent experimental points.

nent being given three times the weight of the para component because of the three possible positions of the nuclear spin of the former. The resultant agrees very well with the experimental points of Fig. 9-2, showing that ordinary hydrogen consists of a combination of these two gases.

It was a great triumph of the new quantum mechanics when in 1929 Bonhoeffer and Harteck were able to separate ortho and para hydrogen and to prove that the specific heat curves of the individual gases agreed with those predicted by theory. Because of the differences in the specific heats of ortho and para hydrogen, their vapor pressures are slightly different. By making use of this slight difference and by the aid of the adsorptive action of charcoal, it was possible to prepare para hydrogen about 98 per cent pure. Thus, wave mechanics has revealed an entirely

new concept: the division of elements into what might be called sub-elements or spin isomers with different physical properties.

3. Rotational Band Spectra

Location of spectral lines. In deriving equation 4 the assumption was made, for the sake of simplicity, that the molecule rotates about a fixed axis in space. In reality this axis is not fixed, and a complete wave-mechanical calculation shows that the above expression must be changed to read as follows:

$$E_K = K(K + 1)h^2/8\pi^2I \quad (5)$$

This can also be written in the form

$$E_K = \frac{(K + \frac{1}{2})^2 h^2}{8\pi^2I} - \frac{1}{4} \frac{h^2}{8\pi^2I} \quad (6)$$

which differs from the first expression derived only in that the quantum numbers are increased by half integers and that a constant energy term is subtracted. The constant term does not affect the *differences* between values of the spectral terms.

It was known before the introduction of wave mechanics that reasonable interpretations of rotational energy levels require half-integral quantum numbers, but the origin of the half integers was very obscure. The natural introduction or explanation of half-integral quantum numbers was one of the earliest successes of wave mechanics.

Whenever an atomic system changes spontaneously from one state to another, there is an emission or absorption of light having a frequency given by the condition $h\nu = E_1 - E_2$. The same is true for emissions and absorptions involving molecular transitions. In molecules, however, the numbers of possible changes are much greater than in atoms. For each electronic motion there are many levels belonging to the different quantized vibrational and rotational motions of the nuclei. Of all the energy changes in the molecule, those connected with transitions from one rotational state to another are the smallest.

According to wave mechanics, in transitions between rotational states that occur by radiation, the rotational quantum number K can change by only one unit. This selection rule holds only for spontaneous emission or absorption of radiant energy, as distinguished from the collision phenomena treated earlier. The frequencies of the emitted lines for transitions involving a change of K by one unit are given therefore by

$$\nu_{K+1,K} = \frac{(K + 1)(K + 2)h}{8\pi^2I} - \frac{K(K + 1)h}{8\pi^2I} = \frac{(K + 1)h}{4\pi^2I} \quad (7)$$

Consequently the complete spectrum for this type of change consists of a set of lines equally spaced in frequency from an initial line of frequency $h/4\pi^2I$, as is shown in Fig. 9-6. The same lines may likewise be absorbed when light from a source having a continuous spectrum is passed through the medium under investigation. Since only the rotational energy is involved in these transitions, this emission or absorption spectrum is called the pure rotation spectrum.

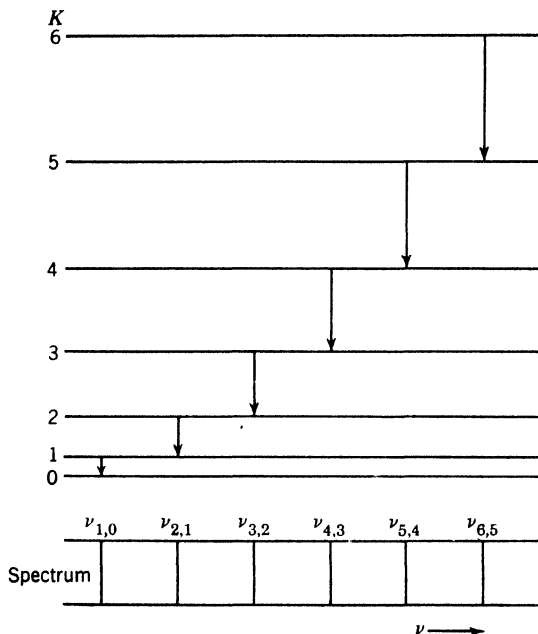


Fig. 9-6. Energy-level diagram for rotational states. The origin of the rotational emission spectrum is shown.

The location of the pure rotation spectrum of a diatomic molecule depends essentially upon its moment of inertia. In all cases investigated thus far, pure rotation spectra have been found to be in the extreme infrared, and their analyses indicate that the distances between individual atoms in the molecules are of the same order of magnitude as the diameters of the atoms themselves. An exact calculation, in accord with the theory given, of the moment of inertia of HCl is considered in Section 4. This simple interpretation of the pure rotation spectra in the far infrared makes measurements in this region extremely valuable, but accurate measurements are difficult because of the small thermal energy available, so the data accumulated are meager compared with those available in the near infrared.

Far infrared spectroscopy. Infrared spectroscopy differs in many essential points from spectroscopy in the visible region. For the far infrared, arbitrarily taken as wavelengths greater than $50\ \mu$, the general arrangement of an apparatus used to investigate the absorption spectra is shown in Fig. 9-7. The source of radiation, for which the Welsbach gas mantle, a "Globar," or a Nernst filament is often used, is imaged on a slit at S . After passing through the slit, the radiation is reflected

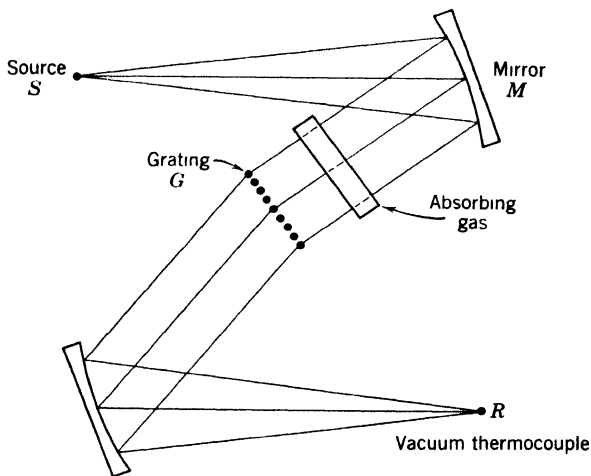


Fig. 9-7. Experimental arrangement for obtaining absorption spectra in the extreme infrared.

from a mirror M which makes the beam parallel. It then passes through the absorbing gas in a cell with quartz or rock-salt windows and strikes the diffraction grating G . Finally it is condensed on a detector at R ; bolometers, vacuum thermocouples, and radiometers have been used. It is unfortunate that photographic plates are not sensitive in this region since they have the property of building up a weak impression when long exposures are used. Accurate measurements in the far infrared were made by Czerny. He studied the absorption of HCl extending to wavelengths as great as $120\ \mu$. The wave numbers of the lines he observed are listed in Table 9-1. They are in good agreement with the empirical formula

$$\bar{\nu} = 20.794M - 0.00164M^3 \quad (8)$$

where M takes integral values as we go from line to line.

It will be noticed that this formula contains a term in M^3 which does not occur in equation 7. A more complete analysis shows that this

TABLE 9-1

Integral Number Used to Designate Line M	Wave Numbers (in waves/cm)	
	Observed	Calculated by Formula 8
4	83.03	83.07
5	103.77
6	124.30	124.41
7	145.03	145.00
8	165.63	165.51
9	185.86	185.95
10	206.38	206.30
11	226.50	226.55

term arises from an increase in the moment of inertia resulting from the stretching of the diatomic molecule when rotating with high angular velocities. Comparing the term in M with equation 7, we find agreement when $K = M - 1$ and $h/4\pi^2 Ic = 20.794 \text{ cm}^{-1}$. The moment of inertia of HCl thus found directly is $2.66 \times 10^{-40} \text{ gm cm}^2$. Knowing the masses of the hydrogen and chlorine atoms, we may therefore calculate that the separation of the two atoms in a molecule of HCl is $1.28 \times 10^{-8} \text{ cm}$.

4. Vibration-Rotation Bands

Theory. The attractive forces which hold two atoms together to form a molecule are of many kinds, as discussed on p. 230. In order to form a stable molecule the potential energy of the system must be a minimum for some particular distance. A typical example for the variation of the potential energy with the distance between the nuclei is shown in Fig. 9-8. Near the minimum, this potential-energy curve approaches very nearly the shape of a parabola, which is the potential-energy curve for a linear harmonic oscillator.

Regarding a diatomic molecule as a linear oscillator, we have for its quantized energy levels (see p. 186)

$$E_v = (v + \frac{1}{2})h\omega_e \quad v = 0, 1, 2, 3, \dots$$

where ω_e is the frequency of vibration about the equilibrium position and v is the vibrational quantum number. Such energy levels are indicated by the dotted lines in Fig. 9-8. The presence of the term $\frac{1}{2}$ in the expression for the quantized energy levels requires that, even in the

lowest state, the atoms must vibrate with small amplitude. Since the potential-energy curve is not exactly that of a linear oscillator the energy levels are not separated by exactly equal intervals, but, instead, the upper levels are usually closer together.

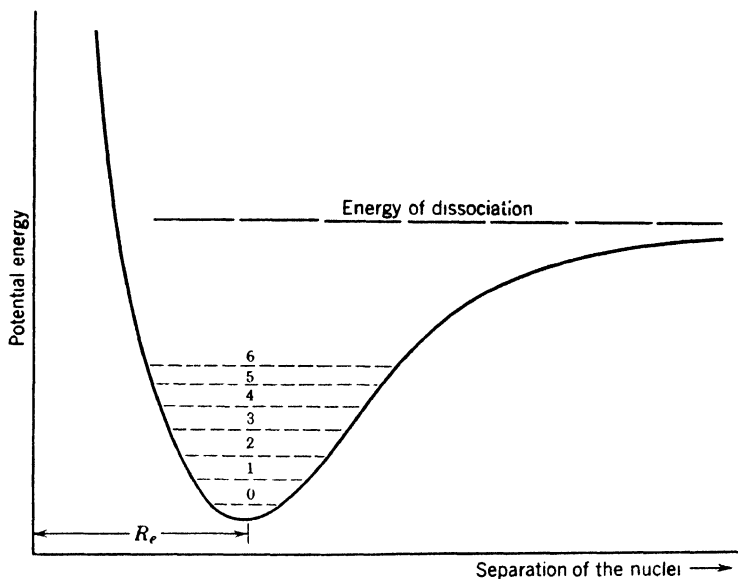


Fig. 9-8. Potential-energy curve for a diatomic molecule. The dashed lines represent quantized vibrational levels.

If the interaction forces resulting from the presence of both vibration and rotation are neglected, the total energy of a rotating vibrating molecule may be approximately expressed by

$$E = (v + \frac{1}{2})h\omega_e + K(K + 1)h^2/8\pi^2I \quad (9)$$

The frequencies of the spectral lines which are emitted or absorbed are accordingly given by

$$(E' - E'')/h = (v' - v'')\omega_e + (h/8\pi^2I)(\pm 2K'' \pm 1 + 1) \quad (10)$$

where the primes and the double primes represent, respectively, the upper and lower levels, and where the plus signs are used if K decreases by one unit and the minus signs if K increases by one unit. These frequencies are illustrated in Fig. 9-9. The vibrational energy change represented by the first term of the expression on the right of the equality sign is very much greater than the rotational energy change which is represented by the second term. The vibrational part determines,

therefore, the spectral region in which the vibration-rotation spectra lie; the rotational part determines the fine structure, that is, the separation of the individual lines. The set of rotational lines belonging to a single vibrational transition is called a band or, more exactly, a vibration-rotation band. The entire group of bands is called a band system.

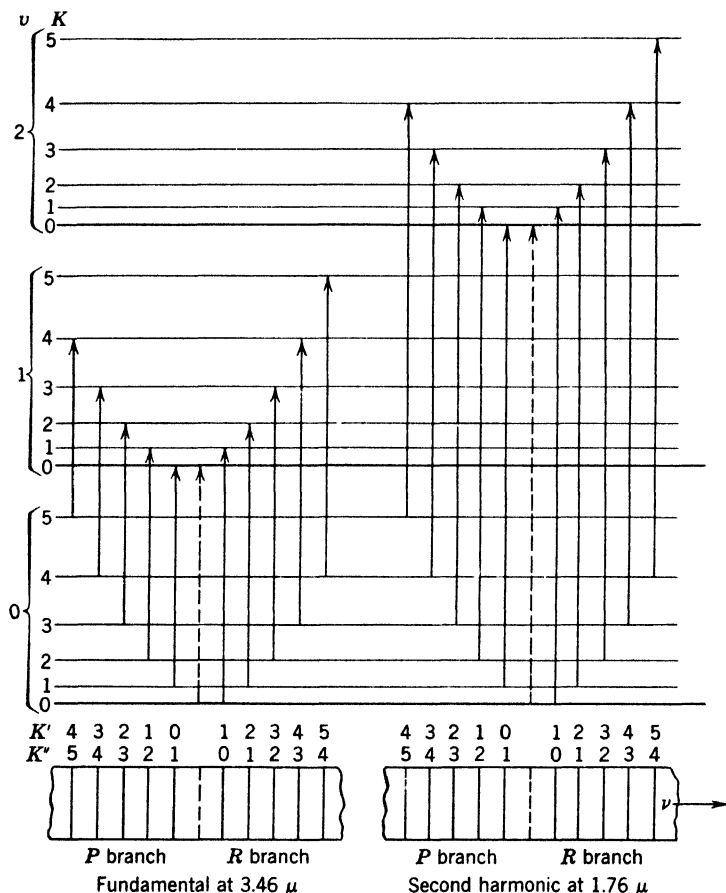


Fig. 9-9. Energy levels of HCl with various vibrational and rotational quantum numbers are shown, though not to scale. In emission or absorption (as shown) increases or decreases of one in K occur. No cases of a zero change in K have been observed. It is interesting that lines corresponding to such zero changes, were they present, would fill exactly the place of the "missing" line of the observed spectrum.

On the basis of the classical theory a linear oscillator can emit waves of only one frequency. A good example is a tuning fork which emits sound of only a single pitch. However, if we load it unevenly or if we

strike it too hard, other frequencies accompany the fundamental. The quantum theory predicts also that a linear oscillator will emit or absorb radiation of only one frequency by limiting the change in v to ± 1 . In an actual molecule, however, the potential energy is not strictly that of a linear oscillator, so that it behaves like a loaded tuning fork and emits frequencies other than the fundamental. These are characterized by changes in v of more than one unit, but the intensity of these bands is very small compared with that of the fundamental. Those bands in which v changes by 2, 3, or 4 are called, respectively, the second, third, or fourth harmonics.

The energy changes and the frequencies associated with the vibrational spectrum are much larger than those associated with the pure rotational spectrum; hence the former spectrum lies much closer to the visible region than the latter. The fundamental vibration-rotation bands lie between 8000 Å and 50,000 Å for large numbers of molecules.

★ **Near infrared spectroscopy.** In the region from about 50 μ to the visible, gratings or prisms may be used, depending on the resolution desired. Most measurements are made from absorption spectra. A typical example of a near infrared absorption spectrogram, that of the

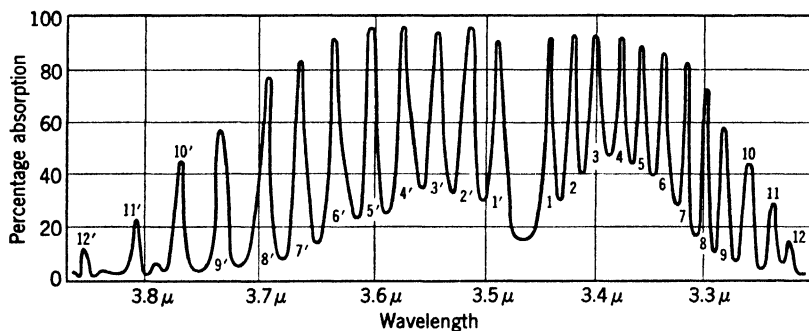


Fig. 9-10. Absorption spectrogram of the fundamental rotation-vibration band of HCl. (After the data of E. S. Imes.)

fundamental band of HCl, is shown in Fig. 9-10. That the spectrogram shows a pronged structure instead of a series of isolated lines with a definite law of separation is a consequence of the rather low resolving power which the conditions of the experiment have imposed. For further discussion the line structure may be logically assumed. The center of the band evidently occurs at 3.46 μ , and the spacing of the lines near the center is about 250 Å. A significant feature of this HCl band is the missing line at the middle of the spectrogram. The explanation for its absence is apparent from the energy-level diagram, Fig. 9-9.

Such a transition, in which the rotational quantum number does not change, is excluded by the selection principle for K .

★ Using equation 10, it is easily verified that the rotational factor ($\pm 2K'' \pm 1 + 1$) takes on values such as to give lines which are equally spaced on either side of the position of the missing line. Those lines for which $K' - K'' = 1$ are said to form the positive or " R " branch; those for which $K' - K'' = -1$ are said to form the negative or " P " branch.

★ **The effect of isotopes on rotation-vibration spectra.** Besides the fundamental band of HCl at 3.46μ which has just been described, the second harmonic band due to a change in v of two units has also been observed. The frequency of this band is just about double that of the fundamental, so that it occurs at 1.76μ . Associated with this band are rotational peaks corresponding exactly with those of Fig. 9-10. It is found that at the side of each of the peaks of the harmonic band are small secondary peaks (see also peaks in Fig. 9-10 at 3.79μ and 3.84μ). These are present because there are two isotopes of the chlorine atom having atomic weights of 35 and 37. Molecules formed from atoms having unequal masses have different vibrational frequencies, just as two unequal masses oscillate with different frequencies when hung upon similar springs. The change in frequency of oscillation carries with it an alteration of the energy levels. Therefore, the frequencies of the spectral lines are altered, and we obtain a separate set of peaks in the spectrum for each isotope. From the heights of these peaks the relative abundance of the isotopes can be estimated; it is found to be in good agreement with the value determined from the resultant atomic weight of chlorine.

★ In concluding this section, it should be remarked that the spectra of polyatomic molecules are dealt with by methods like those above. The complications are greater. There are three rotational degrees of freedom. Subtracting these degrees and the three degrees corresponding to translation of the molecule as a whole, we have $3n - 6$ remaining degrees for a molecule composed of n atoms. This implies that there may be $3n - 6$ independent types of vibration, or so-called normal vibrations. A normal vibration is a state of motion in which all atoms of the molecule move with a single frequency. For example, CO_2 is a linear molecule, with three possible normal vibrations. Let the molecular axis be along the X axis. In one normal vibration, the molecule bends. In another, the oxygens move out and in together along the molecular axis, with the carbon atom remaining at rest. In the third, the motion is also along the axis; but, when the right-hand oxygen moves toward the right, the carbon goes to the left and the left-hand

oxygen toward the right. The reader may wish to write the equations of motion for one of these vibrations and to verify that all the atoms can move with the same frequency. The model to be employed is simply a set of three balls connected by two springs of equal stiffness.

5. Electronic Bands

In Chapter 7 the complex groups of lines resulting from transitions of an electron from excited states of an atom to more stable states were described. Because the electronic structure of a molecule is similar to that of an atom it is natural to expect the energy levels of a molecule to be split up into sublevels in the same manner as are atomic levels. However, besides the sublevels caused by the electronic motion we have the further sublevels arising from rotational and vibrational motion of the nuclei. It is fortunate that the energy changes which occur for each of these motions are of different orders of magnitude, so that it is usually easy to classify the transitions which occur. Most of the spectra involving electronic transitions lie in either the visible or ultraviolet regions.

★ Following the procedure used in analyzing atomic spectra, we should expect to be able to classify molecular spectra into different types depending on both the orbital angular momenta of the electrons and their spin angular momenta. Much progress has been made in such classification, but the results are too complex for inclusion here. In the following discussions, therefore, the electronic change in energy will be considered as a constant factor. On this basis the frequency ν of any line appearing in an electronic band spectrum is given by the following expression:

$$h\nu = h\nu_0 + (E'_{\text{vib}} - E''_{\text{vib}}) + (E'_{\text{rot}} - E''_{\text{rot}}) \quad (11)$$

where $h\nu_0$ represents the electronic change in energy, assuming no interaction of electronic and nuclear motions. The values of the latter terms in this expression are considerably different from the corresponding terms in the rotation-vibration spectra, because the nuclear binding (and thus the vibrational frequency) and the moment of inertia are different in the initial and final states.

★ Using the above relation it is only necessary to substitute the quantized values of the energies in order to obtain a formula which represents all possible spectral lines. An idealized energy-level diagram will help us to form a picture of these changes. In Fig. 9-11, for simplicity, transitions between two electronic levels, *A* and *B*, are represented. Associated with each of these are a few vibrational levels whose spacing enables us to conclude that the binding force is greater in the

upper state than in the lower state. Superposed on these levels are the rotational levels which are spaced at unequal intervals since the energy depends essentially on the square of the rotational quantum number. The spacings of corresponding rotational levels, belonging to the upper and lower electronic levels, are quite different, because the separations of the nuclei (and therefore the moments of inertia) are usually different in the various electronic levels.

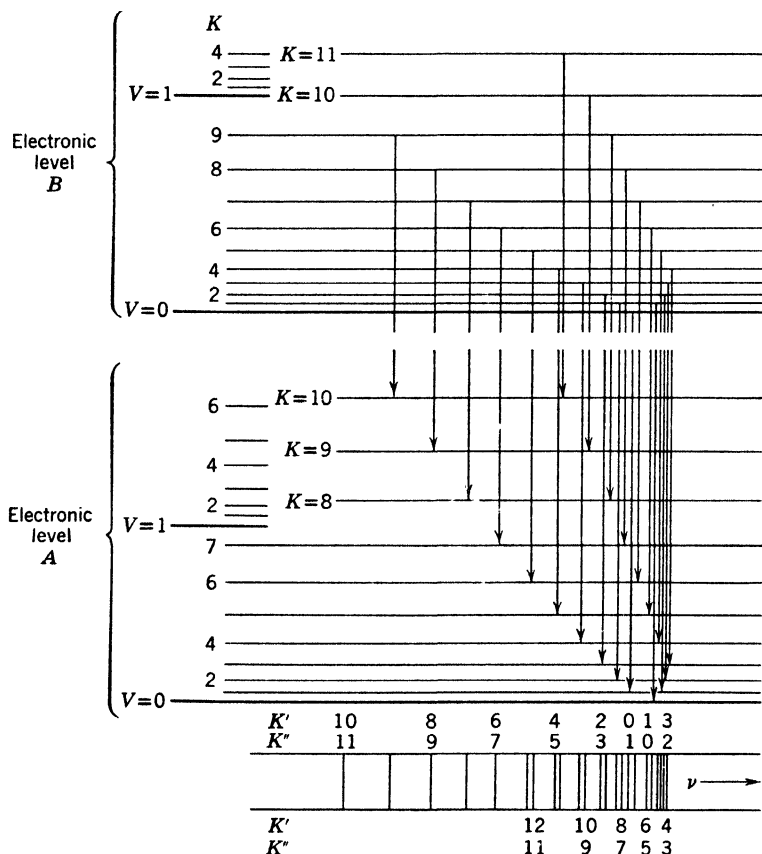


Fig. 9-11. Energy-level diagram showing the convergence of lines to form a head in an electronic band.

★ The distribution of rotational spectral lines in Fig. 9-11 is seen to be quite different from that in Fig. 9-9. The reason for this difference is that in Fig. 9-9 the electronic level, and therefore the moment of inertia, is the same for both the initial and final states, whereas just the converse is true for the spectral levels of Fig. 9-11.

★ The position of a line in a spectrum is determined by the energy change of the molecule as a whole; this is represented in the figure by the length of the vertical line connecting the two states involved. Because the separations of the rotational levels are different in the upper and lower states of Fig. 9-11, these lines for a particular electronic band are seen to grow longer as the quantum numbers increase until the longest is reached at the line for which $K'' = 3$ in the positive branch

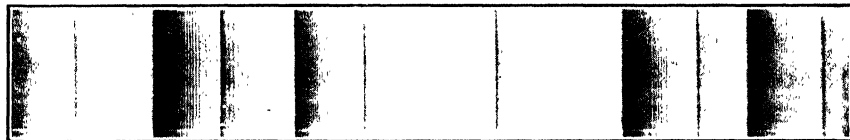


Fig. 9-12. A band spectrum of boron oxide (after R. S. Mulliken). The frequency ν increases toward the left.

($K' - K'' = +1$). The lengths of the vertical lines representing transitions then begin to decrease again. The fact that the frequency of the light passes through a maximum as the quantum number increases gives the appearance of a crowding at one side of the band. The rotational spectral line at the end is called the head of the band. Photographs of typical electronic bands are shown in Figs. 9-12 and 9-13, and the latter illustrates clearly the crowding at a band head.

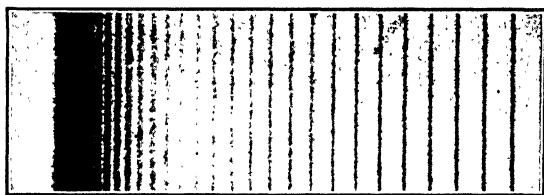


Fig. 9-13. The line structure of a single band of silicon nitride (after F. A. Jenkins). The frequency ν increases toward the left.

★ When the vibrational quantum numbers involved are 1 and 0 or 2 and 1 instead of 0 and 0, new bands are produced. If the vibrational frequency is greater in the upper state than in the lower state, the 2 to 1 band will have a greater frequency than the 1 to 0, and will therefore lie on its violet side.

★ Thus, by classifying the motions of the component parts of the molecule into nuclear rotation, nuclear vibration, and electronic motion, it is possible to bring order out of the chaos of lines which occur. The analysis of these spectra in the manner outlined has provided many of

the physical dimensions of molecules which otherwise would remain unknown, and has allowed us to discover and estimate relative amounts of isotopes. Further, the theory gives us an insight into the behavior of the individual electrons in the molecule and thus provides a new stepping stone in the path toward a mathematical theory of the formation of chemical compounds.

6. Raman Spectra

All materials scatter light in all directions, and it is readily found that the scattered light contains the identical wavelengths which were present in the incident beam. It is, however, reasonable to inquire whether a *part* W of the energy of a photon $h\nu_0$ might not be utilized to excite an atom or molecule to a higher state, the remainder being scattered as a photon of lower frequency, so that

$$h\nu' = h\nu_0 - W \quad (12)$$

Again, an atom or molecule in an excited state might contribute an energy W in a scattering process, so that the emergent photon would have an energy

$$h\nu' = h\nu_0 + W \quad (13)$$

A search for such lines in atomic spectra was reported by Foote and Ruark in 1924, and Smekal made similar suggestions. The effect was found in 1928 by Raman and Krishnan; also by Landsberg and Mandelstam. It was obtained by scattering monochromatic light from suitable molecules. Weak lines are found on both sides of the incident line, due to changes of the rotational quantum number. The spacing of rotational levels is small, so that many molecules may reside in higher rotational states. On the other hand, the spacing of vibrational levels is usually so large that few molecules are in higher vibrational states at ordinary temperatures. Hence, Raman lines corresponding to a change of the vibrational number usually lie on the lower frequency side of the exciting line. The general nature of the rotational effect can be seen from Rasetti's photograph in Fig. 9-14.

The chief interest of the Raman effect lies in the fact that it reveals some frequencies which do not occur in infrared spectra. For example, the symmetrical vibration of CO_2 described on p. 248 does not produce an electric moment and therefore does not yield spontaneous radiation. Yet it is easily demonstrated in scattered light.

A great advantage is that the wavelength of the incident light can be chosen in a region convenient for observation.

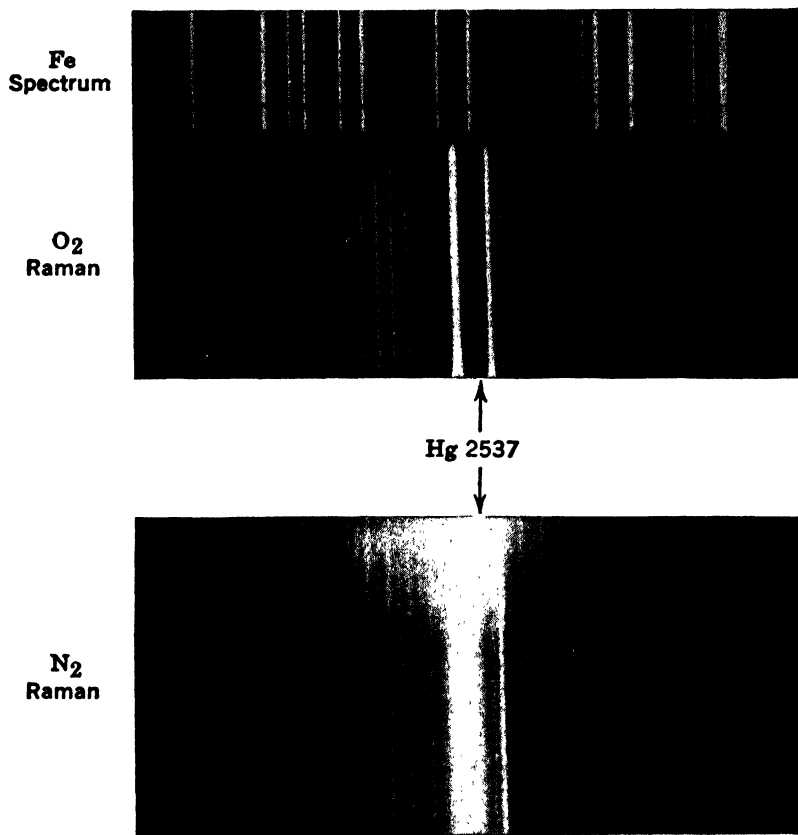


Fig. 9-14. Rotational Raman spectra of N₂ and O₂ (after Rasetti). The exciting line 2537 Å of mercury and a weaker mercury line (which produces no observable effects) are easily distinguished from the scattered radiations of altered wavelength.

7. Microwave Spectroscopy

Since 1934, and particularly since 1945, a new branch of spectroscopy has developed in the microwave region, which has led to the observation and measurement in molecules of energy changes of a much smaller magnitude than is possible by optical methods. The microwave region may be taken to extend over the range of electromagnetic wavelengths from about 2 mm to 16 cm. In this range frequencies can be measured with great precision by electronic methods. When a molecule absorbs a photon of wavelength 3 cm, for example, it suffers a change of energy amounting to only $10^{10} h$ ergs, or about 4×10^{-5} ev. These figures

may be compared with absorption in the visible region of a photon of wavelength 6000 Å, corresponding approximately to an energy change of 2 eV. In the microwave region, therefore, exceedingly close energy levels, when they exist, can be observed and mapped.

Microwave spectroscopy deals entirely with absorption effects, because emission spectra in the microwave range are completely masked by normal temperature radiation. We have no space here even to suggest what experimental methods are used to observe microwave absorption spectra. One set of results will be quoted as an illustration.

★ Consider a linear molecule composed of one atom of iodine and one of chlorine, and think of it as rotating about an axis which is perpendicular to the line joining the two atoms. In the absence of special constraints, the axis of rotation must pass through the center of mass of the system. Using the rotational quantum number K , the change of energy when the molecule passes from the state K to $K + 1$ is, by equation 7

$$\Delta E_{K+1, K} = (h^2/4\pi^2 I)(K + 1) \quad (14)$$

where I is the moment of inertia of the molecule about the axis specified above. Setting this energy change equal to $h\nu$, we find that the change corresponds to a wavelength given approximately by

$$\lambda = \frac{10^{40} I}{56(K + 1)} \quad (15)$$

★ Now the value of I can be computed with reasonable accuracy, since we know the masses of the iodine and chlorine atoms, and may take their separation as 2.3 Å. The result is, roughly, $I = 240 \times 10^{-40}$ gm cm². Hence $\lambda \simeq 4/(K + 1)$, and if K is a small integer, the radiation will occur in the microwave region. Whether or not the expected radiation due to changes in the rotational energy of a simple linear molecule falls in the microwave region is thus seen to depend on the value of the moment of inertia. If the value is up or down within a factor of about 8 from the value 2×10^{-38} gm cm², absorption may be expected in the microwave region. Only molecules with fairly heavy atomic components need, therefore, be considered. If one or both of the component atoms of a diatomic molecule is very light, then the moment of inertia will be small. Only massive molecules such as ICN, ClCH and ICl lead to lines in a region accessible to commonly available microwave apparatus.

Energy changes in the rotational spectra of moderately heavy molecules are not alone in being measured by microwave spectroscopy. Information concerning the structures of paramagnetic and ferromagnetic

substances, the magnitudes of electric fields within crystals, and the values of quadrupole moments arising from non-spherical distributions of nuclear charge or of nuclear matter can be deduced from appropriate absorption measurements. The methods of microwave spectroscopy possess the sensitivity needed to measure these delicate effects.

8. Dipole Moments and Dielectric Constants

We consider now an additional method of determining some features of the charge distribution in certain types of molecules. A simple free atom like hydrogen consists of two parts, an electron carrying a negative charge, and a proton with a positive charge. If the electron were not continuously rotating round the proton (or in the language of quantum mechanics, if the electron's charge were not symmetrically distributed about the nucleus) the orientation of the atom could be controlled by the application of a macroscopic external field. An extension of the argument can be used to demonstrate that a symmetrical molecule like CCl_4 cannot be preferentially orientated by an external electric field.

Many molecules, however, like H_2O or HCl , are not thus immune to the influence of external fields. Such molecules are said to possess electric dipole moments, even though it is not always possible to state precisely how much electric charge has been shifted by any particular amount. In these cases an external electric field tends to turn the molecule so that its electric axis lies parallel to the field, and to hold it in that position, in the same way as a bar magnet tends to align itself with an applied magnetic field.

★ Suppose that a dipole consists of two charges, $+q$ and $-q$, separated by a distance d . The electric dipole moment is defined as the product qd . Suppose further that the dipole is instantaneously at rest with its axis perpendicular to an electric field of intensity F . Now let the dipole be turned round to a position 90° from that which it formerly occupied. The work E needed for this maneuver is

$$\begin{aligned} E &= \pm 2 \times qF \times (d/2) \\ &= \pm Fqd \end{aligned} \tag{16}$$

the product of the electric field strength and the dipole moment. As the signs indicate, work may be done either on or by the dipole, depending on the direction of turning. The quantity E is termed the maximum interaction energy between the dipole and the field F .

★ In practice, of course, it usually happens that a molecule which possesses a dipole moment, being part of a gas or liquid or solid, is not

absolutely free to respond to the external electric field. A partial orientation may then occur, with the result that the body of which the molecule is a part acquires a macroscopic electric moment that persists as long as the external field is present. The material is then said to be *polarized*.

★ There is another way in which the field produces an electric moment, namely, by the slight displacement of nuclei in the direction of the field and displacement of electrons in the opposite direction. This effect is universally present, but the electric moment of an atom or molecule produced by electric fields of magnitudes easily available in the laboratory is *ordinarily small* compared with the permanent moments of the highly polar molecules mentioned above. For example, the electric moment produced in a xenon atom by a field of 1 esu (or 300 volts/cm) is about 4×10^{-24} esu cm. A field of, say, 10^4 volts/cm could readily be applied to xenon at atmospheric pressure, giving a moment of about

$$1.21 \times 10^{-22} \text{ esu cm}$$

This may be compared with the permanent moment of an HCl molecule,

$$1.03 \times 10^{-18} \text{ esu cm}$$

★ The polarization P represents numerically the total dipole moment per cm^3 induced by the external field within the body of the material. Such behavior is characteristic of dielectrics, and the response of the dielectric to the external field is measured by the dielectric constant κ .

★ Dielectric constants can, of course, be measured in a variety of ways. For a material that contains molecules that are permanent dipoles (though not permanently orientated in any one direction) there is a simple relationship (proved, for example in ref. 80, Appendix 9, p. 51) between the dielectric constant κ , the polarization P , and the external field F , namely,

$$(\kappa - 1)/4\pi = P/F \quad (17)$$

Thus, if κ is measured, and F is known, a value of P may be deduced. Proceeding farther, P may be expressed in terms of the number of molecules per cm^3 of the material, the familiar quantity $\frac{1}{2}kT$, and the dipole moment per molecule qd . Since it is reasonable, in the case of a molecule like HCl to ascribe the observed dipole moment to the separation of positive and negative charge caused by the migration of one electron part way from one of the component atoms toward the other, the effective separation of the charges can be found.

★ The induced polarization is substantially independent of temperature over considerable ranges. To alter it, we have to change the distribution of the atoms over the various quantum states available to them. On the other hand, the portion of the polarization coming from orientation of permanent dipoles is strongly dependent on the temperature because molecular collisions tend to distribute the directions of the dipole axes uniformly, opposing the ordering effect of the external electric field.

9. Energy Levels of Solids; Electric Conduction

In this section we give a very brief introduction to the physics of the solid state by considering some of the special properties of metal crystals.

The pattern of energy levels in a molecule is different from that in one of its component atoms. Further modifications of the pattern will occur as additional atoms are attached to the structure to make a more complicated molecule. For example, the energy levels of the H atom are not the same as those of the H_2 molecule; the latter differ from those of water, H_2O , and still more from those of H_2O_2 , hydrogen peroxide. Reasoning in this way, we might expect a crystal of pure copper to have some of the properties of a gigantic molecule, since every new Cu atom added must necessarily modify to some extent the previous pattern of forces existing throughout the solid metal. However, once the crystal, though still submicroscopic, has grown to contain a large number of atoms, say 10^6 , the addition of an extra atom has little effect on the energy levels of the total structure.

The crystal is composed of nuclei, more or less fixed in position relative to the center of gravity of the structure, and the more mobile electrons. The latter do not fill any closed shells, since the neighboring atoms are identical and each already possesses only partly filled shells. Under these circumstances, very little energy is needed to move some electrons from their normal positions to more extensive orbits—so little, indeed, that it is customary to regard a solid metal crystal as containing “free” electrons. It follows immediately that metals so conceived *should* possess a high electric conductivity because a very tiny potential difference would be enough to cause the requisite drift of the free electrons through the lattice structure.

Up to the year 1928, students of the behavior of metals were confronted with a dilemma. There was some evidence that, in a univalent metal like sodium or copper, all the valence electrons are sufficiently free to respond to very minute applied voltages. In fact, Drude and Lorentz had proposed that the valence electrons be treated as though they were

a gas enclosed in a box. On this basis, the electric conductivity could be accounted for, assuming that the average kinetic energy of an electron is $\frac{3}{2}kT$. But if this view were correct, the electrons should contribute a term $\frac{3}{2}R$ to the molar heat of the metal where R is the universal gas constant (p. 9). This was not verified. True enough, it has been shown that a *small* fraction of the specific heat of a metal at high temperature comes from heating up the electrons, but the magnitude of the effect is in flat contradiction with the perfect-gas picture.

The solution of the puzzle was found by Fermi and was beautifully developed by Sommerfeld, who considered the matter waves associated with the electrons. On p. 172 we discussed the possible energy levels of electrons moving freely between two leak-proof walls. The situation is like that which would exist in a *hypothetical* metal able to permit free flow along one axis only. Suppose, for simplicity, that we neglect the repulsive forces between electrons, on the basis that the fields of the positive ions will, on the average, nearly cancel such repulsions. We assume, however, that the potential energy of the electrons has a constant negative value inside the metal. Of course, the barriers that prevent escape at ordinary temperatures are not infinitely high, but for simplicity, we shall speak, momentarily, as though they were. Then one would think that at the absolute zero of temperature, all the electrons would be in the lowest quantum state, whose standing-wave function is depicted on p. 173. Further, it would seem reasonable that at any finite temperature they would be distributed over the various states, approximately in the fashion of the Maxwellian distribution of velocities (p. 6).

★ But we must recall that, according to the Pauli principle, there will be only two electrons in each quantum state. One of these may have a spin number of $+\frac{1}{2}$ and the other $-\frac{1}{2}$ (being oriented relative to a magnetic field applied for our convenience, just as in the discussion of the reason why there are only two electrons in the K shell of an atom). Those which cannot get into states already preempted by others must go into higher states. Thus, *at the absolute zero of temperature, the valence electrons already have a great stock of kinetic energy*. The highest state occupied will be the one with a quantum number $N/2$, where N is the total number of electrons in the block. The momentum for this highest state (p. 173) is

$$p = \frac{(N/2)\hbar}{2a} \quad (18)$$

where a is the distance between the barriers, the faces of the block. Thus the highest energy an electron will possess at absolute zero is

$(h^2/2m)(N^2/16a^2)$. Suppose that the cross section of our hypothetical metal block, perpendicular to the X axis, is 1 cm^2 . If N_0 is the number of electrons per unit length of this column, $N = N_0a$, and the highest energy is

$$E_{\max} = (h^2/2m)(N_0^2/16) \quad (19)$$

This highest energy is independent of the length of the block, as it should be. We notice that if we double the length of the block *there are twice as many electrons to be accommodated, but the uniform separation of the quantum states in the momentum scale is reduced by a factor 2*, so twice as many states occur in the range of momentum from zero up to the highest value, namely, $N_0h/4$.

★ Now consider an *actual* metal, in which the electrons can move in all directions on the basis of classical theory. Then matter waves can pass in a great variety of directions in (say) a centimeter cube of the material; but not in all directions, for the reason that the wave function must always be zero at the boundary. As before, *two* electrons go into each state, and the new value of maximum energy, replacing the one in equation 19, is

$$E_{\max} = (h^2/2m)N_1^{2/3}(3/8\pi)^{2/3} \quad (20)$$

N_1 is the number of valence electrons per cm^3 .

Figures 9-15*a* and *b* show the occupancy of the states at absolute zero and at a finite temperature. They are momentum diagrams, and a little circle placed on an energy level indicates an electron that occupies it. Figure 9-15*c* portrays the distribution of electron energies for absolute zero and for a temperature about 1500°K . The abscissa is proportional to the number of electrons per unit interval of energy. We note the smallness of $\frac{3}{2}kT$, compared with the total range of energies occupied by the electron gas. This range, 5 eV, is roughly correct for the case of sodium; for other metals the values run from 2 to 14 eV. The distributions shown are commonly called Fermi distributions. Looking at the curve labeled 0°K we note that there are definite percentages of free electrons with kinetic energies up to the value E_{\max} and *none with higher energies*. Such a distribution is in strong contrast to the Maxwell-Boltzmann distribution; according to the latter, at 0°K all electrons would be in the lowest energy state.

Suppose now that an electron rather low down in this band of filled levels were to receive an increment of energy of the order kT from the lattice of positive ions, or from the surroundings. To what state or energy level could the electron go? The answer is that unless the electron were to gain enough energy to raise it completely above the

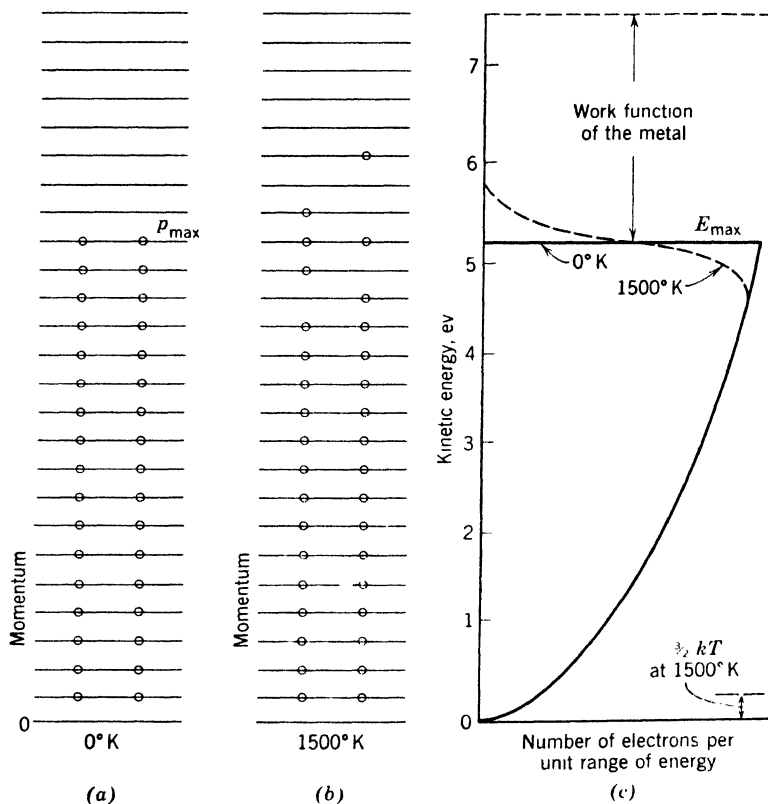


Fig. 9-15. (a) The occupation of different quantized momentum values by electrons at the absolute zero of temperature, in a substance that permits motion of the electrons only parallel to a single direction; (b) the same, for a finite temperature; (c) the energy distributions at the two chosen temperatures are indicated by the abscissas of the curves, respectively. The unoccupied energy levels terminate at a value that corresponds to having a free electron just outside the metal. In a centimeter cube of any real metal the actual number of occupied levels is very great, so great that they may be considered to form a continuous band.

filled band, it cannot go to any new state, and hence cannot accept the increment of energy at all. Therefore, if the temperature of a metal is raised slightly, the only electrons that are able to move to new energy levels are those already near the top of the band, which then occupy states a little higher than E_{\max} . The main population of electrons is unaffected by the small rise in temperature.

Even at what we think of as high temperatures such as 1500°K, the distribution departs only slightly from that at 0°K. The dotted curve

shows the effect that is found. Most important is the tailing off at slightly higher values than E_{\max} . Instead of an abrupt cutoff at energy E_{\max} there are now some electrons with slightly higher energies, and a few with much higher energies, since the dashed tail approaches the vertical axis gradually. It is electrons from within this tapering tail that are emitted thermionically when a filament is heated. At low temperatures, of course, practically no thermionic emission occurs. Electrons can, however, be liberated from a metal even at low temperatures if they are given an increment of energy by radiation, as in the photoelectric effect (Chapter 3). Such an increment moves an electron upward in Fig. 9-15c.

We see here, indeed, the beginning of a gradual transition from the Fermi distribution for 0°K to the Maxwell-Boltzmann type. In actual fact, for very high temperatures the Fermi distribution approaches the Maxwell-Boltzmann distribution, but long before this occurs the boiling points of all materials are far exceeded. The change-over is not complete for an electron gas until the density becomes small compared with that in a metal and the temperature has reached a few tens of thousands of degrees, temperatures that are only known in the stars, in nuclear fission explosions, and in electric discharges.

The inability of the great majority of the electrons to accept thermal energy means, of course, that their contribution to the specific heat is relatively small, in agreement with experiment. We said at the outset that the theory of Drude and Lorentz predicted the electric conductivity in order of magnitude, but failed to explain the specific heat. Now the shoe is on the other foot. The low electronic specific heat is explained by the Fermi-Sommerfeld model. Can the model yield correct values of the electric conductivity when only the electrons of very high energy can accept energy effectively from a small applied electric field? To answer this question we must compute the mean free paths of these fast electrons, because it is collisions with positive ions and other electrons which limit their acquired velocities and provide a finite conductivity for the metal. The mean free paths have been reevaluated. The resultant values of conductivity are in fair agreement with experimental values.

Further improvement of the energy levels is obtained by using a better model of the potential in which the electrons move. This potential is, of course, periodic in space, since the ions are arranged in a crystal-line lattice. It is found that the change to a periodic potential causes the energy levels to occur in separate groups or bands. That is to say, there are regions of energy within which levels can lie, separated by regions in which no levels occur. These gaps between allowed regions

may be several electron volts wide. Then, if the available electrons happen to fill an allowed region, ordinary thermal collisions cannot promote them to higher energies and we have an excellent insulator. If the electrons fall a little short of the number needed to fill a band, few are able to move to slightly higher energies, so we have a poor electric conductor. For all materials, the Pauli principle is the sure guide to understanding thermal, and electrical and magnetic properties. It provides explanations of many effects which cannot be treated by classical theory.

We must now consider whether similar behavior is found for other elementary particles. When a system of exactly similar particles is treated by wave mechanics, it is found that there are only two possibilities, which are mutually exclusive. *Either* the particles obey the Fermi distribution law, so that only a limited number go into a given energy state; *or* they obey a distribution law named for Bose and Einstein, and the number that can occupy a given energy state is unlimited. In the former case, the number that can enter a given energy state is $2s + 1$, where s is the spin of a particle.

This situation is briefly stated by saying that a particle obeys Fermi statistics, or Bose statistics, as the case may be.

Up to the present it has been found that particles with spin $1/2$ obey the Fermi distribution law, while photons, with spin 1 according to certain theories, follow the Bose distribution. (See Appendix 3.) However, it is not known whether there is a necessary correlation between the spin and the type of statistics, applying to all particles.

The fact that photons obey the Bose statistics is the basic explanation of the Planck distribution of the energy of black-body radiation. In a sense Bose particles act as though they encourage each other to enter the same energy state. Just as in the case of the Fermi particles, which act as though they "avoided" each other, the effect is wave mechanical. It has no counterpart in classical mechanics and should not be described as the action of a force.

REFERENCES

Appendix 9, refs. 47, 58, 73, 80, 81.

PROBLEMS

1. By chemical analysis, a gas is found to contain 14 parts by weight of nitrogen and 16 parts of oxygen. What is the correct chemical formula if the gas has a density under standard conditions of 0.00268 gm/cm^3 ?

2. Determine the ratio of the specific heat at constant pressure to the specific heat at constant volume for a gas with six degrees of freedom (three of translation and three of rotation).

3. At what temperature is the average kinetic energy of translation of the hydrogen molecule equal to the energy of rotation in the second quantum state? Assume the moment of inertia of the hydrogen molecule to be 0.48×10^{-40} gm cm².

4. Determine the separation of the lines, expressed in cm⁻¹, in the pure rotation band of HBr, given that the distance between the nuclei is 1.42×10^{-8} cm. Assume that the heavy bromine nucleus remains fixed in space.

5. Calculate the ratio of the energy differences between the first two vibrational levels and the first two rotational levels of HF, whose moment of inertia is 1.35×10^{-40} gm cm² and whose vibrational wave number is 3987 cm⁻¹.

6. Chlorine is known to have isotopes with atomic weights of 35 and 37. Assuming that the oscillations of the nuclei are simple harmonic and that the vibration wave number of the Cl³⁵Cl³⁶ molecule is 2940.8 cm⁻¹, calculate that of the Cl³⁶Cl³⁷ molecule. What separation of the spectral lines, expressed in wave numbers, does the isotope effect produce in the fundamental band?

7. Draw an energy-level diagram showing the convergence of the lines of an electronic band to a head.

8. For the molecule of HBr, predict the pattern of rotational Raman lines in the neighborhood of an exciting line. Obtain the necessary data from problem 4, and give only the distances of a few lines from the parent line, in cm⁻¹. What would be learned by photographing these Raman lines?

9. Could the rotational spectrum of the loosely bound molecule Hg₂ be investigated by microwave methods? If so, in what region would it lie?

10. Compute the dielectric constant of xenon gas at normal temperature and pressure.

11. Look up the density of potassium at very low temperature. Calculate the number of valence electrons per cm³, and calculate the highest kinetic energy that will occur in the Fermi distribution. Also look up the photoelectric threshold of potassium. Thence, find the depth of the simple potential well that represents the metal.

ANSWERS TO PROBLEMS

1. N₂O₂.

2. 1.33.

3. 110°K.

4. 16.5 cm⁻¹. It is necessary first to calculate the moment of inertia of the molecule.

5. 96.

6. 2900.8 cm⁻¹; the difference of emission frequencies is 40.0 cm⁻¹.

8. The lines will occur on either side of the parent line. Each group will resemble the rotational spectrum of HBr, one group being the mirror image of the other.

10. 1.00136. The polarization P per atom is given in the text. The polarization per cm³ must first be derived from it.

11. Approx. 0.90 gm/cm³ at 100°K; 1.35×10^{22} electrons/cm³; 2.1 eV; 4.16 eV for 6000-Å threshold.

Radioactivity

1. Brief Survey

We now begin the study of the atomic nucleus, a complex structure within the atom itself, and of the fundamental particles. The nucleus is an aggregate of protons and neutrons, moving very close to one another under the action of forces that give them velocities comparable with the velocity of light. The nuclei of several heavy elements are unstable. Spontaneously, they emit charged particles of high energy, and, in many cases, electromagnetic radiations of short wavelength, and are therefore said to be radioactive. Other radioactive nuclei can be created from stable nuclei by bombardment with neutrons, protons, etc.

It would seem logical to commence with the properties of energetic elementary particles, and then to deal with the nucleus as a composite structure. However, it is more convenient to begin this chapter with a brief study of the naturally radioactive elements. Then we discuss the energies of the particles they emit, and draw some conclusions concerning nuclear energy levels. Chapter 11 is devoted to methods for detection of individual particles, and to their properties. This paves the way for discussing nuclear reactions and structure in Chapter 12, with the applications segregated in Chapter 13. Finally, Chapter 14 takes up cosmic rays; it is mainly a study of particles and nuclei endowed with energies higher than any yet conferred on them by man.

Natural radioactivity. The entities emitted by naturally radioactive substances fall into three classes as follows:

1. Some radioactive substances emit helium nuclei, called *alpha particles*, and such substances are called alpha rayers.
2. Others emit fast electrons, called *beta particles*, and such substances are called beta rayers.
3. Certain substances of both types also emit *gamma rays*, which consist of photons, usually much more energetic and penetrating than the characteristic X-rays of heavy elements (p. 137).

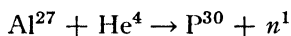
Following general usage, we shall often speak of alpha and beta *rays*, rather than alpha and beta particles. All three types of rays are agents for the study of changes occurring within the nucleus. From 1896 to 1919 radioactive investigations were concerned almost entirely with their properties, but little progress was made in regard to nuclear structure because of the undeveloped state of quantum theory. In retrospect, some of the early findings clearly indicated that the general principles of quantum mechanics are valid within the nucleus. Alpha particles from a given nuclear species have well-defined energies; this means there are stationary energy states within the nucleus. Also, gamma rays form a spectrum of monochromatic lines. Their wavelengths can be measured by the crystal method (p. 281), and the energy given up by a nucleus that emits a gamma ray of frequency ν is $h\nu$. Such nuclear spectra can be analyzed in the same way as spectra emitted by the planetary electrons, and thus we can determine the quantized energy states of a nucleus. Gradually it became clear that rapid progress was dependent on success in attacking the nucleus with high-speed particles.

Transmutation with alpha particles. In 1919, Rutherford was successful in breaking up nuclei artificially. Bombarding nitrogen with energetic alpha particles from a naturally radioactive element, he caused the nitrogen to emit protons. In these experiments the alpha particle, of atomic mass 4, joined the nitrogen nucleus of atomic mass 14, and the structure thus formed emitted a proton. The nucleus left behind was that of a hitherto unknown type of oxygen, having an atomic mass of 17 instead of the value 16. This was the first case of transmutation of the elements, the dream of the alchemist. Between 1920 and 1930, several other light elements were transmuted by alpha particles, but progress was slow because the nucleus is a very tiny target. In the most favorable cases many million alpha particles were required to enable one of them to achieve a single disintegration.

Artificial sources of energetic particles. Stronger sources of high-energy atomic projectiles were urgently required. Physicists saw that it should be possible to impart the necessary speeds to positive ions in high-voltage vacuum tubes. Experiments in this direction were undertaken by the American physicists Breit, Tuve, Hafstad, Lauritsen and Lawrence, and by Cockroft and Walton in England, in the years immediately preceding 1930. The first transmutations by particles that had fallen through a high voltage drop were announced by Cockroft and Walton in 1930. Then began a period of intensive activity, resulting in the discovery of a great variety of transmutations. Charged particles used for bombardment are usually protons and deuterons, for a simple reason. The smaller the positive charge of the projectile, the less it is

repelled by the electric field of any nucleus that it strikes, so that protons and deuterons of given energy are more easily employed than other particles of the same energy, but of higher charge.

Neutrons; induced radioactivity; neutrinos. Work on artificial disintegration led to the discovery of the neutron in 1932. Chadwick followed up some very suggestive work of Bothe and of M. and Mme. Curie-Joliot, and demonstrated the existence of this particle, having a mass slightly greater than that of the proton and no detectable electric charge. Then in 1934 the Curie-Joliot made a very important discovery. On bombarding aluminum with alpha particles, they obtained phosphorus and neutrons, according to the reaction-equation



where n stands for a neutron and the superscripts are the mass numbers. The phosphorus thus formed is unstable, and is capable of emitting rays and particles just as the heavy radioactive elements do.

Fermi linked these two discoveries, showing that neutrons can be used to transmute elements lying in all parts of the periodic system, and that in many cases the isotopes formed are radioactive. Neutrons are highly efficient in causing transmutations, simply because they have no charge and are therefore able to approach close to a nucleus of any atomic number whatever. Indeed, at small distances they are attracted.

In this same period came the suggestion that, when a beta ray is emitted, a neutral particle called the neutrino also leaves the nucleus.

The positron. In 1932, Anderson discovered the positive electron, or *positron*. In the atomic debris called cosmic rays there are gamma rays of high energy. Anderson found that these are capable of producing positrons and electrons, in pairs. Then the production of pairs in the laboratory was soon accomplished, using gamma rays from radioactive materials. This process is not creation of matter out of nothing at all; it is the direct conversion of electromagnetic energy into energy in the form of matter; it can occur only in the strong field close to a charged particle. The nucleus serves as a catalyzer. The converse process also occurs, in which a positron collides with an electron near a nucleus. The positron and electron are annihilated and a gamma ray is produced. However, another mode of annihilation is much more frequent; a positron collides with an electron, which is substantially free; two gamma rays emerge from the scene of the collision.

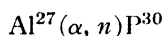
Mesons. In 1937, mesons, both positive and negative, were found in cosmic rays by Anderson and Neddermeyer and by Street and Stevenson, independently. These charged particles are unstable. They have masses intermediate between those of the electron and the proton. In

1947, Lattes, Muirhead, Occhialini, and Powell, at Bristol, established the existence of two types, pi mesons and mu mesons. This was the beginning of a new field of study, described in Chapter 14.

Notation for nuclear reactions. We denote the customary bombarding particles by the symbols

$$p, \quad d, \quad \alpha, \quad n, \quad \text{and} \quad \gamma$$

standing for proton, deuteron, alpha particle, neutron, and gamma ray, respectively. The symbol ν denotes the neutrino. A brief notation for reactions is often convenient; for example, the reaction between aluminum and an alpha particle by which phosphorus and a neutron are created is written as



2. The Discovery of Radioactivity

Radioactivity of uranium and thorium. The discovery of radioactivity was inspired by Röntgen's experiments in 1895 which showed that X-rays are produced when cathode rays strike the glass walls of a discharge tube. A few weeks later it occurred to Henri Becquerel that the X-rays might be connected with the phosphorescence of the glass. He undertook to find out whether phosphorescent substances emit penetrating rays of similar character. His procedure was to render a substance phosphorescent by exposure to strong light, and to lay it on top of a photographic plate wrapped in black paper. In February, 1896, Becquerel announced that he had obtained positive results with a salt of uranium. Within a few days, however, he recognized that the phenomenon had nothing to do with phosphorescence, since non-phosphorescent compounds of uranium also affected the plate. He realized that uranium is a natural source of penetrating rays and coined the word "radioactive" to describe this property. The intensity of the rays from various uranium salts was found proportional to their content of this element, aside from minor variations caused by absorption in the material itself.

The ability of the rays to ionize the surrounding atmosphere was soon demonstrated with an electroscope like that in Fig. 10-1.

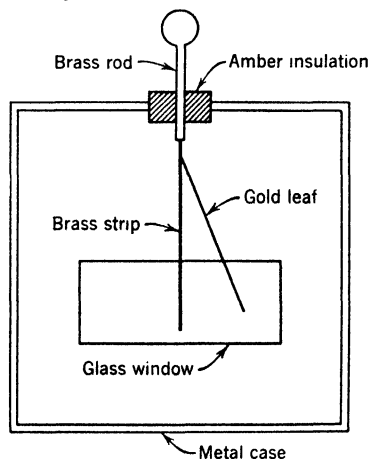


Fig. 10-1. A simple electroscope.

A metal case, provided with windows, contains a vertical metal strip. This is supported on a rod which passes through a bushing of amber. The upper end of a rectangular piece of gold leaf is attached to the metal strip. If the strip and foil are charged, the strip repels the leaf, which assumes the position shown. If now a radioactive substance is brought near, ions are produced inside the electroscope. Those of one sign go to the wall; those of the other to the strip and leaf. The charge on the insulated system is gradually neutralized, and the leaf collapses. The motion may be followed with a long-focus microscope, having an eyepiece scale on which the image of the leaf is seen. In this way measurements of the rate of ionization may be made with an accuracy of about 1 per cent. The electroscopic method of detection was found extremely sensitive compared with the photographic plate, and was employed in seeking for other radioactive elements.

Discovery of radium. In April, 1898, G. C. Schmidt and Mme. Curie announced the radioactivity of thorium. Mme. Curie then made a systematic investigation of many minerals, but only those containing thorium or uranium showed activity. She noted that certain uranium minerals possess an activity several times higher, gram for gram, than that of uranium metal. This observation suggested the presence of a new element, more active than uranium. She and her husband, Pierre Curie, set out to isolate this element by a straightforward but laborious chemical procedure. They traced the active substance, by the electrical method, through a great number of fractionations and precipitations. Late in 1898, the Curies, together with Bémont, announced the discovery of *radium*, a very active element belonging to the second column of the periodic table.

Other discoveries of natural activities. By 1918 nearly 40 radioactive isotopes had been found (Fig. 10-3), with mass numbers greater than 206 and atomic numbers greater than 80. In addition, potassium, rubidium, and three elements in the sixth period of the table (Appendix 5) have isotopes which are slightly radioactive. Radioactive materials are manufactured all the time in the atmosphere and near the earth's surface, by cosmic ray bombardment, but the effects due to decay of such material are so minute that their detection is a specialized art.

Some elements are not found in the earth's crust because all their isotopes are so short lived that they have decayed to insignificance in the course of geologic time. By means of bombardment, or by the use of chain-reacting piles, as the case may be, the "missing" elements 43, 61, 85, 87, and the elements 93 to 100, inclusive, have been produced.

3. The Breakdown of Radioactive Elements

The decay law. If a solution containing radium is placed in a closed glass vessel, after a few days it is found that the air above the solution shows a faint glow when examined in the dark. If the air is pumped away, the glow goes with it. This shows that a gas is produced when radium disintegrates and that this gas itself is radioactive. Radium has chemical properties like those of barium. The charge of the radium nucleus is $88e$. Further, its disintegration process consists in the emission of an alpha particle, with a charge $2e$, from the nucleus. Thus the charge of the residual nucleus is $86e$, and the planetary electrons are now too numerous. If the newly formed atom is to be neutral, two of them must leave, and so they do. By analogy with the elements preceding barium in the periodic table, the new substance must be a rare gas. The name originally given to this gas was radium emanation, but now it is called radon.

Radon in its turn breaks down with emission of an alpha particle, but there is a striking difference between its behavior and that of radium. Whereas the amount of radium in a given preparation decreases only 0.06 per cent in a year, a sample of radon isolated from its parent radium decays to one-half the original amount in 3.825 days. What is still more striking, the half remaining will be half gone after another period of 3.825 days, and so on. The law according to which the strength of the preparation decreases is simple. The average number of radon atoms that decay in a time interval Δt , very small compared with 3.8 days, is

$$-\Delta N = \lambda N \Delta t \quad (1)$$

where N is the number present at the beginning of the interval and λ is a constant. The same type of law holds for all radioactive elements. The meaning of λ is seen at once if we put $N = 1$ and $\Delta t = 1$ sec. It is the chance that a single atom will disintegrate in 1 sec and is called the *decay constant* for the element in question. If the atoms in the preparation are very numerous, it can be shown from expression 1, as on p. 114, that

$$N = N_0 e^{-\lambda t} \quad (2)$$

N being the number of atoms that survive at a time t and N_0 the number present at time zero. Figure 10-2 shows the type of variation represented by equation 2.

The half-life and average life. The larger λ is, the smaller will be the *half-life*—the time T required for the element to decay to one-half

its original amount. To find the half-life we write $N = N_0/2$. Then $\frac{1}{2} = e^{-\lambda T}$, and

$$T = \frac{\log_e 2}{\lambda} = \frac{0.693}{\lambda} \quad (3)$$

This must not be confused with the *average life*, which is found to be $1/\lambda$.

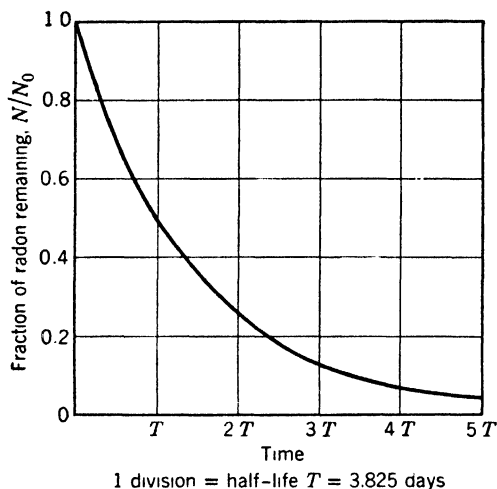


Fig. 10-2. Decay curve of radon.

Radioactive equilibrium. If radium is sealed up, radon will accumulate until the number of atoms which decay per unit of time is equal to the number which are formed from the radium per unit of time; that is, by equation 1,

$$\lambda_1 N_1 = \lambda_2 N_2$$

where the subscripts 1 and 2 refer to radium and radon, respectively. When this relation holds true we say that equilibrium has been established. More generally, when several substances in a radioactive series are in equilibrium, the product of the number of atoms and the decay constant is the same for all of them.

★ **The curie, a unit of activity.** The user of a radioactive preparation is more interested in the number of disintegrations per unit of time than in the number of atoms present. Direct experiments have shown that, in 1 gm of radium element, 3.71×10^{10} atoms decay each second. Any source that gives this number of decays per second is said to have an activity of 1 curie. Earlier, a narrower definition, applying

only to radon, was current. In medical work, the millicurie is the commonly used unit.

★ **How the decay constant of a long-lived element is determined.** For an element of very great life, such as uranium, it would be difficult to observe the decrease in the amount present even if we could follow the weight of a sample from the dawn of human history up to the present. To determine T , a counting method is used. Uranium consists of three isotopes, uranium 234, 235, and 238, which emit alpha particles of different ranges. It is found that a gram of uranium 238 emits 1.2×10^4 alpha particles per second, and the number of atoms per gram of uranium 238 is 2.55×10^{21} . By equation 1 the chance for an individual atom to die in 1 sec is:

$$\frac{1.2 \times 10^4}{2.55 \times 10^{21}} = 4.7 \times 10^{-18} \text{ sec}^{-1}$$

This is the value of the decay constant, and by equation 3 the half-life is 4.6 billion years. This datum is used in determining the ages of rocks by determining the lead produced (Fig. 10-3) from the uranium present at the time of formation. The older the mineral, the greater the ratio of the lead to the present uranium content, provided it has not suffered differential solution. In this fashion, it is established that the time which has elapsed since the solidification of the earth's crust is at least 1.8 billion years. At present, about 3 billion years is favored as an estimate of crustal age.

4. Statistical Character of Radioactive Decay

The decay equation, 2, is only a statistical law holding true for a large number of atoms. If we study the decay of a small amount of radioactive material by any method that records the disintegration of individual atoms, we find fluctuations in the intervals between successive breakdowns. The question arises: are the sizes of these intervals distributed in the way we should expect if the chance of disintegration in a given time is *independent* of the age of the atoms? Experiments on the distribution of interval sizes indicate that the probability of breakdown does not depend on age. For example, in radon, the chances are equal for any atom to die, or to survive, in the period of 3.825 days after we begin to study its behavior, regardless of the length of time it has already lived. It is as though the atoms experience no aging effect (indeed, this seems quite reasonable) but are caused to disintegrate by some agency operating on the laws of chance. *We cannot tell what will happen*

to an individual atom. Only when we are dealing with a number of atoms sufficiently large to smooth out individual variations do we arrive at the simple relations described above.

5. The Natural Radioactive Elements

The uranium family. We have discussed the production of radon by the disintegration of radium. The atomic mass of radium is 226, and its daughter atom of radon should have an atomic mass of 222 because an alpha particle has been lost. This transformation fits into an interesting scheme. Figure 10-3 shows the genetic relations between the natural radioactive elements, which fall into three groups, the uranium series, the thorium series, and the actinium series. The actinium series arises from an isotope 235 of uranium. In the figure, the atomic number is plotted horizontally and the atomic mass vertically.

The atomic masses in the three series are of the types $4n + 2$, $4n$, and $4n + 3$, respectively, where n is an integer. Members of a fourth series, with masses of the type $4n + 1$, were first prepared by neutron bombardment of thorium, by Curie-Joliot, Halban, and Preiswerk. The short half-lives they found show that we cannot expect to find these substances in natural radioactive minerals. They are members of a chain headed by neptunium 237, so we call this chain the neptunium family. There is also a side chain headed by Pa^{230} , delineated by Studier and Hyde. We omit these series from Fig. 10-3 for simplicity.

The three naturally occurring series are quite similar, so we may concentrate on the uranium family. Uranium 238 has atomic number 92. It is an alpha ray, which gives rise to a beta-raying short-lived isotope, uranium X_1 , of atomic mass 234 and atomic number 90. (This substance is *not* a uranium isotope, since the atomic number is different; and neither are radium A, B, etc., isotopes of radium.) Uranium X_2 differs in mass from uranium X_1 only by the mass of the emitted electron; the net charge on the nucleus should be 91 units. Uranium X_2 is also a beta ray, and similar arguments lead to the conclusion that its product should have atomic mass 234 and atomic number 92; in other words, it should be an isotope of uranium. This identification is confirmed by chemical evidence. Successive emission of two more alpha particles brings us to radium. This element should have an atomic number of 88 and an atomic weight of 226, in agreement with experiment.

The displacement law. These facts are illustrations of the radioactive displacement laws due to Soddy, Fajans, and Russell: *When an element undergoes alpha disintegration there is a loss of two units of positive nuclear charge and four units of atomic mass. The nucleus moves down two*

places in the periodic table. In beta-ray disintegration an electron is lost. The nucleus moves up one place in the periodic table and the atomic mass remains constant, save for the loss of the electron.

Today these laws are obvious, but originally this was not so, and

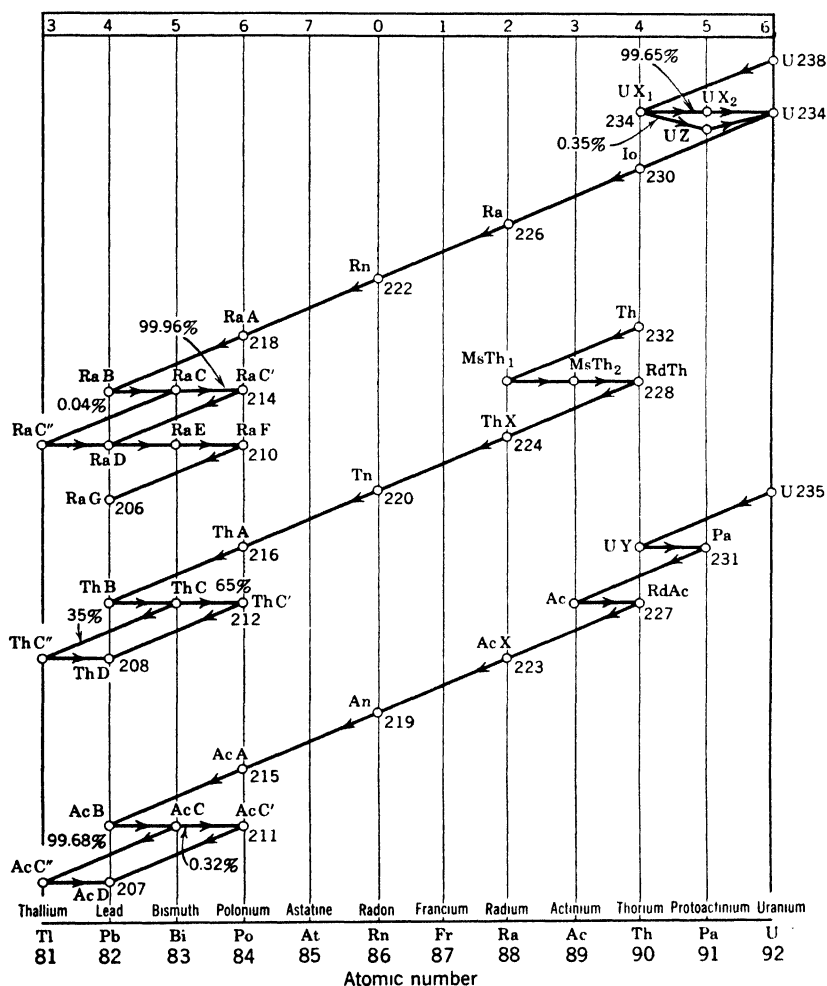


Fig. 10-3. Genetic relations of the natural radioactive elements. Alpha-particle emission is denoted by a two-unit diagonal arrow to the left, beta-particle emission by a one-unit horizontal arrow to the right. All atoms on one vertical line are isotopes of the same element. For example, Ra C, Ra E, Th C, and Ac C are the same as Bi 214, Bi 210, Bi 212, and Bi 211, respectively. Names like radioactinium (Rd Ac), ionium (Io), mesothorium (Ms Th), and actinon (An) have survived from early studies on radioactivity.

their discovery brought system into a field which had been chaotic. They pointed the way to the discovery of new radioactive substances and non-radioactive isotopes. They showed that lead from minerals rich in uranium should have an atomic mass different from that of lead taken from thorium minerals. Figure 10-3 shows that radium G, the end product of the uranium family, is an isotope of lead, with an atomic mass 206. Radium G does not decay, so far as can be detected. Therefore, if all the lead in a uranium mineral were derived by the breakdown of uranium the atomic mass should be 206, in round numbers. Similarly, the atomic mass of lead derived from the disintegration of thorium should be 208. As a matter of fact, some uranium minerals have yielded atomic weight values lower than 206.0, and a certain thorite gave 207.9. In general, a radioactive mineral contains lead produced by all three radioactive series, and also ordinary lead which was present originally. This original lead is a mixture of the isotopes 206, 207, and 208, with an atomic weight of 207.2.

★ **Branching.** When radon is stored in a vessel for a few hours and is then pumped out, the vessel is still able to affect an electroscope. Indeed, practically all the gamma-ray activity remains with the vessel, but this activity falls off rapidly compared with that of radon, decreasing to half the original value in an hour. This means that the products of the decay of radon have remained on the walls and that they have short half-lives. The first two products, radium A and radium B, require no comment, but at radium C we have a branching of the series. This substance can emit either an alpha or a beta particle. Out of 10,000 atoms that break down, only four give alpha particles. Those which do so form atoms of radium C'', which then undergo a beta transformation. On the other hand, if a radium C atom emits a beta particle, forming radium C', this atom almost immediately emits an alpha particle. In both cases the residue is an atom of radium D. Similar competition between alternative decay processes occurs in the thorium and actinium families, and in many other cases.

6. Energy of Individual Particles and Gamma Rays

In dealing with the energies of the particles and gamma rays emitted by radioactive materials, it is convenient to use one million electron volts (1 Mev) as a unit of energy; 1 Mev is equivalent to 1.6×10^{-6} erg. Another unit, widely used in dealing with electrons so fast that their change of mass must be considered, is m_0c^2 , the rest energy of the electron, equivalent to 0.511 Mev.

In general, alpha particles are much more energetic than beta particles and gamma rays. Aside from certain complications considered in Section 9, the energy of the alpha particles from a given nucleus is a well-defined quantity. In the uranium series it ranges from about 4 to about 8 Mev. Table 10-1 presents data on the decay properties of radium and several of its descendants. The energies of the alpha particles and their ranges in air are shown. The nucleus recoils when a particle (or a photon) is emitted, because the total momentum of the nucleus-particle system must be conserved. The moving nucleus is called a recoil atom. In the case of alpha-particle emission, the energy of the recoiling nucleus is not to be ignored.

TABLE 10-1. Decay Properties of Radium and a Few of Its Descendants

Element	Half-Life	Decay Constant (per sec)	Particle Emitted	Energy of Alpha Ray (Mev)	Range in Air at 15°C and 760 mm pressure (cm)
Radium	1600 yr	1.37×10^{-11}	Alpha	4.74	3.39
Radon	3.82 days	2.10×10^{-6}	Alpha	5.44	4.12
Radium A	3.05 min	3.79×10^{-3}	Alpha	5.97	4.72
Radium B	26.8 min	4.31×10^{-4}	Beta	—	—
Radium C	19.7 min	5.86×10^{-4}	Alpha or beta	5.45–5.51	4.04–3.97
Radium C'	10^{-6} sec	10^6 , approx.	Alpha	7.68	6.97
Radium C''	1.32 min	8.75×10^{-3}	Beta	—	—
Radium D	25 yr	1.37×10^{-9}	Beta	—	—

Beta particles fall into two classes. First, beta-raying nuclei emit particles having a *continuous spectrum* of energies, between zero and a maximum value characteristic of the substance. Second, in the case of both alpha rayers and beta rayers, the nucleus is often left in an excited state after it decays. As we shall see in Sections 10 and 11, gamma rays are then emitted. These act on the planetary electrons of the atom, a sort of inner photoeffect; the ejected planetary electrons have definite energies and form the so-called secondary beta ray spectrum, or *line spectrum*. The electrons forming the continuous spectrum are considerably more numerous than those of the line spectrum.

As for the gamma rays, the nucleus may emit one or several in succession; they are monochromatic. The gamma-ray spectrum may con-

tain any number of lines from 1 to possibly 50, but in general the number is small.

The energies of nuclear beta rays, and of gamma rays, range from a few kev to several Mev. These remarks apply to gamma rays emitted by a nucleus. Electrons and other particles from high-energy accelerators can produce electromagnetic radiations of still shorter wavelength, when decelerated by collisions in a target (Chapter 5).

Heat effects. The production of swiftly moving particles and gamma rays keeps a tube of radium at a temperature slightly higher than its surroundings; a gram of radium, together with its products, emits 140 gram cal/hr. Most of this heat is produced by dissipation of the kinetic energy of the alpha particles and their parent atoms. The distribution is as follows:

Alpha particles and recoil atoms	124 cal/hr
Beta particles	6.3 cal/hr
Gamma rays	9.4 cal/hr

7. Magnetic Spectrographs

Much light has been thrown on the mechanism of radioactive disintegration by studying the emission velocities of the alpha and beta particles. A suitable instrument for this purpose is the magnetic spectrograph. We first describe a form suitable for beta-ray measurements. This instrument separates a beam of electrons into what may be called a velocity spectrum, by using the fact that the deflection of an electron in a magnetic field depends upon its velocity. When an electron of velocity v moves perpendicular to the lines of force of a uniform magnetic field of strength H , it experiences a force Hev at right angles to the field and to its own velocity (p. 32). The electron moves on a circle of radius R , such that

$$Hev = mv^2/R \quad (4)$$

where e and H are expressed in electromagnetic units. This equation expresses the fact that the deflecting force is equal to the mass times the acceleration toward the center. Therefore,

$$v = HR(e/m) \quad (5)$$

Since e/m is known and H can be measured, the velocity of a fast electron can be determined if we can find the radius of its path. This is accomplished in a flat, highly evacuated chamber placed between the pole pieces of a large magnet, as shown in Fig. 10-4. Q is a source of beta particles, usually a wire coated with radioactive material. A pencil

of beta particles is selected by the broad slit S . The magnetic field is perpendicular to the plane of the page, and a photographic plate is placed in the position shown. It is shielded by a lead block from the direct action of gamma rays. Precautions must be taken to keep the strength of the field constant during an exposure, which may last for hours or days. In the figure, we show three possible paths for an electron of given velocity, QAO , QBO , and QCO ; all these are circles having the same radius. The points at which three electrons traversing these three paths, respectively, would hit the plate are very close together, for all

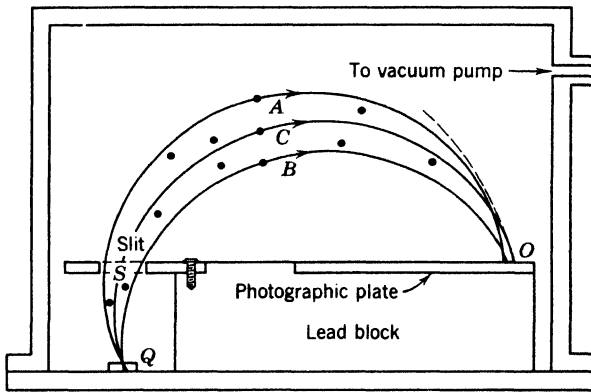


Fig. 10-4. A magnetic spectrograph.

the circles must touch their envelope (the dashed arc) in the neighborhood of O . This "focusing property" of the apparatus makes it an instrument of precision. If the beam is composed of electrons of a single definite velocity we shall see at point O a black line, sharp on the side farthest from the source and fading off gradually on the other side, where electrons strike after following such paths as QAO and QBO . Rays of other velocities would, of course, be focused at other points. Figure 10-9, a typical photograph, is discussed on p. 282. The "lines" are designated by giving the corresponding values of IIR .

★ On p. 33, we saw that the mass m of a particle increases with its velocity v , according to the relation $m = m_0 / \sqrt{1 - \beta^2}$, where m_0 is the mass in a state of rest and β is v/c . The variability of mass does not alter equation 4 in our discussion of the magnetic spectrograph. Equation 5 is also correct, but, since m depends on v , a few more steps are required to obtain the velocity. Always, the momentum is given by eHR .

In Chapter 2, Section 4, we showed that the kinetic energy of a fast particle is

$$T = mc^2 - m_0c^2 = m_0c^2 \left[\frac{1}{\sqrt{1-\beta^2}} - 1 \right] \quad (6)$$

which reduces to $\frac{1}{2}m_0v^2$ when v is small compared with c .

8. Alpha-Ray Spectra

The magnetic spectrograph has been used to measure the energies of alpha rays. Owing to their great momentum, the product HR is much higher than for beta rays and so the apparatus must be larger and the field stronger. Indeed, Rosenblum employed a spectrograph 75 cm in diameter, placing it between the poles of a large electromagnet. His results threw new light on alpha-ray emission. For a long time it was believed that all the alpha particles emitted by a radioactive substance have the same range and therefore the same energy. While this is true for many alpha rayers, there are exceptions of two types.



Fig. 10-5. Alpha-ray spectrum of thorium C (after Rosenblum).

First, Rosenblum found that some alpha rayers emit several groups of particles of different energies rather close together. Figure 10-5 exhibits the groups from thorium C. For the sake of simplicity we shall discuss the spectrum of radium, which emits only two groups. From the velocities of these rays we can show that, when radium disintegrates, the kinetic energy of alpha particle and recoiling nucleus is either 4.869 or 4.684 Mev. The accepted interpretation is illustrated by the exaggerated energy diagram in Fig. 10-6. For simplicity, we neglect the relatively small kinetic energy of the recoiling nucleus. If a "fast" particle is emitted the daughter nucleus of radon is left in its normal state; if a "slow" particle is emitted the daughter nucleus is left in an excited state, lying 4.869 - 4.684, or 0.185, Mev above the normal state. Therefore, the excited radon nucleus should give out a gamma ray with an energy of 0.185 Mev. In fact, the gamma-ray spectrum emitted in the disintegration of radium consists of a single line of energy 0.189 Mev, agreeing with expectation when the limits of error are considered.

Second, there are three very short-lived alpha rayers, $\text{Ra C}'$, $\text{Th C}'$, and $\text{Ac C}'$, which emit a few particles having ranges much greater than that of their "normal" alpha particles, as shown on p. 293. The expla-

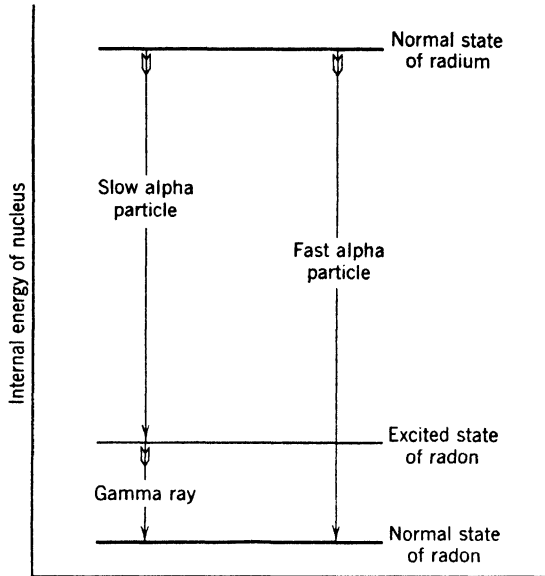


Fig. 10-6. Energy losses associated with the emission of (1) a fast alpha particle or (2) a slow alpha particle and a gamma ray, in the disintegration of radium.

nation is illustrated by Fig. 10-7. When Th C disintegrates, the daughter $\text{Th C}'$ nucleus is usually left in the normal state and emits alpha particles of 8.6-cm range, but infrequently it is left in an excited state. A gamma ray can then be emitted, but $\text{Th C}'$ is so short lived that it may emit an alpha particle before the loss of a gamma ray can take place. In this case we get a long-range particle with energy equal to that of the gamma ray plus that of the "normal" alpha particle.

The important point is that there are energy levels of the nucleus, and *we can find the distances between nuclear energy levels directly from measurements of alpha-ray energies*, with due allowance for the calculated kinetic energy of the recoiling nucleus.

9. Gamma-Ray Spectra

Nuclear energy levels can also be found by studies of gamma rays, using crystal methods like those employed in the X-ray domain. The wavelengths are so short that specialized apparatus is necessary. In

an arrangement devised by Rutherford and Andrade (Fig. 10-8) a beam of gamma rays from a needle-shaped tube of radium passes through a broad slit between the lead blocks *L*. In this divergent beam there will be photons corresponding to a given wavelength, which are moving in the correct direction to satisfy the Bragg condition (p. 124) for reflection at crystal planes parallel to the axis of the figure and *perpen-*

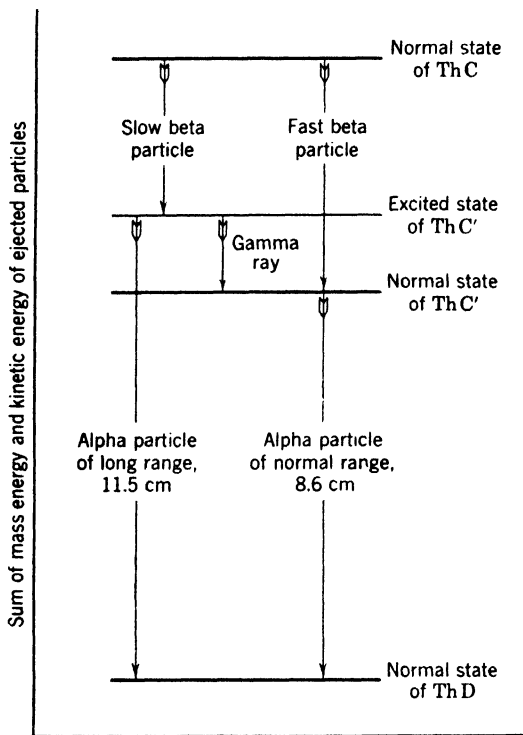


Fig. 10-7. Energy losses associated with the formation of the thorium C' nucleus, either in an excited state, or in its normal state. When in an excited state this nucleus can emit an alpha particle of greater energy than the "normal" ones. In both cases the daughter atom is thorium D.

dicular to the plane of the diagram. By symmetry, quanta of all wavelengths will pass through a slit *F* just as far behind the crystal as the source is in front of it. After passing this slit, formed by lead screens to cut off stray radiation, the rays diverge and produce blackening on a photographic plate at a considerable distance behind *F*. Geiger counters (p. 290) may also be used. Since the reflection angle may be measured, we can determine the wavelengths of the gamma-ray lines.

TABLE 10-2. Gamma Rays of a Radium B Source (after Ellis)

Wavelength (X-units)	Energy (Mev)	Number of Beta-Ray Lines due to Gamma Ray
232.8	0.0529	8
51.2	0.2406	3
47.9	0.2571	2
41.9	0.2937	2
35.2	0.3499	4

★ By this method, and by another explained in Section 10, it is found that a radium B source emits gamma rays having the energies shown in Table 10-2. Others are doubtless present. These lines are, of course, due to the *daughter* atom, radium C. Such an array of lines can be

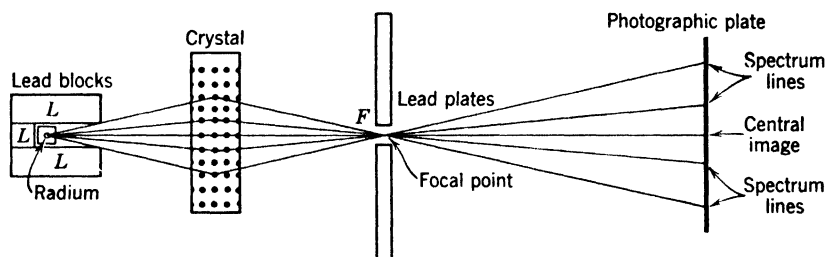


Fig. 10-8. The Rutherford-Andrade gamma-ray spectrograph.

analyzed, just as we analyze an optical spectrum, to determine the energy levels of the nucleus that emits them. We note, for example, that the energy of the fourth line in the table is the sum of those of the first and second lines, within the limits of experimental error. This relationship indicates the existence of three levels separated by the intervals 0.0529 and 0.2406 Mev. Another case is described on p. 317.

10. Beta-Ray Line Spectra

As we said in Section 6, beta rays are of two kinds: secondary electrons ejected from the planetary shells by the photoelectric action of gamma rays from the nucleus, and disintegration electrons coming directly from the nucleus and having a continuous distribution of velocities. Figure 10-9 shows the beta-ray spectrum of radium D, as obtained by Curtiss. There are five lines in this spectrum, each representing the impact on the plate of secondary electrons of a definite velocity. In addition, there

is general blackening. The disintegration electrons of Ra D have energies much lower than those forming the lines, but they are very numerous relative to the latter. Disintegration electrons scattered by slits and other parts of the apparatus contribute to the background.

If W is the energy required to remove a secondary electron, its kinetic energy T is given by the equation for the photoelectric effect (p. 86),

$$T = h\nu - W \quad (7)$$

Here we are dealing with high electron speeds so we must use expression 6 for the kinetic energy.

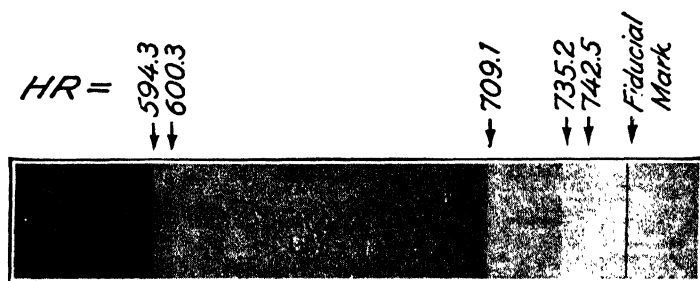


Fig. 10-9. Beta-ray spectrum of radium D (after Curtiss). This is the appearance of the exposed and developed plate of Fig. 10-4, looking down upon it.

If the photoelectron comes from the K shell, the energy required to separate it from the atom will be called W_K ; if it comes from the L shell, W_L , and so on. Thus, gamma rays of a given frequency can produce photoelectrons having several different velocities; that is, they can give rise to a group of lines in the beta-ray spectrum. If several frequencies are present, there will be many such groups. The spectrum in Fig. 10-9 is simple, being produced by gamma rays of a single energy. It happens that this energy is not great enough to eject K electrons. In all cases so far examined, the gamma rays and secondary electrons are emitted after the ejection of the primary electron from the nucleus.

The reasoning that leads to this conclusion can be illustrated by a study of the figure. When a gamma ray ejects a secondary electron from the M shell, its kinetic energy is

$$T_M = h\nu - W_M \quad (7a)$$

When a gamma ray of the same frequency ejects an electron from the L shell, its kinetic energy is

$$T_L = h\nu - W_L \quad (7b)$$

Subtracting, we find there should be two groups of electrons that differ in energy by the amount $W_L - W_M$. If ejection of the secondary electron occurs after disintegration, the difference $W_L - W_M$ should be that appropriate to the *daughter element*, radium E, which is an isotope of bismuth. There are two strong groups for which the values of HR , the field strength times the radius, are 594.3 and 709.1, respectively. They differ in energy by 12,380 ev. From X-ray evidence like that presented on p. 140, $W_L - W_M$ is known to be 12,400 ev for radium E, whereas the corresponding value for the parent substance, radium D, is 12,020 volts. The agreement for radium E is closer than we might expect from the experimental errors. This evidence shows that the extranuclear electrons have adjusted themselves to the condition appropriate to an element of atomic number 83 after the disintegration, before the nuclear gamma ray is emitted.

Working backward from the known ionization potentials of the different electron shells (p. 138) and the measured velocities of secondary electrons, we can determine the frequencies of nuclear gamma rays with the aid of equations 6 and 7. For example, the strongest line in Fig. 10-9, at the extreme left, arises from the ejection of electrons from the L_I shell of radium E, the ionization potential of this shell being 16,360 ev. The energy of the ejected electrons is 30,330 ev. Adding these, we obtain the energy of the gamma-ray quantum; it is 46,690 ev, corresponding to a wavelength of 264 X-units, or 0.264 Å.

11. Continuous Beta-Ray Spectra

The continuous spectrum of beta particles is investigated by replacing the photographic plate in a magnetic spectrograph with an ionization chamber (or a Geiger counter) behind a narrow slit covered with a diaphragm thin enough to transmit the incident particles. The magnetic field is first set at a given value, and particles of a certain energy enter the slit; the field is then altered and particles of another energy enter. Thus, step by step, we can determine the relative numbers of electrons of different velocities. Figure 10-10 exhibits Scott's curve for radium E. The highest energy occurring in a beta spectrum is quite difficult to determine, but several investigations more recent than that of Scott are in agreement. The fastest electrons emitted by this nucleus have an energy of 1.17 Mev and the average energy is 0.39 Mev. A. C. G. Mitchell and his colleagues have contributed much to our experimental knowledge of continuous beta spectra. For example, a 1949 paper of Langer and Price contains precise measurements of the shape of a number of spectra. Some of these conform closely to a shape

predicted by a theory of Fermi. Other spectra, including that of radium E, conform to modified theories because of changes of nuclear spin associated with beta emission.

To explain such spectra, it was originally assumed that disintegration electrons having energy less than the maximum had been slowed down by passing through the gross matter of the source; but this cannot be true, for the secondary electrons would also be slowed down and we would not observe the groups of definite energy discussed in Section 10.

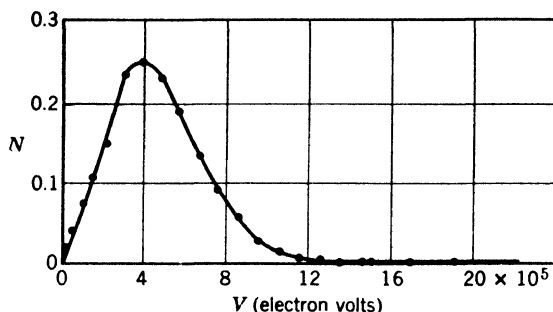


Fig. 10-10. Energy distribution of disintegration electrons from radium E (after Scott).

Furthermore, if the average disintegration electron frittered away a large percentage of its energy in collisions, this energy would appear as heat. Ellis and Wooster proved by calorimetric measurements of the total heat liberated by radium E that this is not the case. They found that when radium E disintegrates the average *observable* energy liberated per atom is 0.390 Mev. It is now generally believed that the difference between the maximum possible energy and the actual energy of a beta particle is carried away by a neutral particle, the neutrino, which was not stopped and absorbed in Ellis and Wooster's calorimeter and therefore contributed nothing to the heating effect. Evidence for this view is discussed on p. 317.

REFERENCES

Appendix 9, refs. 19, 43, 49, 55, 61, 79, 88, 98.

PROBLEMS AND EXERCISES

1. Compare the charge and mass of the alpha particle with those of the proton.
2. Explain the terms beta ray and gamma ray.
3. What process of search and deduction led to the discovery of radium?

4. State the equation describing the decay of a radioactive substance, defining all the symbols used.

5. Using Avogadro's number and a table of atomic weights, show that a gram of radium element contains about 2.6×10^{21} atoms.

6. By actual counting experiments, 1 gm of radium element gives out 3.71×10^{10} alpha particles per second. Find the decay constant, the half-life, and the average life.

7. How much helium is produced in 1 yr by a gram of radium element? Neglect the production of helium by the daughter products.

8. The half-life of radon is 3.825 days. What is (a) its decay constant λ ? (b) Its average life?

9. One millicurie of radon is sealed at time zero. At what time will 1/10 millicurie be present?

10. What is the volume of 1 millicurie of radon at 0°C and 76 cm pressure?

11. Suppose we have just four atoms of a substance whose half-life is 5 min. What is the chance that all four survive at the end of 5 min?

12. State the radioactive displacement law. Use it to find what is produced by the beta ray disintegration of potassium.

13. Use the radioactive displacement law to show that the isotopes produced by the disintegration of $\text{Ra C}'$ and $\text{Ra C}''$ are identical.

14. The velocity of the alpha particles from polonium is 1.6×10^9 cm/sec, and the atomic weight of polonium is 210. What is the velocity of the recoil atom?

15. The velocity of an alpha particle from radium C' is 1.92×10^9 cm/sec. Neglecting the change of mass with velocity, calculate its energy in ergs.

16. Roughly compare the energy of a million-volt particle with that released when a common pin is stopped after falling 1 mm from rest.

17. The internal energy of an electron at rest is m_0c^2 . Express this in ergs and in units of one million electron volts (Mev).

18. What is the HR product for an electron whose speed is $0.9c$? What is the path radius in a magnetic field of 3000 oersteds?

19. A beta particle has a speed 0.99 times the velocity of light. Find its kinetic energy in ergs and compare with its rest energy.

20. Through what voltage drop must an electron fall to gain a speed 0.99 times that of light?

21. A magnet for obtaining velocity spectra of alpha particles is desired. For reasons of expense, the pole-piece diameter should not exceed 75 cm. What field will be required to bend the paths of alpha particles from radium C' to a radius of 30 cm? Their velocity is 1.92×10^9 cm/sec.

22. At what angle will gamma rays with a wavelength of 0.01 Å be reflected in the first Bragg order, if they fall on a set of crystal planes with a spacing of 3 Å?

23. In a beta-ray spectrograph, a strong beta-ray line of radium B occurs at a position corresponding to a radius of curvature of 6 cm, when the magnetic field strength H is 323 oersteds. (a) What is the kinetic energy of the beta particles forming the line, if we neglect change of mass with velocity? (b) What is the energy according to the correct "relativity" expression?

24. Analysis shows that the beta particles of problem 23 come from the K shell of the daughter atom, radium C. The ionization potential of this shell is 0.899×10^6 ev. (a) What is the energy of the nuclear gamma ray that ejects these particles? (b) What is its wavelength in angstroms?

25. What is the evidence that gamma rays are emitted *after* the nucleus has undergone a disintegration?

ANSWERS TO PROBLEMS

6. 1.38×10^{-11} per sec; half-life = 1590 yr; average life = 2295 yr.
7. $0.0432 \text{ cm}^3/\text{yr}$.
8. (a) 2.10×10^{-6} per sec; (b) 5.52 days.
9. 12.7 days.
10. $6.53 \times 10^{-7} \text{ cm}^3$.
11. $1/16$.
12. Calcium.
13. $3.1 \times 10^7 \text{ cm/sec}$.
14. $12.2 \times 10^{-6} \text{ erg}$.
15. Energy of particle is roughly one-millionth that of the pin.
16. $8.19 \times 10^{-7} \text{ erg}$; 0.511 Mev.
17. $HR = 3520$; 1.17 cm. The relativistic mass should be used.
18. $4.98 \times 10^{-6} \text{ erg}$, or 6.1 times the rest energy.
19. 3.11 Mev.
20. 13,300 oersteds.
21. $1.7 \times 10^{-3} \text{ rad}$.
22. (a) $5.28 \times 10^{-7} \text{ erg}$; (b) $4.20 \times 10^{-7} \text{ erg}$.
23. (a) $5.64 \times 10^{-7} \text{ erg}$; (b) 0.0355 A.

Elementary Particles

1. The List of Elementary Particles

Our present understanding of the elementary particles has been gained largely from nuclear-bombardment studies and cosmic-ray investigations. There is little use in tracing the record chronologically. We shall make the best progress by listing the actors in this atomic drama, describing the instruments for their detection, and discussing separately the properties of each particle. The discussion of mesons, however, is conveniently postponed to Chapter 14.

We apply the adjective "elementary" to these particles, in the sense that they are the smallest entities we have learned to recognize. Eventually, perhaps some of them will be split into things still smaller. Appendix 3 shows the properties of all particles whose existence seemed well assured in 1953. Throughout this chapter, we shall be developing the story of the interaction of each type of particle with radiation and with other particles. The leading features are summarized in tabular form in Appendix 4, to which the reader should refer frequently.

Why does Nature show great preference for particular packets of energy in the construction of stable matter? Here we stand at the frontier of knowledge, so it may be useful to say a few words about what we do *not* know. We do not know why the charges of the positron and the electron are equal, but on p. 315 we discuss Dirac's view that the positron is merely an electron in a state of negative energy. It is not yet well established that the charges of the mesons so far discovered are equal to those of electrons, but this seems very likely to be true. The neutron is unstable, decaying into a proton and a negative electron. On this basis, the equality of the charges of proton and electron follows automatically.

We do not have any simple theory to explain the ratio of the proton mass to the electron mass, or the corresponding ratios for the mesons. Eddington has given a theory for calculating the proton-to-electron

mass ratio M_p/m_0 , and several other ratios that occur in atomic physics. His concepts are so novel and far reaching that their acceptance, rejection, or modification is a matter for the future.

The intrinsic magnetic moment of a particle of mass m is of the order $(h/2\pi)(e/2mc)$. The non-integral multiples of this quantity occurring in the proton and neutron (Appendix 3) have occasioned some surprise, and there is no generally accepted theory by which they can be computed.

Finally, we do not know the forces between proton and neutron, save in order of magnitude; hence there is no accurate theory of the simplest composite nucleus, the deuteron, analogous to the Bohr theory of the hydrogen atom.

In view of the general tendency to associate a field with each type of particle known to us, the reader may wonder whether there is any evidence for a "graviton" particle, belonging to the gravitational field, or for a free magnetic pole. Both have been much discussed. Physicists seem disinclined to consider the neutron as a fundamental particle of gravitational nature, since it is able to split into two charges. Perhaps the neutrino should be considered as the particle associated with the gravitational field alone, but this is not certain. The weakness of gravitational force has prevented the observation of any true gravitons resulting from the acceleration of bodies by gravitational forces alone. Experiments designed to discover a free magnetic pole have been performed with negative results. Further experimentation on these subjects is desirable.

2. Detection of Individual Particles and Photons

All the particles listed in Appendix 3 can be detected individually, in a variety of ways. Often the choice of a detector is based on simplicity, compactness, and response speed, rather than sensitivity. All the methods now to be described make use of the ionization produced by the particles to be detected, or by electrons and nuclei which they set in motion by collision.

★ **Sensitive electroscopes and amplifiers.** The classical instruments for radioactive measurements were the electroscope (p. 267) and the quadrant electrometer. They were ordinarily used at sensitivities much below those necessary for the study of individual alpha particles; yet both of them can be constructed to detect the individual alpha particle, and to measure with an error of a few per cent the number of ions it produces. These instruments were superseded by the electrometer tube and the linear amplifier, which are used substantially as shown in Fig. 11-1a. The former is a single tube of very high current ampli-

cation, so designed that great stability of operation can be attained. Leakage currents to the grid are suppressed by very thorough evacuation and by keeping all potential differences below the ionization potential of the residual gas, with the result that currents of a few hundred electrons per second can be measured. The tube is also a highly sensitive detector of small amounts of charge. A single alpha particle having an energy of a few Mev produces one to two hundred thousand ion pairs when it runs its full course in ordinary air. If the ions of one sign are caught by the grid of an electrometer tube, the grid voltage change is several milli-

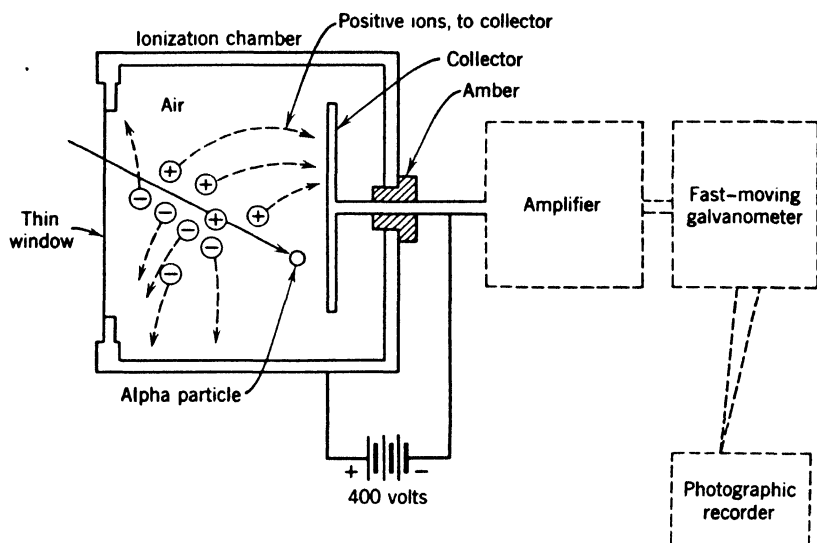


Fig. 11-1a. The amplification of ionization produced by a single particle.

volts and the change of plate current can cause a large deflection of a sensitive galvanometer. This tube has its place in some investigations for it pushes the sensitivity down to the limit set by heat fluctuations. For most purposes it can be replaced by a multistage low-noise linear amplifier. Voltage gains of 10^6 or more can be had for recording particles passing through small ionization chambers.

★ **Scintillation counters.** The scintillation screen is made by spreading a thin translucent layer of phosphorescent zinc sulfide crystals on a glass plate smeared with castor oil, which serves as a cement. When the screen is bombarded with alpha particles we can, with a microscope, see a tiny flash of light wherever a particle strikes. This effect can be shown with most watches having luminous dials. One observes the flashes through a low-power magnifier after resting the eye a few minutes

in the dark. It is difficult to make accurate visual counts of scintillations; hence the method fell into disuse in the late 1920's; but it was clear that it would be useful if the eye could be replaced by a suitable phototube. Ordinary phototubes do not have the sensitivity required. However, the photomultiplier, a tube with internal provision for great amplification, is satisfactory for this purpose. It was discovered that anthracene and other crystals give pulses of fluorescence under the action of electrons and gamma rays. The great advantage of such scintillators is their high gamma-ray efficiency, for example, 20 per cent, as compared with less than 1 per cent for ordinary Geiger counters. The use of the crystal provides a relatively large volume for absorption of the rays.

★ **Conductivity-crystal counters.** These scintillating crystals should be distinguished from another type of crystal counter, exemplified by silver chloride and diamond, in which an ionization pulse produced by release of electrons in the crystal is detected by means of applied electrodes. These devices commonly require a liquid-air temperature for satisfactory operation, and effort is being devoted to getting around this defect.

★ **Tube counters.** The Geiger-Müller counter, or tube counter, (Fig. 11-1b) is a highly versatile instrument for detecting both charged

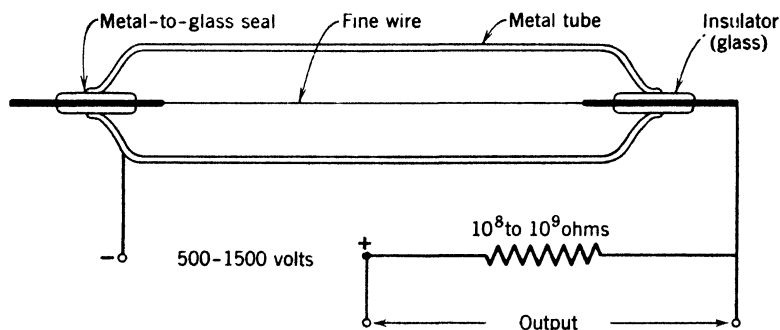


Fig. 11-1b. A tube counter and the original very simple circuit for operating it. This circuit has a long recovery time, and quenching circuits or self-quenching gas mixtures are now nearly always used to permit high counting rates.

particles and gamma rays. In its original form it consisted of a metal tube with insulating plugs at each end, which supported a thin wire passing down the center. Between the central wire and the outer case, a battery with an emf of several hundred volts is connected. A resistance of 10^8 or 10^9 ohms limits the current. The tube is filled with any common gas at a pressure of a few cm of Hg, and the voltage is adjusted to

a value below that at which a spontaneous discharge would occur. If an alpha or beta particle enters the tube, the ions produced are swept toward the cylinder and the wire. These ions produce others by collision, thus initiating a current sufficient to produce a drop of several volts across the series resistance. The current is sufficient to give a loud click in a telephone receiver in series with the resistance, but it is customary to amplify the effects so that mechanical recorders can be used.

★ When current flows, there is a voltage drop across the high resistance. If this drop is large enough, the voltage across the gas-filled space between the counter electrodes falls below the value required to maintain the discharge. The discharge ceases, the voltage across the counter rises to its original value, and the counter is ready to operate again. The simple device in the figure has undergone a number of successive improvements. Quenching circuits are used to put the discharge out more rapidly, or hydrocarbon vapors can be added to make the counter self-quenching. Thin windows are used to admit slow beta particles. With a coating of boron inside the tube, neutrons can be detected, for they cause disintegration of boron, with emission of alpha particles. If a gamma ray is absorbed in the walls of the cylinder, it may eject a fast secondary electron, which can actuate the counter. Indeed, a single ion pair in the gas suffices to start an avalanche of ions. Recombination can be held down to a point such that the efficiency in counting electrons is 98 per cent. Using tubes with a light-sensitive inner surface, Rajewsky found it easy to detect individual photons of ordinary light. (Some of the photons liberate photoelectrons which are accelerated in the strong field between the counter electrodes, producing other ions and operating the counter.)

★ **Coincidence counters.** There are many instances in which we wish to know whether two particles have been generated within a very small time interval, in order to judge whether or not they may be causally connected. Again, in the study of cosmic rays, it is important to have information about the number of particles that strike a horizontal square centimeter per second, and the directions from which they come. Such information has been obtained by making use of the fact that cosmic ray particles can penetrate several tube counters, while electrons of shorter range from radioactive materials can penetrate only one, provided that the wall-thickness is properly chosen. Similarly, thin-walled counters may be employed to detect coincidences, in work with radioactive substances.

★ Suppose that two counters, I and II, are arranged with their axes parallel, (Fig. 11-2) and that their outer cylinders are connected to the grids of a tetrode tube, the grids being normally negative. If a count

occurs in counter I alone (or in counter II alone) it raises the potential of the grid to which it is connected, but the negative potential of the other grid prevents an increase of plate current. If both counters are excited at the same time, both grids become positive, and current passes, sending an impulse to some recording mechanism. Such an event is called a coincidence. In practice, other circuits are employed and several counters may be used.

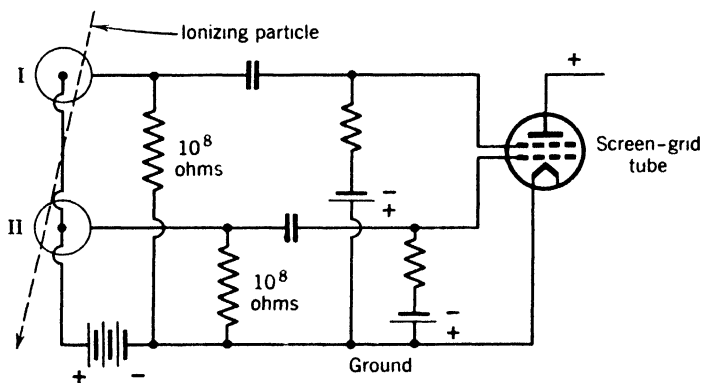


Fig. 11-2. Simple arrangement for amplifying coincident pulses in two counters.

★ Coincidences can be produced by the passage of an ionizing particle through both counters, or by the accidental arrival of two independent particles, one in each counter, at nearly the same time. To determine the correction for accidentals, we move the two counters far apart. The chance that a cosmic-ray particle passes through both of them becomes negligible, since each subtends a small solid angle when viewed from the other. Only the accidental coincidences remain.

The Wilson cloud chamber. C. T. R. Wilson showed in 1911 that, if alpha rays pass through air sufficiently supersaturated with water vapor, minute drops of water condense on the ions produced, and, if a strong source of light shines on the trail of water drops, they are seen by its scattered light as a continuous track. Figure 11-3 is a diagram of the type of cloud chamber used by early workers. The top is a plate of glass. A blackened piston below is suddenly forced downward by a spring when a catch is released. This motion expands moist gas in the chamber, so that the sudden cooling tends to condense the water vapor. The expansion is stopped just short of the point at which a general fog would be produced. To maintain the air in a saturated condition the piston may be coated with a layer of wet gelatin. Near

the end of the expansion, a source of alpha particles is uncovered by the motion of a small shutter containing a narrow slit which passes in front of the source. While the slit is open a few alpha particles can pass into the chamber through a thin sheet of mica. Since the air is in a super-

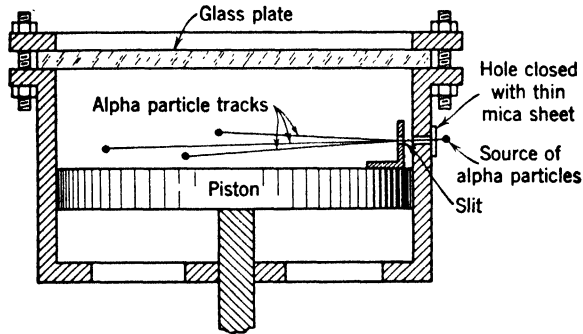


Fig. 11-3. Diagram of a Wilson cloud chamber.

saturated condition, tracks of water droplets are produced. Images of these may be recorded on motion-picture film. To obtain good photographs the illumination must occur for only a brief interval just after the tracks are formed, for they quickly become diffuse.

Thorium C' alpha particles are shown in Fig. 11-4. It is apparent that practically all the alpha particles have about the same range, and the occurrence of the long-range track is discussed on p. 279. The straightness of the typical alpha trail is due to the comparatively large mass of the particle. Though not appreciably deflected by electrons

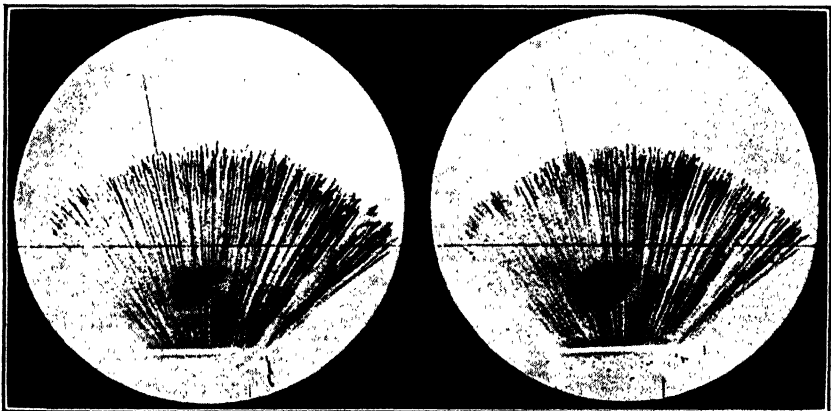


Fig. 11-4. Tracks of alpha particles from thorium C'. (After Meitner and Freitag.)

that lie along its path, it loses energy rapidly by ionizing and exciting the atoms it encounters, until finally it is no longer able to release electrons and the short remaining portion of its track is invisible.

The photography of electron tracks reveals much interesting detail. In air at normal temperature and pressure a fast electron produces about 60 ion pairs per centimeter, but unless proper precautions are taken some may be missed, for condensation occurs over a greater range of conditions on negative than on positive ions. Although the droplets are usually less than 0.001 in. in diameter, good photographs can be made if the illumination is well planned. X-rays and gamma rays are recognized by the results of their primary interactions with matter—the production of electrons by the photoelectric and Compton effects. In Fig. 3-14 an old photograph of C. T. R. Wilson's shows photoelectrons ejected by a narrow pencil of X-rays traveling from left to right. Since the electric vector of the radiation is at right angles to the beam, we might expect the electrons to be ejected at right angles to the beam.



Fig. 11-5. Individual ion pairs along electron tracks. Photography delayed to permit the positive and negative ions to drift apart. Magnified a few diameters for reproduction. (*After P. I. Dee.*)

Quantum theory modifies this expectation, predicting, however, that ejected photoelectrons are more frequent at large angles with the beam direction. Clearly the photograph supports this statement. While the track of an electron of moderate velocity is extremely devious, that of an electron with an energy of 0.3 Mev or more is nearly straight over distances of several inches in normal air. The loss of energy per ion pair is small, about 30 ev, for these energetic electrons, so the speed is reduced

very little in a distance of this order of magnitude. We know that the number of ion pairs per centimeter produced by a fast electron increases as its speed diminishes. The increased density of the tracks near their ends is clearly apparent. More detail can be seen in Fig. 11-5, in which positive and negative droplets were allowed to drift apart before the photograph was taken. While we cannot expect a droplet to form on every ion, it is known that under proper conditions the efficiency of the cloud chamber in revealing individual ions is high.

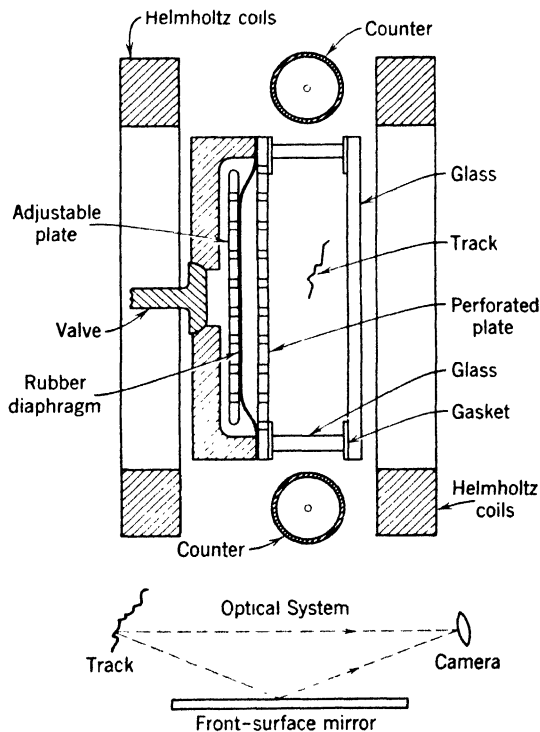


Fig. 11-6. Diagram of a versatile cloud chamber apparatus. The Helmholtz coils produce a magnetic field which is nearly uniform over the body of the chamber. The camera views the chamber and its image in a mirror, so that tracks can be seen in space with a stereoscopic viewer.

★ Several accessories have greatly increased the versatility and convenience of the Wilson chamber. Rubber diaphragms constrained to move between suitable grids have replaced the piston, and automatic operation is practically universal. Application of a strong magnetic field makes it possible to determine the sign of a particle's charge, and

its momentum. With the aid of coincidence counters (Fig. 11-2) placed above and below the chamber, it is possible to trigger its expansion when and only when an ionizing particle has passed through. This practically insures a track on every picture. The Wilson chamber is the court of last resort in nuclear physics; seeing is believing. Stereoscopic photography makes it possible to see the form of tracks in space, and to measure angles of scattering and path radii. An arrangement which provides for applying a magnetic field to the chamber and for stereoscopic photography is diagrammed in Fig. 11-6.

We list here the pages on which additional cloud-chamber pictures are reproduced, so that the reader may perceive at once the range and power of this method:

	Page
Disintegration of nitrogen by alpha particles	339
Products of bombarding deuterium with deuterons	355
Discovery of the positron	310
Electron-pair production	311
Fission fragments	382
Recoil protons produced by neutrons	326
Decay of a mu meson	413
Cosmic-ray shower	439

Photographic detection. It has been known for a long time that an alpha particle passing through an ordinary photographic emulsion produces a few developable silver bromide grains. Originally photographic emulsions were not suitable for studies of individual particles; but early observations led to the development of special fine-grain plates with thick layers of emulsion. Today the individual tracks of mesons and protons can be recorded well, and those of electrons with fair clarity. For particles whose ranges exceed the thickness of the emulsion, it is usually most convenient to use grazing incidence and to choose for examination only those tracks that happen to lie entirely in the emulsion. The method has been especially useful in studies of nuclear disintegrations produced by cosmic rays, p. 424, and of mesons, p. 412. By exposing plates on mountains, and sending them up on high-flying balloons, much interesting information on cosmic-ray phenomena at great altitudes has been accumulated. For additional pictures, the reader may consult references 91 and 111 (Appendix 9).

3. Scattering and Absorption of Particles and Gamma Rays

Ionization effects. The goal of this section is to describe and interpret some of the chief facts concerning the scattering and energy loss of fast particles passing through matter. The cloud-chamber photographs of Section 2 show the great differences between the ionizing effects of alpha particles, electrons, and X-ray or gamma ray photons in gases.

★ An alpha particle of radium C' produces more than 200,000 pairs of ions in air, before it comes to rest. The number of ion pairs per centimeter is greater near the end of the track than at the beginning.

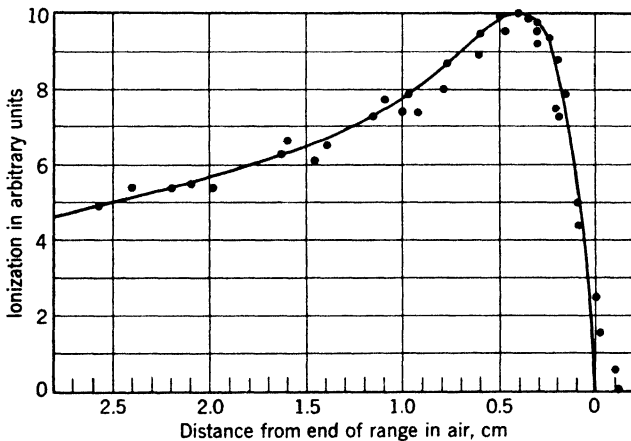


Fig. 11-7. The Bragg curve for a single alpha particle. (After Holloway and Livingston.)

Figure 11-7 shows the ionization per centimeter, as a function of residual range. This plot is called the Bragg curve. The behavior of other light nuclei is similar. For a proton with its smaller charge, the ordinates would be lower and the range figures would be about four times as great. The explanation of the Bragg curve is that when the particle is moving very rapidly it passes the gas atoms so quickly that their electrons are not able to respond to the forces it exerts; they do not pick up sufficient momentum to leave their parent atoms before the alpha particle has passed on. At smaller speeds this is not so. The number of ion pairs per centimeter may rise to more than twice the value appropriate to the beginning of the track, only to fall again at the very end. The ionization along the path of a typical beta particle is smaller, mainly because of its much higher velocity. The total number of ion pairs it

can produce in air is of the order of ten thousand. Since the range is great compared with that of an alpha particle, we should expect that only a few ion pairs are produced per centimeter. In fact, the number ranges from several hundred per centimeter for slow beta particles, down to about 60 for particles whose velocity approaches that of light.

★ **Penetrating power.** These differences in ionization are reflected in the relative abilities of these particles to penetrate gross matter. Rutherford says, "As a rough working rule, it may be taken that the beta rays are about one hundred times as penetrating as the alpha rays, and the gamma rays from ten to one hundred times as penetrating as the beta rays." In practical terms, an ordinary sheet of paper will absorb the fastest alpha rays. The beta particles slip through more easily, the faster ones being able to penetrate several millimeters of aluminum or a millimeter of lead, and gamma rays can pass through several centimeters of metal before they are reduced to half intensity.

One significant difference comes to light at once. The alpha and beta particles fritter their energy away in frequent dribbles. The high-energy photons suffer effective collisions much less frequently, but in those collisions they are either absorbed by atoms, with production of photoelectrons, or they are scattered, giving energy to the recoil electrons. The higher the energy of the photon, the greater, on the average, is the fraction of its energy which is lost in each scattering process. These facts lead to the description of the alpha particle and the electron as "range particles"; that is, the alpha particle has a definite range. The beta particle, though greatly deflected in its encounters with fellow electrons, has a quite definite range, measured along its track. But monochromatic gamma rays have no definite range; they disappear all along the beam, or are thrown completely out of the beam by scattering. Their law of decrease is the exponential one described for X-rays on p. 114. In passing through a thickness x , the intensity is reduced from I_0 to the value

$$I = I_0 e^{-\mu x}$$

where μ is called the linear absorption coefficient. In the absence of a definite range, we can state the mean path traveled by a photon before it is scattered or absorbed. This is $1/\mu$, in which distance the intensity of the beam is reduced by a factor e . Of course, if the beam is not monochromatic, the softer parts characterized by small values of $1/\mu$ are filtered out first (p. 115). Thus the effective absorption coefficient falls as we increase the thickness of the absorber.

★ Figure 11-8 presents range-energy curves which will cover most of the cases met with in studying the emissions of radioactive elements although much greater energies are encountered in work with very large

accelerators. The upper graph shows the mean ranges of alpha particles and protons in air, at 15°C and 760 mm pressure. The lower graph shows ranges of electrons in aluminum and mean free paths of photons in copper. For gamma rays in lead the corresponding curve (not shown)

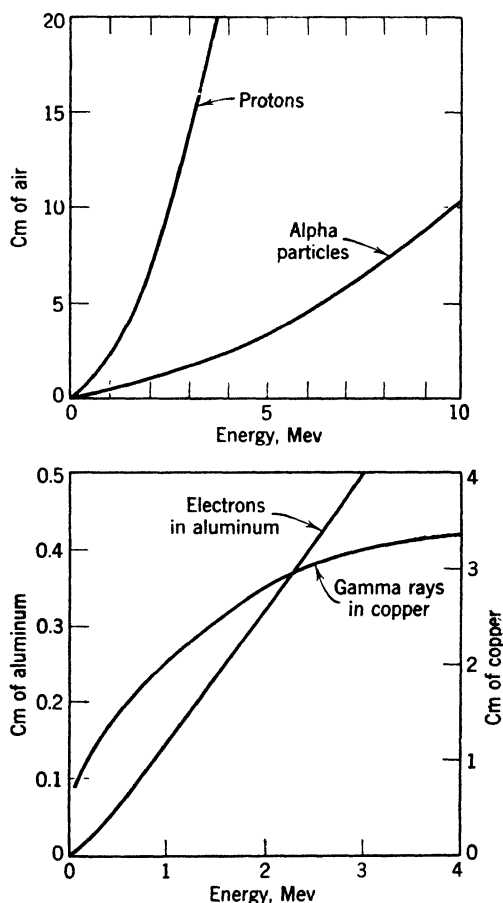


Fig. 11-8. Upper diagram: ranges of protons and alpha particles in air at 15°C and 760 mm pressure. Lower diagram: ranges of electrons in aluminum and mean free paths of gamma ray quanta in copper.

passes through a maximum value of 2 cm, for an energy of about 5 Mev. At lower energies, frequent scattering and absorption reduce the mean free path, while at higher energies the increasing frequency of pair production (p. 311) cuts it down. Thus, lead has a maximum trans-

parency for photons of energy about 5 Mev. For materials of lower atomic numbers, the maximum lies at much higher energy so that the curve for copper continues to rise at energies even higher than those included in the figure.

★ From the curves for alpha particles, protons, and electrons, it is possible to obtain the loss of kinetic energy per centimeter. To understand these matters qualitatively we must now study collisions. Strictly speaking, these collisions are usually inelastic, for energy is expended in exciting and ionizing the atoms of the medium. However, much light is obtained by considering the changes of direction and the transfer of energy occurring in elastic collisions between free particles, in which momentum and energy are conserved.

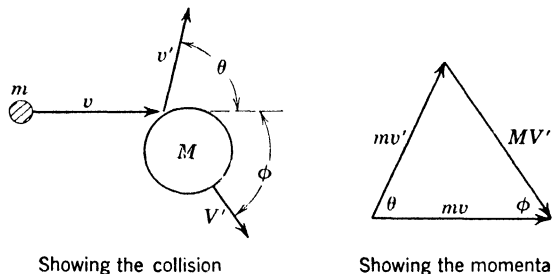


Fig. 11-9. Elastic collision of two particles.

★ **Elastic collisions.** In Fig. 11-9, a resting particle of mass M is struck by a particle of mass m , velocity v , momentum $p = mv$, and kinetic energy $t = p^2/2m$. After the collision, m and M are moving at angles θ and ϕ , relative to the original direction of m . Their final velocities, momenta, and energies will be called, respectively,

$$v', \quad p', \quad t'; \quad V', \quad P', \quad T'$$

There are some conclusions we can get from the conservation laws, without any regard to the nature of the particles. In the figure, the triangle illustrates the conservation of momentum. Resolving the momenta parallel and perpendicular to the x axis, we have

$$p = p' \cos \theta + P' \cos \phi \quad (1)$$

$$0 = p' \sin \theta - P' \sin \phi \quad (2)$$

and by the conservation of energy we get

$$p^2/2m = p'^2/2m + P'^2/2M \quad (3)$$

We can eliminate p' and θ from these relations, obtaining P' as a function of t and ϕ . First of all,

$$p' \cos \theta = p - P' \cos \phi$$

$$p' \sin \theta = P' \sin \phi$$

We square these equations, add the results, and use $\cos^2 \theta + \sin^2 \theta = 1$ to rid the equations of θ . The result is:

$$\frac{T'}{t} = \frac{4r \cos^2 \phi}{(1 + r)^2} \quad (4)$$

where $r = m/M$. This is the fraction of the original energy which is handed over to the struck particle. Now $\cos^2 \phi$ cannot exceed 1; it attains this value only when the collision is head on. Thus the fraction of the energy that is handed on is certainly less than $4r/(1 + r)^2$. This fraction is zero when $r = 0$, has a maximum value of 1 when $r = 1$, and falls off toward zero again as r goes to infinity. This is a quantitative description of what we know from common observation. The collision partners must be well matched to achieve good transfer. In head-on collisions of elastic spheres, a ball of small mass will rebound from a large one with little loss of energy. When the masses are equal, the striking ball stops while the struck ball moves away with all the energy. When the striking ball has much greater mass, the smaller one separates from it with a speed of about v , or, in other words, the smaller ball has a speed of nearly $2v$ with respect to the observer. It carries away, however, a comparatively small amount of energy. We apply this result to several cases shown in the accompanying table.

Projectile	Particle Struck	r	$\frac{4r}{(1 + r)^2}$	Remarks
Electron	Helium nucleus	1/7340	1/1830	Back scatter occurs
Electron	Electron	1	1	{ No back scatter; $\theta = 90^\circ - \phi$
Proton	Proton	1	1	
Alpha	Electron	7340	1/1830	No back scatter; θ always small

★ Thus we see that the *maximum* energy lost by a 10^5 -ev electron in colliding with a nucleus of helium is only about 50 ev. An alpha particle of 5 Mev colliding with an electron might give it 2500 volts. There are in fact some short spurs, the tracks of recoil electrons of thousand-

volt energy, along the track of an alpha particle, but these are infrequent. Typically, the value of $\cos^2 \phi$ is quite small. We have stated before that the average energy required to form an ion pair in air is about 30 ev, and this includes excitation energy handed over to atoms that are not ionized. The detailed treatment of such inelastic collisions is quite complex.

In studying collisions, conditions are simplified by viewing the collision from a vehicle moving with the center of mass of the two particles, that is, with the speed $v \times m/(M + m)$. The total momentum of the particles is zero, and must remain so. The two particles simply rebound from each other, retaining their original velocities, but moving along new lines. In the elastic collision of light nuclei the distribution of emerging particles is often close to uniform over the surface of a surrounding sphere, *when viewed* from the center-of-mass frame.

★ **Collisions of equal balls.** The slowing down of neutrons by protons (p. 328) is usually treated as a collision of hard frictionless balls of equal mass. In this case it can be shown that all values of $\cos^2 \phi$ have equal probability and that the average of $\cos^2 \phi$ is $1/2$. By equation 4, the average loss of energy of the neutron is one-half its kinetic energy before the collision.

★ **Impossibility of direct combination of two particles without change of internal energy.** Equations 1 to 4, which presuppose the conservation of momentum and of energy, show that there is no type of *elastic* collision in which *two* particles simply come together and move off with common velocity. We leave the algebraic proof to the reader, because the result is obvious when we use the center-of-mass coordinate frame. In that frame, the particles would stick together and remain at rest. The situation is relieved if at least one of the particles has internal energy which can be altered in the collision. Then, in place of equation 3, we put

$$\frac{p^2}{2m} = \frac{p'^2}{2m} + \frac{P'^2}{2M} + E$$

where E is the energy diverted into the interior. At first sight, the presence of E appears to make direct combination possible in all cases, but the reader can easily convince himself that, for a given v and θ , E is fully determined. If atoms did not have definite quantum states, they could combine for any value of v , but, as matters are in Nature, E must be the difference between two allowed energy levels.

★ There are many applications. Hydrogen atoms do not combine in the gaseous state to form diatomic hydrogen molecules except in triple collisions. In nuclear bombardment, the projectile does not

merely join the nucleus; something else is thrown out. There may be trivial exceptions, but we do not know of any. For example, neutrons are captured to some extent by nearly all nuclei, but in such cases a gamma ray is emitted.

★ The above discussion was based on Newtonian mechanics. Let us consider a simple example using relativity mechanics. Can a photon combine with a free electron? If so, the two conservation laws of momentum and energy would say respectively,

$$\frac{h\nu}{c} = \frac{m_0 v}{\sqrt{1 - \beta^2}} \quad h\nu = \frac{m_0 c^2}{\sqrt{1 - \beta^2}}$$

where m_0 is the mass of the electron. If these equations were simultaneously valid, they would imply that $v = c$, but a free electron cannot attain the velocity c . Thus the photoeffect, in which a photon is absorbed, occurs only when the electron is bound in an atom. This is the basic physical reason why the Compton effect predominates over the photoeffect when $h\nu$ is high and the binding energy of the electrons is small, as is so in atoms of low atomic number.

Cross sections. We have met with the idea of target area, or cross section, in considering molecular collisions, on p. 16. There we spoke of billiard-ball molecules of diameter d . To make a collision, a molecule must move so that its center will come within the distance d from the center of another molecule. Then we say the cross section for the collision is πd^2 . It is useful to extend the concept to collisions of real atoms, nuclei, etc., which have fields of force and may interact at any distance.

We shall give a definition commonly used in nuclear physics. Let N_b bombarding particles fall on a foil of thickness t containing N_t targets of the kind in which we are interested, per cm^2 . We consider a particular process—ionization, transmutation, etc. The number of processes occurring is N_p . Then the yield fraction is N_p/N_b , and the cross section S for the process is defined by the relation

$$N_p/N_b = N_t S$$

$$\text{or} \quad S = \frac{N_p}{N_b} \frac{1}{N_t} \quad (5)$$

Referring to Fig. 11-10a, we can say: *the number of processes is the same as though the bombarding particles had negligible diameter and the targets were hard spheres of cross section S so that they occupy a fraction $N_t S$ of the total area bombarded.*

If the target material has density ρ and atomic weight A , the number of nuclei, or atoms, per cm^2 of a foil of thickness t is

$$N_t = \frac{\rho}{A} N_0 t$$

where N_0 is Avogadro's number, 6.02×10^{23} . The number of electrons is Z times as great. Accordingly, for a process involving a nucleus,

$$S = \frac{N_p/N_b}{(\rho/A) N_0 t} \quad (6a)$$

and for a process involving an electron as a target,

$$S = \frac{N_p/N_b}{Z(\rho/A) N_0 t} \quad (6b)$$

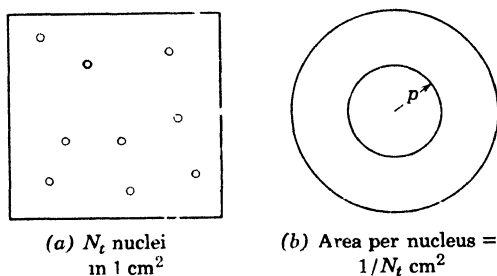


Fig. 11-10. (a) The concept of cross section. (b) How to obtain the fraction of alpha particles that passes within a given distance from a nucleus in a foil.

We give some numerical values illustrating equation 6a in the accompanying table. For reactions carried on by charged particles, a cross section of 10^{-27} cm^2 would be considered high, although in a few cases the value is several thousand times larger.

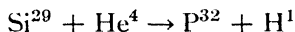
Element	Density (grams/ cm^3)	Nuclei/ cm^3	Number of Processes per <i>Million</i> Bombarding Particles, per cm^3 if the Cross Section is 10^{-27} cm^2
Be	1.85	12.4×10^{22}	120
Si	2.42	5.2×10^{22}	52
Cu	8.89	8.5×10^{22}	85
Au	18.9	5.8×10^{22}	58

★ The accurate determination of cross sections as a function of the bombarding energy is laborious, since the bombarding particles lose energy as they pass along. "Thin" targets are required, and corrections are troublesome; but determination of a rough average value is often all that is necessary. The usefulness of cross sections is obvious, for they are quantities characteristic of the nuclear process.

To avoid large powers of 10 in writing cross sections it has become customary to use a unit of area called the *barn*. One barn is 10^{-24} cm². The name is a bit of wartime slang. The barn happens to be about equal to the "geometric area" of a nucleus of medium atomic weight, say 40. The geometric radius is usually taken as about $1.5 \times 10^{-13} A^{1/3}$ cm.

★ In many experiments the currents used in bombarding beams are only a few microamperes (to avoid undue target heating). One microampere of alpha particles amounts to 3×10^{12} particles/sec. If alpha particles could be passed into a gas of bare nuclei, they would lose their energy in scattering by the nuclei, and in production of transmutations. Now, the electrons of a target material have a great influence in reducing the yield of transmutations by charged particles. They rob the bombarding particles of their energy, sharply reducing the number of nuclei that can be attacked. The situation is much more favorable for transmutation in neutron bombardment, since neutrons do not interact appreciably with the electrons. The net result is to raise the efficiency of transmutation by a large factor, usually much larger than 10^6 .

★ When the order of magnitude of a cross section is known, equations 6 can be used to calculate the yield in any proposed experiment. For example, when alpha particles with energy about 7.8 Mev bombard silicon, the yield of radioactive phosphorus (P^{32}) is about one atom per million particles. What is the approximate cross section? The figure given refers to a target whose thickness is greater than the range of the alpha particles. Therefore, the cross section is an average over the range of the bombardment energies from 7.8 Mev down to a threshold of about 1.6 Mev, below which the reaction does not occur. The distance an alpha particle runs in silicon in coming down from 7.8 to 1.6 Mev is about 0.0035 cm. From the table on p. 304, $(\rho/A)N_0 = 5.2 \times 10^{22}$ nuclei/cm³ for silicon; but the reaction is



and only 6 per cent of the nuclei are those of Si^{29} , the remainder being chiefly Si^{28} . Therefore in equation 6a we must put $5.2 \times 10^{22} \times 0.06$, or 3.1×10^{21} , in place of $(\rho/A)N_0$. Finally,

$$S = \frac{10^{-6}}{(3.1 \times 10^{21})(0.0035)} = 9 \times 10^{-26} \text{ cm}^2$$

With this value in hand we can now answer such questions as: "About what number of P^{32} atoms will be obtained if we bombard a sample of ordinary silicon 0.001 cm thick with $1\text{ }\mu\text{a}$ of 8-Mev alpha particles for 1000 sec?"

Large-angle scattering of alpha particles. On p. 47 we described experiments in which alpha particles fell on foils sufficiently thin to transmit them. In such experiments practically all particles are deflected a little. The most probable scattering angle is only a few degrees at the most. Small deflections can be explained as due to multiple scattering in successive collisions with the electrons, and some nuclear collisions at relatively large distances.

The electron has a mass so small that it cannot deflect an alpha particle through a large angle. It is possible to use foils so thin that cumulative multiple scattering to produce large deviations becomes very improbable. But, when such foils are employed, particles *are* scattered through large angles. Some, indeed, are turned through angles greater than 90° , so that they emerge on the side of the foil turned toward the incident beam. As noted on p. 48, a satisfactory explanation is that each particle has been deflected in a single encounter with

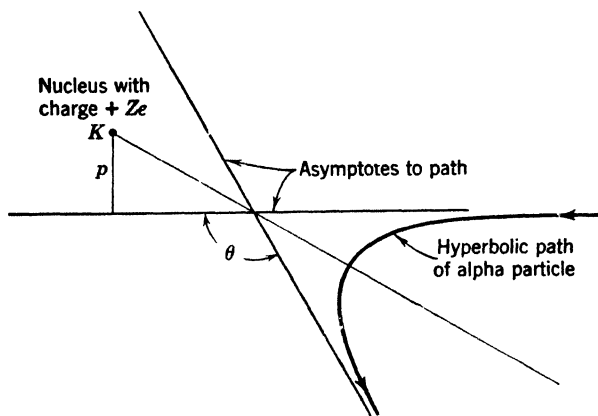


Fig. 11-11. Scattering of an alpha particle by a heavy nucleus.

a massive nucleus. The fraction of the particles deflected through an angle greater than θ will be called $G(\theta)$. We desire to know G for a collision between an alpha particle of mass m and a heavy nucleus with atomic number Z . We assume that the nucleus remains at rest, an assumption that will introduce only a small error if we are dealing with foils of gold or platinum. In Fig. 11-11 the alpha particle comes from the right and moves on a hyperbolic path, with the nucleus at one focus

K. When we observe the scattered particle, it is moving parallel to one of the asymptotes of this curve. Let p be the distance between the nucleus and the initial line of motion of the particle. It can be shown that, if the inverse square law of force is obeyed, the relation between p and the angle θ is

$$p = \frac{2Ze^2}{Mv^2 \tan(\theta/2)} \quad (7)$$

To find the relative frequency with which we shall observe a particle scattered at an angle greater than θ we consider the magnified projection of a unit area of foil, shown in Fig. 11-10a. Let all the particles pass through this area, containing N_t nuclei. Large-angle scattering is so infrequent that overlapping of the spheres of action of the nuclei may be neglected. We assign the area $1/N_t$ to each nucleus, and consider just the particles that pass through a circle whose area is $1/N_t$, centered on a chosen nucleus. The fraction that passes through a circle of radius p around the nucleus will be deflected through an angle greater than θ . This fraction is simply the area of the circle of radius p , divided by the whole area available for scattering by this nucleus. In other words,

$$G = \frac{\pi p^2}{(1/N_t)} = N_t \frac{4\pi Z^2 e^4}{M^2 v^4 \tan^2(\theta/2)} \quad (8)$$

We speak of πp^2 as the *cross section* of the nucleus for scattering the alpha particle through an angle greater than θ . By this we mean simply that, if the nuclei were replaced by disks of radius p , and if the deflection were greater than θ when such a disk is hit, and less than θ when such a disk is not hit, then G would have the value realized in Nature. The formula cannot be applied at small angles where multiple scattering is the real mechanism.

The single-scattering cross section given above approaches infinity as θ approaches zero. This makes common sense, because every particle is deflected to some extent, since the field of force of the scattering nucleus extends throughout all space. However, for sufficiently large p values, screening by the electrons of the atom cuts down the scattering. In practice, we confine our attention to scattering at angles above some minimum value, determined by the extent to which we can reduce the angular spread of the bombarding beam, and by the presence of multiple scattering.

The gist of the above argument is that the cross section can be determined by studying the mechanics of the collisions. For comparison with experiment it is convenient to put the result in a different form.

By differentiation, we find that the fraction of the particles scattered into a small range of angles, θ to $\theta + \Delta\theta$, is

$$\Delta G = N_t \frac{4\pi Z^2 e^4 \Delta\theta}{M^2 v^4 \tan^2(\theta/2) \sin^2(\theta/2)} \quad (9)$$

Geiger and Marsden determined the relative numbers of particles scattered into such small ranges of angle by a foil of gold. In Fig. 11-12, the plotted points represent their results and the curve is drawn on the

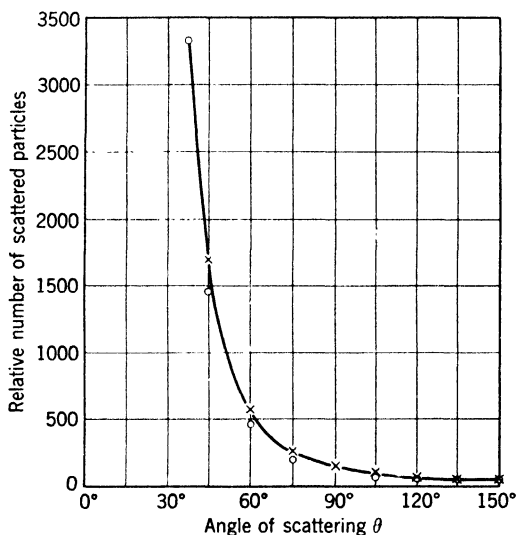


Fig. 11-12. How the number of alpha particles scattered by gold at a given angle depends on that angle.

basis of theory. It was so adjusted as to run through the plotted point for which $\theta = 37.5^\circ$. The theory can be tested by using equation 8 to compute Z from the results of scattering experiments. In this way Chadwick found the charges on the nuclei of copper, silver, and platinum to be 29.3, 46.3, and 77.4, while the atomic numbers are 29, 47, and 78, respectively. Still more important, experiments of this kind may be used to test the inverse square law of force down to very small distances. The alpha particle approaches closest to the nucleus when the collision is head on; then the minimum distance of approach is $4Ze^2/Mv^2$ if the inverse square law holds true. If we find that equation 9 is obeyed for scattering angles in the neighborhood of 180° , we may conclude that the inverse square law is applicable, and that the minimum approach distance can be considered as an upper limit for the "combined radii"

of alpha particle and nucleus. In the case of gold the equation *is* obeyed, and the calculated minimum distance of approach is about 3×10^{-12} cm for the alpha particles of radium C'.

Since the minimum distance is proportional to the atomic number, it is pertinent to use Al or some other element of low Z to investigate the force law at smaller distances. Scattering by the light elements from H to Al differs considerably from that predicted by equation 9, or rather, by a similar formula which takes account of the velocity imparted to the nucleus. The discrepancy increases with the angle of scattering, since a large scattering angle is associated with a close collision. This means that the inverse-square law of force is not valid at the distances involved—a conclusion we should expect. Since protons and neutrons can form stable nuclei, attractive forces must come into play at small distances.

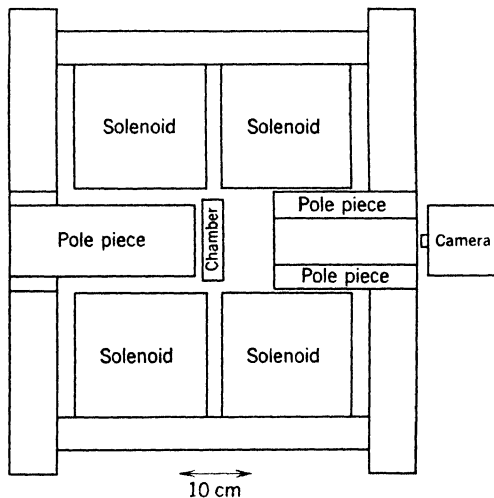


Fig. 11-13. Cloud chamber in the field of a large electromagnet, as used by Anderson to study the tracks of fast positrons and negatrons.

4. Electrons and Positrons

Discovery of the positron. In August 1932, Carl Anderson of the California Institute of Technology discovered the positive electron, whose electric charge (except for sign) is equal to that of the negative electron. The names *positron* and *negatron* were coined by Anderson to replace the terms positive electron and negative electron. He was engaged, with Neddermeyer, in studying the energy of fast cosmic-ray

electrons by Skobelzyn's method (Fig. 11-13). A shallow cloud chamber is placed between the poles of a magnet. The glass face is in a vertical position to favor the observation of particles entering the chamber from above. One of the magnet poles is made hollow so that with the aid of a mirror two stereoscopic photographs of the cloud tracks can be taken through the hole. Charged particles entering the chamber in directions roughly parallel to the glass front are deflected by the magnetic field. Each particle follows a very nearly circular path, and the energy can be obtained from the radius of the path, if we know the value of e/m for the particle. In order to distinguish between particles coming from above and those coming from below, Anderson placed a 6-mm horizontal lead plate inside the chamber. In passing through the plate any particle is slowed down; thereafter it moves on a circle of smaller radius.

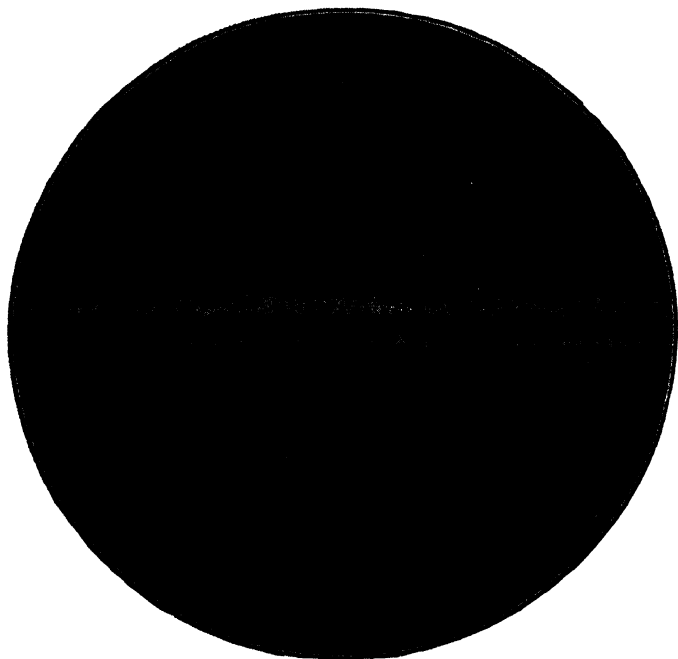


Fig. 11-14. Anderson's photograph which proved the existence of the positron. A positron, coming from below, is forced to the left by the magnetic field.

Figure 11-14 is the famous photograph that revealed the existence of the positron. A particle traversed the chamber from bottom to top. A negative electron coming from below should be bent toward the reader's

right, because the lines of magnetic force point into the paper; but the particle whose track is shown is deflected to the reader's left. Other photographs confirmed the frequent occurrence of particles showing this behavior. Only positive charges could behave in this way, and the question is: What is their mass? Anderson showed that they are not protons by studying the density of ionization along the track. The density corresponds to that expected for negative electrons of similar energy. Later on, Thibaud used a magnetic spectrograph to measure the e/m ratio for positrons, obtaining a value in agreement with that for negative electrons. Other investigations made it possible to determine both e and m . Within the limits of experimental error, the mass of the positron is equal to that of the negatron.

Pair creation and annihilation. Anderson, and also Blackett and Occhialini, found cases in which positrons were produced in a lead plate placed across a cloud chamber, by some entity that left no track in the gas. Often, a positron track and a negatron track appeared to come



Fig. 11-15. Electron pair produced by gamma rays of Th C'' in a Wilson chamber (after M. and Mme. Curie-Joliot).

from the same point in the lead. Such experiments on *pair production* by cosmic rays are supported by others which are easier to interpret. Anderson and Neddermeyer and other groups of investigators showed independently that hard gamma rays are able to eject positron-negatron pairs from lead and other materials. Figure 11-15, obtained by the

Curie-Joliot, is reproduced for its historical interest. It shows a pair produced when a gamma ray with energy 2.6 Mev struck a nucleus in the gas of a cloud chamber. *This important phenomenon, called pair production, consists in the actual creation of a positron and a negatron, out of a gamma-ray photon which disappears in the process. Annihilation of positrons, by junction with negative electrons, also occurs, with production of one, or more commonly two, gamma rays.*

As to Production. 1. Pair production occurs only in regions occupied by a strong field of force, such as the neighborhood of a nucleus or an electron (Fig. 11-16a). The reason is that both energy and momentum

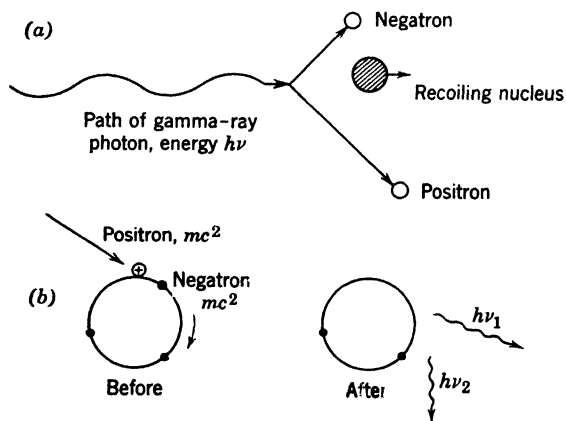


Fig. 11-16. (a) The production of a positron-negatron pair in the field of force near a nucleus. (b) Annihilation of a positron and a negatron, giving rise to two gamma rays.

must be conserved in the process of pair production. This cannot be done in empty space. The nucleus or electron recoils, as it were, from the incoming gamma ray, and makes the creation of the pair possible.

2. Pair production in the neighborhood of a nucleus is a phenomenon much more frequent and more easily observed than production near an electron. To a first approximation, nuclear pair production per atom is proportional to Z^2 , and electronic production to Z , so heavy elements like lead are favorable for pair production.

3. The probability of nuclear pair production increases with the energy of the gamma ray.

4. Other processes of pair production are also possible, but are less prominent. For example, a pair can be produced by collision of a high-energy electron with a nucleus or an electron.

As to Annihilation. 1. When fast positrons strike any material, they produce ionization to about the same extent as negatrons of the same

speed. The mechanism is different since the positron *attracts* the negative electrons.

2. When the positrons have slowed down sufficiently, they join with planetary electrons, each one annihilating the other, with production of electromagnetic radiation.

3. Two gamma-ray photons are usually produced, for reasons of energy and momentum conservation (Fig. 11-16*b*). Thus the commonest process for positron destruction is *not* the inverse of the most frequent process of production. Usually a nucleus is not close by to accept momentum. Such acceptance is necessary if a single photon is emitted.

4. Exceptionally, the positron is caught by an electron so close to a nucleus that a single photon is emitted.

These discoveries, beautiful in their simplicity, emphasize the fact that gross matter can be considered as a form of energy in accordance with Einstein's equation 7, p. 33. They demonstrate that under suitable conditions radiant energy and matter energy are completely interconvertible. Let us now examine experiments that extend our knowledge of materialization and annihilation of matter.

★ High-energy gamma rays are able to produce photoelectrons and Compton recoil electrons, as well as positron-negatron pairs. Anderson allowed the 2.6-Mev rays of Th C'' to encounter a sheet of lead $\frac{1}{4}$ mm thick. He got about 1400 single negatrons, 100 single positrons, and 60 pairs. The single positrons are to be interpreted as members of pairs, the corresponding negatrons being too slow to struggle out of the lead. If both the positron and the negatron emerge from the lead, almost without exception the sum of their kinetic energies is below 1.6 Mev. Now, in pair production, the energy of the gamma-ray quantum is divided into several parts, as follows:

1. Rest energy of the negatron, m_0c^2 .
2. Rest energy of the positron, m_0c^2 .
3. Kinetic energy of the negatron, T_1 .
4. Kinetic energy of the positron, T_2 .
5. Kinetic energy of the nucleus in whose field the pair is formed.

The last term can be neglected, so we can write, for Th C'' gamma rays,

$$\begin{aligned} T_1 + T_2 &= h\nu - 2m_0c^2 \\ &= 2.6 \text{ Mev} - 1.02 \text{ Mev} = 1.6 \text{ Mev} \end{aligned} \tag{10}$$

This is the maximum kinetic energy to be expected; it applies to pairs formed at the surface of the lead. This simple theory gives a satisfactory account of the results.

Why does pair production occur only in the presence of a nucleus, or some other particle? The equations of energy and momentum conservation for pair production in empty space lead to physical inconsistencies. Before the pair is produced we have only a photon. For any photon, momentum over energy equals $1/c$. If the pair were produced in free space we would have only charged particles present. For any material particle momentum over energy equals $mv/mc^2 = v/c^2$, which is less than $1/c$. For any system of material particles, momentum over energy is less than $1/c$. Therefore, if energy is conserved momentum cannot be; that is, a pair cannot be produced unless there is some way to exchange energy with another particle or photon.

Working the argument backward, a positron and a negatron cannot combine to form a single photon without the intervention of another particle. However, energy and momentum can both be conserved if two quanta are produced. It is interesting to examine the case in which a positron and an electron collide, with energies so small that the momentum of the system can be set equal to zero. Then the pair of photons produced must have zero resultant momentum; that is, they must have equal energies and must travel in opposite directions. The energy equation is

$$2m_0c^2 = 2h\nu \quad (11)$$

Then $h\nu = 0.51$ Mev, and the wavelength of each photon is 0.024 Å. Radiation of approximately this frequency is produced when positrons impinge on matter. It is called *annihilation radiation*; it appears as a part of the "scattered rays" whenever hard gamma radiation is directed at a block of matter, and its nature was a puzzle until pair annihilation was understood. Thereafter, Thibaud focused known currents of positive electrons on foils of heavy metal, and thus determined the average number of photons produced by the annihilation of a positron and an electron. The results are rough, but the number is close to *two*, in agreement with the above ideas.

★ **Positronium.** Ruark and also Saha called attention to the possible transient existence of an atom composed of a positron and an electron (Fig. 11-17). The name "positronium" was suggested. The spectrum lines of this interesting configuration lie at wavelengths about twice as great as the corresponding lines of atomic hydrogen. The reason is that the reduced mass is substantially one-half the reduced mass for a hydrogen atom. Wheeler discussed the lifetime of such a combination, which would decay by self-annihilation. He showed that the lifetime depends strongly on the relative orientation of the spins of the two particles. If their spin angular momenta are antiparallel, the life is very short,

but if they are parallel it is about 10^{-7} sec, for the lowest state, because selection principles come into operation. Then decay can only occur by the emission of three photons (rather than two), and this is a relatively improbable event. Deutsch has demonstrated the presence of positronium in nitrogen gas through which positrons are passing. This advance has led to much research because the properties of positronium offer an opportunity to check some very fine details of the quantum theory of two-particle systems.

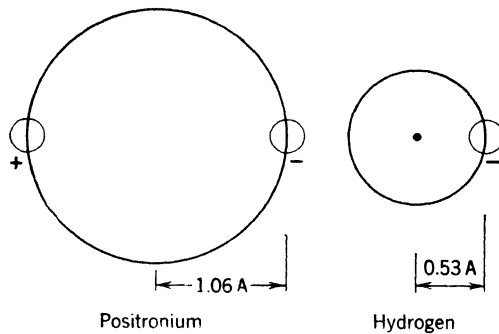


Fig. 11-17. Comparison of positronium with the hydrogen atom. The energy levels of positronium are half as far apart as those of hydrogen, and so the first line of its Lyman series would be at 2430 Å. The orbital radius is twice as great as the value for hydrogen.

★ **Slight interaction of two photons.** In a process inverse to two-quantum annihilation, two gamma rays would collide, producing a pair. This process should exist, but theory shows that it would be very infrequent. Still, its *possibility* proves the existence of an interaction between photons, requiring very tiny corrections to the electromagnetic theory of light.

Dirac's theory of positrons and negatrons. Before the discovery of the positron, Dirac had predicted its existence, in a certain sense. He had discovered a set of equations governing the behavior of the electron, which are now recognized as fundamental. We know from ordinary mechanics that a free electron can have any total energy equal to or greater than its rest energy m_0c^2 ; but it is a consequence of Dirac's equations that it can equally well have a *negative* energy value of $-m_0c^2$ or any lower value down to negative infinity. Furthermore, if we apply a force to an electron of negative energy, that is, negative mass, it will move in a direction exactly opposite to that in which an ordinary electron will move.

Dirac boldly assumed that, in addition to negative electrons of positive

energy as we know them in matter, all space is almost uniformly filled with negative electrons of negative energy, and that we are not ordinarily aware of them simply because they are everywhere. Suppose, however, that a gamma-ray photon of energy greater than $2m_0c^2$ encounters one of these electrons and changes its energy from a negative value to a positive value greater than m_0c^2 . Then it will speed away, leaving behind it a tiny hole in the all-pervading sea of negative charge. What shall we say of such a hole? The absence of negative charge will appear to us as a positive charge; the hole will be a positron.

In this way, at one fell blow, Dirac gives a plausible explanation of the existence of two kinds of electric charge, and an illuminating interpretation of pair production. His concept, though revolutionary, has been

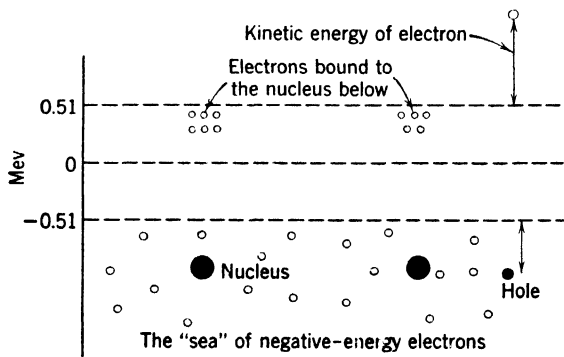


Fig. 11-18. Dirac's hole theory.

useful in theoretical physics. Figure 11-18 helps to visualize the hole interpretation, but must not be taken too seriously. The abscissa is meant to represent all the coordinates of ordinary space, while the ordinate represents electron energy. Positive-energy states are filled at only a few locations, where we have a free electron, or electrons bound to a nucleus. The latter have total energies lying somewhat below m_0c^2 , since their potential energy is negative. At the right we show a hole in the body of negative-energy electrons, produced by a gamma ray which approached a nucleus. The diagram is not meant to show the energies of these nuclei; they are simply placed at random. It must be clearly understood that this picture is *alternative* to the simpler one in which there *is* no filled-up sea of negative-energy electrons. On the latter view, pair production is simply the creation of an electron of positive energy and another of negative energy.

★ **The magnetic moment of the electron.** On p. 198 we discussed the angular momentum of the electron. A charged body that is spinning

is equivalent to a system of circular currents, and should have a magnetic moment proportional to its angular momentum, $h/2\pi$. Experiments on the spectra of atoms in a magnetic field indicate that the electron has a magnetic moment, and that its magnitude is

$$M = \frac{h}{2\pi} \frac{e}{2m_0c} \quad (12)$$

$$= (1.04 \times 10^{-27}) \frac{4.8 \times 10^{-10}}{2(9 \times 10^{-28})(3 \times 10^{10})} = 9.2 \times 10^{-21} \text{ erg/oersted}$$

This quantity is called the *Bohr magneton*. It is possible to construct a classical model of a spinning electron which will have an angular momentum of $h/4\pi$ and a magnetic moment of 1 Bohr magneton. Abraham showed, in fact, that we can vary the ratio of angular momentum and magnetic moment within wide limits by changes in the model. But such models are out of favor. It is a great merit of Dirac's theory that it predicts the correct spin and magnetic moment of the electron without making any mention of a model.

5. The Neutrino

Further discussion of beta-ray spectra. On p. 284 we discussed evidence for the view that a neutrino is emitted in beta decay. We saw that disintegration electrons emerge from the nucleus with any energy from zero up to a certain maximum value, E_{\max} . Three types of explanation have been considered at various times:

1. The difference between E_{\max} and the energy of a particular electron may be carried away by a particle of small mass, no charge, and high penetrating power, capable of escaping observation in the experiment of Ellis and Wooster.

2. All parent nuclei and all daughter nuclei have identical energies, but the law of conservation of energy may not hold during beta decay.

3. The parent nuclei (and/or daughter nuclei) are not all identical in energy content, even though we have failed to detect any differences of behavior associated with this energy difference.

As to (3), there is good evidence that the energy levels of the beta emitter and the daughter nucleus are sharply defined, and that they are separated by an energy difference $m_0c^2 + E_{\max}$.

★ Figure 11-19 shows a case well adapted to prove this. Scandium 46 exists in either of two energy levels. The more energetic form passes into the other by emission of a gamma ray, 0.18 Mev. From the lower level beta decay occurs in *two* ways, and emission of gamma rays of the daughter nucleus follows. There are two superimposed beta-ray spec-

tra, with upper limits of 0.36 Mev and 1.49 Mev. But the difference between these two numbers is equal to the energy of the 1.12-Mev

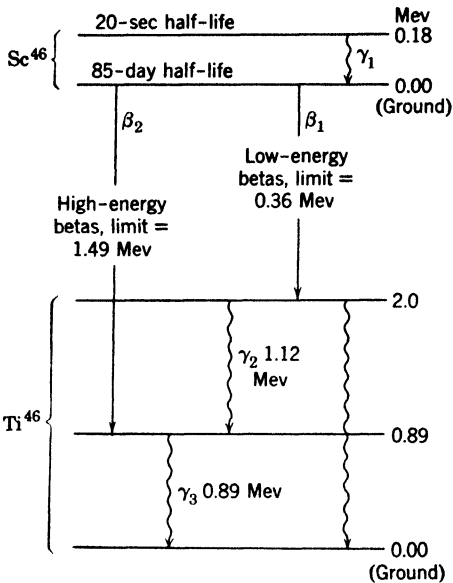
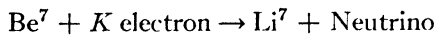


Fig. 11-19. Beta and gamma rays of the decay of scandium 46. Beta emission may leave the daughter atom, titanium 46, in either of two energy levels. The gamma ray labeled γ_2 has an energy equal to the difference between the upper limits of the two beta-ray spectra.

gamma ray of the daughter nucleus. Further, Journey showed that this gamma ray is emitted only when a slow beta ray has occurred. We must infer that the initial and final energy levels are at least as well defined as the energies of the highly monochromatic gamma rays.

Detection of the neutrino.

Attempts have been made to detect collisions of neutrinos with electrons, or with protons, by means of ionization chambers; all have failed. There is, however, direct evidence for their production, obtained by J. S. Allen. To understand his method, we must describe *K capture*. In some cases a nucleus is able to absorb a *K* electron of the atom in which it resides, and in the process a neutrino is emitted. An example is

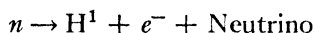


The method of detection usually depends on the fact that, after the *K* electron has been imprisoned, there is a vacancy in the *K* shell, so that the *K*-series X-rays of the daughter atom are emitted; but this does not, in itself, show the presence or absence of a neutrino. What Allen looked for was the recoil of the Li^7 nucleus, whose momentum should be equal to that of the neutrino. Because of the low mass of lithium, the recoil energy should be 58 ev, which makes the direct detection of the recoil nuclei feasible. In this difficult experiment Allen observed recoil nuclei with energies up to about 45 ev. Why cannot the evidence be strengthened by exposing Li^7 to neutrinos and demonstrating the production of Be^7 ? Computation shows that the effects would be too minute for detection by present methods. The success of Allen's experi-

ment is just as good evidence for the existence of the neutrino as would be the demonstration of its direct capture by lithium.

Properties. The rest mass of the neutrino is dependent on the exact shape of curves showing the distribution of beta-ray energies (p. 284). Study of these shapes for various cases of beta emission does not permit an accurate mass determination, but it is clear that the hypothetical mass of the neutrino must be quite small compared with the electron mass. Often it is assumed that the mass is zero.

The neutron decays (Section 6) according to the scheme



The neutron, proton, and electron all have the spin 1/2. The reader may convince himself that the only possible value for the spin of the neutrino is 1/2, unless we assume that the proton and the electron have orbital angular momentum around the mass center, which is unlikely. Consideration of many other cases supports the value 1/2.

We may think of the neutrino as an elusive first cousin of the photon. It probably moves with the velocity of light. It obeys the Pauli exclusion principle; the photon does not. It interacts with an electron and a nucleus jointly, but we have no experimental evidence of its independent interaction with electrons or with nuclei individually.

6. The Neutron

Discovery. In 1930, Bothe and Becker found that, when alpha particles from polonium fall on beryllium or boron, a very penetrating radiation is emitted. Naturally they assumed that this was gamma radiation of very high energy. M. and Mme. Curie-Joliot observed that this radiation is able to eject protons from material containing hydrogen. They thought the protons were recoils produced by scattering of photons. In 1932, Chadwick pointed out that the frequency with which protons are ejected is thousands of times greater than that predicted by wave mechanics, and that the assumed gamma radiation of beryllium would have to possess a quantum energy of 50 Mev. These difficulties led him to assume that the recoiling protons are produced by material particles of great energy.

The problem that confronted him was the measurement of their charge and mass. He made experiments that showed clearly that they are neutrons, possessing no detectable charge, and having a mass nearly equal to that of a proton. A disk carrying polonium was placed close to one of beryllium, so that the latter was bombarded by great numbers of alpha particles, as in Fig. 11-20. Behind the beryllium was an

ionization chamber closed by a sheet of gold foil. The amplified output of this chamber operated an oscillograph. Each ionizing particle which entered the chamber caused a definite deflection of the oscillograph element, recording the occurrence of several heavily ionizing particles per minute. It was assumed that these were atoms of nitrogen or oxygen set in motion by the neutrons. They arose from the air between the beryllium and the chamber, or in the chamber itself, and their maximum velocity was about 4.7×10^8 cm/sec. Feather soon confirmed this

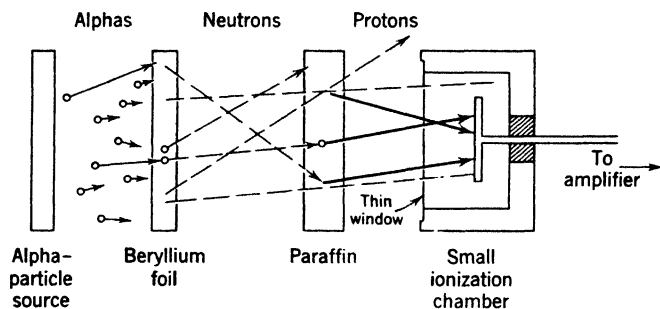


Fig. 11-20. Chadwick's apparatus for discovery of the neutron.

assumption by cloud-chamber observations of the recoiling nuclei. Chadwick placed a sheet of solid paraffin between the beryllium and the ionization chamber, and the number of deflections per minute was *increased*, the increase being due to protons ejected from the paraffin. The protons thrown directly forward had a range of 40 cm in air, which corresponds to an initial velocity of 3.3×10^9 cm/sec, or an energy of about 5.7 Mev. From these two sets of data on nitrogen, oxygen, and protons, referring to head-on collisions of the fastest neutrons, we can get their mass M and their maximum velocity V , since momentum and energy are conserved. From Chadwick's result it became clear that the reactions producing the neutrons from beryllium and boron are



This opened up a better way to obtain the neutron mass, M . Mass is conserved, provided that we take into account the mass equivalent of the kinetic energies of all moving particles (p. 33). Let us write T_α for the mass equivalent of the alpha-particle energy and similar symbols referring to the other particles. Then, in the case of boron, letting an atomic symbol stand for the rest mass thereof, we have

$$\text{B}^{11} + \alpha + T_\alpha = \text{N}^{14} + T_{14} + M + T_n \qquad (13)$$

The masses B^{11} , α , and N^{14} are obtained from mass-spectrograph results; T_α is found from the range of the alpha particle; and T_{14} and T_n are computed from the fact that energy and momentum are conserved in the collision, so we know everything except M . Chadwick found the value 1.010, and the presently accepted value is 1.00894. The neutron is definitely heavier than the proton for which the current value is 1.00812. These results are on the "physical" scale in which the mass of O^{16} is exactly 16.

The neutron as a nuclear building stone. Before the discovery of the neutron it was supposed that the nucleus is composed of protons and electrons, and that many of these are grouped into alpha particles. The alpha particle was thought of as a very stable aggregate of four protons and two electrons. Lithium 6, for example, was described as an alpha particle, two protons, and one electron. This view was suggested by the emission of alpha and beta particles from the heavy radioactive elements, but it failed when attempts were made to draw conclusions as to the behavior of electrons in the nucleus. For example, before Chadwick's discovery, a number of writers suggested the existence of the neutron. Langer and Rosen pointed out that an electron might be able to combine closely with a proton, forming a system of nuclear dimensions. If so, energy would be emitted, and because of the equivalence of mass and energy the mass of the neutron would be less than the sum of the electron and proton mass. However, this prediction does not agree with fact.

★ It is possible to show that electrons cannot exist in the nucleus, provided that the usual principles of quantum mechanics can be applied. There is a theorem, related to the uncertainty principle of p. 179, which says that, if a particle is confined in a region whose radius is X , its average momentum p will be at least as large as $h/4\pi X$. For the heaviest nuclei the radius is about 10^{-12} cm, and the corresponding value of p is about 5×10^{-16} gm cm/sec. From equation 4 on p. 419 we find that the kinetic energy of such an electron would be about 9.0 Mev. For smaller nuclei, much greater values would be encountered. We have no inherent objection to the occurrence of such large kinetic energies, for the field of nuclear force *might* be such as to hold the lively electron in spite of its great momentum. However, the accelerations of the electron in its encounters with the heavy nuclear particles should give rise to intense radiation or to pair production, at the expense of the energy of the electron. Thereby its momentum would quickly be reduced. The de Broglie wavelength would grow to values exceeding nuclear dimensions, and the electron simply could not remain long in the nucleus.

The discovery of the neutron relieved this difficulty, for it led to the view that the nucleus is composed entirely of neutrons and protons. The alpha particle, for example, is thought of as two protons and two neutrons. The question then arises: How can electrons and neutrinos be emitted? The answer, crudely speaking, is that they are manufactured at the moment of emission. Heisenberg put forward the view that a neutron in the nucleus can sometimes be transformed into an electron, a neutrino, and a proton, after which the two light particles escape. The idea may be made clearer by considering the birth of a planet. Before its material separates from the parent sun, one cannot say the planet exists, as such. Similarly, one cannot say that a neutron within the nucleus contains an electron, neutrino and proton, even though it may split up into these particles.

We like to deal with the nucleus *as though* it were an aggregation of neutrons and protons, even though we realize that it may be more correct to treat the nucleus as a melting pot in which these particles lose their identity to a certain extent.

★ **Chief methods for producing neutrons.** There are so many reactions for neutron production that the choice of a method depends on yield and on the neutron energy desired. Some reactions yield a wide spectrum of energies, and others supply us with monoenergetic neutrons. Increasing the energy of the bombarder naturally shifts the neutron energies upward. Table 11-1 lists some of the more important reactions. The energy figures refer to conditions easily employed in cyclotron laboratories. Yields depend greatly on the bombardment energy.

TABLE 11-1. Neutron Production

Reaction	Approximate Neutron Energies; Yields; Remarks
$\text{H}^2(d, n)\text{He}^3$	2.4 Mev. Heavy-ice target. No gamma rays are emitted. Yield is large at relatively low deuteron energies, a few hundred kev.
$\text{Be}^9(d, n)\text{B}^{10}$	0.9 Mev at bombardment energy of 5 Mev. Great yield.
$\text{Li}^7(d, n)\text{Be}^8$	0-20 Mev. Large yield.
$\text{H}^2(\gamma, p)\text{H}^1$	Monoenergetic neutrons, Energy = $h\nu - 2$ Mev. Small yield.
Fission in piles	0-3 Mev. Presence of slowing material reduces neutrons to low velocities.

Roster of the interactions of neutrons with matter. The behavior of neutrons in gross matter depends greatly on their velocity.

They do not interact with electrons to any extent that is easily measured. The only force between a neutron and an electron is the interaction of their magnetic moments, so far as we can see at present. But the neutron interacts strongly with protons and other neutrons, showing the existence of nuclear fields distinct from the familiar electromagnetic ones (p. 375).

As neutrons slow down by collisions with nuclei they pass through different ranges of velocity, corresponding to different patterns of behavior. While no exact boundaries can be defined, it is convenient to use the following adjectives:

Fast	1-10	Mev
Intermediate	0.001-1	Mev
Resonance	0.05-1000	ev
Thermal	0.025-0.05	ev

(The words "slow neutron" are ambiguous in present practice. Sometimes the thermal region is meant; sometimes the term includes the region up to several electron volts. We shall use it in the second sense.) The main reason for the change of behavior as neutrons slow down is change of the de Broglie wavelength, relative to the dimensions of the nucleus. The wavelength runs from the order of nuclear dimensions up to values of several angstroms. Table 11-2 is useful in understanding much that follows.

TABLE 11-2. Properties of Neutrons at Various Energies

Energy	Speed (cm/sec)	Time To Go 1 m (μ sec)	Wavelength (angstroms)	Approximate Number of Proton Collisions Needed to Reach Thermal Velocity
1 Mev	1.4×10^9	0.072	3×10^{-4}	25
1000 ev	4.4×10^7	2.3	9×10^{-8}	15
1 ev	1.4×10^6	72	0.29	5
0.025 ev (thermal)	2.2×10^5	460	1.8	—
0.01 ev	1.4×10^5	720	2.9	—

★ 1. The fast and intermediate regions. The chief interactions with nuclei in approximate order of decreasing importance are these:

(a) Scattering (and energy loss) in elastic collisions. In substances of low average atomic mass like paraffin or water, the scattering process is tremendously effective in reducing the speed to thermal values. On the average, a neutron loses half its energy in a collision with a proton.

(b) Capture by nuclei with ejection of particles, or gamma rays. The nuclei formed may be either stable or radioactive.

(c) Inelastic scattering, resulting in excitation of the nucleus. Not a prominent effect except in some heavy elements.

For the intermediate region, the phenomena are the same, except that the energy may not be sufficient for production of many nuclear reactions, and inelastic scattering should be omitted.

★ **2. Resonance region.** When a neutron approaches a nucleus there is no Coulomb barrier to oppose its entry. In fact, the nucleus attracts it. *When the total energy of the system matches an excited quantum state of the nucleus produced by the capture, the probability of successful entry rises to high values.* The nucleus and the neutron are “in tune,” and the cross section for capture may rise to hundreds or thousands of barns (p. 305), a value tremendous compared with the “geometric” cross section. This is called resonance capture. How the cross section varies with speed is illustrated in Fig. 11-21*a*, referring to cadmium.

★ **3. Thermal region.** If resonance capture does not occur the neutron slows down until it comes into thermal equilibrium with the medium. Here the cross section for capture usually varies with $1/v$, as in Fig. 11-21*b*, referring to boron.

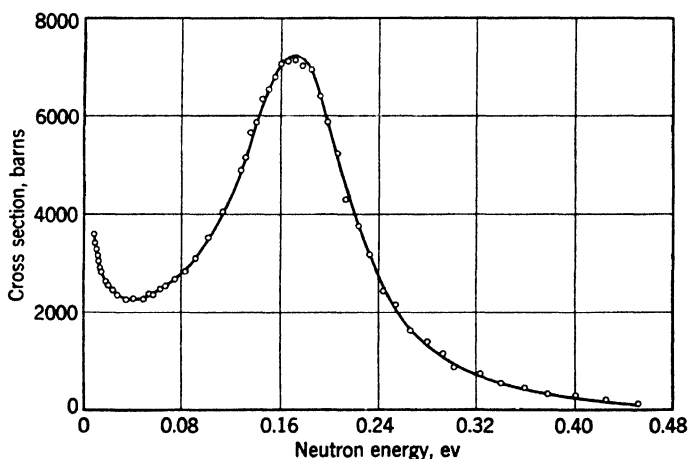


Fig. 11-21(*a*).

Fig. 11-21. The slow neutron cross sections of (*a*) cadmium, showing strong resonance, and (*b*) boron, the latter showing the inverse velocity relation associated with absence of a low neutron level in the compound nucleus. The large cross section of boron is due to the isotope 10. The time of flight of the neutrons (over a fixed distance) is, of course, proportional to the reciprocal of the velocity. The order of magnitude of the energies is indicated. (After Rainwater, Dunning, et al.)

Eventually the neutron will be absorbed. Junction with a nucleus is the normal fate. We now consider these matters in more detail.

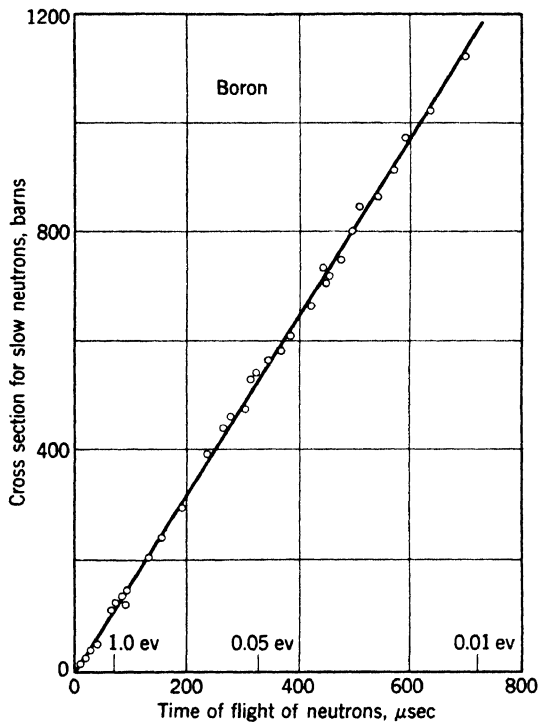


Fig. 11-21(b).

Neutron scattering. 1. *The Interaction with Electrons and with Nuclei.* The almost complete failure of the neutron to interact with electrons is shown by cloud-chamber investigations. It is comparatively easy to obtain large numbers of tracks produced by atoms recoiling from neutrons, because the neutron itself produces almost no ions at all in traversing an expansion chamber of ordinary dimensions. Dee states that the ionization along the path of a neutron is less than one ion pair in 3 m of air. Accordingly, vast numbers of neutrons may be allowed to enter a Wilson chamber during the time of photographic exposure, so that there is a fair chance of photographing a recoil nucleus (Fig. 11-22) in each expansion.

2. *Scattering Experiments.* Outstanding early work in this field was done by Dunning, Pegram, Fink, and Mitchell, at Columbia. In many of the experiments the arrangement shown in Fig. 11-23 was used. The

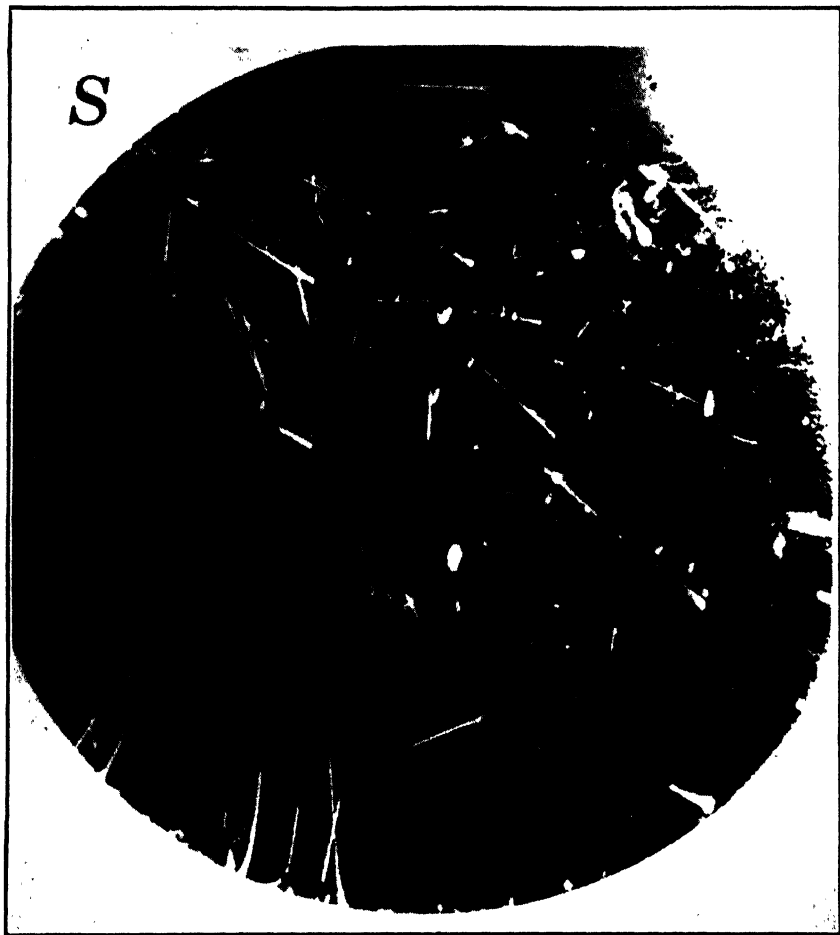


Fig. 11-22. Recoil protons produced by neutrons with energy of about 2.4 Mev (after Dee and Gilbert). The source is at the upper left.

source is a glass tube *N* packed with beryllium filings, and filled with the radon obtainable from several grams of radium. A platinum container surrounds the source, and a block of lead *G* cuts down the gamma radiation emitted toward the scattering block *S*. *P* is a paraffin block, from which protons are ejected by the neutrons that strike it, and the detector *C* is a shallow ionization chamber, attached to an amplifier, which operates an oscillograph and also a mechanical counter. The electric system is designed so that spurts of ionization due to protons (Fig. 11-24) can be distinguished from stray effects. All parts of the

apparatus are supported on wires or thin rods to reduce the effect of neutrons scattered by nearby objects.

A block of paraffin 3 to 4 cm thick scatters about half the fast neutrons by amounts sufficient to keep them from reaching the ionization cham-

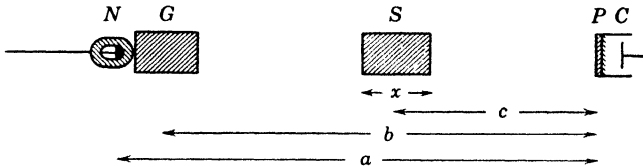


Fig. 11-23. Dunning's apparatus for studying scattering of neutrons.

ber. From the scattering data one calculates the mean free path of a neutron and the scattering cross section (p. 303).

3. *The Fast Scattering Cross Section.* For neutrons with energies of 1 Mev or more the scattering cross section of medium and heavy nuclei is roughly πR^2 , where R is the nuclear radius. The condition for thus neglecting the wave nature of the neutrons and using the "geometric cross section" of the obstacle is that R shall be large compared with $\lambda/2\pi$, where λ is the de Broglie wavelength. At 1 Mev, $\lambda/2\pi$ is 5×10^{-13}

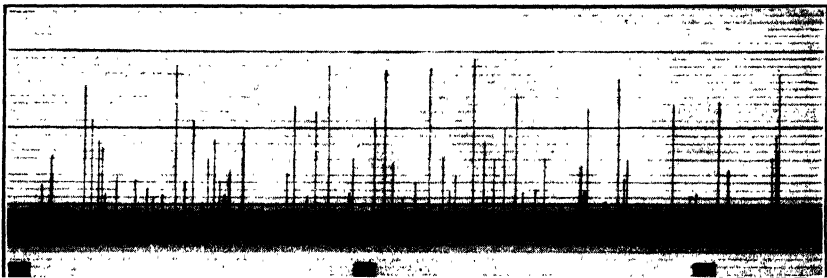


Fig. 11-24. An oscillograph record of kicks due to protons recoiling from neutrons (after Dunning). The film moved horizontally. Each proton entering the ionization chamber deflected the oscillograph mirror by an amount proportional to the number of ions produced. Each vertical line is the record of such a deflection.

cm. Several lines of evidence give the following formula for the nuclear radius:

$$R = 1.5 \times 10^{-13} A^{1/2} \quad (14)$$

If A , the atomic mass, is 33, R barely exceeds $\lambda/2\pi$, and the condition above is not very well satisfied. Still, the above formula yields cross

sections which agree well with experiments on fast neutrons in the medium and heavy domains. The fast scattering cross section goes from 1.6 to 5.3 barns as the atomic number goes from 1 to 82.

The capture of neutrons by nuclei can be studied by measuring their absorption in solid spheres surrounding the neutron source. The results show that scattering of fast neutrons is a much more frequent phenomenon than their capture.

4. *Angular Distribution of Scattered Neutrons.* If, in a cloud-chamber experiment, the direction of flight of the neutrons is known, one can measure the angle A between this direction and the track of each recoil nucleus (Fig. 11-25). Then the angle B through which the neutron is scattered can be computed by using the equations expressing the conservation of energy and of momentum. For many of the elements, the relative numbers of neutrons scattered at various angles agree fairly well with those that would be obtained if the neutron and the struck nucleus behaved like hard spheres.

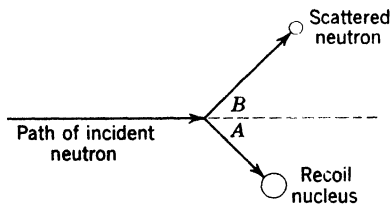


Fig. 11-25. Elastic collision between a neutron and a nucleus. Only the track of the nucleus is seen in a cloud-chamber photograph.

5. *How the Energy Distribution of a Neutron Source Can Be Obtained.* From the range of the recoil nucleus its velocity can be obtained, using the known relation between range and velocity for a particle of given charge and mass. Then the velocity of the scattered neutron can be computed from our knowledge of the angle B and the fact that momentum must be conserved in the collision. Finally, calculating the kinetic energies of the scattered neutron and the nucleus, their sum gives us the *kinetic energy of the incident neutron*. Among the neutrons from a Po-Be source (i.e., beryllium bombarded with alpha particles from polonium) we find some neutrons with energies up to 12 Mev, a strong group with maximum energy of 4.8 Mev, and several groups of lower energy.

Slowing down. In an elastic collision with a nucleus of mass M , a particle of mass m retains only a part of its energy. Let us treat both of them as hard spheres, using classical mechanics (p. 300). Considering all types of collisions, from head-on to glancing, the average value of the final energy over the initial energy is found to be

$$F = 1 - \frac{2mM}{(M + m)^2} \quad (15)$$

We may as well use atomic masses. Putting $m = 1$ for the neutron, we obtain the following illustrative values of F :

H	C	O	Pb
$F = 0.5$	0.858	0.889	0.9904

After ten collisions with protons, the neutron energy would be down by a factor of 1000, while after ten collisions with lead the loss is only a few per cent. Thus we can see the great influence of atomic weight on the behavior of neutrons, diffusing from a point source in a body which is large compared with the scattering free path.

The farther they go, the slower they are. Other things being equal, a low value of M makes the material very effective in slowing the neutrons down to those velocities at which they can easily be absorbed. In getting rid of neutrons, *low M and high absorption coefficient at low velocities are the two prime factors.* Paraffin and water are commonly used as slowing agents. When the neutrons have been brought to thermal velocities, thin tubes and slotted sheets of cadmium permit us to form neutron beams. Those that hit the cadmium are strongly absorbed by it. By the operation of chance, some fast neutrons fail to lose much energy in a slowing medium. Then cadmium does not stop them. A slow neutron beam is always contaminated with this fast residue.

An Illustration. After n collisions, the energy retained by a neutron would be

$$E' = E_0 F^n$$

if the average loss occurred in every collision. Thus,

$$\log (E_0/E') = n \log (1/F)$$

We wish to know what thickness of carbon will be necessary to slow 2-Mev neutrons down to 1 ev. Consider the unfavorable case in which all scattering angles are fairly small. Assume a scattering free path of 0.15 cm; then we need a thickness somewhat less than $0.15n$ cm, or

$$T = \frac{(0.15) \log (2 \times 10^6)}{\log (1/0.86)} = \frac{(0.15)(6.3)}{0.064} = 15 \text{ cm, approximately}$$

In actuality, the mean scattering path decreases as the velocity goes down. We have used a rough average path to obtain an approximate answer.

The resonance region and the slow region. The greatest resonance cross sections occur when the resonance energy is low. Cadmium

has a very low resonance (as such things go), lying at 0.18 ev. Figure 11-21 shows that the cross section below this resonance never falls below 2000 barns, so Cd is a very effective absorber of thermal neutrons. Boron is a second strong absorber of interest. It has been found that the absorption cross section of boron is proportional to $1/v$ over a wide range—from 0.01 to 50,000 ev. It is, in fact, given by

$$S_a = 118/E^{1/2} \text{ barns}$$

with E expressed in electron volts. Therefore, observations of the absorption of slow neutrons in boron provide a means for measuring their energy.

★ The proportionality of the cross section to $1/v$ is predicted by a theory of Breit and Wigner, for any case in which there is no resonance near the region of interest. The resonances occur more or less at random as we ascend the periodic system. For any isotope there may be several, and several isotopes of a given element may have them. The result is irregular variation in the behavior of the elements toward slow neutrons.

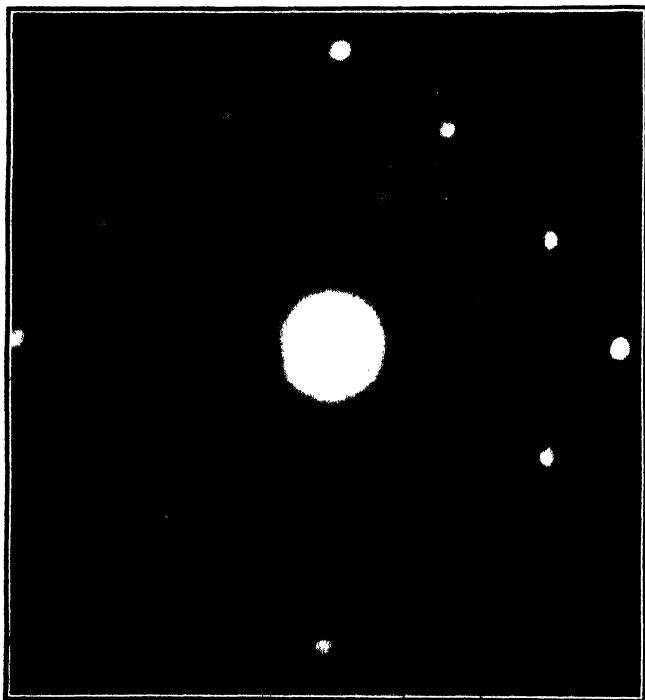


Fig. 11-26. Laue pattern for NaCl, illustrating the diffraction of neutrons by the crystal lattice. (After Shull, Marney and Wollan.)

The task of measuring the neutron scattering and absorption cross sections of separated isotopes is still in progress, and the methods used are interesting. For the range from a few thousand electron volts up to millions of volts, carefully controlled high-voltage generators are used to bombard targets which yield monoenergetic neutrons. For slow neutrons the methods are the crystal spectrometer and the velocity spectrometer.

Mitchell and Powers showed in 1936 that neutrons are diffracted from crystals according to the Bragg formula, just as though they were X-rays. Thus a beam of neutrons having a range of velocities can be spread into a velocity spectrum by reflecting them from a crystal. The wavelength is, of course, computed from de Broglie's relation. From Table 11-2 we see that for slow neutrons it lies in a convenient region. A Laue pattern obtained by Shull, Marney, and Wollan at Oak Ridge is shown in Fig. 11-26. Work like this requires the neutron intensity provided by a reactor. Neutron diffraction is used to deal with certain obstinate problems of crystal structure. The *X-ray* scattering power of light elements is very small; in contrast the neutron is strongly scattered by light elements. Thus it is possible with neutrons to determine the positions of the hydrogens and other light atoms in ice and in organic compounds.

A second method for sorting out the effects of a heterogeneous beam of neutrons is the velocity spectrometer. In the simplest form (Fig. 11-27) two cadmium disks provided with slots rotate on a common axle. Their speed of rotation can be varied. Neutrons pass a fixed slot and fall on the first disk. When a moving slot passes by the fixed slot, a bunch of neutrons passes through. Suppose it contains three groups, *S*, *M*, and *F*—slow, medium, and fast. They spread out in space as they go toward the right. The rotation speed can be so adjusted that the *F* group arrives too early to get through the second moving slit. The *M* group gets through, and the *S* group arrives too late. (If the source is a cyclotron, another method is used. The cyclotron is pulsed, that is, made to operate intermittently for very brief periods; and a detector, placed a suitable distance away, is arranged to be sensitive only during slightly later periods, to record neutrons in a small speed range.)

Spontaneous disintegration of the neutron. It has long been assumed that the neutron and proton are not unbreakable or fundamental particles, and that the neutron should be able to form a proton, an electron, and a neutrino, by beta decay. From the masses in Appendix 2, the maximum kinetic energy of the electrons should be about 0.8 Mev, computed as follows:

Mass difference of neutron and proton	0.00136 mass unit
Rest-mass of electron	0.00055 mass unit
	<hr/>
Kinetic energy	0.00081 mass unit
Equivalent to	0.755 Mev

A very recent evaluation of the data leads to the figure 0.782 Mev. Rough calculations indicated that the half-life might be of the order of 10 min or more. This time is large enough to make the experiment of measuring it very difficult, even when the strong beam of slow neutrons from a pile is employed.

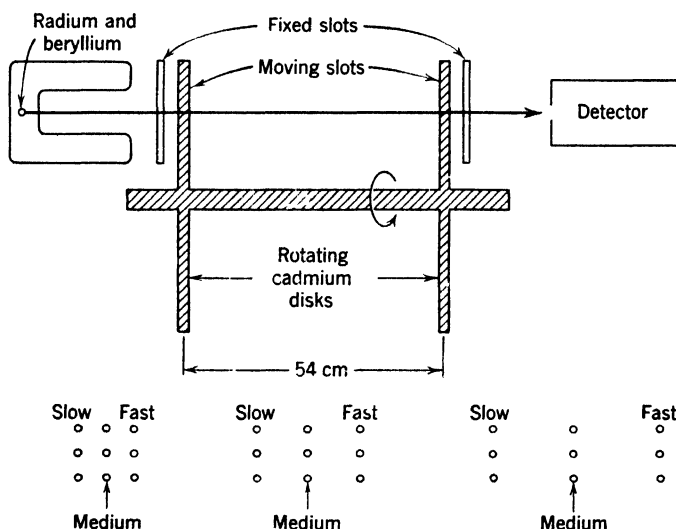


Fig. 11-27. Velocity spectrometer for determining scattering and absorption cross sections of relatively slow neutrons. At the foot, we illustrate the separation of slow-, medium-, and high-speed neutrons as they travel.

Neutron decay has recently been demonstrated (1951). Snell, Pleasanton, and McCord (aided earlier by Shrader, Saxon, and Miller) employed thermal neutrons from the Oak Ridge graphite pile, while Robson used the pile at Chalk River, Canada. The thermal neutron beam passes through a semicylindrical electrode, as indicated in the diagram of Snell's apparatus in Fig. 11-28. In his case, protons from neutrons decaying in flight are caught by an electron-multiplier tube above, while a portion of the decay electrons passes through coincidence counters *A* and *B*. Coincidences between *AB* and the proton counter

are looked for. It is necessary to delay the action of the circuits recording the output of *A* and *B*, because the protons take about $0.25 \mu\text{sec}$ to pass from the neutron beam to the proton counter. In Robson's experiment, two magnetic spectrographs were suitably placed, to receive the protons and the electrons, respectively. He was able to determine the

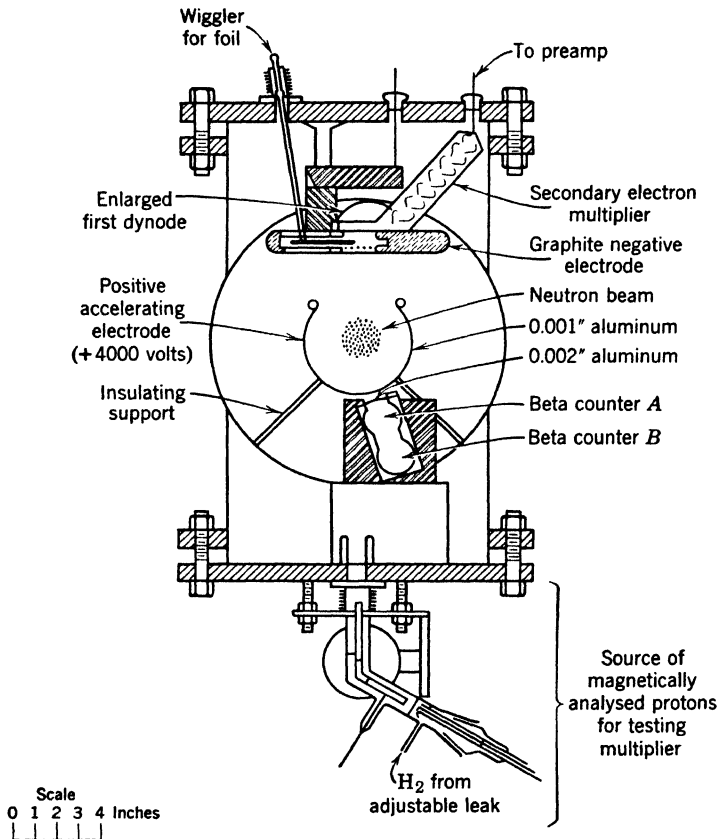


Fig. 11-28. Apparatus of Snell, Pleasanton and Miller, for detecting the beta decay of the neutron [reproduced from *Phys. Rev.* **78**, 310 (1950)].

shape of the beta-ray spectrum, which agrees well with expectations (see p. 284). His value for the end point is $0.782 \pm 0.013 \text{ Mev}$. The half-life is between 10 and 30 min according to Snell. Robson's value is $12.8 \pm 2.5 \text{ min}$.

The reader will appreciate that this decay is suppressed when the neutron is in a stable nucleus. The detailed understanding of the suppression is a challenge to theoreticians.

7. Pictorial Summary

To conclude this chapter we present Fig. 11-29, which may help the reader to visualize the spin, charge, and mass relations of most of the known elementary particles. In considering reactions between them, certain general principles can be kept in mind:

1. Conservation of charge.
2. Conservation of energy.
3. Conservation of angular momentum.
4. Conservation of the statistical character of the system.
5. Conservation of parity.

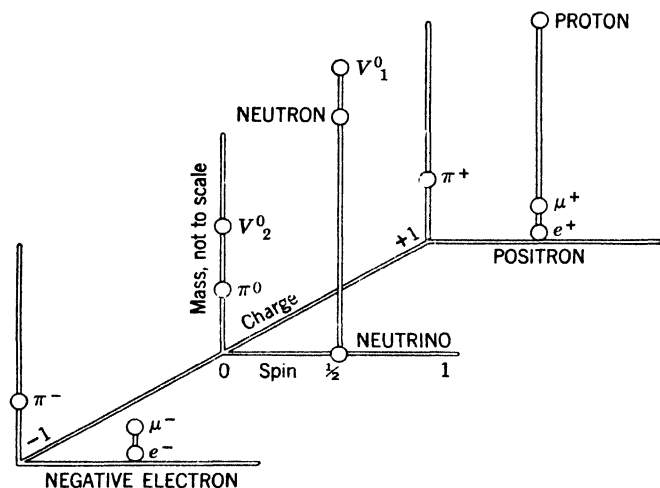


Fig. 11-29. A model for visualizing the spins, charges, and masses of the better-known elementary particles.

The last two items have not been mentioned before. Let several particles of Fermi type and of Bose type (p. 262) react, forming others in the process. Let the number -1 be assigned to each particle of Fermi type, and the number $+1$ to each Bose-type particle. Then the product of these numbers for a system of particles determines the statistical character of the system, and the rule is that *in a reaction the statistical character of the system is unaltered*. For example, if a positron and an electron annihilate each other, giving rise to two photons, the initial character is

$$-1 \times -1 = +1$$

because each of the reactants is a Fermi particle. For the two photons, the character is

$$1 \times 1 = +1$$

Again, when a neutron disintegrates, the initial statistical character is -1 . Suppose that the products were merely a proton and a negative electron; then the final character would be $+1$. This is forbidden, so an additional particle must be formed. It must obey Fermi statistics, so that the character of the system after reaction may be

$$-1 \times -1 \times -1 = -1$$

In this way, we conclude that the neutrino must be a Fermi particle.

Let us now consider the quantity called parity. It happens that the wave function of any particle either stays the same when we pass from a point x, y, z to a point $-x, -y, -z$, in Fig. 11-29 or else it changes sign. In the former case the parity is even, in the latter case, odd. Now the parity of any system of particles is defined as the product of the parities of the particles it contains. When old particles disappear and new ones are born, the parity of the system must remain the same. For example, an electron making a close collision with a positron has odd parity; similarly for the positron. The system's parity is even. If this pair gives rise to two photons, the parity for the photons should be even, and so it is, because each photon has even parity. In this case we arrive at the same result which was obtained by considering the statistical character. But the conservation of parity must not be confused with the conservation of statistical character. The principle of parity is capable of forbidding certain types of reactions which might be expected to occur if only the other four principles were considered.

The reader will note the general emptiness of Fig. 11-29; we have, so far, no indication that particles of spin 1 occur in Nature, except that certain theories yield this value for the photon.

REFERENCES

Appendix 9, refs. 34, 60, 88, 91, 98, 111.

PROBLEMS

1. How can a gamma-ray photon be responsible for a track in a Wilson cloud chamber? (Describe the *atomic processes* involved.)
2. A certain alpha particle produces 100,000 pairs of ions in the ionization chamber of a linear amplifier. If all the ions of one sign could be collected by the electrode connected to the grid of the first tube, how much charge would it receive? What would be its change of potential if its capacity is 6 micromicrofarads?
3. The effective collision cross section of a certain neutron moving through hydrogen at 0°C and 76 cm pressure is $2 \times 10^{-24} \text{ cm}^2$. What is its mean free path? (Remember that there are two protons in each molecule, and allow for the motion of the molecules by using equation 14 on p. 17.)

4. What thickness of lead is required to reduce the intensity of hard gamma rays from thorium C'' to one-hundredth of their original intensity? For the absorption coefficient, use the value 0.45 cm^{-1} .

5. What is the closest distance of approach of a radium C' alpha particle to a uranium nucleus in a head-on collision?

6. What must the wavelength and energy of a gamma ray be, if it is barely able to produce a positron-electron pair?

7. A gamma ray of energy 7 Mev produces a positron and an electron. What is the sum of their kinetic energies? Of their total energies?

8. A positron and an electron, moving with negligible speed, combine, producing two gamma-ray photons. (a) Their frequencies are equal. Why? (b) What is the energy of each photon, in Mev?

9. Discuss the annihilation of a positron and an electron from the standpoint of Dirac's theory of positrons and negatrons.

10. Referring to p. 283 for data, what will be the energy of the neutrino if a nucleus of Ra E emits an electron of energy 0.4 Mev?

11. Copper 64 can decay to nickel 64, either by emitting a positron or by capturing a K electron. In parallel columns, show the fate of the nucleus, the outside electron shells, and the emitted particles and rays for each of these processes.

12. How would you employ a cloud chamber to determine the velocities of neutrons ejected from beryllium by alpha particles?

13. What is the velocity of a nitrogen nucleus thrown directly forward by the impact of a 4-Mev neutron?

14. Suppose that neutrons with an initial speed of 10^9 cm/sec move through hydrogen gas, and that in each collision by chance, one of them loses exactly $1/3$ of its speed. How many collisions must it make before its speed is reduced below the average speed of a hydrogen molecule at 20°C ?

15. A particle of mass 1 gm and charge $+1 \text{ abcoulomb}$ is shot directly toward a fixed particle of charge $+1000 \text{ abcoulomb}$ from a comparatively long distance, with a speed of 50 cm/sec . (a) Find the closest distance of approach, neglecting all gravitational effects. (b) Make a graph showing the potential energy as a function of the distance from the fixed particle. (c) Make a graph showing potential energy against distance in the event that the fixed particle had a charge -1000 abcoulomb .

ANSWERS TO PROBLEMS

2. $4.80 \times 10^{-5} \text{ escoulomb}$ or $1.60 \times 10^{-14} \text{ coulomb}$; 2.67 mv.

3. 6570 cm.

8. (b) 0.51 Mev.

4. 10.2 cm.

10. 0.77 Mev.

5. $3.46 \times 10^{-12} \text{ cm}$.

13. $3.7 \times 10^8 \text{ cm/sec}$.

6. 0.012 A; $1.02 \times 10^6 \text{ ev}$.

14. 22 collisions.

7. 5.98 Mev; 7 Mev.

15. (a) 0.8 cm.

Transmutation and Nuclear Structure

1. Disintegration by Alpha Particles

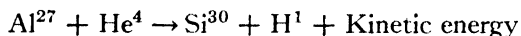
In considering alpha-particle scattering we have assumed for simplicity that the struck nucleus can be treated as a charged particle. This is far from true, since an alpha particle falling on a material of low atomic number sometimes penetrates a nucleus and causes it to emit a particle of different character, either a proton or a neutron. The discovery of such artificial disintegration came about as follows. When alpha particles impinge on a layer of some material containing hydrogen, such as paraffin, sufficiently thick to stop them, particles capable of producing scintillations nevertheless emerge on the other side. These are the "natural H particles," which are not products of disintegration, but simply protons that have been thrown forward with high velocities by the alpha particles. They are also produced when alpha particles pass through hydrogen gas. If the collision is head on, the velocity of such a proton should be 1.6 times that of the alpha particle before the collision, and its range should be 4.1 times the range of the alpha particles. The range of a Ra C' alpha particle in air at 15°C and 76 cm of Hg pressure is 6.97 cm, and the maximum range of the H particles is 29 cm, which is an excellent check.

If protons having a range greater than 29 cm are produced by bombarding a substance with radium C' alpha particles, they must be due to disruption of the atomic nuclei. In 1919, Rutherford found such protons emitted by nitrogen. Other disintegrations were soon discovered by workers in Cambridge, England, and in Vienna.

A representative apparatus used by Kirsch and Pettersson for studying disintegration by the scintillation method is shown in Fig. 12-1. The ring *S* with open center *C* is a strong source of alpha particles which are allowed to fall on a thin layer *T* of the substance to be investigated. Several different substances can be brought over the source in succession by rotating the disk at the top of the figure. Some of the protons

liberated move downward like H through calibrated absorbing foils mounted on the smaller disk, and strike the scintillation screen Z , which is made by applying zinc sulfide directly to the objective of a low-power, wide-aperture microscope; through this the scintillations are observed. The tube of the microscope is composed of two parts with a right-angled prism at their junction, for, if the tube were straight, gamma rays from the source would enter the eye of the observer. The introduction of the prism makes it possible to provide lead screens for his protection.

Experiments of this kind showed that alpha particles of radium C' are able to eject protons from the elements of atomic number 5, 7, 9, and 11 to 19 inclusive, and possibly a few others. The failure of the early workers to disintegrate substances of high atomic number was to be expected, for the alpha particle cannot penetrate the strong repulsive field of force, Ze^2/r^2 , when Z is high. A typical disintegration is that of aluminum,



Some of the protons ejected forward from aluminum have a range of 90 cm in air.

The efficiency of disintegration by alpha particles is very low. Rutherford, Chadwick, and Ellis estimated that one million alpha particles of radium C' may liberate about 20 protons when they are completely absorbed in nitrogen, or 8 protons in the case of aluminum. The efficiency depends markedly on the velocity of the alpha particles. For example, Pose found that about 60 disintegrations were produced by 100 million of the relatively slow alpha particles of polonium when they fell on a foil of aluminum sufficiently thick to stop them. He also showed that the protons from aluminum have several distinct ranges, which means that the daughter element is left in any one of several excited levels.

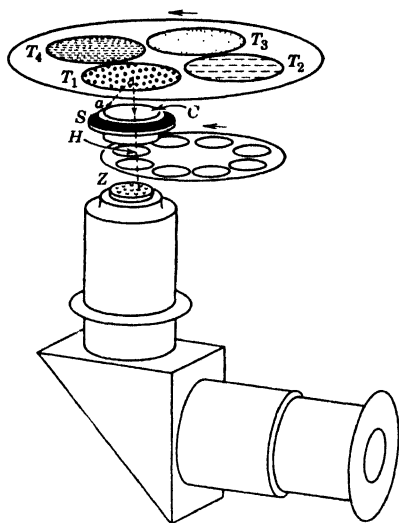


Fig. 12-1. Kirsch and Petterson's apparatus for studying artificial disintegrations by counting scintillations.

Considerable light is thrown on these relationships by stereoscopic Wilson cloud-chamber photographs obtained by Blackett (Fig. 12-2). They show the impact of an alpha particle on an atom of nitrogen. We see the track of the ejected proton and that of the recoiling atom, but there is no evidence that the alpha particle got away after the collision. Similar photographs obtained by Harkins confirm this conclusion entirely. If the nitrogen nucleus captures the alpha particle and loses a proton, the resultant nucleus should have an atomic weight of 17 and

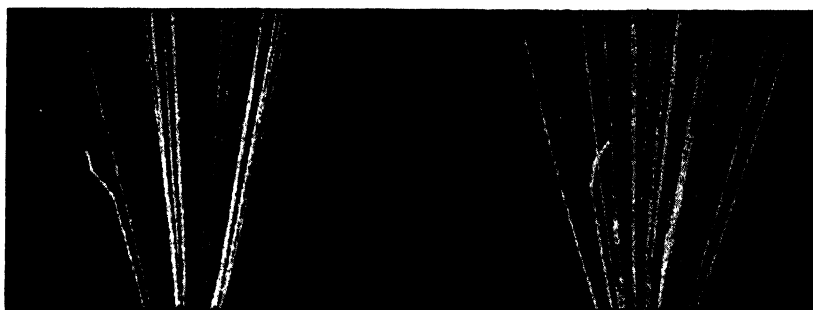


Fig. 12-2. Stereoscopic cloud-chamber photograph showing ejection of a proton from a nitrogen nucleus by an alpha particle. The collision occurred at the fork. The faint track is that of the proton. The other is the track of the O^{17} nucleus.

a nuclear charge of 8; in other words, it should be an isotope of oxygen. This interpretation is supported by determination of the angles between each pair of the three tracks in the photograph, which of course must obey certain relationships if energy and momentum are conserved in the collision. As explained on p. 302, simple capture of the alpha particle cannot in general occur.

2. Production of Fast Charged Particles

The rapid progress of nuclear physics since about 1930 has been largely due to the development of apparatus for producing positive ions of very high energy. The advantages possessed by bombardment methods, in comparison with methods using natural alpha particles, are impressive. Great increases in the numbers of disintegrations are obtained. Higher energies become available; new isotopes, stable and unstable, are produced. Neutrons, positrons, and gamma rays become available in quantity, and the energy and angular distribution of emerging particles can be controlled and measured with greater facility.

Natural sources yielding 10^7 to 10^9 alpha particles per second were the usual thing in the 1920's. On the other hand, a current of $1 \mu\text{a}$ corresponds to the transport of 6×10^{12} singly charged ions per second. If only one ion in 100 million causes a disintegration in a target, the yield is many thousand transmutations per second.

The methods of ion acceleration fall into two classes—those in which high voltages are applied across a long vacuum tube, and those in which moderate voltages are used to give a number of successive energy increments to the ions. Each class has its advantages. Roughly, the high-voltage generators give excellent control of energy, rather low intensity, and low background of dangerous stray products. Repeated-acceleration devices give poorer control, strong beams, and a background that requires the use of thick radiation shields and remote-control methods. Currently, only machines of the second class can be used to attain energies of 100 Mev or more. The others are limited to a few Mev, about 1 to 10, depending on bulk and cost. The following list classifies these machines and gives the names of some pioneers:

High-Voltage Types

Transformers	Breit, Tuve, and Dahl; Cockroft and Walton; Lauritsen
Electrostatic generator	Van de Graaff; Tuve, Hafstad, and Dahl; Herb

Synchronized-Push Types

Linear accelerator	Lawrence and Sloan· Beams
Cyclotron	Lawrence and Livingston
Betatron (p. 150)	Kerst
Synchrotron, or synchro-cyclotron	McMillan; Veksler

The Van de Graaff generator. In its simplest form this device consists of a large sphere mounted on insulating supports, which is raised to a high potential by charges carried to it on a belt made of insulating material. Figure 12-3 shows a compact recent model, enclosed in a tank that permits increase of the voltage range by the use of gas at a pressure of several atmospheres. To avoid unnecessary complication we shall describe an early form (Figs. 12-4 and 12-5) developed by Tuve, Hafstad, and Dahl at the Department of Terrestrial Magnetism of the Carnegie Institution of Washington. This generator develops 1.3 Mev.

★ A silk belt runs over a motor-driven pulley, past a device that sprays charge onto the belt, and into the sphere, where it gives up its charge. This sequence of events is accomplished as follows: Close to

the belt there is a grounded plate P and opposite this is a "comb" of sharp points, connected to one terminal of a kenotron set (let us say the positive one), supplying 10,000 to 30,000 volts. At this voltage

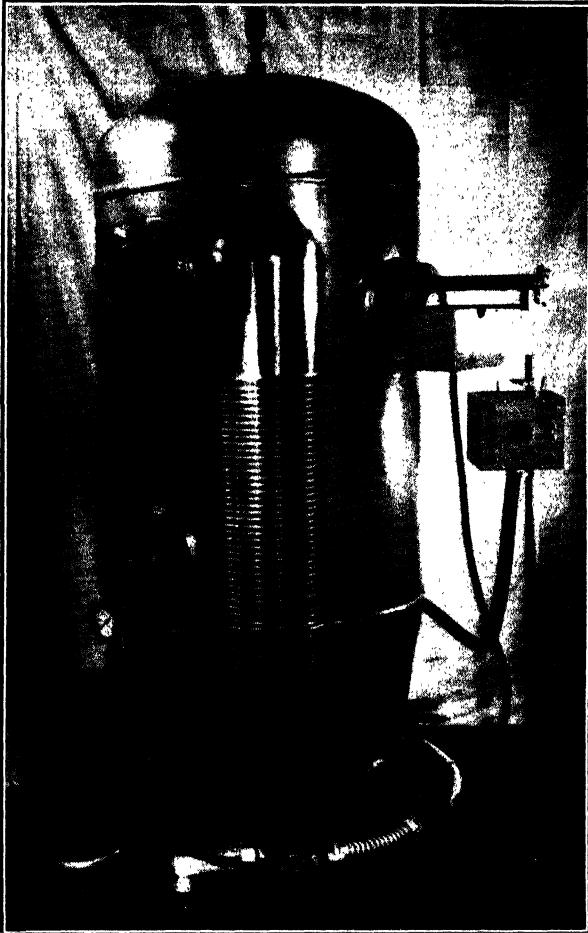


Fig. 12-3. Two-million-volt pressure-type Van de Graaff machine shown as though the tank were transparent. The over-all height is about 7 ft. (*Courtesy of R. J. Van de Graaff and the High Voltage Engineering Corporation.*)

there is a large leak of charge, or corona loss, by ionization in the neighborhood of the points. Some of this charge, on its way to the grounded plate, is retained on the belt, and is carried upward. Inside the sphere there is a similar collector which sprays negative charge on to the belt.

Since this negative charge comes from the sphere, the outside of the sphere becomes more and more positive. The potential of the sphere rises until the incoming current is balanced by corona losses and surface leakage over the belt and supports. Whether or not current is intentionally drawn off for transmutation experiments, the losses set a limit to the highest potential that can be attained. A current-doubling device is employed. The metal comb *A* sprays negative charge onto the incoming belt. This comb is connected to plate *B*, near the belt at the place where it leaves the sphere. The positive charge on *B* pulls nega-

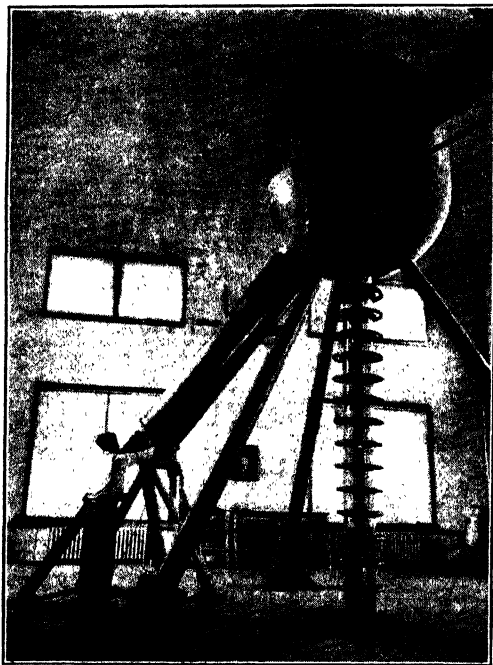


Fig. 12-4. Electrostatic generator and vacuum tube at the Department of Terrestrial Magnetism, Carnegie Institution of Washington. This apparatus yields 1.2 million volts, constant within 1 per cent. The large tube at the left contains a bank of resistors totaling 10^{10} ohms, for voltage measurements.

tive charge from the comb *C* connected to the sphere. Some of the negative charge is retained on the belt, so it serves to carry negative charge away as well as to bring positive in. The negative charge is removed, at the bottom, by the comb and plate *Q*.

★ The interior of the sphere houses much accessory apparatus. There must be gas reservoirs, and leaks for admitting hydrogen, deuterium, or

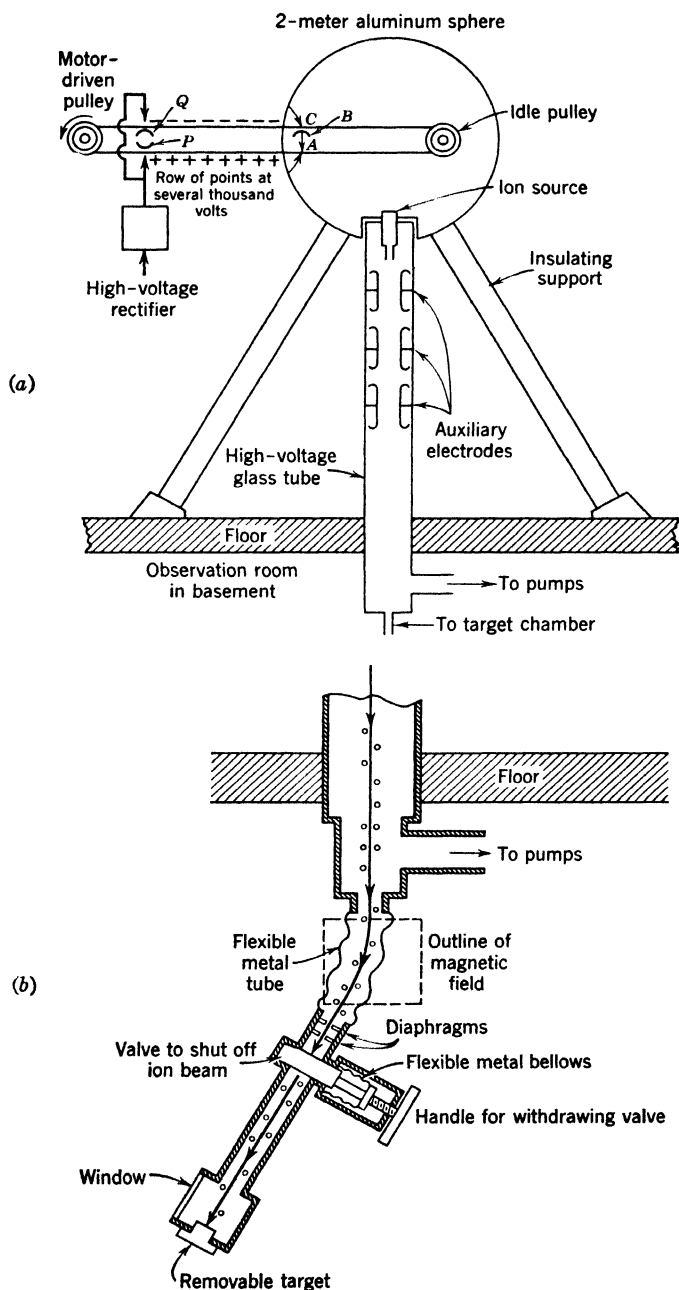


Fig. 12-5. (a) Diagram of the generator in Fig. 12-4. (b) Target arrangements for the generator in Fig. 12-4.

helium to a positive-ion source at the head of the vacuum tube. This source is a low-voltage hot cathode arc, from which an ion beam escapes to the accelerating tube through a canal. The canal must be small, for the pressure in the accelerating tube must be kept low enough, by constant pumping, to prevent an excessive number of collisions between residual gas atoms and the beam of ions. Intermediate electrodes are so disposed along the tube that the ion beam is focused on the material to be disintegrated. Figure 12-5*b* shows the target end of the tube. The ion beam passes between the poles of an electromagnet which separates the constituents with different values of e/m . By varying the strength of the field a single type of ion can be caused to strike the target. Thin windows are provided so that particles and photons emitted by disintegrating atoms can be led out to an amplifier or a cloud chamber.

The linear accelerator and the cyclotron. These machines depend on the idea of applying repeated accelerations to an ion, raising its energy a relatively modest amount at each application. Figure 12-6

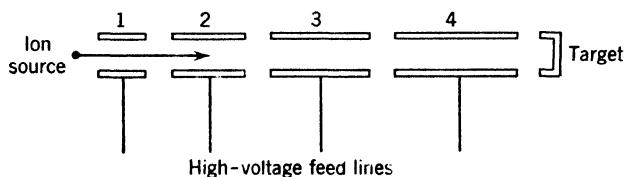


Fig. 12-6. Structure of a linear accelerator.

shows the bare fundamentals of the electrode system for a linear accelerator. Let the successive electrodes be fed with alternating voltage. At time zero, let the potential between the ion source and the electrode 1 be at its maximum value, with the source negative. Let an ion leave the source at this instant. If the time of flight through electrode 1 is one half-cycle of the applied potential the ion will arrive at the gap between electrodes 1 and 2 just in time to find a maximum potential difference directed from left to right, and so on down the line. The electrodes must increase in length as we pass from left to right since the speed of the ion increases as it moves. This principle was developed with some success by Lawrence and Sloan, and also by Beams. However, the instrument described has the defect that particles are easily lost from the beam. Improved versions have been completed since 1950. The Alvarez linear accelerator at Berkeley produces a well-focused beam of 30-Mev protons.

Another ingenious solution of the repeated-acceleration problem will now be described. Lawrence discovered the cyclotron principle in 1931. A flat cylindrical box, evacuated, is mounted horizontally between the poles of a large electromagnet, so that the lines of force traverse it vertically. Inside, there are two insulated electrodes called dees because of their shape, like the halves of a great pill box cut in two (Fig. 12-7). Leads are brought in from an oscillator operating in the 10-megacycle domain, so that the electrodes can be alternately charged positively and negatively, the peak potential being several thousand volts. An ion source is located at the center, in the gap between the electrodes. In the magnetic field the positive ions move on spirals, one of which is shown. Consider an instant when the left electrode is positive and the right one negative. A positive ion produced near the source F is accelerated across the gap and into the space between the semi-circular plates of the right-hand electrode. This space is practically free of electric field, and the ion moves on a circle, emerging at B . If the frequency of the oscillator is adjusted so that the field reverses in the time required for the ion to travel from F to B , then the right plate is positive and the left negative. The ion is again accelerated across the gap and traverses the arc CD inside the left electrode. Figure 12-8 is a small cyclotron chamber used at Cornell, with cover removed to show the dees.

From the equation $mv^2/R = HZe v$, which gives the radius of the path, we find that the time required for an ion of charge Ze to complete a half revolution is

$$t = \pi R/v = \pi m/HZe \quad (1)$$

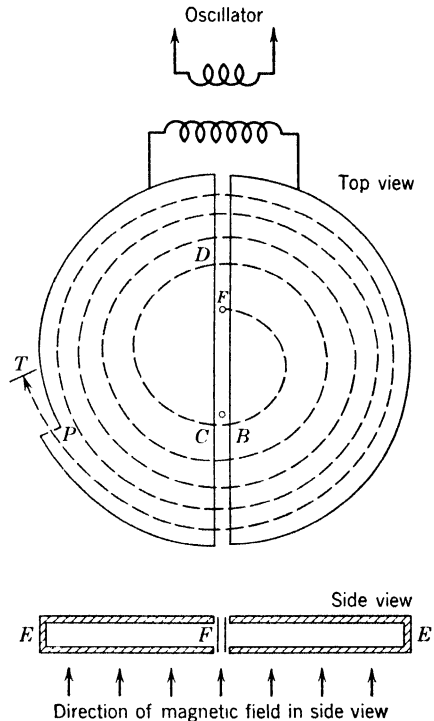


Fig. 12-7. Simplified diagram of the cyclotron. F , source of positive ions. T indicates the target and a Faraday chamber for measuring the ion output.

with H and e expressed in emu. Since this time is independent of the radius R and the velocity v , the ion is accelerated every time it crosses the gap. The frequency required of the oscillator is

$$f = HZe/2\pi m \quad (2)$$

For a proton, $e/m = 9560$ emu/gm. If we put $H = 10^4$ gauss, we obtain $f = 15$ megacycles.

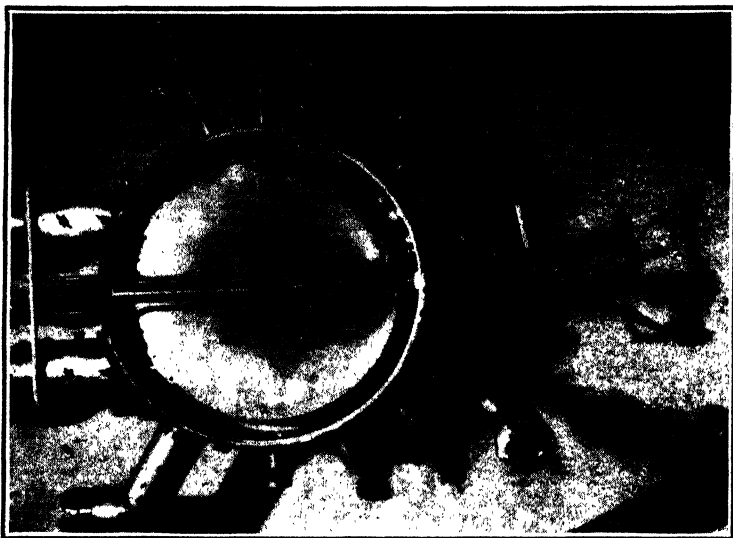


Fig. 12-8. Cyclotron chamber at Cornell University. (Courtesy of M. S. Livingston.)

★ A high magnetic field is advantageous because it gives close spacing of the turns in the spiral path. The energy gain per turn is constant, with given oscillator voltage, so the greater the magnetic field, the greater the final energy of the ion. The reader may show that for an ion at a radius R ,

$$\text{Energy in Mev} = 4.8 \times 10^{-11} (HRZ)^2/A \quad (3)$$

where A is the atomic weight of the ion. For example, deuterons of 12 Mev can be had in a machine of about 20-in. radius. The magnetic field is limited by the properties of iron and the necessity of having a reasonable gap between the poles in which to place the dees. It is impossible to keep the ions traveling in the central plane of the dees because of deflections by molecules of the residual gas. Fortunately, however, the lines of force are not quite straight, so an ion that departs

from the central plane is subjected to a magnetic force, which causes it to oscillate across that plane. In the production of a strong beam, it is essential to utilize this focusing property. The ion current striking the target may be $20\text{ }\mu\text{a}$ or more, so that heating of the target may constitute a limitation.

★ Since the magnetic field is limited, increase of the particle energy requires increase of the radius, but this measure alone is not enough. When the change of mass with velocity becomes significant, the particles, being heavier in the outer parts of the apparatus, cannot keep pace with the alternations of the oscillator. They fall out of step and are not properly accelerated. This is the reason why the cyclotron, in former years, was not used for the acceleration of electrons, since their mass increases appreciably at energies of about 10^5 ev . Similar remarks apply to positive ions with energies of 100 Mev or more. A satisfactory way to evade this problem was devised by McMillan and by Veksler,

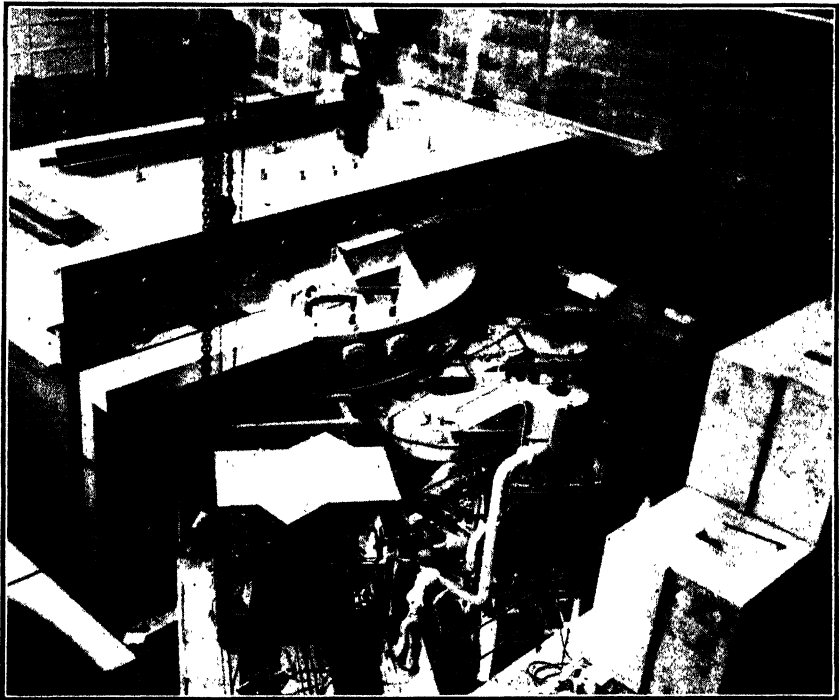


Fig. 12-9. The synchro-cyclotron of Columbia University, financed by the Office of Naval Research and Atomic Energy Commission. At the left, the radio-frequency oscillator; at the right, pumps; in the foreground, shielding blocks. (Courtesy of the Nevis Cyclotron Laboratory.)

independently, in 1945. The very simple solution lies in frequency modulation of the oscillator, or variation of the magnetic field, or both, depending on design requirements. Suppose a burst of ions is provided by pulsing the source. Parallel with this action, a relatively slow decrease of the oscillator frequency is initiated, at such a pace that the ions are always provided with an accelerating voltage when they cross the gap. This plan is used at Berkeley and Columbia for accelerating positive ions. By throwing the burden of synchronization on the oscillators, it is unnecessary to vary the magnetic field—thereby avoiding the use of a laminated magnet. The name synchro-cyclotron is often

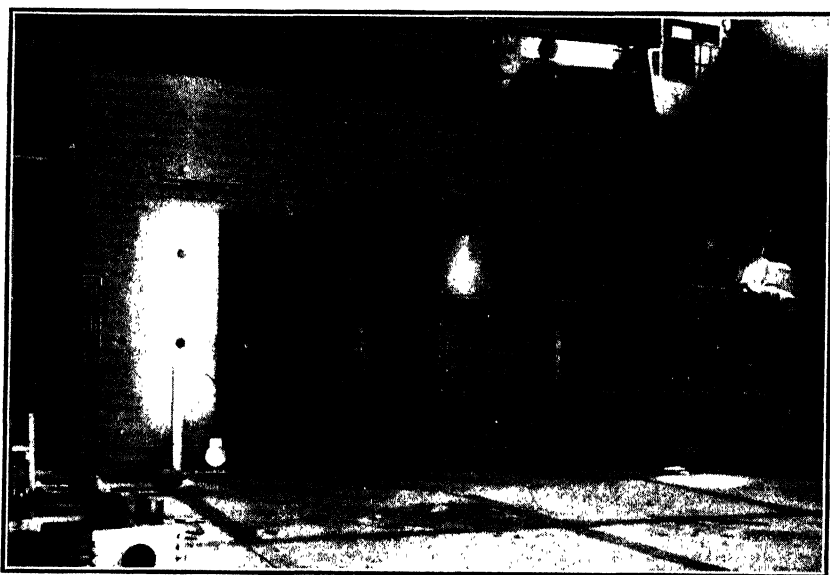


Fig. 12-10. The forward or beam face of the Columbia University synchro-cyclotron.
(Courtesy of the Nevis Cyclotron Laboratory.)

used for these machines, while the name synchrotron is applied to those in which the magnetic field is also varied during the time of acceleration. Figures 12-9 and 12-10 are views of the Columbia synchro-cyclotron.

★ As of 1953, more than twenty machines for 100 Mev or more were being planned or constructed. There were just three which had for a few years produced particles with energies of 300 Mev or more: the Berkeley and Columbia synchro-cyclotrons and an electron synchrotron at Berkeley. Two other machines—one completed, one nearly ready—were available for accelerating protons into the range above 1 Bev

(billion electron volts). These giant synchrotrons are given special names:

At Brookhaven, the Cosmotron, designed for 2.5–3 Bev (Fig. 12-11).

At Berkeley, the Bevatron, designed for 5–7 Bev.

The Cosmotron came into operation in 1952, quickly yielding protons at 2.3 Bev, which can be increased somewhat by further adjustments.



Fig. 12-11. Photograph of the Cosmotron at Brookhaven National Laboratory, from approximately the angle at which protons enter the machine. At the lower left is the steel tank that houses a Van de Graaff generator supplying protons at more than 3 Mev, which the Cosmotron accelerates to more than 2 Bev. Three quadrants of the principal magnets (light colored) are shown. They provide a magnetic field directed vertically downward so that the pencil of protons travels horizontally in a path approximately circular. One of 12 similar vacuum pumps is seen as a dark cylindrical fixture a little to the left and below the center of the picture. (Courtesy of Brookhaven National Laboratory.)

★ In deciding the voltage to be aimed at in such machines, the mass-energy relation is used. To “make” a pi meson of mass $276 m_0$, the voltage requirement is from 165 to 200 Mev, depending on the mass of the projectile and that of the light nucleus bombarded. In practice, the desire for increased yield leads to the use of voltages higher than

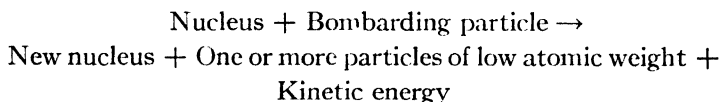
300 Mev. As a matter of fact, the original production of mesons by 390-Mev alpha particles in the Berkeley cyclotron was accomplished by a rather close margin. The simultaneous production of a pair of protons, negative and positive, if it can be done, will require *more* than 1.86 Bev, since the bombarding particle cannot pass all its energy into the nucleus struck. In order to have comfortable safety factors, the design voltages of the Bev machines have been chosen as shown above.

Improvements in particle-focusing methods are being continuously explored and evaluated, and it appears that eventually machines of much higher voltage rating than the Cosmotron and Bevatron will be feasible.

3. Transmutation Processes and Artificial Radioactivity

The availability of positive ions for nuclear bombardment has led to the accomplishment of a great variety of transmutations. In the majority of cases the bombarding ions are protons, deuterons, or alpha particles. The interpretation of results is simpler than it would be if heavier projectiles were used. Also, the small charges of these light projectiles make it easier for them to penetrate the repulsive electric field of a heavy nucleus. In the first few years of bombardment work the list of reactions was rather limited, because some required greater ion energies than the early accelerators could produce. Now, however, it is customary to assume that any desired rearrangement of the nuclear particles can be accomplished if the principles of conservation of energy, momentum, and angular momentum are obeyed, and if each product has a charge-mass ratio not too far from the values characteristic of stable isotopes. The main consideration is the cross section for the process.

Several hundred nuclear reactions produced by charged particles have now been studied. In general, at bombarding energies of a few Mev, the process to be considered is of the type



If the new nucleus is identical with the old one, we speak of scattering, elastic or inelastic, depending on whether the nucleus is left in the ground state of energy or has been raised to a higher state. There are cases in which more than two particles emerge from the collision: for example, bombardment of B^{11} with protons yields three alpha particles.

The new nucleus may be either stable or radioactive. On p. 317 we

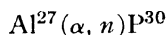
presented a case of nuclear *isomerism*; Sc^{46} may exist in either of two states, both of which are unstable, with measurable half-lives. Many pairs of isomers are now known.

★ We meet with both exothermic and endothermic reactions. An example of the latter is

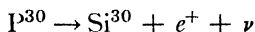


Here the kinetic energy of the alpha particle T_α exceeds the sum of kinetic energies of the boron recoil and the neutron by 2.78 Mev. Therefore we say the "energy release" Q is -2.78 Mev, or the reaction threshold is 2.78 Mev. However, this does not mean that alpha particles with this low energy would produce the reaction at a measurable rate, because of the Coulomb barrier which impedes their penetration of Li^7 . The "photodisintegration" of a nucleus by gamma rays is always endothermic. The cases of deuterium and beryllium are the classic examples.

Artificial radioactivity. In January 1934, M. and Mme. Curie-Joliot announced the discovery of artificial radioactivity. On bombarding B, Mg, and Al with alpha particles they found that after the removal of the source the target continues to emit ionizing particles. Al emits protons, the final product being stable Si^{30} , and also neutrons, the reaction being



Phosphorus has only one stable isotope, of atomic weight 31. The isotope 30 decays with emission of positrons, according to the equation

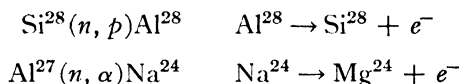


with a half-life of 3.25 min. The nuclei formed in these experiments have a relatively large ratio of charge to mass, so they all emit positrons, thus reducing the charge-mass ratio to a normal value and forming stable isotopes.

The Curie-Joliot's carefully established the chemical nature of the artificially radioactive bodies they found. For example, they bombarded the compound BN with alpha particles. On treating the target with NaOH, gaseous ammonia (NH_3) was formed, and it was found that the activity is carried away with the ammonia. This proved that the active body is N^{13} , formed from the boron, since the protons in the ammonia could not be radioactive.

It is now possible to produce unstable nuclei in all parts of the periodic system by bombardment with charged particles. However, the neutron

is a more convenient bombarding tool for heavy elements, since it does not have to overcome a Coulomb-force barrier in approaching a nucleus. The subject was greatly advanced when Fermi recognized this fact in 1934, opening the way at one stroke to transmutation of nearly all the elements. Three types of neutron reactions, among others, will be mentioned: (1) Neutron capture with emission of gamma rays; (2) capture with emission of a proton; and (3) capture with emission of an alpha particle. Typically, the products are beta rays. We have discussed the first of these reactions on p. 324. Illustrations of the other two processes are



★ **Nuclear reactions at 100 Mev or more.** With projectiles in this range of energy, nuclei can be split into many pieces. The photographic plate becomes a convenient detector for such nuclear debris. It does not make much difference whether the bombarder is a proton or a neutron; hence in many studies the plates can simply be exposed to neutrons, outside the vacuum chamber of an accelerator.

★ The earliest operations of the Berkeley synchro-cyclotron showed that the products of bombardment contain large numbers of new isotopes, both proton-deficient and neutron-deficient. Small “chips” are knocked out of the bombarded nucleus. This process, a mere variation of the one above, is called spallation.

★ In fast-proton bombardment of nuclei it is observed that many fast neutrons are thrown forward, with nearly as much energy as the incident protons—and vice versa in neutron bombardment. These events are not interpreted merely as head-on collisions. The detailed evidence is believed to show that charge exchange may occur. For example, an incident proton may become a neutron by handing its charge to a neutron of the target nucleus.

★ Serber has given a picture of these occurrences which explains many features simply and directly. The beginning of the collision process may be thought of as a collision between the bombarder and just one particle of the nucleus. Most of these collisions will be fairly wide “misses” of the center of the target nucleon, so that the velocity of the struck particle will be nearly at right angles to the direction of the incident beam. It turns out that the average momentum transfer will be approximately $h/2\pi a$, where a is the range of the nuclear forces. This means that the momentum of the struck particle will not be large compared with the average momentum of the particles in the nucleus. Therefore it is not correct to think of the struck particle as free, in spite

of the great energy of the bombardier. The struck particle will share its energy with the others; the "temperature" will be raised and eventually fragments of various sizes may be boiled off.

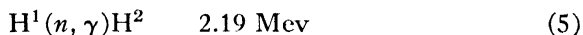
★ This picture leads to the estimate that a particle striking a nucleus of moderate or large Z will experience several collisions inside and may not emerge at all. It is reasonable to speak of a mean free path in the nuclear material, namely, about 4×10^{-13} cm.

The phenomena observed with large accelerators are complex, so that machines yielding a few Mev will continue to play useful roles for a long time to come.

4. Reactions of a Few Light Elements

We shall now consider a few reactions, learning thereby some of the rules of transmutation.

Reactions of hydrogen, deuterium, and tritium. Protons capture neutrons with emission of gamma rays and formation of deuterium. Putting the energy release after the reaction symbols, we write

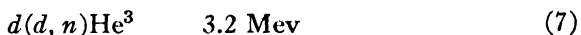
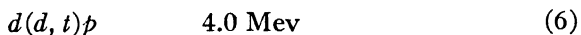


Bombardment of protons with protons leads only to scattering. The reaction $\text{H}^1 + \text{H}^1 \rightarrow \text{H}^2 + e^+ + \nu$ is possible, but has a small cross section. Let us simplify matters by using the symbols p , d , and t for the proton and for the deuterium and tritium nuclei. The reactions of these nuclei with each other can be summarized by showing the reaction products (Table 12-1).

TABLE 12-1

Bombarder	Bombardee		
	p	d	t
p	d, e^+	$\text{He}^3, h\nu$	$\text{He}^4, h\nu$
d	$\text{He}^3, h\nu$	p, t He^3, n	He^4, n
t	$\text{He}^4, h\nu$	He^4, n	$\text{He}^4, 2n$

The following reactions have extraordinarily high yields:



Note that the first reaction yields the tritium nucleus, which is beta unstable, with a life of about 11 years. It decays according to the scheme



He^3 is stable; it represents about 0.01 per cent of terrestrial helium.

The kinetic energy 4 Mev liberated in reaction 6 is, of course, divided between the proton and the triton. The former should have a range in air of 14 cm, and the latter a range of 1.5 cm. This was confirmed by Dee. In his apparatus, Fig. 12-12, the target to be bombarded was

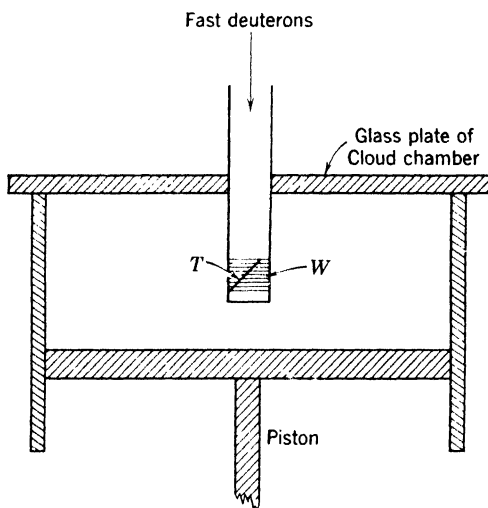


Fig. 12-12. Cloud chamber of Dee and Walton for detecting production of protons and tritons when deuterons bombard a target T containing deuterium. W is a thin window stretched over a supporting screen to admit the disintegration products to the cloud chamber.

located in a tube which passed through the top glass plate of a cloud chamber. The disintegration products were admitted to the cloud chamber through thin windows in the wall of the tube. Figure 12-13 shows the expected pair of tracks, due to p and t , respectively. Reactions 6, 7, and 8 have been followed down to bombarding potentials of a few thousand volts; at 100,000 volts the yield of 6 is about one transmutation per million bombarding ions. Reactions 6 and 7 are about equally probable, but 8 has a cross section roughly 100 *times greater*, amounting to 5 barns at 100 kev.

Deuterium can also be disintegrated by gamma rays, a nuclear photo-electric effect, which is the converse of process 5. When gamma rays from Th C'' are employed we have



The energies of the neutrons and protons were measured by Chadwick and Goldhaber, and the value 0.5 Mev for the sum of these energies is their experimental result. From it we can obtain the neutron mass.

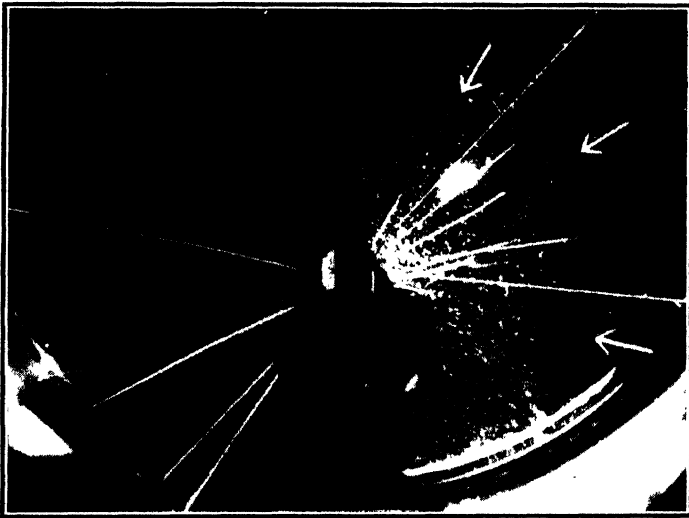


Fig. 12-13. Protons of 14-cm range and tritons of 1.6-cm range, produced by bombarding deuterium with deuterons. The arrows mark the tritons. (Courtesy of P. I. Dee.)

Writing all energies in terms of mass units (where 0.001 mass unit is equivalent to 0.931 Mev), we have

$$\begin{aligned} n &= H^2 + \gamma - H^1 - 0.00055 \\ &= 2.01472 + 0.00278 - 1.00813 - 0.00055 \\ &= 1.00882 \end{aligned}$$

Within the error limits of the reaction energy this agrees with the accepted value 1.00894, which is obtained from similar study of many reactions involving neutrons. In writing out mass-balance equations of this kind, we can use nuclear masses or atomic masses, whichever we please, because the planetary electrons balance out of the equation. (This neglects change of the kinetic and potential energy of the electrons,

due to change of atomic number, which is about ten times too small to show up, in our present state of knowledge of atomic masses.) There is one exception, positron emission, whose detailed consideration is left to the reader.

★ **Helium.** The binding energy of the alpha particle is so large, 28 Mev, that considerable energies are required for its disruption. This coherence adds to its utility as a bombardier. We shall not discuss the numerous reactions of He^3 and He^4 , considered as targets, though some of them are interesting.

★ **Lithium.** The isotopes of lithium show a rich variety of reactions. Early attempts at interpretation were facilitated by work of Oliphant, Shire, and Crowther, who separated the isotopes Li^6 and Li^7 by a mass-spectrograph method, in quantities sufficient to make thin targets for bombardment experiments. Breit, Tuve, and Hafstad and more recently Inglis, Hanna, and their colleagues have contributed extensively to our understanding of the reactions of lithium and its neighbor elements. Only a few of the lithium reactions will be listed:

$\text{Li}^7(d, p)\text{Li}^8$. This leads to a unique disintegration. Li^8 produces Be^8 by beta decay. The energy release is great, the highest energy of the electron being 12 Mev. Be^8 goes quickly into two alpha particles.

$\text{Li}^7(p, n)\text{Be}^7$. Be^7 is the lightest isotope that decays by K capture (p. 318), going to Li^7 . Thus it possesses much theoretical interest.

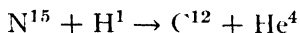
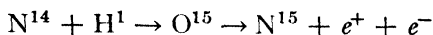
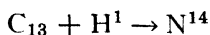
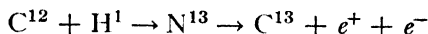
$\text{Li}^7(n, \gamma)\text{Li}^8$. This gives an alternative way to obtain Li^8 . It is often desirable to confirm the nature of reaction products by making them in several ways.

$\text{Li}^7(p, \alpha)\text{He}^4$; 17 Mev. This reaction was the first one carried out with accelerated ions. The yield is high, and the reaction can be detected down to bombarding energies of 20,000 volts or less. The evolution of energy is large, because the sum of the masses of Li^7 and H^1 is considerably greater than that of two alpha particles.

The deuteron bombardment of Li^6 gives rise to two alphas and involves a still larger energy release, 22 Mev.

The carbon cycle. After it was realized that the source of solar energy must be some subatomic process, there was a period of uncertainty as to the main reactions responsible. Because of the abundance of hydrogen it was clear that protons would play a part. The step-by-step reaction of four protons to form helium was considered, but this process does not proceed at a sufficient rate. A set of reactions which fits the specifications was found by Bethe. Systematically, he considered all reactions of the light elements which might play a significant part. As information on nuclear cross sections came to his hands, the possibilities narrowed, because some reactions went much too fast and others much

too slowly. In 1938 he asserted that the main source of solar energy is the chain



The symbols refer to neutral atoms for convenience, even though the reaction is carried on by atoms wholly or partially stripped of electrons. Therefore we indicate that in a positron emission the positron must combine with a planetary electron. After adding all these equations together we see that, when four hydrogens have reacted with C^{12} and its successive products, and two positrons have been emitted, a helium atom has been formed and a C^{12} atom regenerated; the C^{12} atom is merely the necessary catalyst.

Recently, Frieman and Motz have indicated that the reaction $p + p \rightarrow d + e^+ + \nu$ may play a considerable part in stars like our sun. Earlier, Bethe rejected this reaction because of belief that its cross section was too small.

5. The Compound Nucleus

Whenever a physical system undergoes reorganization, a finite time is required for the process. This point was often neglected in the original development of quantum theory. In discussing the Bohr theory of the atom, for example, we have spoken as though a change of quantum state were instantaneous. It happens that in the case of nuclear reactions this point of view is not allowable. Bohr pointed out in 1935 that, when a sufficiently energetic particle enters the nucleus, the energy of excitation is gradually redistributed. We speak of a compound nucleus, which may endure many million times as long as the brief interval required for the incident particle to cross the nucleus. The compound nucleus is in a transitional state. These states are continuously distributed, a feature characteristic of systems which have enough energy to disintegrate. Eventually the configuration will reach a stage at which some nucleon has sufficient energy to depart, or perhaps a gamma ray will be emitted. After this, the residual nucleus is sometimes in an excited state, and sometimes in the ground state.

This view leads to an interesting consequence, which is fully borne out by experiment. The break-up of the compound nucleus does not depend on the way in which it is formed. If it can disintegrate in several

ways, the relative probabilities of these ways are quite independent of the manner in which it acquired its energy. It can be appreciated that this independence simplifies nuclear experimentation.

The reaction diagram. Consider, for example, the bombardment of deuterium with deuterons. We plot a diagram in which the ordinate is energy. In Fig. 12-14, the solid line plotted at the left represents the *sum* of the rest-energies of the bombarding and bombarded deuterons. Thence the upward arrow portrays the kinetic energy of the bombarder.

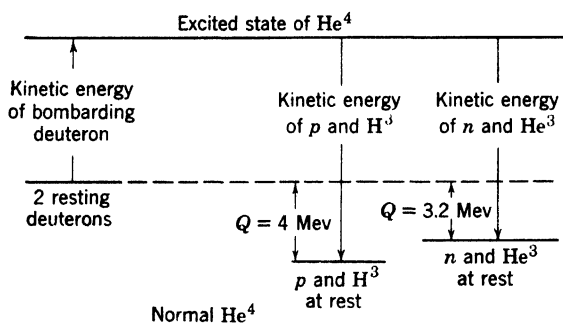


Fig. 12-14. Energy diagram for the dd reactions, involving He^4 as a compound nucleus. Vertical scale is not true because of space limitations.

Hence the energy of the compound nucleus lies at the level of the arrow tip. Disintegration into a proton and a triton gives the kinetic energy indicated by the appropriately marked downward arrow. Elaborations and variations of this diagram are commonly used; it should not be confused with the energy diagram of a single nucleus, Fig. 10-6 or 10-7.

6. The Geiger-Nuttall Law and the Barrier Model

The most striking regularity of radioactive breakdown involving alpha rays is described by the Geiger-Nuttall law. Since about 1912 it has been quoted frequently in the simple form

$$\log \lambda = A + B \log R$$

where A and B are constants for a given radioactive family and R is the range of the alpha particle in air at 15°C and at standard pressure. In order to present this equation in modern form we must bring two additional relationships to bear upon it.

First, ample experimental evidence demonstrates that the range R is, with fair accuracy, proportional to the $3/2$ power of the initial energy

E of the alpha particle; hence $\log R$ can be written as a function of E , and R will no longer appear in the equation. Second, the constants A and B can be calculated by wave mechanics for each radioactive family and for a particular nuclear model in terms of the appropriate atomic number Z , the nuclear radius r_0 , and the energy E . Thus $\log \lambda$ can be expressed as a function of Z , r_0 , and E .

A relation of this type given by Gamow is:

$$\log_{10} \lambda = 21.7 + 4.08 \times 10^{-6} (Z - 2)^{1/2} r_0^{1/2} - 1.72 (Z - 2) / E^{1/2} \quad (11)$$

provided E is measured in Mev. Within the limits of a natural radioactive series $r_0^{1/2}$ does not vary much, so that an average value of this quantity can be substituted in equation 11. Similarly, an average value

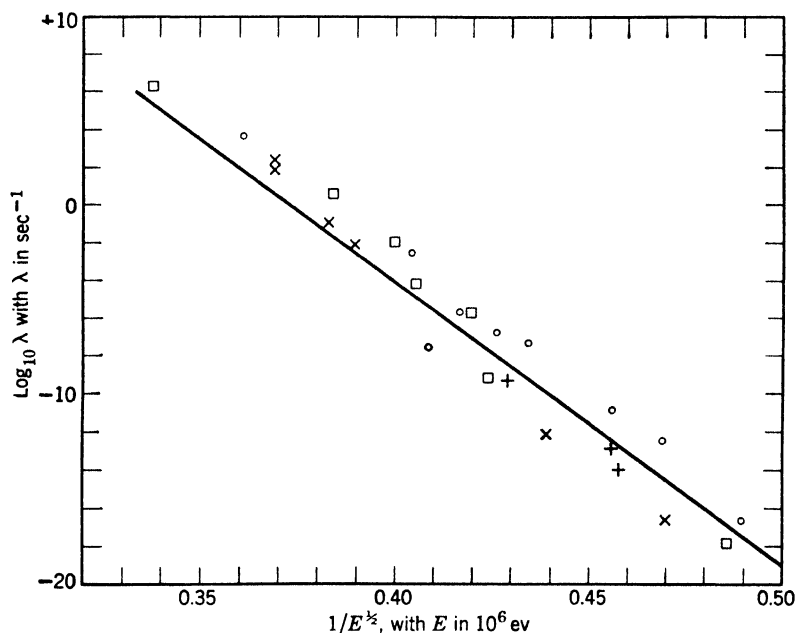


Fig. 12-15. Geiger-Nuttall law. Points belonging to radioactive elements with atomic weights of the forms $4n$, $4n + 1$, $4n + 2$, and $4n + 3$ are indicated by squares, Greek crosses, circles, and diagonal crosses, respectively.

of Z can be employed. Choosing $r_0 = 8.1 \times 10^{-13}$ cm and $Z = 89$, the right-hand side of equation 11 reduces to $55.9 - 150/E^{1/2}$. This expression is plotted in Fig. 12-15, where the abscissa is $1/E^{1/2}$. In spite of the use of average values of r_0 and Z in making the comparison between experiment and equation 11, the general agreement is excellent,

since the values of λ in the graph cover the range from 10^{-18} to 10^6 sec^{-1} . Few physical laws have been tested over such a tremendous range. All attempts to explain this law on a classical basis were futile.

The difficulty is surmounted by a quantized nuclear model which can explain the facts of radioactive disintegration and of transmutation. Except in the case of the deuteron, the problem of the nucleus is a problem of many bodies. There is ample evidence that these particles are closely packed under the influence of forces varying rapidly with the distance. The reader will recall that in the case of atoms we made great progress by singling out one electron and discussing its behavior in a field of radial force representing the average effect of all others. A "one-body" nuclear model of this kind was proposed independently by Gurney and Condon and by Gamow in 1928. It led to an explanation of alpha-particle emission in striking agreement with the facts.

First, we must make an assumption as to the force between the chosen particle P and the center of the nucleus. If P is an alpha particle we know from scattering experiments (p. 48) that the force is a repulsion of magnitude $Ze(2e/r^2)$, when r is several times the radius of the nucleus.

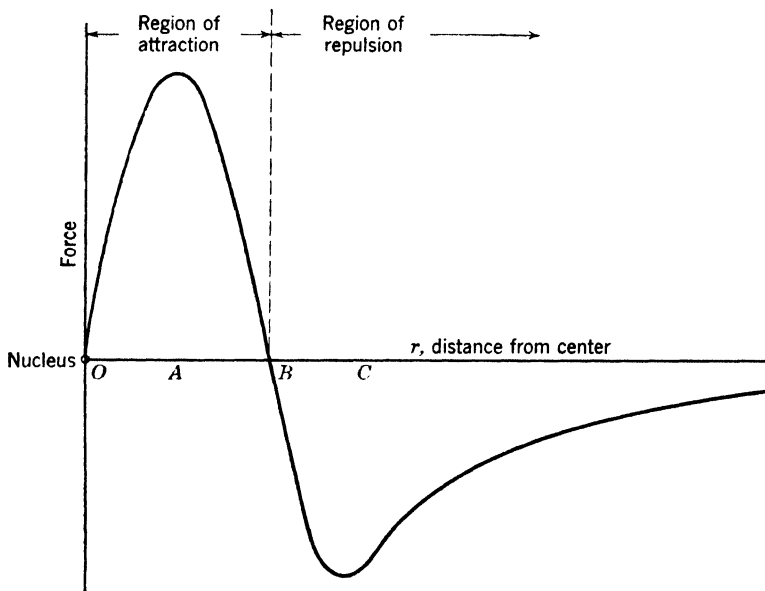


Fig. 12-16. Force between an alpha particle and a nucleus. As the particle approaches the repulsion increases, but in the neighborhood of C an attractive force begins to neutralize the repulsion. At B , the two forces balance. The resultant attraction is large near A , but at the center O the force becomes zero. The nuclear model has spherical symmetry.

At smaller distances, the force must be attractive, since otherwise the particles in the nucleus would fly apart immediately. Figure 12-16 shows the general way in which the force depends on the distance r . An alpha particle at a distance less than OB is attracted and can move on a stable orbit.

Consider the behavior of an alpha particle approaching a nucleus. It is convenient to plot a curve (dashed in Fig. 12-17) showing its potential

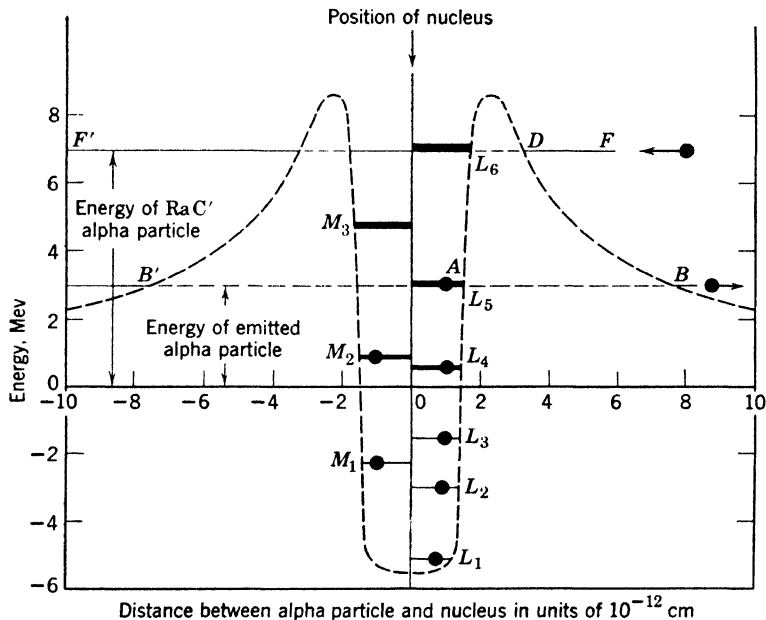


Fig. 12-17. Idealized potential-energy curve for an alpha particle in or near a heavy nucleus. L_1 , L_2 , etc., are energy levels for imprisoned alpha particles; M_1 , M_2 , etc., are energy levels of imprisoned protons; and similar levels might be drawn for neutrons in the nucleus.

energy V as a function of its distance from the center of the nucleus. If we draw a horizontal line FF' at a height equal to the total energy of the particle, the vertical distance from FF' to the potential-energy curve is always equal to the kinetic energy. The projectile must force its way "uphill" as it approaches. Thus, as it comes nearer, the kinetic energy decreases while the potential energy is augmented, until at D the kinetic energy is exhausted. According to ordinary mechanics, the velocity will reverse and the particle will fly away.

Experiments on the scattering of the fast alpha particles of Ra C' by heavy nuclei tell us that the inverse-square law holds true down to the closest distance of approach (namely, 4×10^{-12} cm for uranium), but they yield no information as to the law of force at positions closer to the nucleus than this. Here a second fact is significant, namely, that uranium nuclei are very stable structures that disintegrate very rarely indeed. This means that the potential wall or barrier is so high that the particles inside have but little chance to escape. It must, in fact, be higher than the energy of a Ra C' alpha particle, namely, 7.8 Mev, since this particle does not penetrate the nucleus. The curve of Fig. 12-17 is plotted taking these facts into account. It might then be expected that the alpha particles ejected when uranium disintegrates would be more energetic than those of Ra C', since otherwise they should not be able to surmount the barrier. However, their energy is only 4.1 Mev. Classical mechanics affords no explanation of this fact, but a means of escape is provided by wave mechanics. To understand the explanation the reader should turn back to the wave theory of an oscillator, on p. 185, noting that the maximum displacement of a vibrating pendulum is sharply limited according to classical mechanics, whereas according to quantum mechanics there is no sharply defined limit. Thus at times it may move outward to a position where its potential energy is greater than the total energy. Consider, now, an alpha particle imprisoned in a uranium nucleus, its total energy being 4.1 Mev. Despite the fact that this energy is less than the height of the barrier *there is a small but finite probability that it will be outside rather than inside the barrier. This means there is a small probability for it to pass from the inside to the outside in any given period of time, say one second.* Some writers speak, in a jocular way, of the alpha particle passing through a private tunnel in the potential barrier. However, one should not try to form a classical picture of the escape, for the kinetic energy would have to be negative between *A* and *B*. We are in the presence of new facts, and must accept them, instead of clinging to ideas based on the behavior of matter in bulk.

According to this concept of alpha emission, *each particle appears outside the nucleus with a kinetic energy equal to the total energy—both kinetic and potential—which it possessed inside the nucleus.* Therefore, if a nucleus emits several groups of alpha rays, they give us direct information as to the energy levels of the *nucleus* that emits them. According to the model, these energy levels would refer to the alpha particle, moving in a static field of force. This type of description must not be taken too seriously. Always, an energy level belongs to the system as a whole.

Let us see how the above ideas lead to the Geiger-Nuttall law. It can be shown that, when an imprisoned particle strikes the interior of the barrier, the chance of penetration is approximately

$$e^{-(4\pi/h)WP} \quad (12)$$

Here, W is the width of the barrier at the level BB' , corresponding to escape energy E , or $\frac{1}{2}mv_i^2$; and P is the average value of $[2m(V - E)]^{1/2}$ over this width. The number of collisions with the barrier per second can be determined from the velocity v_i inside the nucleus as follows: The de Broglie wavelength is of the same order as the radius r_0 of the inner wall of the barrier. That is, $h/mv_i = r_0$, roughly, so that f , the number of collisions per second, is given approximately by

$$f = v_i/2r_0 = h/(2mr_0^2) \quad (13)$$

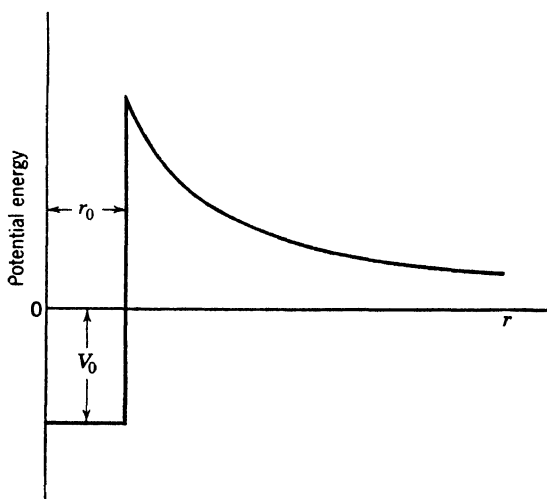


Fig. 12-18. Simple potential-energy curve used by Gamow. The sloping portion corresponds to an inverse-square force, holding good down to distance r_0 .

Now the disintegration constant is the chance of escape per second, or the chance per hit times the number of hits per second:

$$\lambda = \frac{h}{2mr_0^2} e^{-(4\pi/h)WP} \quad (14)$$

Gamow carried out the calculation for a barrier shaped as in Fig. 12-18; the approximate result is equation 11.

Using reasonable values of the nuclear radius r_0 , suggested by the results of scattering experiments, this relation works well for all three radioactive families. Since the radius r_0 is the only adjustable constant and there is not much latitude in choosing values for it, the agreement is a striking demonstration of the usefulness of wave mechanics as applied to the nucleus.

7. Regularities in Beta Decay

★ The reader will wonder whether beta decay can be treated along the same lines as alpha decay. The answer is no. Electrons have no permanent existence inside the nucleus (p. 321). A theory of beta decay must tell us the rate at which electrons are formed, along with their neutrino mates, by an unstable nucleus. They escape at once; there is no barrier to prevent it. Fermi made a bold assumption as to the frequency of formation. The theory is basically like that of the emission of light by moving charges.

The two chief predictions of this theory are the energy distribution of the electrons, and a relation containing the decay constant. Provided the maximum energy E_0 of the disintegration electrons was known, Fermi was able to predict with reasonable accuracy the distribution of energy among those electrons. His theory also gave a plausible explanation of smooth curves known as Sargent curves, which represent relations between the decay constants λ of beta rays and the maximum energies E_0 of their disintegration electrons. Such curves had been found experimentally but had been given no adequate interpretation.

8. Yield Curves for Artificial Disintegration

Wave mechanics enables us to make approximate predictions about the efficiency of artificial disintegration. Even when simplifying assumptions are made, the mathematical theory is too lengthy for inclusion here, but the physical ideas involved are simple. Suppose that a $\text{Ra C}'$ alpha particle approaches a light nucleus as shown in Fig. 12-17. Just as an alpha particle inside can pass through the barrier, so the incident particle can penetrate the barrier and reach the interior. As the energy of the incident particle increases, the probability of penetration increases rapidly, until the energy becomes sufficient for entry over the top of the barrier. Beyond this point, the probability is approximately constant, in many cases over a considerable energy range.

We see that the cross section for a chosen type of transmutation is the product of two factors. These are the cross section for formation

of the compound nucleus, and the chance that it will disintegrate with emission of the chosen particle. The situation is particularly simple when there is only one way in which the compound nucleus breaks up. Then only the penetration cross section has to be considered. The penetration probability is given by an expression similar to equation 12.

As an illustration we may consider the cross section for the reaction of two deuterons. As stated before, the probability for formation of H^1 and H^3 is about equal to that for production of He^3 and a neutron. Since 1948 the yield at low bombarding energies has been measured by several groups of investigators: Bretscher, French, and Seidl; Sanders, Moffatt, and Roaf; and Arnold, Phillips, Sawyer, Stovall, and Tuck. Their results for the production of protons and tritons are in close agree-

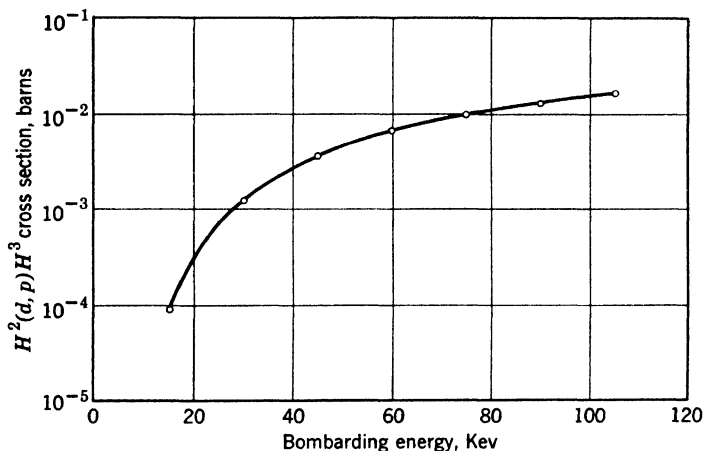
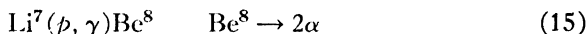


Fig. 12-19. Cross section of the reaction of two deuterons, colliding with low energy to yield protons and tritons. (From the results of Arnold, Phillips, Sawyer, Stovall, and Tuck.) The bombarding energy is measured in the laboratory system.

ment. The essential point for our purpose is not the absolute value, but the trend of yield with energy, shown in Fig. 12-19. This curve can be closely fitted by a formula based on the Gamow penetration idea. The same is true of several other reactions of light nuclei. When we deal with heavier nuclei, troubles arise from basic imperfections of the Gamow model which pictures the nucleus as a simple barrier, neglecting all the real complexity of the compound nucleus. Thus, while the Gamow model has its triumphs, it is not a universal key to nuclear behavior.

Nuclear resonance. The simple description above neglects an important point. If the energy of the bombarding particle happens to

agree with that of an unoccupied level, such as L_6 in Fig. 12-17, the probability of penetration is much greater than it is for energies slightly less or slightly greater. Then the yield of emitted particles or of gamma rays passes through a maximum. This *resonance* effect was first found by Pose, of the University of Halle, who bombarded aluminum with alpha particles and found a yield curve with several maxima. At that time it was customary to say that such studies reveal the positions of energy levels in the initial nucleus. This is a misleading description. The resonance levels are properties of the entire system—the compound nucleus on the one hand, or the initial nucleus *plus* the bombarding particle on the other hand. Similar effects are found when the bombarding particles are protons or deuterons. A well-known case is the reaction



first intensively studied by Hafstad, Heydenburg, and Tuve. When the proton energy is in the neighborhood of 0.44 Mev, the compound

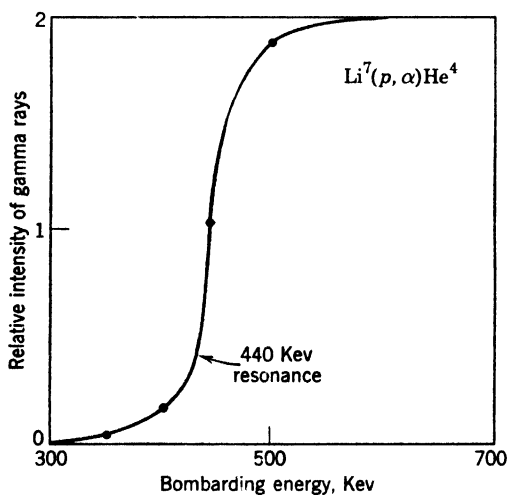


Fig. 12-20. Gamma rays from the reaction of Li^7 with protons. (From the results of Hafstad, Heydenburg, and Tuve.)

nucleus is thrown into an excited state and a gamma ray is emitted before the nucleus breaks up. Figure 12-20 shows roughly the relative numbers of gamma rays emitted, as a function of the bombarding energy. In this case the target was thick, so the gamma rays remain at a high intensity when the energy is made higher than 0.44 Mev; some protons are slowed down to resonance energy as they penetrate

the target. From this type of curve the cross section near the resonance energy can be found. Its equation should be

$$S = \frac{C}{(E - E_r)^2 + \Gamma^2/4} \quad (16)$$

A plot of S versus E in the neighborhood of E_r is called a resonance curve. For the Li reaction, the "width" Γ of the resonance curve is only 0.011 Mev. If there are several resonance levels the equation must be replaced by a more complicated one with several resonance terms.

★ The same equation applies to resonance effects for neutrons, p. 324. We have remarked on several occasions that, when two entities come together, permanent combination is *usually* impossible because of the conservation laws. This fact is an adequate reason why gamma rays should be emitted as the compound nucleus passes to a lower quantized level. The barrier picture of the nucleus helps us to understand why charged particles are not ordinarily emitted—rather than gamma rays—when neutrons of low energy are captured. The emerging charged particle would have to penetrate the barrier.

★ **The angular distribution of the emitted particles.** In the laboratory system of coordinates, the energy of an emitted particle depends on its direction of ejection, as we see by application of the conservation laws. But how is it in the *center-of-mass* system, where the compound nucleus is at rest? In this system the compound breaks into two particles, moving in opposite directions. Focusing attention on one of them, say an alpha particle, will all directions of emission be equally favored? Or will the compound nucleus retain some "memory" as to the direction of the incident beam, so that the number of particles going into a given solid angle will depend on the angle of emission, θ , relative to the axis of bombardment? Both cases are found to occur. For example, in 1940 Young, Ellett, and Plain studied the reaction $\text{Li}^7(p, \alpha)\alpha$, finding a definite departure from spherical symmetry. Heydenburg, Hudson, Inglis, and Whitehead showed that the number of particles per unit of solid angle is proportional to

$$1 + A \cos^2 \theta + B \cos^4 \theta \quad (17)$$

where A and B are functions of the bombardment energy. The absence of odd powers of $\cos \theta$ is easily understood. The emission must be symmetric about 90° , because each alpha particle at angle θ in the center-of-gravity system is accompanied by a mate at angle $\pi - \theta$.

★ These effects bear testimony to the conservation of angular momentum in nuclear collisions, and yield information as to the spin and orbital angular momentum of the compound nucleus. The labor

involved in such experiments is great, which partially explains the late development of this field; it has been cultivated by Inglis, Hanna, and their colleagues, among others.

9. Nuclear Spins and Magnetic Moments

Extensive experiments have shown that nuclei of even atomic mass in their lowest states have angular momenta which are multiples of $\hbar/2\pi$, while those of odd mass have values which are odd half multiples of $\hbar/2\pi$. It has become customary to refer to these multiples as nuclear spins. Of course, they are the vector sums of the angular momenta due to the orbital motion of the nucleons and the spins of these particles. Just as in atoms, the higher states also have characteristic angular momentum values. There is a system of selection rules (p. 379) for transitions between these states.

★ **Hyperfine structure.** The first evidence of this situation came from the existence of hyperfine structure of lines in atomic spectra, a phenomenon observed by Michelson at the turn of the century. Superimposed on the complexities described in Chapter 7, the spectral lines are sometimes made up of several components. The quantum theory of this structure was discussed by Pauli and by Ruark. It is due to the existence of different energy levels, corresponding to the *same electronic structure but to differing orientation of the nuclear spin*, relative to the angular momentum of the atom as a whole.

★ Spinning nuclei possess magnetic moments, which are of the order of a *nuclear magneton*,

$$\frac{\hbar}{2\pi} \frac{e}{2m_p c} = 5.05 \times 10^{-24} \text{ erg/oersted} \quad (18)$$

where m_p is the proton mass, and e is in esu. Stern and Knauer were the first to measure a nuclear magnetic moment, by the method outlined on p. 214. Other methods, of high precision, have been employed by Rabi and his colleagues.

Nuclear magnetic resonance. In 1945 a surprisingly simple method was initiated by Bloch, Hansen, and Packard and by Purcell, Torrey, and Pound, independently. Similar experiments had been tried by Gorter and Broer, but without success, because of differences of technique. We shall describe the method employed by Purcell, Torrey, and Pound. Consider the case of nuclei of spin $1/2$, which have only two orientations in a strong magnetic field. The energy of a magnetic moment MH , oriented parallel or antiparallel to a magnetic field H , is $-MH$ or $+MH$, respectively. The difference being $2MH$, we must

expect that photons of frequency $2MH/h$ will be able to switch nuclei from one of these orientations to the other. If H is several thousand gauss the required frequency will lie in the radio domain, the wavelength being a few meters. Suppose we arrange a resonant circuit (Fig. 12-21) in the field of the electromagnet, and insert a small tube of water into the coil. On tuning through the resonant frequency, protons in the water molecules will switch from one quantized orientation to the other. The oxygen nuclei have zero magnetic moment and therefore are unaffected. There is an absorption of energy at this frequency, which can be detected by ordinary oscillographic methods, since it causes changes in the amplitude and phase of the oscillations. Precise measurements by Zacharias and his colleagues show that the frequency required is $4.2576H$, in kilocycles per second.

★ One point deserves mention: it might appear that the number of protons going from the state of higher energy to that of lower energy would be the same as the number making the reverse transition. Then there would be no net absorption. But there *is* net absorption, because there are more nuclei in the lower orientation state, under conditions of heat equilibrium. As a matter of fact, the lower state becomes impoverished as the experiment proceeds. After a time the numbers in the two states approach equality if the radio-frequency field is sufficiently strong. Thus the reaction on the driving circuit slowly disappears. Then we have to wait awhile, until the protons can be reoriented by random influences. The relaxation time—the average time they dally in the upper state—can be measured with very simple apparatus. Eldridge and Kephart have been able to study the hydrogen resonance, employing a permanent magnet with poles of about 4 in. diameter, taken from an old radar set. This, however, requires careful attention to field shaping, and much larger electromagnets are commonly employed.

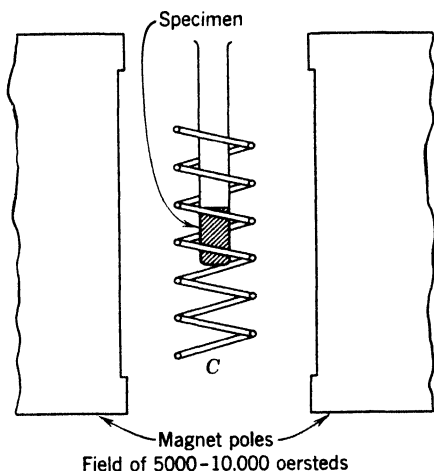


Fig. 12-21. Apparatus for measuring nuclear magnetic resonances in liquids and solids. Nuclei in the specimen switch from one orientation to another when the frequency of the current in coil C is properly adjusted. The coil is exaggerated for clarity. To create a uniform magnetic field the pole pieces are shaped according to a design by M.E. Rose.

★ Figure 12-22 shows the spins and moments of a few light nuclei and of the neutron, first measured by Alvarez and Bloch. The fact that the moments of the proton and the neutron are not integral multiples of the nuclear magneton is evidence that they are complicated structures. Note that the magnetic moment vector of the neutron is

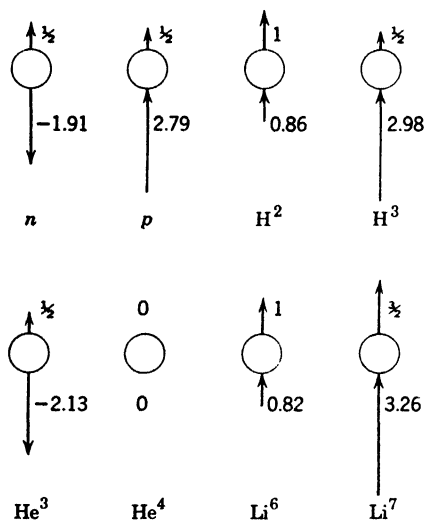


Fig. 12-22. Spins and magnetic moments of the neutron and of light nuclei, spins above, and moments below. The spin is in units $\hbar/2\pi$, and the moment is in nuclear magnetons.

directed opposite to its spin vector, as though it had a negative charge, and that the moment of deuterium is approximately the difference between the proton and neutron moments. This means that the spins of the two constituent particles are parallel, and the magnetic moments substantially antiparallel, in the normal state of the deuteron. Therefore this state is described as a 3S state, by analogy with spectroscopic practice (p. 206).

★ Rabi and his colleagues have shown that the deuteron cannot be treated as a spherical object. It behaves like an egg, spinning around its long axis. This departure from spherical symmetry is expressed by saying that it possesses an electric quadrupole moment.

★ 10. The Deuteron

To construct the theory of the deuteron is an outstanding problem of nuclear physics. (To understand the meaning of a *theory*, think, for example, of Bohr's *theory* of the hydrogen atom, Chapter 4.) Solid progress has been made, but the complete answer still eluded physicists in 1953. Part of the trouble is that, while accurate experimental data are available, they do not suffice to distinguish between a number of possibilities as to the nature of the forces involved. It is as though we were trying to work out the story of the hydrogen atom without knowledge of the Coulomb law. Here we are obliged to confine attention to a few leading facts, and to very simple theories which explain them approximately.

It is highly probable that the deuteron has *only one bound state*. As mentioned above, the evidence from nuclear spins shows that it is a 3S state; that is, the normal deuteron has no orbital angular momentum. The binding energy is $2.185 \text{ Mev} \pm 0.02 \text{ Mev}$. We shall measure energy from the dissociated condition, just as we have done for atoms.

Evidence from scattering of neutrons by protons shows that the absolute value of the energy in the second state, called 1S , is less than 0.07 Mev . The experiments indicate that the state lies above the dissociation limit, which means that it is really in the lower portion of a continuous band of positive-energy states, and not a single state at all. Similarly, it is found that there are no bound states of higher angular momentum.

What does this tell us about the forces acting between nucleons? On p. 173 we saw that the energies of a particle moving in a box of width a are of the form $n^2 h^2 / 8ma^2$. We can increase their spacing as much as we please by making the width smaller. All states except the bottom one can be pushed up, above any chosen energy, by "squeezing the box." The same thing happens in the deuteron. The effective range of the relatively large forces between its particles is small enough to make the level spacing great.

Can we construct an approximate deuteron theory along the lines followed in the Bohr theory of the hydrogenic atom? A dozen reasons can be advanced to show that such a calculation will be crude, but we shall present it before considering a simple wave-mechanical treatment. For the potential energy of the neutron and proton, we shall use

$$V = - \frac{V_0 e^{-r/a}}{r/a} \quad (19)$$

which is an algebraic way of saying that the potential falls to a very small value when the distance r between the two particles is much greater than a . This is the so-called meson potential, discussed in Section 12, where evidence is given that in this model a should have a value about $1.4 \times 10^{-13} \text{ cm}$. We note that the e factor cuts this potential down very rapidly as r increases (Fig. 12-23a). The two particles revolve around the mass center on circular orbits with radii which we shall consider equal, in view of the near equality of their masses. It is easily shown that the mechanical behavior of this system is identical with that of a single particle of mass $m_p/2$, revolving around a fixed center of force under the influence of the potential energy, equation 19. The quantity $m_p/2$ is called the reduced mass, and will be denoted by μ .

Next, we assume that the angular momentum in the lowest state is

$h/2\pi$, neglecting spins, so that

$$\mu v r = h/2\pi \quad (20)$$

This assumption is made in imitation of the Bohr theory of the hydrogen atom, in spite of our knowledge that the deuteron has no orbital angular momentum.

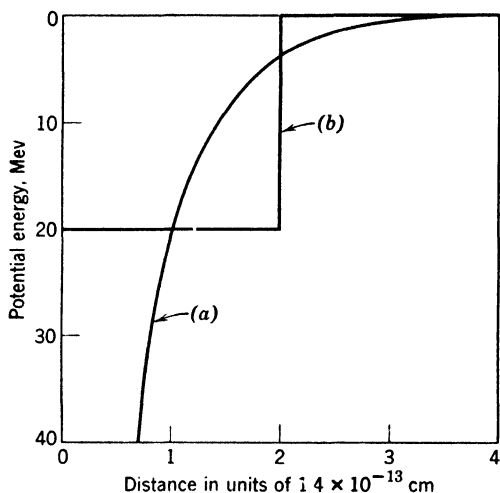


Fig. 12-23. (a) Plot of the potential energy between a neutron and proton, predicted by the meson theory. (b) The square-well potential-energy curve customarily assumed in discussing the deuteron.

Now, the potential, equation 19, corresponds to an attractive force, $-dV/dr$, which we set equal to mass times acceleration:

$$\frac{V_0 e^{-r/a}}{r} [1 + (a/r)] = \frac{\mu v^2}{r} \quad (21)$$

Hence,

$$v = (2\pi/h) r V_0 e^{-r/a} \left(1 + \frac{a}{r}\right)$$

This we substitute back into equation 20, showing that

$$V_0 e^{-r/a} = \frac{(h^2/8\pi^2 \mu a^2)}{(r/a)^2 [1 + (a/r)]} \quad (22)$$

Equations 20 and 22 permit us to simplify the energy, $\frac{1}{2}\mu v^2 + V$.

Writing $r/a = R$, we find that

$$\frac{E}{(\hbar^2/8\pi^2\mu a^2)} = \frac{R-1}{R^3(1+R^{-1})} \quad (23)$$

But $\hbar^2/8\pi^2\mu a^2 = 32 \times 10^{-6}$ erg = 20 Mev, and the energy E is -2.185 Mev, so the left member is -0.1092 . Plotting the right member, we find the equation is satisfied when $R = 0.853$.

Finally, we use this value in equation 22 to get the unknown constant V_0 in the potential energy, which turns out to be about 60 Mev. If a were bigger, V_0 would be smaller. All we really have is a game for finding V_0 when a is given, in other words, a *relation* between V_0 and a . Still, the model is not entirely sterile. The reader may show, if he chooses, that, when V_0 is given the above value, a circular orbit with n equal to 2 or more cannot exist. This means that in such higher quantum states the particles would have sufficient energy to spin their way out of the potential bowl, a behavior that agrees with results mentioned at the beginning of this section.

This calculation illustrates compactly the difficulties of those who have made corresponding wave-mechanical calculations. From the binding energy alone, they can derive only a relation between two constants which always appear in any reasonable-looking potential-energy function. The simplest wave-mechanical treatment of the deuteron makes use of the so-called "square potential well." As illustrated in Fig. 12-23*b*, the potential energy is zero outside a critical radius a , and $-V_0$ inside that radius. The wave function ψ of the lowest state which results from this assumption is simple. The equations of the inside and outside sections are as follows:

$$\begin{aligned} \psi &= A \frac{\sin 2\pi r/\lambda}{2\pi r/\lambda} & \text{for } r < a \\ \psi &= B \frac{e^{-r/b}}{r} & \text{for } r > a \end{aligned} \quad (24)$$

Here λ is the de Broglie wavelength appropriate to the interior of the potential well. It is h divided by the classical momentum, or

$$\lambda = \frac{h}{[2\mu(V_0 - |E|)]^{1/2}} \quad (25)$$

Similarly, the constant b giving the "scale" of the exponential decrease outside the well is $h/[2\mu|E|]$. The constants A and B are so chosen

that the two ψ 's join together smoothly at the nuclear boundary. It is clear that the two particles spend a large fraction of their time at distances apart which are greater than a . In this model the binding energy gives merely the value of $V_0 a^2$. To get information concerning V_0 and a separately, use is made of results on the scattering of neutrons by protons. Fair agreement is obtained with an a value in the neighborhood of 2.8×10^{-13} cm and with V_0 in the neighborhood of 20 Mev.

11. Proton-Proton Scattering

Further information on the force between two nucleons is obtained from experiments on scattering of protons by protons. Such work was first carried out by Tuve, Heydenburg, and Hafstad. The results of their experiments and many later ones have been exhaustively analyzed by Breit and his students. Let it be understood that this scattering does not follow the simple Rutherford law described in Section 1 (with corrections for the motion of the target particle). The influence of the nuclear forces changes the angular distribution of the scattered particles radically. In the simplest type of interpretation, it is supposed that the Coulomb potential holds true outside a certain radius r_0 , and that the "inside" potential energy is a constant, $-V_0$. In other words, the electric inverse-square force is assumed completely absent in the inside region. The question now arises: How does the depth of the well compare with the one above, appropriate for the deuteron, as revealed by neutron-proton scattering?

Here a complication arises. It can be shown that the force between two nucleons depends strongly on the relative orientation of their spins. This effect was passed by, for simplicity, in our previous remarks on the higher state of the deuteron. Actually, the comparison between the neutron-proton potential and the proton-proton potential must be made for the case of opposed spins. The V_0 values, with $a = 2.8 \times 10^{-13}$ cm, are these:

Neutron-proton (1S state): 11.9 Mev

Proton-proton (1S state): 10.5 Mev

With better models, Breit and his colleagues arrived at the important result that, *aside* from the Coulomb force, the force between a proton and a proton is practically identical with that between a neutron and a proton in the 1S state. There is also some evidence that the force between two neutrons is the same. The next section is devoted to attempts to explain the general features of the forces between nucleons.

12. Specific Nuclear Forces

Wigner recognized that the forces between nucleons are probably not "classical" ones, but "exchange" forces of the kind which we have met in explaining the binding energy of the hydrogen molecule. They depend not only on the distance between the centers of the particles but also on the relative orientation of their spins. We have seen that in the lowest state of the deuteron, 3S_1 , the spins of the proton and the neutron are parallel, and the force is an attraction. In the first excited state, 1S_0 , the spins are opposite, and the force between the particles is a much smaller attraction or a slight repulsion.

Originally these ideas were inferred from the occurrence of a sort of saturation, like that found in the case of rare-gas atoms, or that encountered in the study of valence (p. 229). It was noted that the nucleus He^4 is extremely stable, a fact suggesting that in this nucleus the two protons form a closed shell and at the same time the two neutrons form a closed shell, so that in accordance with the Pauli principle another neutron or proton cannot enter these shells. The next particle bound must go into a higher quantum state. Actually, the force between this next particle and the first four is very weak. So far as we can find, the nuclei He^5 and Li^5 do not have an independent existence, but occur only as compound nuclei in bombardment processes. The existence of this saturation phenomenon suggested that *something* is continually being exchanged between any pair of nucleons in proximity, just as electrons are exchanged between the two nuclei of a hydrogen molecule. From this starting point we are led to the following ideas.

Fields and carrier particles. Just as Dirac wrote out the theory of the positron 2 years before it was found, so Yukawa anticipated the discovery of mesons by 2 years under the stimulus of a need for explaining nuclear forces. The idea involved is quite simple. It is natural for us to think of photons as messengers, born only to die again, carrying the energy of an emitting atom to another that can scatter or absorb it. If a photon produces a positron-electron pair, we may think of the positron as a transitory "link" or messenger, from the producing photon to either or both of the two photons produced when the positron is annihilated. It does not seem quite so natural to think of a negative electron as a messenger, because of its permanence under ordinary conditions. However, electrons can be swallowed by some nuclei, a process which is the inverse of beta emission. Such thoughts lead to the plausible assumption that each type of force field involved in the interaction between a chosen pair of particles A , B may be the seat of particles that carry energy from A to B , and vice versa.

Given a field, we look for the carrier particles; given a particle, we look for the field that belongs to it.

Now the question is: *What messengers are responsible for the forces between nucleons?* An early suggestion, based on the existence of beta emission, was that electrons and neutrinos pass back and forth between each pair of nucleons. If, for example, an electron and a neutrino move from a neutron to a proton, the residue of the neutron would be a proton, and the original proton would become a neutron. Since the two nucleons interchange charges, the forces which result from the process can properly be called exchange forces.

Detailed calculation showed that such forces would be about 10^{12} times smaller than the observed attractive forces between particles in the nucleus. This was the situation that confronted Yukawa. He found that the difficulty could be remedied if the messengers between nucleons were particles with a mass of the order $200m_0$. Just as the electric potential energy of two charges q_1 and q_2 is q_1q_2/r , so Yukawa found that the "mesonic" potential energy of two nucleons at rest would be

$$V = \frac{g_1g_2}{r} e^{-r/a} \quad (26)$$

The factor $e^{-r/a}$ arises from Yukawa's desire to insure that the new forces will have a very short range. Here g_1 and g_2 are called the mesonic charges of the two particles. The constant a determines the effective range of the forces. For either a proton or a neutron, the mesonic charge has to be set equal to about 3.6×10^{-9} esu, in order to get binding energies of the order of magnitude found by experiment. Naturally, one of the g 's in equation 26 is made negative. A significant feature of the theory is that

$$a = h/2\pi Mc \quad (27)$$

where M is the mass of the particles carrying the interaction.

There are two types of mesons (p. 427), and both interact with nuclei, but it is now well established that *the heavier ones, the pi mesons, are much more copiously emitted and absorbed than the mu mesons*, under similar conditions. If we use for M the mass of the π meson, we get $a = 1.4 \times 10^{-13}$ cm, which is approximately the linear dimension of the volume per nucleon in any heavy nucleus. This fact is usually considered a strong support for the theory.

The situation described is the basis of the oft-repeated statement that the proton and neutron are not two different particles, but simply different states of the same particle. From the simple picture of

Yukawa many elaborations have arisen, concerned with fitting positive, negative, and neutral mesons into the picture, and with the influence of their spins on the nuclear forces. The subject is in a state of flux at the time of writing. Probably, but not certainly, the conclusions will be that charged π mesons are the principal carriers of the force

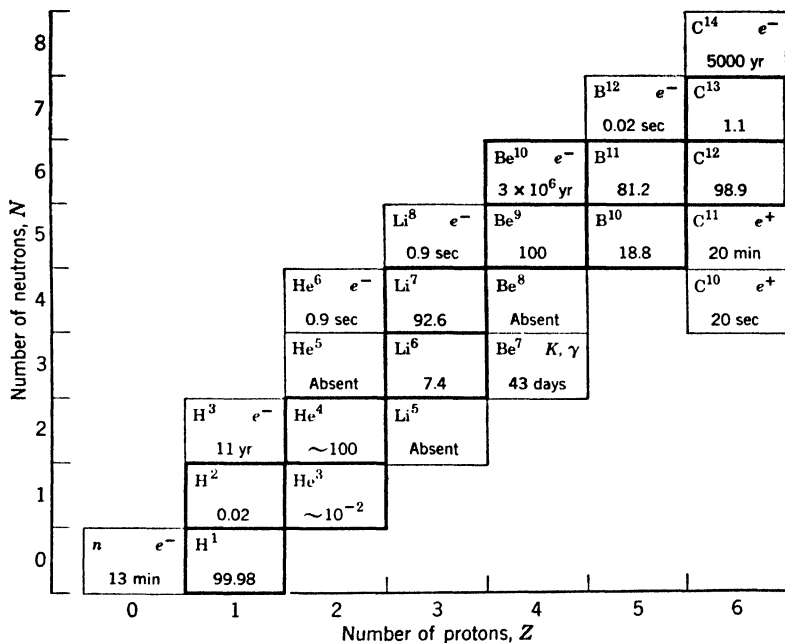


Fig. 12-24. Neutron-proton plot for light elements. The percentage abundances of stable species are shown. For unstable species the emitted particle and half-life are given. Note that an excess of protons leads to positron emission, and an excess of neutrons to negative-electron emission.

between a proton and a neutron; and that neutral π mesons are mainly responsible for the non-electromagnetic force between protons and between neutrons.

13. Regularities in Binding Energies

It is easy to perceive regularities in the abundances and binding energies of the isotopes. There are recurrent patterns in the mode of decay of unstable ones, and in the energies of the particles they emit. Appendix 6 presents abundances, decay data, and binding energies for the first six elements. Precise mass values are still a matter of contro-

versy, and we refrain from discussing the values used. Figure 12-24 is a portion of a type of chart devised by Segrè, in which N and Z , the numbers of neutrons and protons, are used as coordinates. The known isotopes are spotted at the appropriate values of these quantities. For the stable ones, in heavy outlines, we show the approximate abundances. The decay properties of unstable ones are also indicated. Even this small chart and the table in Appendix 6 reveal interesting regularities which can be confirmed by study of a greater part of the periodic table:

1. The *stable* isotopes occupy an ascending band as we ascend the scale of Z . N/Z is never less than 1 for any *stable* isotope, except the proton, of course. N/Z slowly increases to a value of about 1.6, as though the neutrons were a cement, binding the protons together in spite of the Coulomb force. More and more cement is necessary as the charge of the nucleus increases.

2. A deficit of positive charge (or an excess of neutrons) leads to emission of negative electrons; and an excess of positive charge leads to positron emission. C^{14} , C^{11} , and C^{10} show this clearly.

3. The average binding energy per particle rises slowly in the domain of the light nuclei, until a value of about 8 Mev per particle is reached. It remains in this neighborhood over practically the entire remaining range of atomic masses.

4. By considering such pairs as H^3 , He^4 ; B^{11} , C^{12} ; He^3 , He^4 ; etc., we can get the energy required to remove a single proton or neutron from many nuclei. The following results are instructive:

Nucleus	Energy to Remove 1 Proton	Energy to Remove 1 Neutron
H^2	2.19 Mev	2.19 Mev
He^4	19.8	20.5
C^{12}	15.9	18.7

Note the tremendous increase of the removal energy in passing from H^2 to He^4 . This reflects the stability of the alpha particle. Also note the approximate equality of the energies for removal of a proton or a neutron, from either He^4 or C^{12} . While this equality is *not* found in the case of many other light nuclei, its presence in these two cases should convince us that the charge of the removed particle is not a large factor in the energetics of *light* nuclei. It is clear that the specific nuclear forces discussed in earlier sections are dominant.

The great stability of He^4 led many early workers to the view that the alpha particle retains some individuality within the nucleus. This

led to searches for indications of a *system of the nuclei*, that is, indications of larger closed shells of protons and neutrons. For a long time results were slow in coming, but in 1948 Mrs. Mayer published evidence of the specialized stability of the following numbers of protons and neutrons, commonly called the magic numbers: 2, 50, 82, 126. More recently she has presented quite convincing evidence that the list should be written as follows: 2, 8, 20, 28, 50, 82, 126, and that the orbital and spin momenta of the particles within the nucleus can be treated, to a first approximation, by methods like those employed in our discussion of atomic structure in Chapter 7. Similar conclusions were reached, independently, by Haxel, Jensen, and Suess.

REFERENCES

Appendix 9, refs. 6, 38, 43, 77, 89.

PROBLEMS

1. We wish to build a cyclotron that will yield million-volt protons, emerging tangentially at a distance of 15 cm from the center. Find the frequency of the oscillator needed, and the strength of the magnetic field required, assuming that the potential difference of the plates is 10,000 volts when the protons cross the gap between them.

2. Complete the following statements concerning nuclear reactions, and write the reaction equations:

- (a) Deuterium and deuterium yield
- (b) Nitrogen and alpha particle yield proton and
- (c) Alpha particle and Be^9 yield neutron and
- (d) Positron and electron yield
- (e) Neutron combines with isotope 107 of silver to form a new nucleus, namely,
- (f) P^{31} and a neutron yield an alpha particle and
- (g) Unstable Na^{24} emits an electron, yielding

3. Use data on the reaction $\text{Li}^7(p, \alpha)\text{He}^4$ to compute the mass of Li^7 .

4. Use the masses in Appendix 6 to calculate the energy of the gamma ray emitted when a neutron combines with a proton.

5. Explain: natural H particle, Geiger-Nuttall law, nuclear potential barrier.

6. Explain the wave-mechanical picture of alpha-particle emission. What facts show that classical mechanics cannot explain alpha-particle emission?

7. Draw a reaction diagram for at least six reactions involving Li^7 as a compound nucleus. Determine a few of the energy-release values, by using the masses in Appendix 6.

8. Compute the magnetic moment of the neutron in ergs/oersted.

9. At what frequency does the proton resonate in a magnetic field of 5000 oersteds?

10. Accepting equation 26 for the moment, compute the non-electromagnetic potential energy of a positive and negative π meson at a distance of 10^{-12} cm, in ergs, and compare it with the potential energy of a positron and an electron separated by the same distance. What do you learn from this comparison?

11. Speculate on the quantum numbers of the protons and neutrons in the nuclei Li^6 and Li^7 , and on the spin of these nuclei. Check your speculation against the known spins.

12. A proton of energy 1 Mev impinges on a Li^7 atom, causing the reaction $\text{Li}^7 + p \rightarrow \text{He}^4 + \text{He}^4$. (a) What is the total kinetic energy of the two alpha particles as they separate? (b) If 1 gram-atom of Li^7 were thus transformed, how many kilowatt hours of energy would be released?

ANSWERS TO PROBLEMS

1. 14.7 mc/sec; 9540 gauss.
2. 3.49×10^{-6} erg, or 2.18 Mev.
3. 9.47×10^{-24} erg/oersted.
4. 21.298 mc/sec.
5. For the π mesons, -10.6×10^{-9} erg; for the positron and electron, -23.0×10^{-8} erg. The electric force predominates at a distance of 10^{-12} cm.
6. Spin of Li^6 is 1; spin of Li^7 is $3/2$.
7. (a) 18.3 Mev; (b) 4.9×10^5 kw-hr.

Applications of Nuclear Physics

1. Foreword

On p. 44, Fig. 2-10, we gave a curve showing that the mass per nucleon is greater for light nuclei and for heavy nuclei than it is for those of intermediate mass. The energy per nucleon follows the same trend in accordance with the relation $E = mc^2$. Even in the 1920's the idea was often expressed that large amounts of energy might be obtained if we had efficient methods for combining light nuclei, or for splitting heavy ones. It was recognized that natural radioactivity is a demonstration of the relative instability of certain heavy elements. Furthermore, Atkinson, Houtermans, and Eddington had proved that the stars derive their sensible energy from nuclear reactions, maintained in the intensely hot interior. As time went on it became clear that the main problem was to understand how helium could be produced in the stars at the expense of hydrogen. Reactions by which this could be accomplished were described on pp. 353 and 357. Here we discuss the fission of heavy elements. Any means for releasing great amounts of energy carries with it the possibility of destructive uses as well as constructive ones. We prefer to emphasize the benefits that can accrue to mankind from the availability of nuclear energy.

Radioactive and non-radioactive isotopes have been used for many years in a great variety of physical, chemical, and biological investigations. Now they have become available in quantity and variety. It is no idle dream that these substances, created in the recesses of the cyclotron or the nuclear reactor, will enable us to unlock the secrets of nuclei, of large molecules, and of living cells. The field is boundless, and the challenge great.

2. Early Research on Fission

Fermi and his colleagues investigated the action of neutrons on uranium and thorium in 1934. They believed that by neutron absorp-

tion transuranic elements (with atomic numbers greater than 92) were produced. The observed facts were complicated, the results puzzling. In fact, they had produced transuranic elements, but something else was also occurring.

A period ensued in which only a few investigators worked in this field. In general, they accumulated further puzzles. Hahn and Meitner and their colleagues pursued the subject steadily. In 1938, Hahn and Strassmann found that an isotope of barium ($Z = 56$) was produced by bombarding uranium with neutrons. This was the key. Frisch and Meitner quickly suggested that very heavy nuclei could be split into two fragments of about half the original size, which then fly apart with great kinetic energy, of the order 160 Mev for the pair.

The occurrence of a great variety of such reactions was quickly established by numerous investigators. The energetic fragments could easily



Fig. 13-1. Cloud-chamber tracks of two independent fission fragments. (*Courtesy of C. C. and T. Lauritsen.*)

be detected in ionization chambers or in cloud chambers. Figure 13-1 shows a typical event. A uranium compound has been coated on the wall of a cloud chamber, and the entire apparatus has been placed in a neutron beam. When a fission fragment emerges into the gas, its partner recoils in the opposite direction and does not appear. The initial fission fragment is a highly charged and massive nucleus. It may pick up electrons as it travels through the gas, but on the average the charge is high, so that the energy loss per unit distance is also high. The gas in the chamber is argon mixed with water and alcohol vapors,

and the spurs on the tracks are chiefly the tracks of protons ejected in close encounters.

The fragments are radioactive; this is easily established by catching them on foils or thin paper placed close to the source. Usually, they are the parents of short radioactive chains; beta rays are emitted one after another, until a stable nuclear species results.

We do not know who first surmised that in the fission process additional neutrons might be liberated, but Fermi clearly suggested this in January, 1939, remarking that *if enough neutrons were emitted (on the average) a chain reaction might occur in a sufficiently large body of uranium.*

3. General Facts of Fission

Fission can be produced in a variety of nuclei by energetic particles and gamma rays. Figure 2-10 indicates the feasibility of energy release by the approximately equal splitting of any nucleus with atomic number greater than about 40. But energy must be supplied to carry the nucleus over a potential barrier. In uranium, and presumably other elements, production of three or more fragments is possible, though such cases are rare. We shall confine most of our discussion to a relatively small number of important fission processes induced by neutrons. The reader will understand the necessity of this limitation when we state that by 1948 no fewer than 57 isotopes of the elements 90 to 96 had been publicly described. Since that time others have been added, and also isotopes of the elements 97 to 100.

Effects of fast and slow neutrons. Neutron bombardment of uranium, protoactinium, or thorium results in:

1. Production of new isotopes by neutron capture and gamma-ray emission.
2. Fission.

For each bombarded isotope, the relative frequency of these effects depends on the neutron energy. Some isotopes, including U 238,* do not split under the influence of slow neutrons. The slow-neutron fission of uranium is due to the isotope U 235, with possibly a small contribution from U 234. Let us treat the qualitative possibilities before discussing cross sections and the nature of the products.

Figure 13-2 shows a selected group of neutron-capture reactions and subsequent events. Indications are given as to the neutron energies required to produce fission in some especially important isotopes.

*Since isotope symbols occur very frequently in this chapter, the atomic weight and the chemical symbol for the heavy elements will be aligned.

Many other isotopes of the heavy elements have been produced by bombardment. Primarily, the chains of events depicted are produced by slow neutrons, or by ones with energy in a resonance range (p. 324). The black circles identify isotopes that occur in natural sources. All are converted into beta rays, by neutron capture, with the possible exception of U 234, on which we have little information.

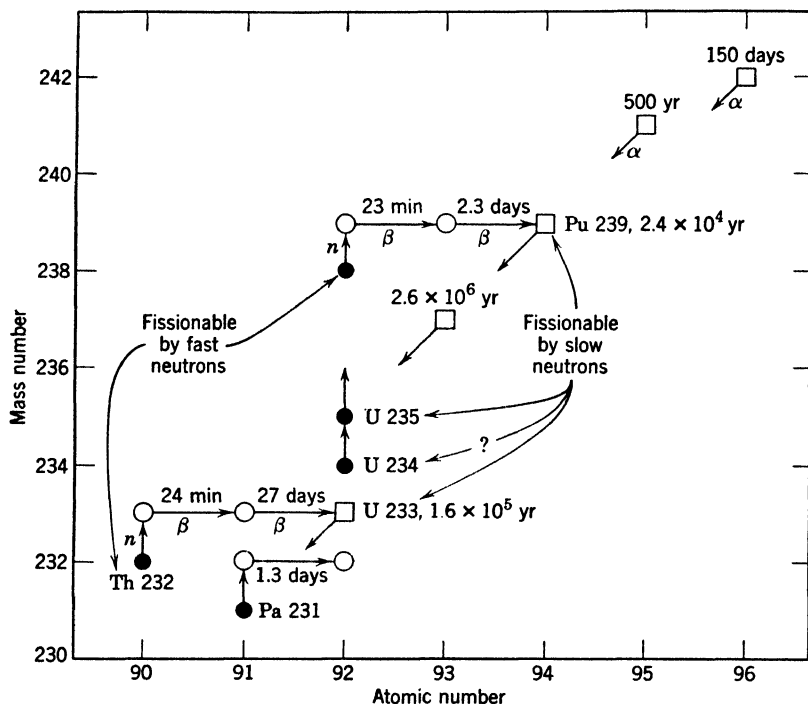


Fig. 13-2. Neutron reactions of some heavy elements. Isotopes available in natural sources are shown by solid circles. The diagram is read as in the following example: U 238 (solid circle) is the abundant uranium isotope. An additional neutron converts it into unstable U 239 (open circle), which then suffers two beta decays of half-lives 23 min and 2.3 days to give plutonium 239 (open square). The diagonal arrow attached to the square indicates that Pu 239 is naturally radioactive.

U 238 is the abundant uranium isotope. It is transformed into neptunium 239. This was the first transuranic isotope to be positively identified, by McMillan and Abelson in 1940. It decays to plutonium 239, which is the isotope produced in quantity in uranium reactors. Note the long half-life of this species, 24,000 years, and note that it can be split by slow neutrons. When it decays, by alpha emission, we

obtain U 235. This chain of events yields a considerable amount of energy, using up a neutron and a U 238 atom to produce a helium atom and an atom of U 235. U 235 is present in natural uranium in the amount of 0.7 per cent. So far as our knowledge goes, when U 235 absorbs a neutron, fission always ensues.

Thorium 232 presents a case of considerable interest. Relatively slow neutrons do not split this material, but it can absorb those which lie in a rather narrow range of velocities. The two ensuing beta decays produce U 233, a long-lived material. The point of interest is that U 233 can be split by slow neutrons, unlike its greatgrandfather, Th 232.

Cross sections. It is clear that the threshold energies for production of fission depend on the nature of the bombarding particle, since the use of different bombarders leads to the production of different compound nuclei. For example, we have the following data:

Reaction	Threshold	Authority
Gamma rays on Th 232	6.2 Mev	Koch
Neutrons on Th 232	1.1 Mev	Haxby, Shoupp, Stephens, Wells, and Goldhaber

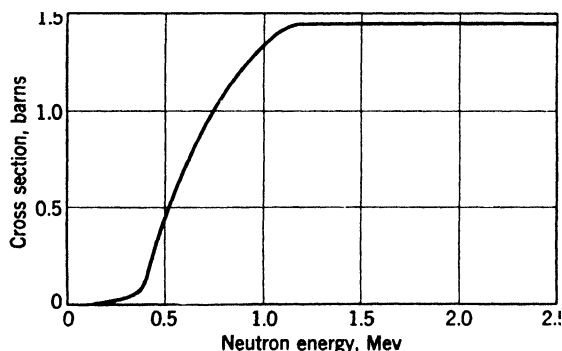


Fig. 13-3. The cross section of neptunium 237 for fission by neutrons. [Based on the data of Klema, Phys. Rev., **72**, 88 (1947).]

We mention this point because of the large fluxes of gamma rays and fast particles in reactors. In general, the energies of the gamma rays are not sufficient to cause photofission, and the large charges of the fission fragments prevent them from causing further fissions; therefore we may concentrate on fission by neutrons. Figure 13-3 shows the

fission yield for neptunium 237. Results for natural uranium and for thorium are similar. Over a wide range of high energies the cross section is sufficiently constant to justify speaking of a definite fast-neutron cross section. Table 13-1 summarizes the situation. Note the *very large cross section, 420 barns, of U 235 for thermal neutrons*. This value, measured by Nier, Booth, Dunning, and Grosse in 1940, enables us to understand, in rough fashion, the potency of U 235 as an explosive. The fission cross section of U 235 follows the $1/v$ law (p. 324).

TABLE 13-1. Thresholds and Cross Sections for Fission by Neutrons

Isotope	Threshold (Mev)	Cross Section (barns)	
		Slow Neutrons	Fast Neutrons
Pa 231	1	—	3
Th 232	1.1	Low	0.1 at 2.4 Mev
U 235	0	420 (thermal)	Varies as $1/v$
U 238	6.35	—	0.5 at 2.4 Mev

The situation for U 238 is quite different. This has neutron resonance levels as low as 5 volts. Their exact positions need not concern us here, so let us speak as though there were just one. It contributes to the efficiency of the capture shown in Fig. 13-2, leading eventually to production of Pu 239. This process uses up neutrons that otherwise would split uranium, so the resonance capture by U 238 is a major factor in determining reactor design.

Fission neutrons. 1. *The Prompt Component.* About 99 per cent of the neutrons liberated by the fission process are emitted very quickly, probably within 10^{-12} sec after separation of the fragments occurs. Experiments of Wilson on the distribution of these neutrons in space indicate that they are simply evaporated from the highly excited moving fragments. Of course, these prompt neutrons have a forward component of velocity, on the average. The reader may visualize this by working out the resultant speeds of fragments from a moving, exploding projectile of spherical shape, relative to an observer on the ground.

2. *The Number of Neutrons per Fission.* This was measured for natural uranium, exposed to *slow* neutrons, by several teams of observers just before World War II. The results varied because methods then available were beset with difficulties.

★ We shall outline just one experiment by Zinn and Szilard, which gave the results:

1.4 neutrons produced per thermal neutron absorbed.

2.3 neutrons produced per fission.

The difference between these results is explicable, in a rough way. The fissions produced were due to U 235, present to the extent of 0.7 per cent. Stray processes of any kind divert neutrons from the fission process. In particular, U 238 can absorb neutrons with velocities in its resonance range. The apparatus is shown in Fig. 13-4. Neutrons from

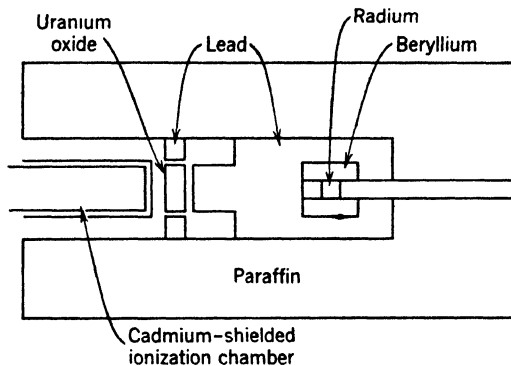


Fig. 13-4. Apparatus of Zinn and Szilard, for finding the number of neutrons produced in the fission of U 238. Radium produces photoneutrons in beryllium. Slowed by the paraffin, these cause fission in the uranium oxide. The lead absorbs much of the gamma radiation. The ionization chamber, shielded from slow neutrons by cadmium sheet, records, substantially, the fast neutrons produced by fission.

a suitable source are slowed by a large body of surrounding paraffin; then they strike uranium oxide. The detector is an ionization chamber containing helium or hydrogen, surrounded by cadmium to shield it from slow neutrons; by this device the chamber is made to detect only *fast* neutrons, produced by fission in the U_3O_8 body; these give rise to fast recoils of the helium or hydrogen atoms. There is also provision, not shown, for insertion of cadmium screens around the uranium oxide, so that corrections for stray effects can be found. After correction, it is found that 45 pulses per min in the ionization chamber are due to the fission neutrons. Two things must now be determined:

Number of fast neutrons from the oxide.

Number of fissions.

As to the first quantity, it is necessary to compute what fraction of the fission neutrons strike the ionization chamber, and then what fraction of these give rise to pulses in the range of heights selected for counting.

The latter fraction depends on the collision cross section of helium (or hydrogen) for fast neutrons. To determine the second quantity, a separate experiment was made. The oxide was removed and a second ionization chamber lined with a thick layer of uranium oxide was prepared. When this was exposed in the same position as the first, 45 fissions per min were observed. The range of the fission fragments in the thick layer is known, so this second experiment enabled the authors to say how many fissions were produced by the neutron source in a *known* volume of oxide. Hence the number produced in the big body of oxide could be found by proportion.

The number of neutrons per fission is, of course, an average over all the various types of splitting that occur. Declassified recent values are,

U 235	2.5 neutrons/fission
Pu 239	3 neutrons/fission

3. *The Energy of the Prompt Neutrons.* Using an apparatus very like Fig. 13-4, Zinn and Szilard studied the energy distribution of the recoil atoms in the ionization chamber, and arrived at partial knowledge of the energy distribution of the fast fission neutrons. The distribution curve descends steeply as the energy rises from 1 to 3.5 Mev. The average energy is about 2 Mev.

4. *Delayed Neutrons.* Roberts, Meyer, and Wang made the important discovery that uranium irradiated with neutrons continues to give out neutrons for a brief period after exposure. They come from the decay of just a few fission products, which are able to emit neutrons spontaneously after an appreciable delay. For laboratory purposes and medical uses, it would be very pleasant to have a variety of long-lived sources, each yielding neutrons of definite energy; but study of the energy relations involved in decay of excited nuclei indicates that the realization of such sources is unlikely. The average decay time of the delayed neutrons of U 235 is about 12 sec. The activity curve has been separated by Hughes, Dabbs, Cahn, and Hall at the Argonne National Laboratory into several components, showing the probable presence of five half-lives ranging from 0.05 to 55 sec. The practical interest of this phenomenon lies in the fact that the delayed neutrons provide a means for controlling the activity of a reactor (p. 395).

The fission fragments. The fission process occurs in many ways, giving rise to fragments distributed over a range of mass numbers, from about 72 to about 158. Symmetrical fission of U 235, which would lead to two nuclei with masses of about 117 and an atomic number of 46, is decidedly rare. This situation leads us to define the *fission yield*; it

is the fraction of all fissions that lead to production of a given pair of masses. The fission yield, expressed in per cent, is shown in Fig. 13-5, referring to the fission of U 235 by thermal neutrons. For example, if this isotope yields fragments with masses 94 and 140 (after emitting two neutrons), we find the relative frequency of this process is about 5 per cent, by looking at the ordinates for either mass 94 or mass 140.

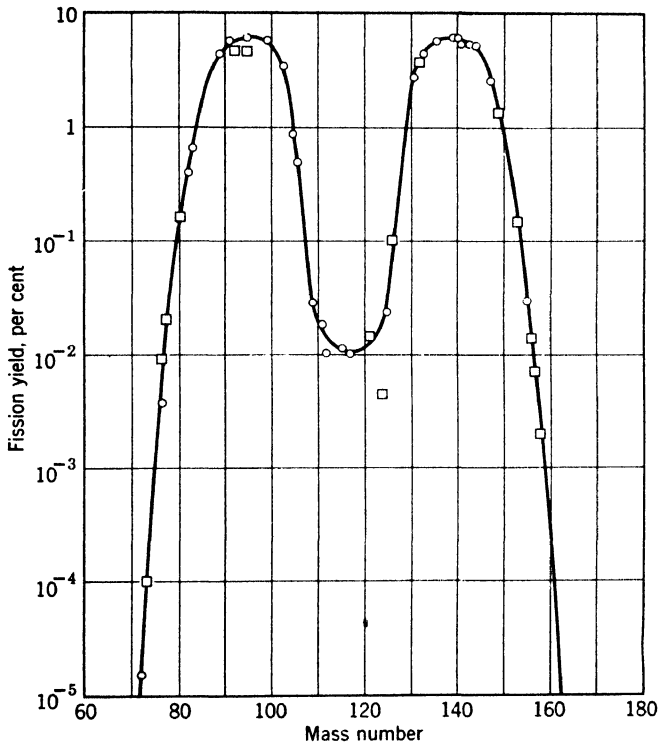


Fig. 13-5. Yields of fission products. (*Based on the Report of the Plutonium Project.*) These data are for uranium 235 under slow neutron bombardment. The curve for plutonium 239 is similar.

Decay of fission products. As we proceed from light to heavy elements in the periodic table, the average value of the ratio of neutrons to protons steadily increases, for stable isotopes. Therefore, when a very heavy isotope undergoes fission, one or both of the fragments will be characterized by a value of this ratio higher than normal. Consider the fission of U 235 with emission of 2 neutrons. If the two fission fragments happen to be Sr 94 and Xe 140, then with the aid of Seaborg's

isotope table (p. 487) we find these are not stable. We may list the successive beta-ray emissions and identify the final products:

Emitters with mass 94	Emitters with mass 140
Sr 2 min	Xe 16 sec
Y 20 min	Cs 40 sec
Zr stable	Ba 12.5 days
	La 40 hr
	Ce stable

Energy released in fission. By direct heat measurements, and other methods, the average energy released in fission is about as follows:

	Mev
Kinetic energy of fragments	159
Kinetic energy of neutrons	7
Beta rays from fission products	11
Gamma rays from fission products	23
Total	<hr/> 200

We see that a significant fraction of the release occurs by delayed radioactive processes. A check on the total energy may be obtained by striking a suitable average of calculations like the following, which refers to one mode of fission, yielding stable zirconium and praseodymium.

Masses of Reactants		Masses of Products	
U 235	235.124	Zr 92	91.942
1 neutron	1.009	Pr 141	140.959
	<hr/> 236.133	3 neutrons	3.027
			<hr/> 235.928

The difference, 0.205 mass units, corresponds to energy release of 190 Mev.

Meitner and Frisch suggested that a fairly consistent theory of fission can be obtained by using a very simple picture of the nucleus suggested by Bohr, in which the nucleus is treated as a liquid droplet.

★ This model is based on the idea that the short-range forces between nucleons give rise to an energy, $-\alpha A$, proportional to the number of

particles A in the nucleus. For the numbers of neutrons and protons we shall write N and Z . At the surface the environment of a typical nuclear particle is different from that of a particle in the interior. Thus there is a positive term in the energy, $\gamma A^{2/3}$, proportional to the surface area. This term is analogous to the surface energy of a liquid droplet. Also, we must insert a positive term $\frac{3}{5}(e^2/a)Z^2A^{-1/3}$, which is a reasonable approximation to the electric energy, a being equal to about 2.8×10^{-13} cm. A correction term $\beta(N-Z)^2/A$ is put in to account for the *decrease* of binding energy that occurs when N and Z are not equal. Finally, if M_p and M_n are the masses of a proton and a neutron, respectively, we have: Mass of nucleus = Mass of its separated constituents — Energy lost when they come together, or,

$$M = (ZM_p + NM_n) - [\alpha A - \gamma A^{2/3} - \frac{3}{5}(e^2/a)Z^2A^{-1/3} - \beta(N-Z)^2/A] \quad (1)$$

As developed by Bohr and Wheeler, the equation gives a way to calculate the energy of a heavy nucleus. Also we can write the sum of the energies of any fragments we wish to consider. Suppose the second energy is greater than the first. Then spontaneous fission into these fragments cannot occur. Exploring all possible fragment pairs, we may ascertain whether spontaneous fission can occur *in any way*. We may repeat the calculation for a compound nucleus obtained by adding a slow neutron to a uranium isotope, determining whether it can split. If it cannot, the kinetic energy which a fast neutron must possess in order to cause fission is, obviously,

Sum of the internal energies of the fission products minus
Energy of the compound nucleus formed by addition of a resting neutron

**TABLE 13-2. Neutron Fission Thresholds
in Million Electron Volts**

Isotope	Computed Threshold	Observed Threshold
Th 230	1.2	?
Th 232	1.7	1.1
Pa 231	0.1	About 1
U 233	-1.7	Slow fission occurs
U 234	-0.4	?
U 235	-1.1	Slow fission occurs
U 238	0.7	0.35
Np 239	0.0	About 8
Pu 239	-1.9	Slow fission occurs

In Table 13-2 we show approximate values of the fission threshold computed about 1940 by Dr. Katharine Way. The correspondence with facts, so far as we know them, is striking, except for Np 239. The slow fission of U 235 and Pu 239 and the existence of thresholds for Th 232 and U 238 are correctly predicted.

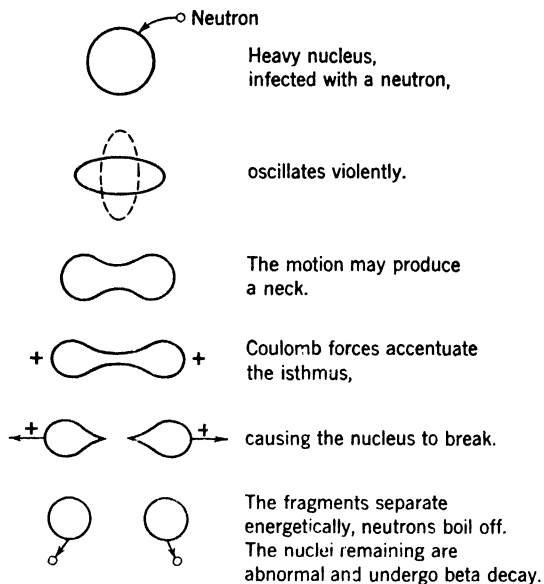


Fig. 13-6. Fission of a heavy nucleus by a fast neutron.

Figure 13-6 shows the sequence of events to be expected on the basis of the droplet model. A fast neutron sets the nucleus into oscillation. If it gets into a shape somewhat like a dumbbell, the Coulomb forces between the two parts conspire with the reduced attractive forces at the small center section to permit further necking-in and final rupture, somewhat like the division of a living cell; hence the name fission, borrowed from biological nomenclature.

4. Large-Scale Utilization of Fission

Isotope-separation devices and reactors yield important new materials and make it feasible to carry out investigations previously impossible. Therefore it is fitting to devote some space to the large-scale developments that have occurred since 1939.

In 1940 American physicists voluntarily agreed to suppress publication on fission. The curtain was partly raised by publication of the Smyth report in the last days of World War II. That report, and the periodic reports of the Atomic Energy Commission, provide the history of each major development. For a balanced account of the scientific gains, the book of Lapp and Andrews (Appendix 9, ref. 61) is useful.

The impetus leading to large-scale work on nuclear energy came mainly from a small group of physicists—Szilard, Wigner, Teller, Weisskopf, and Fermi. Professor G. B. Pegram made contact with the United States Navy early in 1939. A little later Einstein and Alexander Sachs put the matter before President Roosevelt. A Uranium Committee headed by Dr. L. J. Briggs of the Bureau of Standards was appointed. Thereafter the control passed in succession to the National Defense Research Committee, the Office of Scientific Research and Development, and the Manhattan District (an agency of the Army Corps of Engineers). Finally the Atomic Energy Commission was established by Congress in January, 1947, with very broad powers for research, development, operation, and control.

Exploratory period. Work in 1940–1941 was largely devoted to determining the feasibility of various methods for obtaining large amounts of fissionable material and for producing an explosive reaction. The problem was divided into two major categories:

1. Separation of U 235 from natural uranium:
 - (a) By thermal diffusion, using gaseous uranium compounds.
 - (b) By thermal diffusion, using liquid uranium compounds.
 - (c) By centrifuges.
 - (d) By electromagnetic separators—giant mass spectrographs.
2. Plutonium production in large bodies of natural uranium.

It was clear from the start that the mass of U 235 required for production of a fast chain reaction was somewhere between 1 and 100 kg. No worth-while estimate could be made for Pu 239, and it was not clear that a reactor utilizing only natural uranium could be made to operate.

Process and plant development. To increase the probability of success all the methods listed above were carried forward in 1942 and succeeding years. It turned out that all were capable of yielding significant amounts of fissionable material, but they differed in regard to cost and difficulty of operation. For separation of U 235, the gaseous diffusion of uranium hexafluoride proved to be the most economical. This hexafluoride had been known for many years. The great gaseous diffusion plants at Oak Ridge have been improved and expanded since

1945. For a time, the electromagnetic separation plant, called Y-12, at Oak Ridge, operated on a large scale. A part of its equipment is now used for separation of stable isotopes. Isotopes of several dozen elements have been concentrated in quantities sufficient for research purposes and industrial needs.

In December, 1942, a self-sustaining nuclear reaction was first achieved in a uranium-graphite pile at the University of Chicago. This initial success led to the construction of the pilot reactor at Oak Ridge and the production reactors at Hanford in the state of Washington. There are other large reactors at Harwell, England, and at Chalk River, Ontario. Many small ones are in existence also. See Section 6.

5. How a Pile Works

★ **Chain reactions.** Suppose we have a medium composed only of U 235 nuclei, in a hypothetical box from which neutrons cannot escape; and suppose that V , the number of neutrons produced in each fission, is exactly 2. Let us introduce one neutron at zero time to kindle the "fire." For simplicity we may assume that each neutron bounces about with constant speed v , for a uniform small time T , before it produces a fission. Then we may speak of an absorption-mean-free-path, L_a , which is given by

$$L_a = vT \quad (2)$$

★ After a time T the original neutron is absorbed, producing fission, and then we have 2; after time T these 2 are absorbed, producing fission, and then we have 4. After m steps of this kind, the neutron population is 2^m . At time $t = mT$, the population is

$$2^{t/T}$$

Since T may be of the order of 10^{-5} sec, this process leads to explosive reaction of the whole mass, checked only by dispersal of the material, as it explodes, if we do nothing about it.

★ **Control.** By introducing an inert absorbing medium, such as cadmium, at time t , we can check the reaction. In effect, we replace the reproduction factor 2 by another number W , smaller than 1. This is the number of neutrons produced in one fission which manage to produce another fission, on the average. Let us denote by V the actual number of additional neutrons produced at each fission, without regard to their fate. Of these, a number W are used to cause further fission. The remaining neutrons, $V - W$, are taken up by the absorber. Thus the reaction decays; at time t' the number present will be

$$2^{t/T} W^{(t'-t)/T}$$

★ In a more realistic case, a cadmium control rod can be moved back and forth, in response to commands from a counter which indicates the fission rate. In this way the power level can be made to fluctuate slightly in the neighborhood of any desired value.

★ Now, T is very small; even for a thermal neutron, with a speed of 2200 m/sec, the time required for absorption is brief, for example, about 10^{-2} sec in carbon. The response time of the control rods should be considerably shorter than T . In fact, pile control would be difficult or even impossible if it were not eased by a circumstance which we have so far left out of account, namely, the occurrence of delayed neutrons (p. 388). It is possible to arrange matters so that the prompt neutrons *alone* cannot cause a growing chain reaction, while the *total number* available (in the absence of any control measures) exceeds the critical number necessary to insure chain operation. The average time required for emission of a delayed neutron is about 12 sec. Thus it is clear that the fission products produced in a particular step will not make their contributions to the neutron stock until a time of this order has elapsed. Therefore, the full effect of withdrawing a control rod is not felt for several seconds. Thereby, leeway is created for easy handling of fairly massive control devices. This leeway is very desirable, for there must be no mistakes. A slow neutron reactor is nothing like an atomic bomb, whose action depends on the effective utilization of fast neutrons to build up the chain reaction with extreme speed. Nevertheless a reactor out of control would quickly destroy itself.

★ A reactor operating under control of the kind described is said to be below the condition of prompt criticality, but above the condition of delayed criticality. Without further consideration of the complications due to delayed neutrons, we shall now carry through the argument leading to a very rough reactor design.

★ **Design of a spherical pile.** Let us use a homogeneous mixture of U 235 and specially purified graphite as a moderator, or neutron-slowng medium. The advantage of a moderator is easily seen by considering the increase of the fission cross section of U 235 as the neutron velocity decreases. (See p. 324 and Table 13-1.) The fission neutrons are created with an energy of the order 2 Mev, and it pays to make them slow as quickly as possible, using them for fission instead of allowing them to escape from the reactor surface. A price must be paid for this advantage. All stable isotopes absorb neutrons. Carbon has a low absorption cross section—that is why pure graphite is chosen as a moderator—but absorption is far from negligible.

★ Our problem is to find the size of pile which is necessary in order to permit the chain reaction to proceed. This size depends on the per-

centage of U 235 in the mixture. The richer the mixture, the smaller the pile. It is easy to see why a certain minimum size is required. The smaller the sphere, the greater the ratio of its surface to its volume, $3/r$, and the larger the waste of neutrons by escape. In practice, reflectors are added to turn some of them back, but we shall not consider this complication.

★ 1. Although the material is homogeneous, the distribution of the diffusing neutrons is not. Because some neutrons escape, the number per cubic centimeter falls to a low value inside the pile near the surface. It is roughly correct to assume that the surface value of the neutron concentration is zero, as in Fig. 13-7b. Of course, the actual value is finite, for otherwise there would be no outward flow; but the value is small compared with the central concentration when the size is sufficient to insure a chain reaction.

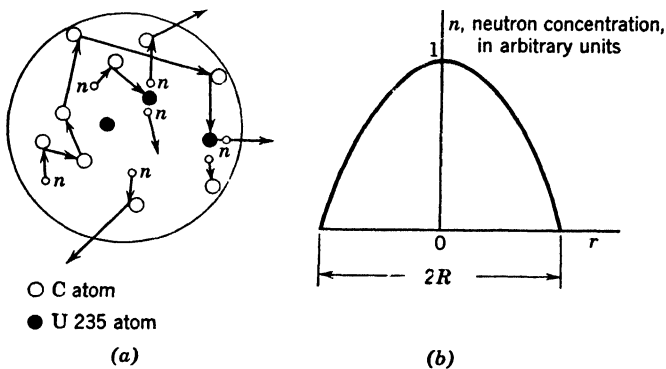


Fig. 13-7. (a) Scattering and absorption in a spherical U 235 pile. (b) Dependence of neutron concentration on distance from the center of a spherical pile.

★ 2. Now we must consider the diffusion of the neutrons. It is more complicated than the diffusion of a stable gas, because they are being absorbed as well as scattered. Scattering helps tremendously to conserve the neutron population, as we can see from Fig. 13-7a. It turns many neutrons back toward the point at which they originated. While others are scattered in a way which facilitates escape, the net effect is very beneficial. Calculation shows that the quantity of importance in an absorbing scatterer is a mean path L called the *diffusion length*, defined in the following way: if neutrons were diffusing from an extended plane source, the number at a distance x from the source would be proportional to $e^{-x/L}$. The formula for L is found to be

$$L^2 = L_t L_a / 3 \quad (3)$$

Here L_t is the average distance a neutron travels parallel to its original direction, per collision with a nucleus, which scatters it. L_a is the average distance it travels before it is absorbed.

★ The following data for thermal neutrons in carbon enable us to appreciate the great importance of scattering:

$$L_t = 1.8 \text{ cm} \quad L_a = 1950 \text{ cm} \quad L = 35 \text{ cm}$$

★ 3. We shall need a quantity K , the *reproduction factor*. It is defined as the number of neutrons created, divided by the total number absorbed in both the U 235 and the graphite. We may allow these numbers to refer to unit time and to 1 cm^3 of material. The *number created* can be written in two ways. First, it is

$$K \times (\text{Number absorbed in U 235 and in graphite})$$

and second it is

$$V \times (\text{Number absorbed in U 235})$$

since V was defined as the number of new neutrons created in one fission process. But, with the pile in steady operation, the total number absorbed is proportional to $N_u S_u + N_c S_c$ where N_u and N_c are the concentrations of U 235 and carbon in atoms per cm^3 ; while the S 's are the absorption cross sections of these materials. S_u is, of course, the fission cross section of U 235. Finally,

$$K(N_u S_u + N_c S_c) = V N_u S_u$$

or

$$K = \frac{V}{1 + (N_c S_c / N_u S_u)} \quad (4)$$

★ 4. A study of the equation governing diffusion of the neutrons proves that the *equilibrium* neutron concentration n in the spherical mass is of the form

$$n = \frac{A}{r} \sin \left[\frac{(K - 1)^{1/2}}{L} r \right] \quad (5)$$

The quantity A is an arbitrary constant, because in this simplified problem any power level can be chosen by putting in the right number of neutrons at the start. We desire to make $n = 0$ at the surface, as we explained above. Also, it is clear that the concentration must drop off steadily from the center to the periphery as shown in Fig. 13-7b. Since $\sin \pi = 0$, we can satisfy both these conditions by choosing a proper value of the reactor radius R , such that

$$(K - 1)^{1/2} R / L = \pi \quad R = \pi L / (K - 1)^{1/2} \quad (6)$$

★ For a given mixture of U 235 and graphite, L and K can be calculated, and then equation 6 yields the radius which will provide, theoretically, for steady operation without either decrease or increase of the activity. (In point of fact, there will be fluctuations.) By adding uranium, or by increasing the size, we get an “overcritical” design, which can then be provided with control devices to yield the desired neutron flux or power level, over a considerable range of values.

★ 5. Let us indicate some of the characteristics of a possible series of designs. It is possible to choose the concentration of U 235 in such a way that a minimum quantity is required. The cost of this material is such that saving is important. The reason why an optimum exists is not hard to see. If we lower N_u sufficiently, a large percentage of the neutrons will be lost in graphite. Then the critical size is large, and it turns out that, in spite of the low uranium concentration, the total uranium required is larger than it would be for a higher value of N_u . If, on the other hand, we increase N_u sufficiently, we get a large percentage of utilization in the uranium and the critical size is small; but then the ratio of surface to volume is high and the leakage increases. It turns out that the quantity of U 235 is approximately minimized when we make

$$N_c S_c / N_u S_u = \frac{4}{8} \quad (7)$$

Then
$$K = \frac{2}{1 + (1/8)} \quad K - 1 = \frac{7}{9}$$

A somewhat refined computation for neutrons of all velocities yields

$$L^2 = 280 \text{ cm}^2 \quad L = 17 \text{ cm}$$

Then the critical radius is

$$R = \frac{17\pi}{(7/9)^{1/2}} = 60 \text{ cm}$$

Putting known values in equation 7, we find N_u , and conclude that the amount of U 235 in this “minimum-uranium” pile would be of the order of 10 lb.

★ 6. *Poisoning.* As the pile works, fission products accumulate, causing less activity and dilution of the uranium content. This “poisoning” effect can be counteracted by the addition of extra uranium to extend the duration of an operating run. Eventually the fission products so diminish the efficiency of the pile that it has to be chemically reconditioned to remove them.

★ A complex problem had to be solved to attain success with the first pile using natural uranium. The difficulty is that resonance capture of neutrons by U 238 interferes with their use for fission by U 235. The solution lay in isolating the uranium in aluminum cans. These are

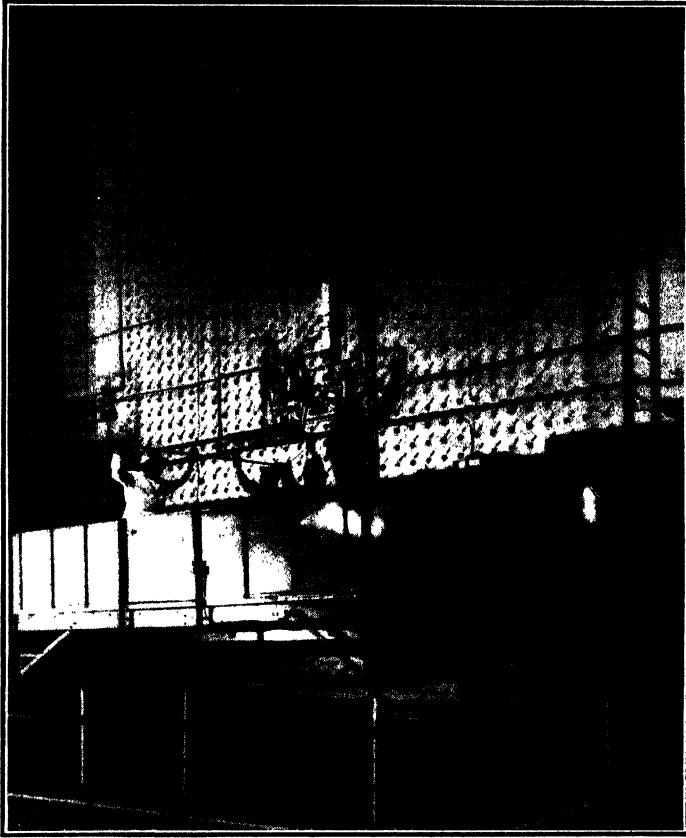


Fig. 13-8. The Clinton X-10 graphite pile, built in 1943 at Oak Ridge. The loading face is shown. The numbered tubes run through the pile. They contain uranium slugs, which are pushed through and fall into water when the time comes to discard them. (Courtesy of Oak Ridge National Laboratory and Carbide and Carbon Chemicals Company.)

arranged in a "lattice" at such distances that a neutron starting from one can is usually slowed down below the resonance energy before entering another. Descriptions are given in a book written by members of the physics faculty of the University of Pennsylvania, and in the Smyth report (Appendix 9, ref. 93 and 97).

6. Recent Reactor Developments

Types of reactors. Specialized reactors can be created to serve a variety of purposes. When a structure exceeds the critical size, there is an excess supply of neutrons. Within limits, there are options as to the way these neutrons are used. We may seek for any of the following features, or desirable combinations of them:

1. Efficient power production.
2. High power production per unit volume, as might be appropriate for powering a seagoing vessel.
3. Convenient experimentation with neutron beams.
4. Production of radioactive materials.
5. Enrichment of the heavier stable isotopes of an element by allowing neutrons to join its lighter isotopes. (Remember, however, that the heavier ones will also absorb neutrons, and thereby destroy themselves, so that the success of this measure will depend on the magnitudes of the absorption cross sections involved.)

6. Breeding. On p. 385 we saw that U 233, which undergoes fission under slow neutron bombardment, can be produced from Th 232. It happens that thorium is present to the extent of about 12 parts per million in the earth's crust; it is about three times as abundant as uranium. Of course, what really matters is the relative availability of "workable" sources of ore. It is clearly important to know whether the supply of fuel for atomic-power installations can be increased by a considerable factor through the use of the U 233 chain. Similarly, it may be possible to operate a natural uranium pile in such a way that we gain more atoms of Pu 239 than the number of U 235 atoms which are lost, while still some power is obtained. An ideal goal would be substantially complete conversion of U 238 into material which could be used in slow-neutron reactors of moderate size.

The American reactor program. A program of developing new reactors was formulated by the Reactor Division of the Atomic Energy Commission, which in 1952 included five reactors. This appeared to be the minimum program to secure advances on all important fronts. The work was under the general guidance of L. R. Hafstad. To minimize risks and disposal problems, a reactor testing station was started near Idaho Falls, Idaho. The general program was this:

- (a) Experimental breeder, Idaho. A fast-neutron reactor. It will produce a little power.
- (b) Materials tester, Idaho. A reactor to subject materials to high neutron flux and learn their behavior quickly.

(c) Submarine thermal reactor, Idaho. For submarine propulsion, using neutrons of thermal energy.

(d) Submarine intermediate reactor, near Schenectady. For submarine propulsion, using neutrons of intermediate energy.

(e) Homogeneous reactor experiment, Oak Ridge. A pilot model to explore possibilities with homogeneous fluid reactors.

One may calculate that the fission energy of 1 lb of U 235 is equivalent to

$$3 \times 10^{13} \text{ Btu, or about } 10^6 \text{ tons of coal}$$

The question arises: Is the millennium of cheap power around the corner? An Oak Ridge estimate of power costs made in 1946 indicated that nuclear power from a plant of the order of 75,000 electrical kilowatts *may* compete with coal at \$10 a ton. The nuclear power industry is still in its early infancy. We may expect that in a decade or two its place in supplying world power needs will become well defined. A good guess is that locations will be found at which breeder-power units of several hundred thousand kilowatts will be useful; also, that these will derive part of their revenue by supplying those isotopes which undergo slow neutron fission to secondary plants in regions not blessed with abundant fuel or water power.

7. Radioactive Isotopes in the Service of Science

When Professor Boltwood of Yale discovered ionium in 1906, he showed that, if it is mixed with thorium, it is impossible to separate them chemically. This was the first proof of the existence of isotopes. At the same time, the experiment opened the possibility of using radioactive materials as tracers. Wherever it is difficult to follow the behavior of a material through a series of chemical or physical manipulations, it is now natural to consider what clarification might be achieved by the addition of a radioactive isotope. The great sensitivity of electroscopic devices and counters enables us to do experiments otherwise unfeasible. This becomes clear from the following:

1. The half-life of Th B is fairly long, 10 hr, yet the electroscope will detect 10^{-16} gm.

2. The life of Po 210 is 137 days; yet a clump of a few thousand Po 210 atoms on a surface will register its presence if the surface is left in contact with a photographic plate for a few hours.

This field was exploited ingeniously by Lind and Bardwell, Hevesy, Paneth, and others, before the discovery of artificial radioactivity. Their work was hampered by the limited number of suitable natural

isotopes, but now radioactive isotopes of a majority of the elements are so cheap and abundant that tracer work has become routine procedure in numerous fields. We shall present only a few illustrations, chosen for their ingenuity and instructive value.

Production of radioisotopes. In the production of radioisotopes, the reactor and the cyclotron must be considered partners, not competitors. The present slow-neutron reactors transmute only a few of the lighter elements at convenient rates. Although the neutron fluxes are very great compared with those available from cyclotrons, the latter are in a general way more suitable for producing reactions in elements above an atomic number of about 25. The fission products, some of which are available in embarrassingly large quantities, form an exception to this trend. Thanks to the existence of an Isotopes Division at Oak Ridge, a wealth of radioactive materials is now available. In laboratories of the Atomic Energy Commission, in university laboratories, and in industry, the synthesis of molecules "tagged" in various ways with radioactive atoms is a growing specialty. In Table 13-3 we present a list of some available radioisotopes which possess special interest. Most of them are beta rayers. To be broadly useful, an isotope should have a half-life superior to 30 min, and preferably much longer than that. Furthermore, its radiations should be sufficiently energetic to insure easy detection.

TABLE 13-3. Brief List of Some Widely Used Radioisotopes

Isotope	Half-Life	Important Uses
H^3	11 yr	As a tag in organic substances.
C^{14}	4700 yr	Basic in the synthesis of a great variety of marked organics. If C^{14} is incorporated in food material, the organism itself will synthesize metabolic products marked with this atom. Useful in dating archaeological items.
Na^{24}	15 hr	Its solubility and chemical properties make it useful in a wide variety of investigations.
P^{32}	14 days	Study of bone metabolism and treatment of blood diseases.
S^{35}	87 days	Numerous chemical and industrial applications.
Co^{60}	5.3 yr	Long-lived. Its strong gamma rays allow it to replace radium in radiography and therapeutics.
I^{130}	12 hr	Thyroid metabolism; treatment of thyroid diseases.
I^{131}	8 days	

Physical applications. 1. The tracer method is well suited for studying the diffusion of one solid into another. In this way the "self-diffusion" of zinc into zinc, among other cases, has been measured.

2. In adsorption studies it is possible to follow the behavior of an amount of material insufficient to form a single molecular layer. Non-uniformity in the distribution of radioactive substances on a surface can be studied by the use of photographic plates.

3. The solubility of lead chromate in water is so slight that it cannot be accurately determined by ordinary analytical methods. Suppose we add a few millicuries of thorium B, a lead isotope, to 10 mg of ordinary lead, and determine the activity of the mixture by means of an electro-scope. The activity can be expressed in arbitrary units. If the activity of the 10 mg is called 10,000 units, then 1 unit will correspond to 0.001 mg of lead. We now prepare a saturated solution of lead chromate from the lead containing thorium B. The activity of the residue obtained by evaporating 100 cm³ is easily measurable. From this activity, we can find the amount of lead in the solution by simple proportion. The value found is 2×10^{-10} moles/cm³. This measurement gives *total* lead while an electrical conductivity measurement would give only the part in ionic form.

Chemical applications. 1. *Exchange Reactions.* There are numerous cases, of chemical and biological interest, in which we wish to know to what extent an element can be exchanged between two of its compounds, present in solution. (Indeed, it is often necessary in radio-chemical work to make sure, by side experiments, that a radioactive atom will stay in the molecule where we want it.) An interesting example is that of the lead oxides. When radioactive PbO and inactive PbO₂ are united in the orange-yellow compound Pb₂O₃, there is no change in the valences of the lead atoms. The units PbO and PbO₂ can be taken out of combination without any measurable indication that lead atoms have exchanged between them.

2. *The Szilard-Chalmers Type Reaction.* These investigators found a clever way to prepare products of neutron capture in very concentrated form, as follows: In irradiating ethyl iodide with neutrons, the product, iodine 128, recoils so violently that it leaves the molecule. Being free, it can be extracted by shaking up with a small amount of an aqueous solvent, leaving nearly all the unactivated iodine in the ethyl iodide, which does not dissolve in the aqueous layer to any bothersome extent.

Biological applications. In this field carbon 14 is probably more widely used than any other isotope. Activity in synthesizing molecules that contain it in known positions is intense. Incorporated in CO₂, it aids in studies of respiration. In the form of radioproteins and radio-

sugars, it will no doubt bring difficult problems of metabolism to satisfactory levels of understanding and control. Special interest centers in the study of nucleoproteins marked with C^{14} , since these substances are abundant in the cell nucleus.

Medical applications. Radiocobalt has come into prominence as a replacement for radium. Cobalt and its alloys can be fabricated before irradiation, in a variety of useful forms (wire, etc.). Thus the problem of locating a source of radiation just where the physician wants it is greatly facilitated. It is stated that any traces of radiocobalt which dissolve in body fluids are quickly and nearly completely eliminated.

REFERENCES

Appendix 9, refs. 3, 11, 39, 48, 89, 93, 95, 97, 99, 105.

PROBLEMS

1. Assuming you possess Pu 239, state what you would do to attempt production of the elements with atomic numbers 98 and 99.
2. Suppose the compound nucleus U 239 undergoes fission and that temporarily the fission fragments retain all neutrons which may finally be emitted. Take the available kinetic energy as 160 Mev. If the mass number of one fragment is x , what is its kinetic energy?
3. Suppose the *total* energy per fission is 200 Mev (including the energy liberated as the fragments decay). Calculate the energy liberated by 1 mole of uranium, and compare it with that of a combustion process yielding 100 kilocal/mole.
4. When U 238 is bombarded with neutrons, U 239 is formed, and it may split into Ba 140 and Kr 99; *suppose* each of these loses one neutron and that beta rays are then emitted until stable isotopes are formed. Work out the course of events, using only a table of stable isotopes. Check your surmise as far as possible by means of the Seaborg-Perlman table (Appendix 9, ref. 89), which gives the radioactive properties of all known nuclei.
5. Calculate the radius of a spherical "minimum-uranium" pile, under the following conditions: U 235 is used, in a carbon moderator, and the number of new neutrons per fission is 2.5.
6. How would you proceed to determine the solubility of $BaSO_4$, using only a natural radioactive substance?

ANSWERS TO PROBLEMS

2. $160(239 - x)/239$ Mev.
3. Fission of 1 mole of uranium yields 4.58×10^7 times as much energy as a chemical process giving 100 kilocal/mole.
5. 48 cm.

Cosmic Rays

I. Essential History

Extremely energetic particles are continually pouring into the earth's atmosphere. Their intensity is practically constant through the day and night. Even the Milky Way, our galaxy, does not have any special effect on the intensity, as measured by directional detectors. It was natural that investigators should apply the name cosmic rays to these entities.

The study of cosmic rays began in 1900, when C. T. R. Wilson and also Elster and Geitel found that there is always a small residual ionization in an electroscope. This could not be attributed to leakage over the insulators because it was considerably reduced by surrounding the electroscope with several inches of lead. At first it was supposed that the penetrating radiation thus cut off was due to radioactive matter present in the soil, but in 1910 Gockel made measurements in a balloon and found the discharge rate aloft was greater than the rate at ground level. Higher flights showed that the radiation comes from above.

In 1921 Millikan and Bowen sent small sounding balloons to heights of nearly ten miles. At sea level, the total ionization due to *penetrating* rays is 1.4 ion pairs per cm^3 per second (written briefly as 1.4 *I*), but at great altitudes the value is hundreds of times greater. The energy brought in by cosmic rays is equivalent to about one-tenth of the total thermal radiation received from the stars.

The total thickness of absorbing material in the path of the rays is often stated by giving the number of meters of water which would produce the same pressure at the observation point. The "water equivalent" of the whole atmosphere is 10.33 m of water. Again, the layer traversed is often expressed in gm/cm^2 , called "atmospheric depth." The approximate connection between height and other useful quantities is given in Table 14-1. The three heights considered are those accessible to ordinary balloons, to special balloons for study of the primaries, and to suitable rockets.

TABLE 14-1

Height			Gm/cm ² of Air Above	Pressure, mm of Hg, Approximate
Feet	Kilometers	Miles		
0	0	0	1033	760
52,000	16	10	105	76
85,000	26	16	21	15
520,000	160	100	Negligible	Negligible

From the altitude variation of the intensity, measured in relatively thin-walled chambers, it is possible to calculate an *effective* absorption coefficient for the ensemble of ionizing agents, namely, $\mu = 0.005/\text{cm}$ of water. This is very small compared with absorption coefficients for ordinary gamma rays. At the time when this value became known, it seemed reasonable to suppose that the primary cosmic rays are very hard gamma rays, and that the ionizing particles observed by our instruments are electrons thrown forward by them. Later, as a result of ingenious work by Bothe and Kolhörster, it was appreciated that *relativistic particles, (i.e., those with velocity near c) have great penetrating power, and their ability to knock other particles forward extends the range at which their effects can be detected.* We now know that the high-energy rays that enter the atmosphere are nuclei, mostly protons.

Cloud-chamber observations showed the presence of very fast electrons and positrons, singly and in droves, but these are not primaries. As early as 1932, Rossi brought forward evidence for the presence of particles much more penetrating than electrons and positrons. For several years the problem of their nature remained unsolved. Finally, in 1937, came the definitive proof that the cosmic rays contain mesons, particles with masses intermediate between those of the proton and the electron. This discovery, by Street and Stevenson, and by Anderson and Neddermeyer, laid the foundation for a new phase of study.

The effects produced by the primaries and their progeny are complex. In analyzing them, the great troubles have been the *smallness* of our instruments, and the inaccessibility of the primaries. Whatever the investigator might find with counters or cloud chambers, he always wanted to know what went on in regions outside the "vision" of his instruments. Rapid recent progress has been largely due to the use of photographic plates (p. 296) exposed on lofty mountains or carried by balloons to still greater altitudes.

Since there have been several first-rate surprises, it would be profitless to develop the subject in chronological order. The complexities have to be approached by stages, so the next section describes the general

features of the rays. This leads up to instrumentation, and to the behavior of particles having relativistic speeds. We shall then consider comprehensively the nuclear and electronic events occurring in our atmosphere, the gross facts of cosmic ray distribution, and, finally, some speculations on their origin.

2. The Nature of the Cosmic Rays

The primaries. Figure 14-5 depicts the more important cosmic-ray processes, secondary as well as primary. The primaries responsible for the bulk of the observed effects are charged particles. Clay obtained the first evidence in this direction. He observed a latitude effect, due to the barrier imposed by the earth's magnetic field. Later, due mainly to the efforts of T. H. Johnson and W. F. G. Swann, it was possible to prove that the primaries contain a considerable excess of positives, leading to the view that they are protons. Recent work by groups at the Universities of Minnesota and Rochester with plates exposed in balloon flights has thrown light on the constitution of the primaries. The great majority are protons, but nuclei with atomic numbers up to 26 or more are also found, the percentage decreasing as Z increases. The flux from outer space does not contain any appreciable amounts of high-energy photons or electrons—less than 1 per cent, according to some lines of evidence. Neutrons are believed to be absent from the primaries, because of their instability. The secondary neutrons have been intensively studied by Korff and his associates in a series of interesting and beautiful experiments.

1. *The Earth's Field—A Barrier.* A charged particle from outer space cannot reach the earth's atmosphere unless it has an energy greater than a certain limiting value, because its path is curved by the earth's magnetic field, except in the case of approach along a radius striking the north or south magnetic polar regions. Broadly speaking, curvature within the atmosphere is unimportant. At the magnetic equator the energies required for vertical entry are as follows:

Electron	15 Bev
Proton	14 Bev
Alpha particle	11 Bev

The figures for points in Europe and the United States are considerably smaller. For a proton traversing the atmosphere vertically and escaping all nuclear collisions, the ionization loss would be about 1.4 Bev. Of course, there will be nuclear collisions, and this figure merely sets a lower limit on the loss. The reader should notice that in the longitude

of central United States the magnetic latitude is about 12° higher than the geographic latitude, because the north magnetic pole is at 78.5° N, 69.1° W, according to J. A. Fleming.

2. *Collisions of the Primaries with Nuclei.* Collisions with nuclei are the principal means of reducing the energy of the primaries, ordinary ionization loss being a minor factor (p. 421) for primary protons, though it is not to be neglected when the bombarder is a nucleus of larger Z . The nuclear collisions are so effective that the process is at a maximum at a height of about 27 km, that is, at "depths" of 20 gm/cm^2 or less.

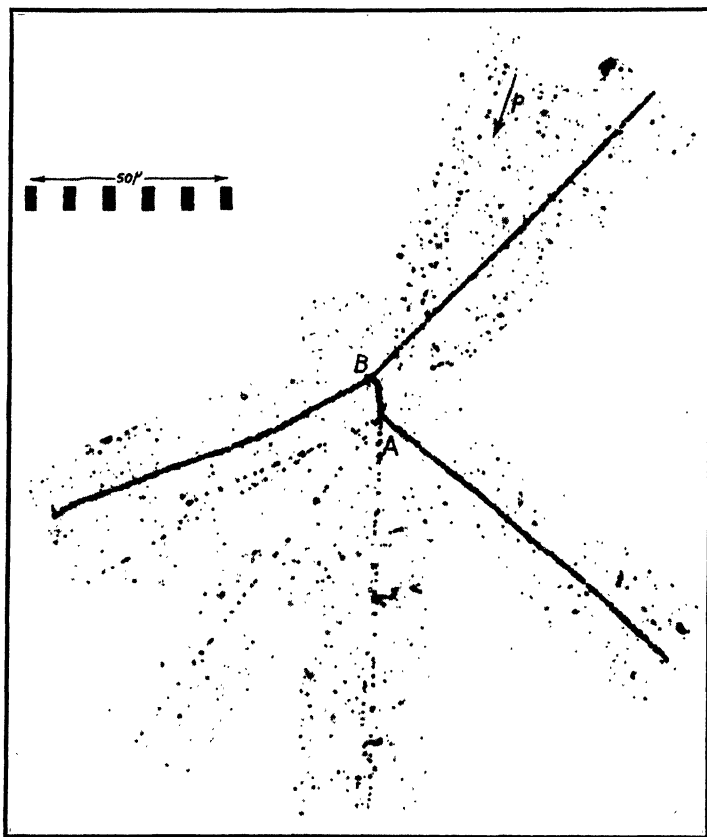
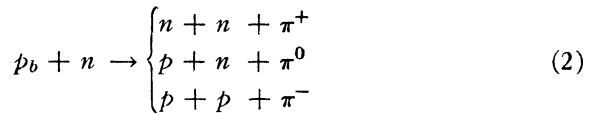
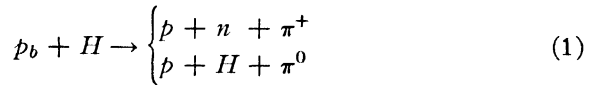


Fig. 14-1. A cosmic-ray star. Disruption of a nucleus, at point A , by a fast proton, marked p , in the emulsion of a photographic plate. A heavy particle and several particles of minimum ionization are emitted. Presumably they are mesons. Also a slow π -minus meson is emitted, and causes a second disintegration at B . (After C. F. Powell, Reports on Progress in Physics, **13** (1950). The Physical Society, London; "Mesons," Plate IV.)

With obvious minor exceptions, primaries able to get through the earth's field have ample energy for complete disruption of the nuclei of nitrogen or oxygen, as well as the nuclei of silver or bromine in the plates employed to study them. The photographic records of such nuclear disruptions are called stars (Fig. 14-1). The events observed range from simple ejection of a proton or neutron up to occasional production of a star containing as many tracks as there are protons in the nucleus. In such a case, it is probable that most of the neutrons have been knocked out. Of course, they are not usually detected within the confines of the emulsion.

Pi mesons. 1. *Production.* Mesons, positive, neutral, and negative, are born in these explosions, sometimes singly and sometimes in groups (Fig. 14-5). The simplest reactions giving rise to π mesons are



Here p_b stands for a bombarding proton. If very energetic protons fall on deuterium, the results may approximate these equations since the binding energy of deuterium is small. When the nuclei of our atmosphere are bombarded, single nucleons are sometimes split off. Also, many more complicated events occur, involving production of several mesons by interaction with one or more nucleons. The cross sections for some of the simpler processes above were discussed by Hamilton, Heitler, and Peng in 1943. In retrospect, it is interesting to see that they predicted many features that are accepted as experimental fact today. Because π mesons are produced copiously in nuclear explosions, we infer that they must be able to interact strongly with nuclei, and so they often do, in the dense matter of photographic plates. Figure 14-2 shows a fast π meson exploding a nucleus and producing other mesons in turn.

These observations were confirmed by the artificial production of charged π mesons at Berkeley, in 1948. Gardner and Lattes bombarded thin targets of a variety of elements with alpha particles of energy 390 Mev. This energy suffices only for the production of single mesons. The paths of the emitted π mesons were curved by the field of the cyclotron. Photographic plates placed at a suitable point showed the characteristic paths of mesons. Some of the tracks ended in stars.

In 1949, York, Moyer, and Bjorklund showed that neutral mesons are produced in cyclotron targets; then Steinberger, Panofsky, and Steller used gamma rays of 330 Mev to produce neutral π mesons.



Fig. 14-2. Collision of a fast π meson with a nucleus. The meson is of negative sign. Three charged particles are emitted. (After C. F. Powell, Reports on Progress in Physics, **13** (1950). The Physical Society, London; "Mesons," Plate II.)

Now an essential point must be grasped. The π mesons are unstable. The positive and negative varieties have half-lives of the order of 2×10^{-8} sec. In this time they can travel only a few hundred centimeters. The half-life of the neutral variety is believed to be of the order 5×10^{-14} sec.

2. *The Lengthening of Life due to Motion.* Here a new feature enters. When a particle moves relative to an observer, time intervals associated

with the behavior of the particle are *increased*, relative to their values when the particle is at rest. The theory of relativity predicts (p. 466) that such events, as judged by this observer, are deemed to be more leisurely. The half-life of the particle is given by

$$T = T_0 / (1 - \beta^2)^{1/2} = T_0 (m/m_0) \quad (3)$$

where T_0 is the half-life when the particle is at rest. A fast meson, therefore, will traverse more matter before decaying than it would traverse if its kinetic energy were small, compared with the rest-energy. Nevertheless, most of the decay of π mesons in the atmosphere will be accomplished within a distance of, say, 1 km from the point of production, because T_0 is so small.

We have, then, two modes of disappearance to consider: absorption by nuclei, and decay. The relative importance of these two modes is under active study. A difference in the behavior of π^+ and π^- mesons is to be expected, because the π^- meson is attracted by nuclei, while the π^+ meson is repelled.

3. *Disappearance of pi Mesons.* A π meson of either sign can decay (Fig. 14-3) to yield a μ meson of the same sign, and a neutral particle of small mass, probably a neutrino. Since the neutrino leaves no track, only the μ meson is observed when decay occurs in a plate. Often the decay occurs after the π meson has been practically brought to rest. Then the energy of the daughter μ meson is *always* about 4 Mev, this being the crucial evidence that only one other particle emerges. In the case of negative π mesons, which are attracted by nuclei, the production of nuclear stars competes strongly with the decay process.

Mu mesons. 1. *Their Life.* At various times the μ mesons were called mesotrons, or yukons, after Yukawa, who predicted their existence. At sea level they outnumber all other ionizing particles by a factor of 2 or 3, depending on latitude. They may be positive or negative. They are unstable, with a half-life of about 2.1×10^{-6} sec, while moving slowly. This instability was brought to light by a peculiar discovery. The absorption of μ mesons in a layer of air weighing D gm/cm² is much greater than that in a layer of water, or other material of low atomic number weighing the same number of gm/cm². Yukawa had predicted that the meson would be unstable, and Kulenkampff pointed out in 1938 that mesons passing through a tenuous medium *appear* to be more strongly absorbed, because some of them die along the path. Nevertheless their half-life, augmented by the relativity effect just described, is great enough so that fast μ mesons liberated in the high atmosphere can penetrate to the earth's surface, in numbers

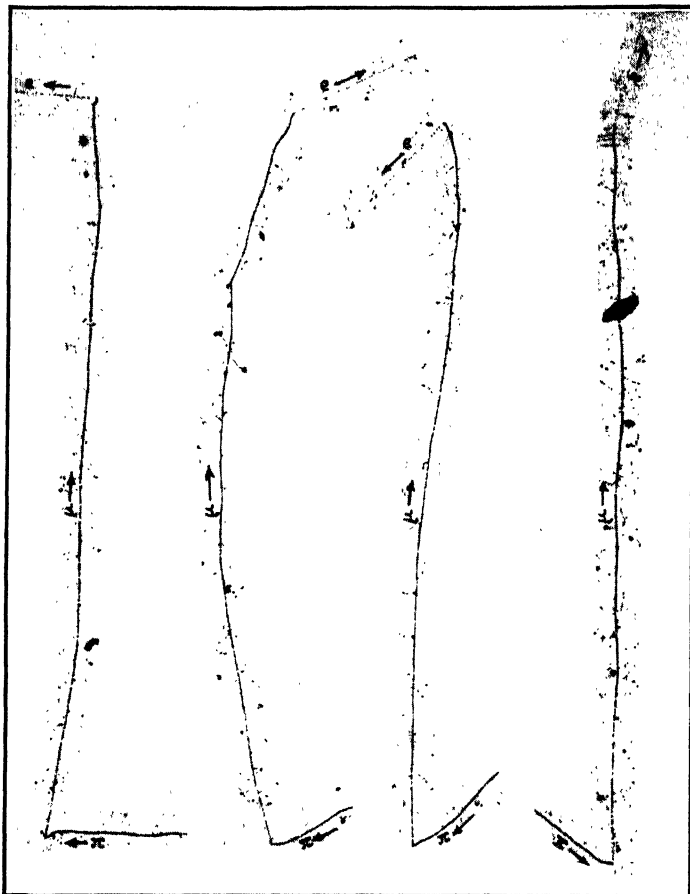


Fig. 14-3. Four examples of the decay of a π meson, practically at rest, and of the resultant μ meson when it has come to rest. Special plates are required to show decay electrons. (After C. F. Powell, Reports on Progress in Physics, **13** (1950). The Physical Society, London; "Mesons," Plate I.)

large enough to make them the most prominent constituent of the sea-level cosmic rays.

Indeed, weak cosmic ray effects are observed in mines at depths of 1000 m or more. Single ionizing particles, showers, and stars are found there. The nature of the *initiating* particles is not fully understood. Very fast mesons are probably the cause, but the existence of neutral entities such as π^0 opens up new possibilities for understanding these effects.

2. *Fate of the Mu Mesons.* Negative charge favors entry into nuclei, and positive charge favors decay. The visible product of disintegration is an electron, Fig. 14-4, of the same charge as the μ meson. Contrary to the situation for π mesons, the energy of this decay electron is *not* definite. In the experiments of Leighton, Anderson, and Seriff, it ranges from 9 up to 55 Mev. Probably the unobserved lower limit is zero. At first sight, it might seem reasonable to assume that we are dealing

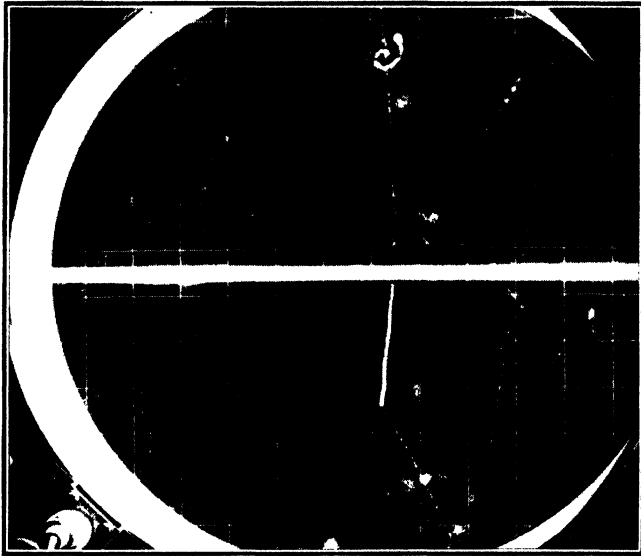


Fig. 14-4. Decay of a μ meson. [After R. W. Thompson, Phys. Rev. **74**, 490 (1948).] A positive μ meson enters the chamber almost vertically from above and barely penetrates the $\frac{1}{4}$ -in. horizontal aluminum plate. The meson stops in the gas and disintegrates, ejecting a decay electron toward the lower right.

with a beta decay, but this view is customarily rejected on the basis that spin would not be properly conserved. The train of reasoning is this: Durbin, Loar, and Steinberger have proved that the charged π meson has zero spin. When it splits into two particles their spins must add up to zero, and therefore must be equal in magnitude. Out of all existing possibilities, the value $1/2$ is most likely, because the invisible partner of the μ meson can then be a neutrino. But, if the μ meson has spin $1/2$, its decay cannot produce just two particles of spin $1/2$, because certain symmetry conditions would be violated. This leads to the inference that in μ -meson decay the electron is accompanied by *two* invisible partners, of nature still unknown. It is fairly well established

that they are not energetic photons, and the best present guess is that they are neutrinos.

Showers. 1. *The Electronic-Photonic Component.* Electrons can be knocked forward by onrushing mesons or by energetic nuclei. Decay of fast-moving μ mesons may also produce fast electrons. No doubt there are also other cosmic-ray processes that set electrons in motion.

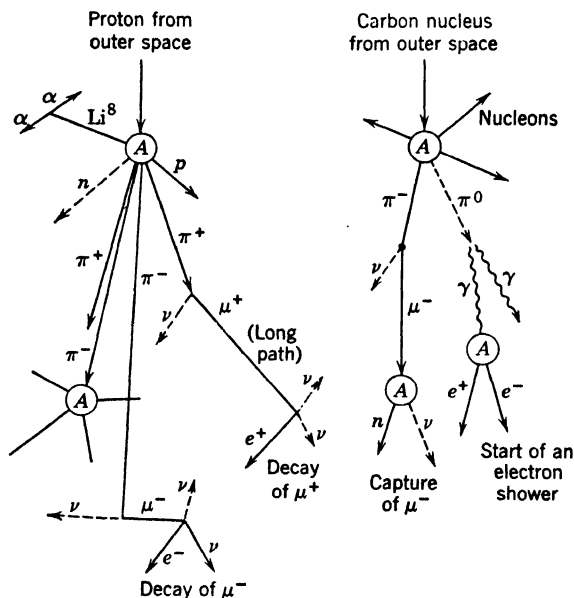


Fig. 14-5. Fast protons and heavier nuclei from outer space split nuclei (A) of the upper atmosphere, and produce π mesons, both singly and in showers. The charged π meson decays, giving rise to a μ meson of similar sign and a neutrino. The neutral π mesons give gamma rays, which can start electron showers. Gamma rays may also originate in other ways. The μ 's have long paths. A positive μ meson decays into a positron and (probably) two neutrinos; a negative μ meson may have a corresponding fate. Alternatively, they may be captured into Bohr orbits, by a nucleus; thence they enter the nucleus, ejecting a neutron and neutrino, according to present evidence.

But fast electrons, in turn, produce energetic gamma rays; these in turn produce more electrons; and so on. A chain of such multiplicative processes is called an electron shower. In general the energy of the individual particles in a shower is low compared with that of the mesons, at ground level. Because of this fact, and because the effective absorption coefficient of the shower particles is greater than that of the typical mesons, the electronic and photonic part of the rays is often called the **soft component** (see Section 3).

2. *Mesonic Showers.* The multiple production of mesons by nucleons and by π mesons leads to showers composed of mesons and their progeny. Any very energetic μ meson in such a shower may in turn produce a subshower of electrons and gamma rays by knock-on processes or by μ -meson decay. Thus a mixed shower can be produced.

3. Experimental Methods

Most of the early cosmic-ray work was confined to measurements of ionization. Later on, methods were worked out for finding the numbers of ionizing particles, their directions of travel, ranges, specific ionizations, and energies.

The description of intensities and absorption properties. Sometimes we are interested in the total *downward flux*, J . This is the number of downward-moving particles that traverse a horizontally placed square centimeter, per second. The *vertical intensity*, I_v , is often measured with directional receivers. Since the particles come from all directions, the number that come *straight* downward is strictly zero, but we can consider the number I_v that come down, through a square centimeter per second, *per unit solid angle*. The number I_A at any zenith angle A is similarly defined. One might think that, at the top of the atmosphere, I would be independent of direction, but this view overlooks the influence of the earth's magnetic field. Nevertheless, it is often assumed, as a rough approximation, that I is independent of direction at great heights. If this were true, then J would be πI . At ground level, where oblique particles have been preferentially screened out, it is a fact that the numbers for J and for I_v are not very different; furthermore, I_A is approximately $I_v \cos^2 A$. Values given in a summary article by Rossi are shown in Table 14-2. For orientation purposes, the reader may keep in mind that in middle latitudes, at sea level, the total downward flux is about 0.018 particles/cm² sec, and that the largest value, at great altitudes, is only about 40 times larger.

★ Arbitrarily, Rossi defines the hard component as the portion able to produce effects behind a shield of lead weighing 167 gm/cm²: that is, about 15 cm thick. The soft component is defined as the part that can produce effects through apparatus walls equivalent to 5 gm/cm² of brass, or about 0.5 cm, *minus* the hard component, of course. (It is necessary to set such an arbitrary lower limit of penetrating power to avoid inclusion of the radioactive background.) Roughly, the hard component corresponds to μ mesons and possibly a very small number of residual protons, and the soft component to electrons and photons. It must be pointed out that the words "hard" and "soft" have been used very loosely in this subject.

TABLE 14-2. Sea-Level Intensities of Cosmic Rays

Component	Horizontal Flux (particles/cm ² sec)	Vertical Intensity (particles/cm ² sec steradian)
Hard	0.0127	0.0083
Soft	0.0052	0.0031
Total	0.0179	0.0114

The rays are not absorbed exponentially. Slant entry, angular divergence, shower production, changes of cross section with energy, and changes of meson life with energy—all these complicate the law of decrease. Nevertheless, in some regions the semilog plot of intensity versus atmospheric depth is reasonably straight (Fig. 14-26), so an effective absorption coefficient, p. 406, can be defined. It has become customary to express the facts by giving the *absorption thickness*, the number of grams per square centimeter that reduces the intensity by a factor e (see Table 14-4, p. 449).

Pressure ionization chambers and the phenomenon of bursts.

It is possible to magnify the weak ionization effects due to cosmic rays by using a thick-walled chamber filled with gas to a pressure of 30 or 40 atm. The gain is not proportional to the gas density because the recombination of ions and the attachment of electrons to gas molecules become more important with increase of pressure, so a smaller proportion of the ions reaches the collecting electrodes. An electrometer attached to a pressure-ionization chamber shows a steady drift, which can be recorded on photographic paper wrapped around a slowly rotating drum. In 1927, Hoffmann found a large jump in such a photographic record, which indicated the sudden production of about 4 *million ion pairs* in the chamber. On the average, about 35 ev are required to produce an ion pair in air, so this burst of ions indicated the sudden liberation of 1.4×10^8 ev in the gas of the chamber. Now the number of ion pairs formed per centimeter along the track of a very fast electron in air at normal pressure and temperature is only about 50, so there are two plausible explanations. Either the cosmic rays disrupted a nucleus, liberating several particles of atomic mass, and probably mesons also, or the chamber was traversed by a great number of particles of electronic mass. Bursts of both types, and intermediate ones, occur. The electronic phenomena predominate near the ground. Hoffmann bursts have been observed in which the energy liberated is certainly 20 Bev and possibly as much as 1000 Bev. In chambers of ordinary size, only a few large bursts occur per day.

Counters in cosmic-ray work. 1. The simple coincidence arrangement of p. 291 is the prototype of more complex arrays employed in studying cosmic rays. Figure 14-6 shows three counters with axes parallel. Suppose we employ a circuit that gives an indication when, and only when, all three counters are activated. The device rejects accidental coincidences more effectively than is possible with only two counters.

With such an arrangement we can find the number of particles that fall on a horizontal square centimeter per second, coming from such directions that they pass through all three counters. Thus the apparatus functions as a cosmic-ray telescope. By turning it to different orientations the angular distribution of the rays can be determined, as well as the *total* number of particles per minute coming from all directions and striking a horizontal square centimeter. In such work, it is necessary to find the efficiency of the counters, for a counter does not respond to *all* the particles which pass through it. A counter may discharge when only a single ion pair is produced inside, but also it may fail to count if practically all the electrons produced become attached to gas molecules. Depending on experimental conditions, the efficiency may run from 40 to about 98 per cent. It is determined by an ingenious method.

In Fig. 14-6, let the circuits be arranged to count the triple coincidences per unit time, N_t , and also the double coincidences N_d in counters I and III alone. Neglecting the accidentals for simplicity, we know that an ionizing particle passes through counter II whenever I and III record a count. Out of N_d cases in which I and III count a particle, counter II responds N_t times. Its efficiency is therefore N_t/N_d . Now, placing counter I in the middle, its efficiency can be determined, etc. Thus it is possible to compute how many triple coincidences would be observed if all three counters were perfectly efficient.

2. *Anticoincidence Method.* In many experiments, it is necessary to have some way of recognizing or excluding events in which a coincidence train is set off by the particles of a shower, rather than by a single particle that passes through all its members. This is done by placing sheets of counters around the sides of the coincidence train. The pulses from these sheets are applied to the recording circuits so as to block the recording of a coincidence whenever one or more of the anticoincidence counters is triggered by a particle.

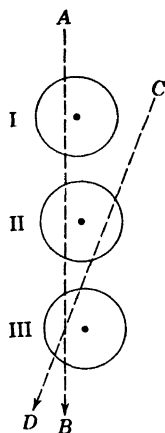


Fig. 14-6. Three coincidence counters in line, forming a cosmic-ray telescope. Particle AB causes a triple coincidence; CD does not.

3. *The Rossi Shower Experiment.* Rossi opened a fruitful field when he performed an experiment on shower production, illustrated by Fig. 14-7. Three or more counters are placed below a block of lead (or any other solid material) in such an arrangement that a single ionizing particle cannot go through more than two of them. Multiple coincidences between the discharges of these counters mean that at least two particles have traversed them and the arrangement is really a recorder

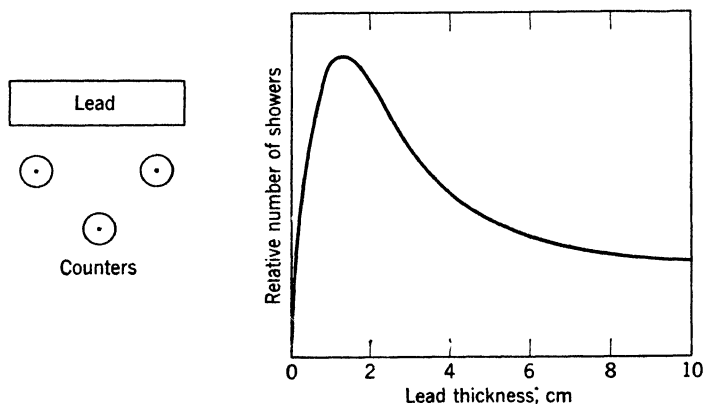


Fig. 14-7. Left: Counters arranged to measure the production of showers in lead. Right: The so-called transition curve giving the dependence of the number of showers on the thickness of the lead.

of showers. If the lead is removed, there are some showers from the atmosphere above, and corrections may be made for these. Beginning with thin plates of lead and increasing the thickness, the number of showers increases, reaches a maximum at a thickness of about 1.6 cm, and decreases again. To simplify matters, suppose the showers are produced by a homogeneous radiation which is absorbed exponentially in lead and that the shower particles are also exponentially absorbed. Then from the shape of the curve in Fig. 14-7 it is possible to read off effective absorption coefficients for the shower particles and for the entities primarily responsible for the showers. It will be noted that a lead thickness of about 2 cm greatly accentuates the electronic showers at our disposal. In the first 1.5 cm the number of shower particles produced increases rapidly on account of the increasing thickness of material. Any additional thickness beyond about 6 cm, however, absorbs about as many of the shower particles as are produced. In other words, a kind of equilibrium has been reached in which each shower producer is accompanied by a number of shower particles appropriate to the nature and

thickness of the absorbing medium. A thickness of about 15 cm of lead is ordinarily considered sufficient to remove the particles of all electronic showers that originated above it. Numerous variations of this experiment have been devised, to study both electronic and mesonic showers.

Cloud-chamber methods. In getting fair samples of the cosmic rays passing through a cloud chamber, expansions must be made according to a plan which pays no attention to the happenings in the rays. We may expand at regular intervals, or quite at random. But often we are interested in a particular class of events. Then (p. 295) counter control is employed. This makes it certain that relevant tracks will be found on nearly every photograph. For example, if we wish to study events in which a particle moving vertically downward creates a shower of at least 3 particles in a plate of lead, we use the arrangement of Fig. 14-7. Plates for absorbing or slowing down the particles are often placed across the chamber. They make it possible to examine the ranges of the particles in solid matter.

4. The Behavior of High-Energy Particles and Photons

In cosmic-ray studies, many of the interesting phenomena involve particles with velocities near c , and therefore, actual masses large enough to justify neglect of the rest mass as a first approximation. We shall discuss the mechanical behavior of such particles and of the photons they produce.

★ **The classical, transition, and relativistic regions.** In dealing with fast particles, it is often useful to employ a simple relation between the *total* energy E and the momentum p , of a free particle moving with the speed βc . Obviously,

$$\frac{1}{1 - \beta^2} = 1 + \frac{\beta^2}{1 - \beta^2}$$

Now, using equation 8, p. 34, and equation 6, p. 33, we note that

$$E/m_0c^2 = (1 - \beta^2)^{-1/2} \quad p/m_0c = \beta/(1 - \beta^2)^{1/2}$$

Substituting in the previous equation, we find that

$$\left(\frac{E}{m_0c^2}\right)^2 = 1 + \left(\frac{p}{m_0c}\right)^2 \tag{4}$$

This tells us that, if E is measured in terms of the very reasonable unit m_0c^2 , and p in terms of m_0c , then

$$(\text{Energy})^2 = 1 + (\text{Momentum})^2$$

where the term 1 really represents the square of the rest energy. For any particle it is convenient to distinguish three regions of kinetic energy in which the behavior is quite different.

Region	$E/m_0c^2 - 1$	v/c
Classical	Small	Small fraction
Transition	About 0.25 to about 5	About 0.6 to 0.98
Relativistic	Large	Practically 1

★ In the classical region the kinetic energy is simply proportional to the square of the momentum. In the transition region the relation is more complex (algebraically speaking), because of the variation of mass with velocity. In the extreme relativistic region, the kinetic energy is so great compared with the rest energy that the latter may be neglected in computing the total energy. Then the energy and momentum are practically proportional to each other, because the speed is nearly equal to c . In this domain, approximately,

$$E = pc = HRZe \quad (5)$$

where H is an applied magnetic field and R the radius of curvature of the path of a particle of charge Ze , moving at right angles to that field (p. 277); e is in electrostatic units, and H in oersteds. Writing E_v for the energy in electron volts, this becomes

$$E_v = 300HRZ \quad (5a)$$

The accurate relation from which this approximation comes is

$$(E_v^2 - E_{v0}^2)^{1/2} = 300HRZ$$

where E_{v0} is the rest energy in electron volts. We see that for particles of given Z and sufficiently high energy, the value of HRZ does not depend on the rest mass, just because the energy is nearly all kinetic. In middle latitudes the average primary cosmic-ray proton has an energy of 6 or 7 Bev, while the rest energy is about 1 Bev. Equation 5a applies well to any 6-Bev particles whose mass is equal to or smaller than that of the proton; the path curvature will be much the same for electrons, mesons, and protons with an energy of several Bev. Also, the ionization losses will be nearly the same. This shows why it is hard to distinguish between very fast particles of charge e , having quite different masses, in cloud chambers or ion chambers. To make a convenient experimental distinction, we have to look for other characteristics, such as the ability of fast π mesons to shatter atomic nuclei.

Energy loss by very fast particles and photons. On p. 298 we have explained that nuclei and electrons with energies of a few million volts fritter away their energy by a succession of small losses, ionizing and exciting the atoms through which they pass; production of radiation is a relatively small effect. Therefore particles with such energies have definite ranges, while gamma rays, losing a relatively large fraction of their energy in a typical Compton scattering, or in pair production, are absorbed according to an exponential law.

The situation is different in the cosmic-ray domain. In Figs. 14-8 to 14-10 we summarize the trend with changing energy of some of the more important losses that are experienced by electrons, photons, and μ mesons moving through air. The nuclear disruptions caused by π mesons and protons make their behavior more complicated. We postpone discussion of these nuclear effects to Sections 6 and 8.

Behavior of electrons and photons. Our understanding of the behavior of electrons and photons is fairly complete up to energies far above that at which they can produce mesons by interacting with nuclei, because the cross section for meson production by these entities is small compared with that for other processes which will now be considered.

1. For fast electrons, either positive or negative, the *average* loss per centimeter, due to ionization and excitation, has been calculated by Bethe. As their energy increases through the range shown in Fig. 14-8, this loss decreases, passes through a minimum in the neighborhood of 10^6 ev, and slowly increases again. (We remind the reader of the Bragg curve, shown for alpha particles on p. 297.)

2. In addition to the frittering away of energy by ionization, an electron with energy much greater than m_0c^2 can lose a large fraction of it by radiation when it is decelerated in a close encounter. This process is the one that gives rise to the continuous X-ray spectrum. The average radiative loss as calculated by Bethe and Heitler is also shown in Fig. 14-8. (The curves refer to water but will serve approximately for air.) At high energies, according to theory, the average radiative loss is large compared with the ionization loss, and a particle can lose a large fraction of its energy in a single radiative act. The nuclei of the medium are the chief cause of radiative loss because the effect varies with the square of the charge of the struck particle.

★ We shall quote the formulas for ionization and radiative loss by very energetic electrons. Let E be the energy of such an electron; and let N_e and N_n denote the number of electrons and nuclei in 1 cm^3 of the medium; and let us write A_e for the conventional area of the electron, namely,

$$A_e = \pi(e^2/m_0c^2)^2 = \pi(2.8 \times 10^{-13})^2 = 2.5 \times 10^{-25} \text{ cm}^2 \quad (6)$$

Then a good approximation for the ionization loss, in ergs per centimeter, is found to be

$$2N_e A_e (m_0 c^2) \log_e \frac{E^3}{2J^2 m_0 c^2} \quad (7)$$

Here, J is an average ionization energy for the atoms affected, and is usually written as 13.5Z (in electron volts).

★ The radiation loss per centimeter due to nuclear collisions is

$$(4/\pi) N_n A_e E [\log_e (183/Z^{1/3}) + (1/18)] \quad (8)$$

provided that $E/m_0 c^2$ is large compared with $137/Z^{1/3}$. For air, we can use the average value $Z = 7.3$, so the bracket is 4.61.

★ Comparing the ionization and radiation losses, we see that in the former the energy occurs in a term which is the logarithm of a large number. Thus the ionization loss rises very slowly in the domain above a few million volts. On the other hand, the radiation loss rises in direct proportion to E . The slow rise of ionization loss results from the alteration of the lines of electric and magnetic force around a fast particle, described on p. 36. Therefore it also occurs in the case of fast mesons and nucleons. Actually, the approximate constancy of the ionization loss presents us with an experimental advantage. Ionization per centimeter is proportional to the square of the charge of the moving particle. Thus, over a very large energy range, the charge of any very fast particle

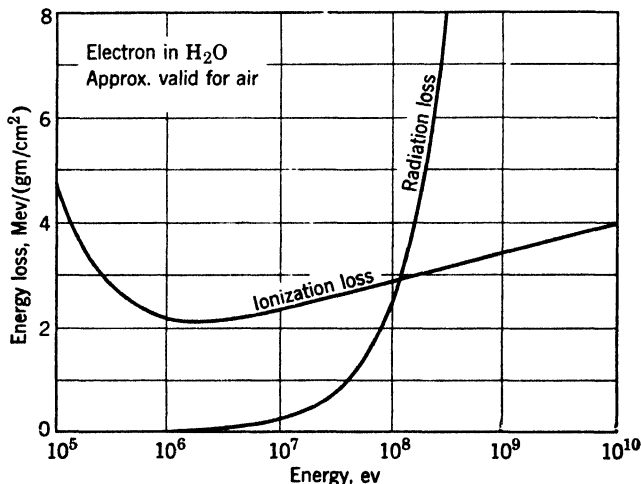


Fig. 14-8. Losses by high-energy electrons in water. The curves are approximately correct for air.

is unambiguously revealed in the cloud chamber, provided that the individual droplets of the track can be counted.

3. As for photons with an energy E large compared with m_0c^2 , the chance of a Compton scattering falls as energy increases. We shall neglect it in this discussion. That of pair production rises (Fig. 14-9), in the same fashion as the probability for radiative loss by an electron. There is an easily understood reason for this. Pair production can be considered as the inverse of radiative loss, in the sense that an electron is thrown from a state of negative energy to a state of positive energy (p. 316).

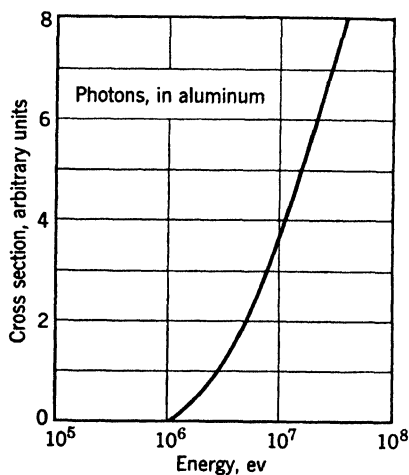


Fig. 14-9. Variation of cross section for high-energy photons in aluminum.

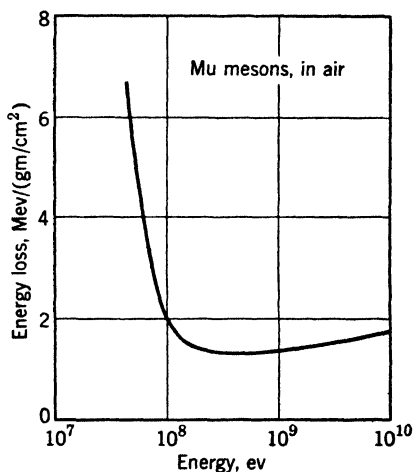


Fig. 14-10. Energy losses by high-energy μ mesons in air, as a function of energy (after Rossi).

★ Since the photon disappears when the pair is produced, it makes no sense to ask: What is the energy loss of a photon per centimeter? However, we can calculate the average energy expended in pair production by a large number, x , of photons in passing through a layer 1 cm thick, and can then divide by x to get an average loss per photon. The result is the *same* as equation 8, except that the last bracket must be replaced by $\frac{7}{8} \log_e (183/Z^{1/2}) - \frac{1}{54}$, which has the value 3.62 for air (E must now be interpreted as the initial energy of the photon.) This expression is not a *local* dissipation of energy into heat, because the pair electrons may create photons a little farther along, and so on and on, until the original energy is frittered away.

Behavior of mesons. In Fig. 14-10, we show the ionization loss for μ mesons in air, after Rossi. There is not much point in drawing a

curve for π mesons. Their lifetime is so short that appreciable ionization loss cannot occur in air before they decay. We omit a curve of radiation loss from Fig. 14-10 because it is relatively minute for either μ mesons or π mesons up to the highest energy shown. Similarly, it is small for protons. A rough explanation is easy. On the basis of classical electrodynamics, the energy radiated per second by an accelerated charge is proportional to the square of its acceleration. But the acceleration of a moving charge by a nucleus is inversely proportional to the mass of that charge. Thus the radiative loss of a particle of mass M should be of the order $(m_0/M)^2$ times the loss by an electron. This argument is not the whole story, because rough calculations show that a meson which experiences a large radiative loss will partly penetrate the target nucleus. Therefore the problem is not entirely one of deceleration by electric forces.

We may conclude that the great penetrating power of fast μ mesons, as compared with electrons of equal *speed*, is mainly due to their greater store of kinetic energy and to the insignificance of radiative loss.

5. The Primaries

It has been clear for a long time that the primaries are mostly protons. Swann concluded from various lines of evidence that a helium component is also necessary to explain the general distribution and properties of the secondary debris. Some very direct evidence was obtained by Pomerantz and Hereford in 1947. With proportional counters on balloons, they established the presence of heavier nuclei among the primaries, using the fact that the ionization by a particle of given speed varies as Z^2 .

Evidence of a more graphic and revealing character was published by Bradt, Freier, Lofgren, Ney, F. Oppenheimer, and Peters, of the Universities of Minnesota and of Rochester. A cloud chamber and photographic plates were carried aloft by balloons which hold considerable loads above 90,000 feet for several hours. At this altitude the air above amounts to only 17 gm/cm². Tracks of heavy nuclei were found, with atomic numbers up to 26, or possibly more. Figure 14-11 shows the general nature of the tracks observed, which can be followed from emulsion to emulsion in a thick stack of plates, by using suitable fiducial marks. Starting with low ionization, the density of secondaries along the path rises to a maximum and then falls off to zero over a length which is known to increase with the atomic number. Thus, the atomic number of the flying particle can be determined (or bracketed within limits) in favorable cases. There are several other ways of determining

the atomic number. For example, for most light nuclei except hydrogen, $A = 2Z$. Assuming this relation, there are several pairs of measurements which yield both the charge of the particle and its energy. The ionization and the range can be measured; or information can be obtained from the number of delta rays, or slow electrons, per centimeter of track, which are thrown out with an energy superior to a chosen limit.

Stars are, of course, produced by the composite nuclei as well as by incoming protons. Indeed, the composites are fragile and may break into a number of pieces in a nuclear collision, so that highly elaborate stars have been observed. Excellent pictures are given in a book by Leprince-Ringuet (Appendix 9, ref. 62), whose group at Paris is also contributing much to our knowledge of the heavy primaries. It is essential to realize that the loss of energy of these heavy particles per unit path is great compared with that of a proton of equal velocity. This means that the air blanket above an observation point discriminates against nuclei of higher atomic number. Also, it discriminates against those which arrive at large zenith angles. For these reasons it is difficult to say much about the percentages having different atomic numbers. Data on this point, quoted below, must be understood as referring to the point of observation, not to conditions in the outside vacuum.

★ The Rochester and Minnesota groups have led the way in obtaining such results as the following:

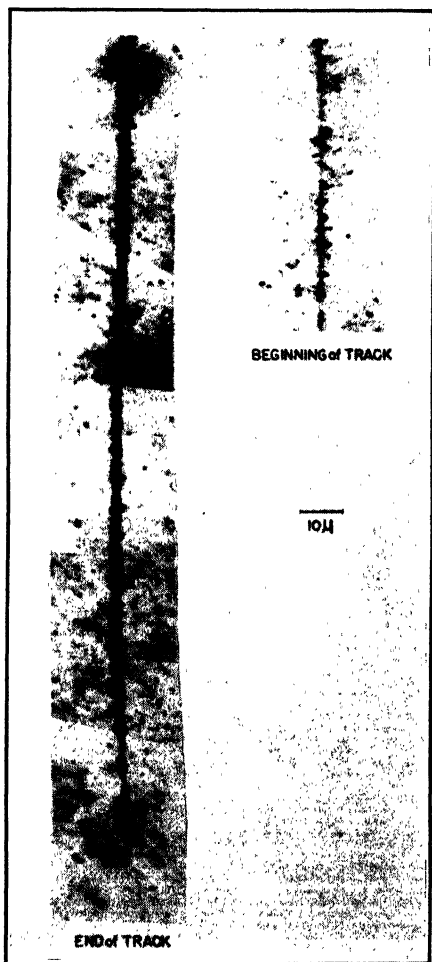


Fig. 14-11. Photomicrograph of a heavy cosmic-ray primary with $Z = 15$ (after Freier, Lofgren, Ney, and F. Oppenheimer). Note the thinning down which occurs after the particle has passed through about 10 gm/cm^2 of glass and emulsion.

1. The kinetic energies of the observed "heavies" usually lie in the range from about 0.4 to 1.5 Bev *per nucleon*. These figures refer to a geomagnetic latitude of about 55° . The lower value is determined by the geomagnetic cutoff. These particles are a low-energy selection for reasons stated above.

2. Nevertheless enough primaries of exceptional energy are found to permit study of their action in disrupting nuclei.

3. All, or practically all, arrive at angles less than 90° from the zenith. For this reason, and for many supporting reasons, they are, predominantly, primaries.

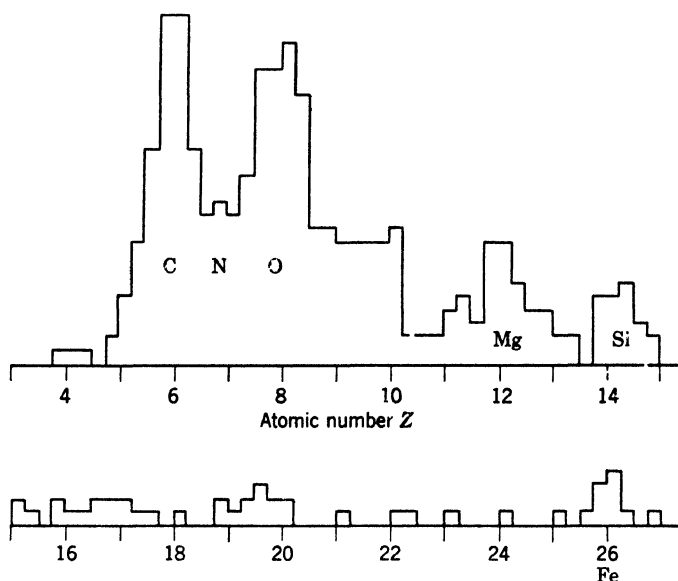


Fig. 14-12. Relative abundance of different atomic numbers in cosmic-ray primaries observed at balloon levels for $Z \geq 6$. (Drawn from the data of Bradt and Peters.)

4. The observed abundances are shown in Fig. 14-12. The method of detection employed discriminates against low atomic numbers, so attention should be paid only to the ordinates for Z equal to or greater than 6. The peaks at the elements C, N, O, Mg, Si, and Fe are notable, these being elements which are astrophysically abundant.

5. The ratio of protons to He nuclei is 3:1 or 4:1.

6. The abundance curve is such that at least half the incoming *mass* is in the form of composite nuclei.

7. According to Bradt and Peters, the general course of the abundances in Fig. 14-12 is roughly similar to that in a certain star of the constellation

Scorpio, discussed by Unsöld. Now the estimated abundance of elements in the solar atmosphere is quite different from figures referring to an "average star." Therefore it is possible that further studies of the Z distribution of the primaries will go far to settle the question whether the cosmic rays originate in the sun or outside the solar system.

★ For discussion of the energy spectrum of the total body of primaries see Section 9. The prominent role played by individual protons must not be overlooked. Our present knowledge of very-high-energy cross sections comes chiefly from study of the behavior of cosmic-ray protons and protons accelerated artificially. Germain has found that the cross section for star production in a photographic emulsion by protons of 0.34 Bev is 0.29 barn per nucleus. This figure illustrates the relatively great frequency of the effect.

6. Pi and Mu Mesons

Discovery of mu mesons and pi mesons. After the discovery of the positron there was much activity in photographing energetic particles in cloud chambers. It was logical to insert absorbing plates in the cloud chamber in order to classify particles as to their penetrating power, and also to observe the growth of electron showers by multiplication in the plates. Experiments of this kind were done by Anderson and Neddermeyer and also by Street and Stevenson, in 1937. They recognized that in addition to electrons and positrons with relatively feeble penetrating power, there were many particles that could traverse thick plates with little energy loss, and that in general these particles did not give rise to energetic secondaries. Further study showed that these particles, the μ mesons, constitute a majority of the single tracks seen at sea level. Near the ends of their tracks they ionize more heavily than electrons, though the ionization at high energies is indistinguishable from that of an electron. These facts lead to the conclusion that they have the charge of an electron, but a much greater mass. Careful studies by Brode and his colleagues, and by others, verified this inference, and in a few cases the mass was measured by determining two of the three quantities curvature, ionization per centimeter, and residual range. The measurements were not easy, and the masses found covered a range from $180m_0$ to about $900m_0$. Eventually they showed a tendency to cluster around $200m_0$.

In 1947, Lattes, Muirhead, Occhialini and Powell, of the University of Bristol, discovered that there is a heavier meson, the π meson. The discovery was made by detection of the pi-mu decay (Fig. 14-3) in nuclear emulsion plates exposed at mountain altitudes. Powell says,

"About 10 per cent of the mesons, when brought to rest, lead to the emission of a second meson. Further, it was established that the range of the secondary particle is always constant within narrow limits."

It was possible soon thereafter to show that the secondary particles satisfy all requirements for being μ mesons. We have mentioned before the production of both charged and neutral π mesons (p. 349) with the synchro-cyclotron at Berkeley. All three varieties are produced with about equal efficiency. Evidence for neutral mesons (sometimes called neutrettos) in the cosmic rays, had also been brought forward by several experimenters. They must be present in large numbers, but observations were difficult. The Berkeley experiments clinched the matter.

To accelerate the story, we present in Table 14-3 the properties of several varieties of mesons, and show their modes of production and disappearance. This table is modeled on one published by Bradner. Where an unseen particle is emitted, we label it as a neutrino, with the warning, that this only means the particle is one of small mass and negligible ionizing power. It may be years before we have conclusive evidence on their nature.

TABLE 14-3. Properties of Mesons

ν stands for a neutrino and γ for a photon. Half-lives are for particles in vacuo and at rest. A stands for a nucleus.

Particle	Spin	Mass m_0	Half-Life (seconds)	Decay Products or Process
π^+	0	273	2.0×10^{-8}	$\mu^+ + \nu$
π^-	0 or 1	273	2.0×10^{-8}	$\pi^- + A \rightarrow \text{Star (75\%)}$
				$\pi^- + p \rightarrow \begin{cases} \pi^0 + n \\ \gamma + n \end{cases}$
π^0	0	262	$< 5 \times 10^{-14}$	2γ
μ^+	1/2	207	1.5×10^{-6}	$e^+ + \nu + \nu$
μ^-	1/2	207	1.5×10^{-6}	$e^- + \nu + \nu$
				$\mu^- + A \rightarrow A' + n + \nu$
V_1^0	?	$2210 \pm$	$(3.5 \pm 1.2)10^{-10}$	$p + \pi^-$
V_1^\pm	?	Heavier than the neutron	?	$n + \pi^\pm$
τ^\pm	?	970	?	3π 's
V_2^0	?	800?	10^{-10} ?	$\pi^+ + \pi^-$
κ^\pm	?	?	Order of 10^{-9}	μ^\pm and 2 neutrals

Laboratory production of pi mesons. The general arrangement for production of π mesons by cyclotron bombardment with charged particles is illustrated by Fig. 14-13. Protons or alpha particles strike a target, which is often carbon about 1/16" thick, placed directly in the vacuum chamber. The energy of the bombarders can be conveniently controlled by changing the radius at which the target intercepts the beam of accelerated particles. Positive and negative mesons are thrown in all directions but are most numerous in forward directions, in accordance with simple momentum considerations. The positives and negatives are separated by the magnetic field of the cyclotron itself.

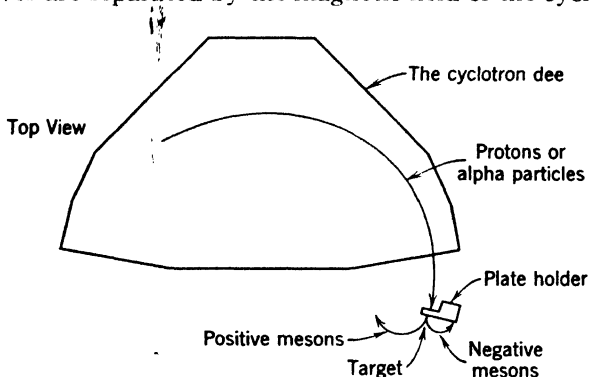


Fig. 14-13. The general arrangement for production of π mesons by bombardment with charged particles in the Berkeley synchro-cyclotron.

Their paths have smaller radii than those of the bombarders, because of their smaller mass, and also because the maximum available energy, say 390 Mev in the case of the Berkeley cyclotron, is not sufficient to give the mesons very great kinetic energy. This is rather convenient, since the mesons can be caught on photographic plates placed within a few inches of the target and heavily shielded with copper, which cuts down stray particles and radiations. The negative ones are more easily studied because they are bent outward, away from the slower bombarders circulating in the cyclotron beam. The number of mesons available is about 10^8 times greater than those available in a cosmic-ray experiment of equal duration. At a considerable sacrifice of intensity (about 1,000,000-fold) it is possible to do the bombardment outside, with the deflected cyclotron beam emerging from a thin window.

Figure 14-14 shows in more detail a simple arrangement for recording the tracks of negative mesons of different energies. A stack of nuclear emulsion plates is employed. The mesons may be allowed to impinge on the edge of the emulsion or to strike it at a small angle.

It has been shown that π mesons are also produced by neutrons and by gamma rays from the Berkeley synchrotron. York, Moyer, and Bjorklund investigated the gamma rays emerging from a target struck by 345-Mev protons. The amount of this gamma radiation was much too large to be explained by the *Bremsstrahlung* of the bombarders, decelerated in their collisions with target nuclei. It was inferred that *a neutral π meson is produced, which decays, with emission of a pair of photons*. Since these photons originated at the target, it was clear that the neutral mesons must have a very short life. A decisive experiment

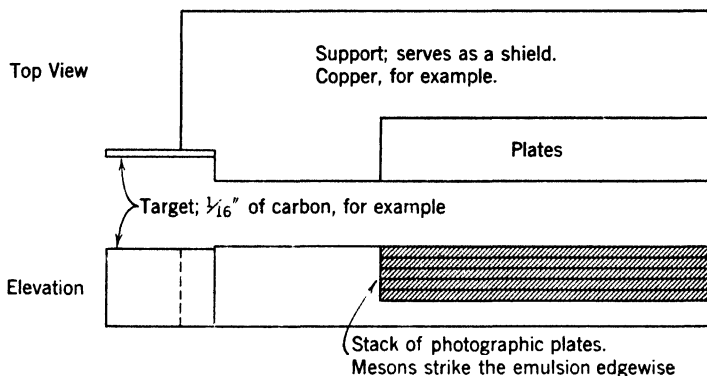


Fig. 14-14. A plate holder used for recording meson tracks in the Berkeley synchro-cyclotron (as described by Bradner).

backing up these conclusions was then made by Panofsky, Aamodt, and York. They arranged to use π^- mesons to bombard a vessel containing hydrogen. Gamma rays from this vessel were detected, and the interpretation is expressed by two modes of interaction:

$$\pi^- + p \rightarrow \begin{cases} n + \pi^0; \pi^0 \rightarrow 2h\nu(70 \text{ Mev}) \\ n + h\nu(140 \text{ Mev}) \end{cases}$$

By study of the energies involved it was possible to determine the mass of the π^0 meson, which now appears to be about $262m_0$.

★ **Multiplicity in meson production.** Heisenberg suggested many years ago that when two nucleons collide with great energy a group of particles, rather than just one particle, should be produced. Many modes of the meson field should be emitted simultaneously, somewhat as a bell, struck heavily, gives voice with many tones. Knowledge as to the truth of this suggestion is considered basic for the construction of a proper theory of nuclear forces and of mesons. It might be thought

that photographs of stars in which several π mesons are produced (Fig. 14-2) would answer the question. Unfortunately, most photographs of this type are unsatisfactory for the purpose, because there is always the possibility that the mesons are produced by plural encounters with several nucleons of the struck nucleus. What is really needed is a collision of a proton of very high energy with hydrogen in a cloud chamber, but even in this case heavier nuclei are always present to provide vapor. In the absence of such a cloud photograph, investigators have been on the lookout for exceptional events in photographic plates. The idea is that in production by plural collision the mesons will emerge over a considerable range of angles. On the other hand, production of several by a collision with a single nucleon should lead to emission of a very narrow bundle of mesons, when the energy of the primary is sufficiently great. A considerable number of events of the general type expected have now been described. Lord, Fainberg, and Schein have published a case which they believe is good evidence for multiple production. A proton of energy 3×10^4 Bev pierced a stack of photographic plates. Figure 14-15 is their reconstruction of the event. There is a bundle of tracks contained in a cone whose width is of the order of 0.2° . Near the struck nucleus this bundle appears like a single track. Farther on, it spreads until the individual tracks can be distinguished.

★ In photographs of narrow bundles, it is sometimes observed that high-energy positron-electron pairs are produced close to the struck nucleus. It is not yet clear whether these are due to decay of neutral mesons, or to direct production of gamma rays in the collision. Probably both causes are active, but it will be difficult to sort them out. The interest of the phenomenon lies in its bearing on the origin of electronic showers of great energy and spatial extent (p. 441).

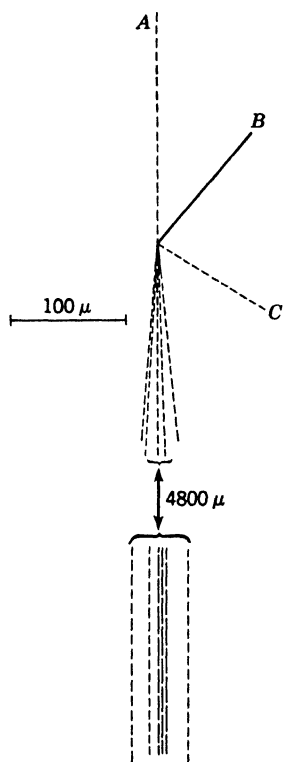


Fig. 14-15. Diagram of an event (described by Lord, Fainberg, and Schein), which they believe to be strong evidence for multiple meson production in an encounter between two nucleons. A proton of 3×10^4 Bev produces this star. A, B, and C are particles of atomic mass. The narrow jet of mesons is the feature of interest.

Behavior of charged pi mesons in the atmosphere and in photographic plates. The lifetime of a charged π meson, positive or negative, is of the order 2×10^{-8} sec. In this time the particle cannot move as much as 6 m. However, if it is born with great energy, say 3 Bev, the half-life will be 20 times the resting half-life. Even then, the meson will decay with a mean path of only 120 m. If the cross section of this meson for producing a star were as high as 1 barn, the chance of an effective nuclear collision in a 120-meter path would be entirely negligible at an atmospheric depth of the order 20 gm/cm², where most of these events go on. For this reason it is generally accepted that the normal fate of π mesons *in the high atmosphere* is decay into a μ meson of the same sign and a neutral particle.

On the other hand, the collisions with nuclei are observed in considerable numbers in the dense matter of photographic plates. Sometimes the breakup of the nucleus is practically complete. For example, a carbon nucleus may give rise to four protons and an alpha particle; they are identified by the densities of their tracks. The four neutrons, of course, leave no visible tracks.

We must carefully note the difference of behavior of the plus and minus varieties of mesons. Positive π mesons are repelled by nuclei. Hence practically all of them decay within the emulsion, just as they do in the high atmosphere; but it was found by Adelman and Jones that in an emulsion 3/4 of the negative π mesons produce stars, while the remaining 1/4 are presumed to interact with a nucleus, with possible emission of a neutron. The original reason for the latter belief is that searches were made for cases in which negative π mesons decayed in the emulsion. Very few were found. This is reasonable, because the time required for stoppage and absorption by a nucleus of the emulsion is minute compared with the half-life. Recently, Sard and others have detected the emitted neutrons.

The fact that negative π mesons interact with nuclei so effectively is the chief basis for the view presented on p. 376 that a field associated with π mesons is the principal means of interaction between nucleons; that it is the "bearer" of the nuclear forces.

★ Pi-mu decay. An interesting problem connected with the decay of negative π mesons at the ends of their tracks is to determine the mass m_ν of the neutral entity emitted. We have the mass equation

$$m_\pi = m_\mu + T/c^2 + m_\nu + T'/c^2 \quad (9)$$

where T is the kinetic energy of the μ meson and T' that of the neutral body. T can be determined quite accurately from the range of the μ meson in the emulsion, which is about 600 microns when the π meson

is substantially at rest at the time of decay. The presently accepted value of T is 4.12 Mev. Now the above equation can be rewritten in the form

$$\frac{m_\nu}{m_\mu} = \frac{m_\pi}{m_\mu} - 1 - \frac{T/c^2}{m_\mu} - \frac{T'/c^2}{m_\mu} \quad (10)$$

The kinetic energy of the unseen neutral particle can be expressed in terms of m_ν/m_μ , m_μ and T by using the fact that the momentum of the neutral particle is equal and opposite to that of the μ meson. Also, the current value of m_π/m_μ is 1.321 ± 0.002 , according to Smith, Birnbaum, and Barkas. Thus we finally have an equation containing only m_ν/m_μ and known quantities. Substituting the known values and taking note of the limits of error, it is found that the mass of the neutral particle may lie anywhere between 0 and 25 electron masses. Thus we are not able to say whether or not it is a neutrino.

The fate of mu mesons. We remind the reader that positive μ mesons decay by emission of a positron and two (or more) neutral particles. Originally, the only way to measure their half-life was to determine their absorption in a long path through the atmosphere and in a path through solid material, containing the same number of grams per square centimeter. Careful experiments of this type were carried out by W. M. Nielsen and his collaborators. They found, as expected, that the absorption on the atmospheric path was greater, since in this case the effect of decay is superimposed on the removal of mesons by collision processes. Originally, it was difficult to confirm the μ -meson decay by observation of the decay positrons in the cloud chamber. In 1940, E. J. Williams and G. E. Roberts finally observed a single positron at the end of a meson track. A similar event photographed by Thompson is shown in Fig. 14-4. Events of this kind remained very scarce until the use of electron-sensitive emulsions placed the matter on a different footing.

★ Rasetti (1941) found another ingenious method for studying the half-life of μ mesons. Figure 14-16 illustrates the principle, not the actual arrangement, which is more complex. The counters marked A detect the passage of mesons, some of which are arrested in block B . Such events are selected by the anticoincidence counters C . The decay electrons (which have high average energy, 35–40 Mev) are emitted a few microseconds later. Some of them operate the counters D . However, the pulses from the counters A are subjected to controllable delay before being combined with those from D , in a coincidence circuit. The number of coincidences decreases as this delay is made greater. The half-life obtained with an absorber of iron, $2.2 \pm 1.0 \mu\text{sec}$, was somewhat

larger than the value accepted today for positive mesons, 1.5×10^{-6} sec. It had been suggested by Tomonaga and Araki in 1940 that positive and negative mesons should behave differently after coming to rest in dense matter, but their suggestion was not fully verified until 1945, when Conversi, Pancini, and Piccioni separated positive and negative mesons by a magnetic field and measured their decays individually, with the following results:

In carbon ($Z = 6$): both positives and negatives decay.

In iron ($Z = 26$): only positives decay.

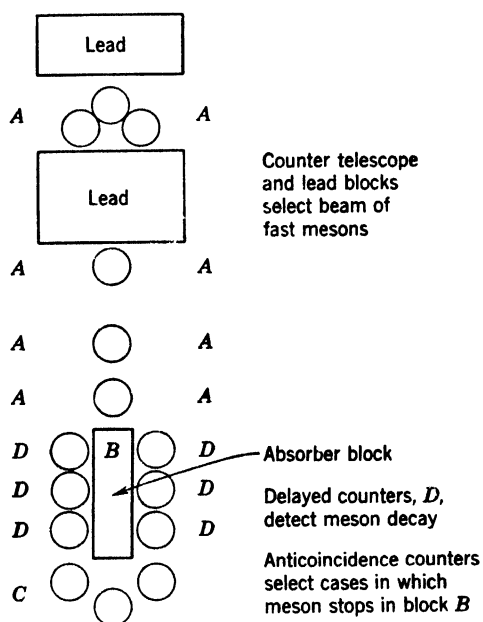


Fig. 14-16. A simplified diagram of Rasetti's arrangement for detecting the decay of μ mesons.

Clearly this means that in iron, by virtue of the greater charge on the nucleus, the negatives are captured before they can decay. For some element with Z between 6 and 26 the decays and nuclear absorptions should occur in comparable numbers. This amounts to saying that the observed half-life in such an element should be less than 1.5×10^{-6} sec. A curve by Valley and Rossi for aluminum (Fig. 14-17) suffices to clinch the matter. Wheeler has developed the detailed picture. Negative mesons are captured in very small Bohr orbits by the nucleus, whence

they may decay, or go to imprisonment in the nucleus. The fraction so captured is proportional to Z^4 , according to his calculations, and experimental results on the variation of effective half-life with Z are in fair agreement with this rule. What happens when μ mesons enter the nucleus? The following is known.

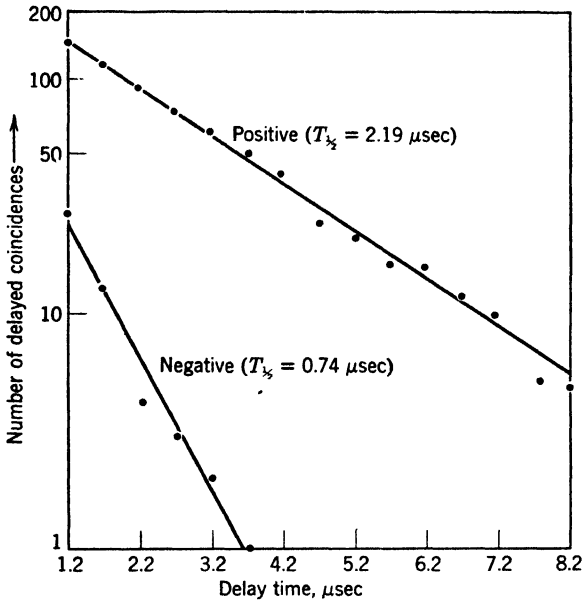
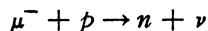


Fig. 14-17. Decay curves for positive and negative μ mesons in aluminum. The steeper the slope, the shorter is the half-life. The number observed after a delay of t sec is evidently proportional to $\exp(-t/T)$, where T is the *average* life. On p. 270 we stated that the half-life is about 0.7 times the average life. (After data by Valley and Rossi.)

1. Charged particles are not emitted in appreciable numbers.
2. High-energy gamma rays are not emitted.
3. According to Sard and his collaborators, about one neutron is emitted for each nuclear absorption. This suggests that the usual process is



If so, the recoil energy of the neutron should be a small fraction of the total energy release. Experiments on the energy of these neutrons will be awaited with interest.

7. Other Unstable Particles

For many years there have been reports of particles with masses ranging from 10 to over 1000 electron masses, in cosmic-ray photographs. Many of the instances were doubtless π or μ mesons whose tracks were badly scattered or distorted. At one time it was rather widely accepted that mesons have a continuous spectrum of masses. It is still possible that a limited fraction of the mesons form such a spectrum. Alikhanian, Alikhanov and Weissenberg interpreted their observations in this way, and called their particles varitrons.

However, the occurrence of several unstable species of definite mass, heavier than π mesons, has now been demonstrated. Two cases of special interest were reported by Rochester and Butler in 1947. They found a forked track associated with a large shower, which appeared to be due to the disintegration of a neutral particle into two charged particles. The observations indicated that the mass of the neutral particle was about $1100m_0$. In the other case, a track was apparently deflected through an angle of about 20° in the gas. In the absence of a track showing a recoiling partner, this was interpreted as decay of a charged particle, yielding a charged particle and one or more neutral ones. The photograph showing these two cases, and several others can be seen in Appendix 9, ref. 84. The decaying entities were called V particles, because of the V formed by the cloud-chamber tracks. The interpretations given by Rochester are as follows:

1. $V_1^0 = p + \pi^-$.
2. $V_2^+ =$ a π meson (or a μ meson) and one or more neutral particles.

Supporting evidence has come from many investigators. At the present time, it appears that there are three main groups of unstable particles. It has been proposed at an international gathering of cosmic-ray physicists that they be designated as follows:

Light mesons, L . π , μ , and any others which may be found in the same mass range.

Heavy mesons, K . Particles heavier than π mesons and lighter than the proton, such as tau mesons, kappa mesons, and V_2^0 particles.

Hyperons, Y . Particles with masses intermediate between those of the proton and the deuteron.

In 1953, V_1^0 particles were produced artificially by the cosmotron at Brookhaven. Fowler, Shutt, Thorndike, and Whittemore showed that V_1^0 particles are made when neutrons with energies up to 2.2 Bev strike materials in the neighborhood of a cloud chamber; they are also found when negative π mesons of 1.5 Bev pass through hydrogen.

From the last result, the sequence of events leading to V_1^0 creation and decay becomes clear. The primary event is

$$\pi^- + p + T_1 = V_1^0 + \text{Another neutral particle} + T_2$$

where T_1 and T_2 stand for kinetic energies. The nature and mass of the second neutral particle has not been ascertained at the time of writing, but it must be present to balance the momentum. The decay process is

$$V_1^0 = p + \pi^- + 35 \text{ to } 40 \text{ Mev}$$

From this equation we find the mass of V_1^0 to be $(2185 \pm 5)m_0$. The combination formed from the proton and the primary π meson behaves

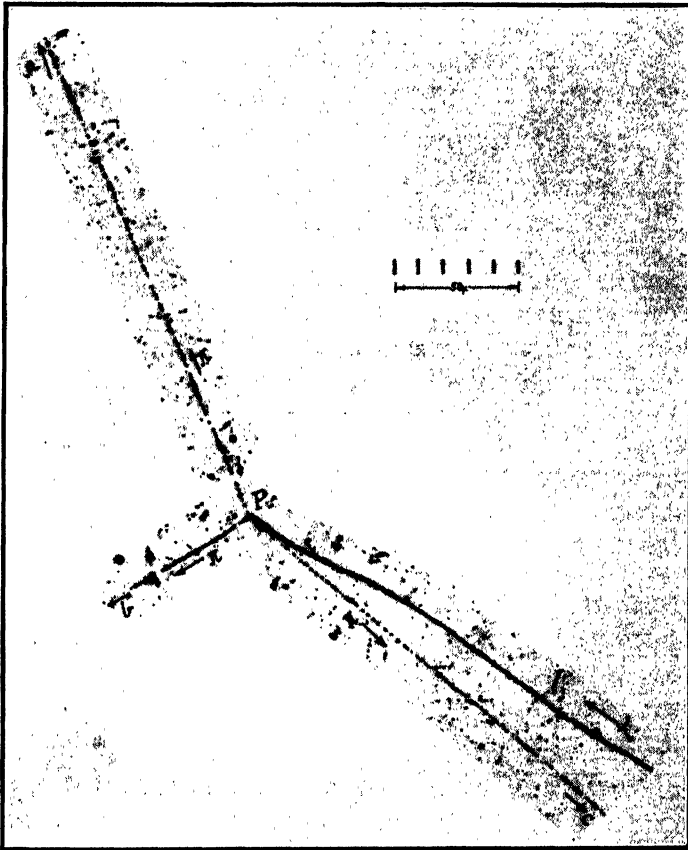


Fig. 14-18. Decay of a charged τ meson into three π mesons. The whole length of the scale is 50 microns. (Courtesy of C. F. Powell.)

just as though it were a compound nucleus. We note that the total energy of the primary meson is not sufficient in these experiments to provide the entire mass of the V particle.

Similarly, Lal, Pal, and Peters, among others, found charged V particles, whose decay is believed to produce a neutron and a π meson.

As to the heavy-meson group K , with masses about $1000m_0$, it is not clear whether there is one particle type with different charges and having various modes of decay, or several different particle types, some of which may decay in several ways. Only a few points will be mentioned:

1. The charged τ meson decays into 3 π mesons (Fig. 14-18). This decay process is well authenticated, and the mass of the τ meson is certainly close to $970m_0$.

2. Another well-established event is

$$V_2^0 = \pi^+ + \pi^- + \text{A neutral particle}$$

3. There are also charged particles, called κ mesons by O'Ceallaigh, which probably decay to yield a μ meson and two neutrals. Figure 14-19 is an illustration provided by C. F. Powell.

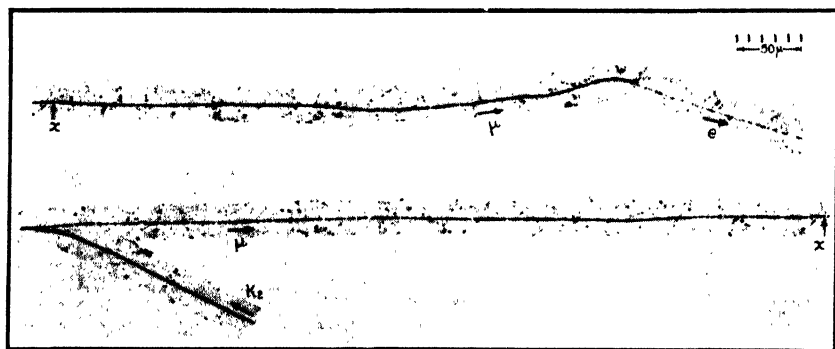


Fig. 14-19. Decay of a κ meson. The two neutral decay particles, of course, leave no tracks. In this case the μ meson remains in the emulsion until it too decays. The whole length of the scale is 50 microns. (Courtesy of C. F. Powell.)

The hyperons and κ mesons are often found in the neighborhood of nuclear explosions, in both the cloud chamber and nuclear plates. If the half-life happens to be such that decay of the particles usually occurs within the chamber (or the emulsion), then the chance of observing them experimentally is good. Particles which are the decay products of others of very short half-life will be expected to appear close to the

birth points of their parents; those which come from relatively long-lived parents will be born outside the cloud chamber or emulsion, and may not thus far have been recognized. It is quite possible that a number of additional unstable entities await discovery.

It is natural to hope that negative protons will be found, emerging from high-energy nuclear disintegrations. Schein believes he has obtained a record of such a particle.

8. Showers

Shower phenomena, beautiful and spectacular, have been both a stimulus and a complication in cosmic-ray work. Let us first consider electronic showers. Figure 14-20 shows the production and growth of

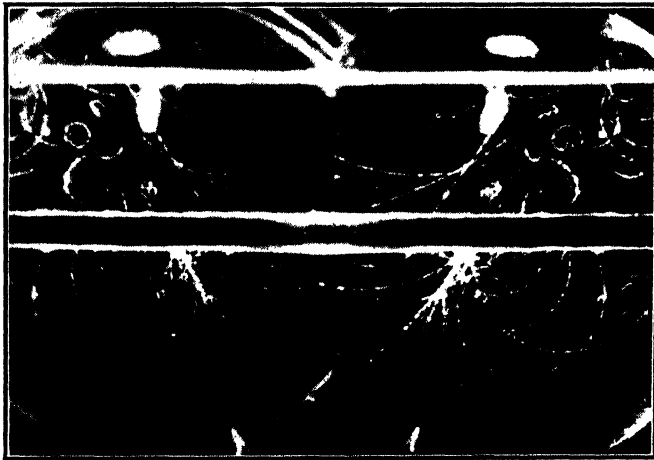


Fig. 14-20. Production of an electron shower in a cloud chamber by a non-ionizing entity. (After Anderson, Millikan, Neddermeyer, and Pickering.) The left-hand exposure is a direct photograph, the other is a reflection for stereoscopic purposes. The tracks in the upper portion are parts of a shower originating outside the chamber.

A shower of 7 positives and 15 negatives originates in the lower lead plate.

such a shower in a cloud chamber, while Fig. 14-21 illustrates the process of multiplication when an electron or positron starts the chain. A fairly good description of electronic showers can be obtained by considering only two processes, production of photons by radiative loss, and pair production by the photons. It makes little difference whether the shower is initiated by a photon or by an electron because of the approximate equality of the energy losses per centimeter for these two processes,

discussed in Section 4. Naturally this simple description breaks down when the energy has been subdivided so far that the average electron in the shower has an ionization loss larger than its radiative loss, and when the average photon has an appreciable chance of losing energy in the Compton process. We see from Fig. 14-8 that ionization loss exceeds radiative loss appreciably at an energy of the order 10^7 ev. At this energy multiplication has effectively ceased, and from that point on, the number of particles and photons decreases. Some of the more significant facts will be outlined.

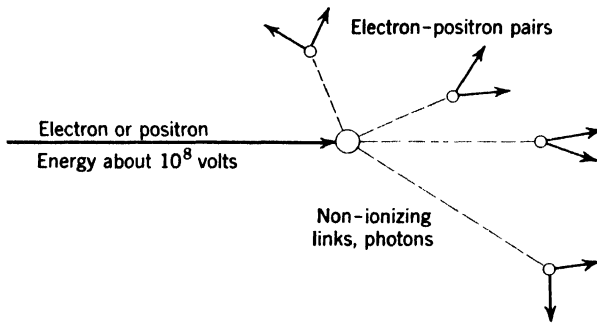


Fig. 14-21. The production of a shower.

1. It is a general feature of high-energy collisions that most of the secondaries are thrown forward, nearly in the same direction as the particle that produced them. This can be roughly understood by imagining that we are moving with the center of gravity of two particles that collide (p. 302). In this frame of reference, the collision products move in opposite directions. Then we may ask: How will they look when we return to a set of axes at rest in the laboratory?

2. W. M. Nielsen and K. Z. Morgan showed that the number of showers produced in plates having the same number of nuclei per square centimeter is proportional to the square of the atomic number of the material. This agrees with predictions from the formulas for radiative loss and pair production on p. 421.

3. The structure and development of electronic showers is well understood. Molière, Arley, and Roberg and Nordheim have all made substantial contributions in this field.

4. The word "penetrating" is used to describe showers in which the effects are mainly due to mesons. In Fig. 14-1 we showed the production of a number of mesons in a star event. Clearly, when the energy of these particles is sufficient, they may produce additional stars. Again, they may produce fast nucleons which in turn can give rise to

more mesons. This alternation of generations makes the process similar to the interplay of electrons and photons in an electronic shower.

5. A few words should be said about the extensive air showers discovered by Auger, Maze, and Grivet-Meyer in 1938. To explore the lateral extension of showers, they moved the counters of a coincidence pair apart, horizontally. As the process went forward the number of coincidences decreased, but background was not reached until the distance had risen to 5 m. It was concluded that showers of 1000 rays spread over 20 m^2 were being observed. Later experiments showed that occasionally the lateral dimension may be hundreds of meters. If such an event, containing possibly 10^4 to 10^6 particles, is due to a single primary, that primary must have an energy of the order 10^{13} to 10^{16} ev, according to the enthusiasm of the estimator. Actually, there is a quite general belief that these events are principally due to single primaries, rather than a number moving in company. Indeed, single protons with an energy of more than 10^{13} ev have been detected through study of the stars they produce. It is not unreasonable to suppose that further search will push the record to higher values. The large showers are, in general, mixed ones. At ground level, the particles in them appear to be mainly electrons, perhaps 50 for each heavy ionizing particle, according to Cocconi and Greisen. Although a few balloon experiments on the large showers were made as early as 1941, it is clearly difficult to track them to their breeding place.

9. Geographic and Depth Distribution of the Cosmic Rays

The latitude effect. In 1927, Clay carried an electroscope on board ship from Holland to Java and found a small decrease of the cosmic radiation as he traveled. This could be explained by assuming that a part of the primaries suffers a significant bending by the earth's magnetic field. In 1931–1935, A. H. Compton directed an extensive survey of cosmic-ray intensities, including observations on mountains and in stratosphere balloons. Progressively, much larger effects than those found by Clay were uncovered. It is convenient to discuss the underlying physics before considering the experimental facts.

The reader will remember that the magnetic field of the earth is essentially that of a dipole, which drops off with the inverse third power of the distance, so that a large part of the bending of the incoming primaries must be accomplished within a few thousand miles from the earth's surface. This can be appreciated from Fig. 14-22. On the other hand, bending of a typical primary inside the atmosphere is relatively insignificant. The path radius for a 6-Bev proton is about 600 km.

Many years ago Störmer studied the paths pursued by charged particles near the earth, in order to explain the aurora borealis. In general, the paths are highly complicated spirals, but it is easy to trace the general nature of the phenomenon by considering simple cases. A proton coming straight into the earth's magnetic pole from the zenith will not be bent at all, but one arriving in the plane of the equator will experience a large deflecting force, and, if singly charged, will not be able to reach the atmosphere unless its energy is superior to about 14 Bev. In order that a proton of this energy may graze the earth's surface (assuming the atmosphere absent, for the moment) it must follow the path depicted in Fig. 14-22. Such a particle comes from the

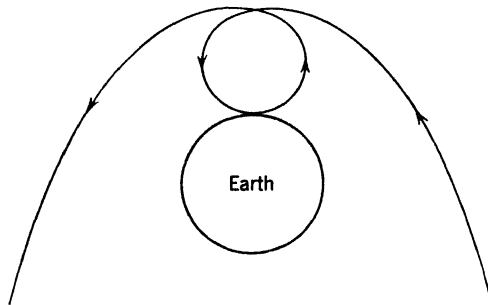


Fig. 14-22. Path of a proton moving in the plane of the earth's magnetic equator (after W. F. G. Swann). We are looking at the south geographic pole, and so the lines of force outside the earth go into the paper. This particle possesses the minimum amount of energy needed to reach the earth in the equatorial plane if the atmosphere were absent. A proton of the same energy coming from any other direction fails to reach the earth.

western horizon. A negative particle of the same mass and energy would have to come from the east. Protons of higher energy will be able to arrive in directions lying in a certain cone (not circular) near the western horizon, whose aperture opens out as the energy increases. Finally, those whose energy lies above a definite value will be able to arrive in any direction. For any other latitude, the situation is similar, but the energy limits are lower; there is a lower limit of energy below which a particle cannot arrive at all, a middle range where certain directions of arrival at the surface are possible, and a high limit beyond which all directions are possible.

We may state the results in another way. Consider particles of given energy, coming uniformly from all directions. Lemaître and Vallarta showed that from the magnetic pole to a certain limiting geomagnetic latitude, they should reach the atmosphere from all directions, but below

this latitude, there are directions of approach—filling the so-called shadow cone—which are forbidden, and the intensity decreases. Of course, if the energy is higher, the latitude at which decrease begins recedes to lower values, and for sufficiently high energies, greater than 20 Bev, the intensity should remain constant from pole to equator.

★ In interpreting the summary of experimental findings at sea level, given in Fig. 14-23, it must be remembered that we are dealing with particles covering a wide range of energy. The intensity increases 15 to 20 per cent in passing from the magnetic equator to 50° N magnetic latitude, and then remains approximately constant to the magnetic pole. The Lemaître-Vallarta theory accounts for this curve fairly well.

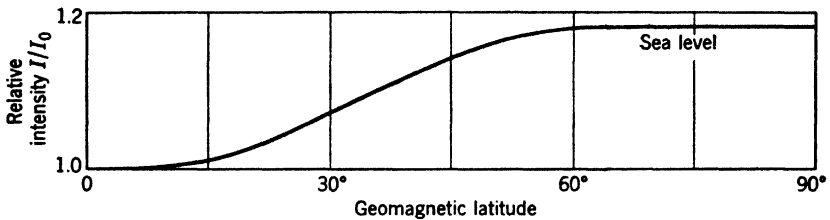


Fig. 14-23. Dependence of cosmic-ray intensity on magnetic latitude, at sea level. (Drawn from data summarized by A. H. Compton.)

At 50°N the earth's field begins to block off singly charged particles whose energy is less than 3 Bev. At any higher latitude, say 55°, slower particles also reach the atmosphere. If some of their progeny get through, their effect would be added to that of the faster particles and the sea level ionization at 55° would be greater than at 50°. This is not true, and we conclude that on the *average* a singly charged particle must have an energy of at least 3 Bev in order to get its secondaries down to ground level. We noted on p. 407 that a proton descending *vertically* would lose 1.4 Bev in traversing the atmosphere.

★ **Latitude effect at rocket-altitudes.** The losses on oblique paths complicate the picture. It is much more instructive to consider conditions at the top of the atmosphere. From rocket experiments of Van Allen and Singer on the vertical intensity of the primaries outside the atmosphere, and related balloon work of Pomerantz and of Winckler et al., we have Fig. 14-24. Figure 14-25 gives an idea of the instrumentation involved. In Fig. 14-24 the ordinate is a measure of the number of rays with energies more than sufficient for vertical entry at the place of observation. The abscissa requires explanation. We recall from p. 420 that $HR = pc/Ze$. It is actually HR that determines whether a particle is admitted or rejected by the field, regardless of the charge

it carries; and the critical value of HR alters with latitude. Since about one-half of the incoming nucleons are tied up in composite nuclei, different energy values correspond to a single HR value. We cannot use energy as an abscissa, so we employ a quantity proportional to HR . To make the magnitudes convenient, pc/Zc is converted to Bev. Thus the abscissa turns out to be $(300/10^9)HR$, which is called magnetic

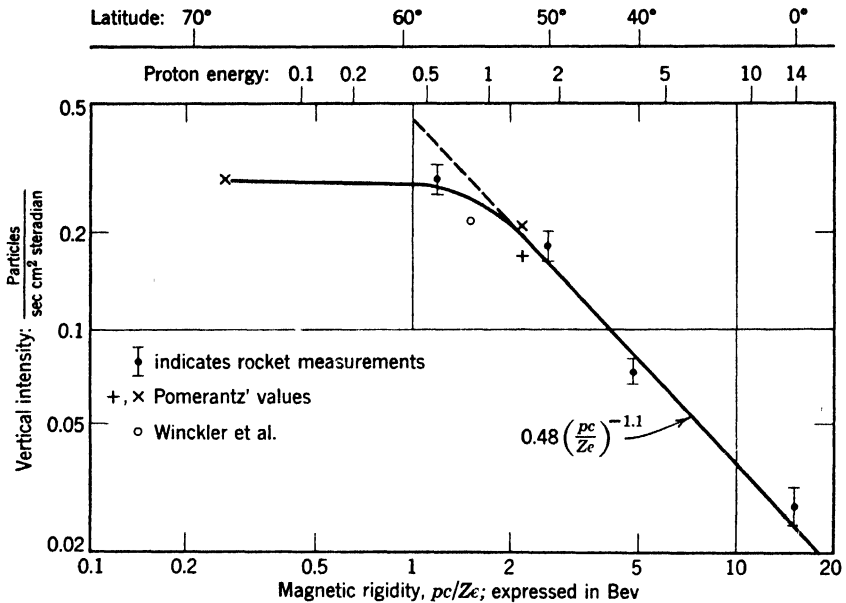
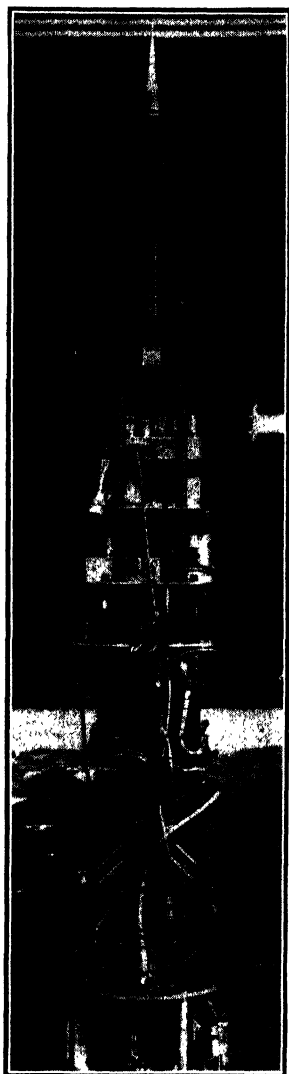


Fig. 14-24. The vertical intensity outside the atmosphere, as a function of the HR value which just allows vertical entry. Scales showing the corresponding proton energy and magnetic latitude are appended. (After Van Allen and Singer.)

rigidity. For protons of very high energy, the magnetic rigidity is practically equal to the energy of the proton in Bev, but at lower energies they are not equal, so we attach a scale of corresponding proton energies at the top border of Fig. 14-24.

★ This figure shows clearly that, at low magnetic latitudes, a great many of the primaries available outside the effective domain of the earth's field are shut off. If the theory is correct, it also shows that no appreciable fraction of the primaries can be neutral. If we could neglect rays scattered upward from the atmosphere to the rocket, the curve would give directly the fraction of the rays, $F(HR)$, having a rigidity greater than any particular abscissa. The equation of the straight



14-25a



14-25b

Fig. 14-25. (a) Instruments for measuring the azimuthal asymmetry of primary cosmic rays above the atmosphere, in an Aerobee rocket. (b) The Aerobee on its way, March, 1948. (Courtesy of the Applied Physics Laboratory of The Johns Hopkins University, and of J. A. Van Allen.)

descending portion is:

$$F = 0.48 V^{-1.1} \text{ particles per sec per cm}^2 \text{ per unit solid angle}$$

This disagrees with earlier formulas, widely quoted, but not so well founded, which predicted steeper drop-off, about proportional to V^{-2} . In fact, it is probable that the drop-off is much steeper beyond the upper limit of the region explored by Van Allen and Singer, so that the range of rigidities responsible for the bulk of the cosmic-ray effects is not much more than a single decade wide. Indeed, study of the total energy dissipated by cosmic rays in the atmosphere and of the number of primaries indicates that the average energy of a primary is of the order 7 Bev at a magnetic latitude of about 50° .

★ **The east-west effect.** If a set of several counters, all in line, is directed so as to receive rays first from a direction west of the zenith, and then from a direction the same amount east of the zenith, the intensity measured in the first direction is greater than that measured in the second direction. T. H. Johnson was particularly active in investigating this effect, at the Bartol Foundation. Lead was usually introduced between the counters to eliminate the effect of low-energy secondaries. The east-west effect is small at sea level in the United States, but increases as one approaches the magnetic equator or goes to high elevations. Indeed, the difference of west and east intensities on high tropical mountains is 10 to 15 per cent of the average. The explanation is that for particles of certain intermediate energies the shadow-cone is in the east for positives and in the west for negatives.

Distribution in depth. In view of the different directions of arrival of the primaries, and the copious production of showers, the decrease of any particular type of event is not exponential when plotted against the overlying air mass per square centimeter, as we descend through the atmosphere. It is possible to cope with these complexities in two ways. First, the use of counter telescopes is a fairly successful expedient in sorting out the vertical component of the harder constituents. We have mentioned the small deflection of these constituents by the earth's field, in traversing the atmosphere. Another factor is the general tendency of very fast particles to throw their secondaries forward.

Second, if we make the rough assumption that particles traveling *in a given direction* are absorbed exponentially, it is possible to find an effective absorption coefficient for any limited portion of a curve of vertical intensity versus depth, such as Fig. 14-26. This adaptation of a figure published by Rossi summarizes the results of a large number of investigators, and provides much information. Let us consider the chief points.

1. The maximum of the soft component at great heights shows that this component is generated by the primaries and their energetic meson secondaries. The generation of the soft component increases as the producing particles encounter air of ever-increasing density. The fact that the maximum occurs at 13 km or about 8 mi shows that the producers have a relatively small absorption thickness.

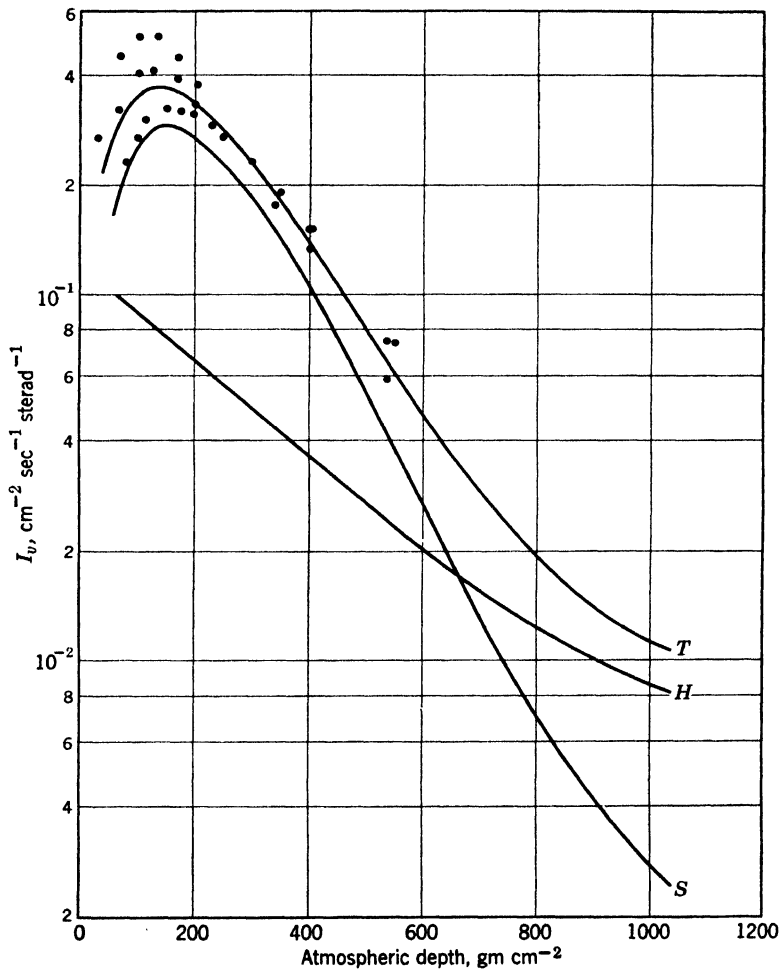


Fig. 14-26. Vertical intensity plotted against atmospheric depth. The curves H , S , and T refer to the hard and soft components and the total corpuscular radiation, at geomagnetic latitudes higher than 45° . For definitions of the hard and soft components, see p. 415. [Adapted from a diagram by Rossi, *Revs. Modern Phys.*, **20**, 540 (1948)].

2. We have mentioned that the hard component consists mostly of μ mesons at sea level and low altitudes; there are few protons at sea level. Observations of Pomerantz show that a maximum does not occur in the intensity recorded behind 6 cm of Pb or more, up to an atmospheric depth of 13 gm/cm^2 . The detailed reasons for this are not yet clear. We can be sure that the μ -meson part of the hard component will show a maximum at some atmospheric depth, because these short-lived particles cannot come from outer space.

3. It should be noted that the soft component falls off more rapidly than the hard as we descend from a height of about 12 km, or an atmospheric depth of 200 gm/cm^2 . Nevertheless, the absorption thickness of the soft part is *far too high* for explanation by means of the known absorption properties of its electrons and photons. The explanation of this fact is slightly complicated. The soft component is produced all the way along, and generally speaking, the electronic showers are mere embroidery on the paths of the more penetrating particles which produce them. Therefore we should expect a reasonably close parallelism between the absorption of the soft component and that of the mélange of particles producing it. Since this is not true, the ability of this mélange to produce the soft component must fall as we come downward.

★ Table 14-4 presents the absorption thicknesses for several types of events and for the hard and soft components as a whole. This table shows some striking features.

(a) The third, fourth, and fifth entries result from star production. The first five entries have substantially the same absorption thickness, 130 gm/cm^2 , which corresponds to a nuclear cross section of 0.18 barn. Now the so-called geometric cross section of a nucleus of atomic weight A is

$$S_{\text{geom}} = (1.7 \times 10^{-13})^2 A^{2/3} \text{ cm}^2 \quad (11)$$

Putting $A = 14.4$ for the atomic weight of air, this is also 0.18 barn.

(b) The μ mesons are more penetrating than the star-producing nucleons and π mesons. Two important reasons can be cited. We recall that fast μ mesons are relatively inefficient in interacting with nuclei. Also, the short life of π mesons acts to decrease their apparent absorption thickness.

(c) The absorption thickness for the soft component at middle altitudes agrees reasonably well with that for the nuclear processes at much higher altitudes. This coincidence simply makes it harder to sort out the various processes responsible for the soft component.

(d) The changes in slope of all the absorption curves in Fig. 14-26

TABLE 14-4. Absorption Thickness for Several Classes of Cosmic-Ray Events in the Atmosphere

Event	Range of Atmospheric Depth Considered (gm/cm ²)	Absorption Thickness (gm/cm ²)
Star production	250-1030	135
Counting rate of unshielded thin-walled ionization chambers	250-1030	138
Slow-neutron density	250-1030	138
Penetrating showers	300-700	125
Bursts in a chamber behind considerable thicknesses of lead	300-700	125
Hard component, interpreted as fast mu mesons (mostly)	60-400 400-760 580-1033	340 360 450
Soft component (electronic showers plus slow mu mesons)	472-614 614-760 700-1000	142 156 240

are difficult to interpret because several influences are at work to change each constituent of the rays. As a heterogeneous group of particles moves downward, the less energetic ones are screened out, so that the residue should be more penetrating; but all are being slowed by collision losses, which reduces the penetrating power. In this fashion, a very complex beam may give a good imitation of exponential absorption over considerable thicknesses, just as though it were composed of one type of particles, all of which are endowed with the same initial energy.

Underground effects. The cosmic rays contain some entities that can penetrate the earth to depths as great as 1 km. Millikan and Cameron constructed self-registering electroscopes, which could be filled with gas at a pressure of several atmospheres to increase their sensitivity. With these instruments the ionization was measured in snow-fed mountain lakes. The water of the sea and of stream-fed lakes contains sufficient radioactive material to make ionization-chamber measurements in such bodies worthless. Observations of this kind were continued by Millikan and his colleagues and by Regener, whose instruments went to a depth of 230 m. Kolhörster performed similar experiments in a mine. The absorption curve flattens as depth increases until, at a depth of 500 m of rock, the effective absorption thickness reaches the tremendous value of 2×10^4 gm/cm², corresponding to a rock thickness of about 80 m.

Since the time of this early work, cloud chambers have been operated underground. E. P. George and J. Evans also studied the effects with electron-sensitive emulsions which were *prepared* and utilized at a depth of 30 m, to avoid recording events due to pre-exposure at the earth's surface. In these ways, soft showers, penetrating showers, and stars have been found underground.

★ While fairly reasonable accounts of these effects at 30 m can be constructed rather easily, the problem is still a difficult one for a depth of 500 m or more. The idea currently pursued (by Greisen, Hayakawa, Tomonaga, and others) is that some charged mesons of sufficiently high energy can last long enough and lose a small enough fraction of their energy to persist to kilometer depths. For example, primary nucleons of 1000 Bev have often been observed at high altitudes. If nearly all the energy of such a primary were relayed to a positive μ meson, its properties would be as follows:

Actual life	10^{-2} sec
Mean path in vacuo	3000 km
Ionization loss in 1 km of rock	About 400 Bev

Thus we can see that some very energetic π mesons may produce μ mesons that are able to penetrate large thicknesses of rock. Barnothy and Forro prefer an explanation based on penetrating neutral particles. The matter requires further study.

10. Origin of the Rays

Millikan made experiments in deep valleys in the High Andes, to see whether there is a daily variation of intensity. If the rays have their origin in the stars of our galaxy they should be more intense in such mountain pockets at certain times of the day, though not necessarily when the Milky Way is overhead, because of bending in the earth's field. Daily fluctuations are small, and can be explained as due to two causes. The first is variation of the mass of air overhead as the barometric pressure changes. The second, pointed out by Ross Gunn, is the daily variation of the earth's magnetic field. Scott Forbush has dealt fully with this matter. The substantial constancy of the primary flux (after such corrections are attended to) is a stubborn fact which opens the way to extensive speculation on the origin of the rays.

The question of origin is really a pair of related questions: *Where* do they come from and *how* do they get their energy? It was proposed by Lemaitre that they arose at the "beginning," at which time a compact ball of neutrons is supposed to have exploded, giving rise to the universe.

Proof and disproof are equally difficult; or shall we say impossible? Present attempts to explain the rays try to assign them to known acceleration processes which may operate within the solar system, within the stars of our galaxy, in the interstellar spaces of our galaxy, or even in much broader reaches of space. Currently, each of these possibilities is fraught with difficulties.

Those who assume that the sun is the origin have a copious source of energy available, but are confronted with the lack of any appreciable daily variation of the rays. They are obliged to suppose that weak magnetic fields extending through the solar system are able to redistribute the directions of motion, so that the flux in all directions is substantially the same. This view, advocated recently by Richtmyer, Teller, and Alfven, is attractive, but requires further development. There are types of experimental work that may aid in deciding the matter. Forbush has consistently investigated the changes of cosmic-ray intensity which accompany magnetic storms and solar flares (local outbursts of strong ultraviolet light). The difficulty is that these events affect moving ionized gases in the neighborhood of the earth, thereby changing the earth's magnetic field, thus introducing an additional variable into the problem.

Now consider the view that the rays come from the stars. An interesting fact is that the cosmic-ray energy hitting the earth is about 1/10 of starlight. But the sun is a typical star; if typical stars are the source of the rays, then cosmic rays should have the intensity of sunlight—a flat contradiction. To avoid the contradiction, a suggestion has been made that the rays come *only* from novae or from supernovae. This suggestion has fallen to the ground for quantitative reasons.

It is necessary to search farther afield if we wish to maintain the view that the rays do not originate in the solar system. Those who assume a galactic origin must deal with the following approximate values of energy densities, reduced to mass densities for convenience.

Density, including kinetic energy, of the cosmic rays in the neighborhood of the earth 3×10^{-10} proton/cm³

Average density of interstellar matter in the galaxy 0.1×10^{-10} proton/cm³

Density of absorbing clouds in the galaxy 1 to 10×10^{-10} proton/cm³

The interstellar material, so far as is known, moves with velocities of a few tens of kilometers per second. Thus its kinetic energy is small compared with its rest energy. The reader will easily find that the energy of the cosmic rays (if uniformly distributed through the galaxy)

is of the order of 1 per cent of the kinetic energy of interstellar matter. If the rays are produced at the expense of that stock of kinetic energy, it is necessary to show the existence of some very effective method of acceleration. Fermi has attempted to do this, pointing out that interstellar clouds probably carry magnetic fields with them, and that protons striking these *moving* fields will experience forces, so that on the average they gain energy, provided that they have an energy of the order 200 Mev in the first place. The problem then is to understand how they can get this "injection energy." This complicated theory is ingenious, but seems overforced.

We have not yet indicated how the rays could obtain their energy within the solar system. Long ago, Swann discussed the possible role of sunspots as gigantic particle accelerators, operating somewhat like a betatron. Alfvén's view is that corpuscular streams from the sun produce moving magnetic fields. Their estimated magnitude is sufficient to give rise to associated electric fields, large enough to provide cosmic-ray energies.

Babcock has found that certain stars possess large magnetic fields which reverse in a period of a few days. Since any changing magnetic field produces an electric field, it is now proposed by Dauvillier and by Terletzki that such stars may be the origin of the rays. Bohm and Gross, on the other hand, consider that fluctuations of the ionized gas clouds in our galaxy may give rise to large-scale potential changes of a type suitable to accelerate ions. In the absence of an understanding of the motion of this gas, this ingenious suggestion is difficult to judge.

Probably the solution will be found when we have sufficient knowledge of the percentages of different nuclear species in the primaries, and the energy spectrum of each species.

REFERENCES

Appendix 9, refs. 15, 41, 45, 54, 62, 72, 78, 85, 86, 103, 109, 110.

PROBLEMS AND EXERCISES

1. Write out equations showing all the reasonably probable ways in which π mesons can be produced if energetic gamma rays fall on deuterium.
2. Do the same for neutrons bombarding deuterium.
3. What is the approximate half-life of a π meson of 10-Bev kinetic energy?
4. In the absence of slowing by collisions, about how far can a 10-Bev μ meson go in its half-life?
5. Calculate the path radius of a cosmic-ray electron of energy 10^9 ev, assuming the average intensity of the earth's magnetic field to be 0.3 gauss.

6. Work out a rough design of an instrument for studying the deflection of cosmic-ray electrons in an electrostatic field. (Employ two parallel plates. What dimensions and voltages are required?)

7. Use equations 7 and 8 to compare the ionization and radiation losses of a 100-Mev electron in a sheet of lead thin enough so that the energy does not change appreciably during the passage. Calculate only the ratio of the expressions 7 and 8.

8. Let a fast primary proton fall on a resting proton near the top of the atmosphere. Draw a labeled chart showing, for a chosen sequence of events, the nature and fate of all the progeny.

9. If the unseen partner in the decay of a resting π meson is a neutrino of zero rest mass, what is its kinetic energy?

ANSWERS TO PROBLEMS

3. $1.4 \mu\text{sec}$.

4. 42 km. The lengthening of life due to motion must be taken into account.

5. 110 km.

6. Consider an electron having energy of 10^9 ev, passing down between plates 300 cm long, separated by 0.5 cm. The particle is between the plates 10^{-8} sec, since it moves with a speed nearly equal to c . In transverse field of intensity X , the acceleration is (Xe/m) and the deflection at the bottom will be $(Xe/m)t^2/2$. Make this 0.5 cm, remembering that m is the actual mass, not the rest mass. Then field must be 37 escoulombs/cm or 11,000 volts/cm, so the voltage needed is 5500.

7. Ionization loss over radiation loss = 4.6.

9. 31 Mev. Start with $E_\nu/c = p_\mu$.

The Theory of Relativity

1. Introduction

Although those best qualified to judge are agreed that the full scope and beauty of the theory of relativity cannot be represented without the aid of much purely mathematical argument, nevertheless it is possible for a non-mathematical reader to comprehend the general nature of the theory and its consequences if he will but regard it as a stimulating challenge to the nimbleness of his mind. As will be shown more completely later, many of the mathematical equations describing the simpler parts of the theory were developed in preresativity days to account for the unexpected results of certain physical experiments. Einstein's theory of relativity (1905) changed not the equations but their interpretation; this change, in turn, can be made to give results that appear at first sight to be paradoxes. These so-called paradoxes are, however, reasonable, though their reasonableness would be doubted without a firm appreciation both of the new ideas introduced by Einstein and of the more limited point of view which prevailed before his time. If the reader will keep an open mind, unprejudiced by the observations of his daily life, he should find in this chapter many occasions for displaying his ingenuity. Its aim is to give no formal treatment of the subject; rather it is to show the nature of the arguments which underlie the theory. Most of the mathematical results will be quoted without proof.

2. Relative Motion

Communication; The velocity of light. The speed of communication between intelligent beings on different parts of this earth has sometimes been taken as a measure of the development of their civilization. Sailing boats and messengers were displaced by mechanically propelled steamboats and trains; the telephone, telegraph, and radio have outdistanced these. Radio waves traveling with the speed of light reach the antipodes in about $1/15$ sec. But here a limit has been

reached, for no speed has ever been observed, whether of a wave signal or of a material particle, which exceeds this velocity of 3×10^{10} cm/sec. True enough, the refractive index of a substance may be less than 1, for certain wavelengths, and this means that any peak or trough of a *monochromatic* light wave travels with a speed greater than c . The speed of such an idealized train of waves is called the *phase* velocity. However, if we wish to use the wave train to transmit knowledge of an event, we must modulate it in some way, must impress a signal on it. This locally modifies the energy of the disturbance, and it is found, by virtue of dispersion, that the recognizable energy change is always propagated with a *signal speed* less than c . In what follows, frequent reference will be made to this maximum speed of communication; hence it is important to remember that, though this speed is enormous, it is finite, and has been measured with an accuracy better than 0.001 per cent.

Motion is relative. Relativity is the theory of relative motion, the elements of which are familiar to all who have begun the study of dynamics. In everyday life all speeds of moving objects are quoted with reference to some object which is considered fixed. Trains and automobiles move at so many miles per hour in relation to the surface of the earth. An airplane has an air speed and a ground speed. If a wind is blowing there is, in general, a numerical difference between these two magnitudes, and usually a difference in their direction. Which of these, then, is the true speed? Which obeys Newton's laws? The answer is that both are true, in the sense that both obey these laws, provided the reference object, or frame of reference, is properly specified.

On foggy nights in the Straits of Belle Isle, at the mouth of the St. Lawrence, passengers on liners cannot tell by observations from a port-hole whether the ship is anchored or whether it is gliding along with the engines shut off. In both cases the water moves past the boat, though it is impossible to decide whether the tide is running past the anchored vessel or the ship is still moving forward. Similarly, were it not for the inevitable jolts and jars, a passenger in a train moving with uniform velocity along a straight track has no means of telling whether he is moving past the earth or whether the earth is moving past him. Both statements are in fact "true." We are accustomed to regard the earth as fixed, and from this point of view it is the train alone that moves. However, it is scarcely fair to limit our outlook thus when astronomy offers a universe of vastly greater extent. Current ideas of relative motion must be adapted to this grander scale. It would serve no useful purpose to return to Ptolemaic astronomy, asserting that the earth is at rest. Everyone knows the great convenience of saying that it moves

at least round the sun. Moreover, an astronomer would be unwilling to admit that the sun is at rest; it moves through space with reference to the "fixed" stars, and even these have peculiar motions among themselves. On this liberal view, therefore, it would be a bold presumption for any particular individual to maintain that he is absolutely at rest in space, and that all motion which he perceives is real. It would place him, unjustifiably, at the pivot of the universe. Hence, all motion must be considered as relative.

Space and the ether. Before we accept without reservation the point of view developed in the preceding paragraph, one important question must be considered. In the nineteenth century, the question was often put in the form: "*Is there any way of deciding by experiment whether an observer (say on the earth) is actually moving with respect to absolute space?*" This presupposes that the words absolute space have a meaning. It is, however, an empty phrase, but for the moment we shall exercise charity and accept it as a groping attempt to express the idea that there *may* be some natural frame of reference possessing characteristics which make it "more useful" to the physicist than any other frame. In deliberating the possibility of finding an answer to this question, we might think of the known properties of light, which can travel through space devoid of matter, whether it is interstellar space or an artificially created vacuum. However, if light is regarded as a wave motion, we find some difficulty in accepting its propagation through emptiness with perfect equanimity; wave motion suggests a periodic vibration; yet in empty space there is by definition nothing, or at least no ordinary matter, which can vibrate. Hence from the earliest days of the undulatory theory of light it has been customary to speak of a "luminiferous ether," or more concisely an "ether" which fills all space, whether that space is occupied by matter or not. Having made this assumption, we can forget our qualms about the propagation of light through space if we replace the word "space" by "ether." To account for the propagation of light and electric and magnetic disturbances through this ether, scientists of the nineteenth century found it necessary to ascribe to it the elastic properties of ordinary matter, thus endowing it with a spurious reality. More recently, the ether, intangible as its name suggests, has come to be regarded as no more than a convenient fiction introduced to ease the minds of physicists. If the doubt expressed at the beginning of this paragraph were reworded, it would become: "Perhaps there is a way of detecting the motion of the earth (carrying an observer) through the ether." Until we reach Section 5, we shall speak in language appropriate to the period before 1905, entertaining the idea of the ether at face value.

3. Uniform Motion through Space. The Michelson-Morley Experiment

Principle of the experiment. A possible experiment is suggested by a simple analogy. Let us suppose that two boatmen of equal speed have a race in a smoothly flowing stream. One is to row straight across and back to his starting point; the other is to go an equivalent distance upstream, then downstream to the same starting point. The important point is that, with respect to the banks of the stream, each competitor is to go the same distance. Will the result be a tie? The answer, as we shall now show, is that he who rows across and back will arrive a little earlier. His rival has lost more time on the upstream path than

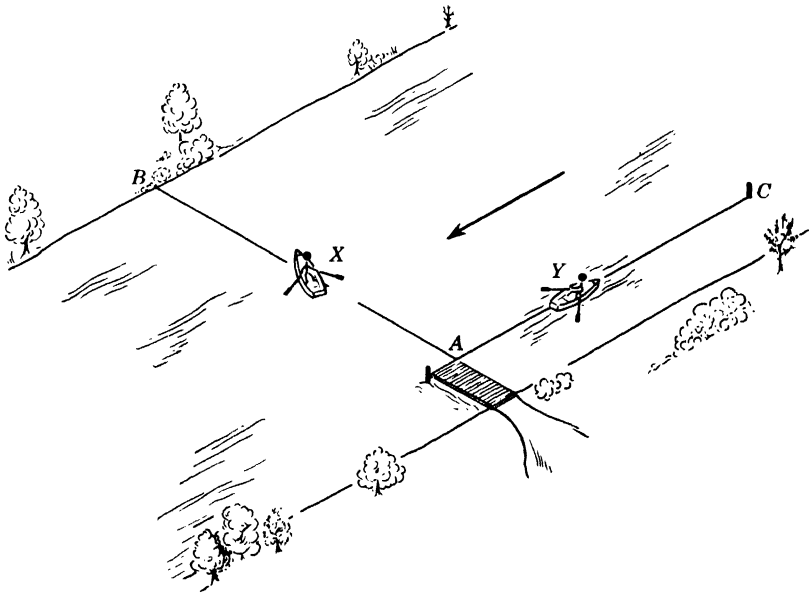


Fig. 15-1. A race between two boatmen on a smoothly flowing stream. Notice that the one who is in midstream has to keep heading slightly upstream, and must row in that direction in order that he may arrive at point *B*, immediately opposite *A*.

he can regain on the downstream lap. By way of illustration, let the course be 50 yd out and back, 100 yd in all, and let the rowers' speed in quiet water be 2 yd/sec. The stream will be supposed to flow at 0.4 yd/sec. The boatman *X* who goes across must direct his path a little upstream, along *AD* (Figs. 15-1 and 15-2) with respect to the water, so that he will arrive at *B*, just opposite *A*. In calculating *AD* we know that $DB/AD = 0.4/2 = 0.2$, and $AD^2 - DB^2 = 50^2$. Hence $AD =$

51.03 yd, while DB is a little over 10.2 yd. Coming back, X must again head a little upstream, so as to return to A . His round-trip distance is 102.06 yd, and his time 51.03 sec. From the standpoint of a man on the bank he moves, of course, out along AB and back again, a total distance of 100 yards, in 51.03 sec. His effective velocity along the line AB is thus less than 2 yd/sec. Meanwhile, Y proceeds upstream at 1.6 yd/sec, returning at 2.4 yd/sec. His total time is easily found to be $31.25 + 20.83$ sec, or 52.08 sec. X therefore wins by 1.05 sec.

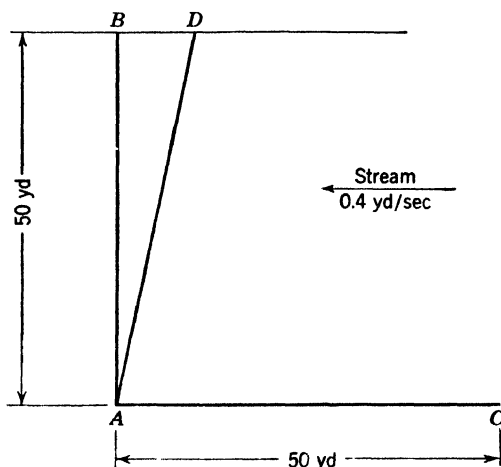


Fig. 15-2. Schematic diagram of the race illustrated in Fig. 15-1.

The argument may be reversed as follows: X and Y are two rowers of equal speed over the same course, who row equal distances in directions at right angles to each other out and back to the starting point. It is observed that X wins. We therefore deduce that a current must have been flowing in the direction of Y 's motion.

Now replace X and Y by two beams of light, which have equal speeds under similar conditions; replace the flowing stream by a stream of ether. It ought to be possible by timing the two beams to decide which one is moving parallel to the ether flow and which is moving perpendicular to it. Such an experiment was devised and carried out in 1887 by Michelson and Morley, using an instrument known as the Michelson interferometer.

The Michelson interferometer. In Figs. 15-3 and 15-4, A and B are identical plane parallel glass plates. A is silvered slightly on the side away from the source of light S . The beam SE falling on A at E is refracted to H . There it divides, part being reflected to F , where

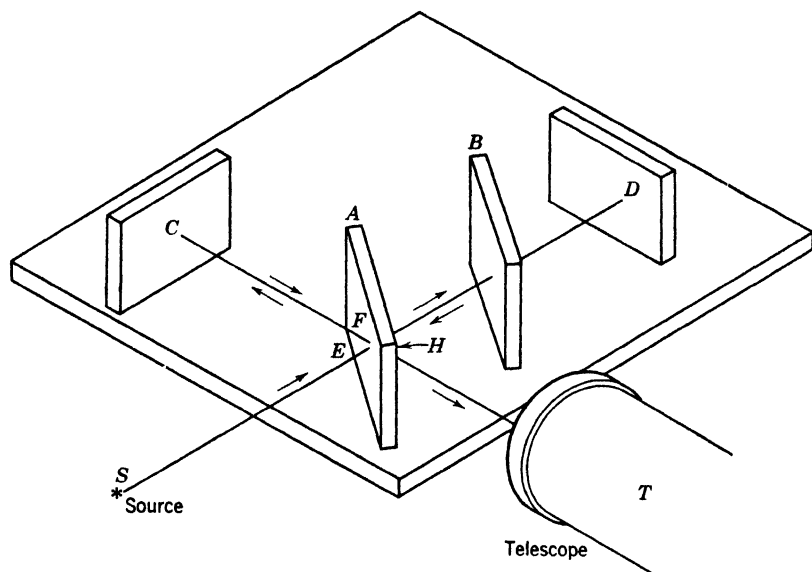


Fig. 15-3. The Michelson interferometer. S is the source of light, T a telescope for observing interference fringes. All devices for adjusting the positions of the various mirrors have been omitted from the picture. The lettering corresponds exactly to that in Fig. 15-4.

refraction changes its direction to FC' , and part being transmitted through the faint silvering towards D . C and D are plane mirrors normal to the light that falls on each. The two parts of the initial beam therefore return to H along their original paths after reflection at C and D . Again partial reflection and transmission occur, so that

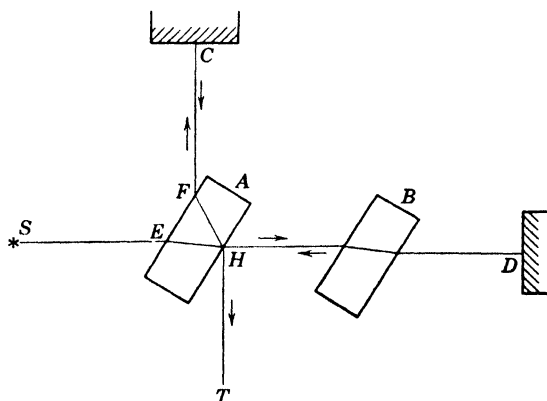


Fig. 15-4. Schematic diagram of a Michelson interferometer.

the light traveling along HT to the telescope consists of a mixture of parts of the two beams which were formed after the first division at H . It is obvious that the light traveling along $IIFCFHT$ passes through two thicknesses of glass; the plate B is therefore introduced between H and D to make conditions the same for the light traveling along $HDHT$. Furthermore, the mirrors C and D are placed so that the distances HFC and IID traveled by the two beams of light are equal, and so that the beams are at right angles to one another. In every essential respect, therefore, the arrangement of the two light beams is the same as that of the two boatmen in our earlier illustration.

If the whole apparatus is at rest in the ether, the two beams, coming originally from the same source, will combine to give a set of interference fringes in the eyepiece of the telescope. Suppose, however, that the earth is moving (with the apparatus) from left to right. This is equivalent to an ether flow from right to left. Relative to the instrument the beam HD traveling in the ether will therefore move more slowly on its outward path and faster on its return path, like a boatman moving first upstream and then down. Along FC the effective velocity, as in the case of the rower X , will be very slightly less than the usual velocity of light, but the change will not be as great as along HD . The result is that the light traveling parallel to the ether stream will arrive at T later than its twin. This will be shown by a shift of the fringes in the eyepiece. By rotating the whole instrument slowly, first one optical path, then the other can be brought parallel to the ether flow, thus doubling the calculated shift of the fringes as they move to and fro. The lag of one beam behind the other can be shown to be lv^2/c^2 , where l is the optical length of the path CH ($=HD$). The use of the optical length means that we allow for the slower passage through the glass. Here v is the known velocity of the earth (and apparatus) in its orbit and c is the velocity of light in the ether at rest. In the original experiment, l was about 10 m, while v and c have values 18.5 and 186,000 mi/sec. Hence lv^2/c^2 was about 10^{-5} cm. This would correspond to a shift of about one-fourth of a fringe. The detection of a lag of this amount in one of the light beams implies an accuracy equivalent to that necessary for measuring the circumference of the earth with an error of not more than 2 ft.

Result of the Michelson-Morley experiment. The result of this great experiment gave a shift of the fringes so small as to be scarcely measurable; it was probably about 3 per cent of what was expected. We shall call this a negative result. Hence there must have been something wrong. The experimental technique was above reproach; perhaps the assumption that the ether was drifting past the earth was wrong.

At the time of Michelson and Morley's work only two possibilities were thought of in explanation: (*a*) that the earth did not move through the ether; (*b*) that the earth carried an envelope of ether with it, somewhat like its atmosphere. The former of these is untenable, for the earth moves at least round the sun, so that it must at some period of the year move relative to the ether, unless we are arrogant enough to believe that this planet is so privileged as to be the hub of the universe. Supposition *b* means that round the earth is a body of ether which adheres to the earth and moves with it. In this form *b* does not sound so probable. It is, in fact, proved impossible by various types of astronomical evidence.

4. Prerelativity Explanations

The Fitzgerald-Lorentz contraction. Here, then, was the dilemma. The experiment was sound; the objections to the theory could not be sustained, so apparently the theory was sound. But theory and experiment disagreed. No advance was possible without drastic action. This came from Fitzgerald and from Lorentz independently in the form of a pure assumption that when a material body moved through the ether the body contracted, in the dimension parallel to its motion, by an amount just sufficient to compensate for the result of the Michelson-Morley experiment; and that it did not contract in a direction perpendicular to this. Thus the negative result of the Michelson-Morley experiment was explained—but let us count the cost. To placate certain unruly equations, an assumption was introduced which had no connection with other physical phenomena. It could not be tested by an observer *moving with the apparatus*, for every measuring stick placed alongside the contracted apparatus would shorten by a corresponding amount. To doubters, it was suggested that interatomic forces would naturally change on account of motion through the ether; hence dimensions would alter; with that they had to be satisfied, for *no* experiment performed by the observer moving with the apparatus could detect this change. Indeed the expected existence of double refraction due to the strain in a piece of glass caused by change in length was never observed. The Fitzgerald-Lorentz contraction was a truly academic explanation. Its greatest service was to permit physicists to keep on believing that motion through absolute space was “real,” and that such a motion modified the velocity of light in space.

★ This change in length should apply not only to gross matter but to its ultimate elements, electrons and nuclei. In these, we are as much concerned with electric and magnetic forces as with mechanical ones. Hence, in order to uphold the principle that the change of length could

not be observed by any experiment, whether mechanical or electrical, performed by the moving observer, Maxwell's equations, the governing equations of the electromagnetic field, would have to be valid, in the same mathematical form, for an observer in uniform motion through the ether as they are for an observer at rest in it. The difficulty that confronted physicists was therefore a fundamental dilemma, which may be reviewed as follows:

1. According to the Michelson-Morley experiment, the electromagnetic theory of light is so cunningly devised that optical experiments cannot show any uniform motion of our apparatus through our ether. This requires that Maxwell's equations governing light in a matter-free region must have the same form in two frames of reference, each of which moves uniformly relative to the other.

2. All previous mechanical experience suggests that the relation between the two frames is

$$x' = x - vt$$

where x is the coordinate of some happening, observed at time t in our laboratory frame, and x' is the coordinate of the same happening, observed in a frame moving along the positive X axis with speed v . For convenience, we have provided that the origins coincide at time $t = 0$.

3. All previous mechanical experience suggests that time measurements in the two frames will agree:

$$t' = t$$

Let it be clearly understood that observers in both frames are provided with standard meter sticks and watches which have previously been compared in ordinary laboratory fashion, while at rest in one frame. This comparison may be made in *either* frame.

4. When the independent variables in Maxwell's equations are shifted from x, t to x', t' , in accordance with the relations above, the equations do *not* retain their original form.

5. This situation led to the suggestion of Fitzgerald and Lorentz, and thence to the problem, what transformation of the coordinates and the time will lead to perfect similarity of electromagnetic behavior in the two frames, that is, to identical forms of the Maxwell equations?

★ **The Lorentz transformation equations.** Lorentz solved this mathematical problem by discovering a new set of transformation equations for the coordinates and the time. Imagine an observer A at rest

with respect to an apparatus which he is manipulating. In his apparatus an object is moving along a straight line which he calls the X axis. He can assign a coordinate x to a certain happening and say that it occurs at an instant t (by his watch).

★ Let there be another observer B in uniform motion with velocity v relative to A , in a direction along the X axis. B will naturally observe the same happening at a different coordinate x' , but will, perhaps intuitively, expect that the instant of its occurrence will be given by the same number t when recorded by his own watch. Lorentz's equations state that the quantities x, x' are related thus:

$$x' = k(x - vt) \quad (1)$$

where

$$k = \frac{1}{\left(1 - \frac{v^2}{c^2}\right)^{1/2}}$$

which, it should be noted, is always greater than 1. This equation, which implies that an observer moving with respect to an object fixed in the ether does not measure its true length, is in harmony with the Fitzgerald-Lorentz assumption of contraction. But this equation is not in itself sufficient. Lorentz found it desirable, in achieving an elegant mathematical discussion of certain electrical and optical experiments, to introduce what he called a fictitious time t' for the moving observer which differed from that of the observer who was at rest in space, such that

$$t' = k\left(t - \frac{vx}{c^2}\right) \quad (2)$$

This was the value to be used in the calculations, but it was not doubted that the moving observer would, by his watch, measure the same time instant t as the fixed observer. The use of t' rather than t in the equations was merely a pretty mathematical trick.

Thus the theory of relative motion, before the advent of Einstein's relativity, was in a highly artificial state, complicated by an assumption (the Fitzgerald-Lorentz contraction) without which the former theory could not be made logically consistent with the negative result of the Michelson-Morley experiment. Since this point of view did not throw any light on the physical basis of the theory, it was intellectually unsatisfying.

5. Einstein's Solution

A new point of view. Einstein (1905) cleared up the difficulties by taking a much more liberal view of the whole situation. His argument was, "If a thing cannot be observed, why should it be necessary to assume its existence?"—a point of view similar to that adopted by Heisenberg 20 years later in developing a mathematical theory of spectra. The Michelson-Morley experiment detected no ether flow past the interferometer. Einstein assumed that there is no ether, so that it makes no sense to say that any particular observer is or is not at rest with respect to such an entity. Hence any one of a set of observers in relative motion may assert with equal propriety that it is he alone who is at rest in the ether and may proceed to discuss any experiment on this basis; or he may simply refrain from any mention of ether, without loss. Each observer may go farther; he may determine the velocity of light with an apparatus of his own. The reader will scarcely be surprised to learn that all observers, whatever their motion, would arrive at the same numerical result. This independence of the velocity of light on an observer's motion is one of the fundamental postulates of Einstein's theory.

The theory of relative motion was thus given a reciprocal aspect in that the observations which *A* makes upon a moving observer *B* are identical with those which *B* makes upon the moving observer *A*. It is now the relative motion, not the absolute motion through space, which counts. If we have found a frame in which the laws of mechanics are obeyed, all frames which move uniformly with respect to it are equivalent for the description of physical phenomena; and it is impossible by any conceivable experiment to detect any absolute uniform rectilinear motion through space, or the difference between one state of uniform rectilinear motion and any other. Only the relative velocity, not the absolute velocity, can be observed. As this discussion is restricted to uniform motion in a straight line, the principle is known as the *restricted* (or *special*) *theory* of relativity. The *general* theory, discussed later, which deals with accelerated motion, includes the special as a particular case.

The negative result of the Michelson-Morley experiment can now be construed as showing that it was erroneous to correct the velocity of light on account of a supposed ether flow past the apparatus. The ether flow has disappeared; the correction must also vanish. Hence the velocity of light in free space must be accepted as a constant independent of the motion of the source, or of the observer. Thus the analogy of a rower going first upstream and then down was altogether misleading.

In that case, the assumed result could have been checked by an outside observer standing on the bank of the stream; in the case of the ether flow one cannot place an assistant on the bank of the "ether river" to verify the calculated results. There is no such thing now as an "outside" observer.

Consequences of Einstein's postulates. Acceptance of the ideas outlined above makes no change in the mathematical form of the Lorentz transformation equations. They are still valid, but they are interpreted in a different manner. Appendix 7 shows how they are derived, from the relativistic point of view.

In Appendix 8 a simple equation, $L = kL'$, is deduced from the Lorentz transformation equations. To understand its meaning, let us return for a moment to consider the two observers A and B . The former is at rest (with respect to us) while B moves rapidly past A . Both A and B are supposed to be measuring the length of a line in a piece of A 's apparatus, the line being parallel to the direction of the relative motion. L is the length of the line as measured by A , or by any one else at rest in A 's laboratory. L' is the length as perceived by B while he is in motion relative to A . The equation tells that the measurements made by B and by A do not give the same result. A 's answer is larger than B 's by a factor k , which, we have noted, is always greater than 1. Thus, under the specified conditions, B sees an object which is moving rapidly past him *apparently* contracted in the dimension parallel to the relative motion. At the same time, A is measuring the object in his laboratory, and sees it in its "natural" shape. To take a simple illustration, suppose that A is observing a square, which B notices as he rushes past. To A , the figure appears as a square, but to B it is a rectangle whose shorter dimension is parallel to the direction of relative motion of A and B . Thus the Fitzgerald-Lorentz contraction arises naturally out of the theory of relativity, from which the equation $L = kL'$ is deduced.

It becomes necessary, however, from Einstein's point of view, to regard the t' in Lorentz's equations as the actual time which both observers would read (A with the help of a telescope), on B 's watch, and not as a mathematical figment. A numerical (but hypothetical) example will make clearer the reciprocal nature of the process. Suppose that A prepares two rods, a and b , each 60 cm long, measured by standards at rest. He gives b together with a standard meter to B , who proceeds with it to some other frame of reference, which is moving at 81,000 mi/sec past A . B , quite undisturbed by his high speed, sets his rod parallel to the direction of his motion relative to A . Earthbound A does the same thing. (See Fig. 15-5.) B now measures b with his own standard

ruler, and, as he flashes past A , he measures a . Observer A performs the two corresponding operations with his own standard scale. The results are as follows:

Observer A		Observer B	
Measuring a	Measuring b	Measuring a	Measuring b
60 cm	54 cm	54 cm	60 cm

Thus a appears shortened to B and b appears shortened (by the same amount) to A , whereas each observes that his own rod is 60 cm long.

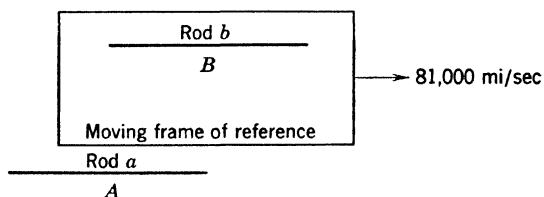


Fig. 15-5. Relative motion of two frames of reference. The observer B with his apparatus b moves relative to A . However, B is at rest with respect to his own apparatus b .

This is a necessary consequence of the reciprocal nature of Einstein's postulates, for instead of saying that B is moving past A we are equally justified in stating that A is moving past B . Hence any change in the appearance of a noted by B must be the same as the change in the appearance of b noted by A .

Relativity of time. There occur interesting and at first sight paradoxical relations between the times shown on the watches which A and B carry. It is mainly because of these curious relations that the theory of relativity is thought by the average person to be unintelligible, even though he finds it amusing to read:

There was once a young fellow named Bright
 Who traveled much faster than light.
 He set out one day
 In a Relative way
 And returned on the previous night.

We know, however, that the suggestion of the verse cannot be realized because no signal or material particle can travel faster than light.

Equation 1 shows that x and x' are connected by a relationship involving time and velocity. We might therefore expect time to depend on position and velocity. The nature of this dependence is controlled by

two things: first, a new point of view concerning simultaneity in which allowance must be made for the finite time of transit of any signal traveling with the velocity of light; and second, the equation

$$t_2' - t_1' = k(t_2 - t_1) \quad (3)$$

which is proved in Appendix 8. To interpret the equation we think of A and B in relative motion at 81,000 mi/sec, and assume that each carries a watch. A , using a telescope, can read B 's watch as well as his own. Suppose now that we are concerned with timing a sequence of events *occurring in apparatus which is at rest in A 's laboratory*. There are three, and only three, possible timetables for the events, one according to A 's watch, another according to B 's watch as read by A , the third according to B 's watch as read by B , the readings being inferred by A , or communicated to him afterward. Equation 3 tells what A deduces that B 's watch reads to B , compared with A 's reading of his own watch. The equation states that the interval $(t_2' - t_1')$ between two events as read by B on B 's watch is k times as long as the interval $(t_2 - t_1)$ between the same two events as read by A on A 's watch. In other words, a minute on B 's watch, as deduced by A , is longer than a minute on A 's watch. This is the slowing down of time frequently referred to in elementary accounts of Einstein's theory.

★ To make the matter clearer, we copy a numerical example from Eddington. Suppose that, as A and B pass each other, both light identical cigarettes which normally last 10 min. At the end of 10 min, A throws away his cigarette. A knows, of course, that B cannot notice this at once, for the signal has a long way to go to catch up with B . We watch A while he calculates when the signal will overtake B . Let x , he writes, be the unknown time, in minutes. Then, since B had 10 minutes' start, and was traveling at 81,000 mi/sec,

$$(60x)(186,000) \text{ mi} = 60(10 + x)(81,000) \text{ mi}$$

Hence $x = 7.7$ min, and A knows that his own watch will show 17.7 minutes when B sees him throw away his cigarette.

★ Being familiar with Einstein's theory, A is aware that a minute as B reads it on B 's watch is longer to A than a minute as A reads it on A 's watch— k times as long, in fact. In this particular case $k = 1/\sqrt{1 - 0.19} = 1/\sqrt{0.81} = 1.11$. Therefore, 17.7 min on A 's watch are equivalent to 17.7/1.11 min on B 's watch. This gives 15.9 min as the time B reads on his own watch when he receives (and perhaps acknowledges) the signal. (Since B 's signal acknowledging that he had seen A throw away his cigarette has to travel back a long distance to

A , it will not, of course, reach A until much later, but this is not pertinent to this discussion.)

★ The timetable, from A 's point of view, is given in Table 15-1.

TABLE 15-1. Timetable of Observations in Frames of Reference Moving with a Relative Velocity of 81,000 mi/sec

Action	A , Observing		B , Looking at B 's Watch, as Inferred by A (min)
	A 's Watch (min)	B 's Watch Simultaneously (min)	
Cigarettes are lit	0	0	0
A finishes cigarette	10.0	6.3	9.0
B finishes cigarette	11.1	7.0	10.0
A receives signal B 's cigarette finished	15.9	10.0	14.3
B receives signal A 's cigarette finished	17.7	11.1	15.9

★ At the risk of repeating what has already been said, let us read across the fourth line of the table. *A receives signal B 's cigarette finished.* Looking at his own watch, A notes that 15.9 min have passed since the start of the observations. Simultaneously, he is looking at B 's watch through a telescope, and finds that it reads 10.0 min, which was, of course, the time when B threw away his cigarette, which lasted 10 min, according to B 's watch. That is, the signal A receives at 15.9 min was sent out by B when B 's but not A 's watch said 10.0 min. The extra time was occupied by the signal traveling back to A . When A receives this signal at 15.9 min, he knows that B does not read that time on B 's watch at that instant; but knowing that B 's watch goes only 9/10 as fast as his own, A deduces that B 's watch reads 9/10 of 15.9, or 14.3 min. The last entry in line four of the table is therefore not an *observation* made by A , but a *deduction from theory* concerning the behavior of B 's watch, as read by B . A 's *observations* are in the first and second columns of figures.

★ So far, we have been looking at things from the point of view of A . Let us now think of B . His timetable is in the extreme right column of Table 15-1. He actually sees A throw away his cigarette at 15.9 min, but B knows that this is not really the instant of A 's signal, because he has made no allowance for the time of transit of the signal. So B proceeds to calculate the duration of A 's smoke. He says, in effect: A has traveled away from me at 81,000 mi/sec, and after n minutes sent me a signal which reaches me after 15.9 min. Problem: find n .

Therefore B writes:

$$60n \times 81,000 \text{ mi} = 60(15.9 - n) \times 186,000 \text{ mi}$$

whence $n = 11.1$ min. Thus B infers that A 's cigarette lasted 11.1 min, or $10/9$ as long as his own, just as A inferred that B 's cigarette lasted $10/9$ as long as his own. Indeed, a timetable written from B 's point of view can be set up by merely interchanging the letters A and B everywhere in Table 15-1.

It is essential, for a complete understanding of the table, to keep in mind the following points:

1. Einstein's postulates deny absolute motion through space, as an observable thing; hence all motion must be regarded as relative; thus any modification of A 's appearance as seen by B must be the same as the modification of B 's appearance seen by A .

2. All motion is relative; there is no absolute motion through space; hence it is impossible to correct the velocity of light to take account of the motion of the source. Therefore the watch carried by B will not appear to A to keep time with A 's watch.

3. The everyday notion of simultaneity cannot be used in describing two events occurring in frames of reference moving with respect to one another. A new definition of simultaneity is needed to take account of the differences in the apparent rates of passage of time, and of the distance separating the two events in space. This is evident from equation 7, Appendix 8.

The special theory of relativity therefore clears away the artificial assumptions which formerly underlay the theory of relative motion. It introduces results that are not encountered in the happenings of everyday life. The velocities with which men can move on the earth are so puny in comparison with the velocity of light that the effects of velocity on the dimensions of objects and on the periods of vibration are not appreciable. Though terrestrial happenings cannot in general be used as a test of the theory, they detract in no way from its elegance. Proofs are more easily found in astronomical observations, or better still, within the atom.

6. The General Theory of Relativity

Accelerated motion; Mechanical forces. The general theory is more comprehensive than the restricted theory in that it deals with accelerated motion. Einstein developed it from a very simple basis, namely, that *gravitation and accelerated motion are fully equivalent; one cannot be distinguished from the other.* It is now known that this equiva-

lence principle is not universally applicable, but it is true in a wide class of cases, and it can be illustrated by the following considerations: Imagine a large box moving smoothly (along rails, if you like), without jolts or jars. Let an observer be put, while asleep, in the box, which has no windows (but may be provided with electric light). If the box is moving uniformly in a straight line when he awakens, he will be unable to tell whether or not he is at rest with respect to the earth. Truth to tell, it matters not, as we emphasized earlier in this chapter. Every experiment he tries to do will work as well as if he were in his usual laboratory. Now let the box go round a sharp curve (unbanked) on its imaginary rails. The observer will be flung towards the outside wall of the box. Will he say, "I am going round a curve," or "Someone has tilted this box"? Either attitude offers an equally valid explanation of his movement towards one side of his prison. In fact, his weight now pulls him not straight down to the floor, but sideways as well. A lamp hanging by a cord from the roof leans over in the same direction.

If, instead of going round a curve, the box were quickly accelerated in a straight line, the observer, sitting quietly in his chair, would probably fall over backwards. His remarks would perhaps suggest that he wished they would keep the box level. Nearly everyone in walking to the rear inside a bus which is starting quickly from rest has experienced the peculiar sensation of appearing to be walking downhill; whereas if he walks in the same direction while the bus is being quickly stopped, he feels as though he were walking up a steep slope.

These examples are sufficient to indicate that the forces due to accelerated motion which we experience are indistinguishable from those due to gravitation. As we stand on the earth, the gravitational pull (our weight) is partially lightened by the centripetal acceleration of the earth as it revolves on its axis. But ordinarily we distinguish these effects only for purposes of calculation.

★ **Electromagnetic forces.** This argument can be amplified to show that, since gravitational forces and those due to acceleration are frequently indistinguishable, then, of any given force, it is impossible to tell what part is gravitational in origin. Hence it is necessary to deny the possibility of detecting absolute acceleration (with respect to space) by means of such mechanical forces. Although electromagnetic and optical experiments show that absolute *uniform motion* is not demonstrable, yet it cannot be asserted unequivocally that such experiments will lead us to deny absolute *acceleration*. It becomes, therefore, a matter for experiment. A beam of light is deviated in going through a non-uniform medium (refraction). We might regard the phenomenon as an acceleration of the beam in a direction at right angles to its path,

due to the electric and magnetic forces in the medium. If there is no such thing as absolute acceleration, it should be possible to create a similar acceleration in a beam of light by making it traverse a gravitational field. For the experiment a very strong gravitational field is necessary. The bending of starlight as it passes the sun has been investigated to clear up this point.

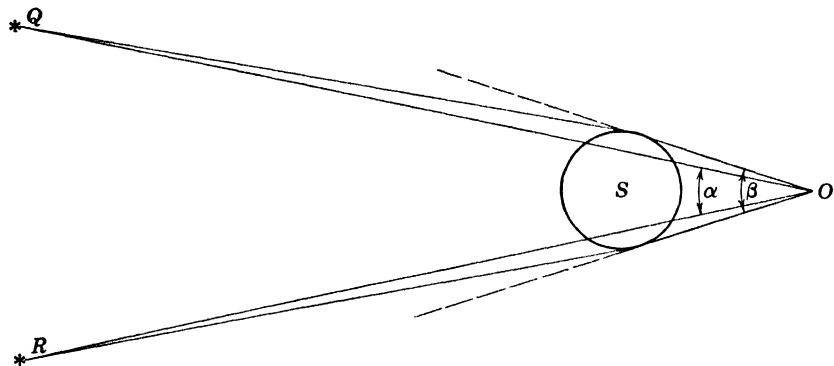


Fig. 15-6. Deflection of starlight in the gravitational field of the sun. When the sun is away, observer O perceives that the stars, Q , R , are separated by an angle α . When the sun is in the position shown, the observer can just see the stars past the edge of the (eclipsed) sun, because the starlight is refracted or bent when it passes close to the sun. Under these circumstances the stars appear to be separated by an angle β , which is larger than α .

★ In Fig. 15-6 let Q , R be fixed stars; S , the sun; O , an observer. If these stars be viewed when the sun is away, they will appear at an angular distance α apart. If their rays are bent as they pass close to the sun the stars will appear to be separated by a larger angular distance β . Here, then, is an experimental test. It can be carried out, however, only at times of total eclipse when the disturbing light from the sun is cut off. The effect sought for is so small that the available experimental results are conflicting. The angle on whose measurement the result depends in this experiment is only 1.7 sec of arc, the angle subtended by the diameter of a 1-in. disk at a distance of 3.2 mi. There is, however, a preponderance of opinion in favor of the shift of the star images to the extent predicted by Einstein's theory.

7. Consequences of the Restricted Theory

Only two of the most important results of the restricted theory are given here. They can, of course, also be deduced from the *general* theory, of which the restricted theory is a special case. The limitation

or restriction is that the velocity is to be uniform; in other words, the acceleration is to be zero.

Variation of mass with velocity. Before the advent of the relativity hypothesis, Lorentz had found it necessary in developing the electrical theory of matter to abandon the concept of a fixed mass for an electron, as pointed out in Chapter 2. The mathematical formulas demanded, in fact, that the mass increase with the velocity, in accordance with the equation

$$m = km_0 = \frac{m_0}{\left(1 - \frac{v^2}{c^2}\right)^{1/2}} \quad (4)$$

where m_0 is the mass of an electron at rest, and v its velocity through the ether; m is the mass as observed (perhaps in a deflection apparatus) by an experimenter who is at rest in the ether.

Relativity considerations require that the mass not only of an electron but of any body vary with velocity in an identical fashion, but the interpretation of the equation is different. If we accept Einstein's principle, it is no longer possible to speak of a velocity v through the ether, or of an observer who is at rest in it. In equation 4, m_0 is now the mass which would be measured by an observer at rest with respect to the body; m is the mass as it appears to another observer moving relatively to the body with velocity v . No question of absolute velocity enters at all. Einstein's theory denies its very existence.

Equivalence of mass and energy. It can be proved that the work done in accelerating a body of original mass m_0 from a condition of rest to a velocity v is $m_0c^2(k - 1)$ while it is obvious from equation 4 that the change in mass due to increase in velocity is $km_0 - m_0$, that is, $m_0(k - 1)$. This leads to the idea that the mass of a body (m_0 at rest) increases to km_0 at velocity v because the body now has more energy. It is therefore reasonable to deduce that the increase in mass and increase in energy are related by the equation

$$\text{Increase in energy} = \text{Increase in mass} \times c^2$$

This equation implies that mass is one aspect of energy, and that all forms of energy have mass. It is now generally accepted that any quantity of energy E is equivalent to a mass m , where

$$E = mc^2 \quad (5)$$

And, as a final corollary: if, by any means, a mass m of matter is made to change to radiation, an amount of energy mc^2 replaces it. This state-

ment does not mean that the mass has vanished entirely, for we have seen that radiation has mass, in the sense that it carries momentum (p. 143). An important application of the relation between mass energy and other forms of energy has been discussed on p. 43 in connection with the structure of the nuclei of atoms. There, for example, it was shown that one helium nucleus has less mass than two neutrons plus two protons. Hence, to split up a helium nucleus into two neutrons and two protons a great deal of energy would have to be supplied. The helium nucleus, or alpha particle, is therefore a very stable entity.

Practical significance of relativity. An understanding of relativity is not essential for the application of physics to everyday life. For all but those scientists who deal with particles of matter moving at many thousands of miles per second, and astronomers who deal with almost incomprehensibly large distances, it is of purely academic interest. We can never hope to make a rifle bullet go fast enough to appreciate its change in mass, or give an automobile the speed necessary for an observable slowing down of the clock. These effects depend on the factor k which is very nearly unity unless v is comparable with the speed of light.

It is evident, however, that if we probe deeply into the fundamental nature of things we must be prepared to modify the Newtonian scheme of natural laws. Euclidean geometry is no longer a true description of the properties of space. In all matters inaccessible to direct observation, investigations must be guided by great principles which are true under the widest possible range of conditions. Among such principles Einstein's theory of relativity takes pride of place.

REFERENCES

Appendix 9, refs. 5, 7, 24, 26, 30, 31, 33, 56, 69, 104.

PROBLEMS

1. Using the equation $L = kL'$, check the results on p. 466.
2. Calculate the mass of an electron which moves with a velocity $1/10$, $9/10$, of the velocity of light.
3. What is the mass of an electron whose kinetic energy is 1.8×10^{-7} erg?
4. What is the velocity of a proton that has a mass of 2.00×10^{-24} gm?
5. Using the equation 5, $E = mc^2$, calculate the amount of energy set free by the annihilation of a positron and an electron.
6. Use the result of problem 5 to find the frequency of a quantum which could produce, simultaneously, a positron and an electron, each possessing a kinetic energy of 5×10^5 ev.
7. What is the energy of the proton of problem 4, in Mev?

8. The lag (in distance) of one beam behind the other in the moving Michelson interferometer is lv^2/c^2 (see p. 460). Using this formula, check the result which is calculated directly in the example of the two boatmen.

9. Prove the formula lv^2/c^2 given on p. 460, assuming that v is small in comparison with c .

ANSWERS TO PROBLEMS

- | | |
|--|-----------------------------------|
| 2. 9.15×10^{-28} gm; 20.9×10^{-28} gm. | 5. 1.638×10^{-6} erg. |
| 3. 11.1×10^{-28} gm. | 6. 4.89×10^{20} per sec. |
| 4. 1.66×10^{10} cm/sec. | 7. 186 Mev. |
| 8. The formula gives 2.00 yd; an exact calculation (p. 458) gives 2.10 yd. | |

APPENDICES

APPENDIX 1

Electrical Units

A. The Electrostatic CGS System

1. The electrostatic cgs unit of charge, sometimes called the esculomb or statcoulomb, is that "point" charge which repels an equal "point" charge at a distance of 1 cm, in a vacuum, with a force of 1 dyne.

2. The electrostatic cgs unit of field strength is that field in which 1 esculomb experiences a force of 1 dyne. It therefore is 1 dyne/escoulomb.

3. The electrostatic cgs unit of potential difference (or esvolt) is the difference of potential between two points such that 1 erg of work is done in carrying 1 esculomb from one point to the other. It is 1 erg/escoulomb.

B. The Electromagnetic CGS System

1. The unit magnetic pole is a "point" pole which repels an equal pole at a distance of 1 cm, in a vacuum, with a force of 1 dyne.

2. The unit magnetic field strength, the oersted, is that field in which a unit pole experiences a force of 1 dyne. It therefore is 1 dyne/unit pole.

3. The absolute unit of current (or abampere) is that current which in a circular wire of 1-cm radius, produces a magnetic field of strength 2π dynes/(unit pole) at the center of the circle. One abampere approximately equals 3×10^{10} esamperes, or 10 amp.

4. The electromagnetic cgs unit of charge (or abcoulomb) is the quantity of electricity passing in 1 sec through any cross section of a conductor carrying a steady current of 1 abampere. One abcoulomb equals 10 coulombs.

5. The electromagnetic cgs unit of potential difference (or abvolt) is a potential difference between two points, such that 1 erg of work is done in transferring 1 abcoulomb from one point to the other. One abvolt = 10^{-8} volt = approximately $1/(3 \times 10^{10})$ esvolt.

C. Practical Electrical Units and Their Equivalents in the Absolute Systems

	<i>Practical</i>	<i>Electrostatic</i> <i>cgs</i>	<i>Electromagnetic</i> <i>cgs</i>
Quantity	1 coulomb	3×10^9 esculombs	1/10 abcoulomb
Current	1 ampere	3×10^9 esamperes	1/10 abampere
Potential difference	1 volt	1/300 esvolt	10^8 abvolts
Electric field strength	1 volt/cm	1/300 dyne/escoulomb	10^8 abvolts/cm

D. Some Energy Relationships

$$1 \text{ esvolt} \times 1 \text{ esculomb} = 1 \text{ erg}$$

$$1 \text{ abvolt} \times 1 \text{ abcoulomb} = 1 \text{ erg}$$

$$1 \text{ volt} \times 1 \text{ coulomb} = 10^7 \text{ ergs} = 1 \text{ joule}$$

The electron volt equals the work done when an electron is moved from one point to another differing in potential by 1 volt.

$$\begin{aligned} 1 \text{ electron volt} &\cong 4.80 \times 10^{-10} \text{ esculomb} \times 1/300 \text{ esvolt} \\ &\cong 1.60 \times 10^{-12} \text{ erg} \end{aligned}$$

APPENDIX 2

Physical Constants and Conversion Factors*

Numerical Constants

e (base of natural logarithms)	2.718
$\log_e 10$	2.303
π^2	9.870

Lengths, Areas

Micron	μ	10^{-4} cm
Angstrom unit	\AA	10^{-8} cm
X-unit	XU	10^{-11} cm
Wavelength of 1-volt photon	—	12,396 \AA
Calcite grating space at 20°C	d	3.036 \AA
Separation of electron and proton in ground state of H	a_0	0.5291×10^{-8} cm
Compton wavelength	h/m_0c	2.426×10^{-10} cm
“Conventional electron radius”, p. 421	e^2/m_0c^2	2.8175×10^{-13} cm
De Broglie wave of 1-volt electron	h/m_0v	12.26 \AA
Barn	—	10^{-24} cm ²

*Values resulting from measurement have been taken principally from a tabulation by J. A. Bearden and H. M. Watts, *Phys. Rev.*, **81**, 73 (1951). With a few exceptions they have been rounded to 4 significant figures although the constants are in most cases known to greater accuracy.

The situation concerning atomic masses is that small differences are often known with considerable accuracy, but some discrepancies have not yet been fully explained. The particular set of mass equivalents presented here comes from Appendix 9, ref. 68.

Masses and Mass Equivalents

Electron	m_0	9.107×10^{-28} gm 5.488×10^{-4} AMU
1/16 mass of O^{16} = Atomic mass unit	AMU	1.6595×10^{-24} gm 931.1 Mev
Proton	M_H	1.6722×10^{-24} gm 1.00758 AMU
Neutron	M_N	1.6744×10^{-24} gm 1.00894 AMU
Deuteron	M_D	3.343×10^{-24} gm 2.01417 AMU
Alpha particle	M_α	6.642×10^{-24} gm 4.00279 AMU
H ¹ atom		1.00813 AMU
H ² atom		2.01472 AMU
He ⁴ atom		4.00389 AMU
Proton mass over electron mass	M_H/m_0	1836.1

Energies and Speeds

Electron volt		
~ 4.80 esculomb $\times 1/300$ esu	ev	1.602×10^{-12} erg
Million electron volts	Mev	1.074×10^{-3} AMU
Energy equivalent of		
electron mass	$m_0 c^2$	0.5110 Mev
Ionization energy of H atom	—	13.60 ev
Speed of 1-volt electron	—	5.931×10^7 cm/sec
Speed of light	c	2.9979×10^{10} cm/sec
	c^2	8.9874×10^{20} (cm/sec) ²

Other Electronic and Atomic Constants

Electronic charge	e	4.802×10^{-10} esu
		1.602×10^{-20} emu
Charge/mass for electron	e/m_0	5.273×10^{17} esu/gm
		1.759×10^7 emu/gm
Planck's constant	h	6.624×10^{-27} erg sec, or
		4.135×10^{-15} ev sec
Unit of angular momentum	$h/2\pi$	1.054×10^{-27} erg sec
Duane's constant (p. 87)	h/e	1.379×10^{-17} erg sec/esu
Rydberg constant		
For H ^I atom		$109,678$ cm ⁻¹
For infinite mass		$109,737$ cm ⁻¹
Bohr magneton	μ_B	9.271×10^{-20} erg/oersted
Fine-structure constant	α	$7.297 \times 10^{-3} = 1/137.04$

Constants Needed in Kinetics and Radiation Theory

Gas constant	R	8.314×10^7 erg/(mole °C)
Boltzmann's constant		
(gas constant for 1 molecule)	$k = R/N$	1.380×10^{-16} erg/(°C molecule)
Molar volume of perfect gas at		
0°C and 760 mm of Hg	V_m	22415 cm ³ /mole
Faraday*	F	9652.2 emu/equivalent
Avogadro's number	$N = F/e$	6.025×10^{23} molecules/mole
Number of molecules in 1 cm ³		
of perfect gas at 0°C and		
760 mm of Hg	F/eV_m	2.687×10^{19} molecules/cm ³
Average kinetic energy of a mole-		
cule at 0°C and 760 mm of Hg		
($T_0 = 273.16^\circ\text{K}$)	$3/2 kT_0$	5.655×10^{-14} erg
	$\sigma = \frac{2\pi^5 k^4}{15h^3 c^2}$	5.669×10^{-5} erg/(cm ² deg ⁴ sec)
Stefan-Boltzmann constant		
First radiation constant (p. 76)	c_1	4.99×10^{-15} erg cm
Second radiation constant	$c_2 = hc/k$	1.439 cm °C

*Based on the "physical" scale of atomic weights, in which $O^{16} = 16$ exactly. On the chemical scale the value 16 refers to the natural mixture of oxygen isotopes. The two differ by 0.018 per cent.

APPENDIX 3

Properties of Elementary Particles

Particle	Charge	Mass	Spin in Units $h/2\pi$	Magnetic Moment	Statistics
Electron	$-e$	m_0	$1/2$	$-\mu_e$	F
Positron	$+e$	m_0	$1/2$	$+\mu_e$	F
Photon	0	0	$1?$	0	B
Neutrino	0	$0?$	$1/2$	0	F
Proton	$+e$	$1836m_0$	$1/2$	$+2.793\mu_n$	F
Neutron	0	$1839m_0$	$1/2$	$-1.914\mu_n$	F
Mesons					
μ type	$\pm e$	$207m_0$	$1/2$	$?$	F
π^+, π^-	$\pm e$	$273m_0$	$0, ?$	$?$	B
π^0	0	$262m_0$	0	$?$	B

Notation

Proton charge = $e = 4.8 \times 10^{-10}$ esu.

Electron mass = $m_0 = 9.11 \times 10^{-28}$ gm.

Unit of spin = $h/2\pi = 1.05 \times 10^{-27}$ erg sec. Values given represent the component parallel to an applied magnetic field. See p. 368 for a discussion of total angular momentum.

In the sixth column, F refers to Fermi and B to Bose statistics. See pp. 262 and 334.

Bohr magneton = $\mu_e = (h/2\pi)(e/2m_0c)$.

Nuclear magneton = $\mu_n = (h/2\pi)(e/m_p c)$, where m_p = proton mass, 1836 electron masses.

APPENDIX 4

Behavior of Elementary Particles

Process	Photons	Electrons	Protons	Neutrons
Production	Deceleration of fast-moving electrons by nuclei. (Collision-radiation) Gamma rays from nuclei. X radiation and light from atoms ionized or excited by any means.	Pair production by gamma rays. Beta radiation. (Remember the neutrino.)	Decay of neutron: $n \rightarrow p + e^- + \bar{\nu}$ Kinetic energy Emission from nuclei.	Reverse of neutron decay, if kinetic energy is available. Emission from nuclei.
Scattering by electrons	Compton process: $h\nu + e^- \text{ at rest} \rightarrow h\nu' + e^- \text{ in motion.}$	Secondary cause of scattering, $\sim Z$; but total energy loss is great.	Deflection by electrons very slight. Main cause of energy loss.	Negligible, because neutron has no charge (slight interaction between magnetic moments).
Scattering by nuclei	Nuclear scattering negligible.	Main cause of scattering, $\sim Z^2$.	Main cause of scattering. Energy loss increases as mass of struck nucleus becomes smaller.	Main cause of scattering. Energy loss becomes smaller.
Elastic	Nuclear scattering negligible.	Electron excites nucleus	Proton excites nucleus.	Neutron excites nucleus.
Gross loss in plate of thickness x	Exponential: $I = I_0 e^{-\mu x}$	Steady drop, definite maximum range. Loss/cm $\sim 1/2$, down to energy of several hundred ev.	Sudden decrease at a nearly definite range.	Approx. exponential for fast neutrons. Slow-neutron loss is complex, since both scattering and absorption occur.
Disappearance	Photoeffect: Increases at each ionization potential of the atom, only to fall again. Steady decrease beyond K limit. Pair production in field of a nucleus, if $h\nu \geq 2mc^2$. Photodisintegration of nucleus.	Pair annihilation, with emission of two 0.5-Mev photons. (One-quantum annihilation in field of nucleus is infrequent.) Electron disintegrates nucleus. K capture.	Enters nuclei if energy is great enough to overcome Coulomb repulsion.	All nuclei absorb neutrons. Broadly, effect increases as v decreases; but resonances cause strong absorption. Resonance cross sections vary tremendously.

APPENDIX 5

Periodic System of the Elements

Period	Group I a	Group II a	Group III a	Group IV a	Group V a	Group VI a	Group VII a	Group VIII a	b
I	1 H 1.0080								2 He 4.003
II	3 Li 6.940	4 Be 9.013	5 B 10.82	6 C 12.010	7 N 14.008	8 O 16.0000	9 F 19.00		10 Ne 20.183
III	11 Na 22.997	12 Mg 24.32	13 Al 26.98	14 Si 28.09	15 P 30.975	16 S 32.066	17 Cl 35.457		18 Ar 39.944
IV	19 K 39.100	20 Ca 40.08	21 Sc 44.96	22 Ti 47.90	23 V 50.95	24 Cr 52.01	25 Mn 54.93	26 Fe 55.85	27 Co 58.94
V	37 Rb 85.48	38 Sr 87.63	39 Y 88.92	40 Zr 91.22	41 Nb 92.91	42 Mo 95.95	43 Tc [99] 98.91	44 Ru 101.7	45 Rh 106.7
VI	55 Cs 132.91	56 Ba 137.36	57 to 71 Rare earths* 81 Tl 204.39	72 Hf 178.6	73 Ta 180.88	74 W 183.92	75 Re 186.31	76 Os 190.2	77 Ir 195.23
VII	87 Fr [223]	88 Ra 226.05	89 to 98 Actinides†						86 Rn 222

*Rare earths: 57 La 138.92 58 Ce 140.13 59 Pr 140.92 60 Nd 144.27 [145] 61 Pm 150.43 62 Sm 152.0 63 Eu 156.9 64 Gd 159.2 65 Tb 162.46 66 Dy 164.94 67 Ho 167.2 68 Er 169.4 69 Tm 173.04 70 Yb 174.99

†Actinides: 89 Ac 227 90 Th 232.12 91 Pa 231 92 U 238.07 [237] 93 Np 237 [242] 94 Pu 242 [243] 95 Am 243 [243] 96 Cm 247 [245] 97 Bk 247 [246] 98 Cf 251 [246]

Atomic weight in square brackets is of the isotope of longest half-life. Elements 99 and 100 were made in 1954 in very small quantities.

APPENDIX 6

Properties of Light Isotopes

Isotope	Per Cent Abundance	Spin, Normal State	Decay	Half-Life	Isotopic Weight of Atom	Binding Energy (Mev)	Binding Energy per Particle (Mev)
${}^1_0\text{H}^0$		1/2	e^-	10 to 30 min	1.00894		
Proton					(1.00758)		
${}^1_1\text{H}^1$	99.98	1/2			1.00813		
${}^2_1\text{H}^2$	0.02	1			2.01472	2.19	1.09
${}^3_1\text{H}^3$		1/2	e^-	11 to 12 yr	3.01703	8.36	2.79
${}^3_2\text{He}^3$	$\sim 10^{-2}$	1/2			3.01701	7.63	2.54
${}^4_2\text{He}^4$	~ 100	0			4.00389	28.2	7.04
${}^6_2\text{He}^6$	—	?	$\alpha + n$	Very short	5.0138	27.3	5.45
${}^6_2\text{He}^6$	—	?	e^-	0.89 sec	6.02073	29.1	4.86
${}^6_3\text{Li}^6$	7.4	1			6.01695	31.9	5.32
${}^7_3\text{Li}^7$	92.6	3/2			7.01820	39.1	5.59
${}^8_3\text{Li}^8$?	$e^-, 2\alpha$	0.9 sec	8.02500	41.0	5.13
${}^7_4\text{Be}^7$	—	?	K, γ	43 to 52 days	7.01916	37.4	5.34
${}^8_4\text{Be}^8$	—	?	2α	Short	8.00781	56.3	7.04
${}^9_4\text{Be}^9$	100	?			9.01499	57.9	6.44
${}^{10}_4\text{Be}^{10}$	—	?	e^-	$2.5-2.9 \times 10^6$ yr	10.01666	64.7	6.47
${}^9_5\text{B}^9$	—	?	$2\alpha + p$	Very short	9.01618	56.1	6.23
${}^{10}_5\text{B}^{10}$	18.8	3			10.01606	64.5	6.45
${}^{11}_5\text{B}^{11}$	81.2	3/2			11.01283	75.8	6.89
${}^{12}_5\text{B}^{12}$	—	?	e^-	0.027 to 0.022 sec	12.01828	79.1	6.59
${}^{12}_6\text{C}^{12}$	—	?	e^+	20 sec	10.02076	59.4	5.94
${}^{13}_6\text{C}^{13}$	—	?	e^+	20 min	11.01498	73.1	6.64
${}^{12}_6\text{C}^{12}$	98.9	0			12.00386	91.8	7.65
${}^{13}_6\text{C}^{13}$	1.1	1/2			13.00758	96.6	7.43
${}^{14}_6\text{C}^{14}$	—	0	e^-	~ 5000 yr	14.00771	104.8	7.49

APPENDIX 7

Derivation of the Lorentz Transformation Equations

Let S and S' be two similar systems, the first containing a fixed set of rectangular axes xyz , the second a parallel set $x'y'z'$. S remains at rest in our laboratory, while S' , which was coincident with the system S at the instant $t = 0$, moves along the x axis toward increasing values of x with a velocity v . Einstein's fundamental postulate states that the velocity of light c is the same in both systems. Suppose that in the system S a point on a spherical wave front starting at $t = 0$ and diverging from the origin reaches a position x, y, z after a time t . Then

$$x^2 + y^2 + z^2 = c^2 t^2 \quad (1)$$

The position x, y, z in system S is described by different coordinates x', y', z' in the system S' . Equation 1, restated for the moving system, thus becomes

$$x'^2 + y'^2 + z'^2 = c^2 t'^2 \quad (2)$$

Our aim is to find relations between $x, y, z, t, x', y', z', t'$ such that equations 1 and 2 shall be consistent. We are guided by the facts that space is homogeneous and that the motion is not accelerated; furthermore the relations between the primed and unprimed coordinates are linear. If they were not, a single event as observed in S would not appear single to observers in S' , and vice versa.

It is clear from symmetry that $y' = y$ and $z' = z$. Also x' must be proportional to $(x - vt)$ because x' is zero when x and t are zero. We shall write

$$x' = k(x - vt) \quad \text{and} \quad t' = \alpha x + \beta y + \gamma z + \delta t \quad (3)$$

where the coefficients $k, \alpha, \beta, \gamma, \delta$ are functions only of the velocity v .

In equation 2, introduce these values of the primed coordinates, giving

$$k^2(x - vt)^2 + y^2 + z^2 = c^2(\alpha x + \beta y + \gamma z + \delta t)^2$$

On expanding and rearranging we obtain

$$(k^2 - c^2\alpha^2)x^2 + (1 - c^2\beta^2)y^2 + (1 - c^2\gamma^2)z^2 - 2c^2\alpha\beta \cdot xy - 2c^2\alpha\gamma \cdot xz - 2c^2\beta\gamma \cdot yz = (c^2\delta^2 - k^2v^2)t^2 + 2(k^2v + c^2\alpha\delta)xt + 2c^2\beta\delta \cdot yt + 2c^2\gamma\delta \cdot zt$$

But this is equivalent to equation 1. Comparing coefficients we find

$$\alpha\beta = \alpha\gamma = \beta\gamma = \beta\delta = \gamma\delta = 0, \quad k^2v + c^2\alpha\delta = 0, \\ k^2 - c^2\alpha^2 = 1, \quad 1 - c^2\beta^2 = 1, \quad 1 - c^2\gamma^2 = 1, \quad c^2\delta^2 - k^2v^2 = c^2$$

Solving for $\alpha, \beta, \gamma, \delta, k$, it follows that

$$\beta = \gamma = 0, \quad \alpha = -kv/c^2, \quad \delta = k, \quad k = (1 - v^2/c^2)^{-1/2}$$

Equations 3 may therefore be rewritten as

$$x' = k(x - vt) \quad t' = k(t - vx/c^2) \quad (4)$$

where $k = 1/\sqrt{1 - v^2/c^2}$.

These are the Lorentz transformation equations as quoted on p. 463.

APPENDIX 8

Derivation of the Length Transformation, $L = kL'$

Let A observe two points, x_1, x_2 , fixed with respect to him, at instants t_1, t_2 . If B observes these, he measures x_1', x_2' at instants t_1' and t_2' .

We have

$$x_1' = k(x_1 - vt_1) \quad (1)$$

$$x_2' = k(x_2 - vt_2) \quad (2)$$

where v is the relative velocity of A and B , and k , as before, is $\left(1 - \frac{v^2}{c^2}\right)^{-1/2}$. Rewriting equation 2, p. 463, for two different instants, we have

$$t_1' = k(t_1 - vx_1/c^2) \quad (3)$$

$$t_2' = k(t_2 - vx_2/c^2) \quad (4)$$

Equations 1 and 3 can be combined to give

$$x_1 = k(x_1' + vt_1') \quad (5)$$

and using this, we find

$$t_1 = k(t_1' + vx_1'/c^2) \quad (6)$$

These refer to the appearance of B as observed by A . The equations are of the same form as 1 and 3 apart from a change from minus to plus. But it must not be forgotten that if B appears to A to move forward, then A appears to B to move backward, so the behavior of A as seen by B is identical with the behavior of B as seen by A .

An expression for a time interval is obtained by subtracting equation 3 from equation 4; that is:

$$t_2' - t_1' = k(t_2 - t_1) - \frac{kv}{c^2}(x_2 - x_1) \quad (7)$$

If the two different instants refer to events happening at the same place, as judged by A , then $x_2 = x_1$, and

$$t_2' - t_1' = k(t_2 - t_1) \quad (8)$$

so that, since k is greater than 1, $(t_2' - t_1')$ is greater than $(t_2 - t_1)$. Hence the interval of time required for a certain occurrence at rest with respect to A is judged to be greater by a moving observer. Further, if equation 5 and its analogue

$$x_2 = k(x_2' + vt_2')$$

refer to events at the same time in the primed system, then $t_1' = t_2'$, and

$$x_2 - x_1 = k(x_2' - x_1') \quad (9)$$

or

$$L = kL' \quad (10)$$

Here L denotes a length in A 's frame of reference as observed by A ; it is greater than the same length observed by B , who is moving relative to A .

APPENDIX 9

Bibliography

1. F. L. Arnot, *Collision Processes in Gases*, 4th ed., Methuen and Co., Ltd., 1950.
2. F. W. Aston, *Mass Spectra and Isotopes*, 2nd ed., Longmans, Green and Co., 1942.
3. Atomic Energy Commission Reports, obtainable from U. S. Government Printing Office, Washington 25, D. C.: Fifth Report, *Atomic Energy Development*, 45 cents; Sixth Report, *Atomic Energy and the Life Sciences*, 45 cents; Seventh Report, *Atomic Energy and the Physical Sciences*, 50 cents; *Isotopes, a Three-Year Summary of U. S. Distribution*, 45 cents (contains extensive bibliography of isotope utilization).
4. L. F. Bates, *Modern Magnetism*, 2nd ed., Cambridge University Press, 1948.
5. P. G. Bergmann, *Introduction to the Theory of Relativity*, Prentice-Hall, 1947.
6. H. A. Bethe, *Elementary Nuclear Theory*, John Wiley & Sons, 1947.
7. H. Bondi, *Cosmology*, Cambridge University Press, 1952.
8. R. M. Bozorth, *Ferromagnetism*, D. Van Nostrand Co., 1951.
9. W. H. and W. L. Bragg, *The Crystalline State*, G. Bell and Sons, 1949.
10. W. H. and W. L. Bragg, *X-Rays and Crystal Structure*, 4th ed., G. Bell and Sons, 1924.
11. British Information Service, *Statement Relating to the Atomic Bomb*, H. M. Stationery Office, London (1945); reprinted in *Rev. Modern Phys.* **17**, 472 (1945).
12. T. B. Brown, *Foundations of Modern Physics*, 2nd ed., John Wiley & Sons, 1949.
13. E. F. Burton and W. H. Kohl, *The Electron Microscope*, 2nd ed., Reinhold Publishing Corp., 1946.
14. G. L. Clark, *Applied X-Rays*, 3rd ed., McGraw-Hill Book Co., 1940.
15. Colston Research Society, *Cosmic Radiation*, Butterworth's Scientific Publications, London, 1949.
16. A. H. Compton and S. K. Allison, *X-Rays in Theory and Experiment*, D. Van Nostrand Co., 1935.
17. K. T. Compton and F. L. Mohler, "Critical Potentials," *Bull. 48, National Research Council*, Washington, D. C., 1924.
18. J. M. Cork, *Heat*, 2nd ed., John Wiley & Sons, 1942.
19. J. M. Cork, *Radioactivity and Nuclear Physics*, D. Van Nostrand Co., 1947.
20. J. A. Crowther, *Ions, Electrons and Ionizing Radiations*, 8th ed., Longmans, Green and Co., 1949.
21. K. K. Darrow, *Introduction to Contemporary Physics*, 2nd ed., D. Van Nostrand Co., 1939.
22. K. K. Darrow, *The Renaissance of Physics*, The Macmillan Co., 1936.
23. S. Dushman, *The Elements of Quantum Mechanics*, John Wiley & Sons, 1938.
24. A. S. Eddington, *Space, Time and Gravitation*, Cambridge University Press, 1923.
25. A. Einstein, *The Meaning of Relativity*, Princeton University Press, 1950.
26. A. Einstein and L. Infeld, *The Evolution of Physics*, Simon and Schuster, 1938.
27. E. Feenberg, *Revs. Modern Phys.*, **19**, 239 (1947).
28. E. Fermi, "Quantum Theory of Radiation," *Revs. Modern Phys.*, **4**, 87 (1932).
29. W. Finkelburg, *Atomic Physics*, McGraw-Hill Book Co., 1950.
30. Philipp Frank, *Between Physics and Philosophy*, Harvard University Press, 1941.

31. Philipp Frank, *Relativity, A Richer Truth*, Beacon Press, 1950.
32. G. Gamow, *Atomic Energy in Cosmic and Human Life*, The Macmillan Co., 1947.
33. G. Gamow, *Mr. Tompkins in Wonderland*, The Macmillan Co., 1940.
34. W. Gentner, H. Maier-Leibnitz, and W. Bothe, *Atlas Typischer Nebelkammer-bilder* (Atlas of Typical Cloud-Chamber Pictures), Springer, Berlin, 1940.
35. O. Glasser, *Dr. W. C. Röntgen*, C. C. Thomas, Springfield, Ill., 1945.
36. O. Glasser and Others, *Physical Foundations of Radiology*, Harper and Brothers, 1950.
37. S. Glasstone and M. C. Edlund, *The Elements of Nuclear Reactor Theory*, D. Van Nostrand Co., 1952.
38. Maria Goeppert-Mayer, papers on the systematic classification of nuclei, *Phys. Rev.*, **74**, 235 (1948), and **78**, 16 and 22 (1950).
39. Clark Goodman, Editor, M.I.T. Staff, *The Science and Engineering of Nuclear Power*, Addison-Wesley Press, Cambridge, Mass., 1947.
40. W. Gordy, W. V. Smith, and R. Trambarulo, *Microwave Spectroscopy*, John Wiley & Sons, 1953.
41. G. W. Gray, "Cosmic Rays" (popular article), *Sci. American*, March, 1949, p. 28.
42. R. W. Gurney, *Elementary Wave Mechanics*, The Macmillan Co., 1935.
43. D. Halliday, *Introductory Nuclear Physics*, John Wiley & Sons, 1950.
44. G. P. Harnwell and J. j. Livingood, *Experimental Atomic Physics*, McGraw-Hill Book Co., 1933.
45. W. Heisenberg, *Cosmic Radiation*, translated by T. H. Johnson, Dover Publications, 1946.
46. G. Herzberg, *Atomic Spectra and Atomic Structure*, 2nd ed., Dover Publications, 1944.
47. G. Herzberg, *Molecular Spectra and Molecular Structure*, Vol. I, *Spectra of Diatomic Molecules*, 2nd ed., D. Van Nostrand Co., 1950.
48. G. von Hevesy, *Radioactive Indicators*, Interscience Publishers, 1948.
49. G. Hevesy and F. Paneth, *A Manual of Radioactivity*, Oxford University Press, 1948.
50. J. B. Hoag and S. A. Korff, *Electron and Nuclear Physics*, 3rd ed., D. Van Nostrand Co., 1948.
51. A. L. Hughes and L. A. DuBridge, *Photoelectric Phenomena*, McGraw-Hill Book Co., 1932.
52. G. F. Hull, *Elementary Survey of Modern Physics*, The Macmillan Co., 1949.
53. R. F. Humphreys and R. Beringer, *First Principles of Atomic Physics*, Harper and Brothers, 1950.
54. L. Janossy, *Cosmic Rays*, Oxford University Press, 1948.
55. G. E. M. Jauncey, *Modern Physics*, 3rd ed., D. Van Nostrand Co., 1948.
56. J. H. Jeans, *The New Background of Science*, The Macmillan Co., 1933.
57. F. A. Jenkins and H. E. White, *Fundamentals of Physical Optics*, McGraw-Hill Book Co., 1937.
58. W. Jevons, *Report on Band Spectra of Diatomic Molecules*, Cambridge University Press, 1932.
59. R. C. Johnson, *Atomic Spectra*, 2nd ed., Methuen and Co., 1950.
60. S. A. Korff, *Electron and Nuclear Counters*, D. Van Nostrand Co., 1946.
61. R. E. Lapp and H. L. Andrews, *Nuclear Radiation Physics*, Prentice-Hall, 1948.

62. L. Leprince-Ringuet, *Cosmic Rays*, translated by Fay Ajzenberg, Prentice-Hall, 1950.
63. L. B. Loeb, *Atomic Structure*, John Wiley & Sons, 1938.
64. L. B. Loeb, *Fundamentals of Electricity and Magnetism*, 3rd ed., John Wiley & Sons, 1947.
65. L. B. Loeb, *Kinetic Theory of Gases*, McGraw-Hill Book Co., 1934.
66. K. Lonsdale, *Crystals and X-Rays*, D. Van Nostrand Co., 1949.
67. J. Mack, "Table of Nuclear Moments," *Revs. Modern Phys.*, **22**, 64 (1950).
68. J. Mattauch and A. Flammersfeld, *Report on Isotopes*, Tubingen, 1949.
69. A. A. Michelson, *Studies in Optics*, University of Chicago Press, 1927.
70. R. A. Millikan, *Electrons (+ and -), Protons, Photons, Neutrons and Cosmic Rays*, revised ed., University of Chicago Press, 1947.
71. A. C. G. Mitchell and M. W. Zemansky, *Resonance Radiation and Excited Atoms*, Cambridge University Press, 1934.
72. D. J. X. Montgomery, *Cosmic Ray Physics*, Princeton University Press, 1949.
73. N. F. Mott and R. W. Gurney, *Electronic Processes in Ionic Crystals*, Oxford University Press, 1948.
74. O. Oldenberg, *Introduction to Atomic Physics*, McGraw-Hill Book Co., 1949.
75. L. A. Pauling and S. A. Goudsmit, *The Structure of Line Spectra*, McGraw-Hill Book Co., 1930.
76. J. Perrin, *Brownian Movements and Molecular Reality*, Taylor and Francis, London, 1910.
77. E. Pollard and W. L. Davidson, *Applied Nuclear Physics*, 2nd ed., John Wiley & Sons, 1951.
78. C. F. Powell and G. P. S. Occhialini, *Nuclear Physics in Photographs*, Oxford University Press, 1947.
79. F. Rasetti, *Elements of Nuclear Physics*, Prentice-Hall, 1936.
80. F. O. Rice and E. Teller, *The Structure of Matter*, John Wiley & Sons, 1949.
81. O. K. Rice, *Electronic Structure and Chemical Binding*, McGraw-Hill Book Co., 1935.
82. F. K. Richtmyer and E. H. Kennard, *Introduction to Modern Physics*, 4th ed., McGraw-Hill Book Co., 1947.
83. J. K. Robertson, *Radiology Physics*, D. Van Nostrand Co., 1948.
84. G. D. Rochester and J. G. Wilson, *Cloud-Chamber Photographs of the Cosmic Radiation*, Academic Press, 1952.
85. B. Rossi, "Cosmic Ray Phenomena," *Revs. Modern Phys.*, **20**, 537 (1948).
86. B. Rossi, *High-Energy Particles*, Prentice-Hall, 1952.
87. A. E. Ruark and H. C. Urey, *Atoms, Molecules and Quanta*, McGraw-Hill Book Co., 1930.
88. E. Rutherford, J. Chadwick, and C. D. Ellis, *Radiations from Radioactive Substances*, The Macmillan Co., 1930.
89. G. T. Seaborg and I. Perlman, "Table of Isotopes," *Revs. Modern Phys.*, **20**, 585 (1948). See also J. M. Hollander, I. Perlman, and G. T. Seaborg, *Revs. Modern Phys.*, **25**, 469 (1953).
90. H. Semat, *Introduction to Atomic Physics*, Rinehart and Co., 1946.
91. M. M. Shapiro, "Tracks of Nuclear Particles in Photographic Emulsion," *Revs. Modern Phys.*, **13**, 58 (1941).
92. M. Siegbahn, *Spectroscopy of X-Rays*, translated by G. A. Lindsay, Oxford University Press, 1925.

93. H. D. Smyth, *Atomic Energy for Military Purposes*, Princeton University Press, 1945; reprinted in *Revs. Modern Phys.*, **17**, 351 (1945).
94. Arnold Sommerfeld, *Atomic Structure and Spectral Lines*, translated by H. L. Brose, Methuen and Co., 1923.
95. H. Soodak and E. C. Campbell, *Elementary Pile Theory*, John Wiley & Sons, 1949.
96. W. T. Sproull, *X-Rays in Practice*, McGraw-Hill Book Co., 1946.
97. W. E. Stephens, editor, Pennsylvania Physics Staff, *Nuclear Fission and Atomic Energy*, Science Press, 1948.
98. J. D. Stranathan, *The Particles of Modern Physics*, The Blakiston Co., 1942.
99. Symposium, *The Use of Isotopes in Biology and Medicine*, University of Wisconsin Press, 1949.
100. Y. K. Syrkin and M. E. Dyatkina, *Structure of Molecules and the Chemical Bond*, Interscience Publishers, 1950.
101. G. P. Thomson, *The Wave Mechanics of Free Electrons*, McGraw-Hill Book Co., 1930.
102. G. P. Thomson and W. Cochran, *Theory and Practice of Electron Diffraction*, The Macmillan Co., 1939.
103. A. M. Thorndike, *Mesons, A Summary of Experimental Facts*, McGraw-Hill Book Co., 1952.
104. R. C. Tolman, *Relativity, Thermodynamics and Cosmology*, Oxford University Press, 1934.
105. L. A. Turner, *Revs. Modern Phys.*, **12**, 150 (1940). Early history of fission and chain-reaction studies.
106. J. Valasek, *Introduction to Theoretical and Experimental Optics*, John Wiley & Sons, 1949.
107. R. L. Weber, *Heat and Temperature Measurement*, Prentice-Hall, 1950.
108. H. E. White, *Introduction to Atomic Spectra*, McGraw-Hill Book Co., 1935.
109. J. G. Wilson, editor, *Progress in Cosmic Ray Physics*, Interscience Publishers, 1952.
110. John G. Wilson, *About Cosmic Rays*, Sigma Books, London, 1948.
111. H. Yagoda, *Radioactive Measurements with Nuclear Emulsions*, John Wiley & Sons, 1949.
112. I. F. Zartman, *Phys. Rev.*, **37**, 383 (1931).
113. M. W. Zemansky, *Heat and Thermodynamics*, 2nd ed., McGraw-Hill Book Co., 1943.

Index

- Aamodt, R. L., 430
Abelson, P. H., 384
Absorption, of gamma rays, 298
 of X-rays, 114
Absorption coefficient, cosmic rays, 406
Absorption edges, X-ray, 142
Absorption spectra, optical, 59
 X-ray, 141 *ff.*
Absorption thickness, cosmic rays, 416, 449
Abundances of isotopes, 378, 482
Actinium series, 272
Adelman, F. L., 432
Alfven, H., 451, 452
Alichanian, A. I., 436
Alikhanov, A. I., 436
Alkalies, spectra of, 194 *ff.*
Alkaline earths, spectra of, 202 *ff.*
Allen, J. S., 318
Alpha particles, 45, 264 *ff.*
 as range particles, 298
 disintegration by, 337 *ff.*
 energy of, 274, 276
 heating effect of, 276
 ions produced by, 297
 large-angle scattering of, 306
 penetration of matter by, 298
 scattering of, 47, 306
 spectrum of, 278
Alvarez, L. W., 344, 370
Amplifier, 288
Anderson, C. D., 266, 309, 310, 313, 406, 413, 427, 439
Andrade, E. N. da C., 280, 281
Andrews, H. L., 393
Angstrom unit, 52
Angular momentum, alkali atom, 200
 in Bohr orbit, 97, 100
 of electron, 199
Annihilation, of matter, 43, 311, 312, 472
 of positrons and electrons, 311
Annihilation radiation, 314
Araki, G., 434
Arley, N. H., 440
Arnold, W. R., 365
Artificial radioactivity, 350 *ff.*
Aston, F. W., 39
Atkinson, R. d'E., 381
Atmospheres, law of, 19
Atomic bomb, 395
Atomic Energy Commission, 114, 393
Atomic number, 41, 135
Auger, P., 441
Avogadro's law, 3
Avogadro's number, 10, 19, 30

Babcock, H. W., 452
Bainbridge, K. T., 31, 40, 41
Balmer series, 93, 194
Band head, 251
Band spectra, electronic, 249
 rotational, 241
 vibration-rotation, 244
Bardwell, D. C., 401
Barkas, W. H., 433
Barkla, C. G., 118
Barn (unit of area), 305
Barnothy, J., 450
Barrier model of nucleus, 358
Beams, J. W., 340, 344
Bearden, J. A., 29, 134, 477
Becquerel, H., 267
Bémont, M. G., 268
Berkelium, 383
Bernoulli, D., 4
Beta decay, 264, 273 *ff.*, 317
 regularities in, 364
Beta particles, 264 *ff.*
 as range particles, 298
 continuous spectrum of, 275, 283
 energy of, 274, 275
 heat effect of, 276
 ions produced by, 297
 line spectrum of, 275, 281
 origin of, 321
 penetration of matter by, 298
 spectrum of, 317
 velocity of, 276
Beta-ray spectrograph, 276

- Betatron, 150, 340
 Bethe, H. A., 356, 421
 Bevatron, 349
 Bibliography, 485
 Bichowsky, F. R., 198
 Binding energy, 46, 377
 of light nuclei, 482
 Birnbaum, M., 433
 Bjorklund, R. F., 409, 430
 Black body, 52, 68 *ff.*
 as standard radiator, 70
 brightness of, 68
 Black-body radiation, 52, 68 *ff.*
 spectrum of, 70 *ff.*
 Stefan-Boltzmann law, 70
 Blackett, P. M. S., 339
 Bloch, F., 368, 370
 Bohm, D., 452
 Bohr, N., 96, 357, 391
 Bohr magneton, 215, 317
 Bohr orbits, 97
 Bohr's theory, elliptic orbits, 100
 extensions of, 100
 fundamental assumptions, 96
 of hydrogen atom, 93, 96
 insufficiency of, 107
 Bolometer, 63
 Boltzmann constant, 10, 30
 Bonhoeffer, K., 240
 Booth, E. T., 386
 Born, M., 89, 157
 Bose-Einstein distribution law, 262
 Bose statistics, 262, 334, 479
 Bothe, W., 266, 406
 Bowen, I. S., 65, 405
 Boyle's law, 9, 14
 Brackett, F. S., 95
 Bradner, H., 428, 430
 Bradt, H. L., 424, 426
 Bragg, W. H., 130, 131, 297
 Bragg, W. H., curve of ionization, 297
 Bragg, W. L., 121
 Bragg's law, 122 *ff.*, 280, 331
 for electrons, 159
 Branching in radioactive series, 274
 Breit, G., 265, 330, 340, 356, 374
 Bremsstrahlung, 149, 430
 Bretscher, E., 365
 Brickwedde, F. G., 105, 106
 Briggs, L. J., 393
 Brode, R. B., 427
 Broer, L. J. F., 368
 Brownian movement, 17
 Bucherer, A. H., 33
 Bursts, cosmic-ray, 416
 Butler, C. C., 436
 Cadmium as neutron absorber, 329
 Cahn, J. H., 388
 Californium, 383
 Cameron, G. H., 449
 Canal rays, 38
 Carbon cycle, 356
 Cario, G., 213
 Carrier particles, 375
 Cell, photoconductive, 64
 Center-of-mass frame of reference, 302, 367
 Chadwick, J., 266, 308, 320, 321, 338, 355
 Characteristic X-rays, 117
 Charge, conservation of, 334
 Charge distribution in hydrogen atom, 190
 Charges of elementary particles, 479
 Charles' law, 9, 14
 Clausius, R., 11
 Clay, J., 407, 441
 Cloud chamber, Wilson, 292, 419
 Cloud-chamber tracks, 79, 292, 295, 296
 Cocconi, G., 441
 Cockroft, J. D., 265
 Coincidence counters, 291
 Collisions, of elastic particles, 300
 of equal balls, 302
 of inelastic particles, 302
 of the second kind, 213
 Combining weight, 3
 Compound nucleus, 357, 391
 Compton, A. H., 143, 441, 443
 Compton effect, 143
 Condon, E. U., 360
 Conduction in solids, electrical, 257
 Conductivity-crystal counter, 290
 Conservation laws in nuclei, 334
 Constants, tables of, 477
 Continuous spectrum, optical, 59
 X-ray, 126
 Contraction due to relative motion, 461 *ff.*
 Conversi, M., 434
 Coolidge, W. D., 110
 Corpuscular theory of light, 51
 Cosmic-ray bursts, 416
 Cosmic-ray showers, 439 *ff.*
 Cosmic rays, 65, 405 *ff.*
 absorption thicknesses of, 448
 at high altitudes, 443
 distribution in depth, 446
 east-west effect, 446
 energy of, 405, 441
 experimental methods, 415 *ff.*
 ionization at sea level, 405
 latitude effect, 441

- Cosmic rays, nature of, 407
 origin of, 450 *ff.*
 primary, 424 *ff.*
 underground, 449
 Cosmotron, 349
 Coulomb, C. A. de, 23
 Counters, coincidence, 291
 conductivity-crystal, 290
 Geiger-Müller, 290
 scintillation, 289
 Crookes' dark space, 31
 Cross section, for collision, 303 *ff.*
 for fast neutron scattering, 327
 for fission, 385
 for single scattering, 307
 for thermal neutron capture, 324
 Crowther, B. M., 356
 Crystal, metallic, 257
 Crystal-structure analysis, Laue method,
 120
 powder method, 133
 Crystals, cubic, 128
 space lattices of, 127
 structure of, 126
 Cubic crystal, body-centered, 128, 129
 face-centered, 128, 129
 simple, 128, 129
 Curie, M. S., 268
 Curie, P., 268
 Curie-Joliot, F., 266, 272, 319, 351
 Curie-Joliot, I., 266, 319, 351
 Curie-Langevin law, 219
 Curie, unit of activity, 270
 Curtis, W. E., 94
 Curtiss, L. F., 281, 282
 Cyclotron, 340, 344
 Czerny, M., 243

 Dabbs, J. W., 388
 Dahl, O., 340
 Dalton, John, 2
 Dauvillier, A., 452
 Davisson, C. J., 156, 159
 de Broglie, L., 155 *ff.*
 de Broglie theory of matter waves, 156
 Debye, P., 133
 Decay, of fission products, 389
 of neutron, 331
 of radioactive atom, 269
 of radium, 269
 Decay constant, 269 *ff.*
 Dee, P. I., 294, 326, 354, 355
 Dee of cyclotron, 345
 Deflection of starlight, 471
 Degenerate levels, 207
 Degrees of freedom, 12
 Degrees of freedom, vibrational, 235
 Delayed neutrons, 388, 395
 Democritus, atomic theory of, 1
 Dempster, A. J., 39
 Detection of particles and photons, 288
 Deuterium, 42, 105, 353
 mass of, 41
 Deuteron, 265
 theory of, 370 *ff.*
 Deutsch, M., 315
 Dewar, J., 61
 Diamagnetism, 217
 Diatomic molecules, 235
 Dielectric constants, 255
 Diffraction, by crystals, 120 *ff.*, 156, 158
 by multiple slits, 57
 effect of, on measurement, 180
 of atoms and molecules, 160
 of electrons, 156, 158
 of neutrons, 331
 of X-rays, 119 *ff.*
 Diffraction grating, 55
 Diffuse series of sodium, 195
 Diffusion of neutrons, 396
 Diffusion length for neutrons, 396
 Dipole moments of molecules, 255
 Dirac, P. A. M., 89, 90, 287, 315, 375
 Dirac's theory of positrons and electrons,
 315
 Disintegration, radioactive, 267 *ff.*
 Displacement law in radioactivity, 272
 Displacement rule in spectra, 209
 Distribution, of black-body radiation, 70
 of electron energy in metals, 257 *ff.*
 of electron momenta in metals, 259
 of molecular velocities, 6
 Doublet levels, 198
 Doublets in alkali spectra, 198
 Droplet model of nucleus, 390, 392
 Drude, P. K. L., 257, 261
 Dubridge, L. A., 88
 Dufay, C. F. de C., 23
 Dunning, J. R., 324, 325, 327, 386
 Durbin, R., 413

 Earth's crust, age of, 271
 Eddington, A. S., 287, 381, 467
 Einstein, A., 18, 33, 85, 155, 393, 454, 464
 Einstein's ghost field, 89, 155
 Einstein's photoelectric equation, 86, 88
 Elastic collisions, 300
 Eldridge, F. R., 369
 Electric dipole moment, 255
 Electric discharge in gas, 30
 Electrical conduction in solids, 257
 Electrical units, 476

- Electrolysis, 24
 Electromagnetic nature of mass, 35
 Electron microscope, 162 *ff.*
 Electron shells, 141, 225 *ff.*
 Electron volt, 30
 Electronic bands, 249 *ff.*
 Electrons, 24 *ff.*
 angular momentum of, 193 *ff.*, 199
 behavior of (table), 480
 charge of, 25 *ff.*, 134
 diffraction of, 156, 158
 distribution in periodic table, 228
 effective mass of, 104
 free, 145, 151, 257
 in cosmic-ray showers, 414
 in metals, 257
 interaction of, with atoms, 148
 magnetic moment of, 198, 316
 mass of, 30 *ff.*
 rest energy of, 30, 274
 size of, 37
 spin of, 193 *ff.*
 variable mass of, 32, 102, 137
 wavelength associated with, 156 *ff.*
 Electroscope, 267, 288
 Electrostatic generator, 340
 Elementary particles, 287 *ff.*
 behavior of (table), 480
 properties of (table), 479
 Elements, chemical properties of, 229
 Ellett, A., 367
 Elliptic orbits, 100
 Ellis, C. D., 284, 338
 Elsasser, W., 155
 Elster, J., 405
 Emission spectra, 59
 X-ray, 134
 Energy, from uranium fission, 400
 Energy-level diagram, hydrogen atom, 101
 nucleus, 278
 sodium atom, 196
 mass equivalence of, 33, 472
 of electrons in metals, 259
 release in nuclear reactions, 351
 solar, 356
 states, hydrogen atom, 97
 Energy levels, hydrogen atom, 99
 of solids, 257
 quantized, 244
 Equipartition of energy, 13
 Equivalence of mass and energy, 33, 472
 Ether, luminiferous, 53
 Evans, J., 450
 Exchange energy, 219
 Exchange forces, 375
 Exchange forces, theory of, 231
 Exclusion principle, 207
 Fainberg, J., 431
 Fajans, K., 272
 Far infrared spectroscopy, 62, 243
 Faraday, M., 3, 24, 35
 Fermi, E., 258, 261, 266, 352, 364, 383, 393, 452
 Fermi distribution law, 261, 262
 Fermi statistics, 262, 334, 479
 Ferromagnetism, 219
 Fink, G. A., 325
 Fission, early research on, 381
 energy release in, 390
 large-scale use of, 392 *ff.*
 of the nucleus, 381 *ff.*
 Fission fragments, 382, 388
 Fission products, decay of, 389
 Fitzgerald, G. F., 461
 Fitzgerald-Lorentz contraction, 461 *ff.*
 Fleming, J. A., 408
 Flint, H. T., 184
 Fluorescent X-rays, 116 *ff.*
 Foote, P. D., 252
 Forbush, S., 450, 451
 Forces between nucleons, 376
 Formation of molecules, 229
 Forro, M., 450
 Foucault, J. L., 51
 Found, C. G., 210
 Fourth-power law of radiation, 70
 Fowler, A., 103
 Fowler, E. C., 436
 Frame of reference, 462 *ff.*
 center-of-mass, 302
 Franck, J., 213
 Franklin, B., 23
 Fraunhofer, J. von, 55, 60
 Fraunhofer lines, 60, 93
 Free electrons, 145, 257
 Free volume, 14
 Freier, P., 424, 425
 Freitag, K., 293
 French, A. P., 365
 Frenkel, J., 199
 Fresnel, A. J., 51
 Friedrich, W., 120
 Frieman, E. A., 357
 Frisch, O. R., 382, 390
 Fukuda, M., 205
 Fundamental series of sodium, 197, 198
 Gamma-ray microscope, 181
 Gamma-ray spectrograph, 280
 Gamma rays, 65, 264 *ff.*

- Gamma rays, absorption of, 298
 detection of, 280, 288 *ff.*
 diffraction by crystals, 279
 energy of, 274, 279
 heating effect of, 276
 intensity measurements, 279, 288 *ff.*
 pair production by, 311
 producing photoelectrons, 281
 scattering of, 143
 spectra of, 279
 wavelengths of, 279
 Gamow, G., 359, 360, 363
 Gardner, E., 409
 Gas constant, Boltzmann's, 10, 478
 molar, 9
 Gases, ideal, 4 *ff.*
 real, 14
 Gay-Lussac, J. L., 2
 Geiger, H., 48
 Geiger counter, efficiency of, 290
 Geiger-Müller counter, 112, 290
 efficiency of, 291
 Geiger-Nuttall law, 358, 363
 Geitel, H., 405
 General theory of relativity, 469
 Generators, high-voltage, 340
 George, E. P., 450
 Gerlach, W., 214
 Germer, L. H., 156, 159
 Gilbert, C. W., 326
 Gilbert, William, 23
 Glancing angle, 123
 Gockel, A., 405
 Golay cell, 64
 Goldhaber, M., 355, 385
 Gorter, C. J., 368
 Goudsmit, S. A., 198
 Gram-molecular volume, 3
 Grating, diffraction, 55 *ff.*
 Grating space, of a crystal, 124 *ff.*
 of sodium chloride, 128
 Gravitation and accelerated motion, 469
 Gravitational deflection of light, 471
 Graviton, 288
 Greisen, K., 441, 450
 Grimaldi, F. M., 51
 Grivet-Meyer, T., 441
 Gross, E. P., 452
 Grosse, A. V., 386
 Gunn, R., 450
 Gurney, R. W., 360

 H particles, 337
 Hafstad, L. R., 265, 340, 356, 374, 466
 Hahn, O., 382
 Halban, H. von, 272

 Half-life, mu meson, 411
 pi meson, 410
 Half-lives, light isotopes, 482
 radioactive substances, 269
 Hall, D., 388
 Hallwachs, W., 78
 Hamilton, J., 409
 Hanna, S. S., 356, 368
 Hansen, W. W., 368
 Harkins, W. D., 339
 Harmonic oscillator, 185
 Harteck, P., 240
 Hartley, W. N., 194
 Hause, C. D., 58
 Haxby, R. O., 385
 Haxel, O., 379
 Hayakawa, G., 450
 Head of a band spectrum, 251
 Heisenberg, W., 179, 219, 322, 430, 464
 Heisenberg's uncertainty principle, 179
 Heitler, W., 231, 409, 421
 Helium, spectrum of, 103
 Herb, R. G., 340
 Hereford, F. L., 424
 Herschel, W., 61
 Hertz, G., 212
 Hertz, H., 53, 77
 Herzberg, G., 194
 Hevesy, G. von, 401
 Heydenburg, N. P., 366, 367, 374
 Hoffmann, G., 416
 Hoffmann cosmic-ray bursts, 416
 Holloway, M. G., 297
 Homopolar molecules, 230
 Hooke, R., 51
 Houtermans, F. G., 381
 Hudson, C. M., 367
 Hughes, D. J., 388
 Hulburt, E. O., 93
 Hull, A. W., 133
 Huygens, C., 51
 Huygens' principle, 56
 Hyde, E. K., 272
 Hydrogen, heavy, 105
 Lyman series of, 95, 100
 molar heats of, 234 *ff.*
 para and ortho, 238
 Paschen series of, 95
 specific heats of, 239
 Hydrogen atom, Bohr's theory, 93 *ff.*
 de Broglie's quantization of, 164
 effect of external fields, 106
 in wave mechanics, 189
 quantization of, 96, 97, 164 *ff.*
 Hyperons, 436

- Ideal gas, 4 *ff.*
 Imes, E. S., 247
 Indetermination, principle of, 182
 Index of refraction, X-rays, 120
 Induced radioactivity, 266
 Infrared radiation, 62
 Inglis, D. R., 356, 367, 368
 Inner quantum number, 199
 Interaction of photons, 315
 Interferometer, Michelson, 458
 Internal energy of reacting particles, 302
 Ionization, by alpha particles, 297
 by beta particles, 294
 by gamma rays, 297
 of mercury vapor, 210
 Ionization chamber, 112
 for cosmic rays, 416
 Ionization loss, by electrons, 421
 by mesons, 423
 Ionization potential, 209
 Ionization spectra of X-rays, 124
 Ionization spectrometer, 124
 Ionizing effects of particles, 297
 Ions in electrolytes, 3, 25
 Isomerism, nuclear, 351
 Isotopes, 38 *ff.*
 effect on band spectra, 248
 scientific uses of, 401 *ff.*
 table, 482
 Isotopic weights, 482

j-j coupling, 207
 Jeans, J. H., 74
 Jenkins, F. A., 251
 Jensen, J. H. D., 379
 Johnson, T. H., 161, 407, 446
 Joliot, F. C., 266, 272, 311, 319, 351
 Jones, S. B., 432
 Joule, J. P., 9
 Journey, E. T., 318

K capture of electrons, 318
K characteristic X-rays, 117, 137 *ff.*
K shell of electrons, 138
 Kappa meson, 438
 Kelvin temperature, 9
 Kephart, D. C., 369
 Kerst, D. W., 150, 340
 Kikuchi, S., 160, 161
 Kinetic energy of a fast particle, 278
 Kinetic theory of gases, 4 *ff.*
 Kirchhoff, G. R., 60
 Kirchhoff's law of radiation, 66
 Kirkpatrick, P., 164
 Kirsch, G., 337
 Klema, E. D., 385

 Knauer, F., 368
 Knipping, P., 120
 Koch, H. W., 385
 Kolhörster, W., 406, 449
 Korff, S. A., 407
 Krishnan, K. S., 252
 Kulenkampff, H., 411

L characteristic X-rays, 117, 137 *ff.*
L shell of electrons, 138
 Lahaye, H., 33
 Lal, D., 438
 Lamb, W. E., 102
 Landsberg, G., 252
 Langer, L. M., 283, 321
 Langmuir, I., 230
 Lapp, R. E., 393
 Larmor, J., 106
 Larmor precession, 106
 Larsson, A., 120
 Lattes, C. M. G., 267, 409, 427
 Laue, M. von, 120
 Laue pattern, 120
 of electrons, 160
 Lauritsen, C. C., 265, 340, 382
 Lauritsen, T., 382
 Lawrence, E. O., 265, 340, 345
 Lead from radioactive minerals, 274
 Leak effect in wave mechanics, 174, 362
 Leighton, R. B., 413
 Lemaître, G., 443, 450
 Leprince-Ringuet, L., 425
 Lewis, G. N., 230
 Light, corpuscular theory of, 51
 velocity of, 454 *ff.*
 wave theory of, 51
 Light and matter, theories of, 157
 Light isotopes, properties of, 482
 Lind, S. C., 401
 Line spectrum, 59
 of alpha particles, 278
 of beta particles, 275, 281
 Line structure of band spectra, 241, 251
 Linear accelerator, 340, 344
 Linear oscillator, 244
 Lithium, nuclear reactions, 356
 Liveing, G. D., 61
 Livingston, M. S., 297, 340, 346
 Loar, H., 413
 Lofgren, E. J., 424, 425
 London, F., 231
 Lord, J. J., 431
 Lorentz, H. A., 33, 37, 257, 261, 462
 Lorentz transformation equations, 462 *ff.*,
 483
 Luminiferous ether, 456

- Lyman, T., 65
Lyman series, 95
- M* characteristic X-rays, 117, 142
Magic numbers, 379
Magnetic moment, 368
 of a particle, 288
 of atom, 214
 of electron, 198, 316
 of elementary particles, 479
 orbital, 199
Magnetic quantum number, 107, 226
Magnetic spectrograph, 276
Magnetron, Bohr, 215, 317
 nuclear, 368
Mandelstam, L., 252
Marney, M. C., 330, 331
Marsden, E., 48
Mass, and energy, equivalence of, 33, 472
 meaning of, 35, 155 *ff.*
 variation with velocity, 32 *ff.*, 102, 277, 303, 472
Mass-energy relationship, 33
Mass spectrograph, 39 *ff.*
Masses of elementary particles, 479
Matter and light, theories of, 157
Matter in bulk, magnetic properties, 215
Matter waves, 155 *ff.*
 and probability, 177
 frequency and velocity of, 168
Maxwell, J. C., 6, 17, 51
Maxwell-Boltzmann distribution of velocities, 7, 261
Maxwell's distribution law of molecular velocities, 6 *ff.*
Mayer, M. G., 379
Maze, R., 441
McCord, R. V., 332
McMillan, E. M., 340, 347, 384
Mean free path, for neutron absorption, 394
 of molecules, 15, 16
 of photons, 298
 in nuclear material, 353
Measurements, limits of accuracy, 182, 184
Meitner, L., 293, 382, 390
Melting points of elements, 224
Mendeléef, D. I., 135, 221
Mendeléef's table, 135, 481
Meson potential, 371, 376
Mesons, 266, 427 *ff.*
 as carrier particles, 376
 discovery of, 266
 heavy, 436
 kappa, 438
 Mesons, light, 436
 mu, 266, 411 *ff.*
 negative, 266
 pi, 266, 409 *ff.*
 pi-mu decay of, 432 *ff.*
 positive, 266
 properties of, 428
 tau, 436
Metals, conduction in, 257
Metastable state, 205
Mev, million electron volts, 30, 274
Meyer, Lothar, 221
Meyer, R. C., 388
Michelson, A. A., 457, 458
Michelson-Morley experiment, 457 *ff.*
Micron, 52
Microscope, electron, 162
 gamma-ray, 181
 X-ray, 163, 164
Microwave spectroscopy, 61, 102, 253
Microwaves, 61, 253
Miller, L. C., 332, 333
Miller indices, 128
Millikan, R. A., 25 *ff.*, 65, 439, 449, 450
Mitchell, A. C. G., 283, 325, 331
Model of atom, vector, 193 *ff.*, 204 *ff.*
Moderator in nuclear reactor, 395
Modified X radiation, 143
Moffat, J., 365
Mohler, F. L., 213
Molar heats of gases, 11 *ff.*
Molar volume, 3
Mole, 3, 24
Molecular diameters, 15
Molecular energy and temperature, 9
Molecular spectra, polyatomic, 248
Molecular structure, 234 *ff.*
Molecular velocities, 4
Molecules, diatomic, 234 *ff.*
 reality of, 17
 rotating-vibrating, 244 *ff.*
Molière, G., 440
Moment, electric dipole, 255
Moment of inertia, of HCl, 244
 of molecules, 238
 in microwave spectroscopy, 254
Momentum, angular quantized, 97
Morgan, K. Z., 440
Morley, E. W., 458
Moseley, H. G. J., 134, 136
Moseley's law, 134
Motion of the nucleus, 103
Motz, L., 357
Moyer, B. J., 409, 430
Mu meson, 266, 411 *ff.*, 427 *ff.*
 half-life of, 411

- Muirhead, H., 267, 427
 Mulliken, R. S., 251
 Multiple proportions, laws of, 2
 Murphy, G. M., 105, 106
- Nacken, M., 33
 Nature of matter, 35, 155 *ff.*
 Nature of radiation, 51 *ff.*
 Near infrared radiation, 63
 spectra, 247
 spectrometer, 71
 Neddermeyer, S. H., 266, 309, 406, 427, 439
 Negative energy, 287, 315
 Negatron, 309
 Neptunium, 384
 Neptunium series, 272
 Nernst, W., 235
 Neutrino, 266, 317 *ff.*
 detection of, 318
 properties of, 319
 spin of, 319
 Neutron absorption, 386
 Neutron-capture reactions, 383
 Neutron-proton potential, 374
 Neutron reactions, 352
 Neutron scattering experiments, 325
 Neutron-velocity spectrometer, 331
 Neutrons, 41, 319 *ff.*
 absorption of, 330
 as components of nuclei, 41, 44, 321
 behavior of (table), 480
 created by fission, 383, 386 *ff.*
 decay of, 331
 delayed, 388
 diffracted from crystals, 331
 discovery of, 266
 energy distribution of, 328
 fast, 323
 fast-scattering cross sections of, 327
 half-life of, 333
 interacting with matter, 322
 mass of, 320
 of intermediate velocity, 323
 production of, 322 *ff.*
 resonance, 324
 resonance cross section of, 329
 scattered, angular distribution of, 328
 scattering of, 325
 slowed down, by collisions, 302, 328
 by protons, 302, 329
 spontaneous disintegration of, 331
 thermal, 323, 324
- Newton, I., 51
 Newtonian mechanics, limitations of, 182
 Ney, E. P., 424, 425
- Nichols, E. F., 62
 Nielsen, W. M., 433, 440
 Nier, A. O., 386
 Noble, R. H., 71
 Noble gases, 222
 Nordheim, L. W., 440
 Notation, spectroscopic, 202
 Nuclear charge, 41, 135, 308
 Nuclear energy, 381 *ff.*
 Nuclear forces, 360, 375 *ff.*
 Nuclear isomerism, 351
 Nuclear magnetic resonance, 368
 Nuclear magneton, 368
 Nuclear particle tracks, in emulsions, 296, 408 *ff.*
 Nuclear reaction, self-sustaining, 394
 Nuclear reaction equations, 355
 Nuclear reactions, notation, 267
 Nuclear reactor, 394, 400
 design of, 395
 Nuclear reactors, U. S. program, 400
 Nuclear resonance, 365
 Nuclear spin, 368
 Nuclear structure, 337 *ff.*, 357 *ff.*, 371
 Nuclear tracks in emulsions, 296, 408 *ff.*
 Nucleon, 46
 Nucleons, forces between, 376
 Nucleus, artificial disintegration of, 265 *ff.*, 337 *ff.*
 barrier model of, 358
 compound, 357
 particles emitted by, 264 *ff.*
 transmutation of, 265 *ff.*, 337 *ff.*
 Nuttall, J. M., 358
- Observation, process of, 179
 Occhialini, G. P. S., 267, 427
 O'Ceallaigh, C., 438
 Oliphant, M. L., 356
 Oppenheimer, F., 424, 425
 Orbital angular momentum, 203
 Orbital magnetic moment, 199
 Orbits in hydrogen atom, 96
 Order of a spectrum, 56, 123, 126
 Origin of quantum theory, 71 *ff.*
 Ortho hydrogen, 238
 Oscillator, linear, 244
 simple harmonic, 185
 Ostwald, Wilhelm, 17
 Oxides of the form R_2O_n , 224
- Packard, M. E., 368
 Packing fraction, 44
 Pair annihilation, 311
 Pair creation, 311
 Pair production, 312, 350

- Pairing, of electrons, 230
- Pairing, of spins, 203 *ff.*
- Pal, Y., 238
- Pancini, E., 434
- Paneth, F. A., 401
- Panofsky, W. K. H., 410, 430
- Para hydrogen, 238
- Paramagnetism, 218
- Parity, conservation of, 334, 335
- Particle in a box, 172
- Particles, elementary, 287 *ff.*, 479, 480
 - high-energy, 419
- Paschen series, 95
- Pauli, W., 193 *ff.*, 368
- Pauli's exclusion principle, 193 *ff.*, 207 *ff.*
 - application to periodic table, 226
- Pegram, G. B., 325, 393
- Peng, H. W., 409
- Periodic system of the elements, 135, 221 *ff.*, 481
- Periodic table, 481
- Permeability, magnetic, 215
- Perrin, J., 17 *ff.*
- Peters, B., 424, 426, 438
- Pettersson, H., 337
- Pfund, A. H., 95
- Phase velocity, 455
 - of matter waves, 169
- Phillips, J. A., 365
- Photoelectric experiments, 80
- Photoelectric work function, 86
- Photoelectricity, 77 *ff.*
 - stopping potentials, 83
- Photoelectrons, 78 *ff.*
 - ejected by gamma rays, 281
 - ejected by X-rays, 79, 138
 - energy of, 80 *ff.*
- Photon, 52 *ff.*
 - behavior of (table), 480
 - mean free path of, 298
 - momentum of, 143
 - scattering of, 143, 181 *ff.*
 - spin of, 262
 - X-ray, 143
- Photons, high-energy, 419
 - interaction of, 315
- Physical constants (table), 477
- Pi meson, 266, 409 *ff.*, 427 *ff.*
 - half-life of, 410
- Piccioni, O., 434
- Pickering, E. C., 103
- Pickering, W. H., 439
- Pile, operation of, 394
- Pi-mu meson decay, 432 *ff.*
- Plain, G. J., 367
- Planck, M., 52 *ff.*, 96
 - Planck's constant, 76, 87, 96, 182
 - best value of, 87
 - determination of, 76, 87
 - Planck's quantum theory of radiation, 74
 - Planck's radiation formula, 74
 - Planetary atom, 96
 - Pleasanton, F., 332, 333
 - Plutonium, 384
 - Point molecule, 12
 - Poisoning of nuclear reactor, 398
 - Polarization, electric, 256
 - of X-rays, 117
 - Polyatomic molecular spectra, 248
 - Pomerantz, M. A., 424, 443, 448
 - Pose, H., 338, 366
 - Positive ions, 38, 39
 - Positron, discovery of, 266, 309
 - Positron-negatron pairs, 311
 - Positrons and negatrons, Dirac's theory, 315
 - Potassium, radioactivity of, 268
 - Potassium chloride, structure of, 130
 - Potential, excitation, 212
 - ionization, 209 *ff.*
 - resonance, 211
 - stopping, 83
 - Potential barrier, 174, 361
 - penetration of, 174, 362
 - Potential-energy diagram, of diatomic molecule, 245
 - of particle in a box, 172
 - of radioactive nucleus, 279
 - of thorium C, 279
 - Potential well, 373
 - Pound, R. V., 368
 - Powder method of crystal-structure analysis, 133
 - Powell, C. F., 267, 408 *ff.*, 427, 437, 438
 - Powers, P. N., 331
 - Precession, Larmor, 106
 - Preiswerk, P., 272
 - Price, H. C., 283
 - Principal quantum number, 102
 - Principal series of sodium, 195, 198
 - Probability in radioactive decay, 269
 - Probability density, 177 *ff.*, 237
 - Prompt neutrons in fission, 386, 388
 - Proton, 24
 - behavior of (table), 480
 - Proton-proton potential, 374
 - Proton-proton scattering, 374
 - Protons, size of, 37
 - transmutation by, 265, 350 *ff.*
 - Prout's hypothesis, 43
 - Purcell, E. M., 368

- Quantization, of hydrogen atom, 98
 of orbital magnetic moment, 226
 of simple harmonic oscillator, 186
 in wave mechanics, 172
- Quantum, 52, 96
- Quantum defect, 196
- Quantum number, 98, 165
 azimuthal, 100, 194
 inner, 199
 magnetic, 106
 orbital, 225
 radial, 102
 spin, 199
 total, 194, 196, 202
- Quantum numbers, assignment of, 225
- Quantum theory, of particle in box, 172
 of radioactive disintegration, 358 *ff.*
 of rotator, 235
 of simple harmonic oscillator, 185
 of specific heats, 235 *ff.*
 Planck's, 74 *ff.*
- Quenching of counter discharge, 291
- Quintuplet terms, 206
- Rabi, I. I., 368, 370
- Radial quantum number, 102
- Radiation, annihilation, 314
 classical theory of, 53 *ff.*
 electromagnetic conception of, 53 *ff.*
 energy density of, 89
 fourth-power law of, 70
 from black-body cavity, 69
 interacting with an atom, 147
 quantum theory of, 71 *ff.*
 temperature, 66
- Radiation loss, by electrons, 421
 by mesons, 423
- Radio waves, 62
- Radioactive decay, 269
 average life, 269
 branching, 274
 half-life, 269
 statistical nature, 271
- Radioactive displacement law, 272
- Radioactive equilibrium, 270
- Radioactive families, 272 *ff.*
- Radioactive isotopes, scientific uses, 401
- Radioactivity, 264 *ff.*
 artificial, 350 *ff.*
 discovery of, 267
 induced, 266
 natural, 264
- Radioisotopes, production of, 402
 table of, 402
- Radium, discovery of, 268
 heating effect of, 276
- Radon, half-life, 269
- Rainwater, J., 324
- Rajewsky, B., 291
- Raman, C. V., 252
- Raman spectra, 252
- Range-energy curves of ionizing particles, 299
- Rasetti, F., 253, 433, 434
- Ratio of specific heats, 12
- Rayleigh, Lord, 73
- Rayleigh-Jeans radiation formula, 71
- Reaction diagram, 358
- Reactor, nuclear, 394
- Real gases, 14
- Recoil electrons, 143, 313
- Recoil nucleus, 278
- Reduced mass, 371
- Refraction of X-rays, 120
- Refractive index of matter waves, 171
- Regener, E., 449
- Relative motion, 454 *ff.*
- Relativistic particles, 406, 419
- Relativity, basic postulates of, 464
 of time, 410, 466
 precession of elliptic orbits, 102
 theory of, 454 *ff.*
- Relaxation time, 369
- Reproduction factor in reactor, 394, 397
- Residual rays, 62
- Resolving power, of a grating, 57
 of a microscope, 162
- Resonance capture of neutrons, 386
- Resonance potential, 211
- Resonance radiation, 211
- Resonance region for neutrons, 324
- Rest energy, electron, 30, 274
- Restricted theory of relativity, 464
- Retherford, R. C., 102
- Reversed spectrum line, 60
- Richardson, O. W., 88, 184
- Richtmyer, R. D., 451
- Ritter, F., 61
- Ritz, W., and combination principle, 95, 99
- Roaf, D., 365
- Roberg, J., 440
- Roberts, G. E., 433
- Roberts, R., 388
- Robson, J., 332
- Rochester, G. D., 436
- Rock salt, structure of, 130
- Röntgen, W. C., 25, 119, 267
- Rose, M. E., 369
- Rosen, B., 321
- Rosenblum, S., 278
- Rossi, B., 406 *ff.*, 423, 434 *ff.*, 447

- Rotating molecules, 13, 241, 244, 254
- Rotation-vibration spectra, 244
- Rotational band spectra, 241
- Ruark, A. E., 184, 252, 314, 368
- Rubens, H., and Nichols, E. F., 62
- Rubidium, radioactivity of, 268
- Russell, A. S., 272
- Russell-Saunders coupling, 206
- Rutherford, E., 48, 265, 280, 281, 298, 337, 338
- Rydberg, J. R., 94, 96, 194
- Rydberg constant, 94, 99, 209
- Rydberg formula, 94, 195
- Sachs, A., 393
- Saha, M. N., 314
- Sanders, J. H., 365
- Sard, R. D., 432, 435
- Sargent curves, 364
- Saunders, F. A., 60
- Sawyer, G. A., 365
- Saxon, D., 332
- Scattered neutrons, angular distribution, 328
- Scattering, of alpha particles, 47, 306
 - of gamma rays, 143, 297
 - of neutrons, 325
 - of photons, 143
 - of X-rays, classical theory, 116 *ff.*
 - quantum theory, 143 *ff.*
- Schein, M., 431, 439
- Scherrer, P., 133
- Schmidt, G. C., 268
- Schroedinger, E., 156 *ff.*
- Schroedinger's equation, 171
- Schumann, V., 65
- Scintillation counter, 289
- Scintillation screen, 338
- Scott, F. A., 283, 284
- Seaborg, G. T., and table of isotopes, 389, 487
- Secondary X-rays, 116
- Segrè, E., 378
- Seidl, F. G. P., 365
- Selection rules, 198, 201
- Serber, R., 151, 352
- Seriff, A. J., 413
- Sharp series of sodium, 195
- Shells of electrons, 138 *ff.*
- Shire, E. S., 356
- Short wavelength limit, 126
- Shoupp, W. E., 385
- Showers, cosmic-ray, 414, 439 *ff.*
 - mesonic, 415
- Shrader, E. F., 332
- Shull, C. G., 330, 331
- Shutt, R. P., 436
- Sidhu, S. S., 121, 134
- Siegbahn, M., 120
- Signal speed, 455
- Simultaneous events, 469
- Singer, S. F., 443, 445, 446
- Singlet levels, 203
- Skobelzyn, D., 310
- Sloan, D. H., 340, 344
- Smekal, A., 252
- Smith, A. E., 58
- Smith, F. M., 433
- Smyth report, 393, 399
- Snell, A. H., 332, 333
- Soddy, F., 272
- Sodium, series in spectrum of, 195
- Sodium chloride, structure of, 130
- Soft component of cosmic rays, 414, 416
- Solar energy, 356
- Sommerfeld, A., 100, 258, 261
- Space, absolute, 456
 - and the ether, 456
 - uniform motion through, 457 *ff.*
- Spallation, 352
- Specific heats of gases, 11 *ff.*, 234 *ff.*
 - classical theory, 234
 - quantum theory, 235
 - ratio of, 12
- Spectra, 54 *ff.*
 - absorption, 59, 247
 - microwave, 253
 - X-ray, 141
 - atomic, 93 *ff.*, 193 *ff.*
 - beta-ray, 284, 317
 - electronic band, 249
 - gamma-ray, 279
 - of alkalies, 194 *ff.*
 - of alpha particles, 278
 - of black-body radiation, 70
 - Raman, 252
 - rotational band, 241
 - rotation-vibration, 244
 - effect of isotopes on, 248
 - types of, 59 *ff.*
 - velocity, 39
 - X-ray, 124 *ff.*, 134 *ff.*
- Spectral displacement rule, 209
- Spectral energy curves, 70
- Spectrograph, magnetic, 276
 - mass, 39
- Spectrometer, infrared, 71
 - ionization, 124
 - neutron velocity, 331
- Spectroscopic notation, 202
- Spectroscopic terms, 95, 196, 202
- Spectroscopy, far infrared, 243

- Spectroscopy, microwave, 253
 near infrared, 247
 Spectrum, electromagnetic, 60, 62
 line, 59, 126
 of sodium, 195
 Spees, A. H., 33
 Spin, nuclear, 368 *ff.*
 Spin quantum number, 199
 Spin vector, 203
 Spins, of elementary particles, 479
 of light nuclei, 482
 Stability of atoms, 44
 Stark effect, 107
 Starke, H., 33
 Stars, cosmic-ray, 409, 425
 Stationary states, 97
 Statistics, Bose, 262
 Fermi, 262
 of elementary particles, 479
 Stefan-Boltzmann law, 70
 Steinberger, J., 410, 413
 Steller, J. S., 410
 Stephens, W. E., 385
 Stern, O., 214, 368
 Stern-Gerlach experiment, 214
 Stevenson, E. C., 266, 406, 427
 Stokes, G. G., 61
 Stokes' law, 27, 28
 Stoney, J., 24, 29
 Störmer, C., 442
 Stovall, E. J., Jr., 365
 Strassmann, F., 382
 Street, J. C., 266, 406, 427
 Studier, M. H., 272
 Suess, H. E., 279
 Susceptibility, magnetic, 215, 219
 Swann, W. F. G., 407, 424, 442, 452
 Sylvén, structure of, 130
 Symmer, R., 24
 Synchro-cyclotron, 340
 Synchrotron, 340
 Szilard, L., 387, 388, 393

 Tau meson, 436 *ff.*
 Tear, J. D., 62
 Teller, E., 393, 451
 Temperature and molecular energy, 9
 Temperature radiation, 66
 Terletski, Y. P., 452
 Terms, spectroscopic, 95, 196, 202
 Thales of Miletus, 23
 Thermal neutrons, 323, 324
 Thermionic work function, 88
 Thermopile, 63
 Thibaud, J., 311, 314
 Thomas, L. H., 199

 Thompson, R. W., 413, 433
 Thomson, G. P., 156, 160
 Thomson, J. J., 25, 38
 Thorium series, 272
 Thorndike, A. M., 436
 Threshold frequency, photoelectric, 78, 87
 Tomonaga, S., 434, 450
 Torrey, H. C., 368
 Total energy, 168
 Townsend, J., 25
 Tracks of particles, in cloud chamber, 296
 in photographic emulsion, 296
 Transmutation, by alpha particles, 265,
 337, 351
 by neutrons, 266, 352 *ff.*
 by protons, 352 *ff.*
 of light elements, 353
 Triplet levels, 203, 204
 Tritium, 105, 353
 Tuck, J. L., 365
 Tuning of matter waves, 166
 Tunnel effect in wave mechanics, 362
 Tuve, M. A., 265, 340, 356, 366, 374

 Uhlenbeck, G. E., 198
 Ultraviolet radiation, 61
 Uncertainty principle, 179
 Uniform motion through space, 457
 United States Atomic Energy Commis-
 sion, 114, 393
 United States nuclear reactors, 400
 Unsöld, A., 427
 Unstable particles, 427 *ff.*, 436 *ff.*
 Uranium, decay constant of, 271
 isotopes of, 271
 separation of, 393
 Uranium series, 272
 Urey, H. C., 105, 106, 198

V particles, 436 *ff.*
 Valence electron, 193, 222 *ff.*
 Valence forces, 229
 Vallarta, M. S., 442
 Valley, G. E., 434, 435
 Van Allen, J. A., 443 *ff.*
 Van de Graaff, R. J., 340, 341
 Van de Graaff generator, 340
 Van der Waals' equation, 15
 Van der Waals' force, 230
 Vector model of atom, 193 *ff.*
 Veksler, V., 340, 347
 Velocity, of light, 456 *ff.*
 of matter waves, 168
 Velocity filter, 39
 Velocity spectrum, 39
 Vibration-rotation band spectra, 244 *ff.*

- Visible radiation, 64
- Waller, I., 120
- Walton, E. T. S., 265, 354
- Wang, P., 388
- Watts, H. M., 477
- Wave amplitude ψ , 167, 169, 172 *ff.*
- Wave equation, 172
- Wave function, 172
 Born's interpretation of, 177
 of harmonic oscillator, 188
- Wave function ψ , 169, 172 *ff.*
- Wave mechanics, 155 *ff.*
 leak effect in, 177, 362
- Wave motion, equation of, 167
- Wave number, 52, 94
- Wave theory, of hydrogen atom, 189
 of light, 53 *ff.*
 of matter, 156 *ff.*
- Wavelengths, in X-ray spectra, 134
 of Balmer series lines, 94
 of Fraunhofer lines, 94, 104
 of ionized helium, 104
 of moving particles, 158
 of X-rays, 109, 137
- Waves associated with material particles, 155 *ff.*
- Way, K., 392
- Weak light experiments, 90
- Weiss, P., 219
- Weissenberg, A., 436
- Weisskopf, V. F., 393
- Wells, W. H., 385
- Wheeler, J. A., 314, 391, 434
- White, H. E., 189, 190
- Whitehead, W. D., Jr., 367
- Whittemore, W. L., 436
- Whole-number rule, 42
- Wien, W., 71
- Wien's displacement law, 72
- Wigner, E., 330, 393
- Williams, E. J., 433
- Williams, Robley C., 165
- Wilson, C. T. R., 79, 405
- Wilson, H. A., 25
- Wilson, R. R., 386
- Wilson cloud chamber, 79, 292
 stereoscopic photographs, 296
- Winckler, J., 443
- Wollan, E. O., 330, 331
- Wood, R. W., 93, 211
- Wooster, W. A., 284
- Work function, photoelectric, 86
- Work function, thermionic, 88
- Wyckoff, R. W. G., 165
- X-ray absorption spectra, 141 *ff.*
- X-ray emission spectra, 134 *ff.*
- X-ray energy-level diagram, 139
- X-ray microscope, 163
- X-ray photon, 143
- X-ray spectrum lines, table of, 137
- X-ray tube, 110, 150
 efficiency of, 110, 150
- X-rays, 61, 109 *ff.*
 absorption coefficient of, 114
 as wave motion, 117
 characteristic, 116, 117
 continuous spectrum of, 126, 149
 diffraction, by crystals, 120 *ff.*
 by ruled gratings, 119
 by slits, 119
 emission spectra of, 134 *ff.*
 energy-level diagram, 139
 fluorescent, 116
 hard, 115, 149
 index of refraction of, 120
 intensity of, 113
 ionization chamber, 112
 ionization spectrum of, 124
 measurement of, 112
 modified, 143
 polarization of, 117
 production of, 110
 refraction of prisms, 120
 safety measures, 111, 114, 115
 scattered, 116, 143
 scattering of, 143
 secondary, 116
 soft, 115
 wavelengths of, 109, 137
- X-unit, 52
- Yield curves, nuclear reactions, 364 *ff.*
- York, H. F., 409, 430
- Young, T., 51
- Young, V. J., 367
- Yukawa, H., 375, 376, 411
- Zacharias, J. R., 369
- Zahn, C. T., 33
- Zartman, I. F., and experimental determination of molecular speeds, 8
- Zeeman effect, 107
- Zinn, W. H., 387, 388

CENTRAL LIBRARY
BIRLA INSTITUTE OF TECHNOLOGY & SCIENCE
PILANI (Rajasthan)

Call No.

Acc. No. *47742*

DATE OF RETURN

--	--	--	--

